TOPOGRAPHIC, HAEMODYNAMIC AND PSYCHOPHYSICAL INVESTIGATION OF GLAUCOMATOUS OPTIC NEUROPATHY

EMMA JANE ROFF

Doctor of Philosophy

THE UNIVERSITY OF ASTON IN BIRMINGHAM

September 1999

The University of Aston in Birmingham
Topographic, Haemodynamic and Psychophysical Investigation of Glaucomatous Optic Neuropathy.
Emma Jane Roff
Doctor of Philosophy
1999

Synopsis

Loss of optic nerve head (ONH) axons in primary open angle glaucoma (POAG) has been attributed to both mechanical and vascular factors. Confocal scanning laser ophthalmoscopy (cSLO) provides a promising tool for the topographic follow-up of the ONH in glaucoma, while scanning laser Doppler flowmetry (SLDF) facilitates the rapid non-invasive assessment of retinal capillary blood flow. The purposes of these investigations were to optimise the techniques and explore their potential to classify and monitor disease.

Preliminary investigations explored the reproducibility and validity of cSLO and SLDF and showed that:
For cSLO:

- In a model eye, measurements are accurate over a range of axial lengths.
- For best reproducibility, seven images per visit are required, with a contour line located on Elschnig's scleral ring and transferred automatically between images.

For SLDF:

- Three perfusion images are required for optimum reproducibility.
- Physiological changes induced by gas perturbation can be measured.

Cross-sectional comparison of groups of normal subjects and early POAG patients showed that:

- cSLO parameters differentiate the early POAG group.
- Blood volume measured by SLDF showed group differences in superior nasal retina only.

Longitudinal investigation of ONH topography, haemodynamic and visual field indices in normal subjects and POAG patients showed that:

- cSLO detects topographical change over time more frequently in the POAG group. Important parameters include: C:D area ratio, cup and rim area, mean depth in contour, volumes above and below reference and surface.
- Factor analysis identified "cup" and "rim" factors that can be used to detect change over time in individual patients.
- Blood flow changes were most apparent in the inferior nasal peripapillary retina of the POAG group.
- Perimetry is of clinical value for the identification of glaucoma but is less sensitive than cSLO for monitoring glaucomatous change.

Keywords: Confocal scanning laser ophthalmoscopy, scanning laser Doppler flowmetry, perimetry.

Acknowledgements

I would like to thank my PhD supervisor Mr D. A. Barnes and my external supervisor, Mr J.M.Gibson, for their time and support. I would also like to thank my associate supervisor Dr S. L. Hosking for her expert guidance and friendship throughout this project. Special thanks are due to Miss Sally Embleton who was so helpful and thoughtful throughout my write up period.

I would also like to thank Professor A. Harris and colleagues at the Glaucoma Research and Diagnostic Centre at Indiana University for welcoming me into their Lab and their continued support and friendship. In particular I would like to thank my friends Mrs A. M. Morrison and Mr P. J. Halter who where both accommodating and professional.

Finally I would like to thank my family for their endless patience and understanding and my loving fiancé Anthony for always having confidence in me.

List of Contents

List of Tables

List of Figures

Chapter 1.

Glaucomatous optic neuropathy and its investigation

1.1. Introduction

Primary Open Angle Glaucoma (POAG) is a disease in which progressive loss of retinal ganglion cells and optic nerve axons results in characteristic disc appearances and visual field defects (Quigley, H. A., 1993). POAG may be further classified into two groups: high-tension glaucoma and normal- or low-tension glaucoma. High-tension glaucoma (HTG) is defined as glaucomatous optic neuropathy in the presence of elevated intraocular pressure (IOP) that results in characteristic visual field defects. Normal-tension glaucoma (NTG) is defined as glaucomatous optic neuropathy with intraocular pressure within the statistically normal range (Geijssen, H. C. & Greve, E. L., 1995).

The absolute aetiology of POAG is unclear and it is probable that the eventual loss of retinal ganglion cells (RGC) and optic nerve head (ONH) axons occurs as a result of several mechanisms. Two principle theories for glaucomatous ONH atrophy have evolved. The vascular theory, which proposes an underlying vascular mechanism that precipitates atrophy, and the mechanical theory, which depicts that a physical process such as increased IOP results in glaucomatous optic neuropathy. Recently investigators have acknowledged the possibility that these theories are not mutually exclusive and that they are both involved, at least to some extent, in the pathogenesis of glaucoma.

There are several tests available for the assessment of glaucomatous optic neuropathy, including visual field analysis, IOP assessment and examination of the ONH. Typically paramedical staff have carried out the former two assessments although the examination of the optic nerve has remained the responsibility of the ophthalmologist. Recent developments in digitised imaging techniques and scanning laser

ophthalmoscopy now provide potential tools for qualitatively and quantitatively assessing the human optic nerve head and retina *in-vivo*. Such developments may facilitate ONH assessment and follow-up with minimal input from the ophthalmologist.

The following review describes the normal ONH and it's pathogenesis in glaucomatous optic neuropathy with particular attention to the vascular and mechanical theories for ONH damage. The epidemiology of POAG is reviewed together with the known risk factors associated with the disease. Three areas of clinical assessment for glaucoma are outlined with specific attention to the examination of the ONH. A detailed review of confocal scanning laser ophthalmoscopy (cSLO) follows, focusing in particular on the Heidelberg Retina Tomograph (HRT). Finally, in response to the increasing likelihood of an underlying vascular mechanism in POAG, several of the techniques currently available for the assessment of ocular blood flow are reviewed.

1.2. The history of glaucoma

As early as 1830, Mackenzie, W. A., identified a link between what was then known to be glaucoma and raised pressure in the eye. At that time the optic disc was assumed to be swollen or bulging. The invention of the ophthalmoscope provided the first clinical tool to properly examine the ONH after which Helmholtz, H. (1851) and Weber, A. (1855) made the important discovery that the optic disc was excavated rather than swollen in glaucoma. Von Graefe recognised cupping of the optic nerve and further divided glaucoma into four sub-groups: acute congestive glaucoma, chronic congestive glaucoma, secondary congestive glaucoma and amaurosis with excavation of the optic nerve (Von Graefe, A., 1857). This early classification of glaucoma came about when only the limited technique of digital tonometry was available. Von Graefe proposed, that with the exception of amaurosis with excavation of the optic nerve, all sub-groups of glaucoma occurred in the presence of elevated pressure. Later, Von Graefe withdrew the concept, possibly at the instigation of Donders, F. C. (1862), who believed that all excavation of the ONH was due to

elevated IOP. It was not until the introduction of indentation tonometry by Schiotz in 1905 that the existence of ONH excavation and atrophy without elevation in IOP was concluded (Schnabel, J., 1905).

At the turn of the century, interest in the normal ONH grew with Elschnig's characterisation of the five different types of disc (Bothman, L., 1947). Extensive attempts to accurately describe and document the glaucomatous ONH followed (Elliot, R. H., 1922; Pickard, R., 1923; Kronfeld, P. C., 1967; Halberg, G. P., 1969). Armaly, M. F. & Sayegh, R. E. (1969) contributed substantially by the introduction of the decimal cup:disc ratio still used today. From this point on, an inexhaustible number of investigators have attempted to distinguish between the normal and glaucomatous ONH.

1.3. Terminology and classification

The term glaucoma refers to a bilateral group of disorders that have certain common features. In particular:

- cupping and atrophy of the ONH:
- characteristic visual field loss; and
- often, but not always, increased IOP.

(Thylefors, B. & Negrel, A.D., 1994)

Several types of glaucoma exist including:

- Primary open angle glaucoma
- Primary angle closure glaucoma
- Secondary forms of glaucoma
- Congenital glaucoma

The two primary forms of glaucoma are discussed in more detail in the following sections.

1.3.1. Primary angle closure glaucoma (PACG)

Primary angle closure glaucoma (PACG) is an acute form of glaucoma that results in pain and visual loss. This condition is very often asymptomatic, resulting from an obstruction to the drain of aqueous fluid from the eye (Quigley, H. A., 1996). PACG can occur bilaterally as a result of increased surface apposition of the lens to the iris. This causes an increase in resistance to the flow of aqueous humour from the posterior to the anterior chamber of the eye, otherwise known as the pupillary block mechanism. The pressure gradient between the two chambers then forces the iris to bow forwards (iris bombé) (Phillips, C. I., 1972). This results in obstruction of the trabecular meshwork and a raise in IOP that can be quite sudden in onset (Rosenberg, L. F., 1995).

PACG is more common in hypermetropic eyes with narrow anterior chamber angles (Harvey, W. J. F., 1997). Occasionally, it can occur in the absence of pupillary block, for example in primary plateau iris where the angle is blocked by the last role of the iris when dilated (Harvey, W. J. F., 1997).

1.3.2. Primary Open Angle Glaucoma (POAG)

Primary open angle glaucoma (POAG) is the chronic progressive from of the disease and is by far the most demanding clinically. This condition is characterised by atrophy of the ONH, loss of peripheral visual function and excavation of the optic disc (Quigley, H. A., 1993). Optic disc findings include enlargement of the central cup, thinning of the neuroretinal rim, and focal abnormalities of the disc rim, such as haemorrhaging and notching (Rosenberg, L. F., 1995). POAG may be further classified into sub-groups:

1.3.2.1. High-tension glaucoma (HTG)

Sometimes referred to as POAG, this sub-class of the disease is characterised by glaucomatous optic neuropathy, with visual field loss, in the presence of elevated IOP above the statistically normal range and an open anterior chamber angle. The mean IOP of a normal population is 15.5mmHg (Moses, R. A., 1975) and it is generally thought that IOP ≥ 22 mmHg may be classed as HTG (Hodapp, E. *et al.*, 1993; Jonas, J. B. & Papastathopoulos, K. I., 1995).

1.3.2.2. Normal- or low-tension glaucoma

Normal-tension glaucoma (NTG) may be defined as glaucomatous optic neuropathy in the presence of abnormal visual fields with IOP within the statistically normal range (< 22mmHg) and an open anterior chamber angle (Hodapp, E. *et al.*, 1993; Geijssen, H. C. & Greve, E. L., 1995).

1.3.2.3. Focal glaucoma

Some authors prefer to characterise glaucoma according to the appearance of the optic disc and corresponding visual fields defects rather than IOP only (Geijssen, H. C. & Greve, E. L., 1990; Spaeth, G. L., 1994a; Gupta, N. & Weinreb, R. N., 1997; Broadway, D. C. *et al.*, 1999). Focal glaucoma, sometimes referred to as focal ischemic glaucoma, refers to glaucoma in the presence of marked focal change of the disc and corresponding focal visual field changes (Emdadi, A. *et al.*, 1998). IOP may be elevated, but is more often normal (Geijssen, H. C. & Greve, E. L., 1990; Spaeth, G. L., 1994a). People diagnosed with focal glaucoma tend to be younger than those diagnosed with POAG, are more often female (Spaeth, G. L., 1994a) and have specific haemodynamic characteristics (Galassi, F. *et al.*, 1997).

1.3.2.4. Suspect Glaucoma

A glaucoma suspect may be defined as a person who is at higher risk than usual of developing glaucomatous optic nerve damage and visual field loss. The absolute classification of suspect glaucoma varies, but the common conditions that place a patient at risk include:

- Increased IOP.
- Large or asymmetric optic cups.
- Margin splinter haemorrhage.
- Unexplained visual field defect consistent with glaucoma.
- Family history of glaucoma. (Hodapp, E. *et al.*, 1993)

A patient that exhibits one or more of these risk factors in the presence of an open and normal anterior angle may be defined as a glaucoma suspect, further definitions exist to define them as low, moderate, or high risk (Hodapp, E. *et al.*, 1993). In this respect patients with elevated IOP only may be regarded as a glaucoma suspect. Other classification systems separate patients with raised IOP into a group called ocular hypertension.

1.3.2.5. Ocular hypertension

Only 10% of patients with increased IOP have glaucoma (Gupta, N. & Weinreb, R. N., 1997). This leaves a large sub-group with raised IOP. Ocular hypertension, or patients diagnosed with elevated IOP only, may be defined as those that have IOP $\geq$ 22mmHg in the presence of an open and normal anterior angle but without ONH abnormalities or visual field loss (Hodapp, E. *et al.*, 1993).

1.4. Epidemiology

Several papers have attempted to determine the global impact of glaucoma. There are a number of difficulties associated with conducting studies that deliver epidemiological facts. Clearly it is impractical to count the number of people with glaucoma world-wide, for that reason estimates are made from examining random samples of the population. The epidemiological data varies from study to study, not only because different samples of the population are examined, but also because different sampling methods are used and different criteria are employed to define the glaucoma groups. With this in mind epidemiological data must be reviewed with caution and may only ever give an approximation of the prevalence and incidence of a disease.

Survey	Beaver Dam	Framing-ham	Barbados	Baltimore	Melton Mowbray	Tierp
Author	(Klein, *et al.* 1992)	(Khan, *et al.* 1977)	(Leske, *et al.* 1994)	(Tielsch, *et al.* 1994)	(Gibson, *et al.* 1985)	(Ekström, 1996)
Age Range	43-84	75-85	40-84	40 +	76 +	65-74
POAG (%)	2.1	7.2	7	8.4	6.6	5.7
PACG (%)	0.4	-	-	1.3	-	-

Table 1.1. Epidemiology data (prevalence (%)) for primary open angle glaucoma (POAG) and primary angle closure glaucoma (PACG).

Table 1.1. outlines the prevalence of POAG and PACG as reported from several epidemiological studies. Clearly POAG is considerably more prevalent than PCAG. In Baltimore alone, approximately 8.4% of people over the age of 40 suffer from POAG compared to 1.3% diagnosed with PACG. Several investigators have attempted to determine the global impact of glaucoma by pooling the available results from the separate epidemiological studies that have been conducted on different populations around the world. From this data Thylefors, B. & Negrel, A.D. (1994) estimated that 3 million people world-wide are blind as a result of glaucoma. Quigley, H. A. (1996) estimated that 2.47 million people in the USA will have POAG by the year 2000 and a

recent HMSO report recommended that POAG is responsible for 21% of registered blindness in the UK (Evans, J., 1991).

1.5. Risk factors in glaucoma

Primary open angle glaucoma is considered a multifactorial disease. Although the aetiology of the disease remains unclear, a number of studies have identified a selection of risk factors associated with the condition. These are summarised in Table 1.2. and some of the more pronounced risk factors are discussed in following sections.

Category	Risk factor
Demographic	Age Gender Race
Ocular	Intraocular pressure (IOP) Myopia
Systemic	Diabetes Systemic hypertension Systemic hypotension Peripheral vascular disease Vasospasm Migraine Hormonal influences
Genetic	Family history of glaucoma
Other	Cigarette smoking Caffeine intake Alcohol intake Socio-economic factors

Table 1.2. Risk factors in glaucoma.

1.5.1. Ocular hypertension

Elevated IOP above the statistically normal range of 21-22mmHg is the most consistent risk factor in the development of glaucomatous optic neuropathy. This statistical value is based on the results of a number of studies and represents the upper bracket of the mean IOP plus two standard deviations (Armaly, M. F., 1965; Hollows, F. C. & Graham, P. A., 1966; Bankes, J. L. K. *et al.*, 1968; Wallece, J. & Lowell, G. G., 1969; Bengtsson, B., 1972).

The importance of raised IOP as a risk factor is reflected in the fact that approximately 50% of patients presenting with POAG have raised IOP at the time of diagnosis. One of the most extensive IOP surveys carried out, the Baltimore survey, elegantly demonstrates this. The IOP of more than 5000 participants were examined and a total of 198 subjects were diagnosed with glaucoma. Of these, 41% were found to have IOP of 22mmHg or over (Sommer, A. *et al.*, 1991b).

A relationship between the level of IOP and optic disc cupping (Rath, E. Z. *et al.*, 1996), and IOP and visual field loss has been identified (Vogel, R. *et al.*, 1990). When IOP is elevated above 21mmHg, visual field loss is reported to progress at a rate of approximately one percent per year (Perkins, E. S., 1973; Kass, M. A., 1983). However, other authors have suggested that the link between IOP and visual field loss is weak and controversial (Lundberg, L. *et al.*, 1980; Crick, R. P. *et al.*, 1989).

Clearly, elevated IOP is an important risk factor in POAG, but there are several facts that imply that there may be further risk factors involved. The existence of NTG suggests a form of glaucomatous optic neuropathy that may be dependent on factors other than raised IOP. Furthermore, the Baltimore survey revealed that the prevalence of POAG is 4.3 times more prominent in black than white people, whereas the average IOP between the two ethnic groups is similar (Sommer, A. *et al.*, 1991b). Additionally although glaucomatous optic neuropathy is known to increase with age (see section 1.5.2.), in Japan IOP is found to decrease with age (Shiose, Y., 1990). Finally, a longitudinal investigation by Lundberg, L. *et al.*, (1980), found that only 30% of patients with elevated IOP showed signs of visual field damage, even when followed up for as long as 20 years. This weak link between the level of IOP and visual field loss implies that there are other factors involved in the pathogenesis of glaucomatous optic neuropathy.

1.5.2. Age

Increasing age is one of the most significant risk factors for POAG. Increased prevalence of POAG with age has been consistently reported in several population studies (Hollows, F. C. & Graham, P. A., 1966; Bankes, J. L. K. *et al.*, 1968; Tielsch, J. M., 1991). Over 2 percent of the population aged over 40 years suffer from glaucoma (Nuzzi, R. & Cerruti, A., 1995) and the prevalence rates increase dramatically with age. POAG is between four and ten times more prevalent in older age groups. Bankes, J. L. K. *et al.*, (1968) showed that, in a cohort of nearly 6,000 people (Bedford Survey), IOP increased with age and that 80% of POAG cases occur over the age of 60.

1.5.3. Gender

There is some evidence to suggest gender as a significant risk factor in POAG. Orgül, S. *et al.*, (1995) reported that NTG is more prevalent in females than males. Wilson, R. *et al.*, (1982) identified an increased rate of visual field loss in women compared to men and increased IOP levels have been reported in females (Armaly, M. F., 1965; Hollows, F. C. & Graham, P. A., 1966; Bankes, J. L. K. *et al.*, 1968). This finding has been attributed to hormonal and menopausal influences (Armaly, M. F., 1965).

1.5.4. Race

Race has been demonstrated as an important risk factor in POAG. Population studies have shown that black people are four times more likely to develop POAG compared to Caucasians (Tielsch, J. M. *et al.*, 1991). Interestingly the average IOP for black and white people is similar (Sommer, A. *et al.*, 1991b).

1.5.5. Diabetes

Diabetes mellitus has been identified as a risk factor for POAG. Studies have shown that people suffering with diabetes have a higher incidence of POAG than people without the disease (Armstrong, J. R. *et al.*, 1960; Klein, B. E. K. *et al.*, 1994). Likewise, studies have shown that POAG patients have a higher incidence of diabetes than found in the normal population (Becker, B., 1971; Wilson, R. *et al.*, 1982). The reasons why people with diabetes mellitus are more prone to POAG are unknown. One theory is that diabetes may be associated with changes in the trabeculum resulting in a decrease in aqueous outflow (Klein, B. E. K. *et al.*, 1994). This rationale is supported by reports of higher IOP in people with older-onset diabetes compared to the normal population (Klein, B. E. K. *et al.*, 1984).

1.5.6. Systemic hypertension

Studies have identified a positive association between systemic hypertension and increased IOP (Leske, M. C. & Podgor, M. J., 1983; Carel, R. S. *et al.*, 1984). The absolute significance between raised IOP and blood pressure remains unclear, however, it is suggested that such a combination may result in decreased perfusion pressure of the eye which is associated with increased risk of POAG (Tielsch, J. M. *et al.*, 1995). The subject remains controversial with some studies reporting a protective effect of raised blood pressure in POAG (Wilson, R. *et al.*, 1982).

1.5.7. Systemic hypotension

Low blood pressure has been identified as a risk factor in POAG (Kaiser, H. J. *et al.*, 1993b; Hayreh, S. S. *et al.*, 1994), particularly NTG (Demailly, P. *et al.*, 1984; Gramer, E. & Tausch, M., 1995). Nocturnal hypotension is more pronounced in NTG compared with patients with anterior ischemic optic neuropathy (Hayreh, S. S. *et al.*,

1994) and normal control subjects (Meyer, J. H. *et al.*, 1996). It has been suggested that although nocturnal hypotension is a physiological phenomenon, drops in blood pressure may contribute to ONH damage in patients that may already have a predisposing vascular insufficiencies (Hayreh, S. S. *et al.*, 1994). A recent paper by Evans, D. W. *et al.*, (1999b) supports this concept as POAG patients where found to display an abnormal ocular circulatory response to the nocturnal pressure dip compared to normal subjects.

1.5.8. Family history of glaucoma

A positive family history has been identified as an important risk factor in POAG (Wilson, R. *et al.*, 1982; Tielsch, J. M. *et al.*, 1994; Booth, A. *et al.*, 1997; Haefliger, I. O. & Flammer, J., 1997). Results from the Baltimore survey showed that the odds ratio for a person developing POAG, who already has siblings with the disease, was 3.69. For those with parents diagnosed with POAG, the odds were 2.17 (Tielsch, J. M. *et al.*, 1994).

1.5.9. Peripheral vascular disease

Drance, S. M. *et al.*, (1973) reported that certain haemodynamic factors are more prevalent in NTG compared to HTG. These included coronary heart disease with shock, heart failure and carotid circulatory deficiencies. Gutman, I. *et al.*, (1993) found abnormalities of the carotid arteries in NTG and Sponsel, W. E. *et al.*, (1997b) has shown that retinal leukocyte velocity is compromised in POAG during IOP elevation when compared to normal subjects. Another study confirmed the higher prevalence of hyperlipidemia in NTG compared to the general population (Winder, A. F. *et al.*, 1974), but this finding is not consistent (Demailly, P. *et al.*, 1984). Neither is the finding that haemodynamic crisis is more prevalent in glaucoma (Demailly, P. *et al.*, 1984).

1.5.10. Vasospasm

Vasospasm may be defined as a reversible constriction or insufficient dilation of ateriosclerotic or otherwise healthy vessels (Flammer, J., 1996). Women are reported to suffer from vasospastic disorders five times more than men (Gasser, P., 1989) and NTG is more predominant in females (see section 1.53.). Harris, A. *et al.*, (1994b) proposed that vasospasm distal to the ophthalmic artery compromises blood flow to the optic nerve in NTG. The measured blood flow resistance in the ophthalmic artery of NTG subjects compared to normal controls was abolished following the administration of a cerebral vasodilator, thus providing evidence for reversible vasospasm in this patient group (Harris, A. *et al.*, 1994b). Interstingly, Rankin, S. J. A. & Drance, S. M. (1996) were unable to identify a significant link between focal peripapillary arteriolar narrowing and vasospasm in glaucoma patients.

1.5.11. Migraine

An association between migraine headache and NTG has been identified (Corbett, J. J. *et al.*, 1985; Phelps, C. D. & Corbett, J. J., 1985). However, in a large population survey, no evidence could be found of a relationship between glaucoma and migraine (Klein, B. E. K. *et al.*, 1993), hence direct evidence supporting the theory is lacking.

1.5.12. Other risk factors

Other proposed risk factors, that are yet to be fully substantiated, include cigarette smoking, caffeine and alcohol intake, myopia and socio-economic factors (Gramer, E. & Tausch, M., 1995; Rosenberg, L. F., 1995; Stewart, W. C., 1995; Fraser, S. G., 1997; Langhans, M. *et al.*, 1997).

1.6. The normal optic nerve head

1.6.1. Anatomy of the optic nerve

The optic nerve has a total length of approximately 50mm, commencing at the optic disc and extending to the optic chiasma. The nerve is made up of RGC axons that are encased within a thin myelin sheath and range between 0.65μm and 1.1μm in diameter, and 689,500 and 1,244,005 in number (Balazsi, A. G. *et al.*, 1984; Quigley, H. A. *et al.*, 1988; Mikelberg, F. S. *et al.*, 1989; Repka, M. X. *et al.*, 1989). The nerve has a well-developed extracellular matrix which is most extensive at the level of the ONH (Evans, A. & Jeffery, G., 1992; Birch, M. *et al.*, 1997). The RGC axons are arranged in bundles or fascicles that are separated by connective tissue and although they are contained within a myelin sheath for the majority of the length of the optic nerve, at the level of the ONH they are non-myelinated. The RGC axons are densest at the inferior temporal sector and thickest at the superior nasal sector (Mikelberg, F. S. *et al.*, 1989). An age -related decline of between 4909 and 6723 RGC axons yearly has been identified in the normal human optic nerve (Johnson, B. M. *et al.*, 1987; Mikelberg, F. S. *et al.*, 1989).

1.6.2. Anatomy of the optic nerve head

The optic nerve head may be divided into four distinct regions:

- Superficial retinal nerve fibre layer (lamina retinalis)
- Prelaminar region (lamina choroidalis)
- Lamina cribrosa (lamina scleralis)
- Retrolaminar region

The underlying anatomy of these areas is discussed in the following sections with the exception of the vascular anatomy, which is reviewed in section 1.7.

1.6.2.1. Superficial retinal nerve fibre layer

The superficial retinal nerve fibre layer (RNFL) occurs at the level of the retina and is otherwise known as the lamina retinalis. The RNFL may be further divided into five sectors according to how the nerve fibres radiate towards the optic nerve from the various locations of the retina (Figure 1.1.):

1. Superior arcuate fibres – originate temporally at the horizontal raphé and travel superiorly in an arc around the papillomacular bundle arriving at the superotemporal portion of the optic disc.
2. Inferior arcuate fibres - originate temporally at the horizontal raphé and travel inferiorly in an arc around the papillomacular bundle arriving at the inferotemporal portion optic disc.
3. Superior radiating fibres – originate in the superonasal region of the retina and radiate towards the optic disc to occupy the superonasal portion.
4. Inferior radiating fibres - originate in the inferonasal region of the retina and radiate towards the optic disc to occupy the inferonasal portion.
5. Papillomacular bundle – fibres originate from the temporal retina where they cluster around the macular above and below the horizontal raphé, they then travel towards the optic nerve to occupy a substantial portion of the temporal optic disc.

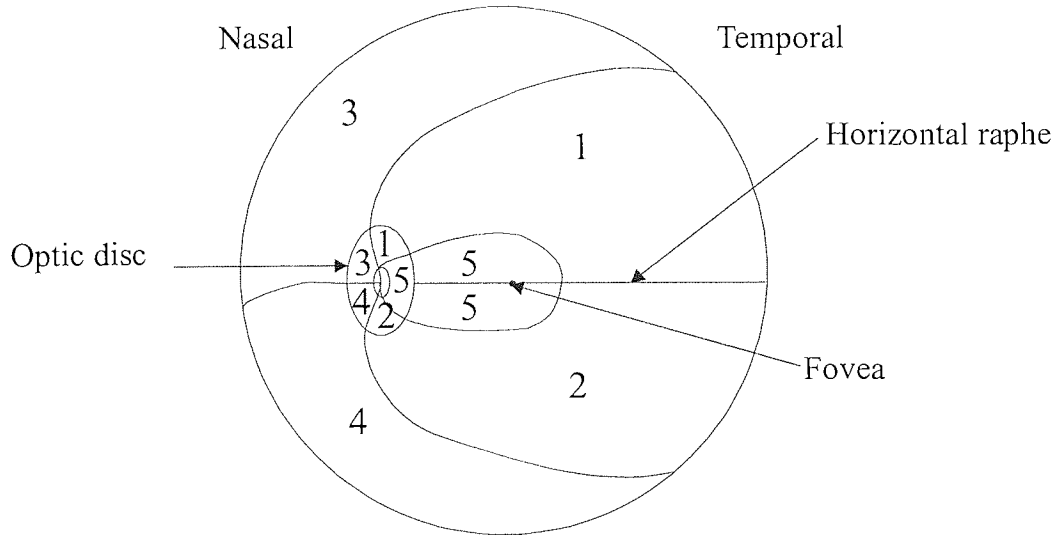

Figure 1.1. Retinal nerve fibres. The pattern of the retinal nerve fibres are shown: superior arcuate fibres (1), inferior arcuate fibres (2), superior radiating fibres (3), inferior radiating fibres (4), papillomacular bundle (5).

At the disc margin, the thickness of the retinal nerve fibres vary between 316μm and 405μm. The thinnest fibres are located at the temporal polar papillomacular bundle (Varma, R. *et al.*, 1996). The distribution of fibres in the retina and localised damage of individual bundles results in characteristic visual field defects in glaucoma (Anderson, D. R., 1983).

1.6.2.2. Prelaminar region

The prelaminar region of the ONH (Figure 1.2.) lies adjacent to the choroid and consists of non-myelinated RGC axons arranged in fascicles and surrounded by an extensive extracellular matrix rich in glial cells (Birch, M. *et al.*, 1997). The fascicles are formed by astrocytes that wrap around the bundles of nerve fibres to form circular tubules. The long processes of the astrocytes extend into the fascicles, which are continuous throughout the lamina cribrosa and retrolaminar regions of the optic nerve.

1.6.2.3. Lamina cribrosa

The lamina cribrosa or lamina scleralis (Figure 1.2.) at the level of the sclera is comprised of ten perforated plates of collagenous extracellular matrix. The extracellular matrix is a compliant tissue that contains numerous elastin fibres and fibrillar collagens and a complex network of filamentous basement membranes (Hernandez, M. R. *et al.*, 1987). The perforations or pores of adjacent cribiform plates are arranged in parallel to form channels that allow the transit of non-myelinated RGC axons (Birch, M. *et al.*, 1997). This facilitates axonal transport, which is defined as the movement of material along an axon either from the cell body to the axon terminal (orthograde), or from the terminal to the cell body (retrograde) (Anderson, D. R., 1977). The pores vary in diameter, those arranged centrally appear to be smaller than others in the periphery and pores in the superior and inferior quadrants are larger than others situated in the nasal and temporal quadrants (Mikelberg, F. S. *et al.*, 1989; Birch, M. *et al.*, 1997). As a result the extracellular matrix appears thicker in the

temporal and nasal areas. When viewed three-dimensionally the collagenous extracellular matrix of the lamina cribrosa often appears to be shaped like a saddle. Consequently, the nasal/temporal axis is situated closer to the surface of the vitreous than the superior and inferior poles.

1.6.2.4. Retrolaminar region

The retrolaminar region of the optic nerve (Figure 1.2.) lies posterior to the lamina cribrosa and is surrounded by the meninges of the central nervous system, namely the pia, arachnoid and dura maters. The RGC axons appear myelinated in this section of the ONH. The individual nerve fibre fascicles are present and are separated by pial septa that provide both nutritional and mechanical support to the RGC axons.

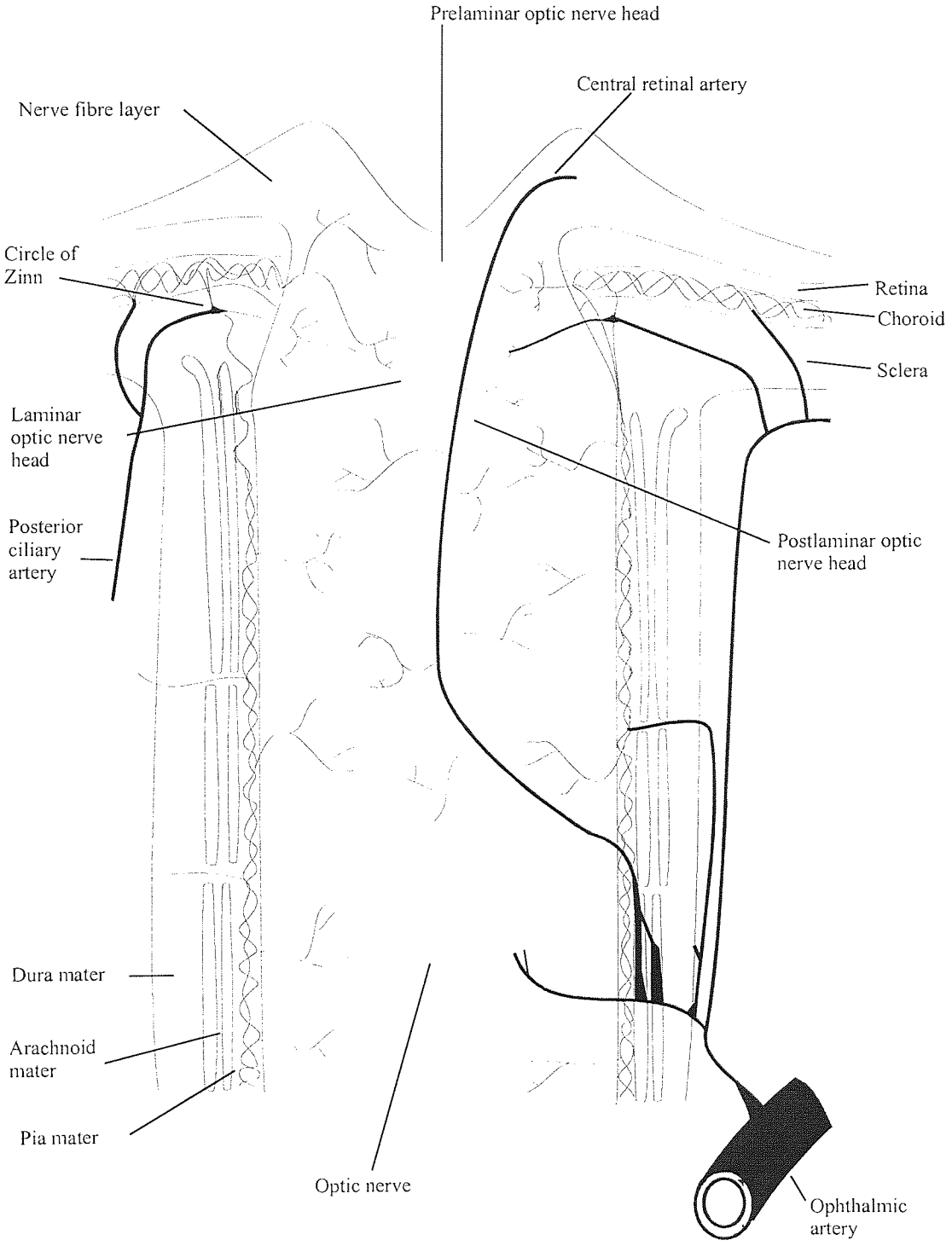

Figure 1.2. Anatomy and blood supply of the optic nerve. (Adapted from Hayes, A., 1997)

1.7. Blood supply to the eye

The human eye is supplied by two systems of blood vessels: the retinal vessels that supply some of the retina, and the uveal or ciliary vessels, which perfuse the remaining retina, choroid, ciliary body and iris. Both sets of blood vessels originate from one source, the ophthalmic artery, which is the only branch of the internal carotid artery outside of the cranium (Hayreh, S. S., 1962) (Figures 1.2. & 1.3.).

1.7.1. Retinal blood supply

The majority of the blood supplied to the retina is through the central retinal artery (CRA); this is usually a branch of the ophthalmic artery (OA), but may occasionally arise from one of the posterior ciliary arteries (PCAs) (Singh, S. & Dass, R., 1960). The CRA penetrates the dural and arachnoid sheaths approximately 10mm posterior to the globe (Figure 1.3.). It then courses in the subarachnoid space before entering the optic nerve where it adopts a central position entering the eye at the ONH (Figure 1.3.). The CRA usually divides to form two branches at the optic disc which then separate to form four trunks that supply the inferior, temporal, superior, and nasal quadrants. These then form arterioles and finally capillaries that perfuse the inner layers of the retina.

The capillary networks perfuse the majority of the retina at three levels. Firstly, at the nerve fibre and ganglion cell layer. Secondly, within the inner nuclear layer and finally at a superficial level around the ONH and along the inferior and superior temporal retinal vessels (Pournaras, C. J., 1996). Occasionally a cilioretinal artery derived from the ciliary circulation may also nourish the inner retinal layers (Bill, A., 1981). Blood from the retinal circulation is drained from the retinal capillaries into venules, veins and eventually the central retinal vein (Figure 1.3.).

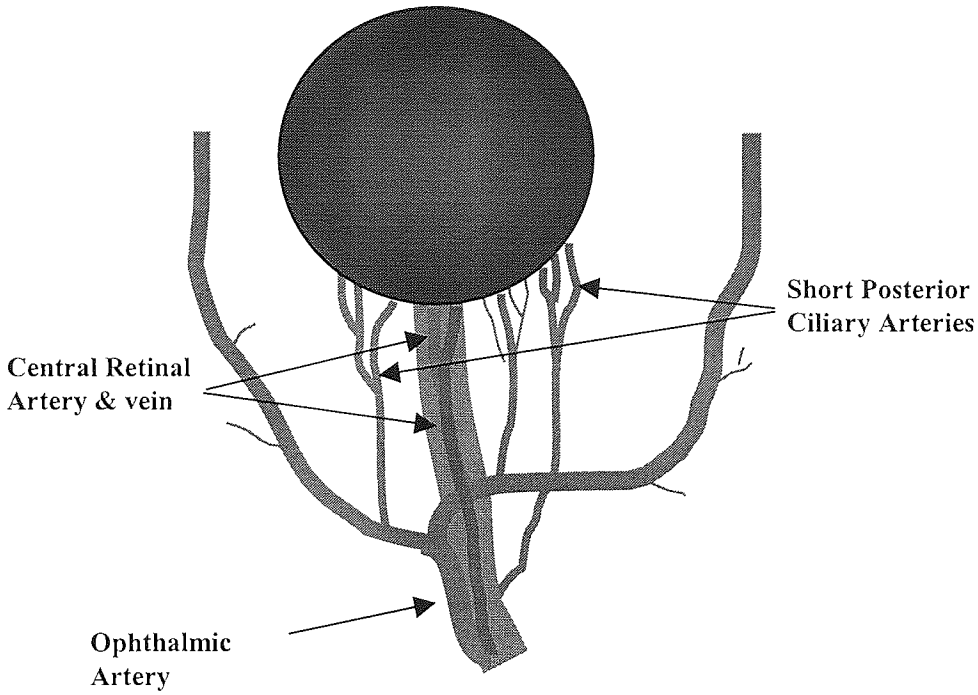

Figure 1.3. Blood supply to the eye. The positions of the retrobulbar vessels relative to the globe are indicated: ophthalmic artery, central retinal artery and vein, short posterior ciliary arteries. Adapted from Harris, H. *et al.*, 1998.

1.7.2. Uveal blood supply

The anterior and posterior ciliary arteries arise from the OA and supply the uvea (Figure 1.3.). Between one and five posterior ciliary arteries (PCAs) derive from the OA in the posterior orbit. Two to four of these then follow an anterior course before forming medial and lateral groups that divide into a number of short PCAs (Hayreh, S. S., 1974; Cioffi, G. A. & Van Buskirk, E. M., 1994; Onda, E. *et al.*, 1995; Büchi, E. R., 1996; Harris, H. *et al.*, 1998). The short PCAs follow a tortuous course and pierce the perineural sclera of the posterior globe. Some of the short PCAs supply the anterior ONH with blood whist others perfuse the choroid forming the choriocapillaris. The transition from arteriole to capillaries is quite sudden, this is a major characteristic of the choriocapillaris which then go on to form a tight network on Bruch's membrane (Hayreh, S. S., 1974). The confluence of branches arising from

the short PCA's gives rise to a non-continuous arterial circle in the sclera, otherwise known as the circle of Zinn-Heller (Figure 1.2.) (Bill, A., 1981). Branches from the arterial circle, along with intrascleral arterioles then perfuse the anterior ONH, peripapillary choroid and pial arterial network (Harris, H. *et al.*, 1998).

Two long PCAs also arise from the PCAs; these travel anteriorly along either side of the globe to the ciliary body where they form the major arterial circle of the iris along with the anterior ciliary arteries. This circle then gives rise to the arteries of the ciliary process, iris and the anterior section of the choriocapillaris (Bill, A., 1981). Blood from the anterior part of the uvea and choroid is drained through the vortex veins that in turn drain into the cavernous sinus. The posterior sclera and occasionally part of the choroid are drained via small posterior ciliary veins and the anterior uvea is drained in part by small anterior ciliary veins.

1.7.3. Vascular supply to the anterior optic nerve

The anterior ONH may be considered as four distinct anatomical regions (see section 1.6.). The superficial layer is largely supplied by the recurrent retinal arterioles of the retinal circulation, however the cilioretinal artery may also contribute when present (Onda, E. *et al.*, 1995). Direct branches of the short PCAs and indirect branches from the circle of Zinn-Haller provide the principle vascular supply to both the prelaminar and lamina cribrosa regions (Anderson, D. R. & Hoyt, W. F., 1969). Occasionally, large arterioles from the peripapillary choroid branch to supply the prelaminar and lamina cribrosa. It should be stressed however, that the choriocapillary network in the peripapillary choroid remains distinct from the ONH (Cioffi, G. A. & Van Buskirk, E. M., 1994). The retrolaminar portion of the optic nerve receives blood from both the CRA and the pial system. The pial system is a network of capillaries that exist in the pia mater, which in turn arises from the circle of Zinn-Haller and occasionally the short PCAs. Branches from the pial system together with branches from the CRA that may anastomose with the pial system extend to nourish the ONH axons (Figure 1.2.) (Lieberman, M. F. *et al.*, 1976).

1.7.4. Regulation of ocular blood flow

Blood flow autoregulation is defined as the ability of a tissue to maintain a relatively constant flow, despite moderate alterations in perfusion pressure (Johnson, P. C., 1980b), or in terms of the eye, ocular perfusion pressure. Perfusion pressure may be defined as the difference between the arterial and venous pressure of a tissue (Bill, A., 1981; Haefliger, I. O. & Anderson, D. R., 1996). Ocular perfusion pressure is defined as either the ocular arterial pressure less the IOP (Harris, A. *et al.*, 1998) or two thirds of the mean arterial pressure less the IOP (Riva, C. E. *et al.*, 1981). In general, the mechanism by which vascular autoregulation is accomplished is either myogenic or metabolic. In tissues controlled by the metabolic mechanism, vascular resistance is modified to enable the level of a certain critical metabolite (i.e. oxygen) to be maintained. Tissues controlled by the myogenic mechanism contain specific cells that detect changes in pressure, these then initiate appropriate adjustments in arteriorlar tone to maintain a constant blood flow (Bill, A., 1981). In the eye, there are a number of specific factors known to be influential in maintaining a constant flow of blood including ocular perfusion pressure, vascular blood velocity and the tone and diameter of resistant vessels and capillaries (Flammer, J., 1996; Pournaras, C. J., 1996). In this regard the eye utilises both metabolic and myogenic mechanisms to maintain a constant blood supply.

Autoregulation is apparent in many organs in the body, often at the precapillary level, and represents the adjustment of the peripheral vasculature in response to changes in the perfusion pressure and/or nutritional flow (Johnson, P. C., 1980a). Precapillary sphincters are largely responsible for regulating capillary closure (Johnson, P. C., 1980a). Regulatory gates are not present in the arterioles of the retina and choroid (Friedman, E. *et al.*, 1964). Due to the lack of precapillary sphincters, physiological stimuli such as neurotransmitters, myogenic or metabolic factors, circulating hormones and endothelium-derived factors affect the vascular tone and diameter of the entire arteriolar network (Haefliger, I. O. & Anderson, D. R., 1996; Meyer, P. *et al.*, 1996).

1.7.4.1. Retina

A number of investigators have demonstrated efficient vascular autoregulatory activity in the retina in response to different physiological stimuli. Raised arterial pressure during exercise has been shown to increase ocular perfusion pressure. Regardless of this, normal levels of blood flow to the retina are maintained within a defined range of mean arterial pressure increases; this is thought to be a direct result of localised vasoconstriction (Robinson, F. *et al.*, 1986; Harris, A. *et al.*, 1996b). The mechanism of autoreguation is probably two-fold, firstly, as a result of increased ocular perfusion pressure and secondly, due to increased sympathetic neural activity (Bill, A., 1981; Harris, A. *et al.*, 1996b). Incremental changes in IOP have also been shown to elicit an autoregulatory response in the retinal circulation through reductions in perfusion pressure within a given range (Sperber, G. O. & Bill, A., 1985; Riva, C. E. *et al.*, 1986).

Both modifications in IOP and mean arterial pressure (MAP) induce changes in ocular perfusion pressure. This in-turn elicits an autoregulatory response of the myogenic type. Retinal blood flow has also demonstrated autoregulatory activity using a metabolic mechanism. When the partial pressure of oxygen (PO_2) in the blood increases (hyperoxia), retinal blood flow decreases as a result of localised vasoconstriction (Riva, C. E. *et al.*, 1983; Fallon, T. J. *et al.*, 1985; Harris, A. *et al.*, 1994a; Langhans, M. *et al.*, 1997; Strenn, K. *et al.*, 1997; Lietz, A. *et al.*, 1998). Other studies have shown that increased levels of PCO_2 (hypercapnia), result in vasodilation and increased blood flow (Tsacopoulos, M. & David, N., 1973; Mansberger, S. *et al.*, 1993). Finally, the importance of CO_2 as a metabolic mediator has been highlighted by investigations into the effect of carbogen breathing (6% CO_2, 94% O_2) on retinal haemodynamics. The results from two separate studies concluded that vascular perfusion preferentially increased via vasodilation during carbogen breathing, thus emphasising the potent effect of CO_2 when compared to O_2 (Arend, O. *et al.*, 1994; Lietz, A. *et al.*, 1998).

1.7.4.2. Optic nerve head

The ONH has been shown to autoregulate effectively during a range of changes in IOP and perfusion pressure in animals (Geijer, C. & Bill, A., 1979; Shonat, R. D. *et al.*, 1992) and humans (Pillunat, E. L. *et al.*, 1996; Riva, C. E. *et al.*, 1997a). Blood flow at the ONH has also been shown to decrease in response to hyperoxia (Harris, A. *et al.*, 1996c; Langhans, M. *et al.*, 1997) and increase during hypercapnia (Harris, A. *et al.*, 1996c).

1.7.4.3. Choroid

The question of choroidal autoregulation is controversial. Early studies into choroidal blood flow were restricted to animal models because of the invasive nature of the procedures used. Trokel, S. (1965) demonstrated decreased choroidal blood flow in rabbits in response to elevated PO_2 and increased blood flow in response to increased PCO_2. A similar study on cats noted increased blood flow in the presence of elevated PCO_2, but no measurable response following increased O_2 breathing unless the mean arterial pressure also increased (Friedman, E., 1970). Studies by Riva, C. E. *et al.*, (1997c) using the laser Doppler flowmetry technique, revealed a bilinear relationship between choroidal blood flow and ocular mean perfusion pressure which is suggestive of autoregulatory activity that is potentially neural or passive in origin.

Kiel, J. W. & Shepherd, A. P. (1992) demonstrated efficient choroidal autoregulation at low intraocular pressures in the rabbit. This finding was consistent with an earlier study which reported a stable flow of blood in the choroid despite changes in blood pressure (Bill, A. & Sperber, G. O., 1990).

1.8. Optic nerve head damage in glaucoma

Recent experimental evidence, using animal models, has shown that RGC axon death in glaucoma occurs due to apoptosis (Quigley, H. A. *et al.*, 1995). Apoptosis,

otherwise known as programmed cell death, constitutes a genetically coded suicide process which is initiated when cells are either damaged or no longer needed (McKinnon, S. J., 1997; Hosking, S. L., 1998a). It is hypothesised that apoptosis may be induced by two main stimuli: neurotrophin withdrawal and glutamate-mediated toxicity. Neurotrophin withdrawal may result due to increased mechanical pressure on orthograde and retrograde transport or may be secondary due to reduced cellular transport caused by ischaemia induced energy depletion. Glutamate-mediated toxicity is known to be a primary response to ischaemia. There are two current theories of how RGC death occurs in glaucoma:

1) The mechanical theory, which proposes that IOP dysfunction causes RGC atrophy due to biochemical or structural damage.
2) The vascular theory, which assumes that the microcirculation is compromised resulting in RGC death.

It is likely that the two theories co-exist in the pathogenesis of glaucomatous optic neuropathy. A model recently proposed for RGC death is given overleaf and shows how the mechanical and vascular theory, either together or exclusively, may be responsible for ONH atrophy (Figure 1.4.).

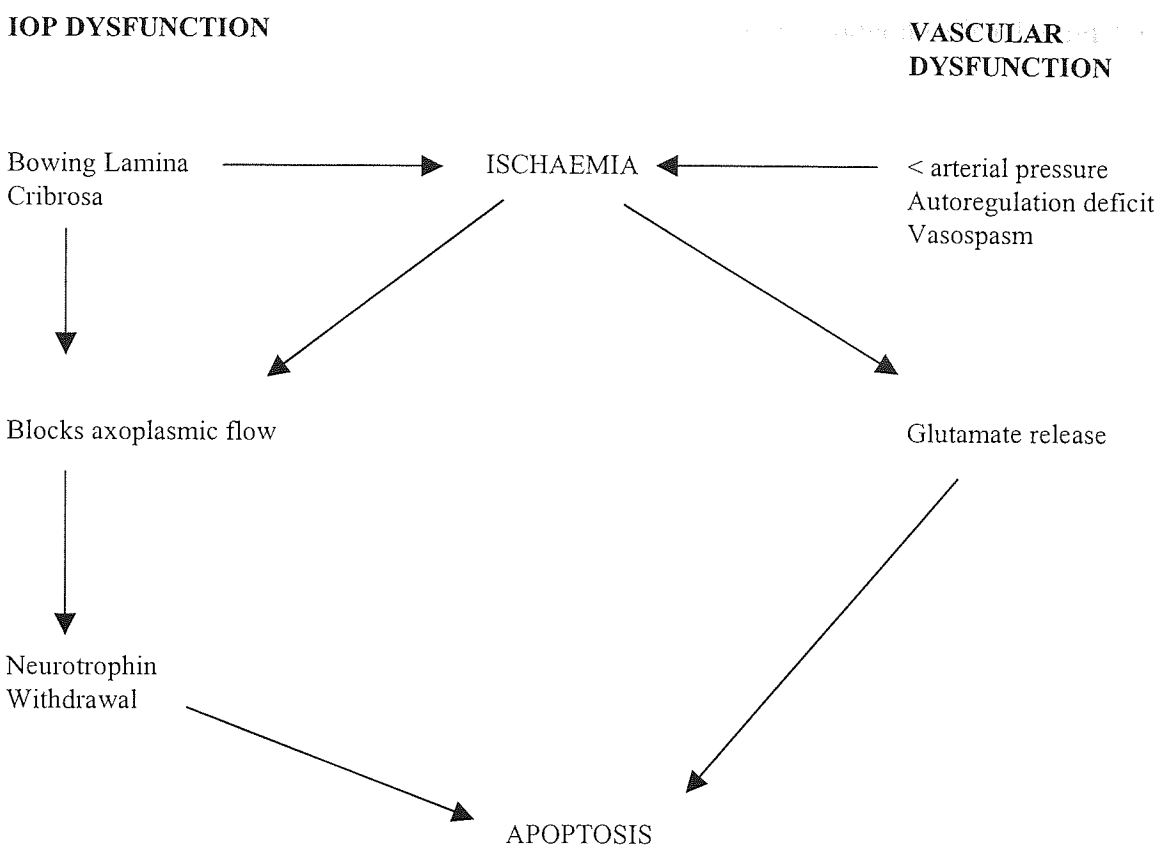

Figure 1.4. A model for ganglion cell death in glaucoma. Adapted from Chung, H. S. *et al.*, 1999a.

1.8.1. The role of elevated IOP in glaucomatous optic neuropathy

The mechanical theory for glaucomatous ONH damage states that RGC loss is related to changes in the connective tissue structure of the ONH induced by increased IOP (Quigley, H. A. *et al.*, 1980). This results in misalignment of lamina cribrosa pores and obstruction of axonal transport (Quigley, H. A. *et al.*, 1979). There are a number of suggested mechanisms by which increased IOP may cause damage at the ONH. The pressure gradient from the vitreous to the optic nerve may increase as IOP elevates. Alternatively, increased tension in the scleral walls may have a compressive effect on RGC axons (Quigley, H. A. *et al.*, 1980). Several changes in the composition of the lamina cribrosa have been identified in the human glaucomatous ONH including:

- Compression of the cribiform plates in patients with moderate visual field loss (Quigley, H. A. *et al.*, 1983).
- Posterior rotation and bowing of the lamina cribrosa in patients with severe glaucomatous optic neuropathy, (Quigley, H. A. *et al.*, 1983).
- Loss of collagen fibres, increased numbers of glial cells, thickening of basement membranes and changes in the elastic fibres including loss of their characteristic tubule appearance have been observed in mild-moderate glaucoma (Hernandez, M. R., 1992).
- Changes in the pores of the lamina cribrosa have been identified in severe glaucoma, including distension along one axis (Miller, K. N. & Quigley, H. A., 1988). This may be related to changes in the collagen and elastic fibres which result in reduced structural support of the RGC axons (Hernandez, M. R., 1992).

The mechanical theory proposes that the changes in the lamina cribrosa evident during glaucoma cause misalignment of the cribiform plates and pores. As a result, the RGC axons that normally pass unhindered through the pores may be put under stress and vital nutrients supplying the nerve fibres may be compromised. A number of studies have identified interruption of axonal transport of neural components in eyes with glaucomatous optic neuropathy (Quigley, H. A. & Anderson, D. R., 1977; Quigley, H. A. *et al.*, 1979; Quigley, H. A. *et al.*, 1980). This has been found to occur predominantly in axons situated in the posterior and inferior poles of the disc, which is consistent with the common from of arcuate glaucomatous visual field damage associated with loss of axons in these areas (Quigley, H. A. & Anderson, D. R., 1977).

A number of specific studies have identified changes in the ONH, including RGC apoptosis, that occurs following experimentally induced changes in IOP in primate eyes (Quigley, H. A. *et al.*, 1980; Levy, N. S. *et al.*, 1981; Quigley, H. A. *et al.*, 1995). Further studies have correlated visual field defects in human glaucomatous eyes with histological changes in the disc (Quigley, H. A. *et al.*, 1982). An association also exists between IOP and visual field loss (Vogel, R. *et al.*, 1990). Fluctuations of IOP in glaucoma have been associated with optic disc cupping (Rath, E. Z. *et al.*, 1996) as have induced IOP changes by use of a suction cup (Azuara-Blanco, A. *et al.*, 1998c;

Yan, D. B. *et al.*, 1998). Acute IOP changes following trabeculectomy have resulted in relative improvements in disc topography (Irak, I. *et al.*, 1996; Lima, M. C. *et al.*, 1999; Topouzis, F. *et al.*, 1999), thought to be due to a reduction in the posterior bowing of the lamina cribrosa (Lusky, M. *et al.*, 1993a). One of the more convincing arguments for a link between increased IOP and ONH damage is the condition of post-traumatic unilateral glaucoma. In such cases, the injured eye with elevated pressure develops glaucomatous damage and the fellow eye remains unaffected (Flammer, J., 1996).

1.8.2. The role of vascular factors in glaucomatous optic neuropathy

As early as 1885, Priestley-Smith characterised glaucomatous ONH damage and suggested the importance of vascular mechanisms in its pathogenesis.

"The excavation of the disc in glaucoma is not a purely mechanical result of exalted pressure; it is, in part at least, an atrophic condition which, though primarily due to pressure, includes vascular changes and impaired nutrition in the substance of the optic disc....which may probably progress even though all excess of pressure be removed."

(Priestly-Smith, 1885)

The fact that some patients go on to develop ONH damage even after IOP has been reduced, together with the existence of normal-tension glaucoma, points to a further mechanism of ONH damage that acts either separately or in conjunction with increased IOP. The possibility of a vascular role has long been considered and a number of vasogenic risk factors have been identified including vasospasm, autoregulatory dysfunction, systemic hypotension and postural- and circadian-related change (Weinreb, R. N., 1992). All are thought to result in reduced perfusion of the retina, choroid and ONH.

The vascular theory for glaucomatous optic neuropathy proposes that decreased perfusion of the optic nerve results in reduced nourishment of RGC axons and eventual axonal dysfunction and death. The exact mechanism by which ischaemia of the optic nerve may arise and whether it is a secondary result of increased IOP or an isolated mechanism of axonal damage is unknown. A number of theories explaining how ischaemia may facilitate glaucomatous ONH atrophy have evolved and are discussed.

1.8.2.1. Ischaemia due to mechanical injury

This theory proposes that ischaemia occurs secondary to IOP damage. Changes in the extracellular matrix, induced through mechanical damage to the ONH may cause blood flow through the capillaries to be compromised. At the lamina cribrosa, capillaries are positioned within the connective tissue plates rather than running parallel with the nerve fibre bundles. Mechanical insult of the surrounding connective tissue may result in stretching or shifting of the perforated plates and cause the capillaries within to become squashed or kinked (Quigley, H. A., 1995).

1.8.2.2. Autoregulatory dysfunction

There is evidence to suggest that the autoregulatory capacity of eyes with POAG is compromised (Alm, A. & Bill, A., 1973; Geijer, C. & Bill, A., 1979; Grunwald, J. E. *et al.*, 1984; Pillunat, L. E. *et al.*, 1985; Zeltan, S. R. *et al.*, 1989; Evans, D. W. *et al.*, 1999a), however the reasons why are not completely understood. It is possible that the vasculature of such patients is already being autoregulated due to another element such as stenosis. Compounded with increased IOP or hypotension, the eye is unable to autoregulate further thus resulting in decreased blood flow and optic nerve damage. Similarly, capillaries may be unable to autoregulate and dilate in response to raised IOP because of an external influence, such as vasospasm, that may be eliciting a vasoconstrictory response. In such a situation the vasculature may preferentially autoregulate to one stimuli. Finally, a phenomena known as vascular steal has been

proposed where one vascular bed (e.g. the choroid) is preferentially perfused over another (e.g. retina) resulting in ischaemia (Anderson, D. R., 1995).

The use of stress tests, particularly IOP modification and blood gas perturbation has allowed the autoregulatory capacity of the normal eye to be compared to that of the glaucomatous eye. Pillunat, L. E. *et al.*, (1985) identified an autoregulatory response in normal eyes in response to artificially raised IOP that was not evident in glaucomatous eyes. Sponsel, W. E. *et al.*, (1997b) measured retinal leukocyte velocity in normal and glaucomatous eyes during increased levels of IOP and noted that whilst blood flow velocities stabilised in normal eyes, indicative of an autoregulatory response, blood flow velocities in the glaucomatous eyes continued to decrease even at high IOP levels. Liu, C. J. *et al.*, (1997) investigated blood flow velocities in glaucoma patients with spontaneously raised IOP and reported decreased flow velocities and increased resistance indices compared to fellow and control eyes.

A gas perturbation study by Harris, A. *et al.*, (1994b) on normal subjects and NTG patients showed that increased CO_2 levels abolished initial differences between the blood flow velocities and resistance indices of the two groups. This finding suggested the presence of reversible vasospasm in NTG patients (section 1.8.2.3.). A later study reported similar results (Hosking, S. L. *et al.*, 1999).

1.8.2.3. Vasospasm

There is evidence that some POAG patients, particularly those NTG, suffer from vasospasm (Phelps, C. D. & Corbett, J. J., 1985; Drance, S. M. *et al.*, 1988; Gasser, P., 1989; Rojanapongpun, P. & Drance, S. M., 1993; Harris, A. *et al.*, 1994b; Broadway, D. C. & Drance, S. M., 1998). A link between a tendency to vasospasm and visual field defects has been found in a number of people without glaucoma, otherwise known as ocular vasospastic syndrome (Flammer, J., 1996). Administration of an anti-vasospastic treatment and/or removal of the stimulus causing the vasospasm (i.e. cold) results in spontaneous visual field improvement (Kaiser, H. J. *et al.*, 1993a). The

visual fields of patients with glaucoma demonstrating similar vasospastic symptoms do not spontaneously reverse.

1.8.2.4. Biochemical abnormalities

This theory is based on a dysfunction in the blood composition of some patients with POAG (Weinreb, R. N., 1992). There is recent evidence to suggest that blood coagulation or platelets are disrupted in some way, possibly resulting in the formation of microthrombi in vessels. This in-turn would result in microvascular occlusion and ischaemia. Interestingly, this finding has not been reported in patients with normal-tension glaucoma (Carter, C. J. *et al.*, 1990).

1.9. Assessment of glaucoma

Current diagnosis, assessment and management of POAG is dependent upon three fundamental factors. The level of IOP, assessment of the ONH and visual field. These are discussed in the following sections.

1.9.1. Intraocular pressure assessment

Raised IOP pressure is the most common risk factor for glaucoma (Gramer, E. & Tausch, M., 1995; Rosenberg, L. F., 1995) and all forms of glaucoma treatment are aimed towards lowering it. For this reason the accurate assessment of IOP is imperative. Tonometry does not give a direct measurement of IOP and the reliability of the different types of tonometers (contact and non-contact) varies. Whilst most optometrists use non-contact tonometry to measure IOP, Goldmann applanation tonometry is considered the reference standard and is commonly used in the hospital environment (Thornburn, W., 1978). The intra- and inter-observer variability of Goldmann measurement has been shown to be low (Bengtsson, B., 1972; Quigley, H. A. & Langham, M. E., 1975; Thornburn, W., 1978; Mackie, S. W. *et al.*, 1996) and superior to other forms of measurement (Mackie, S. W. *et al.*, 1996). The mean

standard deviation of three repeated readings by the same observer has been reported as 0.8mmHg (Dielemans, I. *et al.*, 1994), however repeated applanation causes a decrease in IOP (Wilke, K., 1972).

1.9.2. Visual field assessment

The visual field may be defined as all the space that one eye can see at any one time (Tate, G. & Lynn, J., 1977). The visual field is usually measured in degrees from the line of sight and extends 65° upwards, 75° downwards, 60° nasally and 95° temporally (Henson, D. B., 1983). As axonal damage and neural loss occurs during the chronic course of glaucoma, characteristic visual field loss develops. Investigators have applied a number of tests to determine visual damage. The reasons are twofold, firstly investigators needed to identify a test that gives the earliest indication of ONH damage and secondly the course of the disease and rate of visual loss needs to be monitored.

There are a number of different visual field analysis systems available. Some use a kinetic technique (Goldmann perimeter) whilst others employ a static method (Humphrey Field Analyzer). Automated static perimetry is recommended for the clinical follow-up of glaucoma because it is generally less variable than kinetic perimetry and provides numerical data that facilitates automated comparison between visual fields (Hodapp, E. *et al.*, 1993).

1.9.2.1. Visual field assessment with the Humphrey Field Analyzer

The central 24-2 and 30-2 programs available with the Humphrey Field Analyzer (Zeiss-Humphrey inc.) provide a full threshold program which uses threshold values at four primary points determined at the beginning of the test as starting levels for neighbouring points. The threshold values determined for neighbouring or secondary points are then used to calculate values for subsequent points. In this way, individual

threshold values, including either side of midlines, are determined within the central 24° or 30°.

A staircase strategy is used to threshold points. A stimulus is presented that the patient is expected to see. The intensity of the stimulus is then decreased in 4 decibel (dB) steps until it is no longer seen. To find the exact threshold, the intensity of the stimulus is increased in 2dB increments. The process is repeated if the threshold of a point is 5dB or more below expected sensitivity and the second measurement is expressed in parenthesis on a numerical print-out.

The patient's blind spot is located at the start of the test and is then used to monitor fixation. Approximately 5% of all the points presented throughout the test are located in the blind spot, the subjects responses to which provide an indication of fixation reliability. A fixation loss that exceeds 20% is an indication of poor reliability.

At least one point acts as a false positive trial during the examination. The projector will move as if to present a stimulus, but none will be presented. A false negative trial is also incorporated during which a bright stimulus is presented in an area of previously established intensity. False positive and negative errors that exceed 15% indicate poor reliability.

1.9.2.2. HFA visual field analysis

Statpac 2 single field analysis with the HFA provides several analysis plots. A grey tone representation of the visual field is given where each shade in the pattern corresponds to a 5dB change in sensitivity. A numerical plot is also provided which gives the calculated threshold values for each point. Two total deviation plots are also given. One is numerical and the other is a grey scale representation. The numerical total deviation plot represents the difference between the patients test results and age-corrected normal values for each point tested. The pattern deviation plots are arranged in a similar way, but represent the difference between the patients test results and age-

corrected normal values for each point when adjusted for overall changes in sensitivity. Overall changes in sensitivity may be caused by depressions in the hill of vision due to cataract or small pupils. Alternatively there may be an overall increase in sensitivity for patients who are "supernormal".

Several global indices are given including:

- Mean deviation (MD): the average elevation or depression of the visual field when compared to a normal age matched population.
- Pattern standard deviation (PSD): a measurement of the degree by which the visual field differs to the normal age corrected reference field.
- Short-term fluctuation (SF): an index of the reliability of the responses given throughout testing.
- Corrected pattern standard deviation (CPSD): this provides a measure of the extent by which the total hill of vision differs from a normal hill of vision corrected for age and SF.

The single field analysis provides an indication of whether the visual field is glaucomatous. The glaucoma hemifield test (GHT) examines five zones in the superior visual field and compares these zones to their mirror image in the inferior field. On the basis of this analysis one of three messages are displayed below the grey tone plot:

- GHT within normal limits
- GHT outside normal limits
- GHT borderline

If the patient's visual field is unusually increased or decreased in sensitivity for reasons already discussed then the message may read:

- General reduction of sensitivity
- Abnormally high sensitivity

1.9.2.3. The visual field in glaucoma

Nerve fibre loss in glaucoma results in corresponding visual field loss. The most common visual field defects occuring in glaucoma are small, isolated, scotoma contained within the central 30° (Armaly, M. F., 1971). General constriction and peripheral nasal steps occur less frequently. During progression, the defects enlarge and join with the blind spot resulting in arcuate loss that is characteristic of glaucoma. Studies into the frequency of visual field loss found that loss was most likely to occur in the superior nasal quadrant (Hart, W. M. & Becker, B., 1982; McClure, E., 1988).

A significant relationship has been identified between the rate of visual field loss and level of IOP in POAG (Vogel, R. *et al.*, 1990; Jay, J. L. & Murdoch, J. R., 1993). A correlation between retinal capillary function and central and peripheral function in glaucoma has also been reported (Sponsel, W. E. *et al.*, 1997a). Several studies have identified topographic parameters of the disc that correlate with visual loss (Nyman, K. *et al.*, 1994; Brigatti, L. & Caprioli, J., 1995; Mikelberg, F. S. *et al.*, 1995; Iester, M. *et al.*, 1996; Eid, T. M. *et al.*, 1997; Iester, M. *et al.*, 1997a; Anton, A. *et al.*, 1998; Emdadi, A. *et al.*, 1998; Kono, Y. *et al.*, 1999). Those that relate to cSLO are discussed in section 1.11.2.8.

1.9.2.4. Visual field progression

Visual field examination serves as an important guide as to whether or not a patients condition is stable. Care must be taken when attempting to identify glaucomatous visual field progression. A reduction in visual field sensitivity is associated with increased age (Brenton, R. S. & Phelps, C. D., 1981; Hass, A. *et al.*, 1985; Katz, J. & Sommer, A., 1986). Werner, E. B. *et al.*, (1989) has reported an average physiological variability of 2.8dB over a 12-month period in clinically stable POAG patients. The advanced glaucoma intervention study (AGIS) investigators developed a quantitative method for scoring test reliability and severity of glaucomatous visual field loss. They showed that in 16% of eyes, long-term fluctuations were great enough to suggest

either deterioration or improvement even though the time period was too short for true disease changes to have taken place (Gaasterland, D. E. *et al.*, 1994).

There are a number of ways of determining visual field progression. A minimum criterion for progression is a decline in the global mean deviation parameter that is significant at the 1% level and not due to increasing media opacity or pupillary constriction. A steadily deteriorating CPSD over five visual fields or a decline of ≥ 3dB across all measured points in the visual field that is not related to media opacities or pupil size also indicates progression (Hodapp, E. *et al.*, 1993).

Other methods of measuring progressive field loss include the use of cumulative defect curves, which provide a graphical representation of the visual field and allow a subjective classification of diffuse of localised loss (Chan, A. B. *et al.*, 1997). Cluster analysis, where clusters of points are assessed for increases in depth over time, may also be used to assess progression. Schulzer, M. (1994) characterised glaucomatous visual field loss if a cluster of three or more none edge points declined by ≥ 5dB from the average normal value for the same age group and at least one point decreased ≥ 10dB below normal values. Progression was considered to have occurred if two contiguous points, the same as or adjacent to the baseline visual field defect, declined by ≥ 10dB or a new localised defect appeared. A similar criteria using cluster analysis is outlined by (Hodapp, E. *et al.*, 1993).

A number of statistical analyses have been described for assessing visual field progression including both regression and point-wise linear regression analysis (O'Brien, C. & Schwartz, B., 1993; Fitzke, F. W. & McNaught, A. I., 1994; Katz, J. L. *et al.*, 1997; Wild, J. M. *et al.*, 1997). The glaucoma probability change program provided with the HFA can be used to identify progression. The software compares the average of two baseline fields with subsequent follow-up fields using a point-wise basis. Areas of the visual field that have deteriorated significantly, after taking into account the variability associated with repeated visual fields for stable glaucoma patients, are highlighted. This method has been found to compare favourably with other techniques for measuring progression (Morgan, R. K. *et al.*, 1991).

1.10. Assessment of the optic nerve in glaucoma

1.10.1. History

Early methods of identifying glaucomatous optic neuropathy relied upon the ophthalmoscope. The timely introduction of single exposure fundus photography and later stereoscopic provided a more sophisticated technique for analysing and storing fundus information (Allen, L., 1964; Donaldson, D. D., 1964). Video systems that connected directly to fundus cameras provided a means of assessing the optic nerve without the need to develop films and further advancements in image analysis lead to a surge of ONH analysis systems being marketed in the mid-1980's. Computerised image analysis systems now provide sophisticated techniques for assessing and documenting the glaucomatous ONH. The image analysis systems currently available have evolved in two principle directions: 1) A number of systems such as the Topcon IMAGEnet system and Rodenstock ONH analyser rely on digitising data from fundus photographs (often stereoscopic). 2) Confocal scanning laser ophthalmoscopes (cSLO) (Laser Tomographic Scanner, Heidelberg Retina Tomograph) have been developed that enable direct scanning of the ONH.

Currently, clinical assessment of the ONH is the only investigation of glaucoma that still requires skilled investigation by a trained clinician. With the recent development of image analysers and advancement of scanning laser ophthalmoscopes, there is, more than ever, the real possibility of shared care being implemented in the management and treatment of glaucoma patients.

1.10.2. Ophthalmoscopy

The ONH can be viewed directly via an ophthalmoscope. This technique allows monocular viewing and is the simplest way to examine the ONH (Mikelberg, F. S., 1992). It provides a highly magnified view of the optic nerve, however as it is limited to a two-dimensional view subtle depth and contour changes of the disc that are common in glaucoma are easily missed. All inferences of topography are based on

monocular depth cues. Indirect slit lamp ophthalmoscopy using a 60D, 90D & 78D double aspheric convex lens permits a binocular view of the ONH. This method better facilitates the examination of the ONH as it provides a stereoscopic view where depth and contours can be visualised. There are several features of the disc that are normally assessed including the shape, depth and slope of the margins of the optic cup, the colour of the disc and neuroretinal rim (pallor), the configuration of the disc vessels and the assessment of the RNFL and peripapillary atrophy. Assessment of the RNFL has been shown to be an important indicator of progressive and early glaucoma (see section 1.10.4.)

Direct and indirect ophthalmoscopy both provide rapid means of assessing the ONH. The main disadvantage is that neither method provides a permanent record. For that purpose the clinician must diagrammatically record an impression of the disc; consequently comparison over time is based on semi-quantitative gradings or drawings of the ONH (Harper, R., 1995).

1.10.3. Subjective measurement of cup:disc ratio: inter and intra-observer variability

The ratio between the diameter of the optic cup and the disc is commonly employed to describe the optic nerve (Armaly, M. F. & Sayegh, R. E., 1969; Halberg, G. P., 1969). The cup:disc ratio has been shown to correlate with IOP (Armaly, M. F. & Sayegh, R. E., 1969). Biedner, B. *et al.*, (1983) evaluated the inter-observer variation for the assessment of C:D ratio using indirect ophthalmoscopy and reported 80% agreement between clinicians. Abrams, L. S. *et al.*, (1994) assessed the ability of different clinicians to assess the C:D ratio from disc photographs. Whilst the inter-observer agreement between experienced ophthalmologists was good, with differences of more than 0:2 disc diameters in only 5% of cases, agreement between less experienced optometrists was more variable with differences of more than 0:2 disc diameters in 12% of cases (Abrams, L. S. *et al.*, 1994). Indeed, the consistency of C:D evaluation has been shown to be variable even amongst glaucoma specialists (Lichter, P. R., 1976; Varma, R. *et al.*, 1992). Varma, R. *et al.*, (1992) assessed intra- and inter-

observer agreement during monoscopic and stereoscopic conditions and concluded that experts differed by as much as 0.2 disc diameters monoscopically and 0.166 disc diameters stereoscopically. Tielsch, J. M. *et al.*, (1988) suggested that agreement is optimised by using stereo-photographs and the same observer for clinical follow-up.

The use of slit-lamp biomicroscopy enables the size of the disc to be evaluated and is of value as it allows the clinician to determine whether the size of the optic cup is appropriate for the size of the disc (Spencer, A. F. & Vernon, S. A., 1994; Spencer, A. F. & Vernon, S. A., 1996). Comparison of different indirect methods of examining the optic nerve and planimetry revealed poor correlation between obbservers, but acceptable intra-observer variability for all methods (Spencer, A. F. & Vernon, S. A., 1995). Finally, several studies have compared clinicians and image analysis or scanning laser systems for assessing C:D ratio. Varma, R. *et al.*, (1989) found moderate agreement between clinicians and the IS 2000 image analyser, whereas Zangwill, L. M. *et al.*, (1995) demonstrated good agreement between clinicians and the cSLO.

1.10.4. Assessment of the retinal nerve fibre layer

Retinal nerve fibre layer changes have been identified in nearly 50% of patients diagnosed with ocular hypertension and it has been suggested that RNFL defects may precede visual loss by up to four years (Sommer, A. *et al.*, 1991a; Quigley, H. A. *et al.*, 1992). The normal RNFL appears slightly opaque with an arcuate arrangement of nerve fibres that radiate above and below the macular (Section 1.6.2.1., Figure 1.1.). The RNFL is thickest superiorly and inferiorly (Varma, R. *et al.*, 1996). Glaucomatous optic nerve atrophy results in thinning of the RNFL, particularly in the superior and inferior poles, which results in slit, groove, wedge shaped or diffuse defects (Hoyt, W. F. *et al.*, 1973). The areas affected appear darker and less striated, the location of which is highly correlated with subsequent visual field loss (DeMaio, R. *et al.*, 1992).

The RNFL may be viewed using monochromatic light. Clinically, it can be viewed via the slit-lamp with green (red-free) light. Quigley, H. A. *et al.*, (1993) described a reproducible semi-quantative method for grading the peripapillary RNFL and suggested that such grading should be used in the clinical follow-up of early glaucoma. Caprioli, J. & Miller, J. M. (1989) identified a new parameter of structural ONH damage in glaucoma called the relative nerve fibre layer surface height. The parameter is calculated from magnification-corrected surface measurements of the peripapillary retina made with computerised image analysis of stereoscopic videographic images. A group of normal and glaucomatous eyes were compared and the relative nerve fibre layer surface height was found to be 74μm lower in glaucomatous compared to normal eyes (Caprioli, J. & Miller, J. M., 1989).

A similar measure is available with cSLO (Burk, R. O. W. *et al.*, 1993; Miglior, S. *et al.*, 1994; Eid, T. M. *et al.*, 1997) and measurements of both RNFL thickness and cross-sectional area are available with the HRT. Burk, R. O. W. *et al.*, (1998) reported that RNFL defects could be detected in the reflectivity images of 75% of patients with RNFL defects visible by RNFL photography. Tsai, C. S. *et al.*, (1995) investigated the relationship between peripapillary retinal height and visual field sensitivity in normal and glaucomatous eyes and found a strong association between the two that was particularly evident superior-temporally. A similar study by Eid, T. M. *et al.*, (1997) found RNFL height to correlate well with visual field indices and other topographic parameters. Indeed, it has been suggested that peripapillary height measurements might better reflect the number of RGC axons entering the optic nerve than disc rim area (Caprioli, J. & Miller, J. M., 1989; Tsai, C. S. *et al.*, 1995). Finally, a combined topographic and histological study, carried out using a monkey model, reported that most topographic parameters measured with the HRT correlated with optic nerve fibre number; in particular, mean height in contour, RNFL thickness and cross-sectional area parameters were highlighted as showing a strong correlation (Yücel, Y. H. *et al.*, 1998).

1.11. Scanning laser ophthalmoscopy and tomography

The first SLO, known as the flying-spot TV ophthalmoscope, was designed and introduced by Webb, R. H. *et al.*, (1980). This provided a unique technique that enabled monochromatic viewing and recording of the fundus with an illumination level significantly lower than conventional ophthalmoscopes and cameras (Webb, R. H. *et al.*, 1980; Mainster, M. A. *et al.*, 1982). Early SLOs relied on non-confocal two-dimensional retinal scanning, however by 1987 the conventional SLO had been substantially improved by incorporating confocal optics with the scanning laser principle (Webb, R. H. *et al.*, 1987). This resulted in high contrast stereoscopic viewing of the fundus without loss of resolution or depth of focus irrespective of the illumination level.

1.11.1. Principles of confocal optics

In scanning laser ophthalmoscopy a focussed laser beam is used to scan over the desired area of the fundus with only a single spot illuminated at any one time. The light returning from this spot is deflected by a beam splitter, condensed by a lens, and received by a photodetector housed within the SLO. In a non-confocal system, the photodetector receives all the light returning from the eye (Figure 1.5.). The fundamental disadvantage with this type of arrangement is that some of the light returning from the eye may be scattered due to media opacities or multiple scattering on the fundus (Woon, W. H. *et al.*, 1992), resulting in low contrast images lacking in resolution.

The confocal system overcomes this problem by incorporating a pinhole aperture, or confocal aperture, that only receives light returning directly from the point of focus on the fundus. In its simplest form the term confocal refers to the detection of light returning from the point of focus at or through a focal point which is always conjugate to the illuminated spot on the retina (Webb, R. H. *et al.*, 1987; van Norren, D. & van de Kraats, J., 1989). In the confocal system the aperture is placed conjugate to the

laser focus immediately before the detector. The size of the aperture can vary; if it is very small then only light from the illuminated focus point will reach the detector and all remaining light deflected out the incident beam will be attenuated (Figure 1.6.). A system incorporating a small confocal aperture is said to be tightly confocal (Webb, R. H. *et al.*, 1987).

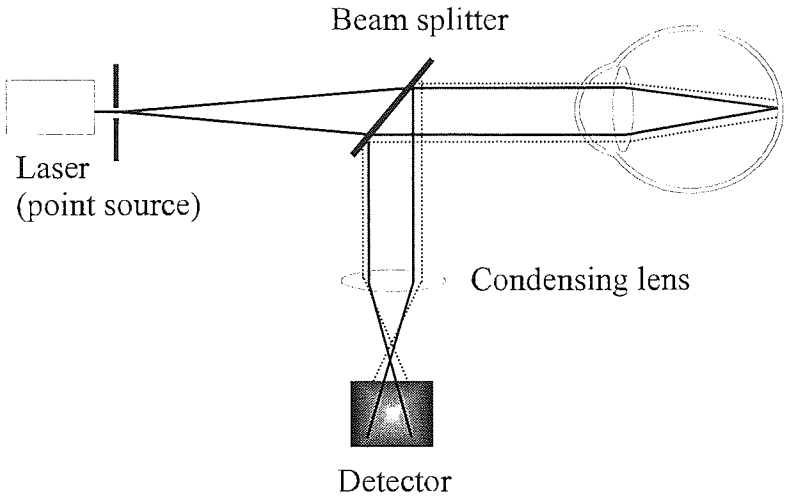

Figure 1.5. Simplified schematic of a non-confocal system. The laser beam is focussed onto the retina (solid line) and all returning light, including scattered light outside the focal plane (dashed line), is deflected off the beam splitter and detected.

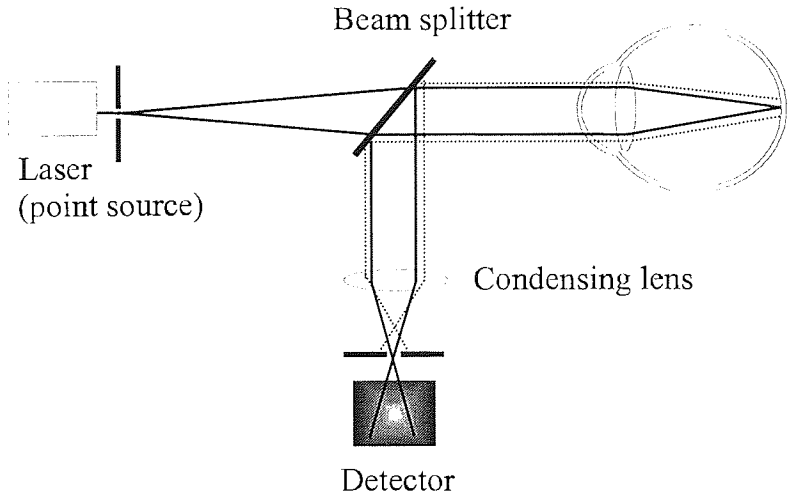

Figure 1.6. Simplified schematic of a confocal system. A confocal pinhole ensures that only light returning from the focal plane (solid line) is detected. All other scattered light outside the focal plane, which would otherwise result in image degradation, is attenuated.

1.11.2. The Heidelberg Retina Tomograph

1.11.2.1. Optics of the HRT

The HRT is a cSLO that uses the confocal optical principle outlined in section 1.11.1. to obtain quantitative and qualitative measurements of the ONH. Measurements with the HRT are based on the assumption that the eye being imaged is of average dimensions. The absolute scaling of a HRT image is determined using the parameters derived from Gullstrand's model 1 eye (Emsley, H. H., 1969). A separate model is used for the crystalline lens which has a gradient index with a resultant focal length of 61.088nm (Blaker, J. W., 1980; Navarro, R. *et al.*, 1985). The degree of ametropia (determined from the divergence of the laser beam) and anterior radius of corneal curvature (determined by keratometry and input manually) are the only variables. Whilst the HRT uses measured values for both ametropia and anterior corneal curvature, other systems use refractive constants for all measures except axial length (Bengtsson, B. & Krakau, C. E. T., 1992; Bennett, A. G. *et al.*, 1994) or ametropia (Bengtsson, B. & Krakau, C. E. T., 1992). A recent paper by Garway-Heath, D. F. *et al.*, (1998) compared several of the current methods available for correcting ocular magnification. The results showed that although methods that used individual axial length measures for each subject result in lower error values, of the methods that did not, the HRT compared favourably.

1.11.2.2. Image acquisition

During one image acquisition a point source diode laser with a wavelength of 670nm is focused onto the retina. The area of interest is scanned sequentially in an x, y direction by means of rotational prisms. The detector receives and measures the intensity of the reflected light via the confocal aperture optically conjugate to the focal plane (Figure 1.6.). The light intensities are then converted into video signals that are recorded by a frame grabber housed within the computer (Thomson, S., 1994). The HRT registers a total of 32 2-dimensional equidistant confocal image sections at varying focal planes perpendicular to the optical axis. The first image section is

located in the vitreous and the remainder are stacked posteriorly into the eye (Figure 1.7.). This process takes 1.6 seconds. The confocal images are then aligned for horizontal and vertical shifts resulting from small eye movements.

Each of the 32 confocal image sections register 65536 pixels (256 × 256 pixels) resulting in 65536 columns of pixels moving posteriorly along the z-axis. The light intensity measurements are compared along the z-axis and the maximum (peak) reflectivity value is used to construct a matrix of numbers. The digital matrix represents the position of the maximum reflectivity value along the z-axis in microns for every x, y location. This is assumed to correspond to the height of the examined structure at each co-ordinate. The matrix is then used to construct a 3-dimentsional topographic map of the scanned object. Simultaneous to the construction of the topographic map a reflectivity map is also generated in which the sum of the reflectance values in each z-axis are used rather than the maximum reflectance values used in the topographic map. The depth of the scan can be varied according to the depth of the structure being examined. If the scan depth is increased then the distance between each of the 32 equally spaced image sections will also increase. Likewise the scan area can be altered between 10°, 15° and 20°. When examining the ONH an image scan area of 10° is recommended (Heidelberg, 1997).

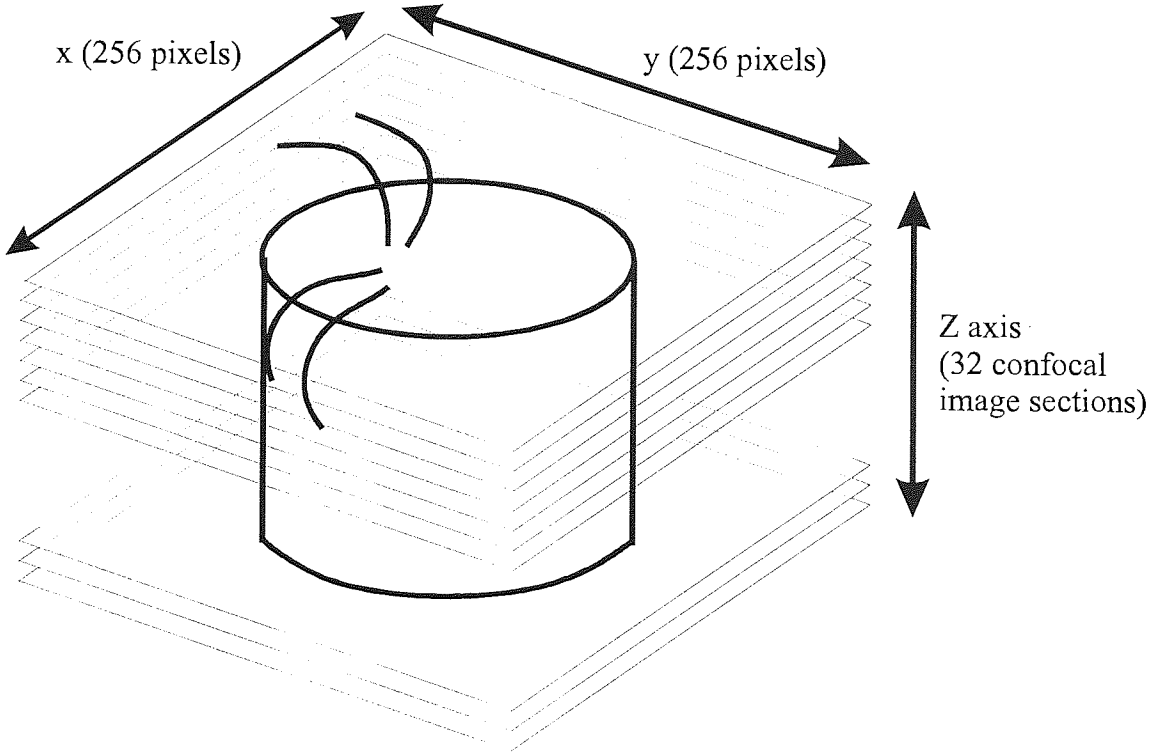

Figure 1.7. Image acquisition with the Heidelberg Retina Tomograph. The HRT registers a total of 32 confocal image sections (256 × 256 pixels) scanned in a x, y direction beginning at the vitreous and moving posteriorly into the eye on the z-axis. Adapted from Janknecht, P. & Funk, J., 1994.

1.11.2.3. Topography image

The topographic image forms the basis for the analysis and quantification of the ONH. A reference ring is located along the margins of the image with an outer diameter that is 94% of the image size and an inner diameter that is 3% of the image size. The reference ring is centred on the image, located on the peripapillary retina, and forms the absolute mean height of the retinal surface. The tilt of the reference plane with respect to the optical axis is used to define the tilted co-ordinate system. The mean height of the reference ring forms the zero-measure for the z-axis and all height and depth measurements are measured with respect to it.

1.11.2.4. Analysis of topography images

The topography image may be analysed interactively or stereometrically. Interactive measurement facilitate height and distance measurements from a cross-section of the topographic image. This form of measurement may prove particularly useful for pathologies other than glaucoma such as localised increased retinal thickness due to diabetic macular oedema. The stereometric analysis software is specifically designed to measure a number of topographic parameters that describe the ONH and is of particular use in the examination of the glaucomatous ONH.

Prior to any stereometric measurements being made from a topography image the area of interest must be clearly defined. For ONH analysis this involves interactively drawing around the edge of the optic disc using Elschnig's ring for reference. This results in a contour line which is then corrected for artefacts such as crossing blood vessels eventuating in the corrected contour line (Figure 1.8.). The HRT system software allows either a contour line to be drawn separately for each individual image, or one contour line, usually drawn on the first image of the series to be exported and imported into subsequent images. This enables successive images of individual patients to be topographically analysed using the same contour line and hence region of interest.

In order for volumetric measurements to be made it is necessary to define locations of the ONH. The HRT software generates two depth-wise reference locations: the curved surface and the reference plane (Figure 1.9.). The curved surface is bound by the contour line and its central point is equal to the mean height of the contour line. The reference plane is located 50μm posterior to the mean height of the contour line between the segments -10° and -4° in the inferior-temporal quadrant (Burk, R. O. W. *et al.*, 1995). This segment is located at the papillo-macular bundle and is thought to be the last area of the papilla to change during the progression of glaucoma. The contour line, curved surface and reference plane together form the basis of the determination of all subsequent stereometric parameters that describe the spatial shape of the ONH.

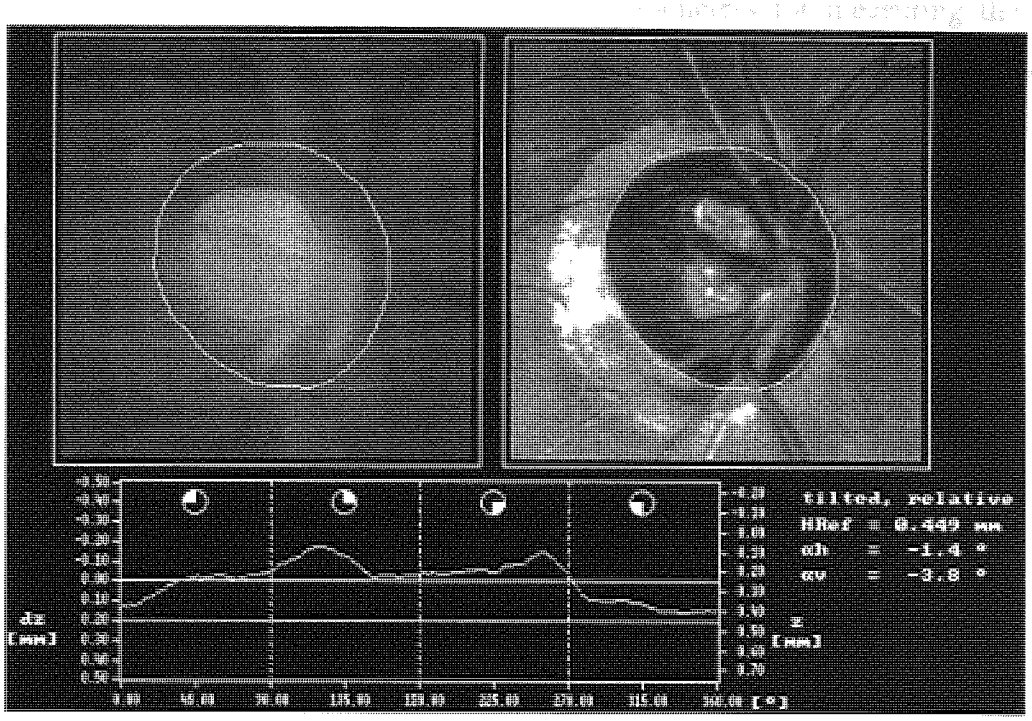

Figure 1.8. Topographic map of the optic nerve head. The area of interest is defined by a contour line and a diagram showing the height profile of the boundary is shown below.

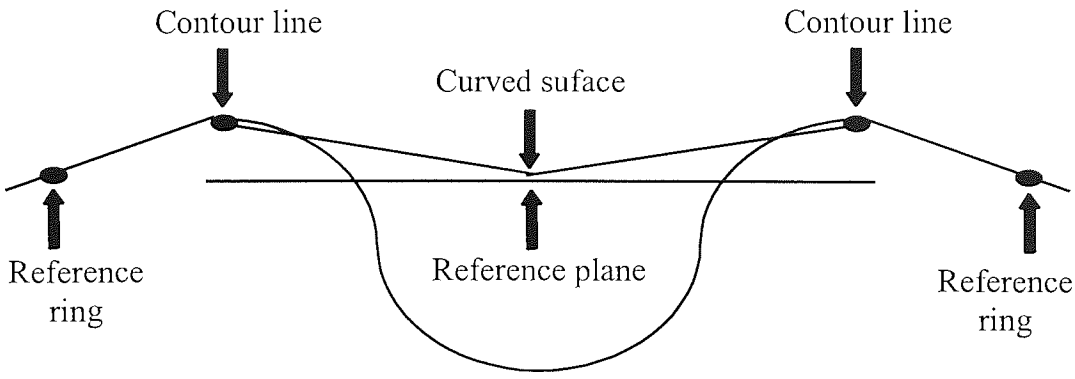

Figure 1.9. Schematic representation of the curved surface, contour line and reference plane.

The HRT provides a number of stereometric parameters for measuring the ONH. Tables 1.3.a., 1.3.b., 1.3.c. list these parameters in relation their points of reference and include a general description according to the HRT manual (software version 2.01, Heidelberg, 1997).

PARAMETER	DESCRIPTION
Reference height	Corresponds to the reference plane (located 50μm posteriorly to the mean height of the contour line between the segments -10° and -4° in the inferior temporal quadrant).
Mean depth in contour	Mean depth within the contour line
Height variation of contour	The difference between the most elevated and most depressed point of the corrected contour line. When the contour line is placed around the ONH, this describes the height variation of the surface of the peripapillary retina, which is dependent on the thickness variation of the nerve fibre layer.
Mean height of contour	Mean height (z-position) of the retinal surface along the contour line. Corresponds to the height of the central point of the curved surface.
Mean radius	Mean radius of the contour line
Disc area	Total area within the contour line

Table 1.3.a. HRT parameters measured with respect to the contour line.

PARAMETER	DESCRIPTION
Rim area	Area within the contour line and above the reference plane
Volume above reference/rim volume	Volume within the contour line and above the reference plane
Area below reference/cup area	Area within the contour line and below the reference plane
Volume below reference/cup volume	Volume within the contour line and below the reference plane
Cup/disc area ratio	Cup area divided by disc area
RNFL cross-sectional area	Mean distance between the retinal surface along the contour line and the reference plane multiplied by the length of the contour line
Mean RNFL thickness	Mean distance between the retinal surface along the contour line and the reference plane

Table 1.3.b. HRT parameters measured with respect to both the contour line and reference plane.

PARAMETER	DESCRIPTION
Effective area	Area within the contour line and below the curved surface (i.e. cup area)
Volume below surface	Volume within the contour line and below the curved surface
Volume above surface	Volume within the contour line and above the curved surface (i.e. neuroretinal rim volume)
Third moment in contour	Third central moment of the frequency distribution of the depth values within the contour line and below the curved surface
Maximum cup depth	Maximum depth inside the contour line relative to the curved surface
Effective mean depth/mean cup depth	Mean depth within the contour line and below the curved surface

Table 1.3.c. HRT parameters measured with respect to the contour line and curved surface alone.

1.11.2.5. Reproducibility of topographic measurement with the HRT

Several investigators have attempted to define the relative reproducibility and clinical efficacy of measurements obtained with the HRT. To this end there have been a number of reports that investigate the reproducibility of both the available topographical parameters (Mikelberg, F. S. *et al.*, 1993; Rohrschneider, K. *et al.*, 1994; Menezes, A. V. *et al.*, 1995; Azuara-Blanco, A. *et al.*, 1998c) and individual pixel height measurements (Lusky, M. *et al.*, 1993b; Weinreb, R. N. *et al.*, 1993; Chauhan, B. C. *et al.*, 1994; Rohrschneider, K. *et al.*, 1994; Chauhan, B. C. & MacDonald, C. A., 1995).

Studies that have considered the mean variability of the height measurements for each of 65, 536 pixels have quoted mean standard deviation values ranging from 28.5μm to 31.8μm for glaucoma patients, 22μm to 30.1μm for normal subjects and 28μm for glaucoma suspects (Lusky, M. *et al.*, 1993b; Weinreb, R. N. *et al.*, 1993; Chauhan, B. C. *et al.*, 1994; Rohrschneider, K. *et al.*, 1994). All of these values are based on the mean standard deviation of 3 topographic images, which has been previously considered the optimum number for maximum reproducibility relative to optimal efficacy within a clinical environment (Weinreb, R. N. *et al.*, 1993).

Although the mean standard deviation of the individual pixels provides a measure of the overall reproducibility of a mean topography image, in terms of the clinicians requirements, it is arguably more useful to know the variability of individual topographic parameters. Several of the studies that have considered the variability of the topographic parameters have quoted coefficient of variation (CV) values only (Rohrschneider, K. *et al.*, 1994; Orgül, S. *et al.*, 1997). It is now clear that this is not the optimal statistical method to use when determining reproducibility as CV becomes elevated when the denominator of the equation is a small value (Mikelberg, F. S. *et al.*, 1993) and cannot be used if the value straddles zero. Some of the parameters do have small denominators, in particular volume above surface and volume above reference and some straddle zero, namely height variation of contour and third

moment in contour. To overcome this problem some studies have quoted intraclass correlation coefficients (ICC) or reproducibility coefficients (RC). These statistical methods use a ratio of the variance due to the patient, and variance due to the patient and measurement effects (Mikelberg, F. S. *et al.*, 1993; Azuara-Blanco, A. *et al.*, 1998a). Table 1.4. summarises the reproducibility of several topographic parameters based on normal control subjects from two studies that quote both CV and ICC/RC values.

PARAMETER	Azuara-Blanco, (1998)		Mikelberg, (1993)	
	Based on mean of 10 images (software version 1.09)		Based on mean of 5 images (software version 1.10)	
	CV	RC	CV	ICC
Mean depth in contour	4.6	98.8	4.6	98.8
Height variation of contour	7.3	91	7.3	91.0
Mean height of contour	49.4	95.4	-	-
Volume above reference/rim volume	4.1	89.9	-	-
Area below reference/cup area	8.1	98.1	-	-
Volume below reference/cup volume	11.2	98.4	-	-
Effective area/cup area	3.8	98.5	4.1	99.2
Volume below surface	4.7	99.3	8	98.5
Volume above surface	20.7	88.2	26	81.3
Third moment in contour	8.9	89.3	30.6	84.4
Maximum cup depth	4.3	96.4	8.2	84.8
Effective mean depth	4.5	97.4	-	-

Table 1.4. Reproducibility values for HRT parameters for normal subjects. CV = Coefficient of variation, ICC = intraclass correlation coefficient, RC = reproducibility coefficient.

Not all of the parameters available in the current software version (2.01) have reproducibility values quoted in Table 1.3. However, of those outlined, volume above surface and third moment in contour consistently show poor reliability. The high variability of volume above surface may be attributable to the small area of tissue being measured (neuroretinal rim), which is contained within the area of the contour line and above the curved surface (Figure 1.9.). Any slight movement in the curved surface would undoubtedly result in large variations in the calculation of this parameter. Cioffi, G. A. *et al.*, (1993) demonstrated that depth measurements with the cSLO are most variable at the slope of the neuroretinal rim. Furthermore, Chauhan, B. C. *et al.*, (1994) demonstrated that during a test-retest variability study of the HRT, pixel height was most variable along the cup border. It was suggested that this may have been due to local topographical slope and software limitations in the alignment procedure. These results may go some way to explaining the low reproducibility of volume above surface and third moment in contour which are both measured from areas with potentially high topographical slope.

Parameters demonstrating high inter-study reproducibility include volume below surface (Figure 1.10.) and effective area. Both of these parameters are measured from the curved surface which may form a more stable surface than the reference plane from which to measure parameters. One possible reason for the increased stability of the curved surface is because its position is derived from the circumference and mean height of the contour line, whereas the reference plane is determined from a relatively small number of pixels in the inferior temporal segment of the contour.

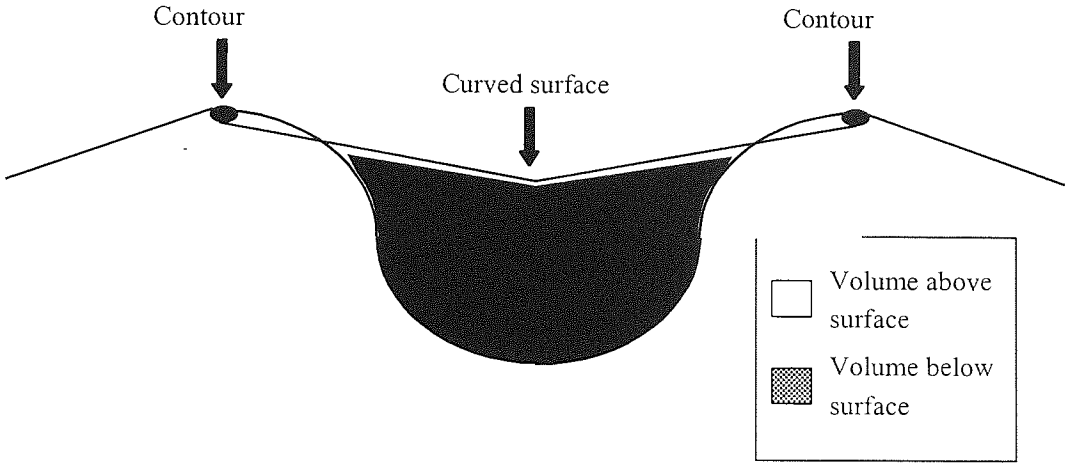

Figure 1.10. HRT parameters: Volume above and below surface

1.11.2.6. Factors affecting reproducibility

In order to detect subtle change over time the reproducibility of the acquired images must be maximised. There are several factors that affect the reproducibility of topographic measurement with the HRT. Hosking, S. L. & Flanagan, J. G. (1996) highlighted the importance of maintaining a constant focus setting for consecutive images of the same patient. Jonescu-Cuypers, C. *et al.*, (1998) highlighted the importance of maintaining a constant scan area for follow-up images of the same subject over time. Orgül, S. *et al.*, (1995) noted that misalignment between the laser scanner and the eye being imaged could be a potential source of variability that could be reduced by increasing the number of images taken at each visit.

The HRT has been specifically designed to allow reproducible images to be obtained even through pupils as small as 1mm (Thomson, S., 1994). A study carried out using the Laser Tomographic Scanner (LTS), predecessor to the HRT, found no significant difference between the reproducibility of topographic measurements obtained from dilated or undilated pupils (Rohrschneider, K. *et al.*, 1990). However, a more recent study highlighted the importance of pupil dilation to reduce variability (Zangwill, L.

et al., 1997). It has been suggested that dilation may reduce accommodation and aid in effective image acquisition in some patients and could be of benefit for the longitudinal follow-up of the ONH, where change in therapy or the development of lens opacity can reduce image quality (Rohrschneider, K. *et al.*, 1990; Zangwill, L. *et al.*, 1997).

Chauhan, B. C. *et al.*, (1994) reported that variability in topographic measurement increased significantly with age and concluded that this may be attributable to increased media opacity with age as it was evident in both a normal and glaucomatous population. Other studies have failed to find a significant correlation between age and the level of reproducibility obtained for topographic images with the HRT (Lusky, M. *et al.*, 1993b) and LTS (Dreher, A. W. *et al.*, 1991). A recent study that incorporated the use of a model eye with simulated media opacity using Bangerter foils reported high reproducibility of topographic measurement with the HRT and superiority over the Rodenstock optic nerve head analyzer even in the presence of poor optical media (Janknecht, P. & Funk, J., 1995). It must be noted however, that the use of Bangerter foils is a gross over simplification of cataract and makes direct comparison difficult.
The alignment of the contour line in subsequent images has been suggested as a contributory factor to topographic variability (Orgül, S. *et al.*, 1997). Results show, however, that the variability due to image acquisition outweighs that due to contour line alignment (Orgül, S. *et al.*, 1997). Finally, cardiac cycle has been highlighted as important in image variability, (Chauhan, B. C. & McCormick, T. A., 1995). It is known that a single bolus of blood is delivered to the eye with each cardiac cycle resulting in an ocular pulse (Langham, M. E., 1975). As a consequence, changes in the appearance of the blood vessels occur during the cardiac cycle (Bailey, P., 1973). Repeat images taken at the same point in the cardiac cycle, by pulse synchronisation with an electrocardiographic signal, have been shown to result in a significant decrease in image variability (Chauhan, B. C. & McCormick, T. A., 1995). The incorporation of pulse synchronisation during image acquisition may improve reproducibility and future software developments may address this issue.

1.11.2.7. Accuracy of topographic measurement with the HRT

Accuracy may be defined as the ability of an instrument to verify the true dimensions of the structure being analysed (Weinreb, R. N. *et al.*, 1990). Unlike establishing the reproducibility of the HRT, which may be adequately determined *in vitro*, accuracy is notoriously difficult to discern on living eyes. For this reason the majority of accuracy studies are carried out using model eyes, or occasionally cadaver eyes.

Dreher, A. W. & Weinreb, R. N. (1991) examined the accuracy of topographic measurement using the LTS, a model eye with sample holes simulating ONHs was used to obtain diameter and depth measurements. The results showed that measurements obtained with the LTS corresponded well with the actual measurements of the sample holes as verified by scanning electron microscopy. Calculated mean relative errors ranged from 2.0% - 3.6% for diameters and 10.1% – 11.7% for depth measurements (Dreher, A. W. & Weinreb, R. N., 1991). A more recent study examined the reproducibility and accuracy of both the HRT and ONH-analyzer (Rodenstock, Germany) (Janknecht, P. & Funk, J., 1994). Unlike earlier studies that measured distances only, this study was able to define the accuracy of two of the three-dimensional topographical parameters available with the HRT: volume below surface and volume above surface. The parameters volume above surface and volume below surface resulted in mean relative errors of 11% and 3.8% respectively, in agreement with the error measurements reported by Dreher, A. W. and Weinreb, R. N., (1991).

A study by Bartz-Schmidt, K. U. *et al.*, (1994) used direct *in vivo* assessment of the ONH in living eyes to assess the accuracy of the HRT. The study sample consisted of eight eyes scheduled for pars plana vitrectomy. Each eye was scanned with the HRT pre-operatively and then during surgery and each ONH measured directly using a modified spatula and high-resolution video system adapted to a Zeiss operation microscope. Using this technique, two-dimensional measurements were obtained for each ONH and compared with corresponding HRT values. The results showed a strong correlation between direct and HRT measurements. Only two-dimensional

measurements could be obtained directly from the optic nerve using the spatula method thus stereometric accuracy could not be evaluated.

1.11.2.8. Clinical application of the HRT

The HRT provides a tool for the potential classification of ONHs and for monitoring the progression of optic neuropathy in POAG. The stereometric analysis software function provides a valuable resource for monitoring the pathogenesis of the disease, however, there is very little published data available to verify the longitudinal follow-up of glaucomatous optic neuropathy. The few published studies that have reported a long-term follow-up (≥ 12-months) are discussed.

During an ongoing ocular hypertensive study at Moorfields Eye Hospital, Kamal, D. S. *et al.*, (1999) identified a group of ocular hypertensive patients who developed glaucomatous visual field loss (n=13). HRT images were examined retrospectively and compared to a normal subject group (n=11) followed for a 12-month period. A selection of HRT parameters were investigated including: cup:disc area ratio, cup area, rim area, cup volume, rim volume and third moment. With the exception of third moment in contour all of the afore mentioned parameters were highlighted as important for the detection of optic nerve change during conversion to POAG. However, it should be noted that the study was limited by the number of patients that had converted to glaucoma and hence group sizes were particularly small. Furthermore, the assumptions were based on the comparison of topographic parameters measured at two visits only. Hosking, S. L. (1998b) followed a cohort of glaucoma suspects (n=68) and POAG subjects (n=27) for a 15-month period. HRT images were obtained at 3-monthly intervals and patients investigated individually for change over time. Of the HRT parameters measured, volume below surface, volume below reference, mean depth in contour and effective mean depth were highlighted as the most important for the detection of change over time (Hosking, S. L. *et al.*, 1997b; Hosking, S. L., 1998b).

Finally, a 1-year follow-up of pre- and post-trabeculectomy ONH topography showed significant changes (relative improvements) in the HRT parameters third moment in contour, cup volume, mean cup depth and height variation in contour (Topouzis, F. *et al.*, 1999).

There are a number of cross-sectional studies that address the clinical validity of the HRT forming two distinct groups: 1) those that attempt to form a diagnostic rationale based on the available topographic parameters that distinguish between glaucomatous, normal and in some cases ocular hypertensive eyes. 2) those that attempt to correlate glaucomatous visual field loss with topographic parameters.

A study by Mikelberg, F. S. *et al.*, (1995) outlined a number of parameters that provide a diagnostic classification of the ONH as normal or glaucomatous. This diagnosis is based on the analysis of cross-sectional data for normal and glaucomatous ONHs. In particular, the parameters: third moment (cup shape measure), volume above reference and height variation in contour appeared important. These have been shown to classify ONHs as glaucomatous with a sensitivity of 87% and specificity of 84% when age corrected and using a reference level based on the papillomacular bundle (Mikelberg, F. S. *et al.*, 1995). Although this diagnostic system has been incorporated into the current HRT software (version 2.01), the sensitivity and specificity levels, combined with the relatively low incidence of POAG make it impractical for use as a mass screening tool.

Iester, M. *et al.*, (1996) used a discriminate analysis formula and described a strong correlation between visual field loss and three parameters highlighted as important (third moment, rim volume and height variation in contour). A second investigation by the same group correlated the amount of visual field loss with the numeric value of the discriminate formula (Iester, M. *et al.*, 1997a). Broadway, D. C. *et al.*, (1998) used the discriminate analysis model and found that diagnostic accuracy varied according to the type of glaucomatous disc. Focal ischemic discs were classified with 93.2% specificity, myopic discs with 81.6% specificity, senile sclerotic discs with 66.7% specificity and discs with generalised enlargement of the cup with 78.6% specificity.

A study by Zangwill, L. M. *et al.*, (1996) compared a number of individual topographic parameters between three age-matched cohorts: POAGs, ocular hypertensives and normal controls. The results showed that the parameters: mean height in contour, rim area, rim volume, disc area and reference plane height differed significantly between normal and ocular hypertensive eyes. Furthermore, every parameter measured, with the exception of reference plane height, showed a significant difference between ocular hypertensive and glaucomatous ONHs. A similar study examining the topographical differences between glaucomatous and normal ONHs identified the importance of RNFL height and cross-sectional parameters in distinguishing between the two groups (Eid, T. M. *et al.*, 1997). Mardin, C. Y. *et al.*, (1999) used the HRT to compare normal, glaucomatous and preperimetric (glaucoma suspect) eyes. The results showed that in most cases the mean values for the HRT parameters differed significantly for the three cohorts, however, there was a significant degree of overlap between the groups thus suggesting that the HRT was not diagnostically useful for separating glaucoma suspect eyes from normal eyes.

All the afore mentioned studies used individual HRT parameters to discriminate between groups. Other methods use cumulative frequency distributions or ranked segment distributions which are based on data from a population of normal ONHs (Asawaphureekorn, S. *et al.*, 1996; Bartz-Schmidt, K. U. *et al.*, 1996). Currently 5th, 50th and 95th percentiles of ranked segment distribution (RSD) curves are provided for the following parameters:

- normalised rim/disc ratio
- rim volume
- rim/disc area ratio
- retinal nerve fibre layer cross-sectional area

A classification of normal or glaucomatous is given according to how the RSD curve for the ONH under examination compares to the normal RSD curves. One study assessed the sensitivity of various HRT parameters to predict glaucomatous loss for different disc sizes. The results showed that the sensitivity of certain parameters such as cup volume, cup area and third moment in contour varied for different disc sizes

whereas the measures of neuroretinal rim area were sensitive for all disc sizes (Mardin, C. Y. & Horn, F. K., 1998). On this basis measures of neuroretinal rim area should provide a good indicator of glaucomatous damage even for small optic discs.

Several investigations have correlated individual parameters to visual field loss in glaucoma. Brigatti, L. & Caprioli, J. (1995) identified a correlation between the cup shape measure (third moment in contour) and visual field indices. This led Brigatti and Caprioli to suggest that third moment in contour is a good indicator of glaucomatous ONH damage, which is in agreement with others (Mikelberg, F. S. *et al.*, 1995; Iester, M. *et al.*, 1997a). Anton, A. *et al.*, (1998) used a sector-based analysis with the HRT and correlated focal disc damage with visual field damage. A new parameter was identified, rim area ratio, derived from the ratio of the rim area in each 10° sector divided by the total rim area. This was correlated with focal field loss. Emdadi, A. *et al.*, (1998) also used sector analysis and correlated early focal glaucomatous visual field loss with focal rim abnormalities in one third of patients, whilst approximately half of the patients had diffuse ONH damage. Furthermore, Kono, Y. *et al.*, (1999) demonstrated a correlation between peripapillary atrophy (specifically zone beta), as measured by the HRT, with a decrease in neuroretinal rim area and an increase in visual loss.

Apart from topographical imaging of the ONH in glaucoma, the HRT has other clinical applications. These include the examination and follow-up of other retinal diseases including diabetic macular oedema (Hudson, C. *et al.*, 1998; Zambarakji, H. J. *et al.*, 1998), macular holes and lesions (Menezes, A. V. *et al.*, 1995; Hudson, C. *et al.*, 1998), retinal tumours and retinal vein occlusion and papilloedema (Mulholland, D. A. *et al.*, 1998).

1.11.2.9. Comparison between cSLO and other techniques for assessing the optic nerve

Several investigations compare topographic measurements obtained with the HRT with other techniques. Absolute measurements for rim area and rim to disc area ratio

were reported as significantly greater for the HRT compared to planimetry (Dichtl, A. *et al.*, 1996; Jonas, J. B. *et al.*, 1998). In contrast, Vihanninjoki, K. *et al.*, (1997) reported that measurements of optic disc areas were significantly smaller for HRT measurements compared to planimetry whilst measures of neuroretinal rim area and cup to disc area ratios were similar. Azuara-Blanco, A. *et al.*, (1999) identified a discrepancy between HRT and computer assisted planimetric measurements of rim area and cup volume, in each case the HRT gave significantly smaller values than the Topcon TRC-SS. It was suggested that the absence of magnification correction between the two systems might have accounted for the differences observed. Regardless of the differences in disc sizes identified between planimetry and cSLO, studies have shown that the inter- and intra-observer variation for the analysis of optic disc images is substantially reduced for cSLO compared to computer assisted planimetric techniques (Garway-Heath, D. F. *et al.*, 1999).

A recent study that compared the HRT with another cSLO (TopSS) reported close agreement for measurements of cup:disc area ratio, cup volume, rim volume and mean cup depth (Okada, M. *et al.*, 1999). Finally, Zangwill, L. M. *et al.*, (1999) showed that the HRT, optical coherence tomographer and GDX Nerve fibre analyser all agreed in their discrimination of normal and glaucomatous subjects.

1.12. Ocular haemodynamic assessment

With renewed interest in vascular dysfunction as a cause of POAG accurate and reproducible assessment of blood flow parameters is imperative. There are several techniques currently available for the non-invasive assessment of ocular blood flow. Some utilise (scanning) laser technology: scanning laser angiography, laser Doppler velocimetry, scanning laser Doppler flowmetry. Some utilise ultrasonography: colour Doppler imaging. Other techniques use fundus photography: fundus photography angiography. Others use changes in intraocular pressure (Langham OBF system, OBF tonometer) to measure the vascular factors related to the perfusion of the eye. Some of these techniques, their application, advantages, disadvantages and clinical usefulness in assessing ocular blood flow in glaucoma are outlined in sections 1.13. – 1.15.

1.13. Colour Doppler Imaging

Christian Doppler (1803-1853) first described the Doppler principle that uses changes in the frequency of reflected waves to measure the velocity of a moving object. This concept was applied to ultrasound in 1957 and since then has been used routinely in clinical practice for imaging blood flow in the heart and major peripheral vessels (Satomura, S., 1957). Technical advances including the colour mapping of flow, which uses colour pixels that represent flow velocities, have improved the visualisation of Doppler imaging. In 1989 the technique of colour Doppler imaging (CDI) was extended to ophthalmology where it provided a unique methodology for visualising and measuring blood flow velocities of the retrobulbar vessels (Erickson, S. J. *et al.*, 1989).

1.13.1. The Doppler effect – ultrasonography

The Doppler effect may be described as a wave phenomenon; if a wave source is moving then the frequency of a receiver at rest is not the same as the source frequency (Bebie, H., 1995). This phenomenon may be applied in several ways including acoustics, microwave physics and optics. Its application in acoustics or ultrasound is perhaps the most easily understood and is simply demonstrated by a police siren that changes pitch according to whether the car is approaching or departing. This example can be extrapolated to light where rays of a given wavelength travelling away from an observer towards a moving object will result in reduced frequency, and increased frequency towards the observer. The Doppler effect using light is discussed in more detail later in relation to the Heidelberg retina flowmeter (see section 1.14.).

When the Doppler effect is applied using ultrasound, the velocity of the moving blood cells can be calculated from the change in frequency of the deflected beam (Equation 1.1.).

$$V = \frac{Dfc}{2FoCosA}$$

Equation 1.1.

Where:

V = Velocity of the blood cells

Df = Doppler frequency shift

c = Propagation frequency shift

Fo = Transmit frequency

A = Angle of incidence of the ultrasound beam to direction of flow

(Williamson, T. H. & Harris, A., 1996)

During the measurement of retrobulbar vessels, the angle of the beam will not always be parallel to the direction of blood flow. For this reason the angle of incidence of the beam is set by the operator who visually determines the course of the vessel. It is imperative that the angle of incidence is set correctly as an error of 45° or more can result in significant error in velocity calculations (Williamson, T. H. & Harris, A., 1996).

1.13.2. Measurement

Various ultrasound scanners are available for CDI, however, for measurement of small orbital vessels a small parts scanner (7.5 MHz linear array transducer) is required. To obtain measurements the transducer probe is covered with sterile coupling gel and gently positioned on the closed eyelid. It is important to ensure that pressure is not placed on the globe as this can cause an elevation in IOP and blood flow changes due to perfusion-pressure dependent haemodynamics (Harris, H. *et al.*, 1998).

The patient is normally in a supine position or 60° recline. Visualisation of the anatomy of the eye is extremely helpful when identifying vessels. For this reason CDI systems combine B-scan imaging with superimposed blood flow in the appropriate

vessels (Figure 1.11.). To obtain velocity measurements, the pulsed Doppler ultrasound beam is directed at the required vessel through a sample gate. The minimum size sample volume is generally used (1.2mm × 1.2mm (Siemens system) (Williamson, T. H. & Harris, A., 1996), or 1.5mm × 1.5mm (Acuson system) (Baxter, G. M. & Williamson, T. H., 1995)). Blood flow in the vessel is visible by colour pixels on the visual display unit which are colour coded according to the direction of flow (ie. towards or away from the transducer). In general red pixels signify arterial flow (towards the probe) and blue represents venous flow (away from the probe). Particularly tortuous vessels such as the PCAs or on occasion, the CRA, may sometimes appear blue due to vessel looping. In this case the pulsatility of the arteriole distinguishes it from the vein which is usually non-pulsatile (Lieb, W. E. *et al.*, 1991). Following the location of a vessel, a few seconds of Doppler frequency shifts are recorded through the sample volume. The resultant spectral analysis calculated from the Doppler frequency shifts of the moving blood cells is then used to obtain a velocity waveform for the measured vessel (Figure 1.11.).

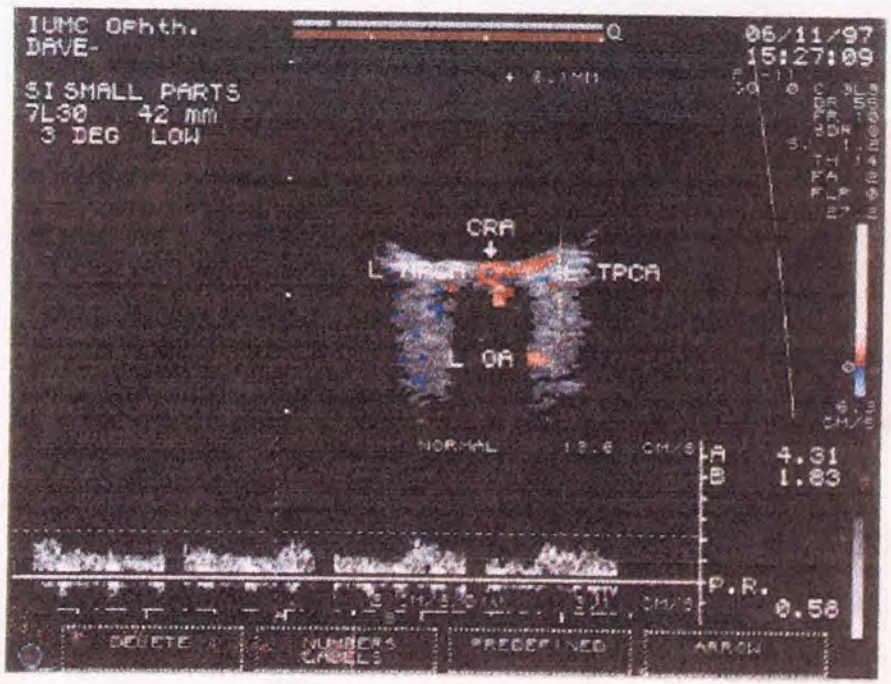

Figure 1.11. Colour Doppler image. Colour Doppler image print out for a normal eye. The OA, CRA and SPCAs are indicated.

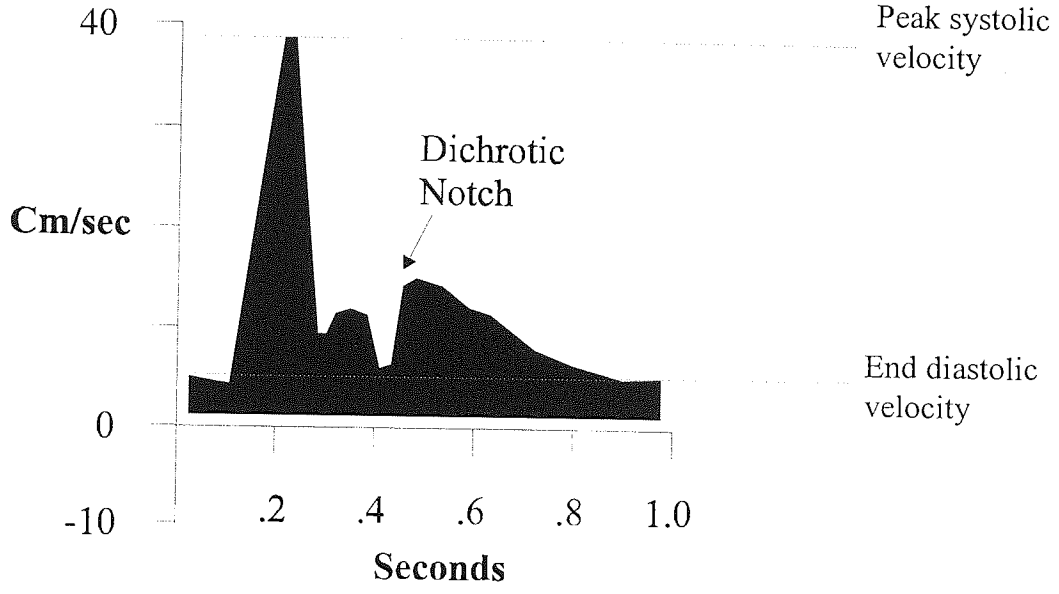

Figure 1.12. Velocity waveform. A graphical representation of a velocity waveform for the OA adapted from Williamson & Harris 1996 (calculated from the spectral analysis of Doppler shift frequencies). Axis x represents time (seconds) and y represents blood cell velocities (cm/sec). Peak systolic velocity and end diastolic velocity (cm/sec) are obtained from the velocities in systole and diastole respectively. Their relative positions are indicated. The dichrotic notch is often visible and represents the closing of the aortic valve of the heart during the cardiac cycle.

The waveform represents all of the blood cell velocities in a given area of the vessel at a given time. In practice the peak velocities are used in calculations. The operator identifies the fastest velocity in systole and diastole (Figure 1.12.) and from this peak systolic velocity (PSV) and end diastolic velocity (EDV) are calculated. Two further parameters are determined that provide an indication of the shape of the waveform and the resistance of flow within the vessel (Pourcelot, L., 1974). These include resistive index, also referred to as Pourcelot's ratio and pulsatility index calculated as follows:

Equation 1.2.

$$\text{Resistive Index} = \frac{(\text{PSV} - \text{EDV})}{\text{PSV}}$$

$$\text{Pulsatility Index} = \frac{(\text{PSV} - \text{EDV})}{\text{Tmax}}$$

Where:

PSV = peak systolic velocity

EDV = end diastolic velocity

The resistive index is often quoted as a percentage, where 0% equals zero resistance increasing to 100% representing maximum resistance. This parameter is particularly useful when measuring small vessels such as in the orbital circulation, whereas the pulsatility index is useful for larger vessels of the peripheral circulation (Williamson, T. H. & Harris, A., 1996). It should be noted however, that only blood flow velocities and measures of vascular resistance can be obtained with CDI. In order to determine measurements of blood flow or volume the diameter of the vessel would need to be determined which is not currently possible with CDI.

When measuring the retrobulbar circulation the vessels that are commonly investigated include the ophthalmic artery (OA), central retinal artery and vein (CRA/V) and posterior ciliary arteries (short (SPCAs) and long (LPCAs) although differentiation is difficult). The relative positions of these vessels are shown in figure 1.3. and the methods used to identify them are outlined in chapter 5. Other vessels which are less commonly measured and notoriously difficult to visualise and assess include the superior ophthalmic vein and vortex vessels (Williamson, T. H. & Harris, A., 1996)

1.13.3. Reproducibility and validity

Few studies report the reproducibility of CDI in the orbital circulation and those that have report the technique as highly reproducible for the measurement of blood flow velocities and resistance indices in the orbital vessels (Tamaki, Y. *et al.*, 1993; Baxter, G. M. & Williamson, T. H., 1995; Harris, A. *et al.*, 1995b; Quaranta, L. *et al.*, 1997). Table 1.5. gives the coefficients of reliability from two recent reproducibility studies (Baxter, G. M. & Williamson, T. H., 1995; Harris, A. *et al.*, 1995b). Evidently, the OA results in some of the lowest coefficients of reliability values indicating good reproducibility. This vessel is the largest of the three most commonly measured, it is easily identified and results in the highest flow velocities of all the vessels in the orbit. Consequently, the resulting waveform for the OA is quite large with well-defined

systolic peaks and diastolic troughs that facilitate accurate measurement of flow velocities (Harris, A. *et al.*, 1995b).

CDI indices measured for the CRA are reproducible, but not as reliable as for the OA. One reason for this may be that the CRA waveforms are broader than for the OA and the peaks and troughs are less well defined. The PCAs are very narrow and hence difficult to locate individually, consequently several PCAs may be contained within the sample area. These vessels follow a tortuous vascular course which makes selection of the angle of incidence difficult and susceptible to greater error in velocity calculations compared to the CRA and OA, which take a more direct route (Harris, A. *et al.*, 1995b).

Of the parameters measured, resistive index (RI) results in lower coefficients of reliability (increased reproducibility) when compared to PSV or EDV (Table 1.5.). The reason for this is that PSV and EDV are both affected by error in the selection of the angle of incidence (see section 1.13.2.). Resistive index, however, forms a ratio of the two velocities and because the angle-dependent error is proportionate between PSV and EDV it is eliminated in the calculation of RI (Harris, A. *et al.*, 1995b).

Author	OA			CRA			PCA		
	PSV	EDV	RI	PSV	EDV	RI	PSV	EDV	RI
Baxter *et al.*1995	6.5	11	4.8	4.8	12.2	6.4	36.6	38.8	10
Harris *et al.* 1995	12	6	4	25	11	11	19	25	38

Table 1.5. Reproducibility of CDI indices. Coefficients of reliability are given for PSV, EDV and RI for three retrobulbar vessels: OA, CRA and PCAs. Results are given for two separate studies, it should be noted that different CDI systems where used.

Few studies have investigated the validity of CDI using *in vitro* models (Miles, R. D. *et al.*, 1987; Von Briba, H. *et al.*, 1990; Spencer, J. A. D. *et al.*, 1991). The relative sparcity of validity data is probably due to the known difficulties of simulating a suitable model for these types of investigations. Doppler measures, however, are used in many clinical disciplines other than ophthalmology including neonatal care where Doppler waveforms are used to measure flow and resistance in the umbilical cord (Ferrazzi, E. *et al.*, 1991). Although non-ophthalmological, a study using an *in vitro*

model to validate Doppler waveform showed excellent correlation between the mean flow for the model and all Doppler measures (Miles, R. D. *et al.*, 1987). Spencer, J. A. D. *et al.*, (1991) carried out a similar investigation and found that resistance and pulsatility index correlated well with known resistance values, but that the systolic/diastolic ratio did not. Although these studies go some way to providing data on the accuracy of the Doppler waveform, further investigations employing the use of models are necessary to further our current knowledge.

1.13.4. CDI applications in ophthalmology - glaucoma

Recently, the application of CDI was extended to the exploration of the vascular basis of glaucoma. Several studies have investigated the effect of IOP, the most prominent risk factor in glaucoma, on blood flow velocities. Three experiments that artificially elevated IOP noted increased resistance indices in the CRA and PCAs (Galassi, F. *et al.*, 1992; Joos, K. M. *et al.*, 1999) and reduced blood flow velocities in the CRA (Guthoff, R. F. *et al.*, 1991; Joos, K. M. *et al.*, 1999). Similarly, a more recent study which investigated the effect of spontaneous elevations in IOP on retrobulbar flow in glaucoma reported reduced blood flow velocities in the CRA and increased resistance indices in the PCAs (Liu, C. J. *et al.*, 1997). The effect of reducing IOP in glaucoma has also been considered. Trible, J. R. *et al.*, (1994) examined the effect of trabeculectomy on Doppler indices measured in the retrobulbar vessels and found that flow velocities significantly increased and vascular resistance decreased in the CRA and PCA's post-operatively as noted by Liu, C. J. *et al.*, (1997).

Other studies have compared flow parameters of glaucoma patients with those of normal subjects. Galassi, F. *et al.*, (1992) noted that glaucoma patients had reduced PSV of the OA when compared to normal subjects. Similarly, Cellini, M. *et al.*, (1996) reported that PSV was reduced and resistance indices increased in both the OA and PCAs. Nicolela, M. T. *et al.*, (1996a) reported decreased blood flow velocities and increased resistance in the CRA and SPCAs of both eyes in patients with asymmetric glaucoma. It was suggested that the presence of reduced blood flow in both eyes of

patients with asymmetric glaucoma compared to normal subjects indicated that circulatory defects in glaucoma that may precede glaucomatous change. Studies on NTG have identified lower PSV values in the OA and CRA (Durcan, F. J. *et al.*, 1993) and increased resistance indices in the OA (Harris, A. *et al.*, 1994b; Butt, Z. A. *et al.*, 1995). Diurnal studies using CDI have shown glaucoma patients to have an abnormal circulatory response during the nocturnal blood pressure dip compared to normal subjects (Evans, D. W. *et al.*, 1999b).

Vasospasm comprises one of the central vascular theories in glaucomatous ONH damage (see section 1.8.2.3.). Colour Doppler imaging has been used to identify NTG patients suffering from vasospasm. A study by Harris, A. *et al.*, (1994b) compared normal and glaucomatous (NTG) eyes and found that the latter had lower EDV and RI values in the OA when compared to normal subjects. In order to determine whether the observed increased vascular resistance was physiological (vasospasm) or anatomical (microvessel loss), increased levels of CO_2, a known vasodilator, was administered. The experimental outcome showed that following increased CO_2 breathing, the flow differences between normal and glaucoma subjects were abolished, thereby suggesting the presence of reversible vasospasm in the OA (Harris, A. *et al.*, 1994b).

Because of the non-invasive nature and relatively high reproducibility of CDI, it provides an ideal method for studying the effect of pharmacological agents on ocular haemodynamics. Furthermore, in view of the substantial evidence that ocular blood flow is compromised in glaucoma a drug that could increase vascular perfusion while decreasing IOP would be of great value. A number of studies have been carried out investigating the effects of various anti-glaucoma ocular hypotensive drugs on ocular circulation.

Harris, A. *et al.*, (1995a) studied the effect of betaxolol and timolol (selective and non-selective β-adrenergic blocking drugs respectively) on ocular blood flow in NTG and found that betaxolol increased EDV and decreased RI in the three orbital vessels measured but no haemodynamic effect was observed for timolol. This finding

contrasted to an earlier study by Baxter, G. M. *et al.*, (1992) which found that the same concentration of timolol resulted in a significant reduction of RI between treated and non-treated eyes suggesting reduced resistance to flow.

A separate study, which looked at the effect of topical dorzolamide on four retrobulbar vessels in normal eyes revealed no effect on blood flow velocities or resistance indices (Harris, A. *et al.*, 1996a). Similarly, nifedipine failed to induce a significant change in blood flow when tested on NTG patients (Wilson, R. P. *et al.*, 1997). A recent study by Harris, A. *et al.*, (1996c) examined the individual and combined effects of acetazolamide and CO_2 on blood flow indices for the OA and CRA, and the internal carotid and middle cerebral arteries. The results showed that acetazolamide alone was ineffective in changing blood flow indices in the orbital arteries, but when combined with CO_2 increased blood flow and decreased vascular resistance was evident in the CRA. In contrast, acetazolamide or CO_2 alone resulted in increased blood flow velocities and decreased resistance indices in the middle cerebral artery. This suggests that in comparison to the brain, the eye is much less responsive to vasodilatory agents.

1.13.4.1. CDI: other applications in ophthalmology

Colour Doppler imaging has many applications in ophthalmology including identification of ocular tumours (Lieb, W. E. *et al.*, 1990) and pseudoexfoliation syndrome following transient ischemic attack (Repo, L. P. *et al.*, 1995). It also provides a useful technique for the investigation and diagnosis of a variety of vascular occlusion diseases such as central retinal vein and artery occlusion (Baxter, G. M. & Williamson, T. H., 1993; Hedges, T. R. *et al.*, 1993), ophthalmic artery stenosis during ocular ischemic syndrome (Ho, A. C. *et al.*, 1992) and reduced blood flow in anterior ischemic optic neuropathy (Flaharty, P. M. *et al.*, 1993).

1.14. Laser Doppler Flowmetry

The technique of laser Doppler flowmetry (LDF), first described by Riva, C. E. *et al.*, (1992), is based on the Doppler effect (see section 1.13.1.). It can be calculated from the following equation.

$$\Delta F = (2\pi / \lambda)(K_S - K_i) \cdot V$$

Equation 1.3.

Were:

ΔF is the frequency shift

λ is the wavelength of the incident light

K_i and K_S are the vectors for the incident and scattered light respectively

V is the velocity vector of the moving particle (red blood cell)

(Riva, C. E. *et al.*, 1992)

The velocity of a moving RBC is minuscule compared to the speed of light and as a consequence the resulting Doppler shift cannot be measured directly. For this reason, an indirect method of measurement is required, achieved by the use of coherent (in-phase) light sources. When a vessel is illuminated the movement of RBCs results in a proportion of the reflected light undergoing a shift in frequency, whereas other light reflected from the motionless surrounding tissue maintains the same frequency as the original source. The outcome is two components of light that are in-phase, but due to their slight difference in frequency demonstrate beat-interference (Figure 1.13.). The detector then measures the intensity of the oscillating light wave, the frequency of which is equal to the difference between the two light components and hence Doppler frequency shift of the moving RBCs.

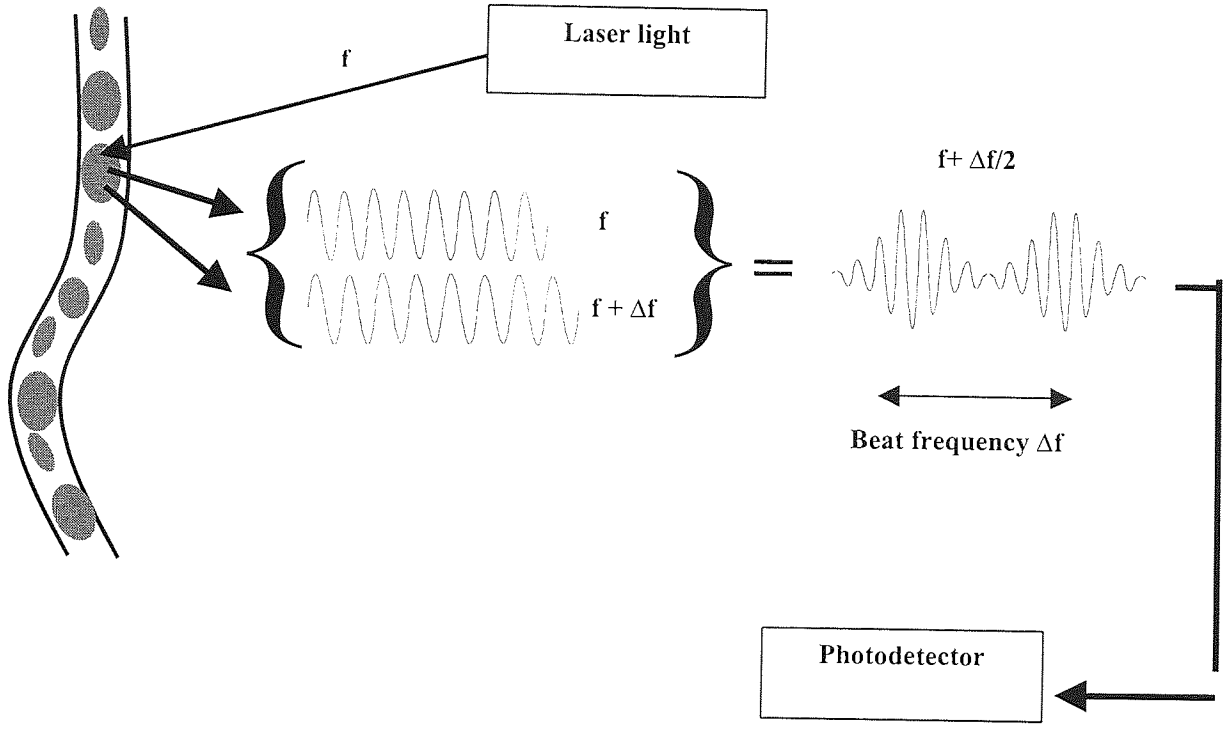

Figure 1.13. The use of coherent light to measure Doppler frequency shift in blood vessels. Coherent laser light is directed at the capillary bed and is deflected off the moving RBCs causing a shift in frequency ΔF. Other remaining light strikes the surrounding tissue and retains the same frequency. Light returning to the photodetector forms an oscillating wave consisting of two components that are in-phase but have different frequencies. It is this wave that is measured, the frequency of the oscillations are equal to the Doppler frequency shift of the original light source caused by the moving RBCs.

Bi-directional laser Doppler velocimetry (LDV), predecessor to LDF, enabled the detection of RBC velocities in the large retinal arteries and veins (Riva, C. E. *et al.*, 1981; Riva, C. E. *et al.*, 1985). The current technique of LDF differs to LDV two fundamental ways:

- LDF measures blood flow velocities of small capillaries where vascular orientation is tortuous forcing the RBCs in different directions (Petrig, B. L. & Riva, C. E., 1996). This contrasts to LDV where RBCs in the larger arteries and veins flow unidirectionally.

- The smaller capillaries measured during LDF contain considerably fewer RBCs than the larger vessels measured with LDV.

During LDF the variation in reflected light intensity is measured as a function of time and computed into Doppler shifted frequencies by Fourier transformation according to the method and algorithm described by Bonner and Nossel (Bonner, R. F. & Nossal, R., 1981; Bonner, R. F. & Nossel, R., 1990). This results in a Doppler shifted power spectrum (DSPS) which represents the various frequencies of the Doppler shifted spectra and the measured intensity of each frequency signal. This may be further regarded in graphical form, where power is proportionate to the volume of moving RBCs and frequency is proportionate to velocity (Figure 1.14.).

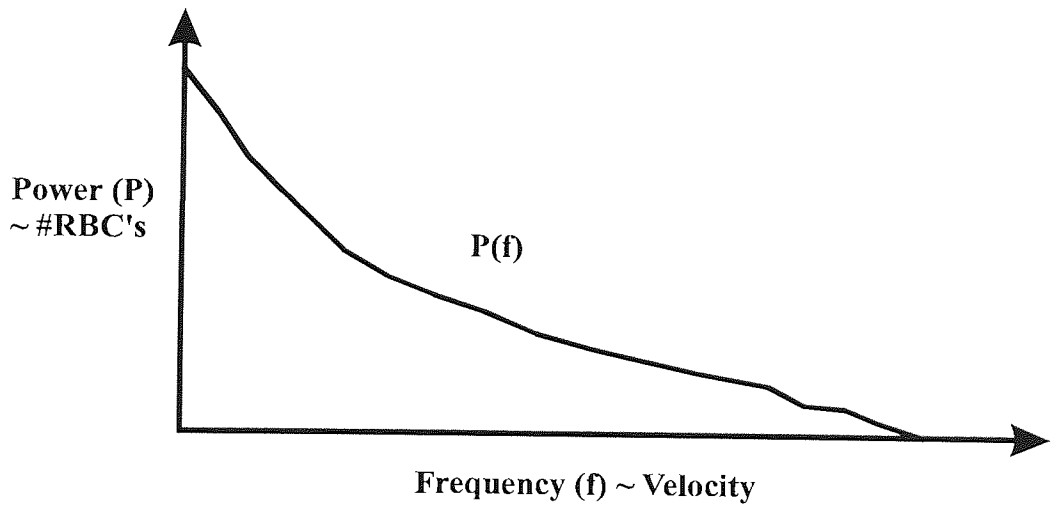

Figure 1.14. Doppler shifted power spectrum. The Doppler shifted power spectrum (DSPS) represents the various frequencies of the Doppler shifted spectra (caused by the moving RBCs) and the measured intensity of each frequency signal. Parameters that may then be extrapolated include power (P) which is proportionate to the volume of moving RBC's and frequency which is proportionate to velocity.

The parameters flow, volume and velocity are determined from the Doppler shifted power spectrum. The calculations of which are given below:

$$w = \frac{2\pi\left(\sum_{125}^{2,000\,Hz} fP(f)df\right)}{P(f=0)}$$

Equation 1.4.

Where:

w = flow

$P(f)df$ = power of the photodetector current associated with a frequency range df about f (given in Hz)

$P(f=0)$ = the DC power in the detected signal

$$x = \frac{2\pi\left(\sum_{125}^{2,000\,Hz} P(f)df\right)}{p(f=0)}$$

Equation 1.5.

Where:

x = volume

$P(f)df$ = power of the photodetector current associated with a frequency range df about f (given in Hz)

$P(f=0)$ = the DC power in the detected signal

$y = w/x$

Equation 1.6.

Where:

y = Velocity

w = Flow (Equation 1.4.)

x = Volume (Equation 1.5.)

(Michelson, G. & Schmauss, B., 1995)

1.15. The Heidelberg Retina Flowmeter (HRF)

The Heidelberg Retina Flowmeter (HRF) is a relatively new technique that combines both laser Doppler flowmetry and laser scanning technology. The instrument is housed within the HRT system. The LDF technique described by Riva, C. E. *et al.*,

(1992) allows the measurement of blood flow indices at a single retinal or ONH location. By incorporating laser scanning technology, the HRF enables multiple LDF measurements over a given scan area. A diode laser with a wavelength of 780nm is used to scan a two-dimensional array of points on the fundus line by line. A total of 64 lines of 256 pixels are scanned 128 times with a scan frequency of 4000 Hz in a two-second time period. The result is a total of 128 reflected light intensity measurements for each location in a 10° × 2.5°, 15°× 2.5° or 20° × 2.5° area. These intensity measurements against time are then used to give the DSPS, which in turn is analysed to give individual perfusion values for each measurement location (256 × 64 pixels). The area of each individual pixel and resolution in the plane of the retina approximates to 10 microns, however the penetration of the laser into the retina and the optical resolution of the HRF relative to the optical axis is much deeper (between 300-400μm). Each perfusion value is expressed as a colour, the lighter the colour the higher the perfusion value for an individual location. The maximum instrument scan frequency is 4000Hz. This limits the detection of correct Doppler frequency shifts to less than 2000Hz and velocity measurements to less than 1 mm/sec in the measurement direction and as a consequence ocular blood flow measurements are restricted to the capillaries. Frequencies of less than 125Hz are also excluded from analysis in order to minimise effects due to breathing movements and cardiac function (Michelson, G. & Schmauss, B., 1995).

In this way a two-dimensional resolved perfusion map is built up which shows the intricate capillary network that would otherwise be undetectable in a normal fundus photograph (Figure 1.15.).

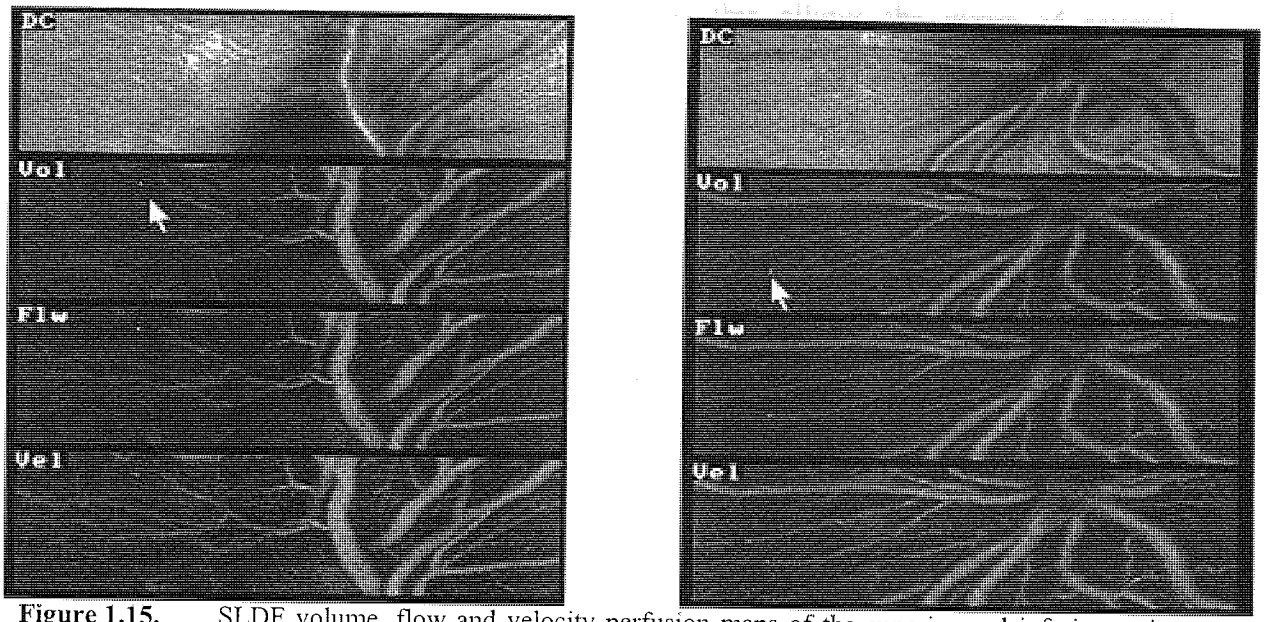

Figure 1.15. SLDF volume, flow and velocity perfusion maps of the superior and inferior optic nerve head and peripapillary retina.

Following the determination of a two-dimensional perfusion map, six images are displayed on the computer for examination:

- Reflectivity image (DC (direct current) component of the Fourier power spectrum) (Figure 1.15.).
- Volume integration to 500 Hz (intermediate result in the determination of perfusion values).
- Volume integration to 1000 Hz (intermediate result in the determination of perfusion values).
- Volume perfusion map (colour coded perfusion map for blood volume at each location) (Figure 1.15.).
- Flow perfusion map (colour coded perfusion map for blood flow at each location) (Figure 1.15.).
- Velocity perfusion map (colour coded perfusion map for blood velocity at each location) (Figure 1.15.).

Further to this the frequency power spectrum is displayed with corresponding data. In order to obtain perfusion measurements from a recorded image an area of interest must be defined. To this end a measurement frame with an area that may be varied from 1 × 1 pixel (approx. 10μm^2) to a maximum of 50 × 50 pixels is placed using the cursor on the desired vascular network. The optimal measurement frame size

recommended is 10 × 10 pixels (100μm^2) as this allows the mean of several measurements to be taken and the avoidance of large vessels (Michelson, G. & Schmauss, B., 1995). The area chosen is dependent upon where the perfusion image is taken, but is usually the peripapillary retina, neuroretinal rim or lamina cribrosa. Care must be taken to avoid the large vessels and any movement microsaccades resulting from eye movements. Following placement of the measurement frame, the average value ± standard deviation for the parameters blood flow, volume and velocity (arbitrary units) are determined. The average reflectance values (DC (direct current) component of the Fourier power spectra) for within the measurement location are also given (Figure 1.14.). The recommended DC range is between 80 –150, if the average DC value for the region of interest is outside this range it should not be used in analysis (Michelson, G. & Schmauss, B., 1995).

1.15.1. Validity and linearity of ocular blood flow measurement with the HRF

Several investigators have investigated the validity and linearity of haemodynamic measurements obtained with the HRF. Michelson, G. *et al.*, (1996b) moved a plane of known velocities in front of the SLDF and compared the observed and expected frequency shifts. A highly significant correlation over a range of velocity values was reported thus suggesting a strong linear relationship between actual and observed frequency shifts.

Chauhan, B. C. & Smith, F. M. (1997) validated the HRF parameters flow and velocity. An *in-vitro* experiment was conducted which used glass capillaries of varying diameters containing skimmed milk over a range of pump flow rates (Chauhan, B. C. & Smith, F. M., 1997). The experimental results identified an operational velocity range of ~0.08 to 1.0mm/sec which agrees with the restricted Doppler frequency range accepted for analysis (Michelson, G. & Schmauss, B., 1995) (see section 1.15.). The measured velocity and flow values given by the HRF correlated linearly with the actual values within this range.

Strenn, K. *et al.*, (1997) used the physiological retinal response to changing levels of oxygen (hypoxia and hyperoxia) to determine the sensitivity of HRF measurement. It is known that retinal blood flow responds to the arterial partial pressure of oxygen, if the PO_2 increases than retinal flow decreases and vice versa (Riva, C. E. *et al.*, 1983). Using this theory, Strenn, K. *et al.*, (1997) found that there was a significant dose dependent change in the measured parameters, thus indicating that the HRF is highly sensitive to alterations in retinal blood flow. Two further studies, one which investigated the effects of hyperoxia on smokers and non-smokers (Langhans, M. *et al.*, 1997), and one which evaluated the effects of both hyperoxia and hypercapnia on normal subjects (Lietz, A. *et al.*, 1998), found similar HRF responses.

1.15.2. Reproducibility of ocular blood flow measurement with the HRF

The clinical usefulness of SLDF to detect changes in blood flow is dependent on the reproducibility of the available blood flow parameters. To this end, several investigators have investigated the reproducibility of velocity, volume and flow measurements. The *in-vitro* model used by Chauhan, B. C. & Smith, F. M. (1997) identified mean coefficients of variation for volume (3.35%), velocity (3.57%) and flow (4.05%). Because these measurements were acquired using an *in-vitro* model, they provide an indication of the instrument-related error. Two other potential sources of error are introduced *in-vivo*:

1) Operator error (due to identifying the same anatomical location for the measurement pixel frame).
2) Physiological error (due to cardiac fluctuations in blood flow).

Michelson, G. & Schmauss, B. (1995) assessed the intra-visit reliability of HRF parameters across five images for 12 normal subjects. Reliability coefficients of 0.84 for retinal velocity and flow and 0.85 for volume where reported thus indicating an error component of 16% for velocity and flow and 15% for volume. A similar study by Chauhan, B. C. (1996) reported slightly lower variability values ranging from 11% - 14%. A further study by Strenn, K. *et al.*, (1997), that investigated the reproducibility of 2 images only, found higher levels of variability.

The inter-visit variability, which is important in the long-term follow-up of blood flow parameters, has also been addressed. Michelson, G. *et al.*, (1996b) estimated the reliability of SLDF by obtaining five images from ten subjects over five days. The reliability coefficients for flow, volume and velocity where reported as 0.82, 0.81 and 0.83 respectively; surprisingly similar to the intra-visit reliability. Nicolela, M. *et al.*, (1997) also assessed the inter-visit reproducibility of HRF parameters across three visits for the retina, neuroretinal rim and lamina cribrosa. The results showed that variability ranged from 18.8% - 25.22%, with the retinal area demonstrating the least variability. The same study also confirmed that the 10 × 10 pixel frame, recommended by Michelson, G. & Schmauss, B. (1995) resulted in more repeatable measurements than the smaller frame option. Finally, a recent study that examined both the intra- and inter-visit reproducibility for blood flow reported coefficients of variation of 7% and 30% respectively. The latter improved to 16% when a pixel by pixel analysis method was used for the whole image instead of the custom pixel measurement frame (Kagemann, L. E. *et al.*, 1998).

1.15.3. Factors affecting reproducibility of HRF measurements

A number of factors have been identified that contribute to the variability of measurements obtained with the HRF:

1.15.3.1. Eye movement

The technique is extremely sensitive to eye movement, even slight movements result in microsaccades where blood flow values are unstable (Michelson, G. & Schmauss, B., 1995).

1.15.3.2. Cardiac rhythm

It has been shown using the blue field technique and scanning laser fluorescein angiography that retinal capillary blood flow is pulsatile (Arend, O. *et al.*, 1995). The

influence of cardiac rhythm results in unavoidable fluctuations in flow, particularly as the measurement time of approximately two seconds incorporates between one and two cardiac cycles. Chauhan, B. C. & McCormick, T. A. (1995) considered the effect of the cardiac cycle on measurements obtained with the HRT and suggested that pulse synchronisation may reduce variability. Sullivan, P. *et al.*, (1999) determined the influence of ocular pulsatility with SLDF and discovered that the alternating bright and dark banding pattern observed during measurement acquisition was related to cardiac pulse and resulted in significant fluctuations in blood flow. Ideally, pulse synchronisation should be incorporated into SLDF to ensure that the measurement time frame occurs at the same point in the cardiac cycle for subsequent measurements of the same individual. A recent study by Michelson, G. *et al.*, (1998b) outlined a new method of analysis for SLDF measurement that does incorporate pulse synchronisation, however the software is still in the early stages of development and not widely available.

1.15.3.3. Camera eye distance

The distance of the laser beam to the eye has been suggested as a potential source of variability which is easily overcome by maintaining a constant distance for all measurements (Kagemann, L. E. *et al.*, 1996).

1.15.3.4. Zero-offset

A large zero-offset of the measured parameters is a potential source of variability. Even when an *in-vitro* model is used and the velocities of moving particles equal zero the corresponding HRF parameters do not. The zero-offset is largely attributable to background noise that is not due to true Doppler shifts. In a clinical situation the size of the zero-offset is impossible to judge and although this is not a problem for measurements made on the same individual subject, studies that compare subjects cross-sectionally must be interpreted with caution (Chauhan, B. C. & Smith, F. M., 1997). A fifth source of variability is associated with the illumination level of SLDF

images. Underexposure can lead to the underestimation of avascular activity and shift the bulk of the measurements towards low values and attenuate high perfusion values (Kagemann, L. E. *et al.*, 1999).

1.15.3.5. The measurement frame

The final source of variability with measurements obtained with the HRF lies with the operator. Placing the pixel measurement frame in the same anatomical position for each perfusion image poses a real problem. Most investigators use a morphological landmark such as a vessel bifurcation to identify the same location (Michelson, G. & Schmauss, B., 1995; Langhans, M. *et al.*, 1997; Nicolela, M. *et al.*, 1997). One group chose to examine the entire image using the 50 × 50-pixel measurement frame (Lietz, A. *et al.*, 1998). This methodology must be questioned however, because it is unlikely that all perfusion data included will fall within the desired DC range and data from large vessels will not be attenuated.

More recently, groups have developed software that allows the whole perfusion image to be analysed and only values that fall within the desired DC range and free from saccades and large vessels are included (Kagemann, L. E. *et al.*, 1998; Michelson, G. *et al.*, 1998b). These methods have been shown to reduce inter-session variability (Kagemann, L. E. *et al.*, 1998; Michelson, G. *et al.*, 1998b).

1.15.4. HRF applications in ophthalmology - glaucoma

The HRF provides a reproducible technique for the measurement of retinal blood flow in the capillaries. This has proved clinically useful in a number of disease conditions where retinal or ONH blood flow is though to be compromised including POAG.

Michelson, G. *et al.*, (1996a) compared retinal and ONH blood flow parameters for an age-matched group of glaucoma and normal subjects. The results showed that in the glaucoma group blood flow parameters measured at both the juxtapapillary retina and

neuroretinal rim were significantly lower than those in the normal control group, thus indicating reduced perfusion in these areas. Furthermore, an inverse relationship has been identified between C:D ratio and ONH blood flow; this is in agreement with previous histological observations which reported a proportionate decrease in capillary area with increasing glaucomatous optic neuropathy (Quigley, H. A. *et al.*, 1984). Michelson, G. *et al.*, (1996a) compared a group of glaucoma patients administering topical therapy with an untreated glaucoma group. A reduction in juxtapapillary retinal flow was observed for both glaucoma groups compared to a normal control group that appeared unrelated to topical therapy. A similar study found that blood flow parameters at the retina and lamina cribrosa but not the neuroretinal rim were significantly reduced in glaucoma patients compared to normal subjects (Nicolela, M. T. *et al.*, 1996b).

Lietz, A. *et al.*, (1998) evaluated the effect of increased IOP on blood flow at the papilla in healthy normal subjects and found that an increase in IOP from 20mmHg to 50mmHg was associated with a decrease in blood flow. A further study by Michelson, G. *et al.*, (1998a) found a significant correlation between decreased blood flow and visual field loss in eyes with glaucomatous damage that was apparent even in early glaucoma.

Other observations for normal subjects show that blood flow is significantly greater in the neuroretinal rim compared to the juxtapapillary retina (Michelson, G. *et al.*, 1996a) and smoking significantly reduces the retinal and ONH haemodynamic response to a known vasoconstrictor (Langhans, M. *et al.*, 1997). Finally, no single investigation has attempted to correlate HRF measurements with age, but a study that compared LDF measurements (Riva technique) of ONH flow with that of the fellow eye found a significant correlation that decreased with increasing age (Cranstoun, S. D. *et al.*, 1994).

1.16. Pulsatile ocular blood flow : ocular blood flow tonography

Blood flow to the eye is not steady but varies according to the arterial pulse, increasing during the systolic phase and decreasing during the diastolic phase of the

cardiac cycle (Silver, D. M. *et al.*, 1989). Each contraction of the heart forces a bolus of blood into the eye via the OA which then spreads rapidly to perfuse the retinal and ciliary vascular network. Blood flow to the eye constitutes two components: a steady continuous component, and a pulsatile component that varies according to the cardiac cycle otherwise known as pulsatile ocular blood flow (POBF).

As POBF varies with cardiac pulse, rhythmic fluctuations of IOP occur. The Langham pneumotonometer, developed in the 1960s, provided the first system for measuring static IOP over a period of time (Langham, M. E. & McCarthy, E., 1968). Using known pressure/volume relationships changes in IOP over time can be used to determine ocular volume as a function of time, thus allowing net pulsatile ocular blood flow to be calculated. Since the development of the pneumotonometer, advancements have been made culminating in a sophisticated system (ocular blood flow tonograph, OBF tonograph) that can monitor IOP 200 times per second thereby enabling ocular pulse waveforms to be obtained and POBF to be derived. Although other systems exist for measuring POBF, they are beyond the scope of this review and hence discussions will be limited to the OBF tonograph.

1.16.1 Blood flow through the eye - elastic chamber model

In order to understand the concept of POBF and how it is measured it is helpful to imagine the eye as an elastic chamber with an inflow and outflow valve. When a bolus of incompressible fluid enters a chamber through an inflow valve the volume of the chamber will increase accordingly. If the outflow valve is then opened, the bolus will leave the chamber and the original chamber volume will be regained (Figure 1.16.a.).

The living eye is not as simple as the elastic chamber model as there are no valves and the pulsatile component of inflow is combined with a second component that is constant and steady (Silver, D. M. *et al.*, 1989). The flow of blood out of the eye is assumed to be non-pulsatile (Riva, C. E. *et al.*, 1985). The venous outflow is made up of two parts: the first is equal to the continuous inflow of blood and the second balances the average pulsatile component of inflow. Variations in the net inflow due

to systole and diastole (ocular pulse) regularly disrupts this equilibrium resulting in changes in ocular volume. In the eye, the sclera is relatively rigid and the vascular network elastic; consequently an increase in the volume of fluid results in slight increase in the overall volume of the eye and a concomitant rise in IOP. Figure 1.16.b. demonstrates this phenomenon and shows the combined pulsatile and steady inflow, the continuous outflow and corresponding changes in ocular volume.

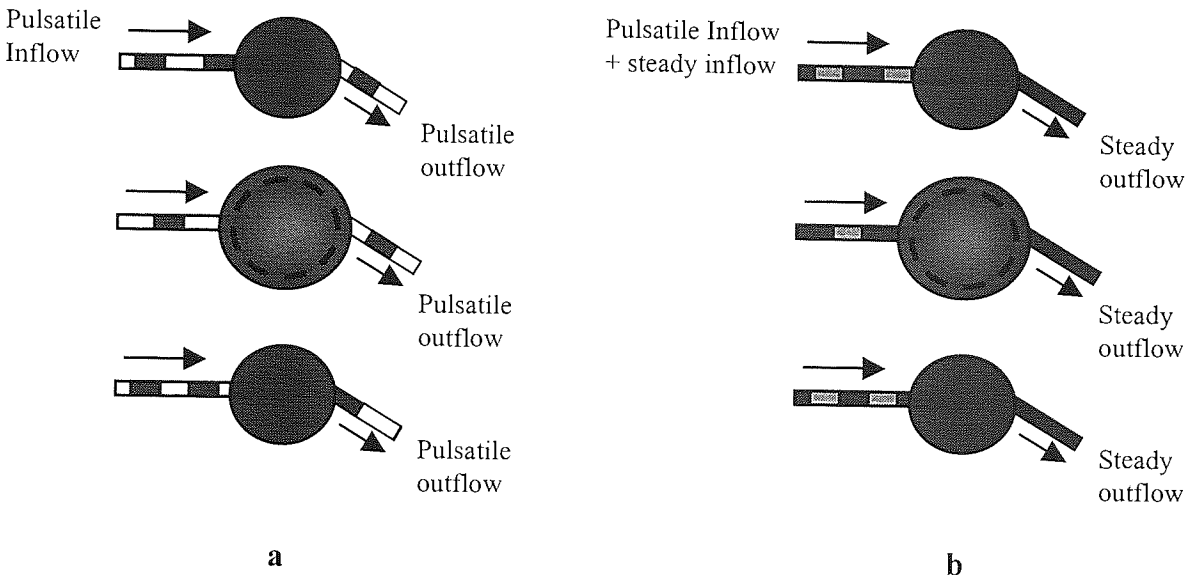

Figure 1.16. Blood flow through the eye: Elastic chamber model. (adapted from Silver, D. M. *et al.*, 1989)

a) A simplified model of an elastic chamber, a bolus of fluid enters the chamber causing an incremental expansion, the bolus then leaves and the chamber returns to its original size. The outflow of fluid is pulsatile.

b) The eye is represented as an elastic chamber. A bolus of blood enters the chamber with continuous flow. During systole, the chamber expands to accommodate a pulsatile component and then returns to its original size during diastole. The outflow of blood is always continuous.

1.16.2 The pressure/volume relationship: calculation of POBF

It is well accepted that changes in the volume of the eye relate to changes in IOP (Friendenwald, J. S., 1937; McBain, E. H., 1958; Eisenlohr, J. E. *et al.*, 1962). This volume/pressure relationship is described by Friendenwalds equation:

$$P_1 = P_0 e^{K\Delta K}$$

Equation 1.7.

Where:

P_0 = initial pressure

P_1 = final pressure change

ΔV = change in volume

K = a constant proportionate to the mean IOP

(Friendenwald, J. S., 1937)

A graph of log P_1 against ΔV results in an approximately linear relation. This fundamental relationship has been examined and validated using a series of direct manometric studies on living human eyes that describe a wide range of induced volumetric changes and corresponding pressure changes (Eisenlohr, J. E. *et al.*, 1962; Langham, M. E., 1967). Investigations by Eisenlohr, J. E. *et al.*, (1962) suggested that the graphical relationship between IOP and volume for living eyes was not linear, but formed a convex curve due to changes in ocular rigidity at varying levels of IOP. However, because the calculation of POBF is determined from very small variations in IOP over a given pulse cycle, the relationship is again approximated to be linear (Krakau, C. E. T., 1992) and is described as:

$$(V_1 - V_2) = k(IOP_1 - IOP_2)$$

Equation 1.8.

Where:

V_1 = initial ocular volume

V_2 = final ocular volume

k = constant

IOP_1 = initial IOP

IOP_2 = final IOP

Using this equation variations in IOP over a given time can be used to determine changes in ocular volume as a function of time. Figure 1.17. shows how IOP measured as a function of time translates to incremental ocular volume changes (pulse amplitude) and subsequently net POBF expressed as µl/min (Silver, D. M. & Farrell, R. A., 1994). At present, the OBF system uses a differentiation technique, which

calculates average net POBF after mathematically fitting a straight line to the increasing net flow and an exponential to the decreasing flow to smooth variability in the data (Silver, D. M. & Farrell, R. A., 1994). More recently, Krakau, C. E. T. (1992) suggested a method that uses the steepest part of an ocular pulse wave (originally derived from a pressure wave) to determine the outflow per second; this value is then multiplied by 60 to give the flow per minute.

Finally net POBF (*v pulsatile*) may be calculated using the following formula:

Equation 1.9.

$$v\ pulsatile = k * f * \left[\frac{dv(t_B)}{dt_B} - \frac{dv(t_A)}{dt_A} \right]$$

The factors in this formula include: *k* which is a constant related to the length of time ($t_B - t_A$) and the period of the pulse (t/(c)-t/(A); f which is the pulse rate; the bracketed expression which represents the incremental volume change at B minus the incremental volume change at A, where A is the trough of the IOP curve and B the peak of the IOP curve (Silver, D. M. *et al.*, 1989; Spraul, C. W. *et al.*, 1998).

There are a number of assumptions that are made when calculating POBF using the OBF system:

- The pulsatile component of blood flow is zero at some point in the pulse cycle and no blood reflux occurs (Krakau, C. E. T., 1992).
- The outflow of blood is steady and not pulsatile (Krakau, C. E. T., 1992; Silver, D. M. & Farrell, R. A., 1994; Krakau, C. E. T., 1995).
- The physical model relating to blood flow in the eye is assumed to be incompressible fluid passing through an elastic chamber (Silver, D. M. & Farrell, R. A., 1994).
- The measurements of IOP and it's variation over time are accurate (Silver, D. M. & Farrell, R. A., 1994).

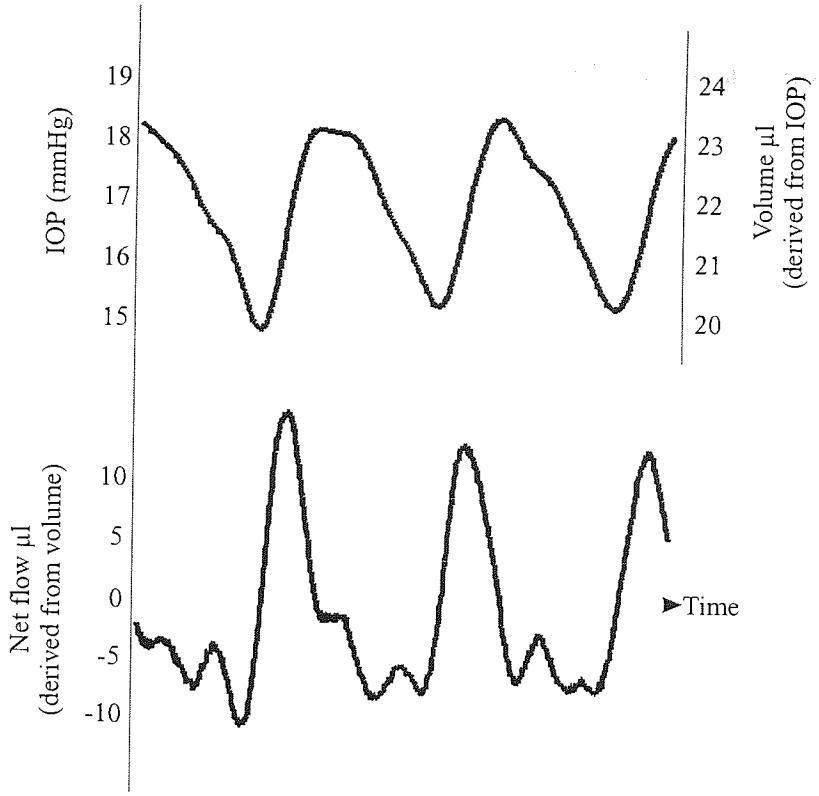

Figure 1.17. Pressure/volume relationship.

1.16.3 The Ocular Blood Flow Tonograph (OBF Tonograph)

The OBF tonograph consists of a pneumatic probe that is capable of taking 200 IOP measurements per second with a resolution of 0.01mmHg (Spry, P., 1996). The pneumatic probe comprises a sensor and silastic membrane tip which forms the end point of a hollow piston mounted on a frictionless air bearing. Gas flows to the tip at an elevated constant pressure through a single plastic pipe consisting of an inlet and outlet lumen. Influx of pressurised gas into the sensor through the inlet lumen causes the piston to force forward and the membrane to bow outwards. To obtain measurements, the tip is applied onto the cornea, this causes the silastic membrane to become depressed thus creating an increase in the pressure within the sensor. As the pressure rises the piston is pushed towards the cornea by the air bearing. The sensor automatically alters the pressure on the piston according to the IOP thereby allowing continuous measurement of IOP. At any given moment the IOP is proportionate to the

pressure in the sensor that is measured via the outlet lumen by a transducer contained within a base unit (Spry, P., 1996).

In order to take measurements a topical anaesthetic must be instilled into the eye. The OBF probe is usually mounted on a slit lamp although it may also be hand held if required. Following contact of the silastic membrane with the cornea an audible tone is heard indicating that IOP measurement has commenced. The test time lasts for a maximum period of 20 seconds or until five similar ocular pulse waves are detected (Figure 1.18.). The five pulse waves are then analysed individually to determine a number of parameters that are averaged; these are outlined in Figure 1.18. Unlike the OBF Tonograph, the Langham OBF system relies on the operator to choose adequate pulse waves for the calculation of POBF.

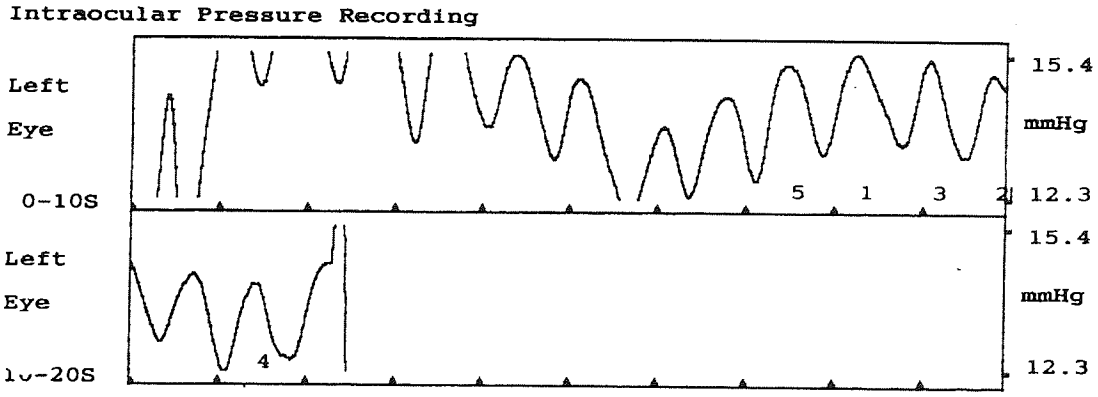

Left Eye	Pulse:	1	2	3	4	5	Average
Minimum Intraocular Pressure	[mmHg]	12.5	11.7	12.0	12.3	11.2	11.9
Maximum Intraocular Pressure	[mmHg]	14.6	13.6	14.0	14.7	12.9	14.0
Average Intraocular Pressure	[mmHg]	13.5	12.6	13.0	13.5	12.0	12.9
Pulse Amplitude	[mmHg]	2.2	1.9	2.0	2.4	1.7	2.0
Pulse volume	[µl]	5.2	4.9	5.0	5.7	4.5	5.0
Systolic Time	[sec]	0.28	0.30	0.29	0.36	0.35	0.31
Diastolic Time	[sec]	0.44	0.44	0.48	0.42	0.40	0.43
Pulse Rate	[/min]	83	81	77	76	80	81
Pulsatile Ocular Blood flow	[µl/min]	834	853	831	866	908	858
OBF % Standard Deviation							3

MNI : 1871 PEQ : 3.2 IDR : 41

Figure 1.18. OBF recording and corresponding data. The IOP recording (pulse pressure wave) for a young healthy subject is given. Five similar pulse waves are chosen for analysis (numbered 1-5). The corresponding data and averaged values for each parameter are detailed in the print out shown. The percentage standard deviation for the five measurements gives an indication of the reproducibility of the recordings.

1.16.4 POBF: what is it measuring?

The vascular supply to the eye may essentially be separated into three fundamental systems including retinal, choroidal and ONH circulation (see section 1.7). There is some controversy over which element of the existing circulation the pulsatile component of total ocular blood flow represents. The total vascular supply to the eye is thought to approximate 900µl per minute (Langham, M. E. *et al.*, 1989b). There is evidence to suggest that the pulsatile component forms a substantial part of the ocular circulation with values varying between 590µl/min (Silver, D. M. *et al.*, 1989) and 724µl/min (Langham, M. E. *et al.*, 1989a) for normal subjects. A recent study that examined normal POBF values using the OBF Tonograph found a mean value of 669.90 ± 233µl/min for males and 841.90 ± 254.6 µl/min for females (Yang, Y. C. *et al.*, 1997a). The significant difference between mean values for male and females has been attributed to the higher pulse rate in females which affects POBF (Yang, Y. C. *et al.*, 1997a).

In monkeys, retinal vasculature flow forms approximately 1/20th of the total ocular circulation with choroidal flow constituting the remainder (Alm, A. & Bill, A., 1973). Studies in the human eye have found similar values of retinal flow (Riva, C. E. *et al.*, 1985). This suggests that the choroidal circulation constitutes approximately 95% of the overall circulation. Consequently, it is proposed that POBF is largely a measure of the choroidal circulation with some influence from the retinal circulation.

1.16.5 Reproducibility and validity

A number of studies have examined the reproducibility of POBF measurements. Some studies are based on the Langham OBF system (Oppenheim, B. *et al.*, 1993; Spraul, C. W. *et al.*, 1998) and others on the OBF Tonograph (Butt, Z. A. & O'Brien, C., 1995; Yang, Y. C. *et al.*, 1997a; Spraul, C. W. *et al.*, 1998). For reasons already discussed in section 1.11.2.5. it is suggested that the coefficient of variation is an inappropriate statistical parameter to use when determining the reproducibility of repeated measures. For this reason studies that use the more statistically viable

coefficient of reliability or intra-class correlation coefficient provide a better determination of reproducibility. Using reliability coefficients, the intra-visit reproducibility based on data from two separate studies (n=83 and n=40) was reported as 0.92 and 0.88 respectively (Yang, Y. C. *et al.*, 1997a; Spraul, C. W. *et al.*, 1998) and the inter-visit reproducibility based on data for 34 subjects was found to be 0.70 (Spraul, C. W. *et al.*, 1998). It was suggested that the majority of the variance associated with POBF measurement was due to intra-subject variability and measurement error of the instrument and not inter-observer variation (Spraul, C. W. *et al.*, 1998).

Although the intra-visit reproducibility of repeated POBF measurements has been reported as good, a number of authors have commented on the substantial range of measurements between individual subjects. In particular, physiological variations such as pulse rate (Trew, D. R. *et al.*, 1991; Yang, Y. C. *et al.*, 1997a), the initial IOP level, systolic and diastolic systemic pressure (Ravalico, G. *et al.*, 1994b), scleral rigidity (Price, E. L. *et al.*, 1999), axial length (Price, E. L. *et al.*, 1999) and refractive error (Kothe, A. C. *et al.*, 1992b) have been highlighted as important.

Other factors that indirectly affect POBF include postural changes (Trew, D. R. & Smith, S. E., 1991a; Kothe, A. C., 1993), age (Kothe, A. C. *et al.*, 1992a; Ravalico, G. *et al.*, 1994b), intrathoracic pressure (Lacey, B. & Rankin, S. J. A., 1997) and diurnal variation (Claridge, K. G. & Smith, S. E., 1994). Postural changes have been studied by a number of workers who have collectively found that although IOP increases when assuming a supine from an upright position, POBF decreases (James, C. B. & Smith, S. E., 1991a; Trew, D. R. & Smith, S. E., 1991a; Trew, D. R. & Smith, S. E., 1991b; Kothe, A. C. *et al.*, 1992a). This postural response in POBF has been found in healthy eyes (Kothe, A. C., 1993), eyes with ocular hypertension (Trew, D. R. & Smith, S. E., 1991a), NTG (James, C. B. & Smith, S. E., 1991b) and POAG (Trew, D. R. & Smith, S. E., 1991b). A decrease in POBF upon adopting the supine position is accompanied by a significant decrease in mean systemic blood pressure and heart rate (James, C. B. & Smith, S. E., 1991a; James, C. B. & Smith, S. E., 1991b; Trew, D. R. & Smith, S. E., 1991a; Trew, D. R. & Smith, S. E., 1991b). In particular, a decrease in

heart rate causes an increase in the diastolic phase of the ocular pulse which is thought to increase the non-pulsatile component of blood flow thus causing a decrease in POBF (Vachon, N. & Kothe, A. C., 1992). A possible shift in the pulsatile/non-pulsatile blood flow ratio on adopting the supine position has been highlighted (James, C. B. & Smith, S. E., 1991a).

As adopting the supine position results in a significant decrease in POBF it may follow that POBF is reduced at night resulting in diurnal variation. It has been shown that although IOP, ocular pulse, blood pressure and heart rate decreased significantly overnight in ocular hypertensives and POAG patients, no significant change in POBF was evident (Claridge, K. G. & Smith, S. E., 1994). Interestingly, when patients were examined individually some exhibited night-time falls in POBF, thus suggesting that some have autoregulatory mechanisms for maintaining POBF nocturnally whilst others do not (Claridge, K. G. & Smith, S. E., 1994).

Finally, the effect of age on POBF has been studied in normal subjects (Kothe, A. C. *et al.*, 1992a; Ravalico, G. *et al.*, 1994b). Kothe, A. C. *et al.*, (1992a) studied the effects of changing posture as a function of age and reported no age-dependent response in healthy individuals. In contrast, a more extensive study by Ravalico, G. *et al.*, (1994b) found that upon changing position POBF declined more in younger subjects than in older subjects. Furthermore, POBF measured in the sitting position decreased significantly with age, however in the supine position, a decreasing trend in POBF was evident only after 50 years (Ravalico, G. *et al.*, 1994b). A number of reasons have been suggested for decreasing POBF with age including reduced ocular pulse, increased vascular resistance and increased scleral rigidity (Ravalico, G. *et al.*, 1994b). The latter must be viewed with caution as there are data to suggest no change in scleral rigidity after 60 years (Friedman, E. *et al.*, 1989).

As POBF is an indirect theoretical measure of pulsatile blood flow in the eye direct validation studies are impossible. In contrast, the accuracy of IOP measurement, which is the basis for the determination of POBF, may be evaluated. The Langham system (Quigley, H. A. & Langham, M. E., 1975) and the OBF tonograph (Spraul, C.

W. *et al.*, 1998) have both been compared favourably to Goldmann applanation tonometry. A series of manometric studies have validated the pressure/volume relationship which is the basis for the determination of POBF (Eisenlohr, J. E. *et al.*, 1962; Langham, M. E., 1967). Furthermore, two independent studies have confirmed the validity of the mathematical formulae used to calculate POBF (Krakau, C. E. T., 1992; Silver, D. M. & Farrell, R. A., 1994).

1.16.6 POBF applications: glaucoma

A number of studies have investigated POBF in NTG (James, C. B. & Smith, S. E., 1991b; Ravalico, G. *et al.*, 1994a; Quaranta, L. *et al.*, 1994; Fontana, L. *et al.*, 1998) HTG (Trew, D. R. & Smith, S. E., 1991b) and ocular hypertension (Trew, D. R. & Smith, S. E., 1991a; Trew, D. R. & Smith, S. E., 1991b). Results showed that POBF was significantly lower in patients with POAG compared to patients diagnosed with ocular hypertension (Trew, D. R. & Smith, S. E., 1991b) and significantly lower in patients with NTG when compared to age- and gender-matched controls (James, C. B. & Smith, S. E., 1991b; Ravalico, G. *et al.*, 1994a; Fontana, L. *et al.*, 1998).

Quaranta, L. *et al.*, (1994) reported that POBF values for NTG patients were significantly lower than that of normal subjects (9.87%) and that incremental increases of IOP (5 and 10mmHg) resulted in substantial decreases in POBF which where considerably more pronounced in the NTG group. Thus NTG patients appear abnormally sensitive to increased IOP which may be explained, in part, by a deficient autoregulatory response (Quaranta, L. *et al.*, 1994). Ravalico, G. *et al.*, (1994a) reported a 32.32% decrease in POBF values for NTG patients when compared to healthy controls, but noted that even when IOP was increased by as much as 30mmHg POBF values for the two groups decreased by similar amounts. This casts doubt on the autoregulatory theory because one would assume that differences in POBF between normal and glaucoma subjects would be more pronounced at higher IOP. Alternatively, the IOP increase of 30mmHg may have been outside the autoregulatory capacity for both groups thus explaining the similar response (Quaranta, L. *et al.*, 1994).

POBF has been used to test the vascular effects of pharmacological agents used in glaucoma therapy. A study which investigated the long-term effect of two beta-blockers, timolol and betaxolol, on POBF in POAG patients reported that although the two drugs had a similar effect on IOP reduction, POBF decreased in patients treated with timolol and remained stable for betaxolol treated patients (Boles Carenini, A. *et al.*, 1994). Although timolol reduces IOP it is also known to increase vascular resistance through vasoconstriction and as a non-cardioselective beta antagonist it decreases systemic arterial pressure and hence has a potential negative effect on ocular haemodynamics (Langham, M. E., 1990; Boles Carenini, A. *et al.*, 1994; Harris, A. & Martin, B. J., 1997). This finding was supported by another study that investigated the effect of topical timolol on normal healthy volunteers. A reduction in POBF was noted in both the treated and untreated fellow eye indicating a systemic effect (Kitaya, N. *et al.*, 1997). In contrast, Betaxolol induced a vasodilatory effect (Langer, S. Z., 1995), that most probably contributed to the stability of observed POBF levels. A separate study investigated the effects of topical pilocarpine on POBF in POAG patients. The authors found no significant difference in POBF values between patients on dual pilocarpine / timolol therapy and patients on only timolol; the conclusion being that pilocarpine had no significant effect on POBF (Claridge, K. G., 1993).

1.16.7 POBF applications: non-glaucomatous disease

POBF measurement has many other applications in ophthalmology other than glaucoma including the investigation of choroidal melanoma where POBF is notably reduced (Yang, Y. C. *et al.*, 1997b). Several studies have also identified a reduction in POBF in other pathologies including diabetes mellitus (Grebe, R. *et al.*, 1989), retinitis pigmentosa (Langham, M. E. & Kramer, T., 1990) and central retinal vein occlusion (Krammer, T. R. & Langham, M. E., 1989).

1.17. Research rationale

1.17.1. Introduction

The aetiology of POAG remains unclear and it is probable that the eventual loss of retinal ganglion cells and ONH axons occurs as a result of several mechanisms. Two principle theories for a mechanism of glaucomatous ONH atrophy have evolved: The vascular theory, which proposes an underlying vascular role that precipitates atrophy by ischaemia, and the mechanical theory, which proposes that a physical process such as increased IOP results in glaucomatous optic neuropathy. Recently, investigators have acknowledged the probability that these two mechanisms are not mutually exclusive but overlap, at least to some extent, in the pathogenesis of glaucoma.

The detection of true change in the ONH during the subtle advancement of glaucomatous optic neuropathy is fundamental for the correct medical management of the disease and prevention of visual loss. There are several methods available for evaluating the ONH. The most widely used include indirect and direct ophthalmoscopy via slit lamp biomicroscopy and planimetry. These methods require a subjective opinion and result in poor documentation that can often be difficult to interpret. Recent advancements in ONH analysis systems such as digitised image analysis and cSLO provide the opportunity to quantitatively and qualitatively detect ONH change over time. These new methods are less subjective and it is proposed that they substantially reduce inter- and intra-observer error (Bishop, K. I. *et al.*, 1988; Kruse, F. E. *et al.*, 1989; Dreher, A. W. *et al.*, 1991; Lusky, M. *et al.*, 1992; Mikelberg, F. S. *et al.*, 1993; Cantor, L. B. *et al.*, 1994; Menezes, A. V. *et al.*, 1995; Azuara-Blanco, A. *et al.*, 1998b; Geyer, O. *et al.*, 1998). The quantitative nature of these methods facilitate the detection of true change over time and the successful application of such methods may lead to routine monitoring of glaucoma by paramedical staff.

Confocal scanning laser ophthalmoscopy provides a promising tool for the assessment of the ONH. There are a number of cross-sectional studies which recommend its

clinical use, however, the relative lack of long-term studies on the follow-up of the normal and glaucomatous optic nerve mean it is still unknown as to whether it is capable of detecting true glaucomatous change.

Several methods for the measurement of ocular blood flow have evolved. More recent techniques include OBF tonography (Silver, D. M. & Farrell, R. A., 1994), LDF (Riva, C. E. *et al.*, 1992) and SLDF (Michelson, G. & Schmauss, B., 1995). The more established technique of CDI was only applied to ophthalmology in 1989 (Erickson, S. J. *et al.*, 1989).

There is still some uncertainty over the ability of ocular blood flow measures to identify abnormalities in individual glaucoma suspects, or if changes in ocular blood flow may be identified during disease progression. A number of studies have compared groups of POAG and normal subjects and have confirmed reduced ocular perfusion in glaucoma (Harris, A. *et al.*, 1994b; Butt, Z. A. *et al.*, 1995; Michelson, G. *et al.*, 1996a; Duijm, H. F. A. *et al.*, 1997; Fontana, L. *et al.*, 1998; Chung, H. S. *et al.*, 1999b). No single study has followed the ocular haemodynamics of a glaucomatous eye and compared it to that of a normal eye to determine whether change over time is apparent.

1.17.2. Research aims

There were five principle aims to this study:

1. To evaluate the reproducibility and accuracy of topographic measurements obtained with cSLO and determine whether the single subjective component of ONH analysis (definition of the ONH) could be improved.
2. To assess the reproducibility of SLDF and to compare the ability of three ocular blood flow measurement techniques to assess a physiologically induced change in ocular blood flow.
3. To quantify ONH topography, retinal blood flow and visual function differences at baseline between a group of normal subjects and a group of glaucoma patients.

4. To investigate the stability of topographic, haemodynamic and visual function measures in a group of normal subjects compared to the change determined in a group of glaucoma patients.
5. To identify topographic, haemodynamic and visual function parameters that may be of value in monitoring change over time in individual glaucoma patients compared to normal subjects.

The five components are outlined below:

1.17.3. Preliminary investigations with cSLO: Reproducibility, accuracy and ONH definition

1.17.3.1. Reproducibility

Weinreb, R. N. *et al.*, (1993) proposed that 3 HRT images were sufficient to provide reproducible measures with optimal efficacy in humans. As a result, many studies using the HRT have based their measurements on the mean of three images (Chauhan, B. C. & MacDonald, C. A., 1995; Spencer, A. F. *et al.*, 1995; Dichtl, A. *et al.*, 1996; Irak, I. *et al.*, 1996; Zangwill, L. M. *et al.*, 1996; Iester, M. *et al.*, 1997a; Azuara-Blanco, A. *et al.*, 1998b). Some doubt still exists regarding the number of images to use, some studies have used 5 images (Mikelberg, F. S. *et al.*, 1993; Menezes, A. V. *et al.*, 1995) and some have used 10 images to assess the repeatability of individual parameters (Azuara-Blanco, A. *et al.*, 1998b).

The reproducibility of HRT measurements has been assessed (Mikelberg, F. S. *et al.*, 1993; Rohrschneider, K. *et al.*, 1994; Menezes, A. V. *et al.*, 1995; Azuara-Blanco, A. *et al.*, 1998b). However, many of these studies used earlier software versions, few images and only assessed a selection of the available HRT parameters. Furthermore, many studies base their assumptions on coefficients of variation, which are not suited to the assessment of reproducibility when mean values vary (Bland, J. M. & Altman, D. G., 1996b).

The aims of this study were twofold: 1) To determine the optimum number of images required to obtain reproducible topographic measurements with minimal measurement error for the complete range of parameters. 2) To determine the reproducibility of each topographic parameter.

1.17.3.2. Accuracy

Few studies report the accuracy of topographic measurement with the HRT (Bartz-Schmidt, K. U. *et al.*, 1994; Janknecht, P. & Funk, J., 1994; Hosking, S. L. & Flanagan, J. G., 1996). The accuracy of cSLO is important for the classification of ONHs and for the longitudinal follow-up of an optic nerve when changes in refraction may occur. In such a case it is important that the inbuilt mechanism for determining the focal length of the eye is robust enough to maintain a reasonable level of accuracy and ensure that the size of the retinal feature under examination is not distorted.

The aims of this study were: 1) To build a model lens system to enable the accuracy of the HRT to be assessed. 2) To determine the ability of the HRT to accurately measure a template of known size and geometry for different refractive errors (axial lengths).

1.17.3.3. Optic nerve head definition

The definition of the contour line is the only subjective aspect of ONH analysis with the HRT. The recommended position of the contour line is on the inner edge of Elschnig's ring which forms the boundary of the optic disc (Heidelberg, 1997). Orgül, S. *et al.*, (1997) suggested that variations in realignment of the contour line on subsequent images may occur because the co-ordinates of the contour must shift by whole numbers of pixels between images. For the longitudinal follow-up of glaucomatous optic neuropathy it is important that the contour line is consistently located on a stable area of tissue. It is possible that Elschnig's ring may not provide the most stable position as it is located at the disc border. The HRT allows one contour line, usually drawn on the first image of a series, to be exported and imported

to subsequent images of an individual subject. Theoretically, using the same contour line for follow-up images will maximise the reproducibility of stereometric parameters and facilitate the detection of real change in the topography of the ONH over time.

The aims of the study were to investigate the optimum position for the location of the contour line relative to Elschnig's scleral ring and determine the best method for contour line transfer between images.

1.17.4. Preliminary investigation with the SLDF: reproducibility and validity

1.17.4.1. Reproducibility

The intra and inter-reproducibility of SLDF has been previously assessed and reported as good (section 1.15.2.) (Michelson, G. & Schmauss, B., 1995; Chauhan, B. C., 1996; Michelson, G. *et al.*, 1996b; Nicolela, M. *et al.*, 1997; Strenn, K. *et al.*, 1997). With the exception of studies that assess the reproducibility, the majority of SLDF investigations have based their assumptions on blood flow values determined from a single perfusion image (Michelson, G. & Schmauss, B., 1995; Nicolela, M. T. *et al.*, 1996b; Langhans, M. *et al.*, 1997). Blood flow is known to be pulsatile and varies with the cardiac cycle (Arend, O. *et al.*, 1995). In the absence of pulse synchronisation it would seem appropriate to take the mean ocular blood flow measurement from a number of perfusion images acquired in a single visit.

The aims of the study were: 1) To determine the optimum number of SLDF images required to obtain a reflective measure of ocular blood flow parameters whilst minimising experimental error. 2) To assess the reproducibility of SLDF parameters.

1.17.4.2. Validity

There are several techniques available for the assessment of ocular blood flow. Different techniques measure different vascular beds. There is still some controversy as to which techniques are best for assessing change. There are several ways to induce changes in blood flow including IOP modification (Riva, C. E. *et al.*, 1997a), and the administration of vasodilatory and vasoconstrictory agents such as CO_2 (Harris, A. *et al.*, 1996c) and O_2 (Schmetterer, L. *et al.*, 1995).

The aims of the study were to evaluate the ability of three ocular blood flow measurement techniques to assess changes in blood flow during hypercapnia and hyperoxia. Parallel to this, the retinal, choroidal and retrobulbar autoregulatory response to hypercapnia and hyperoxia was assessed.

1.17.5. Baseline cross-sectional analysis of ONH topography, retinal blood flow and visual function for a group of normal subjects and glaucoma patients

A number of cross-sectional studies have identified HRT parameters that are important for classifying glaucomatous optic nerve heads (Mikelberg, F. S. *et al.*, 1995; Zangwill, L. M. *et al.*, 1996; Eid, T. M. *et al.*, 1997; Iester, M. *et al.*, 1997a). Many of these studies employed earlier software versions, few images and only assessed a selection of the available HRT parameters. Several studies have used a variety of ocular blood flow techniques to compare groups of POAG and normal subjects and have confirmed reduced ocular perfusion in glaucoma (Harris, A. *et al.*, 1994b; Butt, Z. A. *et al.*, 1995; Michelson, G. *et al.*, 1996a; Duijm, H. F. A. *et al.*, 1997; Fontana, L. *et al.*, 1998; Chung, H. S. *et al.*, 1999b).

The aims of this investigation were to identify cSLO, SLDF and visual function parameters that distinguish between a normal and glaucomatous population. The relative importance of these parameters measured cross-sectionally was compared to

their clinical use for detecting glaucomatous change longitudinally in the following investigation.

1.17.6. The longitudinal follow-up of topographic, ocular haemodynamics and visual function in a group of normal subjects and glaucoma patients.

There are few published longitudinal studies that identify which HRT parameters are best for detecting glaucomatous progression. A one year follow-up of pre and post-trabeculectomy ONH topography showed significant changes (relative improvements) in some HRT parameters (Topouzis, F. *et al.*, 1999). Kamal, D. S. *et al.*, (1999) followed a small group of ocular hypertensive patients and normal subjects for one year and identified cup:disc area ratio, cup area and rim area as important for detecting change during conversion to POAG. Hosking, S. L. *et al.* (1998b) followed a large group of ocular hypertensive and POAG subjects and identified specific parameters that appeared important for the detection of change. To date, there is no published literature that compares a POAG group and normal subject group longitudinally. Clearly, such a study is of value if the clinical viability of the HRT for detecting change over time is to be proved.

Although cross-sectional studies have shown ocular blood flow to be compromised in POAG compared to normal eyes, there is no longitudinal data that investigates haemodynamic change over time in glaucoma. Neither has the long-term variability of ocular blood flow measurements in a normal eye been reported.

The aims of this study were four-fold:

1. To assess the ability of cSLO to detect morphological change over time in patients with progressive glaucomatous optic neuropathy when compared to a cohort of normal subjects and to identify specific topographic parameters that appear important for detecting change.

2. To investigate retinal haemodynamics using SLDF in a normal and POAG group over a study period of 16 months and determine whether regional differences exist in blood flow measurements across the retinal capillary bed.

3. To investigate several visual function indices for the detection of glaucomatous progression and compare these to topographic parameters to detect change.

4. To determine whether topographic and haemodynamic change in patients with POAG can be related to psychophysical change, fluctuations in IOP and treatment changes.

Chapter 2.

Investigation of the reproducibility of topographic parameters with the Heidelberg Retina Tomograph

2.1. Introduction

A number of studies have assessed the reproducibility of the Heidelberg Retina Tomograph (HRT). Some studies have investigated the reliability of available topographic parameters (Mikelberg, F. S. *et al.*, 1993; Rohrschneider, K. *et al.*, 1994; Menezes, A. V. *et al.*, 1995; Azuara-Blanco, A. *et al.*, 1998b). Others have focussed on the reproducibility of individual pixel height measurements that make up the topography (Lusky, M. *et al.*, 1992; Weinreb, R. N. *et al.*, 1993; Chauhan, B. C. *et al.*, 1994; Rohrschneider, K. *et al.*, 1994; Chauhan, B. C. & MacDonald, C. A., 1995).

The mean standard deviation of the pixel heights provides an indication of the overall reproducibility of a topography image. However, the influence of media clarity and eye movement on this measure remains uncertain. In terms of the clinicians requirements, it is arguably more useful to know the variability of the available topographic parameters. There are a number of 2- and 3-dimensional stereometric parameters available with the HRT software. Together they describe the spatial shape of the ONH. These parameters, the tissue they are measuring and the locations they are measured from are described in detail in section 1.13.2.4.

Although the HRT has several applications in ophthalmology, potentially, one of its most effective uses will be the clinical follow-up of the ONH in glaucoma. In order to detect subtle change over time, the reproducibility of the acquired images must be maximised. There are several factors that are known to affect the reproducibility of topographic measurement with the HRT including focus setting (Hosking, S. L. & Flanagan, J. G., 1996), misalignment of the laser scanner (Orgül, S. *et al.*, 1996), age, cardiac cycle (Chauhan, B. C. & McCormick, T. A., 1995) and alignment of the contour line (Orgül, S. *et al.*, 1997).

Previous studies have used varying numbers of images to determine the reproducibility of HRT measurements. Some studies have used 3 images (Orgül, S. *et al.*, 1996; Zambarakji, H. J. *et al.*, 1998), others 5 images (Mikelberg, F. S. *et al.*, 1993; Menezes, A. V. *et al.*, 1995) and some have used 10 images to assess the repeatability of individual parameters (Azuara-Blanco, A. *et al.*, 1998b). When repeated measurements of a given quantity are obtained from the same subject, the measurements, in general, will rarely be the same (Bland, J. M. & Altman, D. G., 1996a). Measured differences may be due to several components including natural variation of that quantity for a subject and variation due to the measurement process. To obtain an interpretation of the measured quantity and reduce the measurement error it is usual to take the mean of several measurements.

Weinreb, R. N. *et al.*, (1993) examined the mean standard deviation of all the pixel elements for 5 images and concluded that 3 images provided measurements of sufficient reproducibility and optimal efficacy in humans. This study was based on small subject samples (5 normal subjects and 5 glaucoma subjects) and it is questionable whether 5 images are enough to determine reproducibility. Furthermore, the mean standard deviations were taken from mean topography images for 2, 3, 4 and 5 images which provided no interpretation of the reproducibility of individual parameters. Regardless of this, many studies using the HRT have based measurements on the mean of three images (Chauhan, B. C. & MacDonald, C. A., 1995; Spencer, A. F. *et al.*, 1995; Dichtl, A. *et al.*, 1996; Irak, I. *et al.*, 1996; Zangwill, L. M. *et al.*, 1996; Iester, M. *et al.*, 1997a; Azuara-Blanco, A. *et al.*, 1998b).

During this study 12 consecutive image series were obtained with the HRT. The optimum number of images required to give an interpretation of a given quantity with minimal measurement error was determined. Using this number of images, the reproducibility of each topographic parameter was determined.

2.2. Aims and objectives

The aims of this experiment were to:

1) Establish the optimum number of images to give an interpretation of a given quantity with minimal measurement error for a range of parameters whilst taking into account clinical practicality.

2) Calculate the intra-class correlation coefficient (reproducibility) for each of the topographic parameters currently available (HRT software version 2.01) using the optimum number of images (previously calculated).

2.3. Materials and methods

2.3.1 Subject sample

The subject sample consisted of 20 normal healthy volunteers and 10 high-tension POAG patients. The normal volunteers were recruited from staff at Birmingham Heartlands and Solihull NHS Trust and the surrounding community. The POAG patients were registered under one consultant ophthalmologist (JMG) at Birmingham Heartlands Hospital. The normal group consisted of 17 Caucasians, one West Indian and one Asian subject. The POAG group consisted of 10 Caucasians. Details of the subject sample are given in the Table 2.1.

	Gender		Test eye		Mean age ± SD (range)
Subject group	**Male**	**Female**	**Right**	**Left**	
Normal group (n=19)	10	10	10	10	60.6 ± 10.9 (40-76)
POAG group (n=10)	4	6	4	6	72.2 ± 6.9 (59-82)

Table 2.1. Subject sample

2.3.2 Inclusion criteria: normal group

- No history of glaucoma or diabetes.
- > 40 years of age.

- Minimal or no lens opacities enabling a clear view of the fundus.
- IOP less than 21mmHg (Goldmann applanation tonometry). The mean IOP of a normal population is 15.5 mmHg (Moses, R. A., 1975) and it is generally thought that IOP of more than 21mmHg may indicate high-tension glaucoma (Jonas, J. B. & Papastathopoulos, K. I., 1995).
- Visual acuity better than 6/9 (Snellen).
- Astigmatism < 1.5 dioptres cylinder.
- Refraction < 6 dioptres (mean sphere).
- Open anterior chamber angle (Shaffer 3-4 where 0 = closed and 4 = open).
- Normal fundus appearance based on:
    - No focal or generalised narrowing or disappearance of the neuroretinal rim with enlarged cupping and/or pallor that may be concentric or eccentric in shape.
    - No notching (focal extension of the cup).
    - Healthy coloured neuroretinal rim (without pallor).
    - No disc haemorrhages.

  (Pawson, P. & Vernon, S. A., 1995; Vernon, S. A., 1996)
- Normal 24-2 visual field assessment (Humphrey Field Analyzer).
- No strabismus.

2.3.3 Inclusion criteria: POAG group

Ten high-tension POAG patients were recruited according to the criteria outlined in section 7.4.2.

2.3.4 Ethical approval

Ethical committee approval was sought and obtained for all experimental procedures which conformed with the tenets of the declaration of Helsinki approved by Birmingham Heartlands and Solihull NHS Trust research and ethics review board.

2.3.5 Methods

2.3.5.1 Preliminary tests

Following informed consent, one operator (ER) obtained measurements for visual acuity (Snellen), distance spectacle prescription (focimetry) and corneal curvature (mm). Systolic and diastolic blood pressure were measured and a brief medical history taken to ensure no ocular disease or cardiac problems. On a separate occasion (prior to study day) each subject was reviewed by an ophthalmologist (JMG) who carried out a full assessment, including anterior chamber depth, IOP assessment ONH assessment. If the ophthalmic assessment was normal and inclusion criteria fulfilled, subjects commenced the study protocol.

2.3.5.2 Dilation

The test eye of all subjects was dilated using one drop of Tropicamide 1% to maximise the reproducibility of the experiment. The subjects were then allowed a period of 20 minutes to ensure full mydriasis (checked by the pupillary light reflex).

2.3.5.3 HRT Image acquisition

In preparation for data acquisition, subject data including refraction and corneal curvature were entered into the database of the HRT. The subjects were requested to place their chin on the chin rest and fixate on a distance target. A scan depth of 1.5mm was routinely used for the first image. The laser head was moved towards the subjects' eye and positioned approximately 1cm from the cornea. The light source of the laser was centred on the pupil and the angle of the laser head manipulated until the ONH was visible and centred on the computer screen. The intensity dial was set to maximum, whilst the sensitivity was adjusted to a level that allowed a bright but not over-exposed view of the fundus. Using the subjects' refraction as a guide, the laser

was focussed onto the retinal vessels and a single image series recorded using a 10° scan field (256 × 256 pixels).

The image series was examined and if necessary the scan depth and focus setting changed to ensure an adequate image series was obtained. An adequate image series consisted of 32 equidistant confocal image sections moving back posteriorly into the eye with the first section positioned on the retinal vessels and the last located deep in the cup. The systems own quality control software "parameters OK" was required for image acceptance.

Following acquisition the individual image sections were examined for eye movements using the software movie option. The HRT automatically corrects for small eye movements but larger movements can result in a poor topography image due to misalignment of the 32 image sections. A quality control form was completed and scores out of 10 given for image quality (clarity and sharpness of the image) and eye movement. A combined total of 15 or more was required for the image to be accepted.

One operator (ER) acquired a total of 12 images for each subject. The focus setting and scan depth was kept constant for consecutive images of the same subject as changing the focus setting has been shown to reduce reproducibility (Hosking, S. L. & Flanagan, J. G., 1996). Throughout the examination each subject was requested to keep his or her chin on the rest. This ensured the distance between the laser and the eye remained constant (Orgül, S. *et al.*, 1996).

Following acquisition of 12 acceptable image series, topography maps were generated using the systems software for each series. The process used to determine the topography maps is detailed in section 1.11.2.3. and includes alignment for horizontal and vertical shifts, rotation and tilt. A contour line was interactively drawn around the edge of the optic disc on the first topography image using Elschnig's scleral ring for reference. The contour height variation diagram was inspected to ensure a classic double hump profile, with peaks corresponding to the superior and inferior poles

indicating thicker rim tissue in those areas (Schuman, J. S. *et al.*, 1995; Weinreb, R. N. *et al.*, 1995).

If the contour line was acceptable, i.e. encompassed the whole optic disc with an adequate height profile, it was exported from the first image and then imported into all subsequent images of the same subject. Using the stereometric software (version 2.01) 7 one-dimensional, 6 two-dimensional and 6 three-dimensional parameters were measured globally for each topography image. A detailed description of the individual parameters, the tissue being measured, and the locations they are measured from is given in section 1.13.2.3.

2.4. Statistical analysis

The standard deviation of repeated measurements on the same subject may be used to determine the measurement error (Bland, J. M. & Altman, D. G., 1996a). In this experiment the mean standard deviation (MSD) of 2-12 images was determined for a range of parameters.

Standard deviation (SD) represents the average deviation from the mean for a number of observations. The unit of expression is the same as the original unit of measurement. The SD (s) is the square root of the variance (s^2) given by:

$$s^2 = \frac{1}{n-1}\left[\sum x_i^2 - \frac{\left(\sum x_i\right)^2}{n}\right]$$

Where:

$n-1$ = degrees of freedom Equation 2.1.

$\left[\sum x_i^2 - \frac{\left(\sum x_i\right)^2}{n}\right]$ = sum of squares

s = standard deviation (Bland, J. M., 1987b).

Following determination of the optimum number of images required, the intra-class correlation coefficient (ICC) was used to determine the reproducibility of each parameter. Whereas MSD gives an indication of the measurement error of individual parameters in their respective units, the ICC gives a measure of the variability. The ICC uses a ratio of the variance due to the patient only, and variance due to the combined effects of the patient and measurement variability. It is thought to provide a better statistical method for assessing reproducibility than the commonly used coefficient of variation, (SD divided by the mean) as it does not become elevated when the denominator of the equation is small.

In order to determine ICC, the subject data were entered into a statistical software package (Statview). A one-way factorial analysis of variance (ANOVA) was determined with subject as the factor (nominal) and the repeated measurements as the dependent variable (continuous). Separate ANOVA was carried out for each parameter. The total sums of squares and the sums of squares between subjects calculated during ANOVA was used to determine the ICC using the following formula.

$$r_1 = \frac{m\mathrm{SS}_B - \mathrm{SS}_T}{(m-1)\mathrm{SS}_T}$$

Where:

r_1 = ICC (finally expressed as a percentage)

m = The number of observations per subject

SS_T = Total sums of squares

SS_B = Sums of squares between subjects

Equation 2.2.

(Bland, J. M. & Altman, D. G., 1996b).

2.5. Results

2.5.1 Determination of the optimum number of images

Mean standard deviation values appear in the same units as the original parameter which makes comparisons between individual parameters difficult. The data were normalised to overcome this problem. The MSD was expressed as a fraction of the maximum MSD observed. Figure 2.1. shows the average MSD profile normalised across 18 HRT parameters for the two groups. It can be seen that, on average, the normalised mean MSD reaches a plateau at 6 images for the normal group and 7 images for the POAG group. Figures 2.2.-2.7. give the normalised mean standard deviation (MSD) values for each HRT parameter for the normal and POAG groups. Summary tables of the normalised MSD data are in Appendix 2.

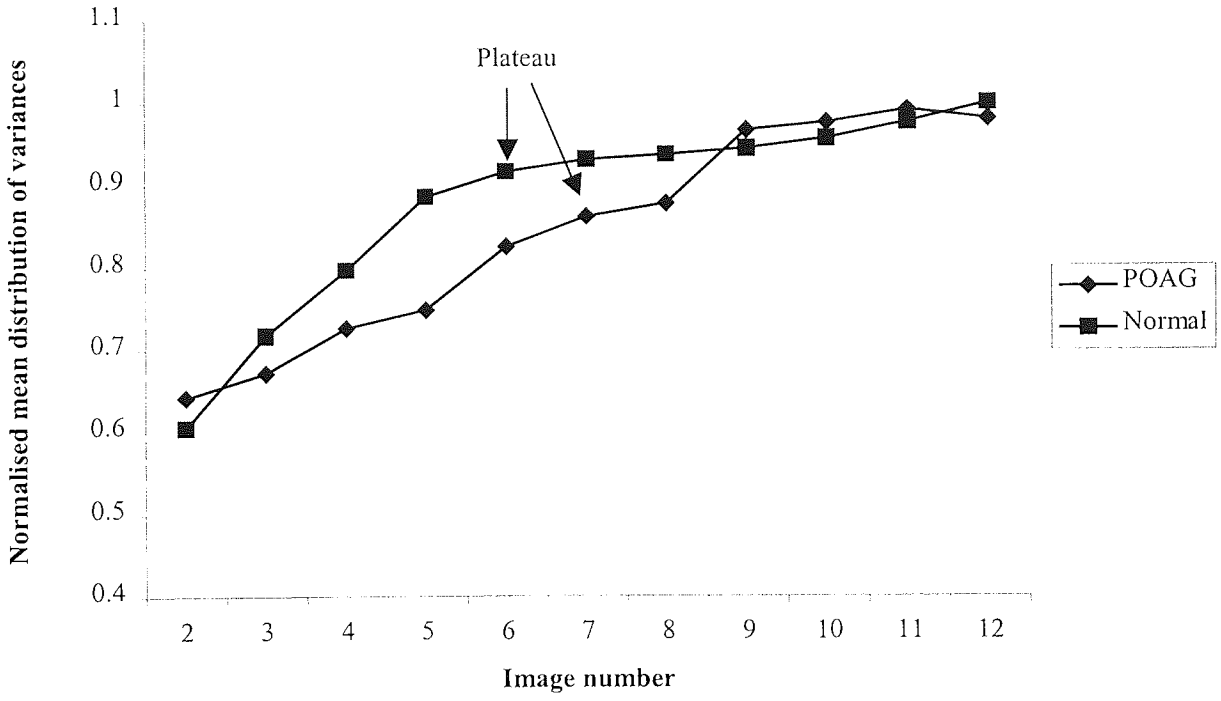

Figure 2.1. Normalised MSD HRT parameter profile for the normal and POAG group (mean of all parameters).

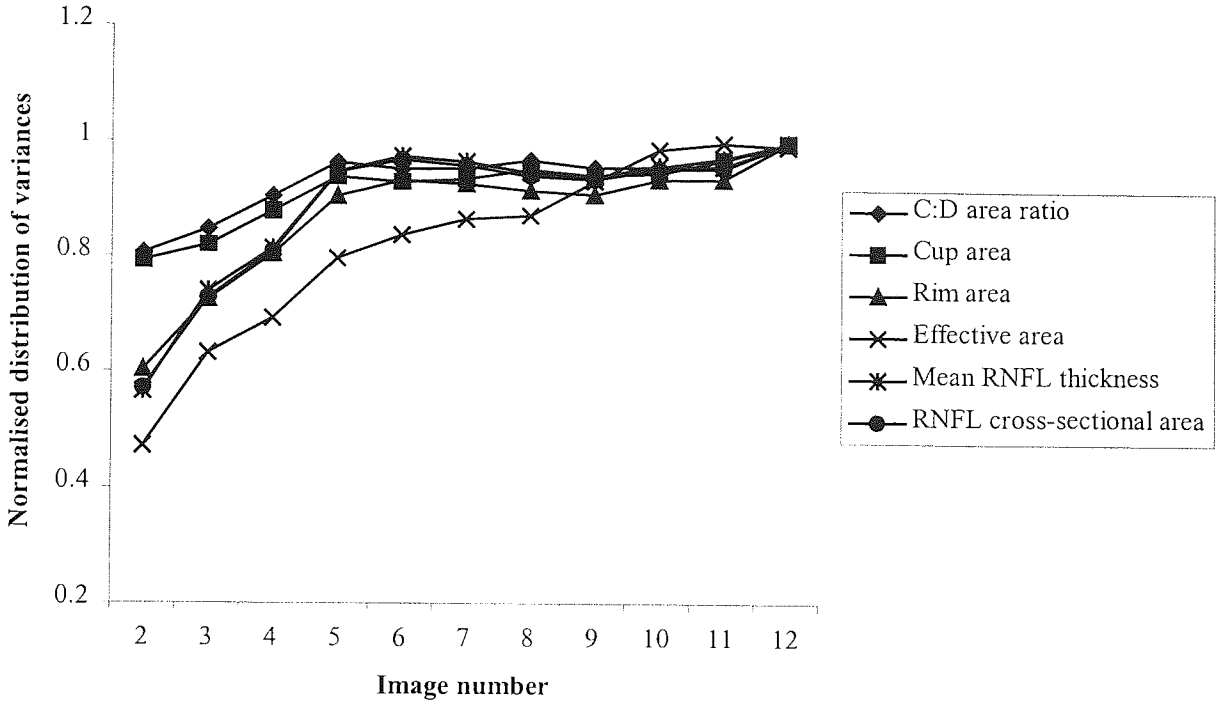

Figure 2.2. Normalised distribution of variances for six HRT parameters measured for the normal subject group.

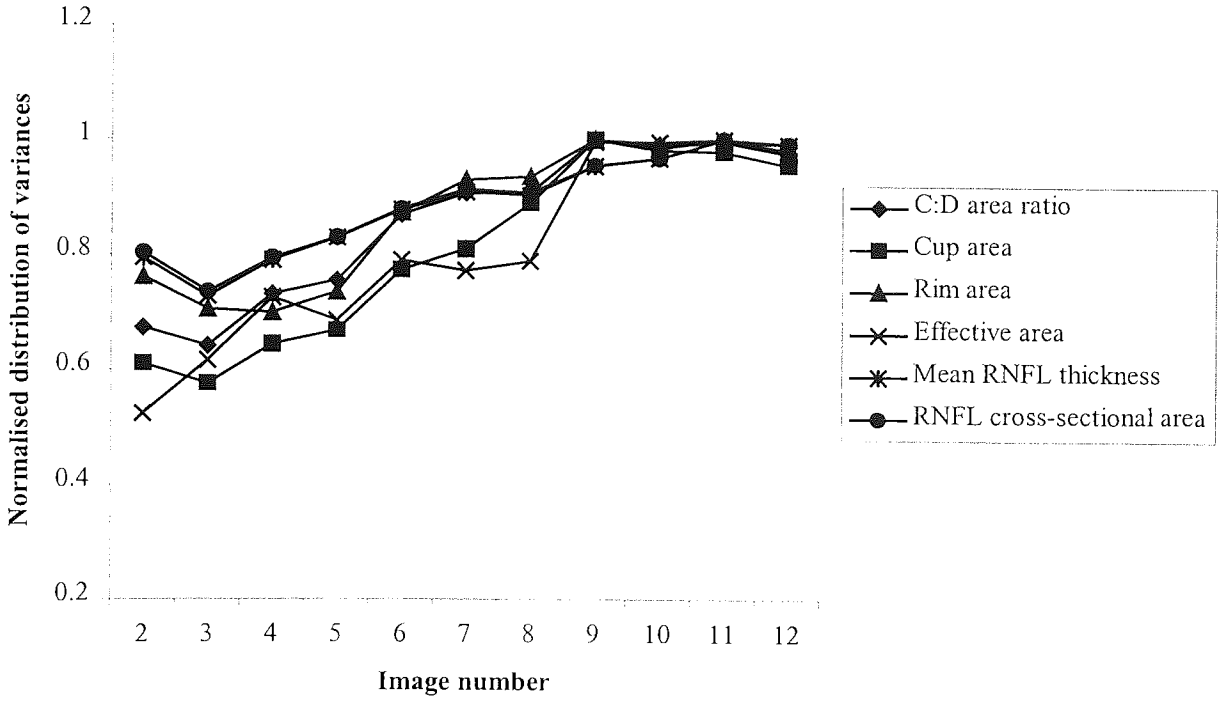

Figure 2.3. Normalised distribution of variances for six HRT parameters measured for the POAG subject group.

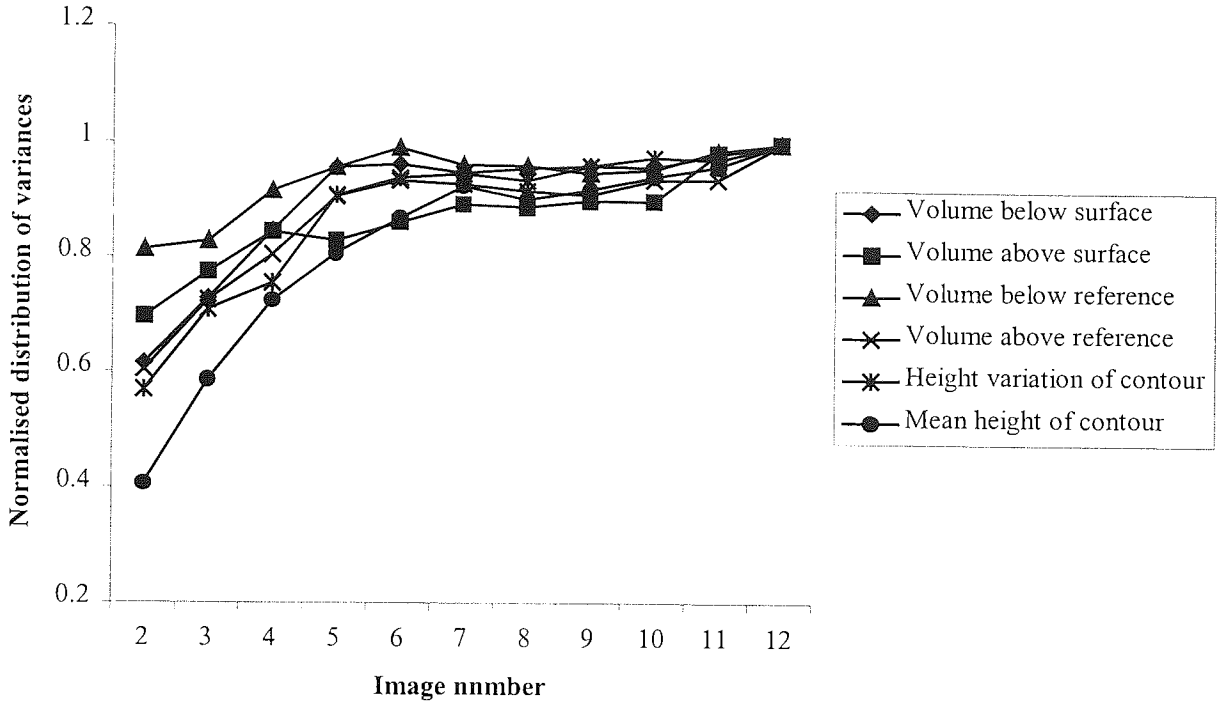

Figure 2.4. Normalised distribution of variances for six HRT parameters measured for the normal subject group.

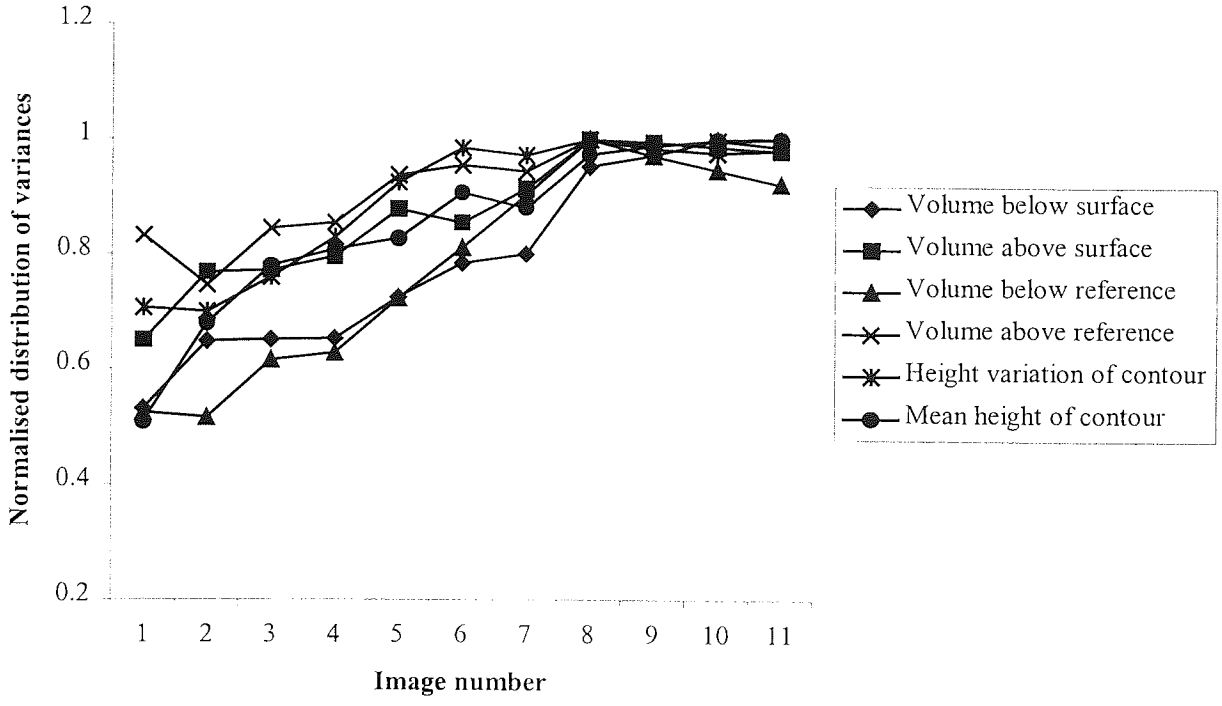

Figure 2.5. Normalised distribution of variances for six HRT parameters measured for the POAG subject group.

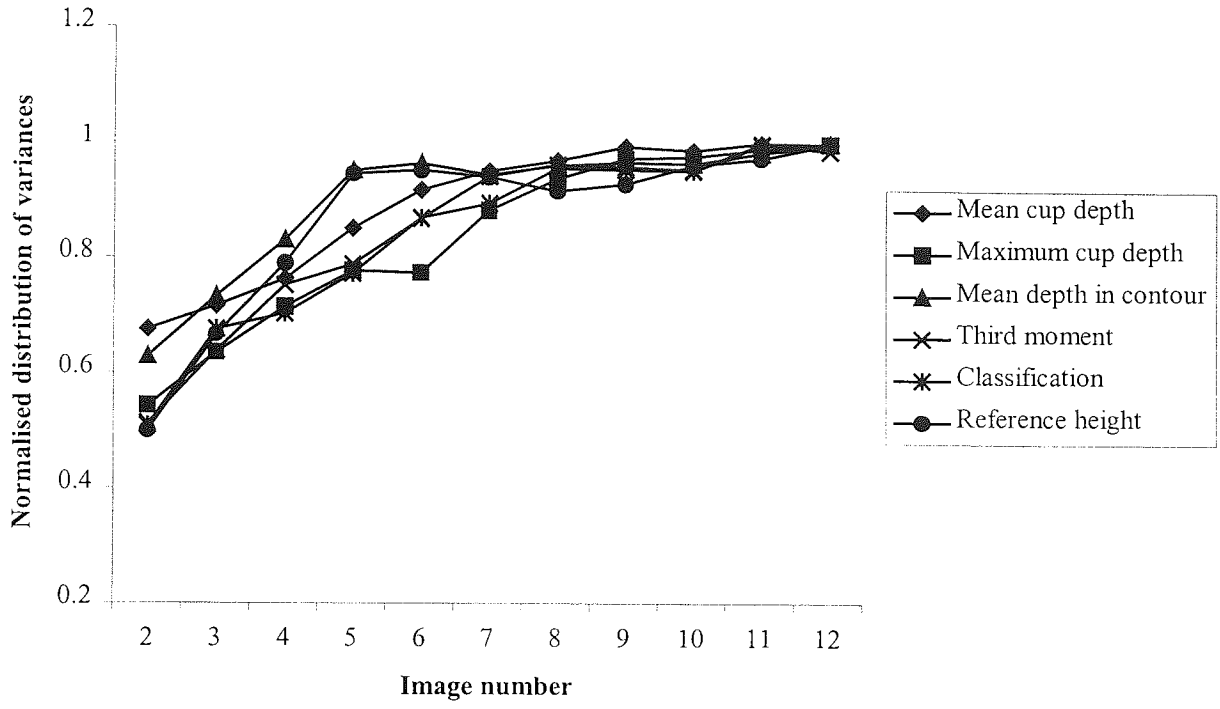

Figure 2.6. Normalised distribution of variances for six HRT parameters measured for the normal subject group.

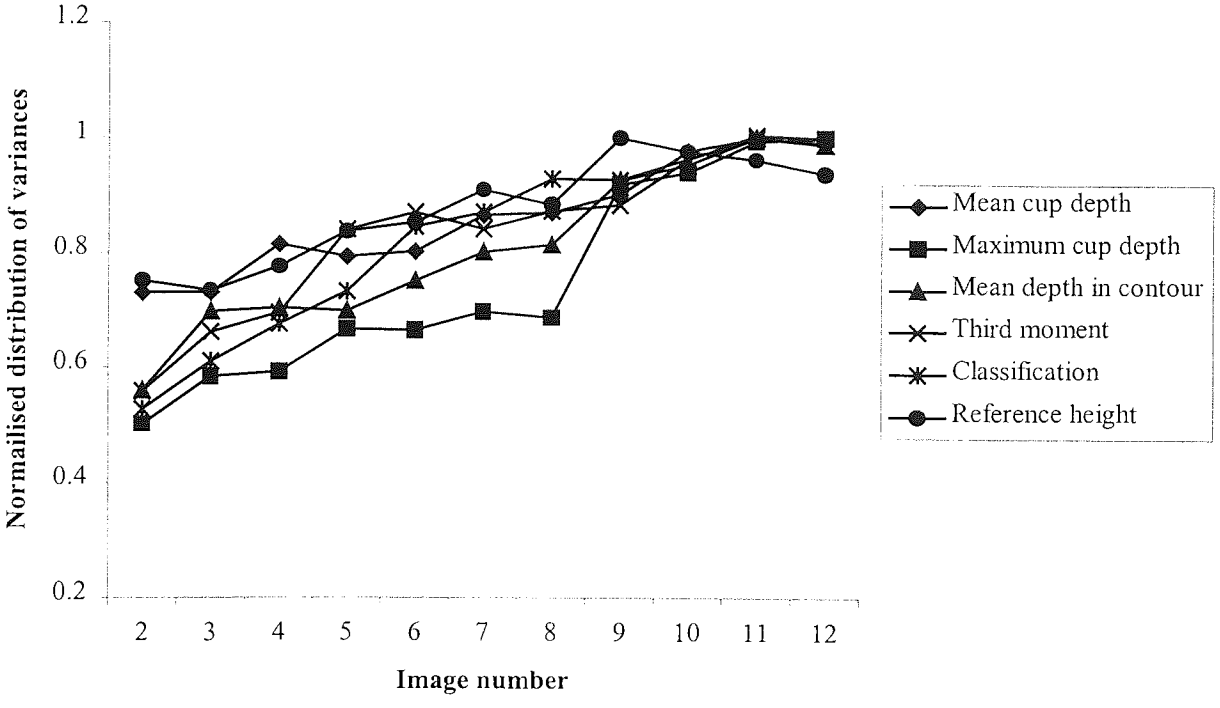

Figure 2.7. Normalised distribution of variances for six HRT parameters measured for the POAG subject group.

2.5.2 Reproducibility of HRT parameters using the optimum number of images

Using 7 images, intra-class correlation coefficients were determined for each parameter. The results are listed in Table 2.2. They give an indication the reproducibility of each individual parameter using the optimum number of images (7). The ANOVA tables resulting from each analysis are given in Appendix 3.

	ICC (r_1) (%)	
Parameter	**Normal group**	**POAG group**
Cup/disc area ratio	98.5	91.9
Cup area	99.0	97.7
Disc area	100.0	100.0
Rim area	96.4	96.2
Height variation of contour	81.5	83.3
Volume below reference	99.2	84.5
Volume above reference	95.2	88.8
Mean cup depth	99.5	95.5
Maximum cup depth	98.1	92.6
Third moment	92.9	91.2
Mean RNFL thickness	89.3	72.3
RNFL cross-sectional area	84.5	75.9
Effective area	99.7	92.6
Mean height of contour	98.6	86.9
Volume below surface	99.7	92.7
Volume above surface	98.4	87.0
Mean depth in contour	99.5	97.2
Classification	95.5	92.4
Reference height	94.9	80.7
Mean	**95.8**	**89.4**

Table 2.2. Intra-class correlation coefficients (ICC) for each of the stereometric HRT parameters measured for the normal and POAG group.

2.6. Discussion

The HRT provides a tool for qualitatively and quantitatively examining the human ONH *in vivo*. Its primary use is in the assessment and follow-up of glaucomatous optic neuropathy; this is reflected in the range of parameters that describe the spatial shape of the ONH. The clinical follow-up of the glaucomatous optic nerve requires the detection of subtle change. In this regard, a technique that is highly reproducible in its measurement will increase the likelihood of detecting real change over time.

2.6.1 Optimum number of images

Recent software developments for the HRT have resulted in added parameters, modifications in the location from which some of the parameters are measured from (i.e. reference plane) and improved contour alignment. No single study has assessed all of the stereometric parameters currently available, therefore, investigation of the reproducibility of each parameter and determination of the optimum number of images required for repeatable measurement will be of use.

In this experiment, controlled conditions were applied to minimise the measurement error of the parameters measured. Focus setting, scan depth, distance between the laser head and the eye and the alignment of the contour line were all kept constant in accordance with current literature (Hosking, S. L. & Flanagan, J. G., 1996; Orgül, S. *et al.*, 1996; Orgül, S. *et al.*, 1997). All of the images were acquired consecutively during one session this minimising the possibility of real change occurring in the measured quantities (areas and volumes of tissue). Consequently, any variation in the measurements obtained was most likely attributable to measurement error of the technique and not physical changes in the measured quantity.

Mean standard deviation curves were not plotted for the parameter disc area. The same contour line was exported from the first image into subsequent images for each subject. Theoretically, given that the same contour line was used the area within it and therefore disc area should remain constant. In reality, the area within the contour does alter slightly because of realignment in subsequent images, but the amount by which it varies is negligible.

Mean standard deviation curves were plotted for the remaining HRT parameters. The results showed that on average the MSD increases and then starts to plateau at 6 images for the normal subject group and 7 images for the POAG subject group (Figure 2.1.). The later plateau observed for the POAG group is indicative of the greater variability for that group. Figures 2.2-2.7. show normalised MSD curves for each

parameter. On an individual basis parameters tend to stabilise more for quickly for the normal group compared to the POAG group.

Weinreb, R. N. *et al.*, (1993) suggested that three images were sufficient to obtain reproducible topographic measurements. For every parameter measured in this study, the MSD was still increasing after 3 images. This implies that three images are insufficient and that the number of images being taken by clinicians should be reviewed. The total image acquisition time for the HRT approximates 1.6 seconds, in view of this, taking the mean of 7 images is a clinically practical option.

2.6.2 Reproducibility of topographic parameters using 7 images

Examination of the MSD curves suggests that 7 images are more appropriate for measurement with the HRT. Consequently, the reproducibility of the topographic parameters was investigated for 7 images. The ICC gives a correlation coefficient which may be expressed as a percentage. This enables the repeatability of individual parameters to be assessed and compared. The commonly used coefficient of variation (CoVar) also facilitates this, but is of limited value because values become elevated when the denominator of the equation is small (Mikelberg, F. S. *et al.*, 1993). Furthermore, the ICC uses a ratio of the variance due to the patient only, and the combined variance occurring as a result of the patient and measurement variability (Bland, J. M. & Altman, D. G., 1996b). This provides an indication of the within-subject measurement error due to the technique rather than the variability between subjects.

The results showed the intra-visit reproducibility of the measured parameters was high across 7 images with ICCs ranging from 81.5% – 100% for the normal subject group and 72.3% – 100% for the POAG group (Table 2.2.). The mean ICC of all the parameters was 95.8% for the normal group and 89.4% for the POAG group. This indicates that, overall, parameters measured for the POAG group were less reproducible than the same parameters measured for a normal subject group. The

variability of topographic measurements may be attributed to many factors including cataract (Janknecht, P. & Funk, J., 1995), miosis, cardiac cycle (Chauhan, B. C. & McCormick, T. A., 1995), eye movement and topographical slope of the ONH borders (Chauhan, B. C. *et al.*, 1994). Other factors more likely to affect inter-visit reproducibility include rotation and tilt of topography images (Chauhan, B. C. *et al.*, 1994), changes in focus setting (Hosking, S. L. & Flanagan, J. G., 1996) and scan depth (Hosking, S. L. *et al.*, 1997a).

The difference in variability observed between the two subject groups may be due to a number of reasons: the mean age for the POAG group was significantly greater than the normal group ($p<0.05$). As such the POAG were more likely to have lenticular changes and miosis. Each subject was dilated thus counteracting miosis. Janknecht, P. & Funk, J. (1995) reported that the relative error of topographic measurements increased with simulated cataract and Chauhan, B. C. *et al.*, (1994) reported that variability in topographic measurement increases significantly with age and concluded that this may be attributable to increased media opacity. In contrast Hosking, S. L., (1998b) suggested that lenticular changes may have a smoothing effect on the topographic contours thereby improving variability. The age difference between the groups may have had an indirect effect on topographic variability. Both groups were accustomed to cSLO measurements, however, the older POAG group may have been less tolerant of the test duration and more prone to eye movement thus increasing variability.

The lower reproducibility observed for the POAG group may have been due to the greater topographic slope of the margin of the cup border resulting from glaucoma. Chauhan, B. C. *et al.*, (1994) demonstrated that during a test-retest variability study of the HRT, pixel height was most variable along the cup border. It was suggested that this may have been due to local topographical slope and software limitations in the alignment procedure.

The least reproducible parameters for both the normal and POAG group included height variation of contour which may be attributable to slight variations in the

position and height of the contour line across images, mean RNFL thickness and RNFL cross-sectional area.

The parameters RNFL cross-sectional area and mean RNFL thickness are both measured with respect to the reference plane and contour line (see section 1.11.2.4., Table 1.2.b). The reference plane is located 50μm posterior to the mean height of the contour line between segments -10° and -4°. Consequently the reference plane is measured from a relatively small portion of the contour line and any small movements in the re-positioning of the contour line may have significant effects on dependant parameters. Interestingly the reference plane height was very reproducible for the normal subject group (94.9%) and less so for the POAG group (80.7%). The poorer reproducibility for the POAG group may account for the greater variability of reference plane dependent parameters compared to the normal group.

The reproducibility of a selection of the available HRT parameters, using previous software versions (1.09, 1.10) have been reported (Mikelberg, F. S. *et al.*, 1993; Menezes, A. V. *et al.*, 1995; Azuara-Blanco, A. *et al.*, 1998b). Of these, Azuara-Blanco, A. *et al.*, (1998b) and Mikelberg, F. S. *et al.*, (1993) used a statistical method comparable with the present study. Their results showed good reproducibility of topographic parameters, however the findings from our data demonstrate better reproducibility in some parameters including volume above surface, third moment in contour, maximum cup depth and mean depth in contour. This may be attributable to improvements in the alignment software, differences in the number of images, or dilation of the test eyes. Extreme care was taken at the image acquisition stage, the focus setting and scan depth was kept constant and the patient was requested to maintain the same head posture throughout, all these factors may have improved reproducibility. A previous study found no effect of dilation on the reproducibly of measurements obtained with the LTS (Rohrschneider, K. *et al.*, 1990). However, it is our opinion that dilation does facilitate effective image acquisition as images appear clearer and brighter through a larger pupil.

The classification parameter was highly reproducible for both groups. This new parameter is calculated from the third moment, cup volume and height variation of contour (see section 1.11.2.8.) and provides a diagnostic classification for ONHs as normal or glaucomatous (Mikelberg, F. S. *et al.*, 1995). The high reproducibility of this parameter is reassuring, but the sensitivity and specificity levels combined with the low incidence of POAG make it impractical for use as a screening tool and as such the results should be viewed with caution.

2.6.3 Summary

A previous study has suggested that the mean of three images is optimal to provide reproducible data with the HRT (Weinreb, R. N. *et al.*, 1993). The findings from this study suggest that three image series are insufficient because the mean standard deviation is still increasing. On average, 6-7 examinations are required for the MSD of the measured parameters to stabilise. Consequently, the mean of 7 image series provides a better interpretation of the measured quantity with minimum error. This number of images is also clinically practical due to the rapid acquisition time of the HRT. An investigation into the clinical reproducibility of the stereometric parameters revealed good reproducibility for all available parameters comparable with previous studies (Mikelberg, F. S. *et al.*, 1993; Azuara-Blanco, A. *et al.*, 1998b). Overall, parameter variability was greater for a POAG group compared to a normal group, this may be attributable to age differences or anatomical differences at the ONH. The high reproducibility of topographic parameters provides reassurance of the measurements obtained with the HRT and supports the possibility that this technique may be capable of detecting subtle changes in the ONH during the progression of glaucomatous optic neuropathy.

Chapter 3.

Accuracy of topographic measurements using a simple lens model with the Heidelberg Retinal Tomograph

3.1 Introduction

Although the reproducibility of the HRT has been extensively investigated, very few studies provide reports on the accuracy of the technique. In 1991 Dreher, A. W. & Weinreb, R. N., (1991) examined the accuracy of topographic measurements made with the LTS, predecessor to the HRT. A model eye with sample holes simulating ONHs (Shields, M. B. *et al.*, 1989) was used to obtain diameter and depth measurements. The results showed that measurements obtained with the LTS corresponded well with actual measurements of sample holes as verified by scanning electron microscopy. Calculated mean relative errors ranged from 2.0% - 3.6% for diameters and 10.1% – 11.7% for depth measurements (Dreher, A. W. & Weinreb, R. N., 1991). A more recent study examined the reproducibility and accuracy of both the HRT and ONH Analyzer (Rodenstock, Germany) (Janknecht, P. & Funk, J., 1994). Unlike earlier studies that measured distances only, this study was able to define the accuracy of two of the three-dimensional topographical parameters available for the HRT: volume below surface and volume above surface. The parameter volume above surface resulted in a mean relative error of 3.8% and volume below surface resulted in a mean relative error of 11%, consistent with the depth measurement error reported by Dreher, A. W. & Weinreb, R. N., (1991).

A study by Bartz-Schmidt, K. U. *et al.*, (1994) used direct *in vivo* assessment of the ONH in living eyes to assess the accuracy of the HRT. The study sample consisted of eight eyes scheduled for pars plana vitrectomy. Each eye was scanned with the HRT pre-operatively. During surgery each ONH was measured directly using a modified spatula and high-resolution video system adapted to a Zeiss operation microscope. Using this technique, two-dimensional measurements were obtained for each ONH,

these were then compared with corresponding HRT values for the structures examined. The results showed that, overall, good agreement was obtained between direct and HRT measurements. Only measurements in the two-dimensional (x, y) plane could be made directly from the optic nerve using the spatula method. Accuracy in the z-plane and hence stereometric measurements could not be evaluated.

Measurements with the HRT are based on the assumption that the eye being imaged is of average dimensions. The absolute scaling of a HRT image is determined using the parameters from Gullstrand's model 1 eye (Emsley, H. H., 1969). A separate model for the crystalline lens is used that has a gradient index with a resultant focal length of 61.088 nm (Blaker, J. W., 1980; Navarro, R. *et al.*, 1985). The degree of ametropia (determined from the divergence of the laser beam) and anterior radius of corneal curvature (determined by keratometry and inputted manually) are the only variables. While the HRT uses measured values for both ametropia and anterior corneal curvature, others use refractive constants for all measures except axial length (Bengtsson, B. & Krakau, C. E. T., 1992; Bennett, A. G. *et al.*, 1994) or ametropia (Bengtsson, B. & Krakau, C. E. T., 1992). A recent paper by Garway-Heath, D. F. *et al.*, (1998) compared several of the current methods available for correcting ocular magnification. The results showed that although methods that use individual axial length measurents for each subject resulted in lower error values, of the methods that did not, the HRT method compares favourably.

Spencer, A. F. *et al.*, (1995) identified discrepancies between measurements obtained with the HRT and planimetric measurements and concluded that the HRT consistently resulted in smaller measurements. In this regard the methods are not freely interchangeable. It could be argued that the longitudinal follow-up of disease progression does not require such a high degree of accuracy for the measurement of optic disc features as in cross-sectional analysis as long as the imaging scaling, and therefore percentage error, remains constant (Hosking, S. L. & Flanagan, J. G., 1996). Such changes in scaling however, may result due to shifts in ametropia. Hosking, S. L. & Flanagan, J. G. (1996) assessed the ability of the HRT to correct for changes in

ametropia that were not axial in origin and showed that for an eye of stable keratometry and axial length, changes in ametropia are assumed to be axial.

This study assessed the accuracy of the HRT using a simplified lens system and template of known geometry. Three different axial lengths and hence refractive errors were simulated by modifications to the lens system. The ability of the HRT to obtain accurate topographic measurements during changes in axial length was determined.

3.2 Aim

1. To construct a simplified lens system and template to investigate topographic measurement with the HRT.
2. To calculate an appropriate magnification correction factor to be applied to HRT measurements.
3. To simulate and assess the accuracy of topographic measurements with the HRT at different axial lengths.

3.3 Materials and methods

3.3.1 Simplified lens system

A simple lens system was constructed to assess the accuracy of HRT measurements at different axial lengths. The apparatus consisted of an optical bench, lens holder containing a five dioptre trial lens, precision made metal plate with gradations of known geometry (template 1) and back plate (template 2) (Figure 3.1.). Figure 3.2. shows the design of template 1 in more detail.

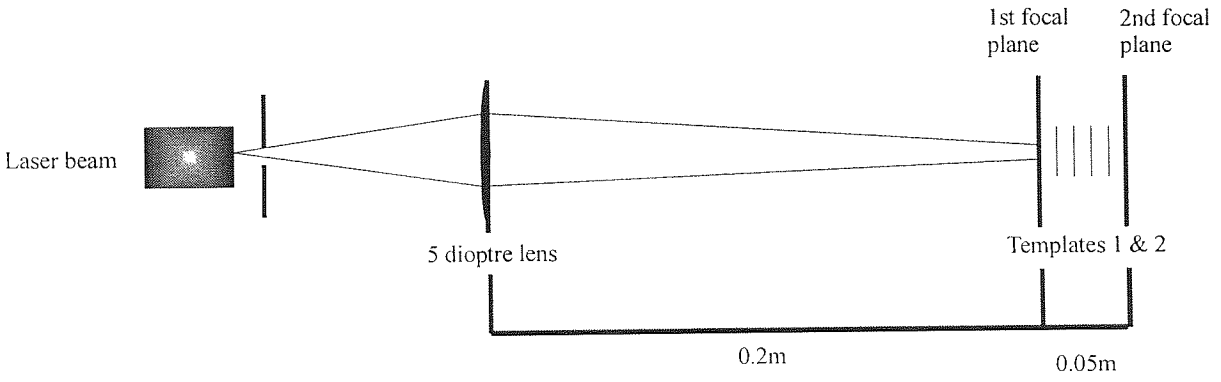

Figure 3.1. Schematic of the simple lens system designed to simulate image acquisition through an ametropic eye.

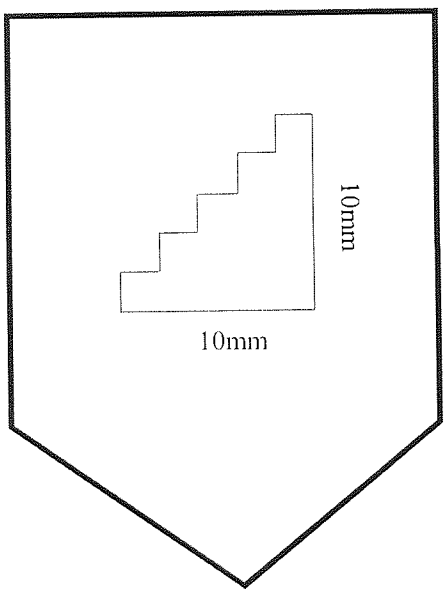

Figure 3.2. Schematic to show the precision made template (template 1) with 2mm gradations (not to scale).

Measurements made with the HRT utilise constants derived from Gullstrand's model eye. The lens system was designed to optically simulate the ametropic eye. Since the lens system used in the study (Figure 3.1) was more simplified than the Gullstrand eye, the optical design resulted in different image scaling between the two systems. A magnification correction factor was determined to allow for these differences such that

linear differences in the x, y plane (two-dimensional scaling) were corrected by factor K. The mathematical determination of K is shown below.

3.3.2 Calculation of magnification correction factor

According to Littmann, H., (1982), one need only be concerned with the posterior section of an eye (primarily the distance between the eye's second principle point and the retina) when dealing with a telecentric system. A recent study confirmed that the HRT is a telecentric system (Rudnicka, A. R. *et al.*, 1998). Based on Gullstrand's schematic model eye, when the optical properties of a simplified ametropic eye subtend a visual angle of 3.43° the retinal image height is 1mm, as shown in the following figure 3.3. and equation (3.1.). (Klingbeil, A. P. U. & Schödel, W. R. C., 1990).

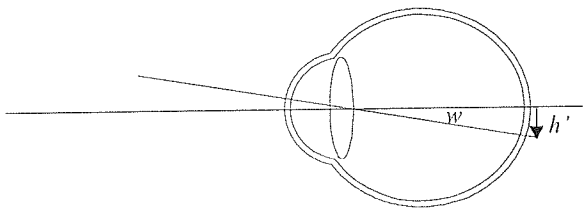

Figure 3.3. The visual angle of Gullstrand's model eye. Schematic showing how a retinal image height (*h'*) of 1mm subtends an angle (*w*) of 3.43°.

$$\underset{=3.43°}{\text{Visual angle}} = \tan^{-1}\left\{\frac{1}{K'-(A,N')}\right\}$$

Equation 3.1.

$$= \tan^{-1}\left\{\frac{1}{24-7.33}\right\}$$

$$= 3.43°.$$

Where:

K' = schematic axial length

A,N' = distance from the nodal point to the schematic corneal surface

The magnification factor K corrects for the retinal image height such that when the visual angle in the optical system is 3.43° the image height is unity. Figure 3.4. shows an optical model in which the focal point is 0.2 m behind the +5.00D lens, equivalent to an ametropic eye, with the retina located at the focal point. When the visual angle is 3.43° the image height, corrected for the magnification factor K is 1mm.

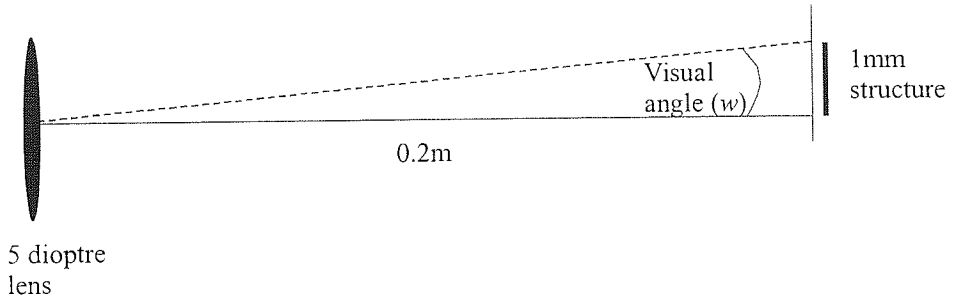

Figure 3.4. The visual angle of a simplified lens system. Schematic showing how a 1mm image located on the focal plane subtends a visual angle (*w*) of 0.286°.

The magnification factor K is simply the ratio of the Gullstrand image height to the actual image height of the system, or may be interpreted as the ratio of the respective visual angles when the image height is the same. It can be seen from Figure 3.4. that the visual angle alpha is given by:

Tan alpha = 1/200 thus alpha = 0.286 degrees.

Hence the magnification factor K is derived from:

$$K = \frac{\text{Visual angle for Gullstrand's model}}{\text{Visual angle of lens system}}$$

$$K = \frac{3.43}{0.286}$$

$$= 11.993$$

Equation 3.2.

The magnification factor K may then be applied to topographic measurements taken with the HRT using the lens system. K was calculated according to the axial length of the lens system and applied to the linear 2-dimensional measurements.

3.3.3 Accuracy of topographic measurements at different axial lengths

Three consecutive 10° images were acquired of the template for each of three axial lengths (Table 3.1.). In each case, the HRT focus setting was set to the corresponding refraction of the model. The sensitivity was set to maximum and the intensity adjusted to allow a bright but not over-exposed image. Figure 3.5. shows the reflectance image for the template and measurement system. The interaction measurement software available with the HRT was used to make linear measurements of the template. Specifically, the cross-wires were used to find the x,y locations at the start and end of the lines and the distance measured. Vertical and horizontal linear measurements were made for 2, 4, 6, 8, and 10mm and multiplied by K to correct for the magnification of the simplified optical system.

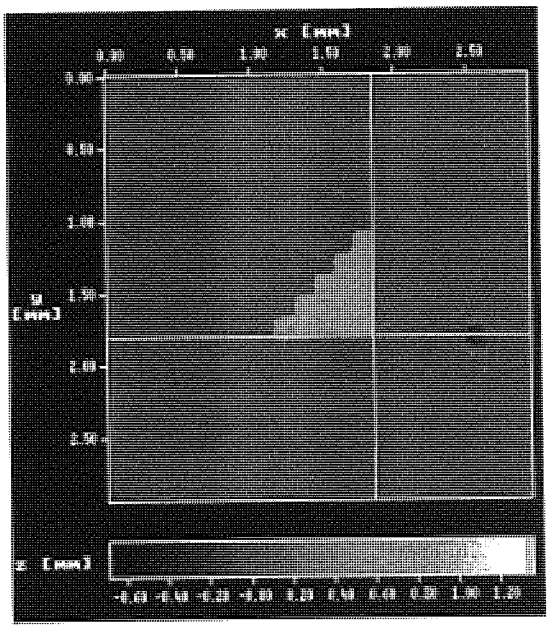

Figure 3.5. HRT reflectance image of a precision made template. The cross-wires are shown and the corresponding x,y locations (mm). The z-axis is represented by a grey scale. Only 2-dimensional measurements were made from the template.

Axial length	Refraction
15 cm	1.67
20 cm	0
25 cm	-1.00

Table 3.1. Axial lengths and corresponding refractions.

3.4 Results

The mean values ± SD (for three images) for linear measurements (horizontal & vertical) multiplied by *K* (to give *SK*) are given in Table 3.2. The true object size (*T*) is also given. Figures 3.6. – 3.7. show the results for *T* and *SK* at the different axial lengths. Table 3.3. gives the r-squared value for the measured image lengths at each axial length.

T		2mm		4mm		6mm		8mm		10mm	
Axial length		**Avg**	**SD**	**Avg**	**SD**	**Avg**	**SD**	**Avg**	**SD**	**Avg**	**SD**
15cm	**V**	1.85	0.06	3.78	0.10	6.05	0.06	7.93	0.11	10.07	0.06
	H	1.94	0.07	4.10	0.11	6.18	0.49	8.20	0.01	9.89	0.01
20cm	**V**	2.07	0.07	4.05	0.11	5.80	0.13	7.91	0.13	9.89	0.07
	H	2.42	0.07	4.41	0.07	6.33	0.40	8.27	0.13	10.02	0.07
25cm	**V**	2.11	0.09	4.09	0.32	6.58	0.09	8.63	0.09	10.86	0.09
	H	1.89	0.13	3.88	0.08	5.95	0.08	8.00	0.08	10.23	0.08

Table 3.2. Average values for horizontal and linear measurements. Values (mean ± SD of three images) are given for the measured image size x K. The true object sizes (*T*) are given in the top row.

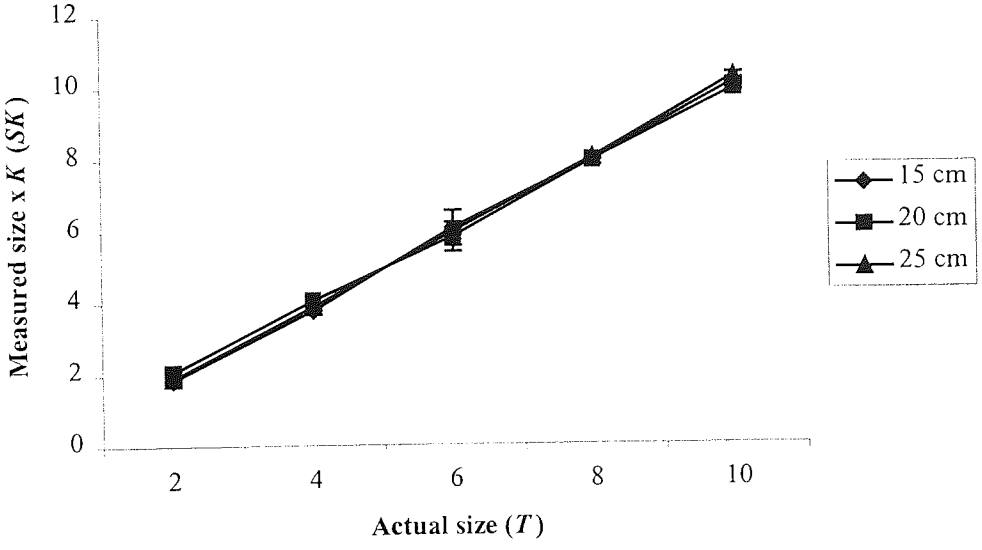

Figure 3.6. Horizontal linear measurements. Magnification corrected image height (SK) (mean ± SD of 3 images) for 3 axial lengths against actual height T.

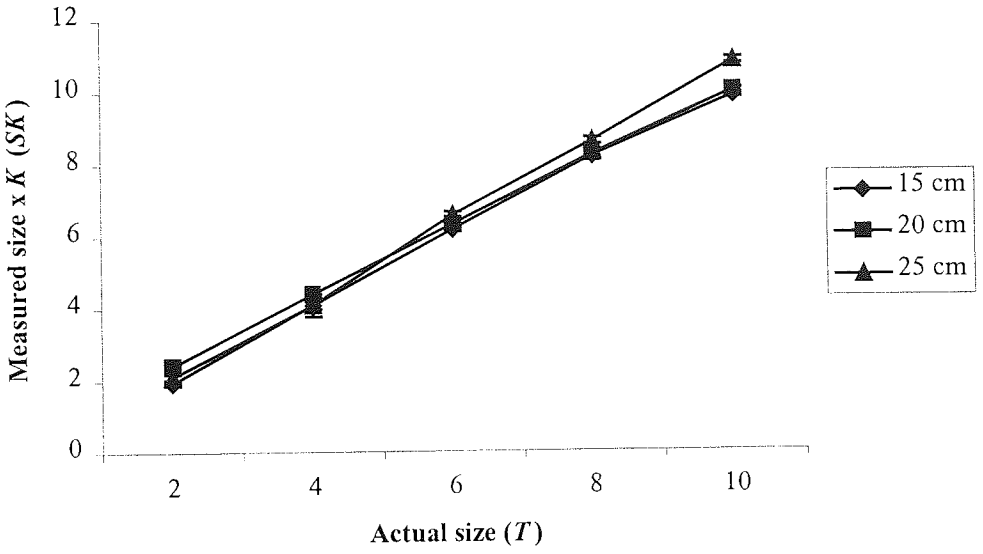

Figure 3.7. Vertical linear measurements. Magnification corrected image height (SK) (mean ± SD of 3 images) for 3 axial lengths against actual height T.

	Axial length		
	15cm	**20cm**	**25cm**
Horizontal (r^2)	0.9992	0.9993	0.9996
Vertical (r^2)	0.9979	0.9995	0.9991

Table 3.3. r-squared values for horizontal and vertical linear measurements at three axial lengths.

3.5 Discussion

3.5.1 The lens system and magnification factor

Other investigations which have assessed the accuracy of the HRT and LTS have used model eyes to make measurements. A model eye optically equal to Gullstrand's is difficult to build and as a result earlier studies have not used Gullstrand's model but have used simplified equivalents with a calculated magnification correction factor to adjust for optical differences (Dreher, A. W. & Weinreb, R. N., 1991; Janknecht, P. & Funk, J., 1994). This study used a simplified lens system, together with a magnification correction factor (*K*), to assess the accuracy of the HRT at different simulated axial lengths. The magnification factor was calculated according to

Littmann, H., (1982), and is similar to that used in other accuracy studies (Dreher, A. W. & Weinreb, R. N., 1991; Janknecht, P. & Funk, J., 1994). The lens system was simple to construct and the large scale used to simulate different refractive errors and axial lengths meant that inaccuracies of a few millimetres that would be important in a small model eye system were negligible.

3.5.2 The accuracy of topographic measurements

The HRT does not require the axial length of an individual eye to be input into the database. Corneal curvature and the divergence of the laser beam are the only data, individual to each subject, that are required for the calculation of focal length. The remaining data are derived from known constants (see section 1.11.2.1). Altering axial length, whilst maintaining the same corneal curvature, tested the ability of the HRT to make accurate topographic measurements for different refractive errors that were axial in origin. A separate study by Hosking, S. L. & Flanagan, J. G., (1996) demonstrated that changes in ametropia in the human eye, that are not axial or keratometry induced (i.e. due to lenticular changes), result in changes in image scaling and hence topography measurements. The simple lens system provided a good model for assessing HRT accuracy of linear measurements during changes in ametropia that were axial in origin. Topographic measurements were made for ametropia, hypermetropia (+1.67) and myopia (-1.00).

There are several potential sources of error that may account for differences observed between actual object sizes and measured object sizes. Firstly, the interactive software function available with the HRT is operator dependent and may result in some error. The observer is required to identify the area or line that is to be measured. In order to minimise this error source the mean of three measurements was taken thus providing a more representative sample in each case. The SD of the mean values are shown in Table 3.2 and figures 3.6.-3.7.

The template posed another potential error source. Although the template was precision built to ± 0.1mm the HRT is more sensitive than this and it is possible that a

discrepancy between the true object size and the measured object size may have been due to errors in the geometry of the template. If measurement discrepancies were due to the template however, the errors would have been consistent for all axial lengths (ie always bigger or always smaller). A final source of error lies with the magnification correction factor. The method used to calculate the magnification correction factor has been used in similar studies and is an accepted way of correcting for the optical differences between a system based on Gullsrand's model eye (HRT) and a simplified system (Klingbeil, U., 1989; Dreher, A. W. & Weinreb, R. N., 1991; Janknecht, P. & Funk, J., 1994). Had there been an error in factor K, then this would have systematically resulted in a constant error for all axial lengths.

The results showed good agreement between the measured value and the true object size for the horizontal and vertical linear measurements for the three different axial lengths. The r-squared value (coefficient of determination) describes the magnitude of the linear association between two variables. An r^2 of 1.0 would have indicated perfect agreement between the actual image size and the measured image size when corrected for magnification. The r^2 values in this study ranged from 0.9970 – 0.9901 for linear measures at the different axial lengths indicating strong, but not perfect, linear associations. Overall, the r^2 values were higher for the horizontal linear measures indicating a greater measurement error in the vertical plane. This finding was not systematic across the different axial lengths suggesting that the difference in measurement error between the two planes was operator dependent and not owing to the instrument or magnification factor.

The r^2 value obtained for both the horizontal and vertical measures was lowest for the shortest axial length (15cm). This axial length resulted in the greatest dioptric shift (1.67 Ds), and was therefore more subject to error if the precise working distance was not achieved. Furthermore, although the refractive error of the optical system was 1.67Ds, the HRT only allows incremental changes of 0.25D and, as such, was not focussed as precisely as with the other axial lengths. In this regard the HRT was unable to completely correct for blur and this may have accounted for the greater measurement error at this axial length.

3.5.3 Conclusion

The principle use of the HRT is for the topographical follow-up of glaucomatous optic neuropathy. One could argue that the accuracy of ONH dimensions is not fundamental for the longitudinal follow-up of glaucoma as long as the detection of change in those dimensions is possible. It could also be argued that accuracy only really becomes an important factor when trying to compare ONHs to classify disease. Potential difficulties can arise longitudinally however, when the refraction of an eye changes. In such a case it is important that the inbuilt mechanism for determining the focal length of the eye is robust enough to maintain a reasonable level of accuracy.

The results from this study suggest that the HRT is capable of accurately measuring objects at different axial lengths with reasonable accuracy. Other studies have assessed the accuracy of the HRT and found to correlate well with actual measurements and compare favourably with other techniques (Bartz-Schmidt, K. U. *et al.*, 1994; Janknecht, P. & Funk, J., 1994). This experiment only allowed linear measurements to be assessed. Many of the topographic measurements made with the HRT are 3-dimensional and include measurements for a z-axis as well as x- and y-axis. The introduction of a third dimension may well increase errors in object measurement. This study has provided only a basic interpretation of the accuracy of the technique, however, the results give reassurance that the imaged objects and subsequent measurements of those objects are true reflections of their size, even during different refractive states. Finally, although axial length is not inputted into the HRT, the calculations used take into account the divergence of the laser beam and are adequate to facilitate accurate measurement.

Chapter 4.

The influence of contour line size and definition on the reproducibility of topographic measurement with the Heidelberg Retina Tomograph

4.1 Introduction

The reproducibility of measurements acquired with the HRT has been investigated by several authors (Mikelberg, F. S. *et al.*, 1993; Chauhan, B. C. *et al.*, 1994; Chauhan, B. C. & MacDonald, C. A., 1995; Azuara-Blanco, A. *et al.*, 1998b; Zambarakji, H. J. *et al.*, 1998). There are a number of factors that may affect the reproducibility of optic nerve measurements taken with the HRT. These include: changes in the focus setting (Hosking, S. L. & Flanagan, J. G., 1996), cardiac cycle (Chauhan, B. C. & McCormick, T. A., 1995), misalignment of the laser head and the eye (Orgül, S. *et al.*, 1996) and variability in the alignment of the contour line (Orgül, S. *et al.*, 1997).

Prior to any stereometric measurements being made from a topography image, the area of interest must be clearly defined. This is done by drawing a contour line around the edge of the optic disc using the inner edge of Elschnig's scleral ring for reference. The scleral ring of Elschnig refers to a thin white band of neuroglial tissue that encircles the optic disc denoting the termination of the retinal pigment epithelium, in this regard it is also referred to the internal limiting membrane of Elschnig (Jonas, J. B. *et al.*, 1992; Pawson, P. & Vernon, S. A., 1995). The contour line is usually between 300-400 pixels in length, dependent on the size of the optic disc (Burk, R. O. W. *et al.*, 1990) and 1 pixel wide. The contour line is corrected for artefacts such as crossing blood vessels, which results in the corrected contour line. An example of a topography image is shown in Figure 1.8. (Chapter 1) together with a diagram that represents the circumferencial height profile of the contour line. The typical double hump appearance of the contour profile represents the height of the retinal nerve fibre layer that is thickest at the superior and inferior poles (Rohrschneider, K. & Burk, R. O. W., 1993).

The HRT allows one contour line, usually drawn on the first image of a series, to be exported and imported to subsequent images of an individual subject. Theoretically, using the same contour line for follow-up images will maximise the reproducibility of stereometric parameters and facilitate the detection of real change in the topography of the ONH over time.

There are a number of stereometric parameters that describe the spatial shape of the ONH all of which are influenced, to some extent, by the position of the contour line. There are three locations from which parameters are measured including:

- Contour line
- Curved surface
- Reference plane

Both the reference plane and curved surface are measured relative to the corrected contour line. The curved surface is bounded by the contour line and its central point forms the mean height of the contour line. The height variation along each line of the curved surface to the contour line is linear (Heidelberg, 1997). The reference plane is located 50μm posterior to the mean height of the contour line in the segment between −10° and -4° (Burk, R. O. W. *et al.*, 1995). This segment is located at the papillo-macular bundle and is considered to be the last area of the papilla to change during the progression of glaucoma. The relative positions of the contour line, curved surface and reference plane are shown in Figure 1.9. section 1.11.2.4.

The reference plane is measured from a relatively small area of the contour line at the inferior temporal quadrant (Burk, R. O. W. *et al.*, 1995). In view of this, correct positioning of the contour line on subsequent images of the same subject may be important. It is likely that slight differences in the positioning of the contour line for follow-up images may result in a change in the location of the reference plane. The curved surface, also located in relation to the contour, is likely to be more stable than the reference plane because it is measured from the mean height of the contour rather

than just one segment. The available stereometric parameters and the locations from which they are measured are listed in Table 1.3a-c. section 1.11.2.4.

Orgül, S. *et al.*, (1997) suggested that variations in realignment of the contour line on subsequent images may occur because the co-ordinates of the contour must shift by whole numbers of pixels between images. During the follow-up of patients with POAG, loss of rim tissue and changes in the topography of the ONH may cause further shifts in the location of the contour line in follow-up images. In the case of normal-tension glaucoma, where optic discs often have a "punched out" appearance, variations in the placement of the contour line may result in substantial differences in the calculation of both the reference plane and curved surface and consequently many of the stereometric parameters. The recommended position of the contour line is on the inner edge of Elschnig's ring which forms the boundary of the optic disc (Heidelberg, 1997). For the longitudinal follow-up of glaucomatous optic neuropathy it is important that the contour line is consistently located on a stable area of tissue. It is possible that Elschnig's ring may not provide the most stable position, as it is located at the disc border.

The HRT software (versions 1.11 & 2.01) has the facility to alter the diameter of an existing contour line by a defined amount while maintaining the same centre co-ordinates. Using this facility, the influence of the overall contour line diameter on the reproducibility of stereometric parameters was investigated. In addition, the effect of using redrawn and imported contour lines on inter- and intra-image parameter variability was determined.

4.2 Aim

The aims of this experiment were:

1) To investigate whether contour line size affects the reproducibility of topographic measurement of the ONH.
2) To determine an optimally reproducible contour line size relative to Elschnig's ring.

3) To investigate whether topographic measurements of the ONH are more reproducible when the contour line is redrawn for each image of a series or exported from the first image into subsequent images.

4.3 Subject sample

Twenty Caucasian patients were recruited forming two subject groups: 1) ten primary open angle glaucoma patients and 2) ten normal healthy volunteers. Subjects for the POAG group were recruited from patients registered at Manchester Royal Eye Hospital. Subjects for the normal control group were recruited from hospital staff. Details of the two subject samples are given in Table 4.1.

	POAG subject group	**Normal subject group**
Number of subjects	10	10
Females	6	6
Males	4	4
Mean age ± S.D.	50.3 ± 6.3	51.1 ± 9.9
Age range	39.1 – 60.9	40.1 – 76.5
Right eyes	2	8
Left eyes	8	2

Table 4.1 Subject sample.

4.4 Inclusion Criteria

4.4.1 Normal subject group

- Visual acuity better than 6/9 (Snellen equivalent)
- No history of glaucoma or diabetes
- No ocular abnormalities
- Open anterior chamber angle (Shaffer 3-4, where 0=closed and 4=open)
- Minimal or no lens opacities enabling a clear view of the fundus
- Intraocular pressures less than 21mmHg (Goldmann applanation tonometry).
- Astigmatism < 1.5 dioptres cylinder

- Refractive error < 6 dioptres (mean sphere)
- > 40 years of age
- No stabismus
- Normal fundus appearance based on:
  - No focal or generalised narrowing or disappearance of the neuroretinal rim with enlarged cupping and/or pallor that may be concentric or eccentric in shape
  - No notching (focal extension of the cup)
  - Healthy coloured neuroretinal rim
  - No disc haemorrhages

(Pawson, P. & Vernon, S. A., 1995; Vernon, S. A., 1996)

4.4.2 POAG subject group

- Visual acuity better than 6/9 (Snellen equivalent)
- Open anterior chamber angle (Shaffer 3-4, where 0=closed and 4=open)
- Astigmatism less than 1.50 dioptres cylinder
- Refractive error < 6 dioptres (mean sphere)
- No diabetes
- IOP > 21mmHg on at least two occasions
- Moderate visual field defect based on:
  - Mean defect (MD) between -6db and -12db.
  - On the pattern deviation plot, between 25% and 50% of the points may be depressed below the 95% probability level, and between 7 and 14 points may be depressed below the 1% probability level.
  - No point in the central 5% may have a sensitivity of 0db.
  - Glaucoma Hemifield Test must be outside normal limits.
  - Reliability, with a fixation loss of < 20% and false negative and false positive rates of <15% must be achieved.

(Hodapp, E. *et al.*, 1993; Park, K. H. *et al.*, 1996)

- Minimal or no lens opacities enabling a clear view of the fundus

4.5 Ethical approval

Ethical committee approval was sought and obtained for all experimental procedures, all of which conformed to the tenets of the declaration of Helsinki approved by the Manchester Royal Eye Hospital research and ethics review board.

4.6 Methods

Following informed consent each subject underwent a full ophthalmic assessment. A registered optometrist assessed the normal subjects and the POAG subjects were reviewed by an ophthalmologist. Measurements were obtained for visual acuity, anterior chamber depth, refraction, corneal curvature and IOP. A complete assessment of the ONH was carried out. Following fulfilment of the inclusion criteria, subjects commenced on the study.

4.6.1 HRT measurement

Subjects with pupils less than 3mm were dilated with one drop of Tropicamide 1%. Although the confocal principle of the HRT enables image acquisition through a pupil as small as 1mm (Thomson, S., 1994), in reality clearer images are obtainable through larger pupils. For those dilated, a minimum of 20 minutes was allowed to ensure complete mydriasis.

Using the HRT (Heidelberg Engineering, Germany), one operator (SH) obtained a total of seven images of the ONH for each subject. Images were taken for one eye only to avoid bias associated with using fellow eyes (see Table 4.1. for test eyes).

To obtain images, subjects were requested to place their chin on the chin rest and fixate on a distant target. A scan depth of 1.5mm was routinely used for the first image. The laser head was moved towards the subjects' eye and positioned

approximately 1cm from the cornea. The light source of the laser was centred on the pupil and the angle of the laser head manipulated until the ONH was visible and centred on the computer screen. The intensity dial was set to maximum, whilst the sensitivity was adjusted to a level that allowed a bright but not saturated view of the fundus. Using the subjects' refraction as a guide, the laser was focused onto the first retinal vessels and a single image series recorded using a 10° scan area (256 × 256 pixels).

The image series was examined and if necessary the scan depth and focus setting changed to ensure that optimum parameter settings were used. An adequate image series consisted of 32 equidistant confocal image sections moving back posteriorly into the eye with the first section positioned on the retinal vessels and the last located deep in the cup. The systems own quality control software "parameters OK" was required for image acceptance.

Focus settings were kept constant for each subject as changes in focus have been shown to affect reproducibility (Hosking, S. L. & Flanagan, J. G., 1996). Scan depth settings were also kept constant, as was the distance between the laser and eye (Orgül, S. *et al.*, 1996).

Following acquisition the individual image sections were examined for eye movements using the software movie option. The HRT automatically corrects for small eye movements but larger movements can result in a poor topography image due to misalignment of the 32 image sections. A quality control form was completed; scores out of 10 given for image quality (clarity and sharpness of the image) and eye movement. A combined total of 15 or more was required for the image to be accepted.

Topography maps were generated using the systems software (version 1.10) for each image series. The process used to determine the topography maps is detailed in section 1.13.2.2. and includes alignment for horizontal and vertical shifts, rotation and tilt.

4.6.2 Analysis of topography images

4.6.2.1 Investigation of the effect of contour line size

Following determination of topography images, a contour line was drawn around the edge of the optic disc on the first image of each series. The inner edge of Elschnig's ring was used to define the optic disc border. The contour line was then imported to the remaining six images for each series.

The radius of the contour line was then:

1. Decreased by 50μm
2. Increased by 50μm
3. Increased by 100μm

Using the original contour line and the three repositioned contour lines, the following stereometric parameters where determined globally.

- Cup volume
- Rim volume
- Retinal nerve fibre layer thickness
- Cup:disc area ratio
- Volume above surface
- Volume below surface
- Reference height

4.6.2.2 Investigation of the export and import function

The following procedures were carried out to determine whether the reproducibility of stereometric parameters is affected using the import and export function verses the redrawn method for contour line definition:

1. The contour line was redrawn separately for each topography image for each subject.

2. The contour line was drawn on the first topography image for each subject and imported into the remaining six images. Heidelberg Instruments recommend this method.
3. In order to determine intra-image reproducibility, a contour line was drawn seven times on a single image for each subject.

For each method, the reproducibility of eight stereometric parameters was determined. The parameters are outlined in section 4.6.2.1.

4.7 Statistical analysis

Results were analysed using the intra-class correlation coefficient (ICC) (see section 2.4. for description).

4.8 Results

4.8.1 Contour line size

Table 4.2. (normal group) and 4.3. (POAG group) give the ICC values (expressed as percentages) for the eight parameters using four contour line diameters: 1) drawn on the inner edge of Elschnig's scleral ring; 2) contour radius decreased by 50μm; 3) contour radius increased by 50μm; 4) contour radius increased by 100μm. The average ICC for the eight parameters is also given as an indication of the overall reproducibility of each contour line position. The results from the one-way ANOVA, which were used to calculate the individual ICC values, are summarised in Appendix 3.

Parameter	-50μm	Elschnig's ring	+50μm	+100μm
C:D area ratio	90.4	93.9	95.7	97.4
Cup vol	93.3	82.5	96.1	97.4
Rim vol	81.6	60.6	81.5	83.8
Rim area	81.2	84.3	93.8	89.7
RNFL thickness	53.4	56.0	67.5	80.8
Vol above surf	98.0	98.3	97.8	97.2
Vol below surf	73.8	71.4	64.4	73.6
Ref height	68.6	66.9	82.8	86.2
Average	**80.0**	**76.7**	**84.9**	**88.3**

Table 4.2. ICC results for the normal subject group the four contour line sizes: 1) Elschnig's scleral ring; 2) radius decreased by 50μm; 3) radius increased by 50μm; 4) radius increased by 100μm.

Parameter	-50μm	Elschnig's ring	+50μm	+100μm
C:D area ratio	98.3	97.1	97.0	97.6
Cup vol	99.5	99.6	99.7	99.6
Rim vol	98.6	97.2	97.8	99.0
Rim area	98.8	95.8	96.6	95.6
RNFL thickness	96.4	94.1	94.6	96.4
Vol above surf	86.3	90.0	90.4	94.8
Vol below surf	66.9	66.8	66.9	66.4
Ref height	96.7	94.7	94.3	93.1
Average	**92.7**	**91.9**	**92.2**	**92.8**

Table 4.3. ICC results for the POAG subject group the four contour line sizes: 1) Elschnig's scleral ring; 2) radius decreased by 50μm; 3) radius increased by 50μm; 4) radius increased by 100μm.

4.8.2 Export and import function

In order to evaluate the reproducibility of the contour line import/export function the radius of the contour line was increased by 50μm for each method. Table 4.4. gives the ICC values (expressed as percentages) for the normal subject group for the eight parameters using three methods: 1) drawing the contour line on the first image of the series and using the export and import function for the remaining 6 images; 2) redrawing the contour line for each of the 7 images; 3) redrawing the contour line on the first image of each series 7 times. The average ICC for the eight parameters using

each method is also shown to give an overall indication of the reproducibility of each method. The corresponding ICC results for the POAG subject group are given in Table 4.5. The results from one way ANOVA, which was used to calculate the individual ICC values, are summarised in appendix 3.

Parameter	Export/import	Redrawn (7 images)	Redrawn (same image)
C:D area ratio	95.7	96.6	97.7
Cup volume	96.1	90.1	98.9
Rim volume	81.5	78.3	87.9
Rim area	93.8	92.2	98.6
RNFL thickness	67.5	70.0	86.1
Volume above surface	97.8	63.4	91.5
Volume below surface	64.4	47.5	99.7
Reference height	82.8	84.3	88.6
Average	**84.9**	**77.8**	**93.6**

Table 4.4. ICC results for the normal subject group during different contour line transfer methods: 1) Using the export and import function; 2) Redrawing for each image; 3) Redrawing repeatedly on the same image.

Parameter	Export/import	Redrawn (7 images)	Redrawn (same image)
C:D area ratio	97.0	97.1	98.8
Cup volume	99.7	99.5	99.9
Rim volume	97.8	81.1	90.1
Rim area	96.6	91.9	94.0
RNFL thickness	94.6	83.3	90.4
Volume above surface	90.4	85.4	98.1
Volume below surface	66.9	99.5	99.9
Reference height	94.3	84.3	94.6
Average	**92.2**	**90.3**	**95.7**

Table 4.5. ICC results for the POAG subject group during different contour line transfer: 1) Using the export and import function; 2) Redrawing for each image; 3) Redrawing repeatedly on the same image.

4.9 Discussion

4.9.1 The effect of contour line size on topographic parameter variability

The results for the normal subject group showed that, on average, the reproducibility of the stereometric parameters improved as the size of the contour line increased. This suggests that parameter variability decreases as the distance between the contour line and the edge of the disc increases. This result was expected as the tissue surrounding the disc beyond Elschnig's ring is flatter and may therefore provide a more stable surface for the location of the contour line than tissue closer to the edge of the disc.

A similar result was expected for the POAG group. Interestingly the reproducibility of topographic parameters measured for the POAG group appeared relatively unaffected by the size of the contour line. This finding was unexpected, however the explanation may be associated with differences in the anatomical structure of the ONH. In particular, differences in disc size or mean contour line height (i.e. retinal surface height) between the two subject groups may account for the observed results.

Following contour line definition for a normal optic disc, the corresponding height profile diagram shows a classic double humped appearance (Figure 4.1.). The two peaks correspond to thicker rim tissue in the superior and inferior poles, typical to a normal ONH (Schuman, J. S. *et al.*, 1995; Weinreb, R. N. *et al.*, 1995). This can also be seen in the wire basket diagram which gives a 3-dimensional representation of the topography of the retina and optic nerve head (Figure 4.1.). Glaucomatous optic neuropathy is characterised by atrophy of the ONH and thinning of the neuroretinal rim (Quigley, H. A., 1993; Rohrschneider, K. & Burk, R. O. W., 1993; Rosenberg, L. F., 1995). As a result, the height profile of the contour line surrounding the optic disc becomes flattened in comparison to a normal ONH. The height profile diagram and corresponding wire frame diagram in Figure 4.2. demonstrate this. It follows that if a contour line is repositioned on a flatter surface, as in the glaucomatous rim, it is likely to be less variable than if it is repositioned on thicker more curved normal rim. It is

therefore possible that flattening of rim tissue in the glaucomatous optic nerve may result in a more stable contour line when compared to normal optic nerve heads which have thicker rim tissue and more defined contours.

The stereometric parameters determined with the HRT are measured from three reference locations: the contour line; curved surface and reference plane. The curved surface and reference plane are measured with respect to the contour line. The reference plane is located 50μm posterior to a small segment of the inferior temporal contour line. The reference height parameter corresponds to the height of the reference plane. The ICC value for reference height for the normal subject group was 68.6% for the smallest contour line size increasing to 88.3% for the largest contour line size. This suggests that reproducibility increases as the contour line size increases and the rim tissue flattens. The POAG group resulted in better reproducibility for the reference plane parameter with values ranging from 93.1% to 96.7% suggesting that reference height was stable at every contour line size. This supports the concept that the contour line and hence reference locations are more stable for the glaucoma group. Some of the parameters measured with respect to the reference plane, particularly rim volume, rim area and retinal nerve fibre layer thickness resulted in higher variability values for the normal group compared to the POAG group. This is a logical finding in view of the less stable reference plane identified for the normal group.

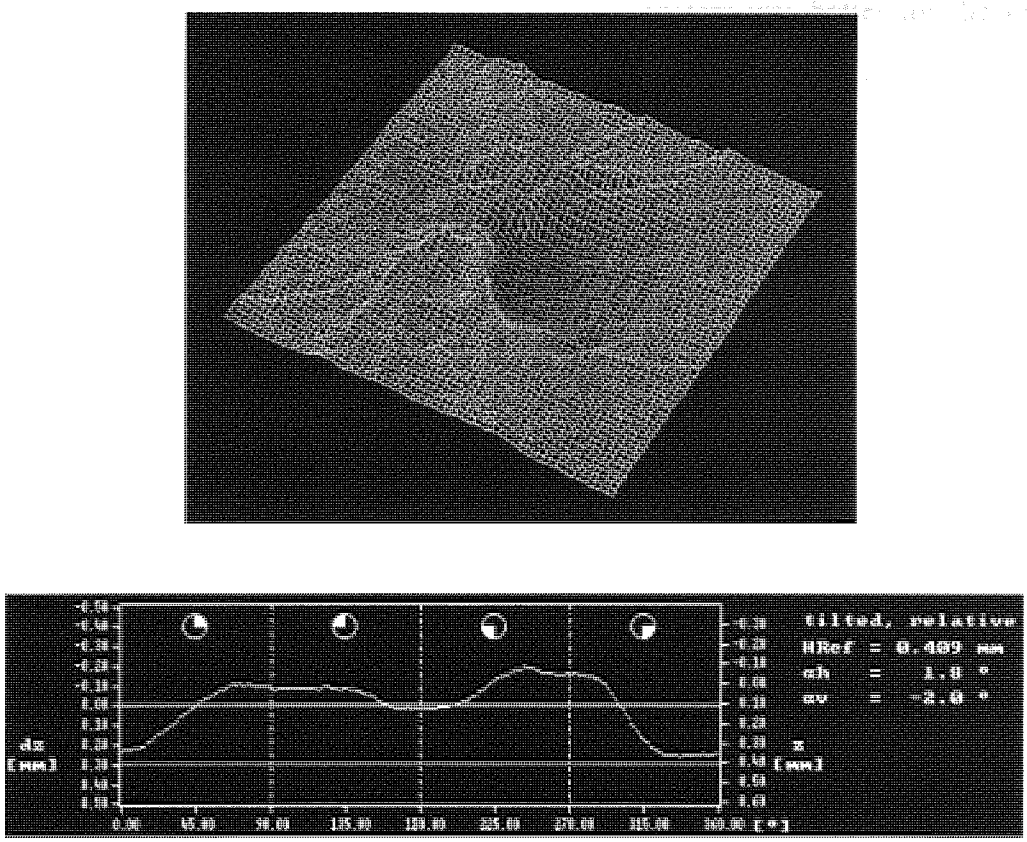

Figure 4.1. Height variation diagram and wire basket plot for a normal ONH.

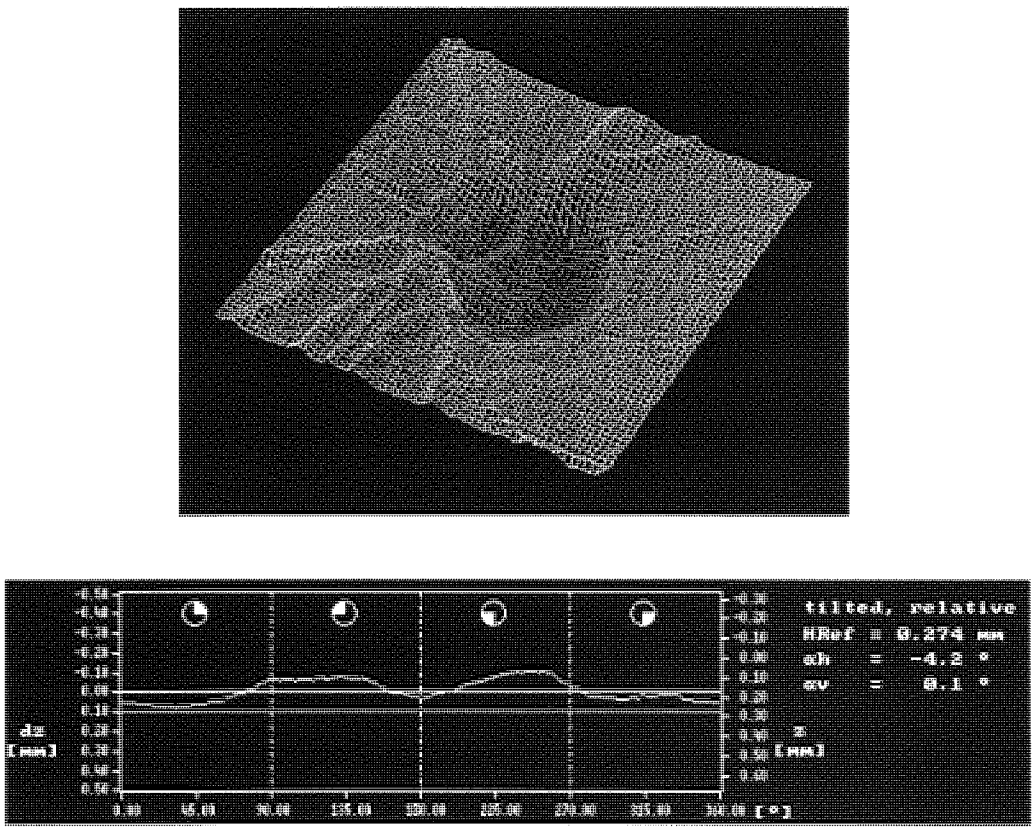

Figure 4.2. Height variation diagram and wire basket plot for a glaucomatous ONH.

Overall, the reproducibility of the topographic parameters was better for the POAG than for normal group at each contour line size. Of the parameters measured for the POAG group, volume below surface demonstrated the poorest reproducibility followed by volume above surface. Both of these parameters are measured with respect to the curved surface. The other remaining parameters are measured with respect to the reference plane. The lower reproducibility values observed for the parameters measured from the curved surface suggest that this reference location was more variable than the reference plane.

Apart from an anatomical explanation there are other reasons which may account for the differences seen in parameter variability between the two groups. The POAG group were more accustomed to ocular assessment and as a consequence better able to fixate resulting in lower parameter variability compared to the normal group. However, a strict quality assessment was applied during image acquisition to ensure good quality images were acquired and each image was assessed for eye movement. Finally, the subject sample sizes were relatively small and may not reliably reflect the normal and glaucomatous population.

4.9.1.1 Summary of the effect of contour line size on parameter variability

The investigation into the effect of contour line size on parameter reproducibility may be summarised by the following:

- The reproducibility of topographic parameters improves as the size of the contour line increases for the normal subject group.
- The reproducibility of topographic parameters for the POAG group seems relatively unaffected by the size of the contour line.
- These results suggest an anatomical explanation that may be related to the thickness of the tissue surrounding the optic disc.

4.9.2 The influence of contour line definition on parameter variability using the import/export function and redraw method

On average, using the import and export function to transport one contour line into follow-up images of the same subject was more reproducible than redrawing the contour line for each separate image. This was true for the normal subject group where the average ICC for all measured parameters increased from 77.8 % for the redraw method to 84.9% for the import/export method, a total increase of 7.1%. For the POAG subject group, the average parameter ICC increased from 90.3% to 92.2%, an improvement of only 1.9%. Although the import/export function improves parameter variability, it does so by a surprisingly small amount, particularly for the POAG group. This suggests that variability of stereometric measurement is largely attributable to differences between topography images, and that differences in the contour line alignment alone are of less importance. This finding is in agreement with an earlier study, which suggested that the variability occurring due to image acquisition is more important than that due to contour line realignment (Orgül, S. *et al.*, 1997).

Similar to the ICC values obtained for the different contour line sizes (Tables 4.2. & 4.3.), the reproducibility of individual parameters was better for POAG group than for the normal group for each contour definition method (Tables 4.4. & 4.5.). In particular, the volume below surface parameter performed poorly for the normal group with ICC's of 64.4% for the import and export function and 47.5% for the redrawing method. Interestingly, an ICC value of 99.7% was obtained for volume below surface when the contour line was repeatedly drawn on the same image. This indicates excellent intra-image reproducibility and suggests that the large majority of the variability seen is due to differences in images and not differences in contour lines.

4.9.2.1 Intra-image reproducibility

When a contour line is repeatedly drawn on a single image the only source of parameter variability is the differences in the contour line size and shape. The intra-image reproducibility was determined by redrawing the contour line repeatedly on a single image for each subject. As expected the observed ICC values demonstrated high intra-image reproducibility for both subject groups (above 85% for all parameters measured). Of the parameters measured volume below surface and cup volume proved the most reproducible (ICC $\geq$ 98.9%). Rim volume and RNFL thickness for both subject groups and reference plane height for the normal group were the least reproducible.

The rim volume and retinal nerve fibre layer thickness parameters are both measured with respect to the reference plane which is located from a relatively small section of the contour line. Changes in the location and hence height profile of the contour line may result in variations in the location of the reference plane. This was apparent in the normal group as the ICC for the reference plane height was less reproducible (88.6%) than some of the other parameters. Parameters located above the reference plane and measured with respect to both the contour line and reference plane (RNFL thickness and rim volume) appeared to be less reproducible than those measured below the reference plane (cup volume).

4.9.2.2 Summary of the effect of contour line definition on parameter reproducibility

The investigation into the import/export method verses the redraw method for contour line definition on parameter reproducibility may be summarised by the following:

1) The intra-image reproducibility was very good.
2) Most of the variability resulting from a series of images is due to differences in topography images, not differences in contour lines.

3) The reproducibility is better if the export/import function is used for contour line definition.

4) The difference between the reproducibility of the two contour line definition methods is surprisingly low.

4.10 Conclusion

An investigation into the influence of resizing the contour line relative to Elschnig's ring revealed little effect for the POAG group. The results obtained from the normal group suggested reproducibility improved as the distance of the contour line relative to the edge of the disc increased. Overall, the parameters measured for the POAG group were less variable than for the normal group. Anatomical differences between the two subject groups relating the thickness of rim tissue may go some way to explaining the results. In view of the high reproducibility measurements obtained for the glaucoma group, it is suggested that both the contour line definition (inner edge of Elschnig's ring) and export and import function recommended by Heidelberg be used for the clinical follow-up of the ONH. Finally, the results from this investigation suggest that the variability of stereometric measurements obtained with the HRT appear to be more dependent on differences in topography images than changes in the location and alignment of the contour line.

Chapter 5.

Evaluation of the ability of three ocular blood flow techniques to detect a physiologically induced change in ocular blood flow

5.1 Introduction

Blood flow autoregulation exists in the eye. Both metabolic and myogenic mechanisms facilitate a constant blood supply to the eye during changes in perfusion pressure and/or nutritional demand (Bill, A., 1981). A stress test may be used to elicit an autoregulatory response and induce a measurable change in blood flow (Ellestad, M. H., 1986). There are several ways to induce an autoregulatory response in the eye. Two of the more commonly used methods include IOP modification and blood gas perturbation. A number of studies have employed the use of a suction cup to alter IOP and consequently perfusion pressure and induce a measurable ocular blood flow response (Grunwald, J. E. *et al.*, 1982; Grunwald, J. E. *et al.*, 1984; Riva, C. E. *et al.*, 1986; Riva, C. E. *et al.*, 1997a). Other groups have used blood gas perturbation, specifically increased levels carbon dioxide, oxygen or nitric oxide to induce an autoregulatory response in the eye (Kety, S. S. & Schmidt, C. F., 1948; Tsacopoulos, M. & David, N., 1973; Harris, H. *et al.*, 1998).

5.1.1 Carbon dioxide: a vasodilator

Carbon dioxide (CO_2) is a known cerebral vasodilator that increases blood flow through arterial and arteriolar vasodilatation (Kety, S. S. & Schmidt, C. F., 1948; Ringelstein, E. B. *et al.*, 1992). Analogous to the brain, both the retina and ONH have been shown to respond to elevated levels of CO_2 (hypercapnia) (Mansberger, S. *et al.*, 1993; Harris, A. *et al.*, 1996c). The exact mechanism by which CO_2 induces a vasodilatory response is incompletely understood. It is possible the CO_2 molecule itself has a direct effect on smooth cell membrane or contractile and metabolic processes (Johnson, P. C., 1980a). Alternatively, increased PCO_2 (partial pressure of

arteriolar CO_2) levels may exhibit an indirect effect through a change in acidity. There is evidence to suggest that the cerebral and retinal response to increased PCO_2 is initiated by a change in pH (Kety, S. S. & Schmidt, C. F., 1948; Tsacopoulos, M. *et al.*, 1976). Tsacopoulos, M. *et al.*, (1976) found that increased levels of PCO_2 reduced interstitial pH in the inner layers of the retina. Interestingly, a study on the effect of increased PCO_2 on the skin of the forearm showed that vasodilation did not alter when the pH level of the blood was returned to normal through chemical induction (Kontos, H., 1971). In this regard, although the mode of vasodilation caused by CO_2 appears to be related to pH levels in the eye and brain, it is unknown whether this is the sole mechanism or a combination of effects.

5.1.1 Nitric Oxide: a vasodilator

A number of studies using animal models have suggested that Nitric Oxide (NO), a potent vasodilatory agent that lowers intracellular calcium levels resulting in relaxation, is released in the brain in response to hypercapnia (Iadecola, C. *et al.*, 1994; Wang, Q. *et al.*, 1995). Schmetterer, L. *et al.*, (1997) investigated the possibility of increased NO activity during hypercapnia in humans by administering an NO synthase inhibitor (L-NMMA). On administering the inhibitor, blood flow that was initially increased through vasodilation in response to hypercapnia was reduced, thereby indicating the presence of increased levels of NO (Schmetterer, L. *et al.*, 1997). Whether the NO released during hypercapnia is neural in origin, released from the endothelial cells that lie between the smooth muscle cells and the circulating blood, or a product of both is unknown (Wang, Q. *et al.*, 1995).

5.1.2 Oxygen: a vasoconstrictor

Increased levels of O_2 (hyperoxia) initiate metabolic autoregulatory activity by decreasing cerebral blood flow through vasoconstriction (Kety, S. S. & Schmidt, C. F., 1948). A similar effect has been demonstrated in ocular tissues (Riva, C. E. *et al.*, 1983; Fallon, T. J. *et al.*, 1985; Harris, A. *et al.*, 1994a). It has been suggested that the

vasoconstrictory action of increased PO_2 is mediated via the retraction of endothelial cells following the release of endothelin-1, a potent vasoconstrictor. As yet though, the exact mechanism by which increased levels of PO_2 induce a vasoconstrictory response remains unclear.

This study investigated the retrobulbar, retinal and chorio-retinal haemodynamic response of the normal eye to changes in ocular blood flow induced by increasing PCO_2 (hypercapnia) and PO_2 (hyperoxia). The ability of three non-invasive ocular blood flow measurement techniques to detect predictable changes in ocular blood flow including scanning laser Doppler flowmetry (SLDF), colour Doppler imaging (CDI) and ocular blood flow tonography (OBF Tonograph) was assessed.

5.2 Aims

1. To carry out a stress test under strictly controlled conditions and elicit an autoregulatory response in the ocular and orbital vasculature.
2. To assess and compare the ability of three ocular blood flow measurement techniques to measure changes in ocular blood flow induced by a stress situation.
3. To investigate the effects of blood gas perturbation (hypercapnia and hyperoxia) on retinal, choroidal and chorio-retinal circulation.

5.3 Materials and Methods

5.3.1 Subject sample

The subjects were recruited from university staff and medical students at the Glaucoma Research and Diagnostic Centre, Indiana University, USA. The sample characteristics are given in Table 5.1.

	Age (years)		Gender		Test eye	
	Mean ±SD	Range	Male	Female	Right	Left
Subject group (n=14)	27 ± 6	18-40	7	7	7	7

Table 5.1. Subject sample.

5.3.2 Inclusion criteria

- No history of glaucoma or diabetes.
- No neurological illness.
- No lens opacities.
- IOP < 21 mmHg.
- Non-smokers (as smoking is known to reduce the level of oxygen uptake and increase heart rate and peripheral vascular resistance through vasoconstriction (Langhans, M. *et al.*, 1997)).
- No medications known to affect blood flow.
- No hypertension or hypotension (as hypertension results in increased vascular resistance due to autoregulatory influences (Robinson, F. *et al.*, 1986) and hypotension induces vasodilatory autoregulatory activity, possibly through adenosine production, on peripheral circulation (Gidday, J. M. & Park, T. S., 1993)).
- Visual acuity better than 6/9.
- Astigmatism < 1.50 dioptres cylinder.
- No asthma or associated respiratory disorders.
- No pregnancy.

5.3.3 Ethical approval

Ethical committee approval was acquired for all experimental procedures. All procedures conformed to the tenets of the declaration of Helsinki and were approved by Indiana University School of Medicine review board. Informed consent was obtained from each subject prior to commencement on the study.

5.3.4 Experimental design

The study consisted of four visits that were randomised according to Ederer, F., (1975) and took place over a two-week time period. Each visit lasted approximately 30 minutes and was carried out at the same time of day to avoid possible diurnal fluctuations in blood flow (Claridge, K. G. & Smith, S. E., 1994) and IOP (Zeimer, R. *et al.*, 1994). Table 5.2. outlines the four visits and gives the combination of blood gas perturbation and ocular blood flow testing carried out.

* Visit	Gas condition	Ocular blood flow measurement Technique
1	Baseline & Hypercapnia	SLDF & CDI
2	Baseline & Hypercapnia	POBF
3	Baseline & Hyperoxia	SLDF & CDI
4	Baseline & Hyperoxia	POBF

Table 5.2. Summary of each visit, gas condition and ocular blood flow measurement. *The order of visits was randomised.

SLDF and CDI were performed in the same session. SLDF measurement always preceded CDI measurement as the process of CDI exerts a small amount of pressure on the eyeball that may affect subsequent blood flow measurements. Measurements with POBF were carried out on a separate day for two reasons:

1. Applanation of the cornea can affect blood flow measurements taken with SLDF.
2. To minimise the amount of time that the subjects underwent gas perturbation thus minimising complications such as hyperventilation.

Measurements were obtained for one eye only. Subjects maintained an upright sitting position throughout testing to avoid localised changes in blood flow known to be associated with shifts in posture (Trew, D. R. & Smith, S. E., 1991b; Kothe, A. C., 1994). Subjects were requested to avoid caffeine based products and vigorous physical activity prior to the initiation of experimental procedures. A single masked operator performed all systemic and ocular blood flow measurements.

5.3.5 Gas conditions

Blood flow measurements were obtained under three test conditions. Baseline, isoxic hypercapnia (increased CO_2 levels whilst maintaining arterial PO_2) and isocapnic hyperoxia (increased O_2 levels whilst maintaining arterial PCO_2) as detailed in sections 5.3.5.1., 5.3.5.2. and 5.3.5.3. respectively. A step-by-step protocol for each gas condition is given in Appendix 4. A schematic illustrating the apparatus used to induce hyperoxia and hypercapnia is given in Figure 5.1.

5.3.5.1 Baseline

Subjects breathed normal room air through a mouthpiece containing a one-way valve to prevent re-breathing of expired air. They were nasally occluded using sterile nose-clips. End-tidal CO_2 and O_2 levels were monitored continuously through a sample line that led from the mouthpiece to a gas analyser (POET II model 602–3, Criticare Systems). Following five minutes acclimatisation individual average end-tidal CO_2 levels were calculated for each subject. Ocular blood flow measurements where then taken.

5.3.5.2 Isoxic hypercapnia

Subjects were nasally occluded and breathed through a sterile mouth-piece. The average end tidal CO_2 level for each subject (previously determined (section 5.3.5.1.)) was raised 15% above baseline by adding CO_2 to room air in a mixing chamber. It is generally accepted in pulmonary physiology that end-tidal CO_2 concentrations are proportionate to arterial PCO_2 concentrations (Rhoades, R., 1995). Hyperventilation may occur during increased CO_2 breathing resulting in a reduction of blood PO_2 levels. This problem was avoided by ensuring that the end-tidal CO_2 content did not increase more than 15% above baseline levels. In the event of hyperventilation O_2 would have been added to the mixing chamber and the CO_2 level reduced thereby re-

establishing isoxia. Fortunately, this was not necessary. Subjects were allowed a minimum of five minutes to acclimatise prior to ocular blood flow measurements being taken.

5.3.5.3 Isocapnic hyperoxia

Subjects were nasally occluded and breathed through a sterile mouth-piece. End-tidal O_2 content was raised 70% above baseline values by breathing 100% O_2. This resulted in a 10-12% increase in arterial PO_2. Breathing excessive amounts of oxygen can cause hyperventilation and reduce arterial PCO_2 levels. To avoid this situation, end-tidal CO_2 content was monitored throughout O_2 breathing; if the end-tidal CO_2 fell below 0.5-1% of individual subjects baseline levels then CO_2 was added to the mixing chamber to prevent hyperventilation and maintain isocapnic conditions. Breathing was allowed to stabilise after the end-tidal O_2 content reached 70% above baseline; blood flow measurements where then taken.

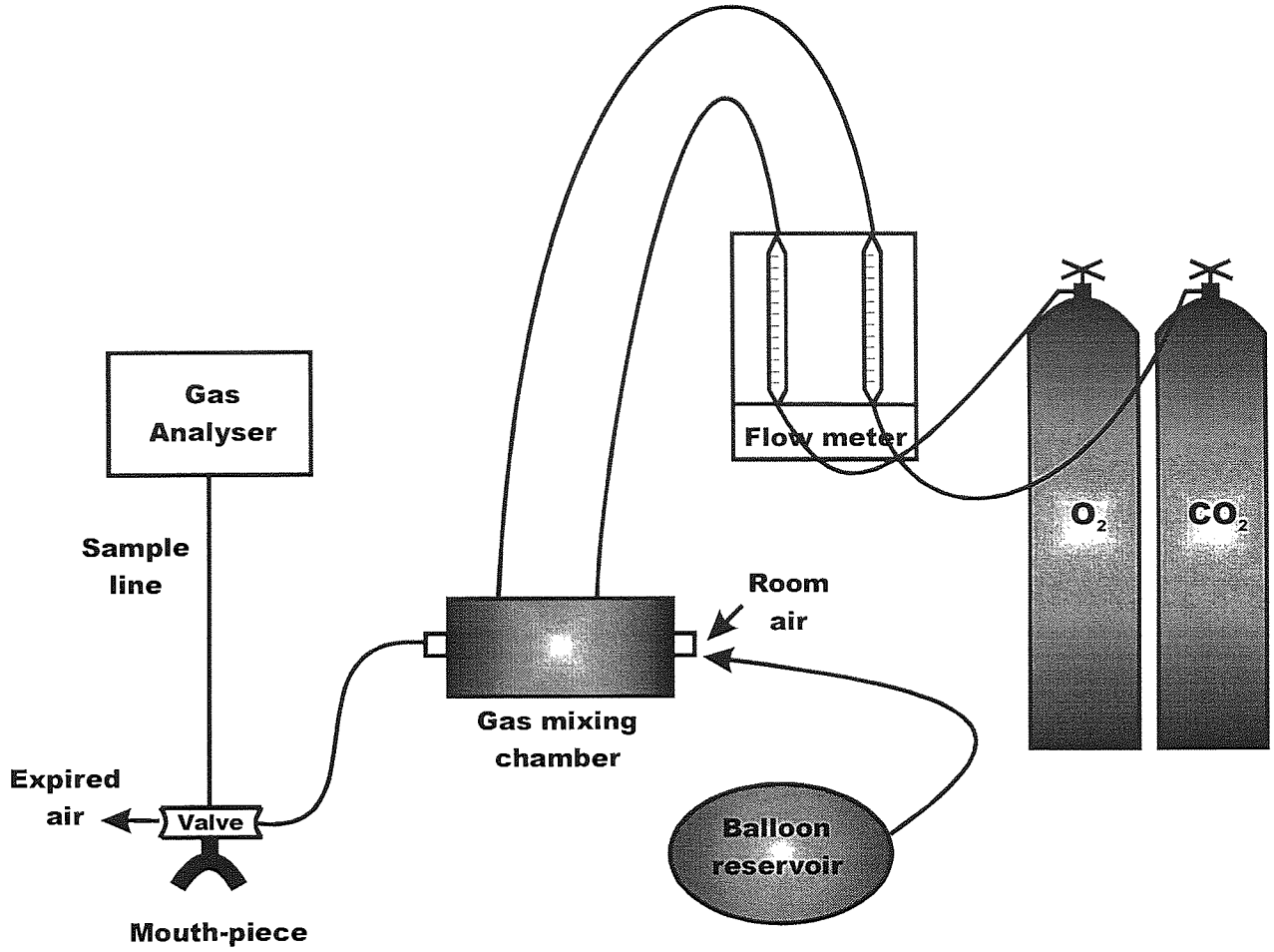

Figure 5.1. Apparatus set-up to induce blood gas perturbation.

- For isoxic hypercapnia, tanked CO_2 was passed through a flowmeter and trickled in a controlled manner into a mixing chamber that also contained room air.
- For isocapnic hyperoxia, an oxygen reservoir (balloon) was attached to the mixing chamber. Tanked O_2 was then passed through a flowmeter to the mixing chamber. For baseline, subjects breathed normal room air through the one-way mouth-piece.

5.3.6 Systemic measurements

During each gas condition a pulse oximeter was placed on the forefinger of the left hand of each subject to provide continuous monitoring of heart rate and O_2 saturation. Blood pressure was measured using a sphygmomanometer during baseline breathing and experimentally induced gas perturbation.

5.3.7 Scanning Laser Doppler Flowmetry (SLDF)

The Heidelberg Retina Flowmeter (HRF, Heidelberg Engineering, Heidelberg, Germany) was used to obtain SLDF measurements. Using a 10 × 2.5 degree field (2.7mm × 0.7mm), one operator (ER) obtained a minimum of two mapped images across the ONH for each experimental condition. Images were focussed on the superficial layer of the retinal capillary bed and the focus setting kept constant for subsequent images to maximise reproducibility. Blood flow, volume and velocity was then measured using a 10 × 10-pixel frame (100μm × 100μm) in four peripapillary retinal locations located 200μm from the disc margin: superior temporal, superior nasal, inferior temporal and inferior nasal. Images were inspected by a single observer (ER) who excluded those of poor quality (defocused, excessive movement).

A blood vessel landmark (usually a vessel bifurcation) was identified and used to ensure that the same retinal locations were used for each image. Large vessels and image areas interrupted by movement saccades were avoided. The exact placement of the pixel frame differed slightly between subjects due to the position of large blood vessels, but for within subject image series every effort was made to keep the location constant.

5.3.8 Colour Doppler imaging (CDI)

The Siemens Quantum 2000 CDI system (Siemens Quantum, Inc., U.S.A.) was used to obtain blood flow measurements for three vessel groups: ophthalmic artery (OA), central retinal artery (CRA) and short posterior ciliary arteries (SPCAs). Peak systolic velocity (PSV), end diastolic velocity (EDV) and Pourcelot's resistive index (RI), which is a measure of peripheral vascular resistance ((PSV – EDV) / PSV), were determined for each vessel group. All CDI measurements were acquired by an experienced technician.

To obtain measurements sterile acoustic coupling gel (steri-ophthalmic methycellulose) was applied to the closed eyelid and a 7.5 MHz linear probe was positioned on the eye with minimal pressure. It is known that increased IOP reduces choroidal blood flow and for this reason pressure on the globe was minimised (Alm, A. & Bill, A., 1973). Williamson, T. H. *et al.*, (1993) demonstrated that the increase in pressure caused by the transducer probe on globe is negligible if carried out by an experienced operator. Subjects were invited to move their eyes until blood flow of the appropriate vessel was clearly identifiable. The shadow of the optic nerve and the surrounding orbit is clearly visible on a horizontal B-scan through the orbit and provides a basis for locating the anatomical positions of each vessel. The OA may be positioned either above or below the optic nerve in the posterior orbit, it then courses forward nasally in a horizontal plane superior to the optic nerve. The CRA is located within the retrolaminar section of the optic nerve visible in the anterior portion of the optic nerve shadow (Lieb, W. E., 1996) and detectable for a length of approximately 10mm. The SPCAs usually originate from the OA 10-20mm posterior to the globe (Figure 1.2.). They then divide into a variable number of branches that follow a tortuous course before piercing the sclera either side of the optic nerve. Care was taken not to sample the closely located choroidal vasculature when measuring the SPCAs.

Apart from their distinct anatomical locations, the blood velocity waveform is unique to each vessel and was used to ensure correct identification. The OA is a branch of the internal carotid artery and exhibits a very similar waveform with a characteristic high PSV spike succeeded by sudden drop in velocity to a low EDV (Williamson, T. H. & Harris, A., 1996). Blood flow in the OA exhibits the highest flow velocities of the ocular vessels. The blood flow velocity of the CRA is flattened compared to the OA. Finally, the SPCA provide a waveform similar to that of the CRA, but with a sharper PSV spike and often a higher EDV which is indicative of the low-resistance vasculature of the choroid lying distal to the measurement site (Lieb, W. E., 1996; Williamson, T. H. & Harris, A., 1996).

Following identification of the appropriate vessel, a sample volume (0.2mm x 0.2mm) was placed over it and a few seconds of pulsed-Doppler signal recorded. After an acceptable recording of Doppler waveform was obtained showing clear peaks and troughs the angle of incidence was selected. When examining the orbit the ultrasound beam is not always parallel to the direction of the flow of blood. For this reason the angle of incidence of the Doppler beam is set by the operator by visually determining the course of the vessel. It is imperative that the angle of incidence is set correctly as an error of 45° or more can result in significant errors in velocity calculations (Williamson, T. H. & Harris, A., 1996). This adjustment is necessary in the calculation of PSV and EDV allowing accurate values up to an angle of incidence of 60° to be obtained. Although in the majority of cases the direction of the vessel and consequently the angle of incidence is clearly identifiable, there are occasions when it is difficult to discerne, especially for the SPCAs. If the direction was not clear then no correction for vessel angle was attempted.

Following sampling of Doppler waveform a single operator selected the peak and trough of the frequency waveform. PSV, EDV and RI was then calculated automatically by the Siemens programme software. A photograph of the waveform was printed out (the PSV, EDV and RI calculations where masked) and used as a visual guide in the obtaining the second CDI measurement. This ensured that the same location was used for each individual vessel under each condition. The technician operating the CDI was unaware of the order of gas conditions to prevent bias.

5.3.9 Pulsatile Ocular Blood Flow (POBF)

POBF, IOP, ocular pulse amplitude, pulse rate and pulse volume were measured using the OBF tonograph (OBF laboratories, Ltd. UK). In order to obtain OBF measurements, one drop of Proparacaine 0.5% was instilled into the subject's eye. The eyelid was then gently held up without placing pressure on the eyeball. A sterile OBF probe was positioned against the cornea and two sequential measurements were

recorded. The mean of the two measurements taken under each gas condition was used for analysis.

5.4 Statistical Analysis

Student's two-tailed paired t-test were used to compare ocular blood flow and systemic indices between baseline and isoxic hypercapnia and baseline and isocapnic hyperoxia. A p-value of less than 0.05 was regarded as statistically significant. The formula for the Student's t-test can be found in section 7.9.2.

5.5 Results

5.5.1 Systemic results: Baseline and CO_2

Mean end-tidal CO_2 was increased significantly from 4.48 ±0.3mmHg to 5.43 ±0.6mmHg during isoxic hypercapnia (Table 5.3.). No statistically significant difference was observed between baseline levels and those obtained under hypercapnia for O_2 saturation, breathing rate or heart rate (Table 5.3.). Similarly there was no significant difference between baseline and hypercapnia for systolic and diastolic blood pressure (Table 5.3.).

5.5.2 Systemic results: Baseline and O_2

Mean end-tidal O_2 increased significantly from 15.0 ±1mmHg at baseline to 77.62 ±8mmHg during hyperoxia (Table 5.4.). Mean O_2 saturation (%) increased significantly from 97.82 ±0.78 at baseline to 98.90 ±0.22 during hyperoxia. Mean systolic and diastolic blood pressure, heart rate and breathing rate did not alter significantly between baseline and isocapnic hyperoxia (Table 5.4.)

Parameter	Baseline	Hypercapnia	Significance (p-value)
End-tidal CO_2 (mmHg)	4.68 ± 0.3	5.43 ± 0.6	<0.001
O_2 saturation (%)	97.7 ± 0.8	98.07 ± 0.65	NS
Systolic blood pressure (mmHg)	112 ± 10	114 ± 10	NS
Diastolic blood pressure (mmHg)	70 ± 7	72 ± 7	NS
Heart rate (beats/min)	77 ± 7	79 ± 7	NS
Breathing rate (breaths/min)	12.71 ± 3.5	12.95 ± 3.36	NS

Table 5.3. Systemic results during baseline and isoxic hypercapnia. Mean ± S D. NS = not significant.

Parameter	Baseline	Hyperoxia	Significance (p-value)
End-tidal O_2 (mm Hg)	15.0 ± 1	77.62 ± 8	<0.001
O_2 saturation (%)	97.82 ± 0.78	98.90 ± 0.22	<0.001
Systolic blood pressure (mmHg)	114 ± 9	114 ± 8	NS
Diastolic blood pressure (mmHg)	74 ± 8	74 ± 8	NS
Heart rate (beats/min)	80 ± 8	77 ± 8	NS
Breathing rate (breaths/min)	11.80 ± 3.36	12.27 ± 2.82	NS

Table 5.4. Mean systemic results during baseline and isocapnic hyperoxia. Mean ± S D. NS = not significant.

5.5.3 Comparative baseline data

Student's paired t-tests were used to compare baseline ocular blood flow values obtained before hyperoxia and before hypercapnia for CDI, SLDF and OBF tonograph measures. There was no significant difference between baseline measures for any parameter. The data is tabulated in Appendix 4.1.

5.5.4 Ocular blood flow measurement results: Baseline and CO_2

5.5.4.1 CDI

SPCAs

A significant (p=0.025) 9% increase in PSV from baseline was observed in the SPCAs during hypercapnia (Table 5.5., Fig. 5.2.a.). Similarly, EDV increased significantly (p=0.006) by 23% (Table 5.5., Fig. 5.2.b.). The calculated RI decreased significantly by 5% (p=0.004) from baseline (Table 5.5., Fig 5.2.c.). These combined results indicate an overall increase in blood flow velocity and decrease in vascular resistance in the SPCAs.

Parameter	Baseline (mean ± SD)	Hypercapnia (mean ± SD)	Change (%)	p-value
PSV (mm/sec)	5.94 ± 0.92	6.43 ± 1.17	9	0.025
EDV (mm/sec)	1.44 ± 0.30	1.78 ± 0.47	23	0.006
RI	0.75 ± 0.00	0.72 ± 0.06	5	0.004

Table 5.5. CDI results (mean values ± SD) for the SPCAs during baseline and hypercapnia.

OA and CRA

No significant change in PSV, EDV or RI was observed for the OA or CRA between baseline and hypercapnia ($p>0.05$) (Tables 5.6. & 5.7).

Parameter	Baseline (mean ± SD)	Hypercapnia (mean ± SD)	Change (%)	p-value
PSV (mm/sec)	32.65 ±	34.93 ± 6.89	6.99	0.06
EDV (mm/sec)	6.79 ± 1.56	7.06 ± 1.30	4.02	0.312
RI	0.79 ± 0.03	0.80 ± 0.02	0.90	0.273

Table 5.6. CDI results for the OA during baseline and hypercapnia. Mean ± SD.

Parameter	Baseline (mean ± SD)	Hypercapnia (mean ± SD)	Change (%)	p-value
PSV (mm/sec)	6.56 ± 1.18	7.06 ± 1.19	7.67	0.199
EDV (mm/sec)	1.34 ± 0.59	1.57 ± 0.44	17.68	0.062
RI	0.80 ± 0.07	0.77 ± 0.06	3.04	0.088

Table 5.7. CDI results for the CRA during baseline and hypercapnia. Mean values ± SD.

5.5.4.2 SLDF

Using SLDF, a significant 13% ($p=0.033$) increase in blood flow and 11% ($p=0.023$) increase in blood velocity was observed following hypercapnia in the peripapillary retina (mean of all quadrants (see Table 5.8.)).

Parameter	Baseline (mean ± SD)	Hypercapnia (mean ± SD)	Change (%)	p-value
Volume (A.U.)	16.93 ± 6.33	18.22 ± 6.54	7.61	0.075
Flow (A.U.)	236.94 ± 113.73	266.86 ± 130.91	12.62	0.033
Velocity (A.U.)	0.83 ± 0.37	0.92 ± 0.42	11.62	0.028

Table 5.8. SLDF results during baseline and hypercapnia (mean of all quadrants). Mean ± SD.

When the blood flow values were examined separately for the individual quadrants (Appendix 4.5.), results showed that the most significant change in blood flow

occurred in the superior temporal quadrant of the peripapillary retina. In this quadrant there was a 39% (p=0.003) increase in flow, a 26% (p=0.004) increase in blood volume and a 34% (p=0.003) increase in velocity from baseline during isoxic hypercapnia (Table 5.9., Figures. 5.3. a-c.).

Parameter	Baseline (mean ± SD)	Hypercapnia (mean ± SD)	Change (%)	p-value
Volume (AU)	18.35 ± 3.95	23.05 ± 6.96	26	0.004
Flow (AU)	252.39 ± 72.30	351.40 ± 144.22	39	0.003
Velocity (AU)	0.89 ± 0.24	1.19 ± 0.45	34	0.003

Table 5.9. SLDF results during baseline and hypercapnia (superior temporal quadrant). Mean ± SD.

5.5.4.3 OBF tonography

No significant change (p>0.05) was observed between baseline and hypercapnia for POBF, IOP, pulse amplitude, pulse volume and pulse rate (Table 5.10.)

Parameter	Baseline	Hypercapnia	% change	p-value
IOP	16.05 ± 2.22	15.25 ± 2.37	4.98	0.052
Pulse amplitude	1.81 ± 0.46	1.85 ± 0.61	2.10	0.321
Pulse volume	3.84 ± 0.82	4.10 ± 1.31	6.73	0.141
Pulse rate	71.25 ± 4.97	72.76 ± 5.06	2.12	0.129
POBF	596.75 ± 131.68	637.83 ± 179.42	6.88	0.232

Table 5.10. OBF tonograph results during baseline and isoxic hypercapnia. Mean ± SD.

5.5.5 Ocular blood flow measurements: baseline and O_2

5.5.5.1 CDI

A significant (p=0.043) 7% decrease in PSV occurred during hyperoxia in the OA (Table 5.11.) (Fig. 5.4.), however, no significant change was evident EDV or RI. No significant difference in PSV, EDV or RI was evident for the CRA or SPCAs (Appendix 4.6.)

Parameter	Baseline	Hyperoxia	% change	p-value
PSV (mm/sec)	35.07 ± 5.77	32.69 ± 6.77	6.79	0.043
EDV (mm/sec)	7.09 ± 1.82	6.39 ± 1.24	9.93	0.07
RI	0.79 ± 0.05	0.80 ± 0.05	0.63	0.578

Table 5.11. CDI results for the OA during baseline and isocapnic hyperoxia. Mean ± SD.

5.5.5.2 SLDF

Overall, for the peripapillary retina (mean of all quadrants) no statistically significant change in blood flow, blood velocity or blood volume was observed following hyperoxia (Appendix 4.5.). When the blood flow values were examined separately for the individual quadrants, results showed that there was a significant change in blood flow in the superior nasal quadrant of the peripapillary retina. In this quadrant there was a 15% decrease (p=001) in flow, an 8% decrease (p=010) in blood volume and a 16% decrease (p=001) in velocity from baseline during isocapnic hyperoxia (Table 5.12.) (Figs. 5.5. a-c.).

Parameter	Baseline	Hyperoxia	% change	p-value
Volume (A.U.)	14.58 ± 4.46	13.46 ± 4.64	7.67	0.01
Flow (A.U.)	211.53 ± 91.56	180.36 ± 91.56	14.74	0.001
Velocity (A.U.)	0.76 ± 0.32	0.64 ± 0.32	14.92	0.001

Table 5.12. SLDF results for the superior nasal quadrant of the peripapillary retina during baseline and isocapnic hyperoxia. Mean ± SD.

5.5.5.3 OBF Tonograph

No significant change in POBF was observed during isocapnic hyperoxia (Fig. 5.6. a & b.). IOP and pulse rate decreased significantly from baseline (Fig. 5.7. a & c.) and pulse volume increased significantly (Fig. 5.7. b.). No change in pulse amplitude was evident between the two conditions (Table 5.13.).

Parameter	Baseline	Hyperoxia	% change	p-value
IOP mmHg	16.03 ± 1.7	13.57 ± 1.39	15.34	0.000
Pulse amplitude	1.94 ± 0.54	1.92 ± 0.43	0.74	0.866
Pulse volume	4.04 ± 1.23	4.64 ± 1.09	14.96	0.008
Pulse rate	73.67 ± 12.23	69.1 ± 11.59	6.2	0.000
POBF (μl/min)	619.96 ± 154.99	652.21 ± 141.40	5.2	0.080

Table 5.13. OBF tonograph results for baseline and isocapnic hyperoxia. Mean ± SD.

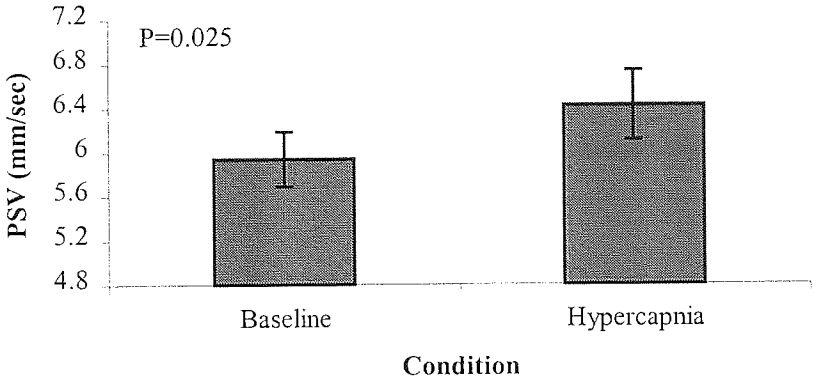

a.

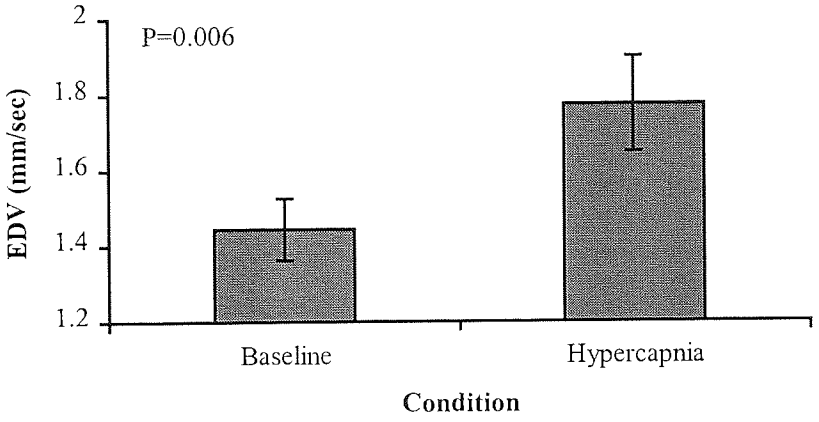

b.

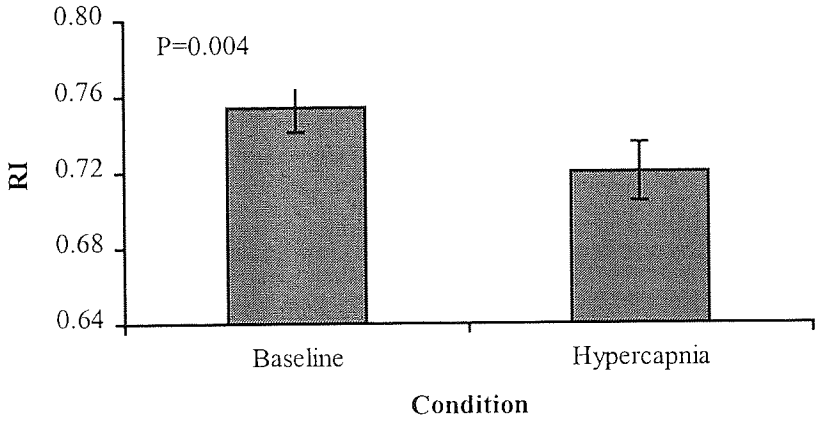

c.

Figure 5.2. SPCA graphs during baseline and hypercapnia.

a. Mean peak systolic velocity (PSV) ± S.E. for the SPCAs during baseline and hypercapnia.
b. Mean end diastolic velocity (EDV) ± S.E. for the SPCAs during baseline and hypercapnia.
c. Mean resistance index (RI) ± S.E. for the SPCAs during baseline and isoxic hypercapnia.

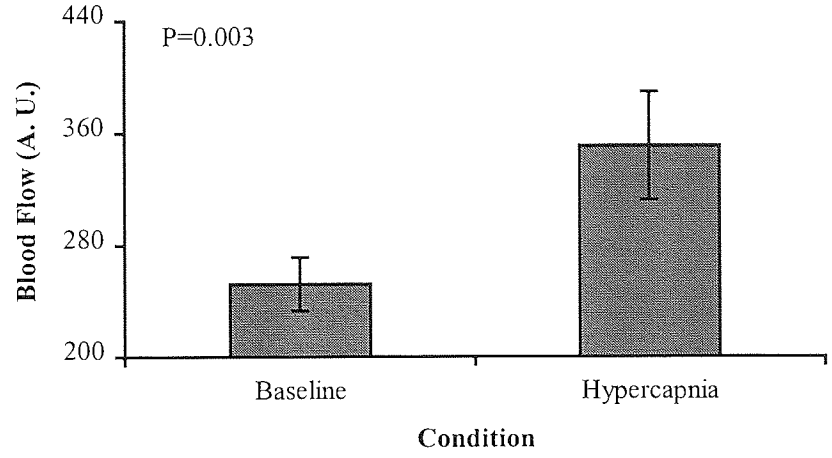

a.

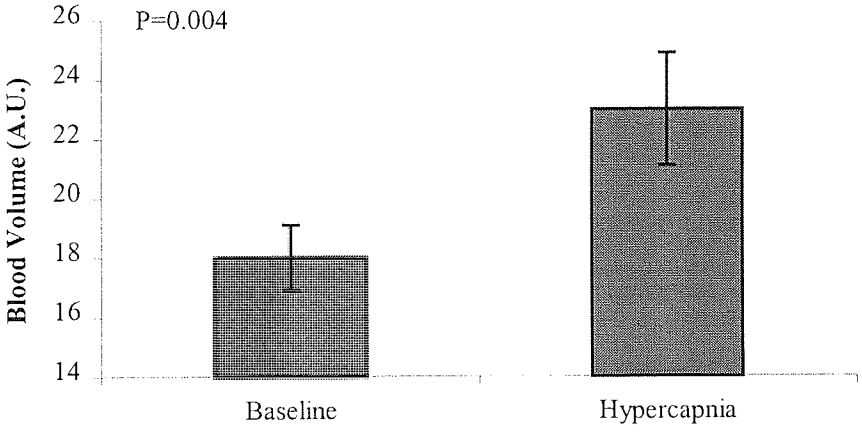

b.

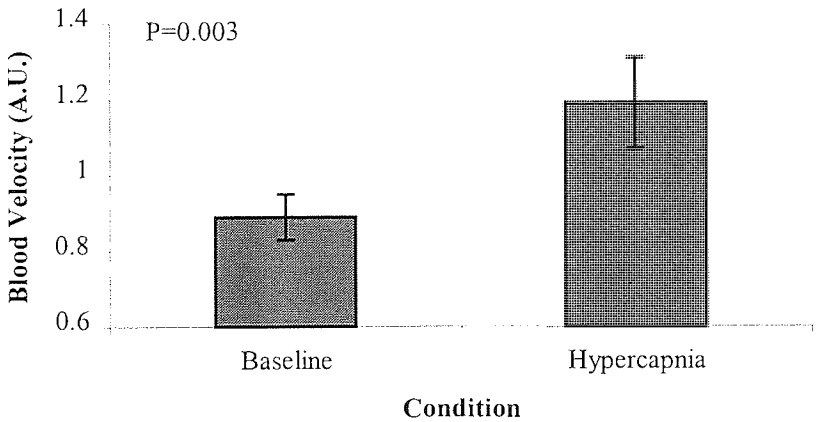

c.

Figure 5.3. SLDF graphs during baseline and hypercapnia.

a. Mean blood flow ± S.E. for the superior temporal quadrant during baseline and hypercapnia.
b. Mean blood volume ± S.E. for the superior temporal quadrant during baseline and hypercapnia.
c. Mean blood velocity ± S.E. for the superior temporal quadrant during baseline and hypercapnia.

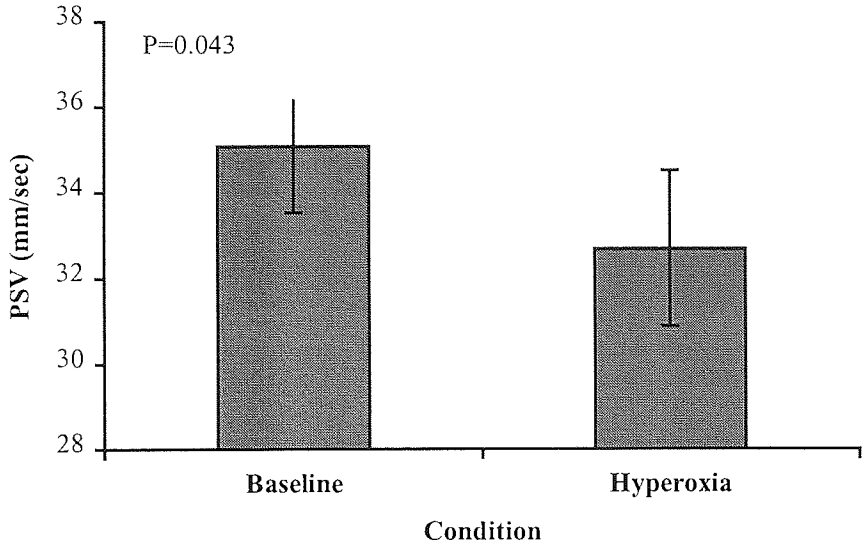

Figure 5.4. OA graph during baseline and hyperoxia.
Peak systolic velocity (PSV) ± S.E. for the ophthalmic artery during baseline and hyperoxia.

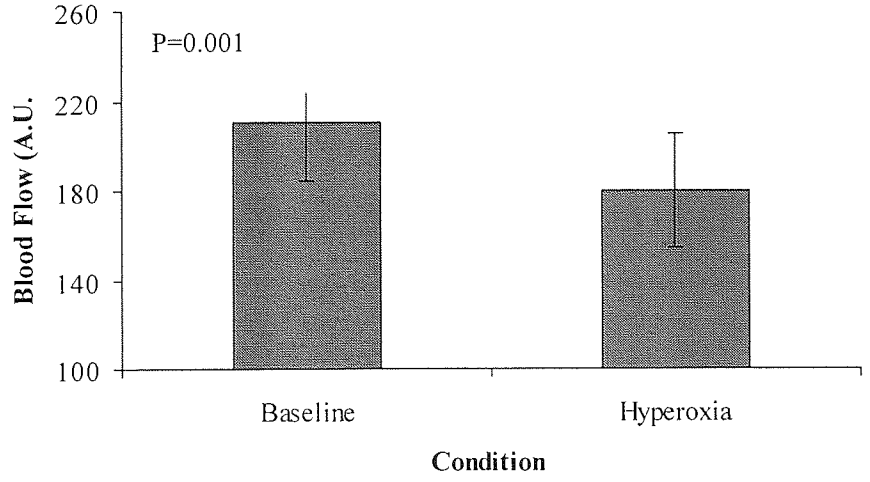

a.

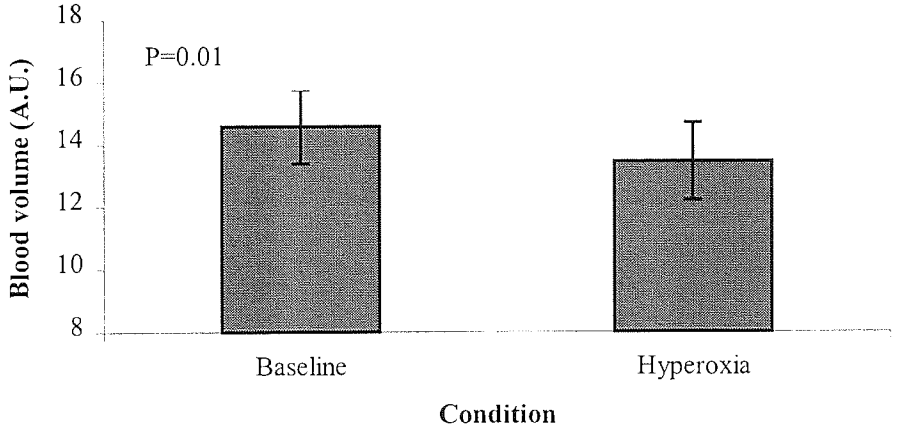

b.

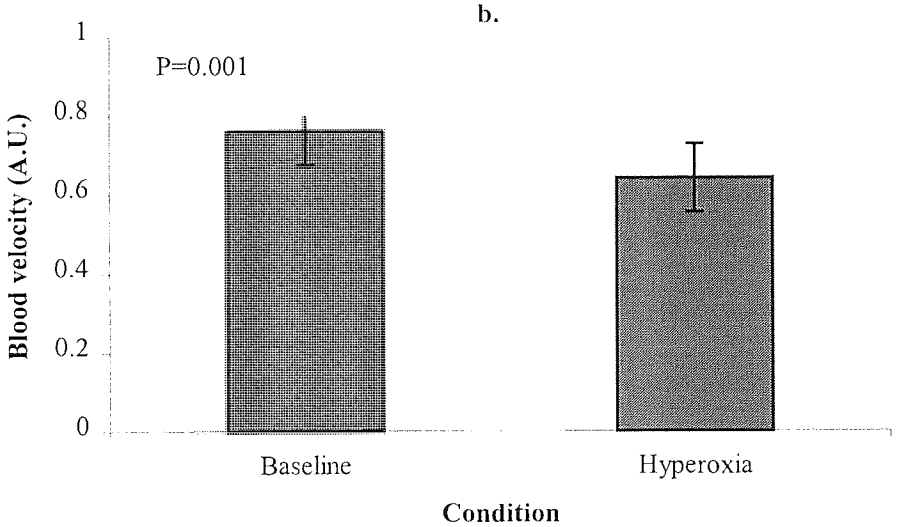

c

Figure 5.5. SLDF graphs during baseline and hyperoxia.

a. Mean blood flow ± S.E. for the superior nasal quadrant during baseline and hyperoxia.

b. Mean blood volume ± S.E. for the superior nasal quadrant during baseline and hyperoxia.

c. Mean blood velocity ± S.E. for the superior nasal quadrant during baseline and hyperoxia.

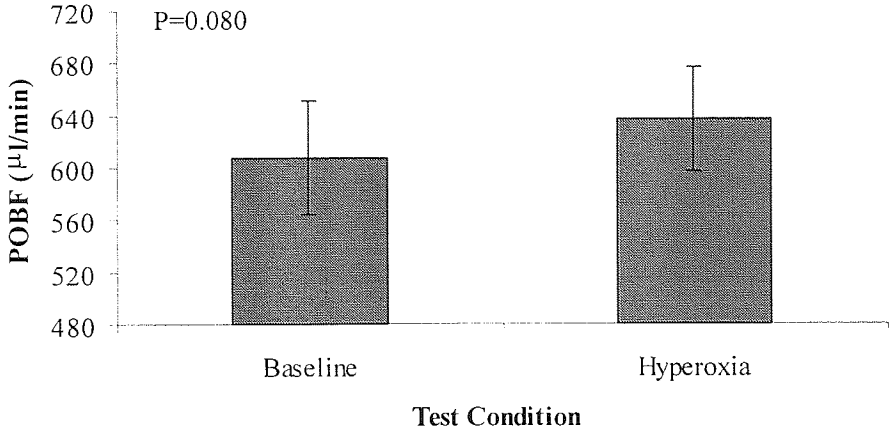

a.

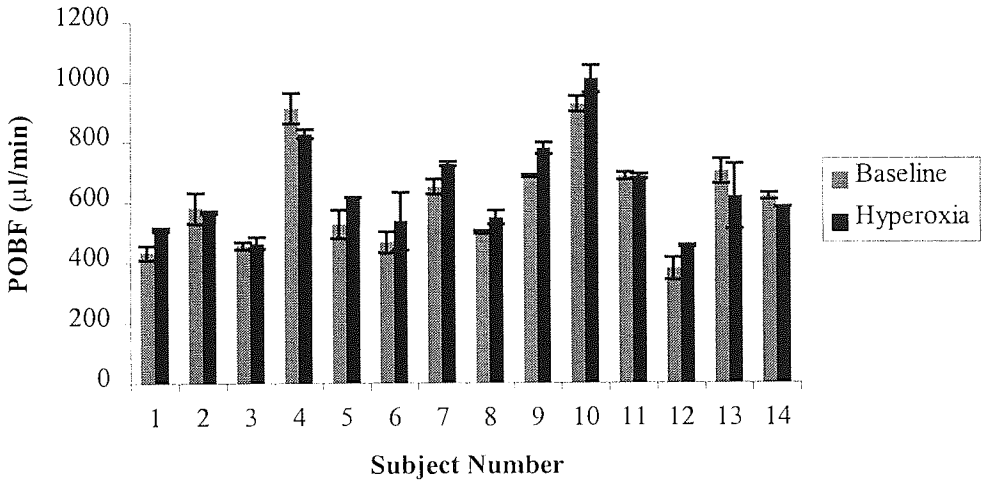

b.

Figure. 5.6. POBF graphs during baseline and hyperoxia.

a. Group mean POBF values ± S.E. for baseline and hyperoxia.
b. Mean POBF values ± S.E. (mean of two values) for 14 subjects under baseline and hyperoxia.

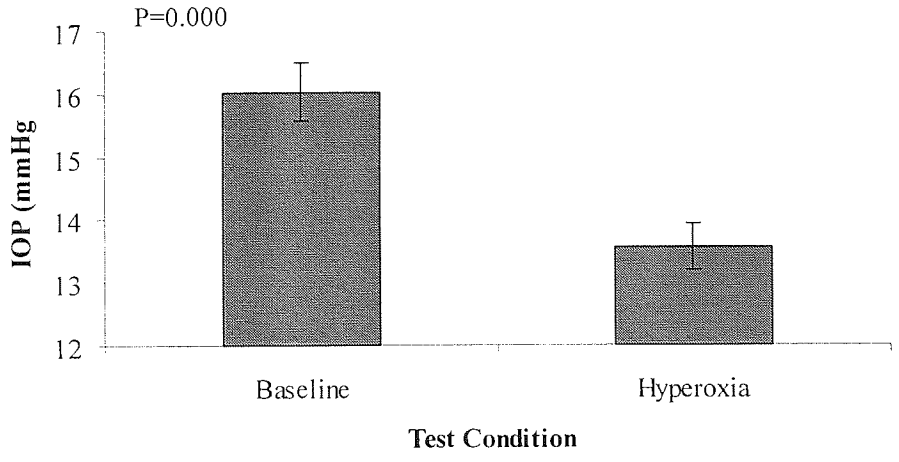

a.

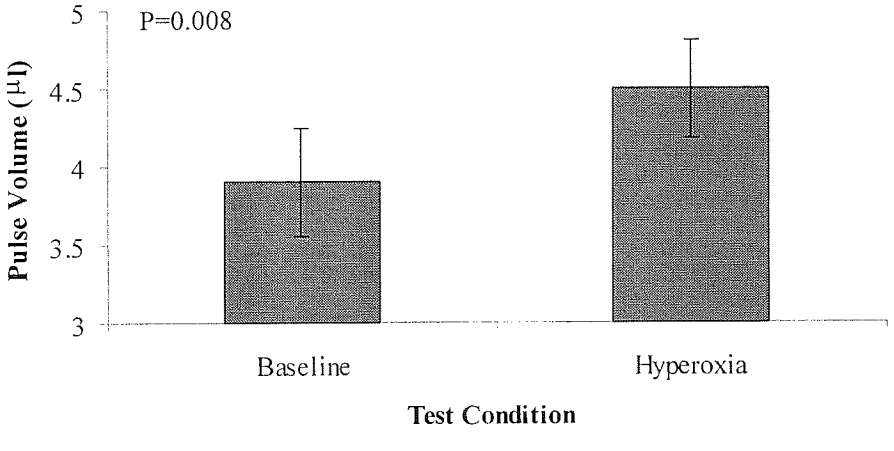

b.

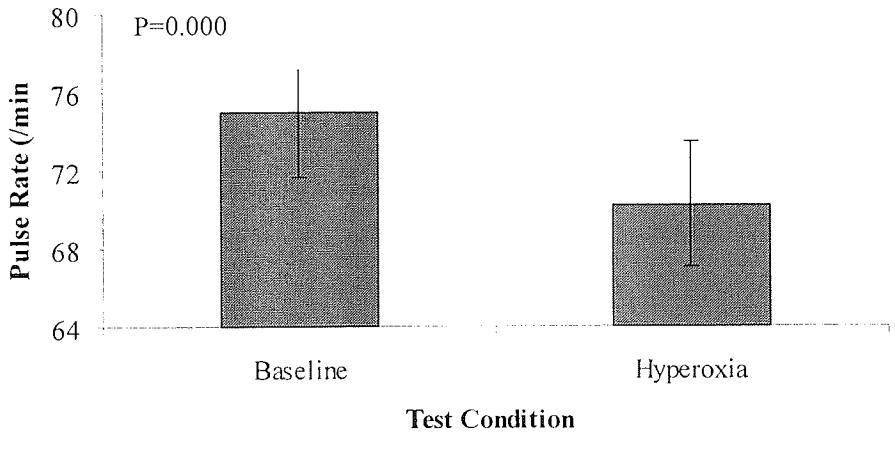

c.

Fig. 5.7. IOP, pulse volume and pulse rate graphs during baseline and hyperoxia.
a. Mean IOP ± S.E. values for baseline and hyperoxia.
b. Mean pulse volume values ± S.E. for baseline and hyperoxia.
c. Mean pulse rate values ± S.E. for baseline and hyperoxia.

5.6 Discussion

5.6.1 Blood gas perturbation – systemic change

Isoxic hypercapnia and isocapnic hyperoxia were successfully created during this study. No significant differences were observed for heart rate or systolic and diastolic blood pressure between baseline and hypercapnia and baseline and hyperoxia. This suggests that the measurable change in ocular blood flow occurred as a direct result of local autoregulatory activity in response to blood gas perturbation and not due to systemic influences that may have resulted in changes in ocular perfusion pressure.

5.6.2 CDI: Retrobulbar haemodynamic response during gas perturbation

5.6.2.1 Hypercapnia

The SPCAs were the smallest orbital vessels measured using CDI and are of particular interest as they are responsible for the supply of blood to the ONH (Hayreh, S. S., 1969; Neetens, A., 1994). Due to their relatively small size, it is difficult to say definitively whether one or several vessels were measured within the area of the sample volume (0.2 x 0.2mm). However, the presence of Doppler spectral waveforms typical of the SPCAs together with the anatomical position of the vessels provided reassurance that blood flow was being measured.

Due to the tortuous nature of the SPCAs, it is difficult to discern and select the angle of incidence. Even for an experienced operator, selecting the angle of the ultrasound beam relative to the flow of blood proves awkward. Previous authors have suggested that RI may be a more reproducible parameter because it is calculated as a ratio of the PSV and EDV and is angle independent (Williamson, T. H. & Harris, A., 1996; Liu, C. J. *et al.*, 1997). However, a review of the current reproducibility data suggests that in practice velocity values are more reproducible than resistance indices in the SPCAs (Harris, A. *et al.*, 1995b). Unlike the SPCAs, the OA and CRA follow a less tortuous vascular course and are considered to provide reproducible data for all parameters (Harris, A. *et al.*, 1995b; Quaranta, L. *et al.*, 1997).

Changes in blood flow velocity and resistance indices measured with CDI must be interpreted with a degree of caution. A parallel increase in PSV and EDV can denote either an increase in blood flow or vessel narrowing (Hayreh, S. S. & Beach, K. W., 1993). Although a decrease in RI indicates reduced vascular resistance distal to the measured vessel, the exact location is unknown (Spencer, J. A. D. *et al.*, 1991). This study showed a significant increase in peak systolic and end diastolic velocities in the SPCAs, coupled with a decrease in RI in response to isoxic hypercapnia. This measured response to elevated arterial PCO_2 suggests an overall increase in blood flow and decrease in vascular resistance in these retrobulbar vessels.

A previous study by Harris, A. *et al.*, (1994b) reported increased PSV in the CRA in response to hypercapnia, but no measurable change in blood velocity or resistance was observed for the SPCAs in normal subjects. In the current study an increase in blood flow velocities and decrease in vascular resistance in the SPCAs was demonstrated. The presence of an autoregulatory response in the SPCAs directly relates to the ONH circulation supplied by these vessels (Hayreh, S. S., 1969). No significant change was observed in the OA or CRA ($p>0.05$), suggesting that there may be variation in the autoregulatory blood flow response during hypercapnia in the orbital vasculature. As such some vessels may preferentially autoregulate in response to a specific vasodilator whilst others do not. These results are in accordance with an earlier study which identified vessels in the brain and eye that respond preferentially to different vasodilators (Harris, A. *et al.*, 1996c). It is possible that measurement error may account for the results obtained, however this seems unlikely as CDI has been shown to be very reproducible and other studies have found similar variability between vessel responses.

5.6.2.2 Hyperoxia

There was a significant decrease in PSV in the OA following isocapnic hyperoxia. This suggests an increase in blood flow resistance, probably due to arterial vasoconstriction. No statistically significant change was observed for other measured

parameters of the OA, CRA or SPCAs during hyperoxia. Analogous to the retrobulbar vessel response to hypercapnia, a variation in autoregulatory activity was also evident during hyperoxia. This finding is consistent with other studies that have reported varying blood flow responses in cerebral and orbital vessels to vasodilatory and vasoconstrictory agents (Faraci, F. M. *et al.*, 1987; Harris, A. *et al.*, 1996c).

5.6.3 SLDF: Retinal haemodynamic response during gas perturbation

5.6.3.1 Hypercapnia

Several studies have documented an increase in retinal blood flow in response to hypercapnia (Tsacopoulos, M. & David, N., 1973; Mansberger, S. *et al.*, 1993). Measurements taken using SLDF during baseline and isoxic hypercapnia showed a significant increase in blood flow, volume and velocity of 39%, 26% and 34% respectively that was localised in the superior temporal quadrant of the disc.

5.6.3.2 Hyperoxia

A number of studies have reported decreased retinal perfusion in response to increased levels of O_2 (Riva, C. E. *et al.*, 1983; Fallon, T. J. *et al.*, 1985; Harris, A. *et al.*, 1994a; Strenn, K. *et al.*, 1997; Lietz, A. *et al.*, 1998). In this study, a significant decrease in blood flow, volume and velocity by 15%, 8% and 16% respectively was detected in the superior nasal quadrant in response to hyperoxia. Consequently, the measured response during increased PCO_2 was more than twice the intensity of the response for increased PO_2. This finding is consistent with Arend, O. *et al.*, (1994) who found that when normal subjects inhaled a carbogen gas mixture (6% CO_2 and 98% O_2), the vasodilatory effect of CO_2 on retinal blood velocity completely outweighed the vasoconstrictory effects of O_2, resulting in increased retinal perfusion.

5.6.3.3 Regional variations of retinal blood flow during a stress situation

Changes in blood flow and consequently autoregulation were measured in the peripapillary retina in response to gas perturbation. This is the first time that possible autoregulation has been demonstrated in this particular area of the retina, contrasting with earlier work that reported high susceptibility of the peripapillary retina in response to changes in IOP (Hayreh, S. S. *et al.*, 1970). Other studies have demonstrated variations in blood flow across the retina under normal conditions. Alm, A. & Bill, A. (1973) showed marked regional variations of blood flow in monkey retina using the radioactively labelled microsphere technique, but possible differences between superior and inferior retinal blood flow were not explored. The finding in this study, that different areas of the retina autoregulate preferentially to certain stimuli is intriguing. Localised variations in the blood flow response to increased PCO_2 in the superior temporal retina and increased PO_2 in the superior nasal retina suggests regional variations in an autoregulatory mechanism which have not previously been reported.

The reasons for regional variations in autoregulation are not fully understood. One possibility is that there may be a gravitational effect on blood flow in the eye. Alternatively, there may be an anatomical explanation. Either way, the inferior retina did not demonstrate the same efficient regulation of blood flow as the superior retina. This anomaly may be of consequence in glaucoma as characteristic visual field loss associated with POAG has been found to commence primarily in the superior nasal quadrant (Hart, W. M. & Becker, B., 1982; McClure, E., 1988). This area corresponds to nerve fibre loss in the inferior retina, which has been shown in this study as having less autoregulatory activity than the more stable superior retina. This diminished autoregulation of blood flow in normal subjects under a stress situation may provide insight to why nerve fibre loss occurs in the inferior retina during early glaucoma; particularly as studies have now shown that the autoregulatory capacity of eyes with

POAG is compromised compared to normal subjects (Geijer, C. & Bill, A., 1979; Grunwald, J. E. *et al.*, 1984).

5.6.4 OBF tonograph: Chorio-retinal haemodynamic response during blood gas perturbation

There is some controversy over which component of the ocular circulation is measured by POBF (see section 1.16.4.). The general consensus appears to be that the chorio-retinal circulation is being measured, of which 95% is choroidal supplied by the SPCAs and the remaining 5% is retinal (Hill, D. W., 1989). The SPCAs supply the choroidal circulation entering the sclera at the posterior pole and forming choroidal arteries that perfuse the choroid (Hayreh, S. S., 1974). Due to the practical difficulties of directly measuring choroidal blood flow, there are few investigations in the literature that report on autoregulation. Some studies have demonstrated a lack of choroidal autoregulation in response to decreases in perfusion pressure caused by body inversion (Lovasik, J. V. & Kergoat, H., 1994), or induced by raising the venous pressure through increased IOP (Friedman, E., 1970; Alm, A. & Bill, A., 1973). Other workers using a catheter insertion into the vitreous of rabbits and the suction cup method in humans to modify IOP have found that choroidal autoregulation does occur dependent on the level of IOP (Kiel, J. W. & Shepherd, A. P., 1992; Riva, C. E. *et al.*, 1997c). The mechanism behind this regulation has been described by some as myogenic (Kiel, J. W. & Shepherd, A. P., 1992) and by others as a passive haemodynamic process (Riva, C. E. *et al.*, 1997c).

5.6.4.1 Hypercapnia

The effect of gas perturbation on choroidal autoregulation is largely unexplored. Some studies, using measurement methods other than POBF (Laser Doppler flowmetry (LDF), Krypton clatherate desaturation technique), have shown that choroidal blood flow responds to increased CO_2 levels (Riva, C. E. *et al.*, 1994). Trokel, S. (1965) used a rabbit model and demonstrated that choroidal blood flow increases during

hypercapnia. Due to the invasive nature of the measurement techniques employed, the majority of choroidal gas perturbation investigations have been carried out on anaesthetised animals. Of the cited literature, only the work by Riva, C. E. *et al.*, (1994) and Schmetterer, L. *et al.*, (1995) consider choroidal blood flow in the human eye. Riva's group applied LDF, a non-invasive technique, to measure choroidal blood flow in the fovea. Results showed that blood flow increased significantly in response to elevated PCO_2. Schmetterer, L. *et al.*, (1995) measured fundus pulsations by laser interferometery in which fundus measurements are directly proportionate to local pulsatile blood flow and showed that the choroid autoregulates during hypercapnia.

The present study demonstrated no measurable change in POBF during increased CO_2 breathing. Increased blood flow was apparent in the SPCAs during hypercapnia and the SPCAs are known to supply the choroid. In view of this, one would expect an increase in blood flow in these retrobulbar vessels to be reflected in the choroidal circulation. The technique used in this study to detect choroidal changes in response to blood gas perturbation differed to those used in other studies. The fact that other studies have reported increased choroidal blood flow using different techniques suggests that change did occur in the choroidal circulation during hypercapnia, but that it was outside the detection limits of the technique.

5.6.4.2 Hyperoxia

Trokel, S. (1965) reported that choroidal blood flow decreases in response to 100% O_2 breathing in rabbits. More recently, hyperoxia has been shown to result in decreased choroidal blood flow in juvenile, but not new born pigs (Hardy, P. *et al.*, 1996). Schmetterer, L. *et al.*, (1995) reported decreased fundus pulsations in response to hyperoxia in humans. Other studies have shown that the choroid does not respond to increased O_2 levels (Friedman, E., 1970; Riva, C. E. *et al.*, 1994). Although the literature supports the hypothesis that the choroid autoregulates during hypercapnia the suggestion of choroidal autoregulation during hyperoxia is controversial and not fully substantiated.

No significant variation in POBF and consequently choroidal blood flow was found in response to hyperoxia in this study. It is impossible to say whether or not autoregulation of the choroidal circulation occurred during hyperoxia, however, the fact that no significant difference in blood flow was evident in the SPCAs, coupled with no change in POBF during increased O_2 breathing, suggests that choroidal blood flow was unaffected. This outcome is consistent with previous studies, which found no significant change in choroidal blood flow during hyperoxia (Riva, C. E. *et al.*, 1994; Schmetterer, L. *et al.*, 1995).

5.6.4.3 IOP, pulse rate and volume

Apart from POBF, other parameters measured with the OBF Tonograph included mean IOP, pulse amplitude, rate and volume. No statistically significant change was observed in these parameters during hypercapnia. However, during hyperoxia, IOP and pulse rate decreased and pulse volume increased significantly from baseline (Figure 5.5); pulse amplitude did not change. Decreased IOP in response to elevated O_2 along with increased scleral rigidity has been reported (Gallin-Cohen, P. F. *et al.*, 1980). This supports the present findings which indicate decreased IOP, and unchanged pulse amplitude and POBF possibly due to the concomitant reduction in scleral rigidity.

5.6.5 Summary

The findings from this study and others suggest that elevated PCO_2 levels significantly increase blood flow in the retrobulbar and retinal vasculature as measured by CDI and SLDF respectively. No change in POBF was detected by the OBF Tonograph during hypercapnia. An increase in choroidal blood flow was expected to occur 1) because blood flow increased in the SPCAs and these vessels are known to perfuse the choroid, and 2) because findings from the current literature suggest that choroidal autoregulation does occur in response to elevated PCO_2 levels (Trokel, S., 1965;

Friedman, E. & Chandra, S. R., 1972; Schmetterer, L. *et al.*, 1995). This suggests that either the choroid did not autoregulate which seems unlikely as changes in blood flow where demonstrated in both the retina and the retrobulbar vessels, or that that the choroid did autoregulate, but at a level outside the detection limits of the technique.

Increased PO_2 resulted in decreased blood flow parameters in the OA and superior nasal peripapillary retina. No change in POBF was evident, although IOP did decrease suggesting that elevated PO_2 resulted in a change in IOP but not in choroidal blood flow. Overall, a more potent autoregulatory response was evident during increased PCO_2 compared to increased O_2, a finding coincident with other studies (Kety, S. S. & Schmidt, C. F., 1948). A variation in blood flow autoregulation during a stress situation was evident in the retrobulbar vessels and retina analogous to cerebral autoregulation which has also been shown to vary in response to different vasodilatory stimuli.

In conclusion, the findings from this study suggest that both CDI and SLDF are able to detect physiologically induced changes in ocular blood flow. The OBF tonograph did not detect changes in flow suggesting that the technique is insensitive to subtle change.

Chapter 6.

Reproducibility of retinal blood flow measurement using scanning laser Doppler flowmetry

6.1 Introduction

Scanning laser Doppler flowmetry (SLDF) provides a promising non-invasive technique that combines confocal laser scanning technology with laser Doppler flowmetry to enable ocular blood flow measurement at the retinal capillary level (Riva, C. E. *et al.*, 1992; Michelson, G. *et al.*, 1996b). The principles of Doppler flowmetry and the clinical application of SLDF are outlined in section 1.14. and 1.15.

There are a number of factors known to directly affect the reproducibility of SLDF measurements including eye movement (Michelson, G. & Schmauss, B., 1995), camera-eye distance (Kagemann, L. E. *et al.*, 1996), a large zero-offset of perfusion values (Chauhan, B. C. & Smith, F. M., 1997) the illumination level (Kagemann, L. E. *et al.*, 1999) and cardiac cycle (Sullivan, P. *et al.*, 1999). Indirectly, errors in the location of the pixel frame used for the analysis of perfusion images may also result in error. Other factors that have been shown to be important in measurements obtained with the HRT such as pupil size (Lusky, M. *et al.*, 1993b), focus setting (Hosking, S. L. & Flanagan, J. G., 1996) and cataract (Janknecht, P. & Funk, J., 1995) may also have a role.

With the exception of studies that assess the reproducibility of SLDF, the majority of investigations have based their assumptions on ocular blood flow values determined from a single perfusion image (Michelson, G. & Schmauss, B., 1995; Nicolela, M. T. *et al.*, 1996b; Langhans, M. *et al.*, 1997). Studies using the blue field technique and scanning laser fluorescein angiography have shown that capillary flow is pulsatile and varies with the cardiac cycle (Arend, O. *et al.*, 1995). In view of this, ocular blood flow measurements of the capillary bed will vary according to the point in the cardiac cycle at which they are recorded. Total acquisition time with the HRF approximates 2

seconds, this represents between one and two cardiac cycles based on a normal heart rate of 70 – 80 beats per minute (Hole, J. W., 1992). Measurements may be recorded during a systolic-diastolic-systolic phase, or potentially, a diastolic-systolic-diastolic phase (Figure 6.1.). The latter would undoubtedly result in lower flow values. This poses a real problem that can only be completely accounted for by incorporating pulse synchronisation, something which has already been suggested for use with the HRT (Chauhan, B. C. & McCormick, T. A., 1995) and more recently for the HRF (Michelson, G. *et al.*, 1998b). In the absence of such technologies it would seem appropriate to use the mean value of several perfusion images to provide a representative value for capillary blood flow across the cardiac cycle. Furthermore, using the mean of several images is likely to account for other factors affecting reproducibility.

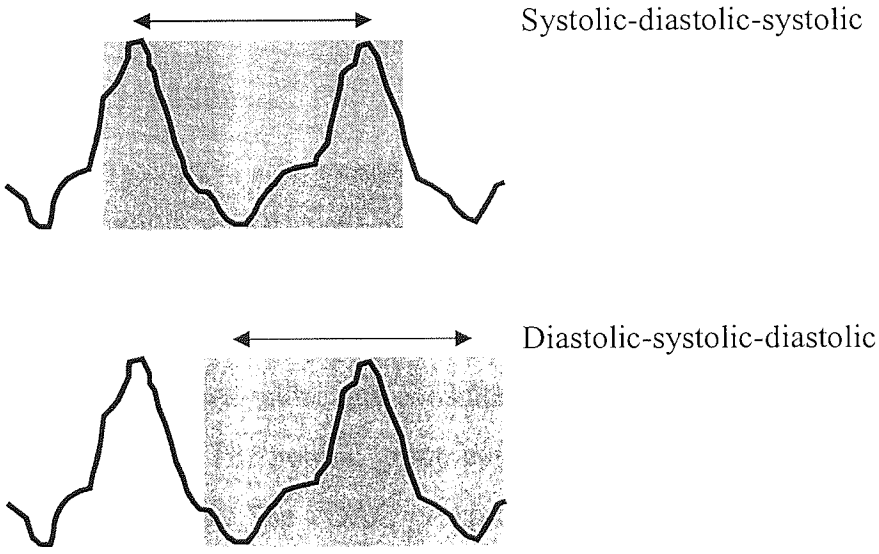

Figure 6.1.
Schematic showing two cardiac cycles and the time interval of 2 seconds where SLDF recording may take occur.

During this study, mean standard deviations for 2-10 images were used to determine the number of perfusion images required to obtain representative values of blood flow, volume and velocity. Further to this intra-class correlation coefficients (ICC) were

determined for six peripapillary retinal locations. This provided an indication of the intra-session reproducibility of SLDF across the peripapillary retina.

6.2 Aim

The aims of this investigation were:

- To determine the optimum number of perfusion images required to give an interpretation of each blood flow parameter whilst minimising experimental error and accounting for clinical practicality.
- To investigate the intra-session reproducibility of ocular blood flow parameters measured using SLDF.

6.3 Materials and methods

6.3.1 Subject sample

The subject sample consisted of 19 normal healthy volunteers and 10 high-tension POAG patients. The normal volunteers were recruited from staff at Birmingham Heartlands and Solihull NHS Trust and the surrounding community. The POAG patients were registered under one consultant ophthalmologist (JMG) at Birmingham Heartlands Hospital. The normal group consisted of 17 Caucasians, one West Indian and one Asian subject. The POAG group consisted of 10 Caucasians. Details of the subject sample are given in the Table 6.1.

	Gender		Test eye		Mean age ± SD (range)
Subject group	**Male**	**Female**	**Right**	**Left**	
Normal group (n=19)	9	10	9	10	60.5 ± 11.2 (40-76)
POAG group (n=10)	4	6	4	6	72.2 ± 6.9 (59-82)

Table 6.1. Subject sample.

6.3.2 Inclusion criteria: normal subject group

- No history of glaucoma or diabetes
- > 40 years of age
- Minimal or no lens opacities enabling a clear view of the fundus
- IOP less than 21mmHg (Goldmann applanation tonometry).
- Visual acuity better than 6/9 (Snellen)
- Astigmatism < 1.5 dioptres cylinder
- Refraction < 6 dioptres (mean sphere)
- Open anterior chamber angle (Shaffer 3-4 where 0 = closed and 4 = open)
- Normal fundus appearance based on:
    - No focal or generalised narrowing or disappearance of the neuroretinal rim with enlarged cupping and/or pallor that may be concentric or eccentric in shape.
    - No notching (focal extension of the cup)
    - Healthy coloured neuroretinal rim (without pallor)
    - No disc haemorrhages

    (Pawson, P. & Vernon, S. A., 1995; Vernon, S. A., 1996).
- No strabismus

6.3.3 Inclusion criteria: POAG group

Ten high-tension POAG patients were recruited according to the criteria outlined in section 7.4.2.

6.3.4 Ethical approval

Ethical committee approval was sought and obtained for all experimental procedures which conformed with the tenets of the declaration of Helsinki approved by Birmingham Heartlands and Solihull NHS Trust research and ethics review board.

6.3.5 Study protocol

Following informed consent, one operator obtained measurements for visual acuity (Snellen), anterior chamber angle depth (Shaffer system), distance spectacle prescription (focimetry) and corneal curvature (mm). Systolic and diastolic blood pressure were measured and a brief medical history taken to ensure no ocular disease or cardiac problems. On a separate occasion (prior to study day) each subject was reviewed by an ophthalmologist (JMG) who carried out a full assessment, including anterior chamber depth, IOP and ONH assessment.

All ocular blood flow measurements were obtained during one visit to determine the intra-visit reproducibility. Each subject was dilated to maximise the reproducibility of the measurements. In order to dilate one drop of 1% Tropicamide was instilled into the test eye, the subjects were then allowed a period of 20 minutes rest to ensure full mydriasis. Prior to ocular blood flow measurement, systolic and diastolic blood pressure was measured using a sphygmomanometer

6.3.5.1 SLDF image acquisition

In preparation for data acquisition, subject data including refraction and corneal curvature (mean radius) were inputted into the SLDF database (Heidelberg Retina Flowmeter, Heidelberg Engineering, Germany). The subject was requested to place their chin on the chin rest and fixate on a distance target.

The laser head was moved towards the subjects' eye and positioned approximately 1cm from the cornea. The laser head was then manipulated until the ONH was visible and centred on the computer screen. The intensity dial was set to maximum, whilst the sensitivity was adjusted to a level that allowed a bright but not saturated view of the fundus. Using the subjects' refraction as a guide, the laser was focused onto the superficial layer of the retinal capillary bed at either the superior, central or inferior region of the fundus. A single image series was then recorded using a 10 × 2.5 degree field (2.7mm × 0.7mm).

One of two operators (ER & SE) obtained a total of 30 images for each subject. These were separated into three sets, which were carried out in a randomised order. The three sets included:

- Ten images located in the superior section of the ONH and peripapillary retina
- Ten images located across centre of the ONH and peripapillary retina
- Ten images located in the inferior section of the ONH and peripapillary retina

Changes in focus setting have been shown to reduce the reproducibility of images obtained with the HRT (Hosking, S. L. & Flanagan, J. G., 1996). On this basis the focus setting was kept constant for consecutive images of the same subject. Throughout the examination each subject was requested to keep his or her chin on the rest. This ensured the distance between the laser beam and the eye, which has been identified as a potential source of variability for both the HRT and HRF, remained constant (Kagemann, L. E. *et al.*, 1996; Orgül, S. *et al.*, 1996).

Following acquisition the individual image sections were examined for horizontal eye movements. Although a small amount of eye movement is acceptable large movements can result in poor quality images with regular interruptions due to saccades. A quality control form was completed and scores out of 10 given for image quality (clarity and sharpness of the image) and eye movement. A combined total of 15 or more was required for the image to be accepted.

6.3.5.2 Analysis of perfusion maps

Following the acquisition of adequate image series, perfusion maps were generated using Fourier transformation. The principles of SLDF and the process by which perfusion maps are generated are outlined in section 1.16. The parameters, blood flow, volume and velocity were then measured using a 10 × 10-pixel frame (100μm × 100μm) by one of two operators (ER, KJ). This pixel frame size is considered optimal because it results in average blood flow values (averaged across a given area) and is small enough to allow avoidance of large vessels (Michelson, G. & Schmauss, B., 1995). Blood flow measurements were obtained in six peripapillary retinal areas located approximately 200μm from the disc margin:

- Superior temporal
- Superior nasal
- Central temporal
- Central nasal
- Inferior temporal
- Inferior nasal.

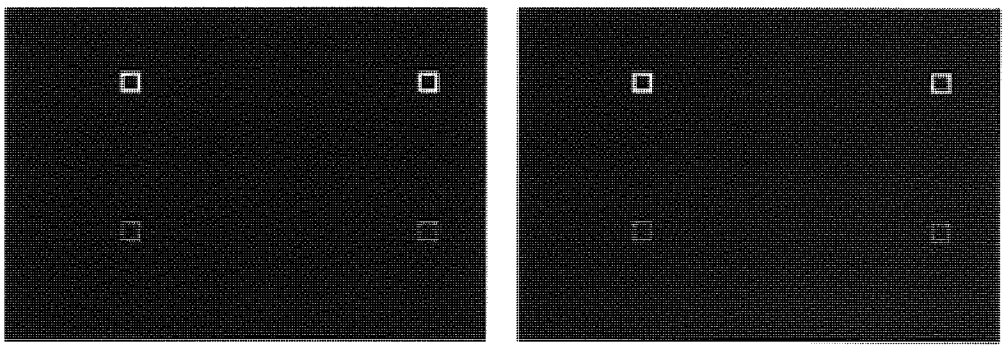

Figure 6.2. Measurement location on SLDF perfusion maps (superior and inferior ONH). The pixel frames (white boxes) indicate where perfusion measurements were taken.

Acetate sheets were used to trace over the retinal vasculature for each fundus and a blood vessel landmark (usually a vessel bifurcation) was identified to ensure that the same retinal locations were used for each image. Using this method the pixel frame

was placed on the previously identified vessel bifurcation and moved pixel by pixel by a defined amount to a location approximately 200μm from the disc margin. Large vessels were avoided. Figure 6.2. shows the measurement frame position for the superior and inferior peripapillary retina. The maximum scan frequency of the HRF is 4000Hz limiting velocity measurements to less than 1mm/sec and hence the small capillaries (Michelson, G. & Schmauss, B., 1995). Image areas interrupted by movement saccades were also avoided. Only blood flow parameters which fell within the recommended DC (reflectivity) range (80-150 A.U.) were included for analysis. The exact placement of the pixel frame differed slightly between subjects due to the position of large blood vessels, but for within subject image series every effort was made to keep the location the same.

6.4 Statistical analysis

The mean standard deviation (MSD) of 2-10 images for 19 normal subjects and 10 POAG subjects was determined for a range of parameters. See section 2.4. for SD formula. Following determination of the optimum number of images required, the ICC was used to determine the reproducibility of each parameter. The formula for ICC is given in section 2.4.

6.5 Results

6.5.1 Systemic measurement

Table 6.2. summarises the systemic measurements for systolic and diastolic blood pressure.

	Systolic BP: mean ± SD (range)	Diastolic BP: mean ± SD (range)
Normal group (n = 19)	121.9 ± 13 (105-150)	76.8 ± 7.1 (66 – 90)
POAG group (n=10)	156.6 ± 15.5 (128 – 178)	85.60 ± 6 (84 – 94)

Table 6.2. Mean ± SD values for systolic and diastolic blood pressure.

6.5.2 Ocular blood flow measurement

6.5.2.1 Determination of the number of images required to obtain representative blood flow values

Figure 6.3. gives the mean standard deviation (MSD) curves (average of all parameters) for 2-10 perfusion images for the normal and POAG subject group. It can be seen that, on average, the mean MSD reaches a plateau at 3-4 images for the normal group and 4 images for the POAG group. Figures 6.4.-6.9. give MSD curves for each SLDF parameter measured nasally and temporally in each region for the normal and POAG groups.

6.5.2.2 Reproducibility of HRF parameters (ICC based on 3 images)

On average a plateau was reached around 3-4 images for the normal group and 4 images for the POAG group (although the plateau was less distinct). Taking into account clinical efficacy, a minimum of three images should be used for SLDF measurements. On this basis ICCs were determined for three perfusion images (Table 6.3.).

Parameter	Volume (A.U.)		Flow (A.U.)		Velocity (A.U.)	
	Normal	POAG	Normal	POAG	Normal	POAG
Superior nasal	87.55	73.95	88.04	59.27	81.25	65.29
Superior temporal	73.84	81.82	71.26	54.52	72.06	52.41
Central nasal	70.57	51.65	62.11	41.56	60.61	43.13
Central temporal	63.33	69.23	67.43	72.23	60.49	52.40
Inferior nasal	62.01	62.91	62.55	64.31	63.28	63.05
Inferior temporal	61.53	76.47	76.39	77.41	63.92	80.22
Average	**69.81**	**69.34**	**71.30**	**61.55**	**66.94**	**59.42**

Table 6.3. ICC (%) for the parameters volume, flow and velocity in the peripapillary retina (based on 3 images) for the normal and POAG subject group.

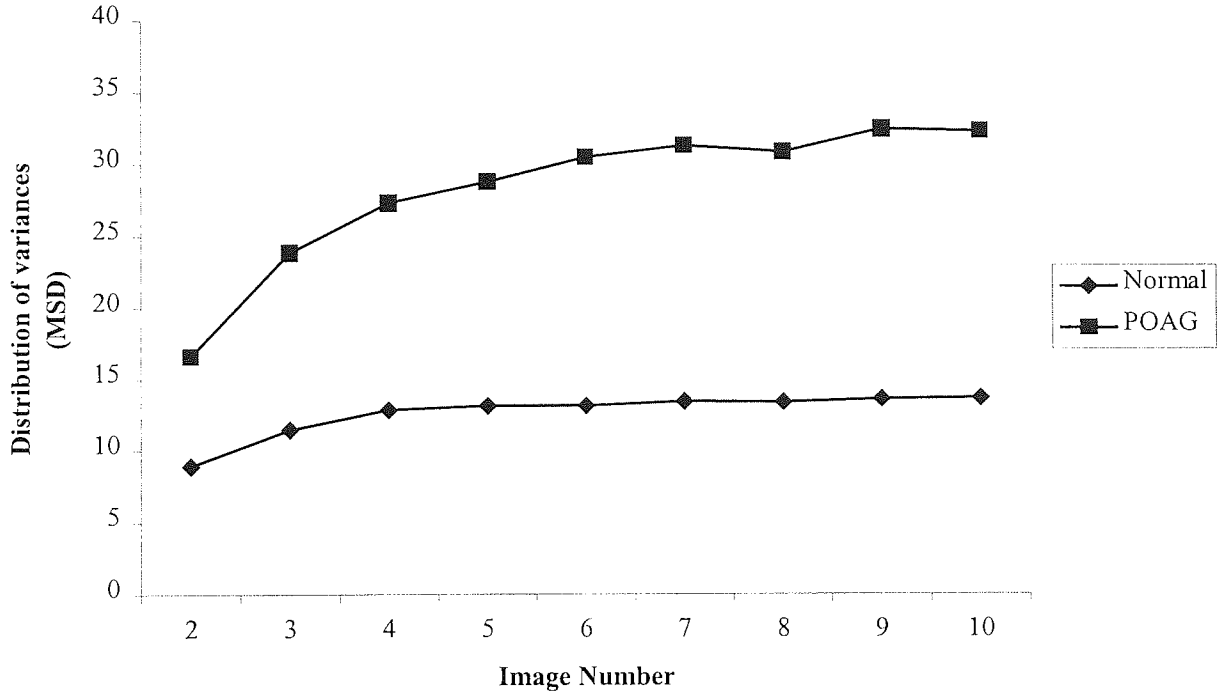

Figure 6.3. MSD curves for the average of all parameters at all locations for 2-10 perfusion images (normal and POAG group).

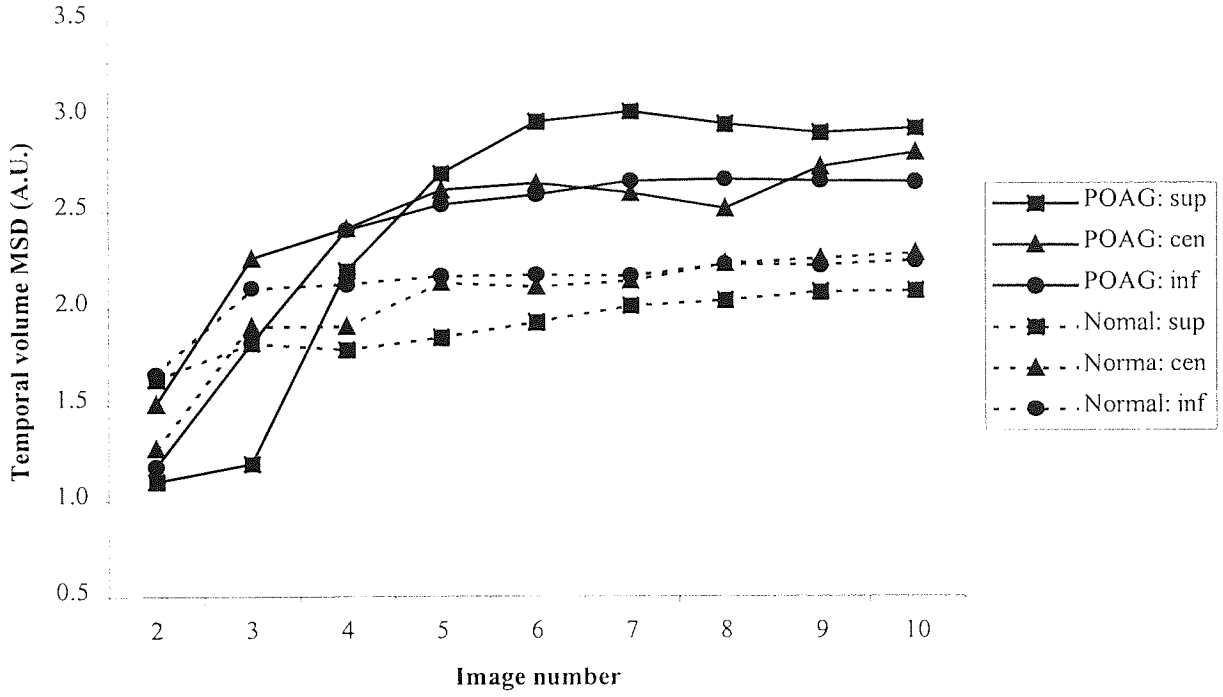

Figure 6.4. Mean standard deviation (MSD) curves for blood volume measured temporally for 2-10 perfusion images (normal and POAG group).

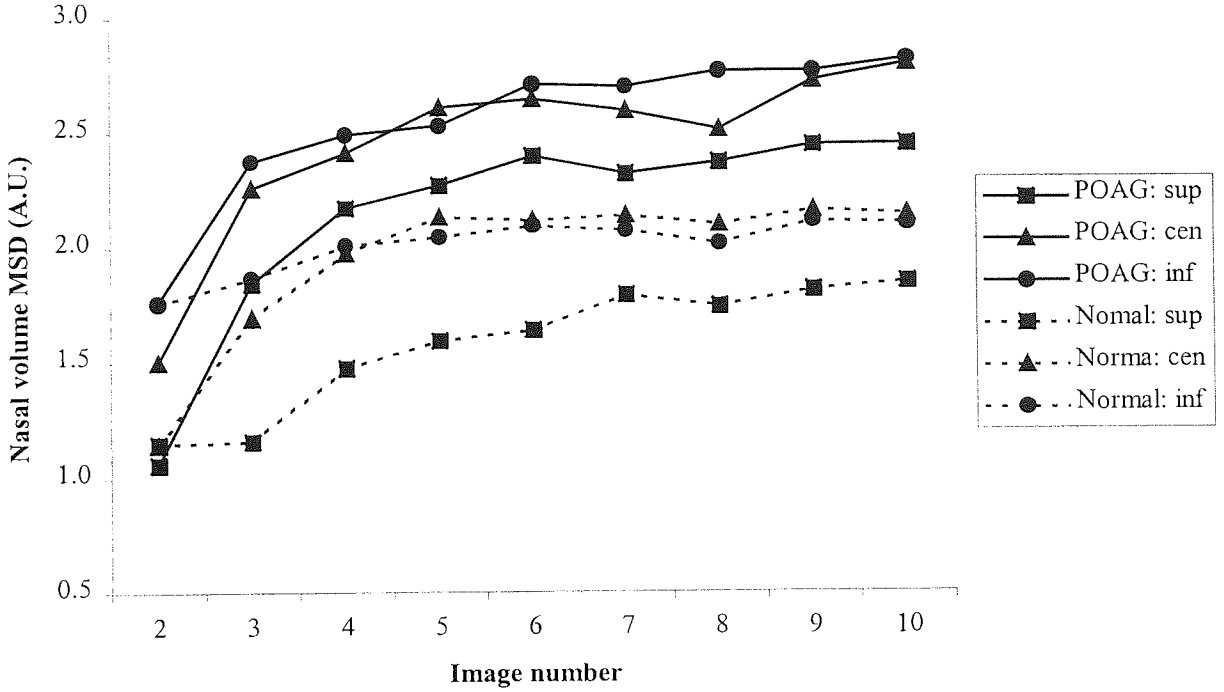

Figure 6.5. Mean standard deviation (MSD) curves for blood volume measured nasally for 2-10 perfusion images (normal and POAG group).

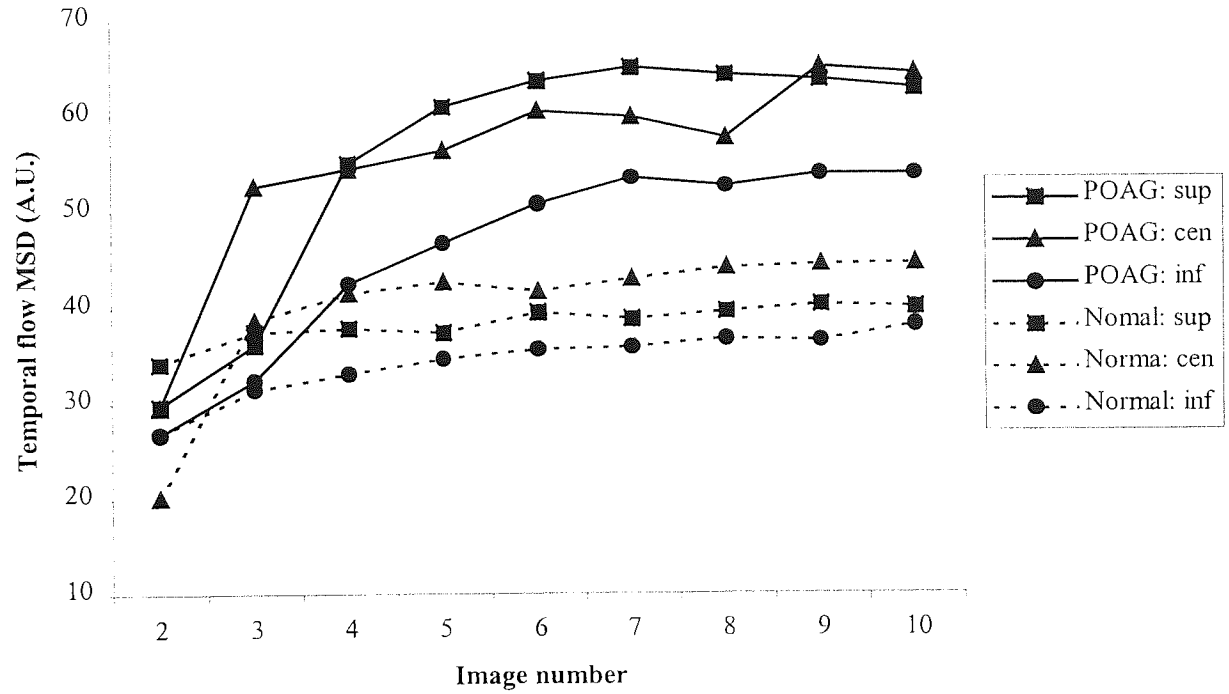

6.6. Mean standard deviation (MSD) curves for blood flow measured temporally for 2-10 perfusion images (normal and POAG group).

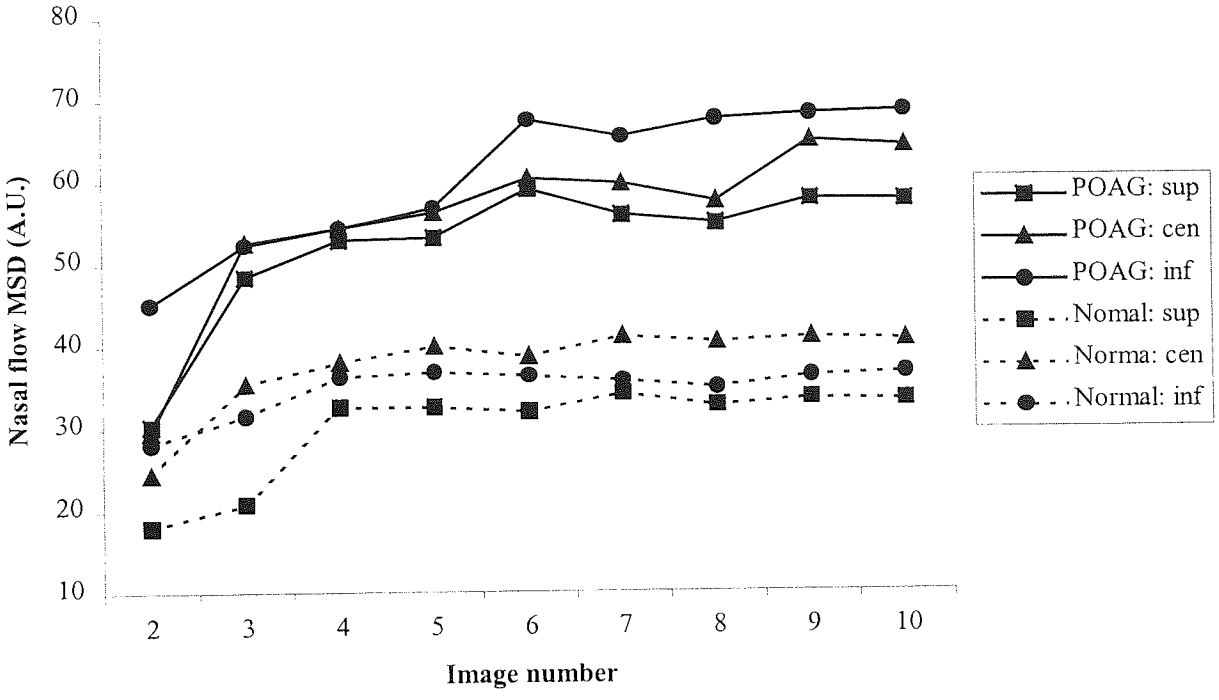

Figure 6.7. Mean standard deviation (MSD) curves for blood flow measured nasally for 2-10 perfusion images (normal and POAG group).

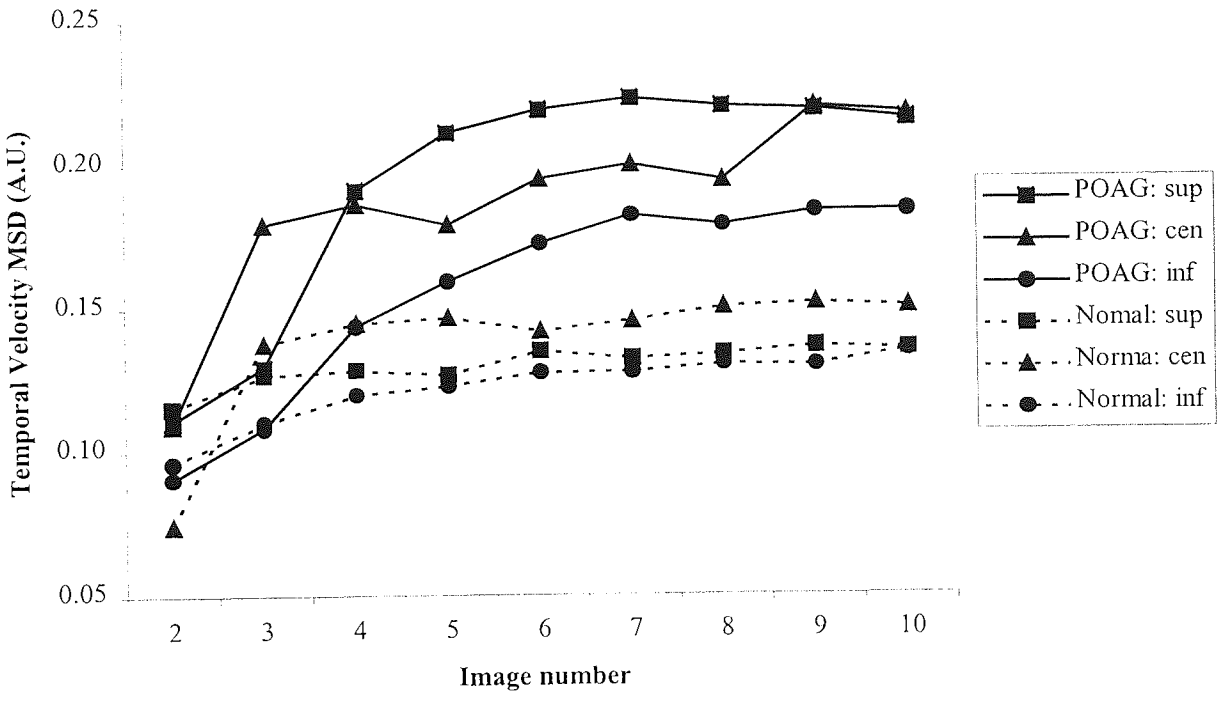

Figure 6.8. Mean standard deviation (MSD) curves for blood velocity measured temporally for 2-10 perfusion images (normal and POAG group).

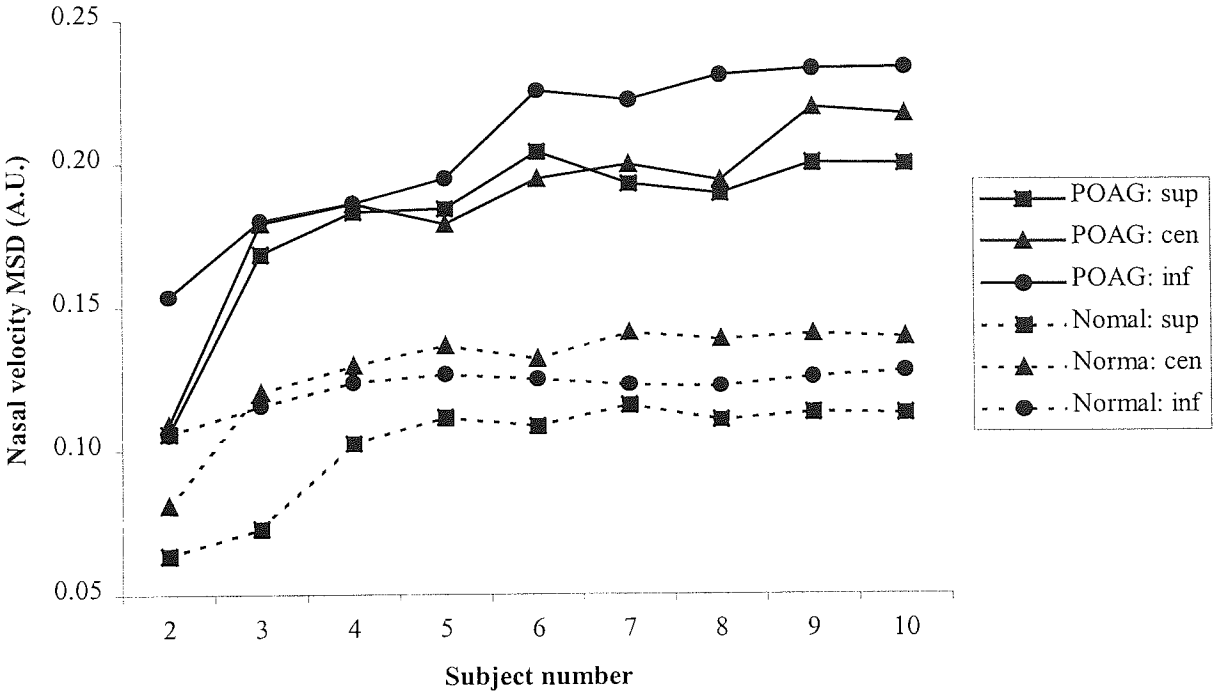

Figure 6.9. Mean standard deviation (MSD) curves for blood velocity measured nasally for 2-10 perfusion images (normal and POAG group).

6.6 Discussion

The majority of investigations that have used SLDF to assess ocular blood flow have based their assumptions on data acquired from a single image. Blood flow is a dynamic entity that varies in response to the environment through local and systemic autoregulatory mechanisms. In the absence of electrocardiograph apparatus the exact point in the cycle at which data acquisition commences is unknown. In this regard SLDF measurement can feasibly fall at any time in the cardiac cycle. This problem may be addressed in two ways: 1) pulse synchronisation may be incorporated into SLDF measurement, 2) the mean blood flow values of a series of images may be taken thereby providing a more representative of blood flow across the cycle.

6.6.1 Optimum number of images

Plotting the mean standard deviation (MSD) curves for 2-10 images based on six retinal locations (Figure 6.2.) revealed a general trend where MSD increased and started to plateau after 3 images for the normal group and after 4 images for the POAG group. The plateau was more distinctive for the normal group compared to the POAG group and the MSD values were lower indicating lower variability of ocular blood flow measures for that group. On this basis, a minimum of three perfusion images should be used for SLDF measurement.

The parameters flow, velocity and volume resulted in similar shaped MSD curves. This was expected as the parameters are interrelated (velocity = flow/volume). Nasal and temporal measurements were made across the retina for the superior, middle and inferior regions. In most cases the superior, or sometimes the inferior region, resulted in the lowest MSD values indicating lower variability for those areas. The effect of cardiac cycle and ocular pulse is likely to be uniform across the retina. Consequently, the differences in the variability of the regional measures may have been observer related. The large superior and inferior retinal vessels provide a host of landmarks from which to make measurements whereas the central region contains relatively few large vessels making repeated measurement difficult. This may explain why the central measures appeared less reproducible.

6.6.2 Reproducibility of blood flow parameters

Chauhan, B. C. & Smith, F. M. (1997) investigated the reproducibility of blood flow parameters measured with SLDF using an *in-vivo* model and reported excellent reliability of repeated measurements with coefficients of variation less than 5%. Additional sources of measurement error are introduced in the clinical environment due to subject variability. Previous studies of the intra-session variability on normal subjects reported reliability coefficients ranging from 67% - 85% for volume, 71% - 84% for flow and 69% - 84% for velocity (Michelson, G. *et al.*, 1996b; Strenn, K. *et al.*, 1997). Similar inter-session reproducibility has been reported based on repeated readings over a five-day period (Michelson, G. *et al.*, 1996b).

The ICC results obtained in this study for the normal subjects ranged from 61.5% - 87.6% for volume, 62.1% - 88% for flow and 60.6% - 81.3% for velocity, and are not dissimilar to values reported in other studies (Michelson, G. *et al.*, 1996b; Strenn, K. *et al.*, 1997). The blood flow values obtained for the POAG group in this study ranged from 51.7% - 81.8% for volume, 41.56% - 77.41% for flow and 43.13% - 80.22% for velocity. These values are lower than reported in previous studies. Clearly, the POAG subjects demonstrated greater variability than the normal subjects. In contrast, a study comparing 5 normal subjects and 6 POAG subjects reported lower variability for the POAG group; it was proposed this finding may have been related to lower flow values in the POAG group (Nicolela, M. *et al.*, 1997).

The mean age for the POAG group was significantly greater than the mean age of the normal group ($P<0.05$). Consequently, the greater variability observed for the POAG group may have been age-related. Lenticular changes are more likely to occur in older age groups and may have contributed to variability. The POAG group, although accustomed to SLDF assessment, may have been more prone to eye movement. Unlike the HRT, the HRF does not correct for eye movements and even slight movements can result in saccades that disrupt the perfusion image.

The differences in the variability of ocular blood flow measurements between the two groups may have been operator dependent. The images were acquired and measured by two different operators: ER (normal group), SE (glaucoma group). Both operators were experienced in image acquisition and followed a strict protocol. For image analysis, one operator was experienced (ER (normal group)) and one was less experienced (KJ (POAG group)). Again a strict protocol was followed, however operator variability may account for some of the error.

6.6.3 Summary

Although the acquisition of perfusion images is in theory very rapid with the HRF, in practice, obtaining good quality images can be time consuming. Unlike the HRT, the

HRF does not correct for eye movements therefore slight movements can result in saccades that appear in the perfusion image and are unacceptable for measurement. Although in some cases the saccades may be located outside the region of interest, extreme care must be taken to ensure the measured area is free from artefacts. Furthermore, the limited scan area of the HRF means that several images are required to encompass the whole of the ONH and peripapillary retina. Clinical practicality is an important consideration and in order to optimise assessment time, avoid subject fatigue and obtain measurements across the entire ONH a minimum series of three images are recommended for SLDF measurement.

The reproducibility of ocular blood flow measurements varies across the retina and is generally best in the superior and inferior regions. This may be attributable to the large retinal vessels located superiorly and inferiorly that provide good landmarks from which to make measurements.

Chapter 7.

Topographic, haemodynamic and psychophysical investigation of glaucomatous optic neuropathy: Introduction, aims and methods

7.1 Introduction

The aetiology of POAG remains unclear and it is probable that the eventual loss of retinal ganglion cells and ONH axons occurs as a result of several mechanisms. Two principle theories for a mechanism of glaucomatous ONH atrophy have evolved: The vascular and the mechanical theory (see section 1.81.-1.82.). Recently, investigators have acknowledged the probability that these two mechanisms are not mutually exclusive but overlap at least to some extent in the pathogenesis of glaucoma.

The detection of true change in the ONH during the subtle advancement of glaucomatous optic neuropathy is fundamental for the correct clinical management of the disease and prevention of visual loss. There are several methods available for evaluating the ONH, many of which require a subjective opinion that result in poor documentation that can be difficult to interpret. Recent advancements in ONH analysis systems such as digitised image analysis and cSLO provide the opportunity to quantitatively and qualitatively detect ONH change over time. These new methods are less subjective and it is proposed that they substantially reduce inter- and intra-observer error (Bishop, K. I. *et al.*, 1988; Kruse, F. E. *et al.*, 1989; Dreher, A. W. *et al.*, 1991; Lusky, M. *et al.*, 1992; Mikelberg, F. S. *et al.*, 1993; Cantor, L. B. *et al.*, 1994; Menezes, A. V. *et al.*, 1995; Azuara-Blanco, A. *et al.*, 1998b; Geyer, O. *et al.*, 1998). It is proposed that the quantitative nature of these methods may facilitate the detection of true change over time and successful application of such methods may lead to routine monitoring of glaucoma by paramedical staff.

Confocal scanning laser ophthalmoscopy provides a promising tool for the assessment of the ONH. There are a number of cross-sectional studies which recommend its

clinical use, however, the relative lack of long-term studies on the follow-up of the normal and glaucomatous optic nerve mean there is uncertainty as to whether it is capable of detecting true glaucomatous change.

Although a number of cross-sectional studies have identified HRT parameters that are important for classifying glaucomatous ONHs (Mikelberg, F. S. *et al.*, 1995; Zangwill, L. M. *et al.*, 1996; Eid, T. M. *et al.*, 1997; Iester, M. *et al.*, 1997a), there are few published longitudinal studies that identify which HRT parameters are best for detecting glaucomatous progression. Section 1.11.2.8. reviews all the cross-sectional and longitudinal studies that have been carried out.

Several methods for the measurement of ocular blood flow have evolved. More recent techniques include OBF tonography (Silver, D. M. & Farrell, R. A., 1994), LDF (Riva, C. E. *et al.*, 1992) and SLDF (Michelson, G. & Schmauss, B., 1995). The more established technique of CDI was only applied to ophthalmology in 1989 (Erickson, S. J. *et al.*, 1989). There is still some uncertainty as to the ability of ocular blood flow measures to identify abnormalities in individual glaucoma suspects, or if changes in ocular blood flow may be identified during disease progression. Although cross-sectional studies have shown ocular blood flow to be compromised in POAG compared to normal eyes (Harris, A. *et al.*, 1994b; Butt, Z. A. *et al.*, 1995; Michelson, G. *et al.*, 1996a; Duijm, H. F. A. *et al.*, 1997; Fontana, L. *et al.*, 1998; Chung, H. S. *et al.*, 1999b), there is no longitudinal study that investigates haemodynamic parameters over time in glaucoma. Neither has the long-term variability of ocular blood flow measurements in a normal eye been reported.

7.2 Aims

1. To quantify ONH topography, retinal blood flow and visual function differences at baseline between a group of normal subjects and a group of glaucoma patients.
2. To investigate the stability of topographic, haemodynamic and visual function measures in a group of normal subjects compared to the change determined in a group of glaucoma patients

3. To identify topographic, haemodynamic and visual function parameters that may be of value in monitoring change over time in individual glaucoma patients compared to normal subjects.

7.3 Subject Sample

The subject sample consisted of two groups:

- Group 1: normal healthy volunteers (n=34).
- Group 2: patients diagnosed with high-tension POAG (n=41).

Data were included for analysis for subjects who completed 4 or more visits. Only a proportion of these subjects completed the study (≥ 4 visits):

- normal healthy volunteers (n=31)
- POAG subjects (n=33)

The basis upon which sample size was determined is given in section 7. 3.1. Subjects for group 1 were recruited from staff at Birmingham Heartlands Hospital and people from the surrounding community. Subjects for group 2 were recruited from patients registered under one consultant (JMG) at Birmingham Heartlands Hospital Ophthalmology Department. Details of the subject sample are given in Table 7.1.

Group	Age		Sex		Eye	
	Mean ± SD	Range	M	F	R	L
Normal group	65 ± 8.3	45 - 77	14	17	16	15
POAG group	71.2 ± 7.6	52 - 84	14	19	17	16

Table 7.1. Subject sample.

7.3.1 Determination of sample size

When the outcome of a study is a quantitative measurement the required sample size can be calculated. Certain indices must be known, including the expected amount of change for the measured parameter (δ) and the variability of the repeated measurements (SD (σ). To compute sample sizes a significance level α and power 1-β

must be specified. The calculations depend on the function (z_α - z_β), where z_α and z_β are the ordinates for a normal distribution. This term is derived from sample size tables. The formula for the determination of sample size (m) is given below:

$$m = \left[\frac{(z_\alpha - z_\beta)^\sigma}{\delta} \right]^2$$

Equation 7.1.

Reproducibility studies have been completed on normal and POAG subjects for both the HRT (Chapter 2) and the HRF (Chapter 6). The mean SD (based on 7 images) for the measured HRT parameters for the normal and POAG group are given Table 7.2.

The average MSD for the measured parameters was 0.048 for the POAG group (0.005-0.338) and 0.018 for the normal group (range was 0.004 – 0.067). The highest average SD was used (0.048). Change was considered to have occurred if the measures differed by one half of the SD (0.024). Taking this value, a power of 80% and a significance level α of 0.05 the sample size is:

$$m = \left[\frac{2.802x0.048}{0.024} \right]^2 = 31.4$$

Equation 7.2.

Parameter	POAG group (MSD)	Normal group (MSD)
Cup area (mm^2)	0.030	0.027
C:D ratio	0.057	0.013
Rim area (mm^2)	0.051	0.027
Height Var Contour (mm)	0.044	0.023
Volume below ref (mm^3)	0.024	0.007
Volume above ref (mm^3)	0.027	0.020
Mean cup depth (mm)	0.012	0.007
Max cup depth (mm)	0.025	0.023
Third moment	0.015	0.016
Mean RNFL thick (mm)	0.024	0.014
RNFL cross-sectional area (mm^2)	0.115	0.067
Classification	0.338	0.026
Effective area (mm^2)	0.030	0.009
Mean Height in Contour (mm)	0.019	0.008
Volume below surface (mm^3)	0.017	0.004
Volume above surface (mm^3)	0.005	0.004
Mean depth in contour (mm)	0.009	0.007
Ref height (mm)	0.033	0.023
Average	**0.048**	**0.018**

Table 7.2. Mean SD values for the HRT parameters. Based on 7 images.

The longitudinal follow-up also included HRF measurement (flow, volume and velocity). The reproducibility of HRF parameters in normal and POAG subjects were determined in Chapter 6. The average SD for the HRF parameters (3 images) are given in Table 7.3. In each case the average MSD was greater for the POAG group and these values were taken forward for sample calculations. The calculated minimum subject samples for flow, volume and velocity, based on a power of 80% and significance level α of 0.05, the average SD for the parameter and an expected change of one half the SD are given below:

$$m(flow) = \left[\frac{(2.802 \times 44.773)}{22.3865}\right]^2 = 31.4$$

$$m(volume) = \left[\frac{2.802 \times 1.92}{0.96}\right]^2 = 31.4$$

$$m(velocity) = \left[\frac{2.802 \times 0.10}{0.5}\right]^2 = 31.4$$

Equation 7.3.

	SD (based on 3 images)		
Parameter	**Region**	**POAG group**	**Normal group**
Flow	Superior nasal	48.49	20.78
	Superior temporal	36.10	37.49
	Middle nasal	52.55	35.41
	Middle temporal	46.85	38.67
	Inferior nasal	52.33	31.58
	Inferior temporal	32.32	31.35
	Average	**44.77**	**32.55**
Volume	Superior nasal	1.84	1.16
	Superior temporal	1.19	1.82
	Middle nasal	2.26	1.69
	Middle temporal	2.01	1.90
	Inferior nasal	2.37	1.86
	Inferior temporal	1.82	2.10
	Average	**1.92**	**1.76**
Velocity	Superior nasal	0.17	0.07
	Superior temporal	0.13	0.13
	Middle nasal	0.18	0.12
	Middle temporal	0.16	0.14
	Inferior nasal	0.18	0.12
	Inferior temporal	0.11	0.11
	Average	**0.10**	**0.11**

Table 7.3. Mean SD values for HRF parameters. Based on 3 images.

Taking into account both HRT and HRF parameters, the minimum sample size is 31 subjects. Due to the longitudinal nature of the study a further 20% was added to the sample to allow for dropout (37 subjects).

A total of 41 POAG subjects and 34 normal subjects were recruited for the study. A greater number of POAG subjects were recruited to account for the greater variability in that group and to ensure the minimal sample size of 31 was maintained despite subsequent dropout. Eight POAG subjects and 3 normal subjects did not complete the study the reasons for which are outlined in section 8.1. The remaining sample of 33 POAG and 31 normal subjects completed the study.

7.4 Inclusion criteria

7.4.1 Group 1 (normal subject group)

- No history or evidence of glaucoma.
- No diabetes.
- No eye surgery.
- No eye disorders known to affect the optic nerve or age related macular degeneration.
- Intraocular pressure <21mmHg (Goldmann applanation tonometry).
- Normal open anterior chamber angle (Shaffer 3-4 where 0 = closed and 4 = open).
- Minimal or no lens opacities allowing a clear view of the fundus.
- Normal fundus appearance based on:
    - No focal or generalised narrowing or disappearance of the neuroretinal rim with enlarged cupping and/or pallor that may be concentric or eccentric in shape
    - No notching (focal extension of the cup)
    - Healthy coloured neuroretinal rim (without pallor)
    - No disc haemorrhages

    (Pawson, P. & Vernon, S. A., 1995; Vernon, S. A., 1996)
- No visual field loss as determined by the Humphrey Field Analyser 640 (Zeiss-Humphrey, Inc.) central 24-2 full threshold standard test strategy and based on:
    - Good reliability, with a fixation loss of <20% and false negative and false positive rates of <15%.
    - Glaucoma Hemifield Test within normal limits.

    (Hodapp, E. *et al.*, 1993; Park, K. H. *et al.*, 1996)
- Astigmatism < 2 dioptres cylinder.
- Refractive error < 6.00 dioptres mean sphere.
- Best corrected visual acuity of 6/12 or better (Snellen).
- > 40 years of age.
- No strabismus.

7.4.2 Group 2 (POAG subject group)

The inclusion criteria may be further differentiated into those that were used to define the high-tension POAG group (mandatory) and those that were chosen to eliminate other conditions and maximise the potential of detecting change over the study period.

7.4.2.1 Mandatory criteria

- Untreated intraocular pressure of more than 22mmHg (Goldmann applanation tonometry) on at least one occasion. This ensured that only high-tension glaucoma subjects were recruited in the study. The mean IOP of a normal population is 15.5 mmHg (Moses, R. A., 1975) and it is generally thought that IOP of more than 21mmHg may be classed as high-tension glaucoma (Jonas, J. B. & Papastathopoulos, K. I., 1995).

- Glaucomatous ONH damage. Defined subjectively by one of two ophthalmologists and based on two of the following:
  - Focal or generalised narrowing or disappearance of the neuroretinal rim.
  - Enlarged cupping and/or pallor that may be concentric or eccentric in shape.
  - Notching (focal extension of the cup).
  - Nasal excavation (concentric enlargement on the nasal side of the disc, indicated by fly-over blood vessels).
  - Pallor of the neuroretinal rim.
- ONH haemorrhages occurring at the disc margin.

  (Pawson, P. & Vernon, S. A., 1995; Park, K. H. *et al.*, 1996; Vernon, S. A., 1996)

- Early or moderate visual field loss as detected by the Humphrey Field Analyser 640 (Zeiss-Humphrey, Inc.) with the central 24-2 full threshold standard test strategy and defined according to Hodapp, E. *et al.*, (1993). Using this classification an early defect was defined as:
  - Mean defect (MD) of less than –6dB.

- On the pattern deviation plot, fewer than 25% of the points are depressed below the 5% level, and fewer than 10 points depressed below the 1% level.
- No point in the central 5° has a sensitivity of less than 15dB.
- Glaucoma Hemifield Test outside normal limits.

A moderate defect was defined as:

- Mean defect (MD) of less than –12dB.
- On the pattern deviation plot, fewer than 50% of the points are depressed below the 5% level, and fewer than 20 points depressed below the 1% level.
- No point in the central 5° has a sensitivity of 0dB.

- Only one hemifield may have a point with sensitivity <15dB within 5° of fixation.

Only reliable visual fields, defined as having a fixation loss of < 20% and false negative and false positive rates of <15%, were used for analysis (Hodapp, E. *et al.*, 1993).

7.4.2.2 Other inclusion criteria

- No history or evidence of any ocular disorder that would cause optic nerve damage other than POAG.
- No diabetes.
- No age related macular degeneration.
- Normal open anterior chamber angle (Shaffer 3-4 where 0 = closed and 4 = open).
- C:D ratio < 0.9 to avoid end-stage POAG and increase the likelihood of observing change throughout the duration of the study.
- Minimal or no lens opacities allowing a clear view of the fundus
- Astigmatism < 2 dioptres cylinder.
- No miotic therapy.
- No eye surgery other than trabeculectomy.
- Refractive error < 6.00 dioptres mean sphere.
- Best corrected visual acuity of 6/12 or better (Snellen).
- No strabismus.

7.5 Ethical Approval

Ethical committee approval was sought and obtained for all experimental procedures, which conformed with the tenets of the declaration of Helsinki approved by Birmingham Heartlands and Solihull NHS Trust research and ethics review board.

7.6 Study Design – visits and follow-up

An initial assessment at baseline was necessary to ensure each subject satisfied the inclusion criterian. Following this subjects were followed-up every 4 months (within a 2 week tolerance) for a total of 16 months (5 research visits). The POAG subject group was also followed clinically by an ophthalmologist (5 clinic visits). The research visit always succeeded the clinic visit by two weeks. Table 7.4. summarises the initial assessment, research and clinic visits. Sections 7.8.1., 7.8.2. and 7.8.10. give a detailed account of the procedures performed during: 1) initial assessment; 2) research visit; 3) clinic visit.

Time (months)	0	0	4	4	8	8	12	12	16	16
Appointment	Init 1	Res 1	Clin 2	Res 2	Clin3	Res 3	Clin 4	Res 4	Clin 5	Res 5
Group 1	⨯	⨯	♦	⨯	♦	⨯	♦	⨯	♦	⨯
Group 2	⨯	⨯	⨯	⨯	⨯	⨯	⨯	⨯	⨯	⨯

Table 7.4. Study Design. Int = Initial ophthalmic assessment, Clin = Clinical appointment (ophthalmologist), Res = Research appointment. ⨯ = Subjects from that group attended, ♦ = Subjects from that group did not attend. Group 1 = normal contgrols, group 2 = POAG patients.

7.7 Determination of test eye

Studies have shown that using data from both eyes of an individual introduces bias into the experiment as data from fellow eyes are more likely to exhibit similarities than data from eyes of different individuals (Murdoch, I. E. *et al.*, 1998). On this basis, only measurements from one eye of each subject were included for analysis. The test eye was chosen randomly for group one. For group two, the test eye was predetermined for patients with unilateral glaucoma. For those patients with bilateral glaucoma, the eye that fulfilled the inclusion criteria was chosen. If both eyes fulfilled

the inclusion criteria, the eye with the best visual acuity was chosen. Table 7.1. outlines the number of right and left eyes in each group.

7.8 Materials and methods

7.8.1 Initial assessment (ophthalmologist)

Medical records were reviewed and potentially suitable patients identified. Following informed consent each subject underwent a full ophthalmic assessment by a consultant ophthalmologist (JMG) including:

1. Visual acuity (Snellen).
2. Complete medical history, including current medication, surgery undergone and family history of medical disorders such as diabetes and glaucoma.
3. Assessment of anterior chamber depth (Shaffer 0-4).
4. Intraocular pressure assessment by Goldmann Applantion Tonometry. One drop containing Lignocaine (4%) and fluorescein (0.25%) was instilled into the test eye. The scale of the tonometer was set at 10mmHg prior to taking the measurement. If the IOP varied with the cardiac pulse then the lowest value was recorded as recommended by Goldmann.
5. ONH assessment. Subjects were dilated using Tropicamide 1%. The ONH was then assessed using slit lamp biomicroscopy with a 60 dioptre lens. A detailed clinic sheet describing the characteristics of the ONH was completed.

7.8.2 Research visit (protocol)

7.8.3 Test sequence

Table 7.5. summarises the test sequence for a research visit. Procedures marked with an asterix denote preliminary tests that were carried out on the first visit only. The individual tests and procedures are outlined in detail in sections 7.8.4.-7.8.9.

Test order	Test
1	Visual acuity*
2	Visual field (test eye first)
3	Keratometry*
4	Dilation
5	cSLO
6	SLDF
7	IOP

Table 7.5. Test sequence. *Tests completed at visit 1 only.

7.8.4 Visual acuity

Uncorrected and best corrected (pin-hole) distance visual acuity was assessed using a Snellen chart.

7.8.5 Keratometry

The radius of curvature was measured for each principle meridian of the cornea (mm) for the test eye (Zeiss (Oberkochen) ophthalmometer). This measurement is required for the optical calculation with the HRT (see section 1.11.2.1.). The mean of two measurements was used for subsequent analysis.

7.8.6 Perimetry

7.8.6.1 Visual field background and protocol

A central program 24-2 full threshold visual field test was completed (Humphrey Field Analyzer (HFA) 640, Zeiss-Humphrey inc.). The technique of visual field assessment using the HFA is described in section 1.9.2.1. The test eye was always assessed first (POAG group) and the non-test eye occluded with an eye patch. A trial lens prescription was calculated using the subjects distance prescription and an addition determined from the date of birth (see table 7.6). The trial lens (including cylinder correction) was placed in the trial frame and positioned close to the patients

eye. If the patient was emmetropic then the appropriate lens addition was used according to the age of the subject (Table 7.6.).

Age	Near Addition
40-44	+ 1.50
45-49	+ 2.00
50-54	+2.50
55+	+3.00

Table 7.6. Refractive Correction for visual field assessment.

Standard parameters were used including:

- Blind spot size of Goldmann III.
- White stimulus size of III.
- Background luminance of 31.5 asb.

The subjects were instructed how to carry out a visual field examination prior to testing. The subject's eye was monitored continuously throughout testing by an internal camera. A 30-second rest was routinely given at five-minute intervals throughout testing. If signs of fatigue were evident (i.e. loss of fixation) then extra rests were given. After the visual field assessment was completed for the test eye, the subject rested before repeating the process for the fellow eye (POAG group only). False-positive and negative errors that exceeded 15% indicated poor reliability and if possible the test was repeated (Hodapp, E. *et al.*, 1993).

7.8.6.2 Visual field analysis

Following visual field testing, a Statpac 2 single field analysis was performed (see section 1.9.2.2.). The following global visual field indices calculated by Statpac 2 were entered into a database for statistical analysis (see section 1.9.2.2. for a complete description of parameters):

- Mean deviation (MD).
- Pattern standard deviation (PSD).
- Short-term fluctuation (SF).

- Corrected pattern standard deviation (CPSD).

7.8.7 Pupil Dilation

The test eye of all subjects was dilated using one drop of Tropicamide 1% instilled into the eye. The subject was allowed a minimum of 20 minutes to ensure complete mydriasis (checked by the pupillary light reflex).

7.8.8 Confocal scanning laser ophthalmoscopy (cSLO)

The Heidelberg Retina Tomograph (HRT, Heidelberg Engineering Germany) was used to obtain topography measurements. The technique and principles of cSLO are described in section 1.11.2.

7.8.8.1 HRT image acquisition

One operator (ER) acquired 7 images of the test eye for each subject in accordance with the method outlined in section 2.3.5.3.

7.8.8.2 HRT image analysis

Following acquisition of 7 acceptable image series, topography maps were generated using the system software. The process used to determine the topography maps is detailed in section 1.13.2.2. and includes alignment for horizontal and vertical shifts, rotation and tilt. A contour line was interactively drawn around the edge of the optic disc on the first topography image using Elschnig's scleral ring for reference. If the contour line was acceptable, i.e. encompassed the whole optic disc with an adequate height profile it was exported from the first image and imported into subsequent images for each individual subject. Using the stereometric software (version 2.01) 15

stereometric parameters were determined globally, and 8 were measured regionally. Table 7.7. outlines the parameters measured globally and regionally. A detailed description of the individual parameters, the tissue being measured, and the locations from which they are measured is given in Chapter 1, section 1.11.2.4.

The topographic parameter data were saved from the HRT to 3.5'' magnetic media. The data were then imported to an Excel database using a Macro programme to ensure that the data were in an appropriate format for statistical analysis.

Parameter	Global 360°	Superior nasal 45°	Superior temporal 45°	Temporal 90°	Nasal 90°	Inferior nasal 45°	Inferior temporal 45°
C:D area ratio	×						
Mean height contour	×	×	×	×	×	×	×
Height variation contour	×	×	×	×	×	×	×
Volume below surface	×	×	×	×	×	×	×
Volume above surface	×	×	×	×	×	×	×
Volume below reference	×	×	×	×	×	×	×
Volume above reference	×	×	×	×	×	×	×
Maximum depth	×	×	×	×	×	×	×
Third moment	×	×	×	×	×	×	×
RNFL thickness	×						
Mean depth contour	×						
Rim area	×						
Cup area	×	×	×	×	×	×	×
Classification	×						
Reference height	×						

Table 7.7. HRT parameters measured globally and regionally.

7.8.8.3 Scanning laser Doppler flowmetry (SLDF)

The Heidelberg Retina Flowmeter (HRF, Heidelberg Engineering Germany) was used to obtain SLDF measurements. The technique and principles of SLDF measurement with the HRF is described in detail in section 1.15.

7.8.8.4 HRF image acquisition

One operator (ER) acquired 6 images of the test eye for each subject in accordance with the method outlined in section 6.5.5.1. The images formed two sets that were completed in a random order:

- 3 images located in the superior section of the ONH and peripapillary retina
- 3 images located in the inferior section of the ONH and peripapillary retina

7.8.8.5 Analysis of perfusion maps

Following the acquisition of adequate image series, perfusion maps were generated automatically by the software using Fourier transformation. The principles of SLDF and the process by which perfusion maps are generated are outlined in section 1.16. The parameters, blood flow, volume and velocity were then measured using a 10 × 10-pixel frame (100μm × 100μm). This pixel frame size is considered optimal because it results in average blood flow values (averaged across a given area) and is small enough to avoid large vessels (Michelson, G. & Schmauss, B., 1995). Blood flow measurements were obtained in four peripapillary retinal areas located approximately 200 μm from the disc margin (Figure 6.2.):

- Superior temporal region.
- Superior nasal region.
- Inferior temporal region.
- Inferior nasal region.

Acetate sheets were used to trace over the retinal vasculature for each fundus and a blood vessel landmark (usually a vessel bifurcation) identified to ensure that the same retinal locations were used for each image. Using this method the pixel frame was placed on the previously identified vessel bifurcation and moved pixel by pixel by a defined amount to a location approximately 200μm from the disc margin. The maximum scan frequency of the HRF is 4000Hz limiting velocity measurements to less than 1mm/sec and hence the small capillaries (Michelson, G. & Schmauss, B., 1995). For this reason, areas containing large vessels were avoided. Image areas interrupted by movement saccades were also avoided. Only blood flow parameters which fell within the recommended DC (reflectivity) range (80-150) were included for analysis (Michelson, G. *et al.*, 1996b). The exact placement of the pixel frame differed slightly between subjects due to the position of large blood vessels, but for within-subject image series every effort was made to keep the location the same.

The blood flow parameter data (flow, volume and velocity for the 6 locations) were saved from the HRF to 3.5'' magnetic media and then imported to an Excel database using a Macro programme.

7.8.9 Intraocular pressure assessment

Following image acquisition, the IOP was assessed in both the test and fellow eye of each subject using Goldmann tonometry. In order to measure IOP the cornea was anaesthetised and made visible by instilling one drop of Lignocaine 4% and Fluorescein 0.25% (minims) into each eye. The subject was instructed to blink and place their chin on the rest. Using a sterile tonometer head the cornea was applanated and the IOP recorded. If the IOP varied with the cardiac pulse then the lowest value was recorded as recommended by Goldmann.

7.8.10 Clinic visit

Clinic visits were carried out for the POAG group only. The patients were followed-up every four months for a total of 16 months (5 clinic visits in total). The clinic visit always succeeded the research visit by approximately 2 weeks. The purpose of the clinic visit was to document the ophthalmologists assessment of the ONH at regular time interval. Subjective measurements and drawings were made of vertical and horizontal C:D ratio, disc size and shape, pallor, peripapillary atrophy and focal rim notching. The configuration of the blood vessels was also noted including bayoneting and fly-over vessels. The clinic visit protocol was identical to the initial visit protocol outlined in section 7.8.1. with the exception of point 4 (assessment of anterior chamber depth). A clinic sheet describing the ONH was completed by the ophthalmologist at each visit to facilitate the detection of change.

7.9 Statistical analysis

A number of statistical tests were used to analyse the different data including Student's unpaired t-tests, (repeated measures) analysis of variance, analysis of covariance, coefficient of determination (r^2) and Pearson's product-moment correlation coefficient (r). These statistical methods are outlined in the sections below. Factor analysis was also performed and this is outlined in section 7.9.9. The way in which the tests were applied to the separate data sets are discussed in section 7.9.9.1 through to section 7.9.13.

7.9.1 Tests for normality

Normally distributed data, when plotted as a frequency histogram, forms a Gaussian or bell-shaped curve and the vast majority of the observations (95%) fall within two standard deviations of the mean (Bland, J. M., 1987a). The Kolmogorov-Smirnov statistical test can be used to test for a normal distribution. If data are not Gaussian,

then the stem and leaf plots are examined for obvious outliers in the data. A Gaussian distribution is a probability distribution of a random variable given by:

$$f(x) = \frac{1}{\sigma\sqrt{2\pi}} \exp\left[\frac{1}{2}\frac{(x-\mu)^2}{\sigma^2}\right] \qquad \text{Equation 7.4.}$$

Where: μ and σ are the mean and variance of the random variable (x).

7.9.2 Student's unpaired t-test

Student's 2-tailed unpaired t-test was carried out to compare the means of two groups unequal in size. The test statistic is given as:

$$t = \frac{\bar{x}_1 = \bar{x}_2}{\sqrt{s^2\left(\frac{1}{n_1} + \frac{1}{n_1}\right)}} \qquad \text{Equation 7.5.}$$

Where:

x_1 and x_2 are means of the sample size n_1 and n_2.

S^2 is an estimate of the assumed common variance given by:

$$s^2 = \frac{(n_1 - 1)s_1^2 + (n_2 - 1)s_2^2}{n_1 + n_2 - 2} \qquad \text{Equation 7.6.}$$

7.9.3 Analysis of variance (ANOVA)

Analysis of variance (ANOVA) studies the effect of one or more nominal independent variables on a continuous dependent variable. This is done by determining how much of the variability in the dependent variable can be explained by the independent

variable. To compute this, a measure that is mathematically very similar to variance (mean square) is calculated by dividing the sum of squares of deviations from the means by the degrees of freedom for the effect. The mean square is then divided by an estimate of variance (residual mean square). This ratio results in an *F*-statistic, the probability (p-value) of which can be used to determine how important an effect is in explaining the behaviour of the dependent variable.

7.9.4 Repeated measures analysis of variance (reANOVA)

ANOVA makes the assumption that each observation in the analysis is independent of other observations. In some cases the observations were not independent, they were repeated observations on the same individual over time. In such a case repeated measures ANOVA (reANOVA) was carried out.

7.9.5 Analysis of covariance (ANCOVA)

In cases where there was an underlying pre-study difference between sets of data (e.g. age) it is possible to equalise the differences by a statistical method. Analysis of covariance (ANCOVA) provides a method for removing pre-study variations from the variable or parameter being assessed before testing for significant differences between the groups (Williams, F., 1992). In this case age was the pre-study difference that existed between the two groups. By using age as a covariate in the ANOVA analysis, the pre-existing difference in the mean age between the two groups that may have otherwise had an effect on parameter behaviour during the study period, was ruled out.

7.9.6 Coefficient of determination (r^2) and correlation coefficient (r).

The coefficient of determination (r^2) gives the square of the Pearson product moment correlation and is expressed as the proportion of the variance in the dependent variable that is explained by the independent variable. In simple terms, this statistical measure provides a value that describes the magnitude of an effect (e.g. time) on a parameter or

variable (e.g. cup area). A value is given between 0-1, where 1 indicates that all of the variance in the dependant variable can be explained by the independent variable. The square root of the r^2 is the correlation coefficient (r). Guilford, J. P. (1956) provided an approximate guide on the interpretation of *r*.

- < 0.20 indicates a slight, almost negligible correlation
- 0.20-0.40 indicates a low correlation that has a definite, but small, relationship
- 0.40-0.70 indicates a moderate correlation with a substantial relationship
- 0.70-0.90 indicates a high correlation with a marked relationship

For this study a significant difference was assumed if $r \geq 0.775$ or $r^2 \geq 0.6$. r^2 was determined from the sums of squares given by ANOVA. The formula for r^2 is:

$$r^2 \frac{SS_{reg}}{SS_{reg} + SS_{res}}$$

Equation 7.7.

Where:

SS_{reg} = sums of squares (regression)

SS_{res}= sums of squares (residual)

7.9.7 Cross-sectional comparison of baseline values

Student's unpaired two-tailed t-test was used to compare baseline measures of HRT, SLDF, IOP and visual function data for the two subject groups. Bonferroni correction was applied because of the repeated measurements on the same tissue, on this basis a p-value < 0.01 was regarded as significantly different (Bland, J. M. & Altman, D. G., 1995). This analysis provided preliminary data for comparing between the two groups and highlighted individual parameters that were different at baseline and important for distinguishing between POAG and normal eyes.

7.9.8 Analysis of HRT data to detect change over time

7.9.8.1 HRT change by group

The regional and global HRT data were tested for normality using the method outlined in section 7.9.1. SAS was used to perform ANCOVA to assess for change over time between the normal and glaucoma subject groups for the global and regional HRT data. In each case age was used as the covariate to correct for a small but significant ($p>0.05$) age difference between the two groups. Group was defined as the independent variable (between factor) and visit was defined as the dependent variable.

Bonferroni correction was applied to the HRT data analysis to guard against increased type I error that can occur a result of multiple testing and to maintain the critical value of alpha (0.05) (Bland, J. M. & Altman, D. G., 1995). On this basis a significant difference was said to exist between the two groups over time if $p < 0.01$ and $r^2 \geq .0.6$. It was also important that the within-visit variation did not demonstrate significant differences ($p>0.01$).

7.9.8.2 HRT change by patient

SAS was used to perform reANOVA to assess for change over time for each individual subject. In each case "visit" was defined as the dependent variable and "parameter" as the independent variable. A significant difference existed between the two groups over time if $p<0.01$ and $r^2 \geq 0.6$ (Bonferroni corrected). It was also important that the within-visit variation did not demonstrate a significant difference ($p>0.01$).

7.9.9 Factor analysis of HRT data to assess change over time

Factor analysis was performed for the regional and global HRT data using the principle components approach available by the factor procedure in SAS. Where there

are a number of related parameters, as with the HRT data, it can be useful to determine whether they may be combined into fewer variables or underlying factors. The technique of factor analysis takes a matrix of inter-correlations from a relatively large number of variables and provides a method for determining a smaller number of hypothetical variables that explain or underlie the original parameters.

The first step of factor analysis is to take the matrix of inter-correlations for the data set and determine how many factors are required to describe the data. This is done by examining the eigenvalues of the correlation matrices, which are indicies of the variance explained by each factor. There are several ways to determine the number of factors required to describe the data. Some investigators choose to include factors with an eigenvalue greater than 1 and consequently the variance of more than one parameter associated with it. This is known as the eigenvalue 1.0 test or Kaiser criterion. This method may be appropriate for data containing a large number of parameters (>50), but for data contained within a smaller number of parameters, as in the present study, it is usual to plot scree plots of the eigenvalues (Cattell's Scree Test). The eigenvalues are plotted and the curve examined to find where the slope of the curve changes from negative to close to zero. The last real factor is the one before the scree begins (the relatively flat portion of the curve).

At this stage in the analysis the number of variables is equal to the number of factors and all of the factors are unrelated (orthogonal). By definition, the most variance is associated with factor one decreasing to the last factor which contains the least amount of variance. The factor matrix gives the correlation associated with each variable and each factor. The variables are said to load onto each factor by a given score.

In order to ensure that the factors reflect the hypothetical variables underlying the various parameters, the factors are rotated (whilst keeping them 90° apart). There are several methods of rotation; the one most commonly used is called varimax. Following rotation the variances are redistributed resulting in the rotated factor matrix. Although the amount of variance associated in the model remains the same, the method of rotation redistributes the variance more equally amongst the factors.

Furthermore, the rotational effect causes individual variables to load more clearly onto specific factors simplifying the final identification of factor content.

The rotated factor matrix is examined to identify which variables or parameters belong with which factor. In most cases variables load clearly onto a single factor, however, occasionally a variable will be factorially complex loading onto more than one factor. In this case it is reasonable for the variable to be removed from the model (Norman, G. R. & Streiner, D. L., 1994). The final result is a reduced number of hypothetical variables (factors) that underlie the data.

7.9.9.1 Factor analysis change by group

ANCOVA was carried out on two predetermined factors for the global and regional data sets to assess for a significant difference between the two groups over time. Age was used as the covariate, group as the independent variable and visit as the dependent variable. Bonferroni correction was not applied as the repeated measurements were already reduced to two variables following factor analysis. Change was considered to have occurred across the five visits if $p<0.05$, $r^2 \geq .0.6$. It was also important that the within-visit variation did not demonstrate significant differences ($p>0.05$).

7.9.9.2 Factor analysis change by patient

ANOVA was carried out on the two factors for the global and regional data sets for each individual subject. Bonferroni correction was not applied for reasons previously outlined. Change was considered to have occurred across the five visits if $p<0.05$, $r^2 \geq 0.6$. It was also important that the within-visit variation did not demonstrate a significant difference ($p>0.05$).

7.9.10 Analysis of HRF data to detect change over time

7.9.10.1 HRF change by group

The HRF data were tested for normality using the method outlined in section 7.9.1. SAS was used to perform ANCOVA to assess for change over time between the normal and glaucoma subject groups for the HRF data. In each case age was used as the covariate to correct for a small but significant age difference between the two groups. "Group" was defined as the independent variable (between factor) and "visit" the dependent variable.

Bonferroni correction was applied to the HRF data analysis to guard against increased type I error and a significant difference was said to exist between the two groups over time if $p<0.01$ and $r^2 \geq .0.6$. It was also important that the within-visit variation did not demonstrate significant a difference ($p>0.01$).

7.9.10.2 HRF change by patient

SAS was used to perform reANOVA to assess for change over time for each individual subject. In each case "visit" was defined as the dependent variable and "parameter" as the independent variable. A significant difference was said to exist between the two groups over time if $p<0.01$ and $r^2 \geq 0.6$ (Bonferroni corrected). It was also important that the within-visit variation did not demonstrate a significant difference ($p>0.01$).

7.9.11 Analysis of IOP to detect change over time

7.9.11.1 IOP change by group

Intraocular pressure is normally distributed. Single IOP measurements were made at each visit for each subject. ANCOVA was then used to assess for change over time between the normal and glaucoma subject groups. Age was used as the covariate, "group" was defined as the independent variable (between factor) and "visit" as the

dependent variable. A significant difference was said to have occurred between the two groups over time if $p<0.05$ and $r^2 \geq 0.6$.

7.9.11.2 IOP change by patient

SAS was used to perform ANCOVA to assess for change over time for each individual subject. In each case "visit" was defined as the dependent variable and "parameter" independent variable. A significant difference was said to exist between the two groups over time if $p<0.05$ and $r^2 \geq 0.6$.

7.9.12 Visual function change over time

7.9.12.1 Visual function change by group

As with the IOP data ANCOVA was used to assess for change over time between the normal and glaucoma subject groups for the visual function parameters MD, PSD and CPSD. Age was used as the covariate, "group" was defined as the independent variable (between factor) and "visit" was defined as the dependent variable. A significant difference was said to have occurred between the two groups over time if $p<0.05$ and $r^2 \geq 0.6$.

7.9.12.2 Visual function change by patient

SAS was used to perform ANCOVA to assess for change over time for each individual subject for each visual function parameter. In each case visit was defined as the dependent variable and parameter as the independent variable. A significant difference was said to have occurred between the two groups over time if $p<0.05$ and $r^2 \geq 0.6$.

7.9.13 Analysis of C:D ratio (subjective assessment) to determine change

Single subjective gradings of horizontal and vertical C:D ratio were carried out at each visit for the POAG subject group only. ANOVA was carried out for the group as a whole to determine whether a change in C:D ratio was detected over the study period. Significant change was considered to exist if $p<0.05$ and $r^2 \geq 0.6$.

Chapter 8.

Topographic and haemodynamic investigation of glaucomatous optic neuropathy: Results

8.1 Subject follow-up

The subject sample consisted of 41 POAG subjects and 34 normal subjects. Of these, 9 POAG subjects and 4 normal subjects did not complete the study. Table 8.1. outlines the number of visits completed and reasons for failure to complete. In accordance with the protocol described in section 7.3., data from subjects who completed less than 4 visits was excluded from the analysis. On this basis data from 33 POAG subjects and 31 normal subjects, who had completed 4 or more visits, was used for subsequent analysis.

Group	No. visits completed	Reason for failing to complete study
POAG	2	Caring for sick spouse
POAG	1	Failed to attend appointment
POAG	3	Illness
POAG	1	Died
POAG	1	Failed to attend appointment
POAG	3	Illness
POAG	1	Failed to attend appointment
POAG	4	Illness
POAG	1	Failed to attend appointment
Normal	2	Bereavement
Normal	2	Died
Normal	4	Illness
Normal	1	Emigrated

Table 8.1. Subject follow-up. Table outlining subjects failing to complete the study, number of visits completed and reasons for failure.

8.2 Medical and surgical changes during follow-up (POAG group)

Subjects diagnosed with POAG and included in the study continued their medical treatment as directed by the consultant ophthalmologist. Of the 33 POAG patients, 31 were being treated with topical therapy at the start of the study. The remaining 2

subjects were not on any treatment following trabeculectomy. Topical therapy consisted of β-blockers, carbonic anhydrase inhibitors, prostaglandin analogues and sympathomimetics. 12 subjects had their treatment modified throughout the study. Three underwent trabeculectomy, the remainder underwent a change in topical therapy due to poorly controlled IOP or drug intolerance. Table 8.2. outlines the medication for those subjects together with any changes in treatment and the visit at which that change was effective.

Subject No.	Treatment at start of study	Modified Treatment	Visit change effective
41	Timolol	Timolol & Dorzolamide	5
44	Timolol & Dorzolamide	Timolol & Brimonidine	2
		Timolol & Latanaprost	3
		Timolol	4
		Trabeculectomy (no Rx)	5
39	Timolol	Brimonidine	4
43	Dorzolamide	Dorzolamide & Brimonidine	3
63	No Rx	Dorzolamide & Brimonidine	2
		Dorzolamide & Latanaprost	3
51	Timolol	Timolol & Brimonidine	3
54	Levobunolol	Trabeculectomy (no Rx)	4
		Levobunolol	5
57	Timolol & Dorzolamide	Timolol	3
		Timolol & Brimonidine	4
		Dorzolamide & Latanaprost	5
61	Levobunolol	Dorzolamide & Levobunolol	5
62	Cartelol & Dorzolamide	Cartelol, Dorzolamide & Latanaprost	5
32	Timolol	Trabeculectomy (no Rx)	5
36	Timolol	Timolol & Dorzolamide	3

Table 8.2. Subject treatment changes. Table summarising the subjects whose treatment was modified throughout the study period.

8.3 Systemic hypertensive medication

Seven (21%) POAG subjects and 8 (26%) normal subjects were diagnosed with systemic hypertension at the start of the study. A further 2 (6%) subjects belonging to the normal group were diagnosed subsequently. All subjects diagnosed with systemic hypertension were on treatment.

8.4 HRT data analysis

8.4.1 Normality statistics for topographic data

Global and regional topographic data recorded with the HRT was transferred directly into an Excel for Windows 95 spreadsheet. The data was separated into 7 sets according to the region of tissue measured:

Data set 1: Global (360°).

Data set 2: Superior nasal (45°).

Data set 3: Superior temporal (45°).

Data set 4: Temporal (90°).

Data set 5: Nasal (90°).

Data set 6: Inferior nasal (45°).

Data set 7: Inferior temporal (45°).

A total of 15 parameters were measured globally, 8 were also measured regionally (see Table 7.7) All of the topographic data was tested for normality by parameter, group and visit. Data was considered Gaussian if $p>0.05$. If the data was not normally distributed then the stem and leaf plots were examined to look for any obvious outliers in the data.

8.4.1.1 Normality results for global topographic data

Data was tested for normality by group and visit. Table 8.3. Summarises the percentage of data that was normally distributed for each parameter measured globally for each group. Overall 54.7% of the data was normally distributed for both the normal and POAG groups. Of the data that did not demonstrate a normal distribution, 19% for the normal group and 22% for the POAG group was associated with a single outlier in the data. This left just 16% for the normal group and 20% for the POAG group that was non-Gaussian without a single outlier. Had a significant proportion of the data been non-Guassian, then a logarithmic transformation of the data would have

been necessary prior to further statistical analysis. A relatively low percentage of the data was non-Guassian and so data transformation was not carried out.

	Normal		Without outliers		With outliers	
Parameter	**Normal**	**POAG**	**Normal**	**POAG**	**Normal**	**POAG**
C:D area ratio	4 [80]	4 [80]			1 [20]	1 [20]
Mean height contour	2 [40]	4 [80]		1 [20]		3 [60]
Height variation contour	5 [100]	2 [40]		1 [20]	2 [40]	
Volume below surface	1 [20]		3 [60]	5 [100]		1 [20]
Volume above surface	1 [20]	1 [20]	3 [60]	1 [20]	3 [60]	1 [20]
Volume below reference			2 [40]	4 [80]	1 [20]	3 [60]
Volume above reference	4 [80]	4 [80]			1 [20]	1 [20]
Maximum depth	4 [80]	2 [40]			3 [60]	1 [20]
Third moment	1 [20]	3 [60]			2 [40]	4 [80]
RNFL thickness	2 [40]	5 [100]	1 [20]			2 [40]
Mean depth contour	3 [60]		2 [40]	2 [40]	3 [60]	
Rim area	4 [80]	5 [100]				1 [20]
Cup area		1 [20]	1 [20]	1 [20]	3 [60]	4 [80]
Classification	5 [100]	5 [100]				
Reference height	5 [100]	5 [100]				
Mean	**41 [54.7%]**	**41 [54.7%]**	**12 [16%]**	**15 [20%]**	**19 [25.3%]**	**22 [29.3%]**

Table 8.3. Normality data for the global HRT parameters. Values correspond to the number of visits [and %] of data that was normally distributed, abnormally distributed without outliers and abnormally distributed with outliers.

	Mean of regional data sets					
	Normal		Without outliers		With outliers	
Parameter	**Normal**	**POAG**	**Normal**	**POAG**	**Normal**	**POAG**
Mean height contour	4.3 [90]	5 [100]	0 [0]	0 [0]	0.7 [14]	0 [0]
Volume below surface	0.7 [14]	1 [20]	2.3 [46]	1.7 [34]	2 [40]	2.3 [46]
Volume above surface	1.4 [28]	0 [0]	1.5 [30]	2.7 [54]	2.5 [50]	2.3 [46]
Volume below reference	0 [0]	0 [0]	4.8 [96]	2.8 [56]	0.4 [8]	2.2 [44]
Volume above reference	5 [100]	3.8 [76]	0 [0]	0.2 [4]	0 [0]	1 [20]
Maximum depth	3.7 [74]	4.5 [90]	0 [0]	0.2 [4]	0.8 [8]	0.3 [6]
Third moment	4.5 [90]	4.5 [90]	0.2 [4]	0 [0]	0.2 [4]	0.5 [10]
Cup area	0.2 [4]	3 [60]	3.8 [76]	0.8 [16]	1.2 [24]	1.2 [24]
Mean	**19.6 [49%]**	**21.8 [54.5%]**	**12.6 [31.5%]**	**8.4 [21%]**	**7.8 [19.5%]**	**9.8 [24.5%]**

Table 8.4. Normality data for the regional HRT parameters. Values correspond to the mean number of visits and [mean %] of data that was normally distributed, abnormally distributed with outliers and abnormally distributed without outliers. The values represent the mean for all regional data sets.

8.4.1.2 Normality results for regional topographic data

Table 8.4. summarises the mean percentage of data that was normally distributed for each parameter measured regionally. Individual tables containing normality data for each separate region can be found in Appendix 6. Overall 49% of data for the normal group and 54.5% of data for the POAG group was Guassian. Of the data that did not demonstrate a normal distribution, 19.5% for the normal group and 24.5% for the POAG group was associated with a single outlier in the data. This left just 31.5% for the normal group and 21% for the POAG that did not follow a normal distribution. On this basis, data transformation was not performed prior to further statistical analysis.

8.4.2 HRT parameters: Baseline values (global data)

Table 8.5. summarises the baseline values (mean of 7 images ± SD values) for the global HRT parameters. The mean values for the normal and POAG were compared

using an unpaired Students 2-tailed t-test. The p-values are given in the table. A significant difference is said to have occurred between the two groups if $p < 0.01$.

	Normal		POAG		
Parameter	**Mean**	**SD**	**Mean**	**SD**	**P-value**
C:D area ratio	0.199	0.115	0.487	0.095	0.000
Disc area	2.06	0.56	2.03	0.60	0.557
Mean height contour	0.010	0.074	0.125	0.051	0.000
Height variation contour	0.335	0.074	0.305	0.080	0.000
Volume below surface	0.190	0.147	0.489	0.241	0.000
Volume above surface	0.065	0.034	0.045	0.022	0.000
Volume below reference	0.076	0.077	0.314	0.201	0.000
Volume above reference	0.350	0.105	0.218	0.082	0.000
Maximum depth	0.477	0.195	0.732	0.171	0.000
Third moment	-0.198	0.054	-0.090	0.049	0.000
RNFL thickness	0.224	0.055	0.171	0.049	0.000
Mean depth contour	0.096	0.061	0.235	0.084	0.000
Rim area	1.391	0.223	1.029	0.209	0.000
Cup area	0.396	0.282	1.004	0.334	0.000
Classification	1.665	1.180	-0.742	1.044	0.000
Reference height	0.227	0.093	0.296	0.071	0.001

Table 8.5. Global HRT parameters at baseline. Average ± SD values for the global HRT parameters for the POAG and normal subject groups. P-values are given (Students unpaired t-test).

8.4.3 Topographical change over time: by group

Topographical parameters measured with the HRT were analysed for change over time between subject groups using repeated measures analysis of covariance (reANCOVA). There was a significant difference between the mean ages of the two groups ($p<0.05$ unpaired 2-tailed t-test). For this reason it was necessary to correct for a possible age effect. Age was used as the covariate and group as the between factor. Change across five visits was assessed for each parameter between the two subject groups and considered significantly different if $p<0.01$ (Bonferroni corrected). It was also necessary that within-visit variation did not demonstrate significant differences ($p>0.01$).

8.4.3.1 Global data set

Table 8.6. gives the significance levels for change in each topographical parameter measured globally. The parameters cup:disc area ratio, volume below surface, volume below reference, mean depth in contour, rim area and cup area demonstrated a significant difference over time between the two subject groups ($p<0.01$). To demonstrate how the change over time differed between the two groups, graphs were plotted of the average values obtained at visits 1-5 (Figures 8.1. – 8.6.). For each graph, standard error bars are given together with a linear trend line and r^2 value. The r^2 value only gives an indication of the linearity of the data as it is based on the group mean for each visit and the repeated measures component of the model is concealed.

Parameter	Global data set (p-value)
C:D area ratio	0.0026 *
Mean height contour	0.0510
Height variation contour	0.2315
Vol below surface	0.0020 *
Vol above surface	0.0273
Vol below reference	0.0065 *
Vol above reference	0.0328
Maximum depth	0.7513
Third moment	0.2433
RNFL thickness	0.3083
Mean depth contour	0.0022 *
Rim area	0.0068 *
Cup area	0.0050 *
Classification	0.1154
Reference height	0.2440

Table 8.6. ANCOVA results for global HRT data showing difference between groups for change over time. P-values significant at the 0.01 level are marked*

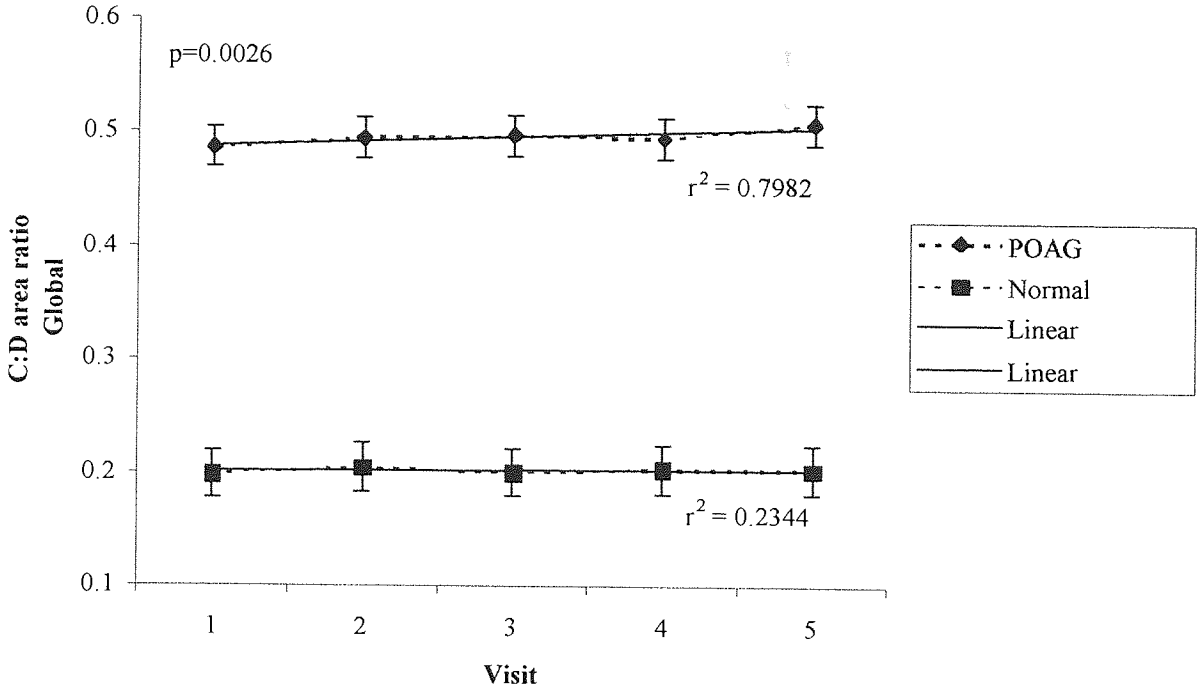

Figure 8.1. Mean values for C:D area ratio at visits 1-5 measured globally for the normal and POAG subject groups. Standard error bars are given together with r^2.

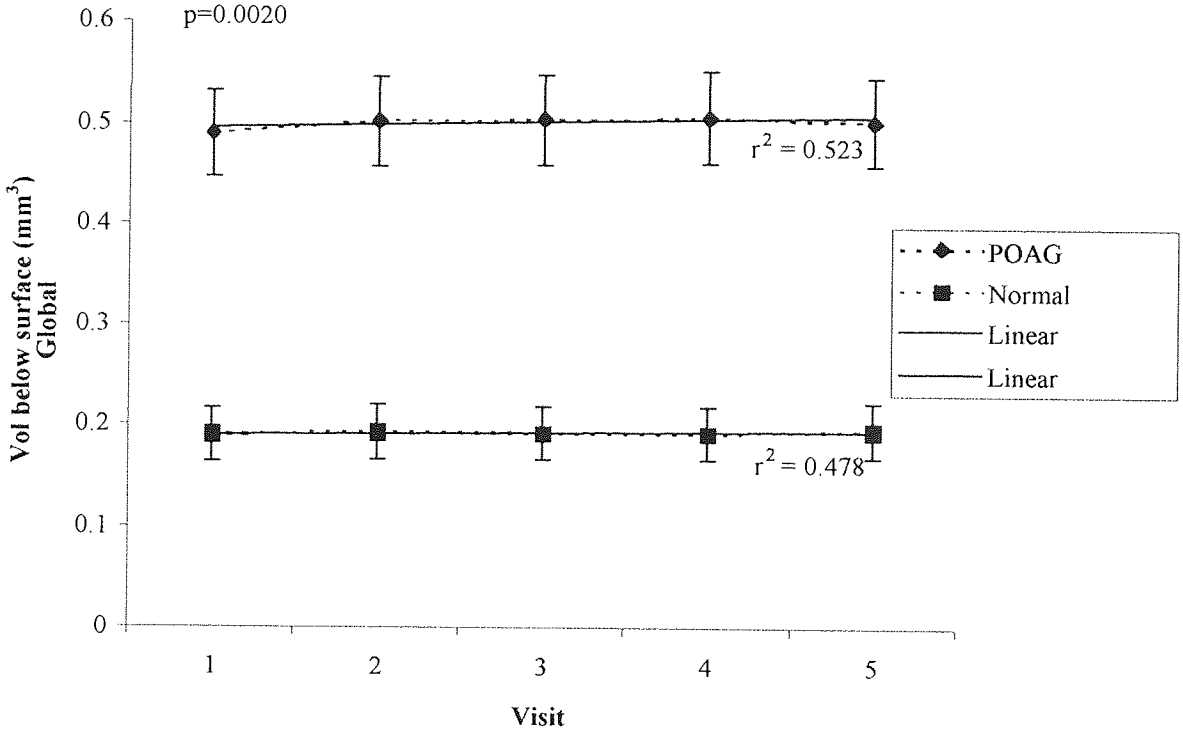

Figure 8.2. Mean values for the HRT parameter volume below surface measured globally at visits 1-5 for the normal and POAG subject groups. Standard error bars are given together with r^2.

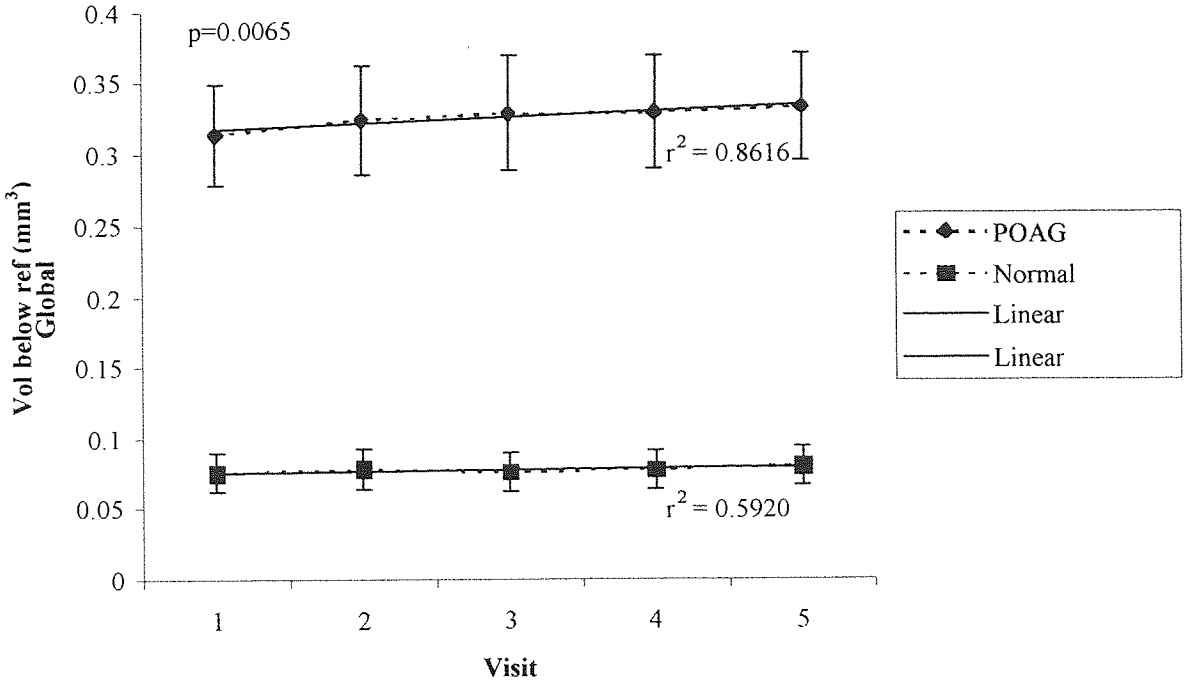

Figure 8.3. Mean values for the HRT parameter volume below reference measured globally at visits 1-5 for the normal and POAG subject groups. Standard error bars are given together with r^2.

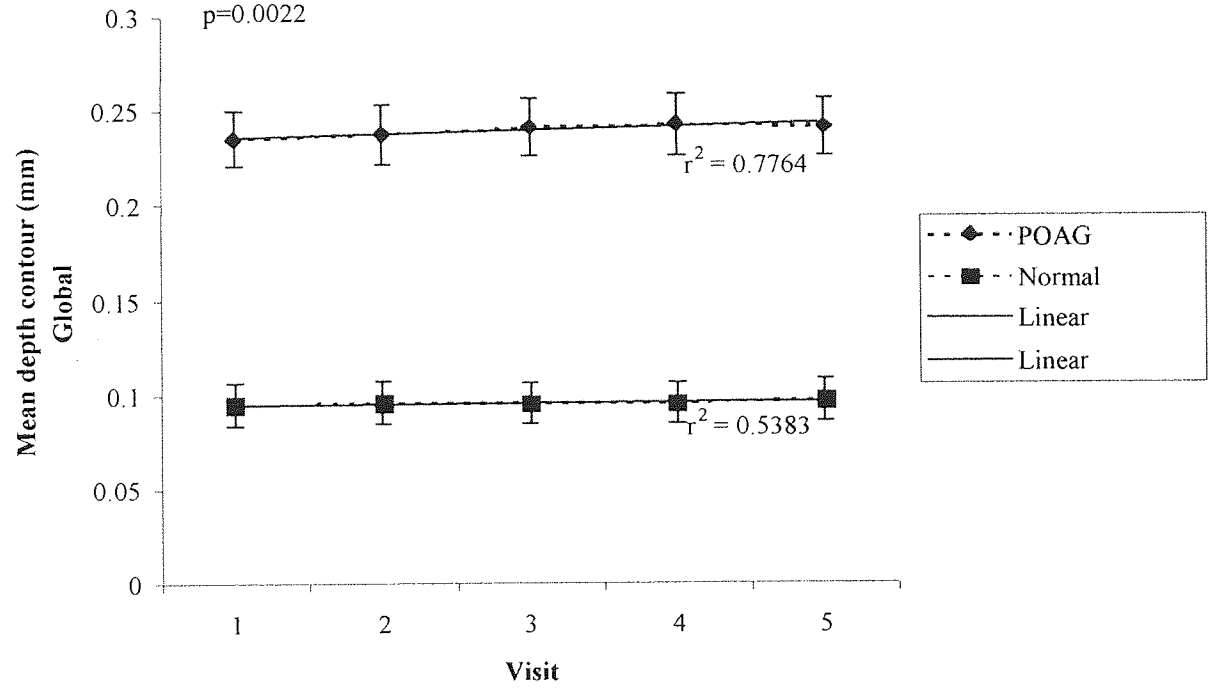

Figure 8.4. Mean values for the HRT parameter mean depth in contour measured globally at visits 1-5 for the normal and POAG subject groups. Standard error bars are given together with r^2.

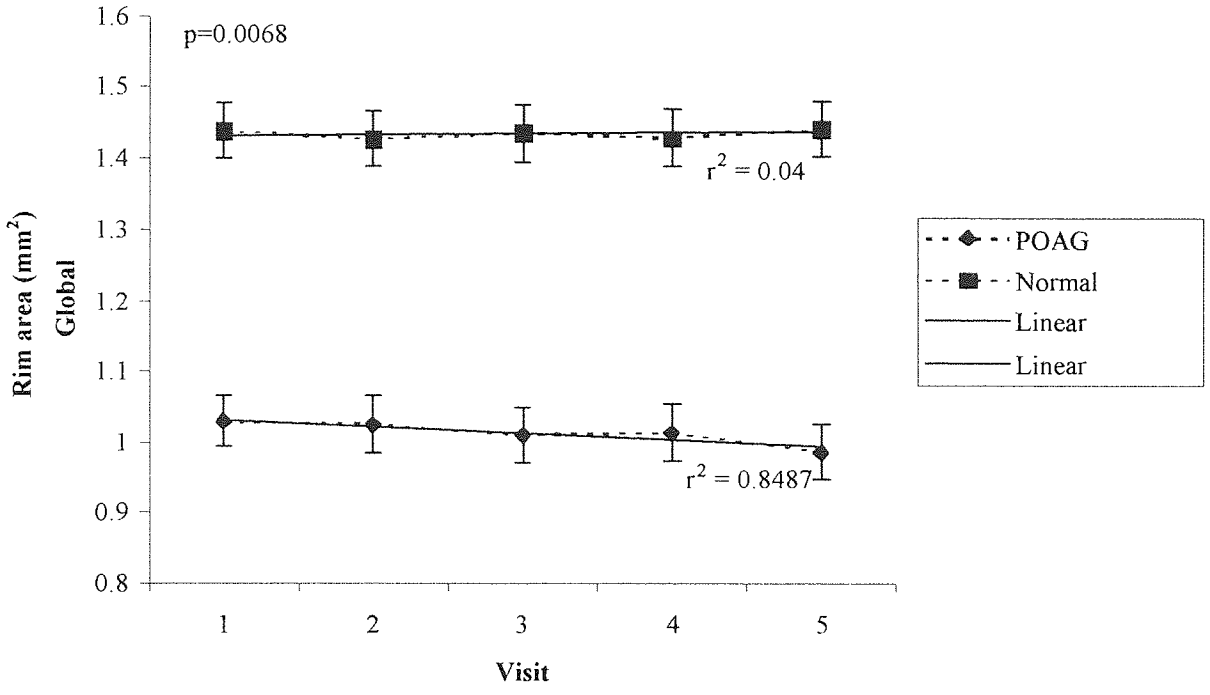

Figure 8.5. Mean values for the HRT parameter rim area measured globally at visits 1-5 for the normal and POAG subject groups. Standard error bars are given together with r^2.

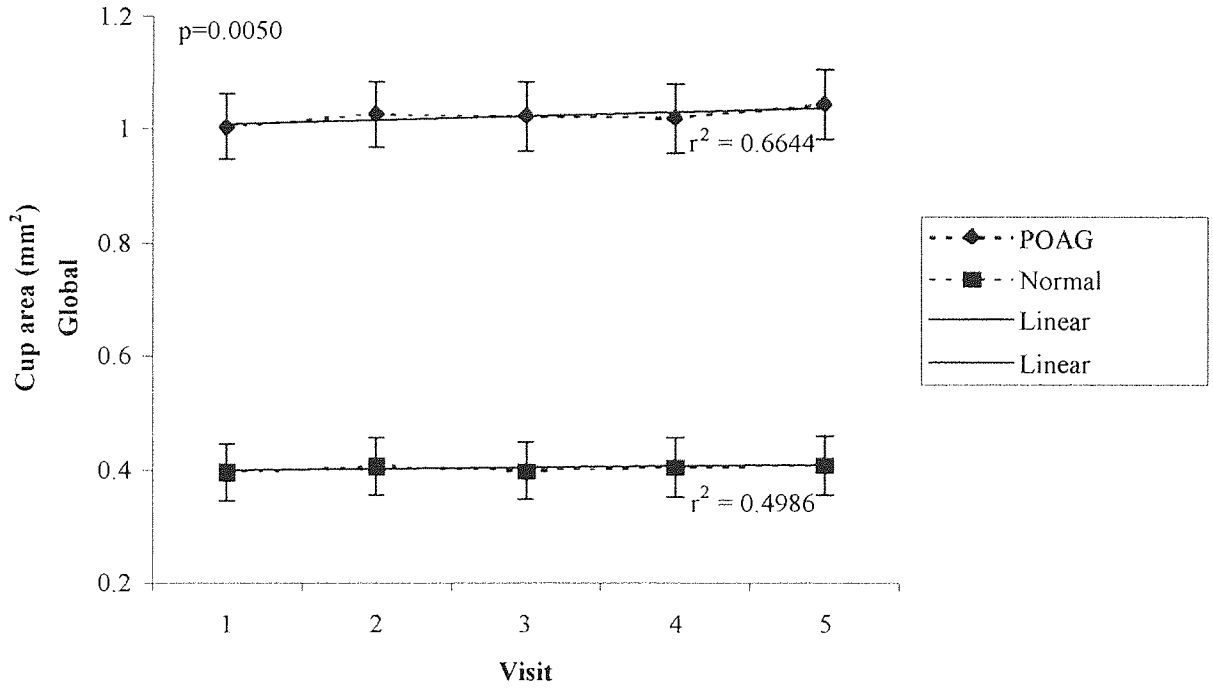

Figure 8.6. Mean values for the HRT parameter cup area measured globally at visits 1-5 for the normal and POAG subject groups. Standard error bars are given together with r^2.

8.4.3.2 Regional data sets

Table 8.7. gives the p-values for change in each measured topographical parameter for the regional data sets. The following parameters measured in both the superior temporal and superior nasal sectors demonstrated a significant difference over time between the two subject groups ($p<0.01$): volume below surface; volume above surface; volume below reference; volume above reference; cup area. No significant difference in parameters between the two groups was observed for the temporal, nasal, inferior nasal and inferior temporal sectors. To demonstrate how the change over time differed between the two groups for the significant parameters, graphs were plotted of the average values obtained at visits 1-5 (Figures 8.7. – 8.16.). For each graph, standard error bars are given together with a linear trend line and r^2 value. The r^2 value gives only an indication of the linearity of the data as it is based on mean values for each visit and the repeated measures component of the model is concealed.

	Data set (region measured)					
Parameter	**Sup nasal (p-value)**	**Sup temp (p-value)**	**Temp (p-value)**	**Nasal (p-value)**	**Inf nasal (p-value)**	**Inf temp (p-value)**
Mean height contour	0.0355	0.0477	0.2526	0.0721	0.2268	0.4473
Vol below surface	0.0033 *	0.0007 *	0.0595	0.0548	0.2327	0.0519
Vol above surface	0.0001 *	0.0001 *	0.1969	0.1807	0.5335	0.3911
Vol below reference	0.0082 *	0.0001 *	0.0659	0.0529	1.1213	0.0275
Vol above reference	0.0065 *	0.0057 *	0.0555	0.1879	0.4538	0.0385
Maximum depth	0.4161	0.3914	0.7085	0.6537	0.4971	0.8098
Third moment	0.9890	0.5376	0.7383	0.1555	0.2115	0.6566
Cup area	0.0003 *	0.0041 *	0.3074	0.0486	0.1852	0.0277

Table 8.7. ANCOVA results for the regional HRT data. P-values significant at the 0.01 level are indicated*.

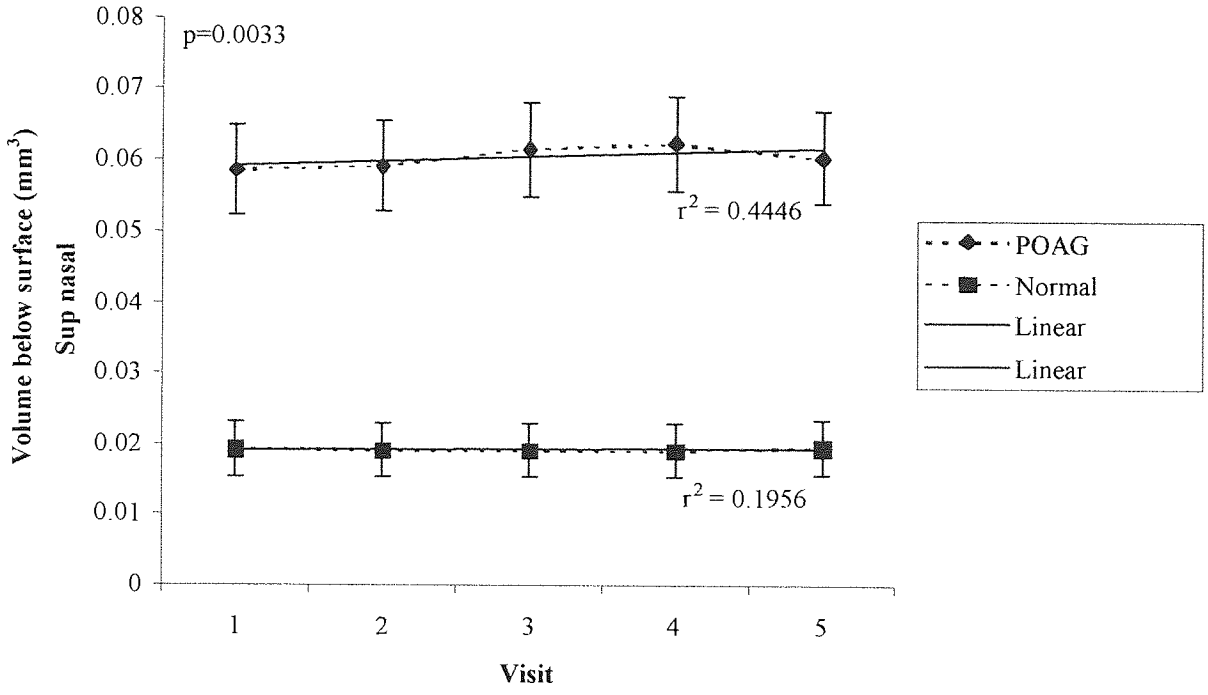

Figure 8.7. Mean values for the HRT parameter volume below surface measured superior nasally at visits 1-5 for the normal and POAG subject groups. Standard error bars are given together with r^2.

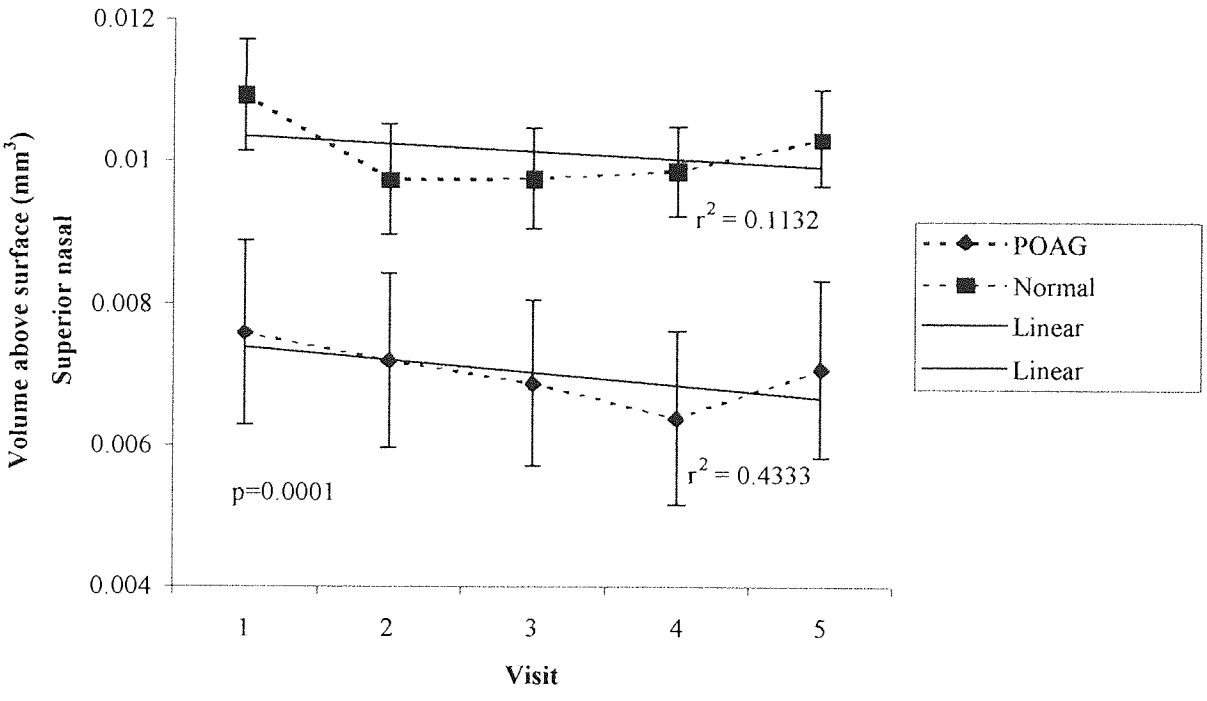

Figure 8.8. Mean values for the HRT parameter volume above surface measured superior nasally at visits 1-5 for the normal and POAG subject groups. Standard error bars are given together with r^2.

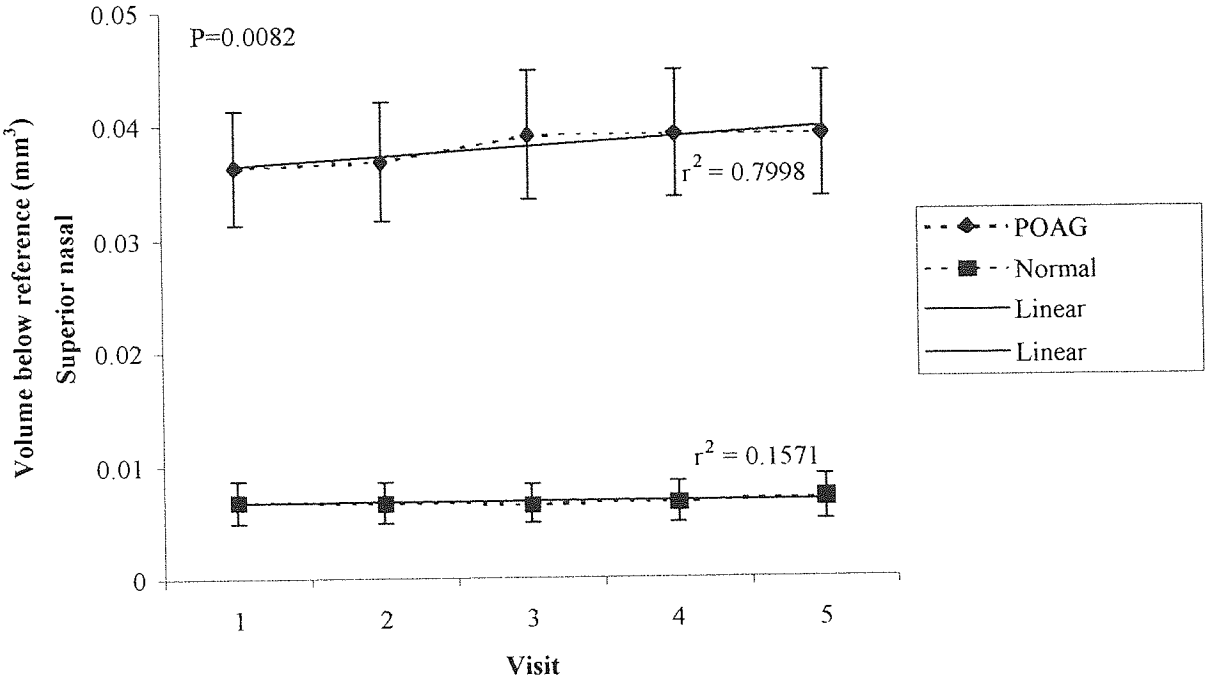

Figure 8.9. Mean values for the HRT parameter volume below reference measured superior nasally at visits 1-5 for the normal and POAG subject groups. Standard error bars are given together with r^2.

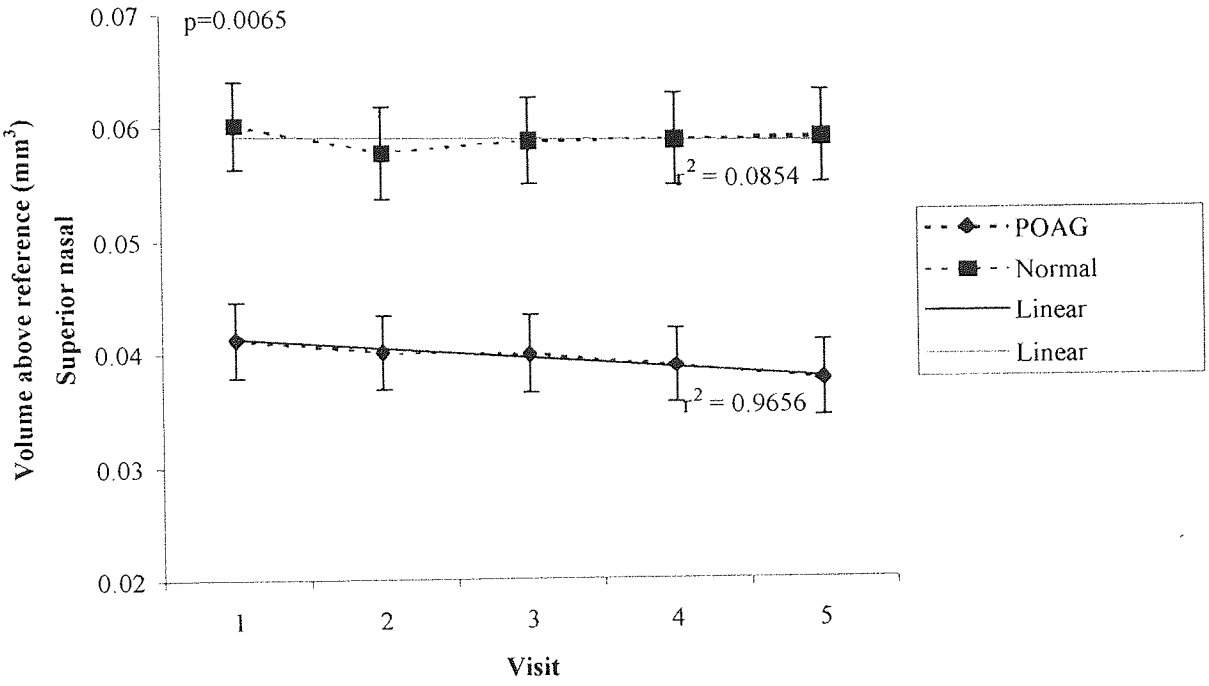

Figure 8.10. Mean values for the HRT parameter volume above reference measured superior nasally at visits 1-5 for the normal and POAG subject groups. Standard error bars are given together with r^2.

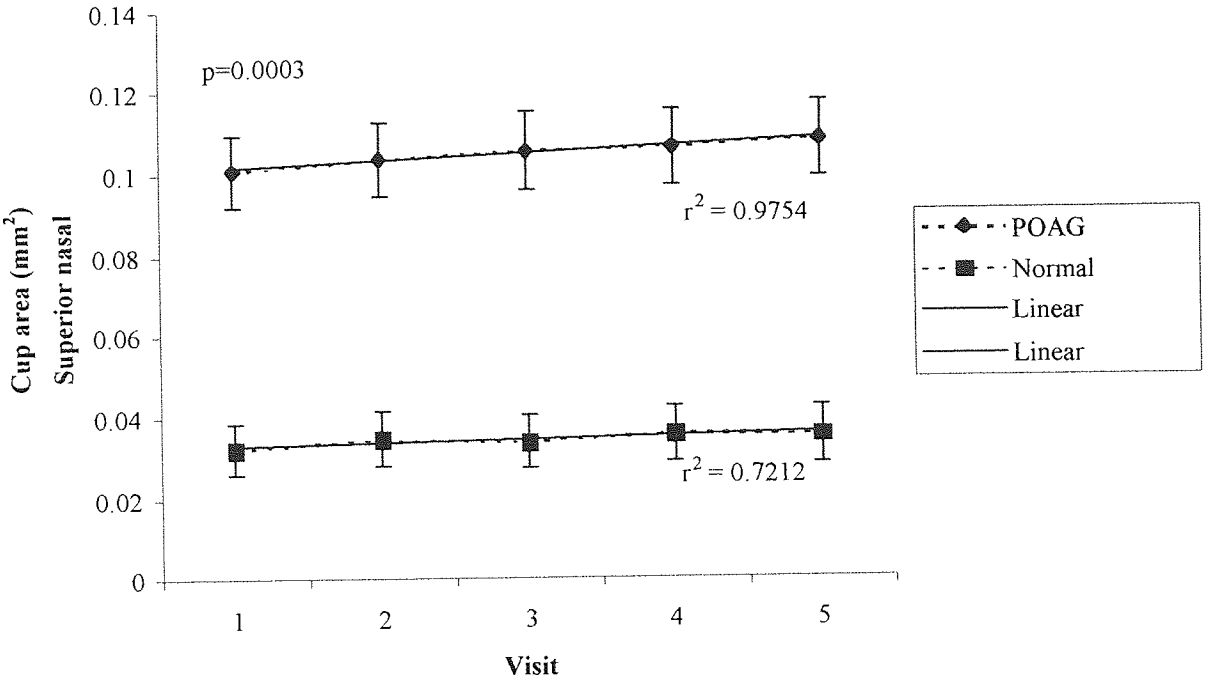

Figure 8.11. Mean values for the HRT parameter cup area measured superior nasally at visits 1-5 for the normal and POAG subject groups. Standard error bars are given together with r^2.

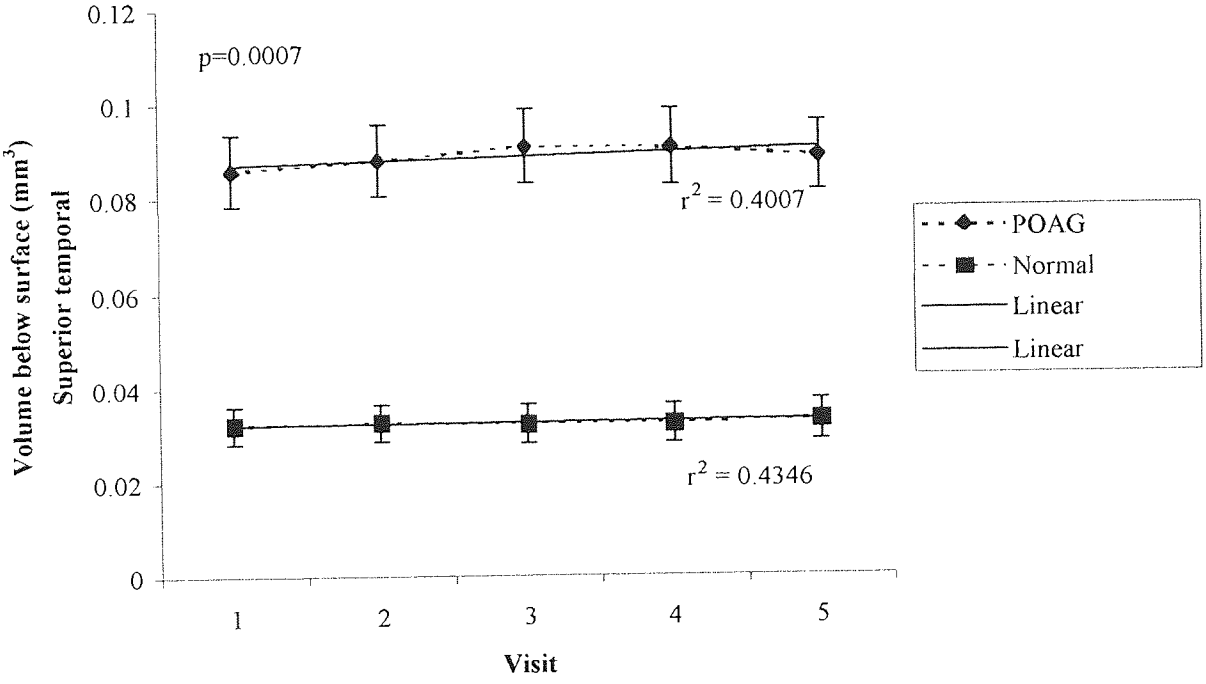

Figure 8.12. Mean values for the HRT parameter volume below surface measured superior temporally at visits 1-5 for the normal and POAG subject groups. Standard error bars are given together with r^2.

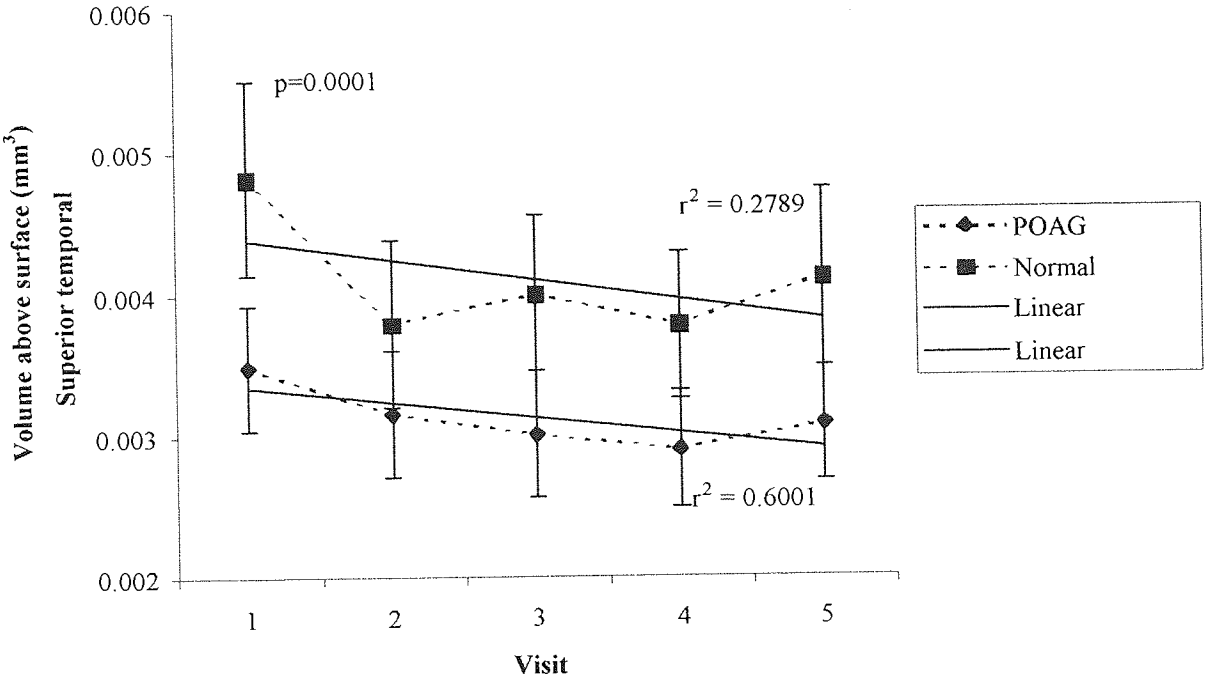

Figure 8.13. Mean values for the HRT parameter volume above surface measured superior temporally at visits 1-5 for the normal and POAG subject groups. Standard error bars are given together with r^2.

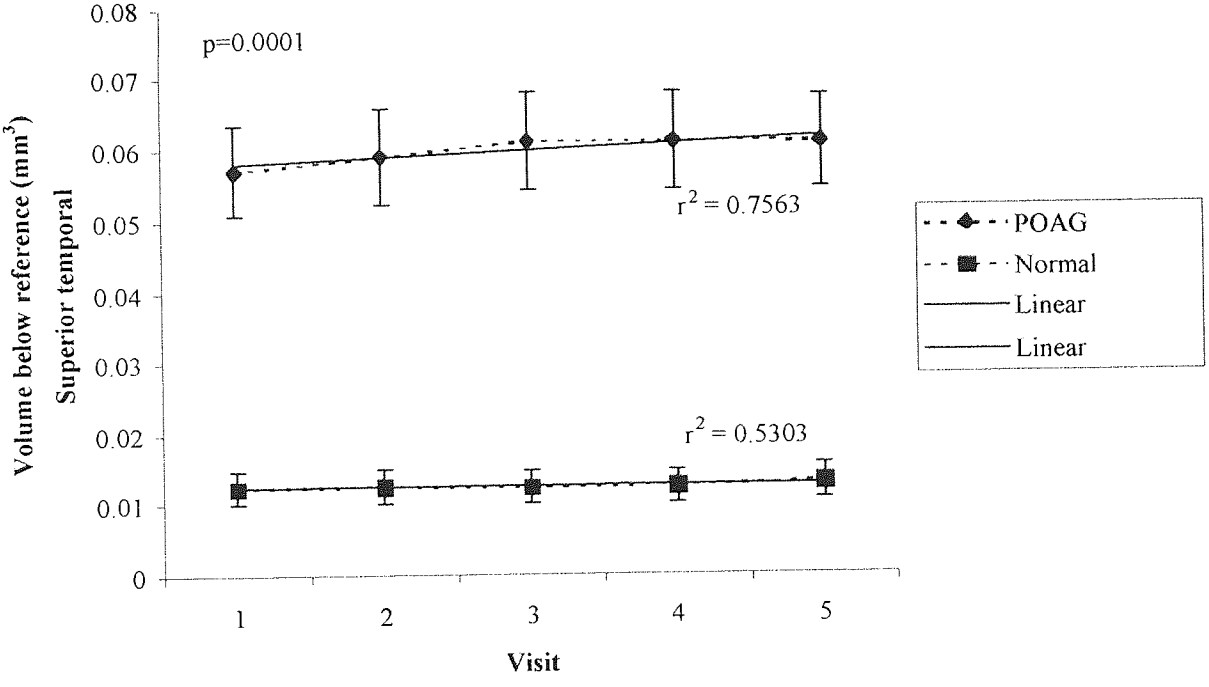

Figure 8.14. Mean values for the HRT parameter volume below reference measured superior temporally at visits 1-5 for the normal and POAG subject groups. Standard error bars are given together with r^2.

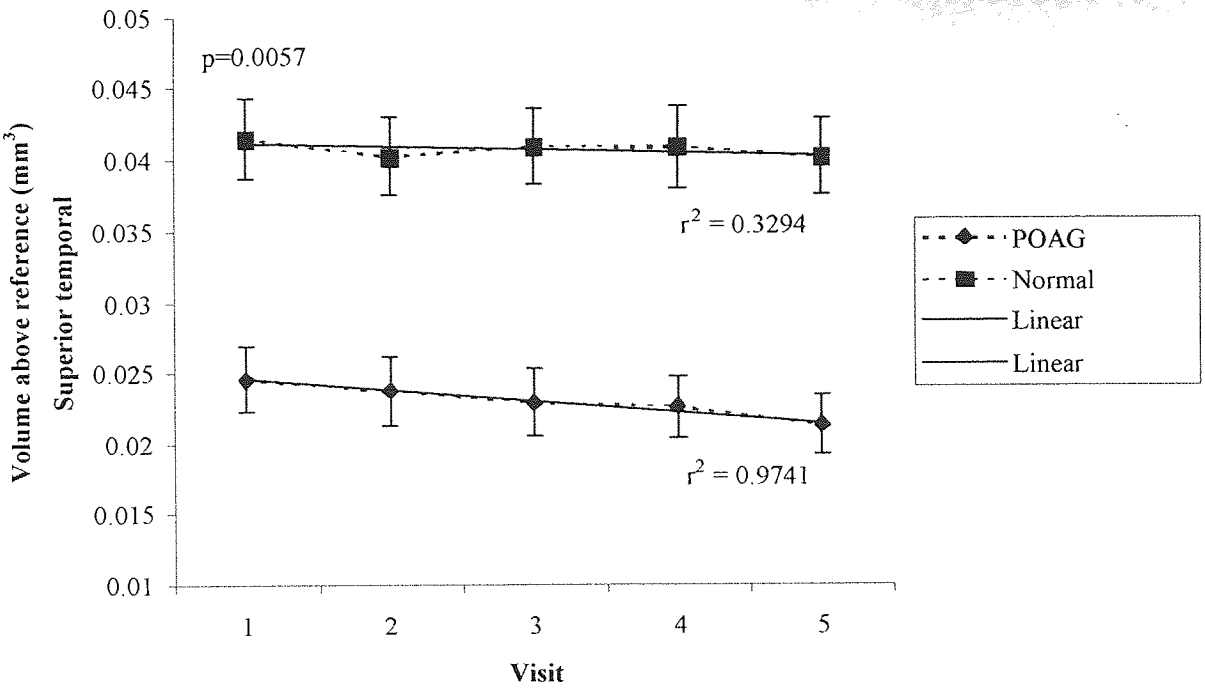

Figure 8.15. Mean values for the HRT parameter volume above reference measured superior temporally at visits 1-5 for the normal and POAG subject groups. Standard error bars are given together with r^2.

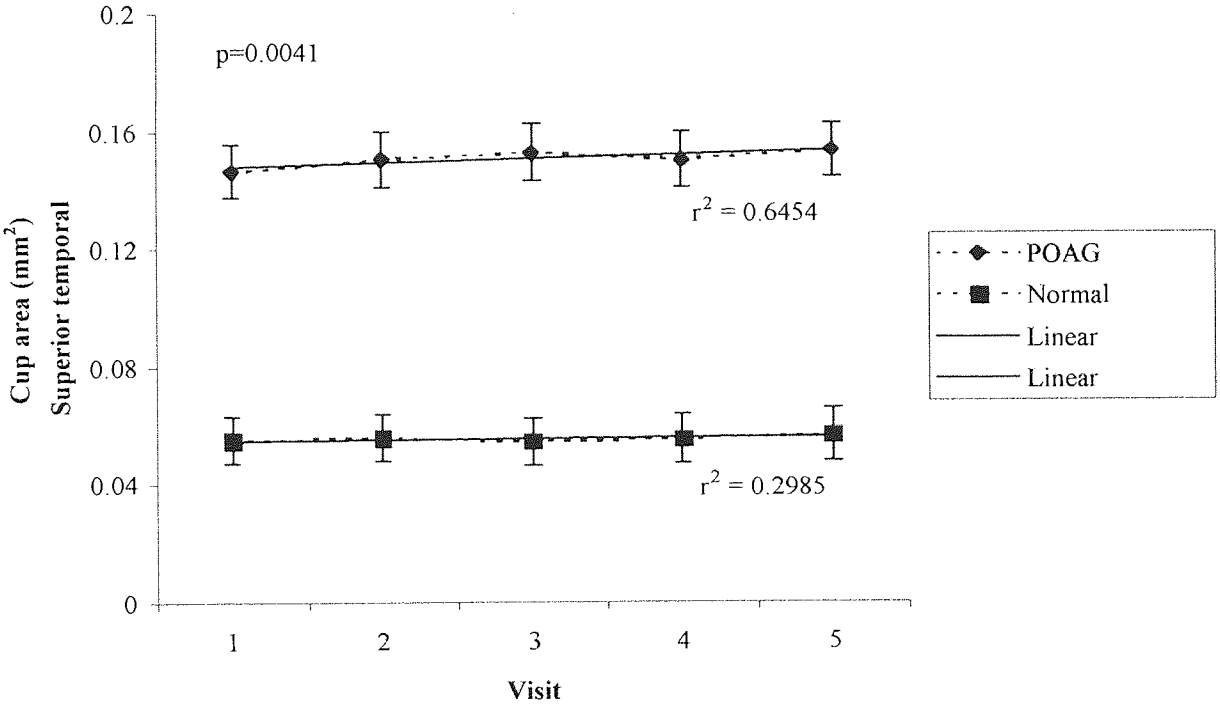

Figure 8.16. Mean values for the HRT parameter cup area measured superior temporally at visits 1-5 for the normal and POAG subject groups. Standard error bars are given together with r^2.

8.4.4 Topographical change over time: by patient

Topographical parameters measured with the HRT were analysed for change over time for each individual subject using repeated measures analysis of variance (reANOVA). As patients were being assessed independently of each other it was not necessary to correct for an age effect. Change over time (5 visits) for each parameter was considered significantly different if $p<0.01$; $r^2 \geq 0.6$. It was also necessary that within visit-variation did not demonstrate significant differences ($p>0.01$) (Bonferroni corrected).

8.4.4.1 Topographic change over time by patient: Global data

Table 8.8. gives the number and percentage of POAG and normal subjects that demonstrated change throughout the study period for each parameter measured globally. The percentage of POAG subjects demonstrating a significant change in individual parameters ranged from 6.1% for third moment in contour to 42.4% for volume below surface. The percentage of normal subjects showing significant change over time ranged from 6.5% (maximum depth in contour & third moment) to 25.8% (C:D ratio & volume above reference).

8.4.4.2 Topographic change over time by patient: Regional data

Tables 8.9. and 8.10. summarise the number and percentage of POAG subjects that demonstrated change throughout the study period for each parameter measured regionally. A significant change over time was demonstrated by at least one subject for every measured parameter (POAG group). For the POAG group, the parameter cup area showed the most change over the study period in the superior nasal, temporal and inferior nasal and temporal quadrants (33.3%, 39.4%, 42.4%, 39.4%). Third moment in contour, measured in the superior nasal sector, showed the least significant change over time with only 2 subjects showing change in this parameter (6.1%).

The percentage of normal subjects demonstrating a significant change over time for measured HRT parameters ranged from 0% (maximum depth in contour in the superior nasal region) to 35.5% (height variation of contour in the superior temporal region, volume above reference in the inferior nasal region).

	Global data Number and [%]	
Parameter	**Normal**	**POAG**
CD ratio	8 [25.8]	12 [36.4]
Mean Height contour	6 [19.35]	12 [36.4]
Height variation contour	5 [16.1]	4 [12.1]
Vol below surf	5 [16.1]	14 [42.4]
Vol above surf	7 [22.6]	8 [24.2]
Vol below ref	5 [16.1]	6 [18.8]
Vol above ref	8 [25.8]	5 [15.2]
Max depth	2 [6.5]	7 [21.2]
Third mom	2 [6.5]	2 [6.1]
RNFL thickness	5 [16.1]	7 [21.2]
Mean depth contour	5 [16.1]	14 [42.4]
Rim area	9 [29]	11 [33.3]
Cup area	9 [29]	10 [30.3]
Classification	3 [9.7]	7 [21.9]
Reference height	6 [19.4]	6 [18.8]

Table 8.8. Number [and %] of POAG and normal subjects showing change in HRT global parameters across 5 visits.

	Data set (region measured)					
Parameter	**Sup nasal**	**Sup temp**	**Temp**	**Nasal**	**Inf nasal**	**Inf temp**
Mean Height cont	5 [15.2]	8 [24.2]	6 [18.2]	8 [24.2]	8 [24.2]	6 [18.2]
Vol bel surf	12 [36.4]	11 [33.3]	8 [24.2]	8 [24.2]	10 [30.3]	5 [15.2]
Vol above surf	3 [9.1]	9 [27.3]	3 [9.1]	7 [21.2]	4 [12.1]	4 [12.1]
Vol bel ref	10 [30.3]	7 [21.2]	5 [15.2]	6 [18.8]	11 [35.5]	7 [21.9]
Vol above ref	5 [15.2]	7 [21.2]	7 [21.2]	5 [15.2]	11 [34.4]	8 [24.2]
Max depth	9 [27.3]	5 [15.2]	8 [24.2]	9 [27.3]	6 [18.2]	8 [24.2]
Third mom	3 [9.1]	7 [21.2]	9 [27.3]	4 [12.1]	7 [21.1]	8 [24.2]
Cup area	11 [33.3]	14 [42.4]	7 [21.2]	7 [21.2]	14 [42.4]	13 [39.4]

Table 8.9. Number [and %] of POAG subjects showing change in regional HRT parameters across 5 visits.

	Data set (region measured)					
Parameter	**Sup nasal**	**Sup temp**	**Temp**	**Nasal**	**Inf nasal**	**Inf temp**
Mean Height cont	6 [19.3]	11 [35.5]	6 [19.3]	5 [16.1]	8 [25.8]	6 [19.3]
Vol bel surf	5 [16.1]	6 [19.3]	6 [19.3]	3 [9.7]	2 [6.5]	2 [6.5]
Vol above surf	5 [16.1]	4 [12.9]	2 [6.5]	6 [19.3]	3 [9.7]	6 [19.3]
Vol bel ref	1 [3.2]	4 [12.9]	7 [22.6]	3 [9.7]	2 [6.5]	3 [9.7]
Vol above ref	6 [19.3]	9 [29.9]	4 [12.9]	6 [19.3]	10 [32.3]	7 [22.6]
Max depth	0 [0]	2 [6.5]	4 [12.9]	1 [3.2]	1 [3.2]	1 [3.2]
Third mom	1 [3.2]	4 [12.9]	3 [9.7]	2 [6.5]	4 [12.9]	0 [0]
Cup area	8 [25.8]	4 [12.9]	3 [9.7]	4 [12.9]	4 [12.9]	7 [22.6]

Table 8.10. Number [and %] of normal subjects showing change across 5 visits regionally.

8.4.5 Factor analysis of topographic data: Factor content and structure

8.4.5.1 Global data

Nine out of the 15 parameters measured globally were included for factor analysis. These are listed below:

- Mean height of contour
- Height variation in contour
- Volume below surface
- Volume below reference
- Volume above reference
- Maximum depth in contour
- Third moment
- RNFL thickness
- Mean depth in contour

The parameters C:D area ratio, rim area and cup area were not included as it was thought that volumetric measures of rim and cup would adequately represent the data. The classification parameter was not included as it was not a true parameter, but a graded measure based on three other parameters. Reference height was not included as it is represents an artificial reference plane from which other parameters are measured, and provided limited information on the ONH itself. Finally, volume above surface was not included, because an initial examination of the factor structure revealed that it did not load clearly into any one factor.

The eigenvalues of the correlation matrices were examined to determine how many factors best described the data set. Eigenvalues are indicies of variance that describe the total amount of variance explained by each factor. The eigenvalues were plotted and the curve examined to find where the slope of the curve changed from negative to close to zero. The last useful factor is the one before the asymptote begins. Figure 8.17, gives the plotted eigenvalues for the 9 factors; note that if there are nine

parameters, the total number of factors is nine and the sum of the eigenvalues for all of these factors is also nine. It is clear that the scree starts after 2 factors. This indicates that the majority of the variance is contained in factors one and two. On this basis 2 factors were used to describe the global data.

Table 8.11. gives the factor weightings for a two factor model following orthogonal rotation. The variance associated with each factor is expressed as a percentage of the overall variance explained by the model. The most variance is contained in factor one, which indicates that this factor carries the greatest weighting.

Data set	Factor 1		Factor 2		Total	
	Variance	Variance %	Variance	Variance %	Variance	Variance %
Global	4.44	49.33	2.99	33.22	7.43	82.56

Table 8.11. Variance explained by each factor and the total variance (actual and percentage) for two factors according to the rotated factor model for the global data set.

The rotated factor pattern was examined for the data set to determine which parameters belong with which factor. Table 8.12. summarises the parameters contained in each factor. The parameter that loaded highest onto a given parameter is at the top of each list, decreasing to the parameter that loaded the least.

Data Set	Factor 1	Factor 2
Global data (Data set 1)	Mean depth contour Vol below surface Maximum depth Vol below reference Mean height contour Third moment	RNFL thickness Height variation contour Vol above reference

Table 8.12. Parameter content for factors 1 and 2 for the global data set.

For the global data, the parameters in factor 1 describe the size, shape and depth of the cup, the parameters in factor 2 describe the rim tissue and retinal nerve fibre layer (RNFL) thickness and profile.

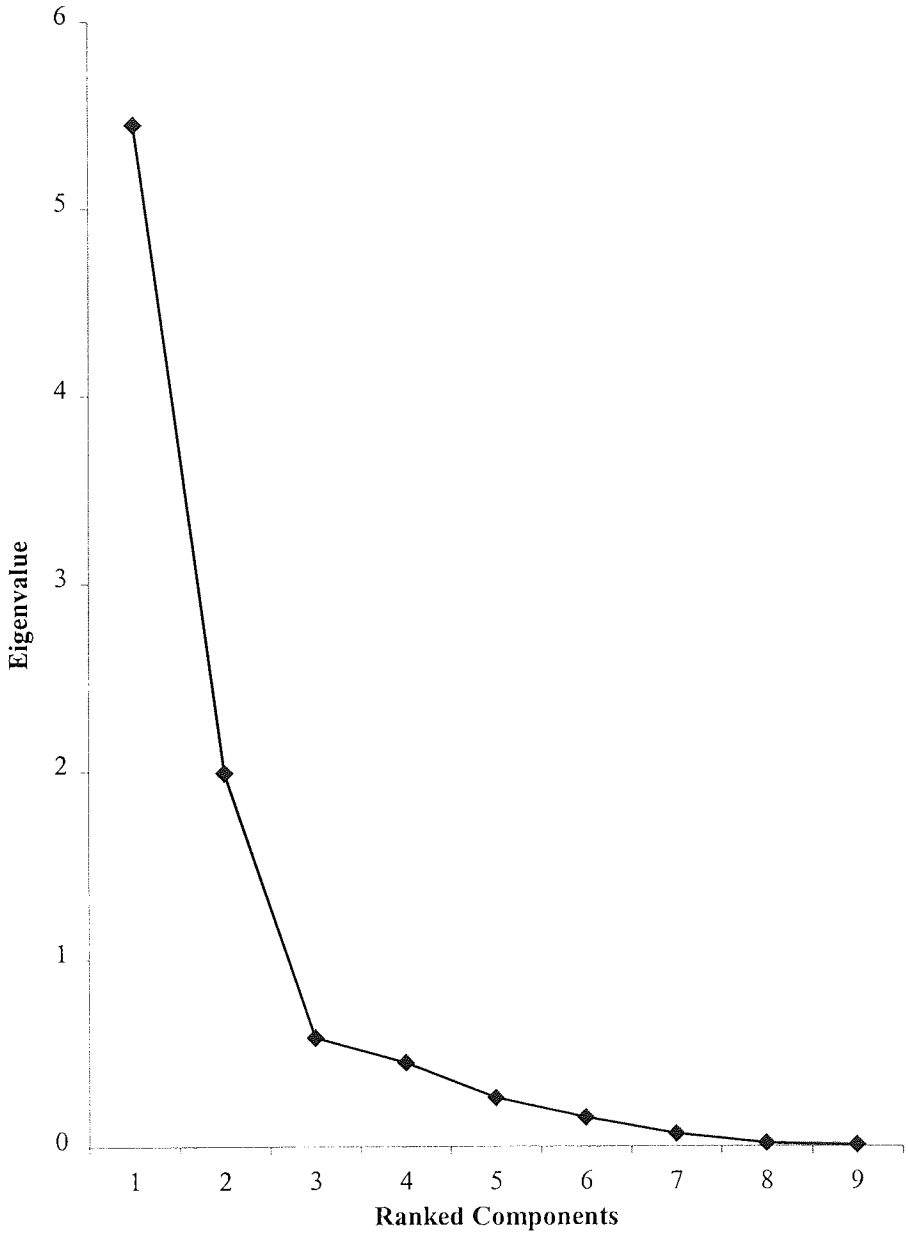

Figure 8.17. Eigenvalues as a function of the ranked component factor for the global data set. The graph represents the eigenvalues for 9 factors contained within the global data set. The most variance is contained in factor 1 and the least in factor 9. The scree begins after 2 factors.

8.4.5.2 Regional data

Six of the 8 parameters measured regionally were included for factor analysis including:

- Volume below surface
- Volume above surface
- Volume below reference
- Volume above reference
- Maximum depth
- Third moment

The parameter, cup area, was not included because of the presence of volumetric measures of the same tissue (volume below reference, volume below surface). Mean height of contour was also excluded because preliminary examination of the factor structure revealed that it did not load clearly onto a single factor.

The eigenvalues were plotted for the six regional data sets. When the scree plots were examined, it was apparent that two factors were appropriate to describe the data (Figure 8.18.).

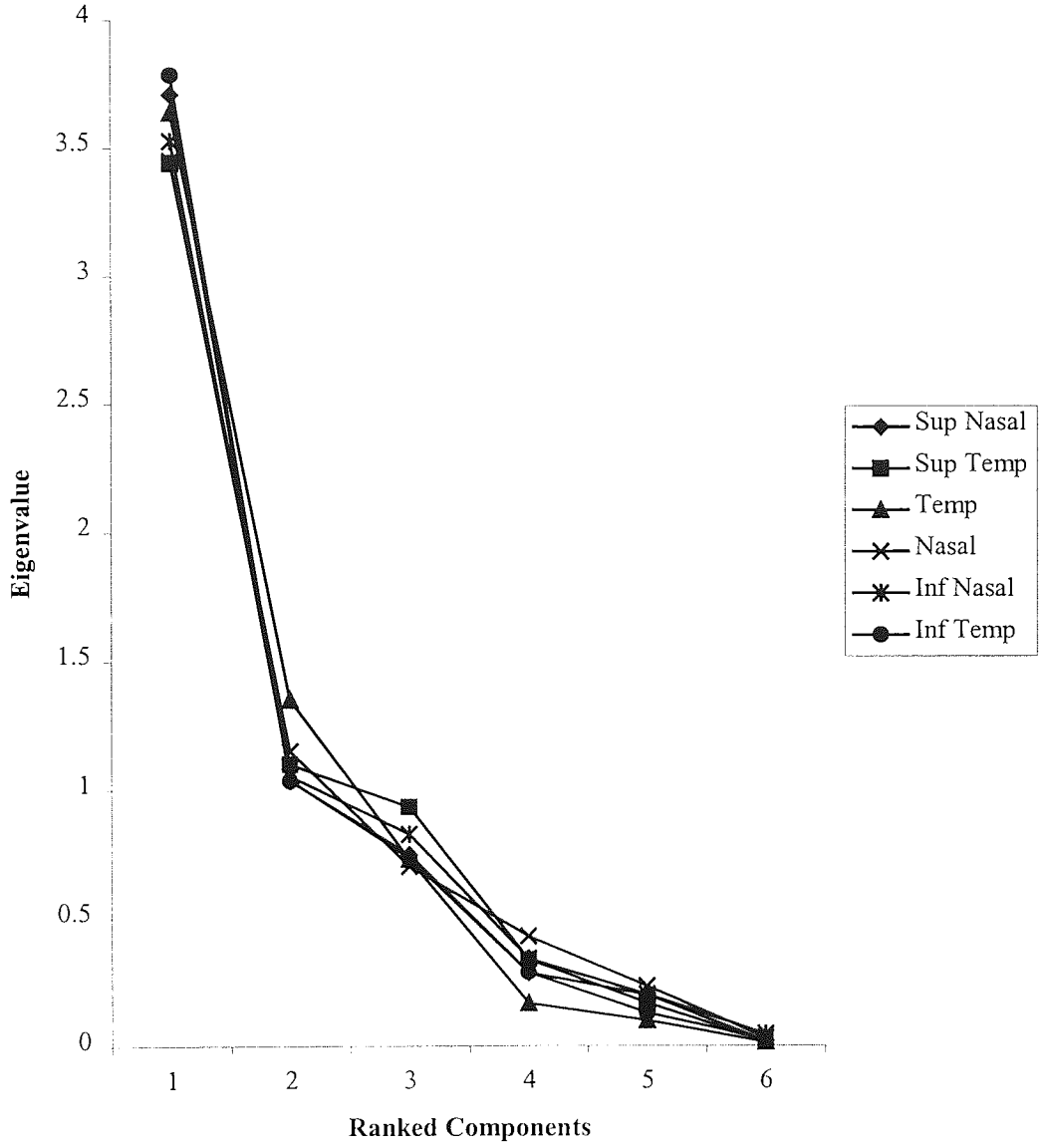

Figure 8.18. Eigenvalues as a function of the ranked component factor for the 6 regional data sets. The graph represents the eigenvalues for 6 factors contained within the 6 regional data sets. The most variance is contained in factor 1 and the least in factor 6. The scree begins after 2 factors.

Six parameters are contained within the regional data sets (2 – 7), therefore the maximum amount of variance that could be expressed by the factors equals 6. Table 8.13. gives the factor weightings for a two factor model following orthogonal rotation. The variance associated with each factor is expressed as a percentage of the overall variance explained by the model. For each data set, the most variance is contained in factor one, which indicates that this factor carries the greatest weighting.

Data set	Factor 1		Factor 2		Total	
	Variance	Variance %	Variance	Variance %	Variance	Variance %
Sup Nasal	2.89	48.17	1.86	31	4.75	79.17
Sup Temporal	3.07	51.17	1.47	24.50	4.54	75.67
Temporal	3.03	50.50	2.0	33.33	5.03	83.83
Nasal	2.41	40.17	2.20	36.67	4.61	76.83
Inf Nasal	2.61	43.50	1.98	33	4.59	76.5
Inf Temporal	3.11	51.83	1.71	28.50	4.82	80.33

Table 8.13. Variance explained by each factor and the total variance (actual and percentage) for two factors according to the rotated factor model for each of the regional data sets.

The rotated factor pattern was examined for each data set to determine which parameters belonged with which factor. The same parameters loaded with factors 1 and 2 for each data set. These are summarised in Table 8.14., the parameters are ranked according to how much they loaded onto any given factor.

Data Set	Factor 1	Factor 2
Regional data (Data sets 2-7)	Vol below reference Vol below surface Maximum depth Third moment	Vol above surface Vol above reference

Table 8.14. Parameter content for factors 1 and 2 for the regional data sets

For the regional data sets (2,3,4,5,6,7), factor 1 describes the size and shape of the cup and factor 2 describes the rim.

8.4.6 Detection of progressive topographical change using factor analysis: By group

The two-factor models were applied to the global and regional data sets. Repeated analysis of covariance (reANCOVA) was used to look for differences over time (5 visits) between the two subject groups. Age was used as a covariate to correct for a potential age effect. The two groups were considered to have changed significantly if $p<0.05$. Bonferroni correction was not applied to the results from the factor reANCOVA's because separating the parameters into factors corrects for repeated analysis.

8.4.6.1 Global data

No significant difference between the two groups was evident for cup (global factor 1) or rim and nerve fibre layer thickness and profile (global factor 2).

8.4.6.2 Regional data

No significant difference between the two groups was evident for cup (regional factor 1) or rim (regional factor 2).

8.4.7 Detection of progressive topographical change using factor analysis: By patient

Analysis of variance (ANOVA) was used to look for change over time for each factor for each individual patient regionally and globally. Significant change was considered to have occurred if $p<0.05$ and $r^2 \geq 0.6$. Bonferroni correction was not applied for reasons mentioned above.

8.4.7.1 Global data

Table 8.15. gives the number and percentage of subjects demonstrating a significant change over time for rim and RNFL (factor 1) and cup (factor 2) measured globally. In total, 10 (33.3%) subjects from the POAG group and just 3 (9.7%) from the normal subject group showed a significant change over time for factor 1.

	Factor 1 (cup)	Factor 2 (Rim and NFL)
Normal	3 [9.7]	7 [22.6]
POAG	10 [33.3]	7 [21.2]

Table 8.15. Number [and percentage] of subjects demonstrating change in factors 1 and 2 globally ($p<0.05$).

8.4.7.2 Regional data

The number and percentage of normal subjects and POAG patients demonstrating a significant change over time for cup (factor 1) and rim (factor 2) are outlined in Tables 8.16. and 8.17. respectively. The percentage of normal subjects showing change in factor 1 (cup) ranged from 3.2% to 16.1%. The percentage showing change in factor 2 (rim) ranged from 3.2% to 22.6%. The percentage of POAG patients demonstrating change in factor 1 (cup) ranged from 12.1% to 24.2%. The percentage showing change in factor 2 (rim) ranged from 3% to 21.1%.

	Normal subject group					
	Sup nasal	**Sup temp**	**Temp**	**Nasal**	**Inf nasal**	**Inf temp**
Factor 1	3 [9.7]	1 [3.2]	5 [16.1]	1 [3.2]	3 [9.7]	2 [6.5]
Factor 2	7 [22.6]	4 [12.9]	2 [6.5]	6 [19.4]	1 [3.2]	4 [12.9]

Table 8.16. Number [and percentage] of normal subjects showing change for factors 1 and 2 regionally

	POAG subject group					
	Sup nasal	**Sup temp**	**Temp**	**Nasal**	**Inf nasal**	**Inf temp**
Factor 1	5 [15.2]	8 [24.2]	8 [24.2]	7 [21.2]	4 [12.1]	7 [21.2]
Factor 2	1 [3]	5 [15.2]	7 [21.2]	4 [12.1]	5 [15.2]	7 [21.2]

Table 8.17. Number [and percentage] of POAG subjects showing change for factors 1 and 2 regionally

8.5 Haemodynamic parameters: tests for normality

Haemodynamic data recorded with the HRF was transferred directly into an Excel for Windows 95 spreadsheet. The data consisted of repeated measures of blood volume, flow and velocity in 4 peripapillary retinal locations. Triplicate measurements were taken (3 images) at each visit (5 visits). The results were tabulated into 4 data sets according to the region of tissue measured:

Data set 1: Superior nasal
Data set 2: Superior temporal
Data set 3: Inferior nasal
Data set 4: Inferior temporal

All of the topographic data was tested for normality by parameter, group and visit. Data was considered Gaussian if $p>0.05$. If the data was not normally distributed then the stem and leaf plots were examined to look for any obvious outliers in the data.

8.5.1 Normality results for haemodynamic data

Tables 8.18. and 8.19. summarise the percentage of data that was normally distributed for each parameter measured for the normal and POAG subject groups respectively. Overall 53.3% of the data was normally distributed for the normal subject group and 51.7% formed a Guassian distribution for the POAG group. Of the data that did not demonstrate a normal distribution, 18.3% for the normal group and 21.7% for the POAG group were associated with single outliers in the data. This left 28.3% for the normal group and 26.6% for the POAG group that were non-Guassian without outliers. As more than half of the data was Guassian, logarithmic transformation of the data was not performed prior to statistical analysis.

Region	Parameter	Normal	Without outliners	With outliers
Superior nasal	Volume	3 [60]	2 [40]	
	Flow	2 [40]	2 [40]	1 [20]
	Velocity	3 [60]	1 [20]	1 [20]
Superior temporal	Volume	1 [20]	3 [60]	1 [20]
	Flow	2 [40]	2 [40]	1 [20]
	Velocity	2 [40]	1 [20]	2 [40]
Inferior nasal	Volume	5 [100]		
	Flow	4 [80]	1 [20]	
	Velocity	3 [60]	1 [20]	1 [20]
Inferior temporal	Volume	3 [60]		2 [40]
	Flow	2 [40]	3 [60]	
	Velocity	2 [40]	1 [20]	2 [40]
	Mean	**32 [53.3%]**	**17 [28.3%]**	**11 [18.3%]**

Table 8.18. Normality data for the HRF parameters (normal group). The number of visits [and %] of data demonstrating a normal distribution and abnormal distribution with and without outliers is given.

Region	Parameter	Normal	Without outliners	With outliers
Superior nasal	Volume	3 [60]	2 [40]	
	Flow	1 [20]	1 [20]	3 [60]
	Velocity	2 [40]	3 [60]	
Superior temporal	Volume	2 [40]	1 [20]	2 [20]
	Flow	3 [60]	2 [20]	
	Velocity	1 [20]	3 [60]	1 [20]
Inferior nasal	Volume	4 [40]	1 [20]	
	Flow	4 [40]		1 [20]
	Velocity	3 [60]		2 [20]
Inferior temporal	Volume	4 [40]	1 [20]	
	Flow	2 [40]	2 [20]	1 [20]
	Velocity	2 [40]		3 [60]
	Mean	**31[51.7%]**	**16 [26.6%]**	**13 [21.7]**

Table 8.19. Normality data for the HRF parameters (POAG group). The number of visits [and %] of data demonstrating a normal distribution and abnormal distribution with and without outliers is given.

8.5.2 Haemodynamic parameters: Baseline values

Table 8.20. summarises the average values obtained at baseline (3 images, 5 visits) for blood volume, flow and velocity for the POAG and normal subject groups.

	Normal		POAG		
Parameter	**Mean**	**SD**	**Mean**	**SD**	**P-value**
Sup temp volume	16.936	5.331	14.767	2.958	0.061
Sup temp flow	262.121	111.894	217.194	44.612	0.042*
Sup temp velocity	0.916	0.371	0.776	0.154	0.059
Sup nasal volume	14.357	3.276	12.506	2.711	0.012*
Sup nasal flow	205.377	66.463	192.512	59.253	0.323
Sup nasal velocity	0.735	0.230	0.699	0.2116	0.407
Inf temp volume	15.954	4.921	15.537	4.921	0.693
Inf temp flow	234.664	85.564	236.781	88.247	0.962
Inf temp velocity	0.823	0.281	0.845	0.298	0.809
Inf nasal volume	11.740	2.908	12.135	3.613	0.689
Inf nasal flow	167.761	49.493	192.213	71.837	0.149
Inf nasal velocity	0.605	0.172	0.697	0.253	0.119

Table 8.20. Baseline values for SLDF parameters. Average ± SD for the haemodynamic parameters, volume, flow and velocity. P-value are shown (Students unpaired t-test). Significant results ($p < 0.05$) are indicated *.

8.5.3 Haemodynamic parameters: change over time between groups

Haemodynamic parameters measured with the HRF were analysed for change over time between subject groups using repeated measures analysis of covariance (reANCOVA). Age was used as the covariate and group as the between factor. Change over time (5 visits) for each parameter between the two subject groups was considered significantly different if $p<0.01$. It was also necessary that within-visit variation did not demonstrate significant differences ($p>0.01$) (Bonferroni corrected).

Table 8.21. gives the results for the reANCOVA analysis (p-values) for each parameter. Results significant to the 95% confidence limit ($p<0.01$) are indicated (Bonferroni corrected). A significant difference between the two subject groups over time was evident for the parameters, blood flow, volume and velocity in the inferior nasal quadrant only. To demonstrate the difference in parameter change between the two groups, graphs were plotted of the average values obtained at visits 1-5 for the significant parameters for the POAG group and normal group (Figures 8.19.-8.21.). For each graph, standard error bars are given together with a linear trend line and r-square value.

Parameter	Data set (region measured)			
	Superior nasal	Superior temporal	Inferior nasal	Inferior temporal
Volume	0.1195	0.4864	0.0073 *	0.3984
Flow	0.4398	0.8330	0.0097 *	0.4822
Velocity	0.2128	0.1615	0.0095 *	0.0151

Table 8.21. ANCOVA results with age as the covariate (p-values) for the parameters blood volume, flow and velocity. Results significant to $p<0.01$ are marked*.

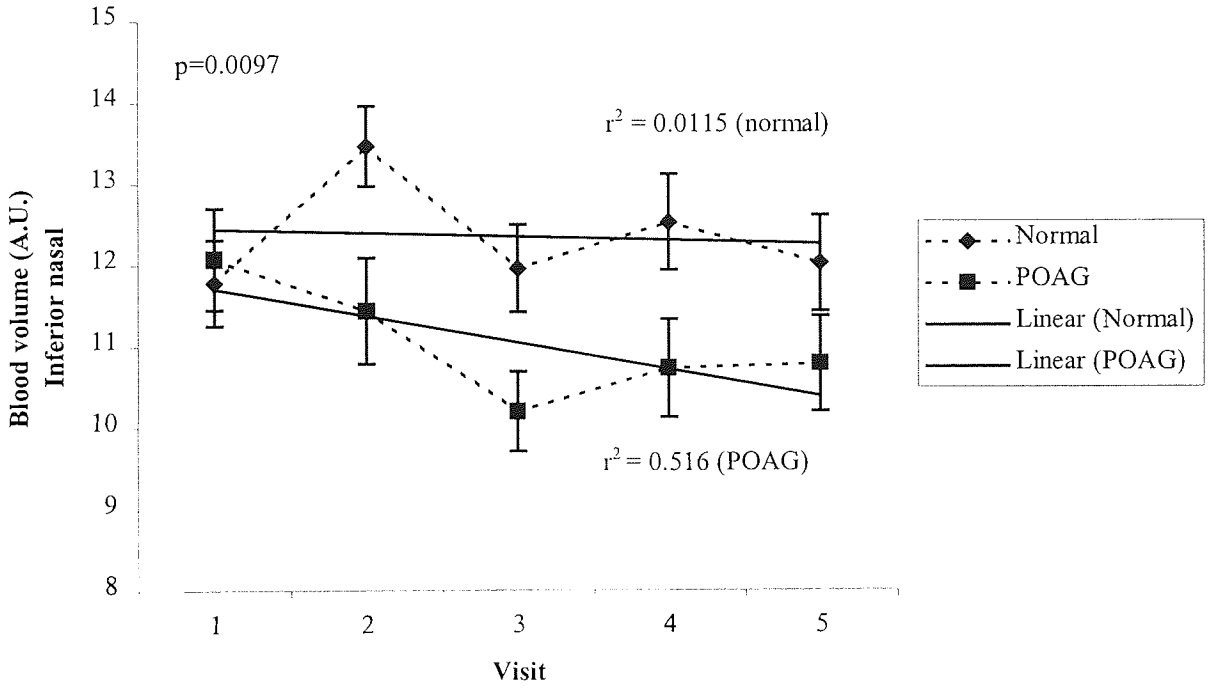

Figure 8.19. Mean values at visits 1-5 for blood volume in the inferior nasal quadrant for the normal and POAG subject groups. Standard error bars are given together with a linear trend line and r^2 value.

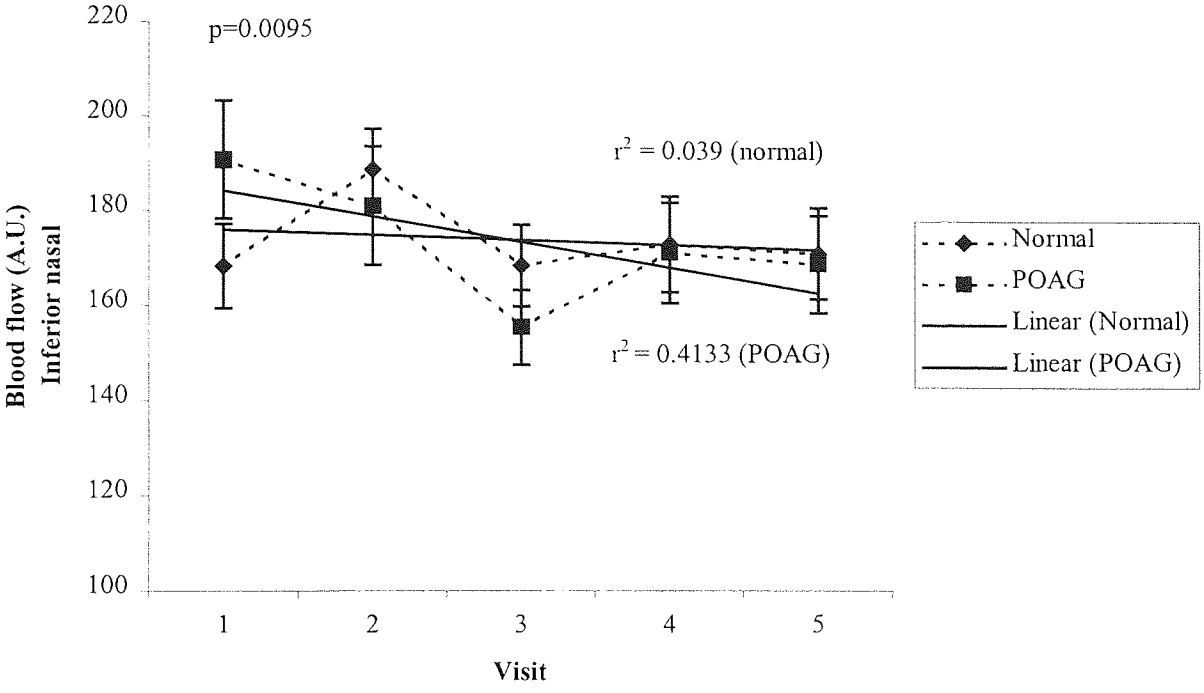

p=0.0073

Figure 8.2(...es at visits 1-5 for blood flow in the inferior nasal quadrant for the normal and POAG subject groups. Standard error bars are given together with a linear trend line and r^2 value.

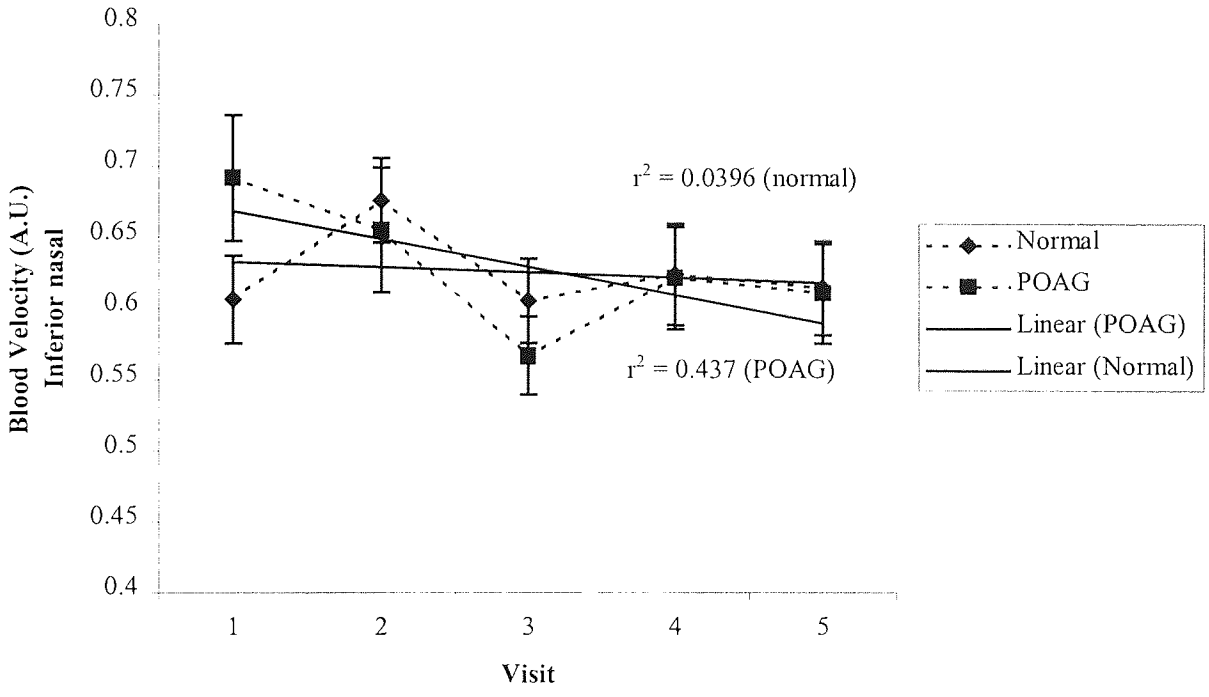

Figure 8.21. Mean values at visits 1-5 for blood velocity in the inferior nasal quadrant for the normal and POAG subject groups. Standard error bars are given together with a linear trend line and r^2 value.

8.5.4 Haemodynamic parameters: change over time by subject

The three haemodynamic parameters (volume, flow and velocity) measured with SLDF were analysed for change over time for each subject using repeated measures analysis of variance (reANOVA). As patients were being assessed independently of each other it was not necessary to correct for an age effect. Change over time (5 visits) for each parameter was considered significantly different if $p<0.01$; $r^2=\geq 0.6$ (Bonferroni corrected). It was also necessary that within visit variation did not demonstrate significant differences ($p>0.01$).

The results are summarised in Tables 8.22. (superior data) and 8.23. (inferior data).

	Superior temporal			Superior nasal		
Parameter	**Vol**	**Flow**	**Vel**	**Vol**	**Flow**	**Vel**
Normal	4 [12.9]	5 [16.1]	5 [16.1]	6 [19.4]	7 [22.6]	8 [25.8]
POAG	9 [27.3]	6 [18.2]	6 [18.2]	8 [24.2]	6 [18.2]	4 [12.1]

Table 8.22. Number [and percentage] of normal and POAG subjects showing change in blood volume, flow and velocity in the superior quadrants.

	Inferior temporal			Inferior nasal		
Parameter	**Vol**	**Flow**	**Vel**	**Vol**	**Flow**	**Vel**
Normal	4 12.9]	5 [16.1]	4 [12.9]	4 [12.9]	2 [6.5]	1 [3.2]
POAG	5 [15.2]	4 [12.1]	4 [12.1]	8 [24.2]	10 [30.3]	11 [33.3]

Table 8.23. Number [and percentage] of normal and POAG subjects showing change in blood volume, flow and velocity in the inferior quadrants.

Change over time for blood flow, volume and velocity was evident for both the normal and POAG subjects in all 4 quadrants. The percentage of normal subjects demonstrating significant change over time ranged from 12.9% (inferior temporal velocity, inferior nasal volume) to 25.8% (superior nasal velocity). The percentage of POAG subjects demonstrating significant change in parameters ranged from 12.1% (inferior temporal flow & velocity) to 33.3% (inferior nasal flow). The greatest

distinction between the number of normal subjects and number of POAG patients that showed change over time was evident in the inferior nasal quadrant. This correlates with the ANCOVA results for the group findings that the blood flow parameters in the inferior nasal quadrant differ between the two groups over time. Figure 8.22. gives the percentage of POAG and normal subjects showing change for each parameter inferior nasally.

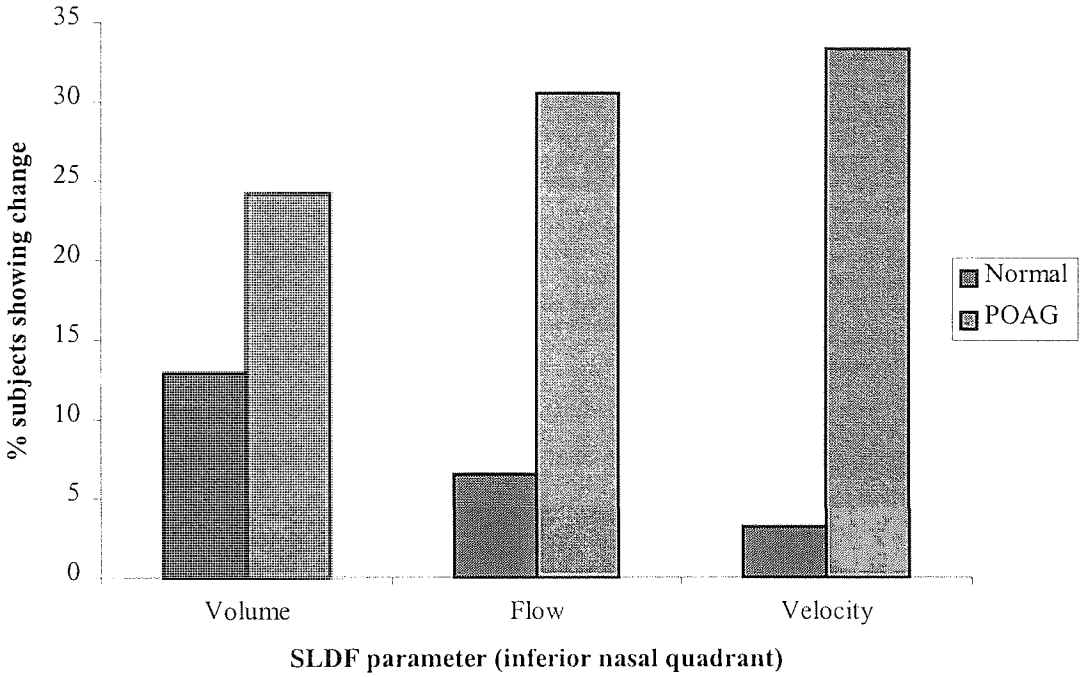

Figure 8.22. Percentage of subjects showing change over time for volume, flow and velocity in the inferior nasal quadrant.

8.6 Visual fields indices

The data for the 3 measured visual field parameters (MD, PSD and CPSD) consisted of 5 discrete measurements, one for each visit. The data was manually input to an Excel spreadsheet.

8.6.1 Visual field indices: Baseline values

The average values at baseline for MD, PSD and CPSD for the POAG and normal subject groups across 5 visits are given in Table 8.24. A Students 2-tailed unpaired t-test was used to compare the two groups. The groups were considered significantly different if $p<0.05$.

	Normal		POAG		
Parameter	**Mean**	**SD**	**Mean**	**SD**	**P-value**
MD	-1.062	1.119	-6.235	1.119	0.000
PSD	2.038	0.700	5.842	0.700	0.000
CPSD	0.992	0.817	5.305	0.818	0.000

Table 8.24. Baseline values (± SD) for MD, PSD & CPSD (5 visits) for the two subject groups.

8.6.2 Visual field indices: Change by group

ANCOVA was used to assess change over time between the two subject groups. Group was used as the between factor and age as the covariate. Significant change was considered to have occurred if $p<0.05$ and $r^2 \geq 0.6$. Table 8.25. outlines the ANCOVA results for the measured visual field indices.

	p-value	r squared
MD	<0.0001	0.9398
PSD	<0.0001	0.9692
CPSD	<0.0001	0.9532

Table 8.25. ANCOVA results for visual field indices. MD: Mean deviation, PSD: pattern standard deviation, CPSD: corrected pattern standard deviation.

ANCOVA revealed a significant difference between the normal and POAG group for change in MD, CPSD and PSD over time. Graphs were plotted for the mean values of visual function indices at visits 1-5 for the POAG and normal subject groups to explore the way in which the two groups differed. Linear regression revealed a significant r^2 for PSD and CPSD for the POAG group (Figures 8.24. & 8.25.). PSD for the normal group decreased significantly over the study period ($r^2=0.6448$) suggestive

of a learning effect (Figure 8.24.). No significant change in MD was evident for the POAG or normal group over the study period (Figure 8.23.).

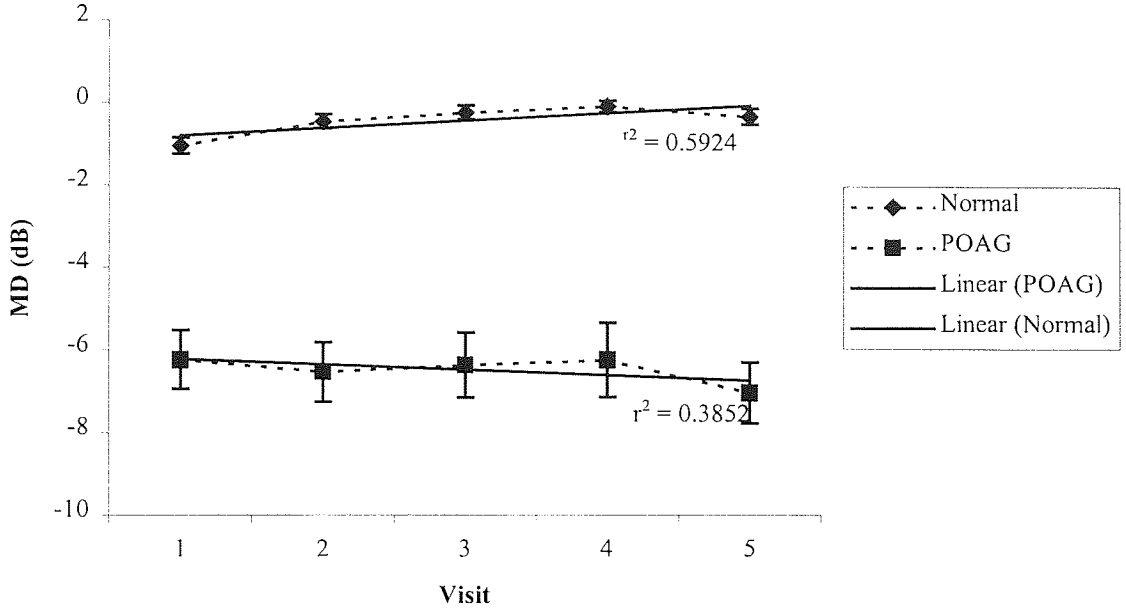

Figure 8.23. Mean values (1-5 visits) for the visual field parameter MD for the POAG and normal subject groups. Linear trend lines together with r^2 and standard error bars are given.

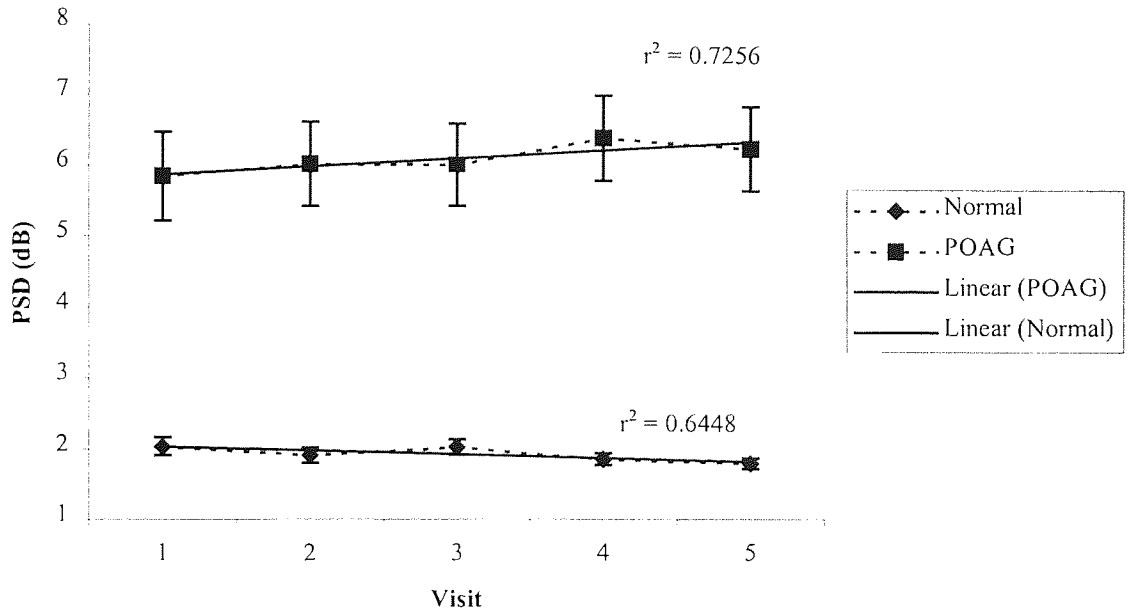

Figure 8.24. Mean values (1-5 visits) for the visual field parameter PSD for the POAG and normal subject groups. Linear trend lines together with r^2 and standard error bars are given.

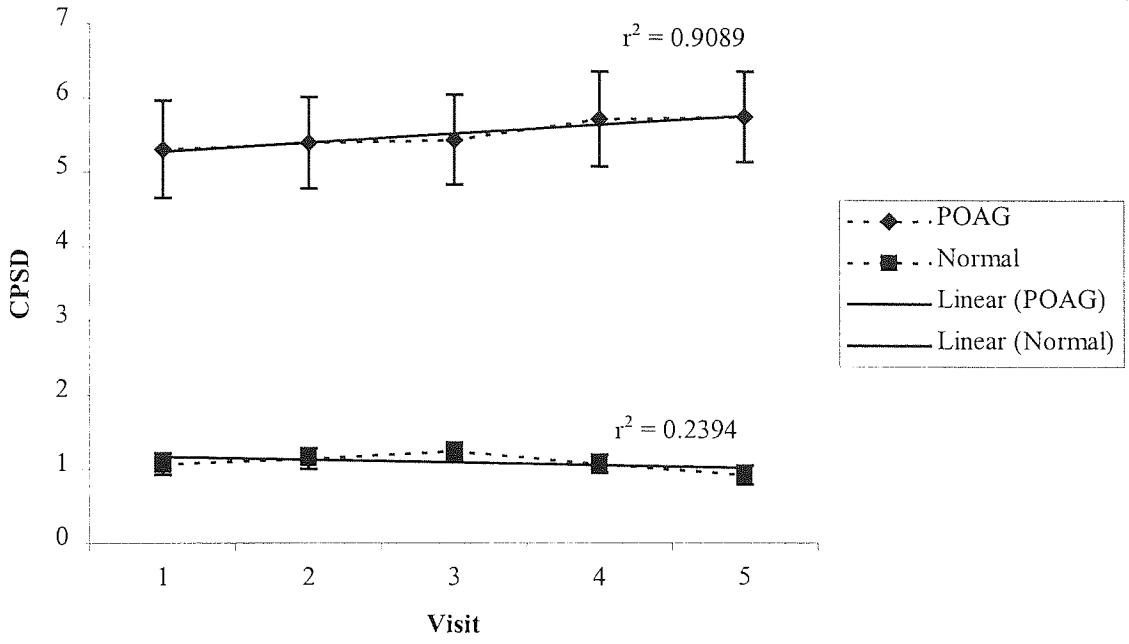

Figure 8.25. Mean values (1-5 visits) for the visual field parameter CPSD for the POAG and normal subject groups. Linear trend lines together with r^2 and standard error bars are given.

8.6.3 Visual field indices: Analysis by subject

ANOVA and linear regression analysis were used to look for change across the 5 visits for each subject for each visual field parameter. Significant change was said to have occurred over the study period if $p<0.05$; $r^2 \geq 0.06$.

In total, 12.9% (4) subjects from the normal group (subjects 7, 13, 15, and 28) and 21.2% (7) subjects from the POAG group (subjects 40, 41, 44, 51, 57, 58 and 62) demonstrated a significant difference over the study period in at least one visual field parameter (Table 8.26.). Of the 7 subjects showing significant change over time for the POAG group, 5 had undergone treatment changes ranging from additional topical therapy (41, 51, 57 and 62) to trabeculectomy (44). Subjects 40 & 51 showed a relative improvement in visual field indices, probably associated with a learning effect. The remaining POAG subjects demonstrated a significant deterioration in visual field parameters (Table 8.27.). Of the subjects demonstrating significant change

over time for the normal group, 3 showed a significant improvement in visual field parameters, only one subject (7) showed deterioration (Table 8.27.).

Parameter	Normal subject group No. and [%] showing change	POAG subject group No. and [%] showing change
MD	2 [6.5]	1 [3]
PSD	0 [0]	3 [9.1%]
CPSD	2 [6.5]	7 [21.2]

Table 8.26. Number and percentage of subjects demonstrating significant change in visual field parameter over the study period.

Subject group	Subject No.	MD	PSD	CPSD
POAG	40			[※]
POAG	41	※	※	※
POAG	44			※
POAG	51			[※]
POAG	57		※	※
POAG	58		※	※
POAG	62			※
Normal	7			※
Normal	13	[※]		
Normal	15			[※]
Normal	28	[※]		

Table 8.27. ※= Individual POAG and normal subjects demonstrating significant differences in visual field parameters over the study period. [※] = indicates a relative improvement.

8.7 IOP

IOP data consisted of 5 discrete measurements, one for each visit. The data was manually inputted into an excel spreadsheet.

8.7.1 IOP: Baseline values

The average IOP values at baseline for the two subject groups (5 visits) are given in Table 8.28. A Students 2-tailed unpaired t-test was used to compare the two groups. The groups were considered significantly different if $p<0.05$.

	Normal		POAG		
Parameter	**Mean**	**SD**	**Mean**	**SD**	**P-value**
IOP	15.225	2.105	18.758	2.105	0.000

Table 8.28. Average (± SD) IOP values at baseline for the two subject groups (5 visits). P-values are given (Students t-test). Values <0.05 indicate a significant difference between the two groups.

8.7.2 IOP: Analysis by group

ANCOVA was used to assess for change over time in IOP between the two subject groups. Group was used as the between factor and age as the covariate. Significant change was considered to have occurred if $p<0.05$ and $r^2 \geq 0.6$.

The results showed a significant difference between the two groups for change in IOP over the 5 visits (p=>0.0001). A graph was plotted of the mean values for the two groups to explore the way in which they differ (Figure 8.26.).

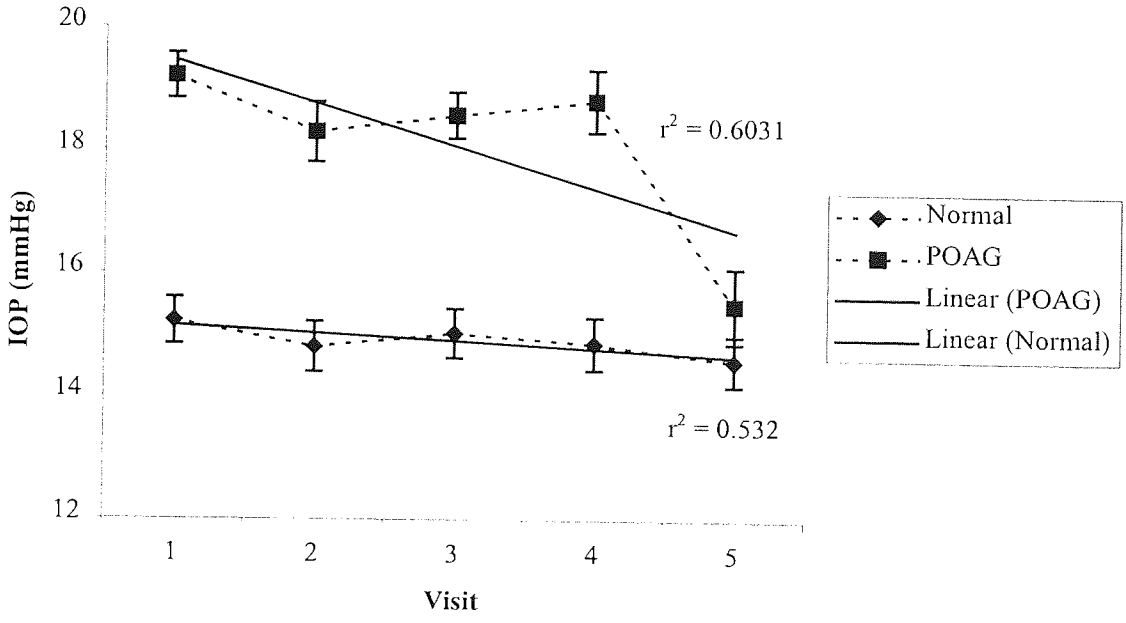

Figure 8.26. Mean values (1-5 visits) for IOP measured in the POAG and normal subject groups. Linear trend lines together with r^2 and standard error bars are given.

8.7.3 IOP: Analysis by subject

Linear regression analysis was used to look for change in IOP across the 5 visits for each subject. Significant change was said to have occurred over the study period if $p<0.05$; $r^2 \geq 0.6$.

No significant differences in IOP across 5 visits were evident for subjects from either group based on linear regression. Three POAG subjects underwent trabeculectomy resulting in a significant decrease in IOP that was not linear over time.

8.8 Cup-disc ratio (subjective measure)

C:D ratio data (horizontal and vertical) was subjectively measured by one of two consultant ophthalmologists and consisted of 5 discrete measurements for the POAG group only, one for each visit. The data was manually inputted into an excel spreadsheet.

8.8.1 Cup-disc ratio: change over time

ANOVA together with linear regression analysis was used to assess for change over time for horizontal and vertical C:D ratio, as measured subjectively by an ophthalmologist (POAG group only). Significant change was considered to have occurred if $p<0.05$ and $r^2 \geq 0.6$. Table 8.29. gives the p-values for the clinically determined parameters. Horizontal C:D ratio changed significantly over time for the group. Vertical C:D ratio, although significant by linear regression, was not significant for the ANOVA analysis. Figure 8.27. shows the mean values for horizontal and vertical C:D ratio for each visit for the POAG group. Standard error bars are given together with a linear trend line and r^2 value.

	C:D ratio	
	Horizontal	**Vertical**
P-Value (ANOVA)	0.0019*	0.1631
R^2 (linear regression)	0.7358	0.6951

Table 8.29. ANOVA and linear regression results for horizontal and vertical C:D ratio as measured clinically by an ophthalmologist. Results are for the POAG group only. Significant results ($p<0.05$; $r^2 \geq 0.6$) are indicated*.

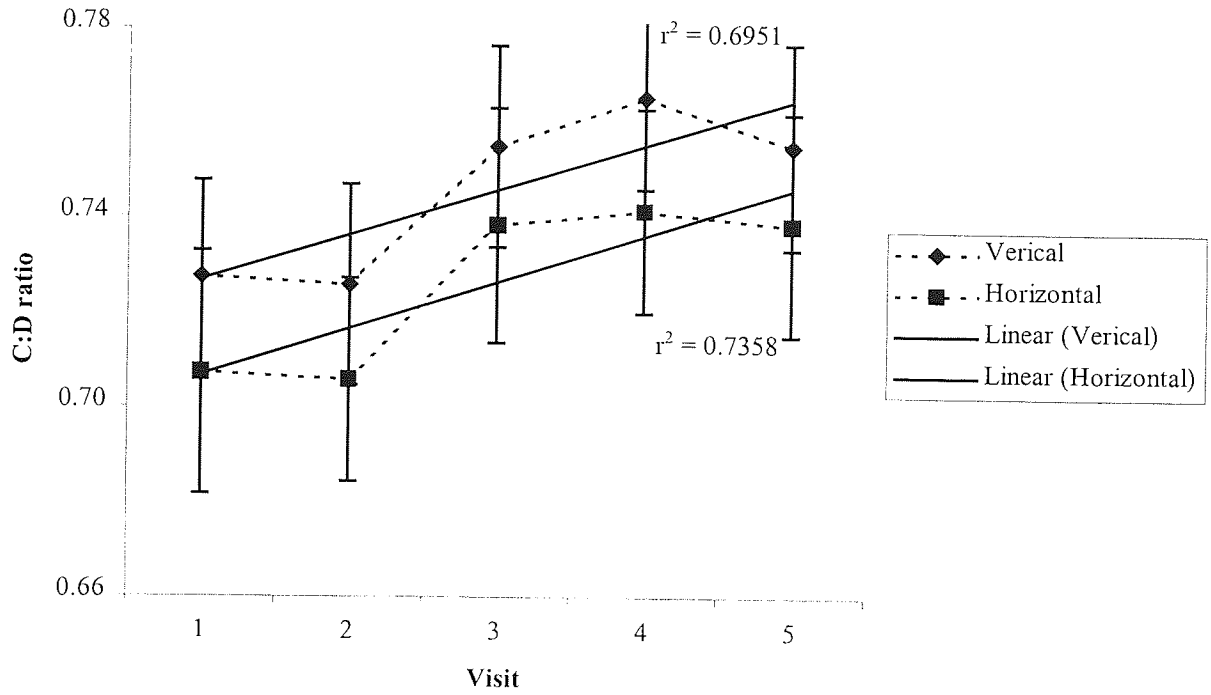

Figure 8.27. Mean values for horizontal and vertical C:D ratio (measured subjectively by a clincian) at each visit for the duration of the study. Data for POAG group only. Linear trend lines are shown together with r^2.

Chapter 9.

Topographic haemodynamic and psychophysical investigation of glaucomatous optic neuropathy: Discussion

9.1 Subject follow-up

The sample for each cohort was determined using sample size calculations as discussed in section 7.3.1. An additional 20% was included in the calculation for each group to allow for dropout. Initial dropout was greater than anticipated and additional subjects were recruited to allow for this. In total, 44 POAG patients and 34 normal subjects were recruited into the study. A drop out rate of 25% for glaucoma patients and 9% for normal subjects occurred during the period of follow-up. The reasons for dropout are shown in Table 8.1. Fortunately, the minimum sample size was maintained for both subject groups throughout the follow-up period of the study. However, for subsequent longitudinal studies, an allowance of at least 25% above the minimum subject sample size is recommended for the diseased group, although this may be subject to local variations.

9.2 Group demographics

Group	Age (yrs)		High BP	Sex		Eye	
	Mean ± SD	Range		M	F	R	L
Normal group	65 ± 8.3	45 – 77	8 [25.8%]	14 [45.2%]	17 [54.8%]	16 [51.6%]	15 [48.4%]
POAG group	71.2 ± 7.6	52 - 84	7 [21.2%]	14 [42.4%]	19 [57.6%]	17 [51.5%]	16 [48.5%]

Table 9.1. Demographic data for the normal and POAG subject group.

9.2.1. Age

The physiological loss of optic nerve axons, which occurs as a consequence of the normal ageing process potentially resulting in changes in disc topography, is well documented (Balazsi, A. G. *et al.*, 1984; Johnson, B. M. *et al.*, 1987; Mikelberg, F. S. *et al.*, 1989; Repka, M. X. *et al.*, 1989; Tsai, C. S. *et al.*, 1992; Roche, M. *et al.*, 1994; Varma, R. *et al.*, 1994). The effects of age on ocular blood flow are less well documented but it is believed that there is a decrease in ocular blood flow with age (Kothe, A. C. *et al.*, 1992a; Ravalico, G. *et al.*, 1994b; Groh, M. J. M. *et al.*, 1996). A negative correlation between age and IOP has been reported in the Asian population (Japanese) (Shiose, Y., 1990), however a positive correlation between age and IOP has been documented in western populations (Armaly, M. F., 1965) suggesting ethnic variability. Finally, a reduction in visual field sensitivity is associated with increased age (Brenton, R. S. & Phelps, C. D., 1981; Hass, A. *et al.*, 1985; Katz, J. & Sommer, A., 1986).

There was a significant difference between the mean age of the two groups ($p=0.003$). The mean age for the POAG group was slightly higher (71.2 ± 7.6 years) than for the normal group (65 ± 8.3 years) (Table 9.1.). A difference in the mean age of the two groups could potentially account for differences in baseline measures. For these reasons a statistical correction was made to account for possible age effects in this study.

9.2.2 Gender

Differences that have been identified between genders are discussed in section 1.5.3. Briefly differences between females and males have been documented for IOP (Armaly, M. F., 1965) and ocular blood flow (Yang, Y. C. *et al.*, 1997a). An increased tendency of females to develop NTG has also been reported (Varma, R. *et al.*, 1994; Orgül, S. *et al.*, 1995).

The gender distribution between the two subject groups was similar for this study. The normal group contained 14 (45.2%) males and 17 (54.8%) females. The POAG group contained 14 (42.4%) males and 19 (57.6%) females (Table 9.1.). Both groups were female biased and this was most probably associated with higher mortality rates in men at older age groups.

9.2.3 Test eye

There were similar numbers of right and left eyes in each group. The POAG group contained 17 (51.5%) right eyes and 16 (48.5%) left eyes and the normal group contained 16 (51.6%) right eyes and 15 (48.4%) left eyes. Although specific differences between topography and haemodynamic indices between right and left eyes have not been identified, randomising the numbers in each group prevented bias (Kahn, H. A. *et al.*, 1975; Murdoch, I. E. *et al.*, 1998).

9.2.4 Systemic blood pressure

Ideally systemic hypertension should have been an exclusion factor for the study to ensure that mean diastolic and systolic blood pressure was not significantly different between the two subject groups. Some studies have identified a positive association between systemic hypertension and increased IOP (Leske, M. C. & Podgor, M. J., 1983; Carel, R. S. *et al.*, 1984). The absolute significance between raised IOP and blood pressure remains unclear, however, it is suggested that such a combination may result in decreased perfusion pressure of the eye which is associated with increased risk of POAG (Tielsch, J. M. *et al.*, 1995). It was considered impractical to include hypertension as an exclusion factor due to the difficulty in finding patients without hypertension, that fitted all other inclusion criteria.

Overall, similar numbers of subjects were diagnosed with hypertension in the normal (n=8, 25.8%) and POAG (n=7, 21.2%) subject groups, all of which were on treatment. On this basis any effect of systemic hypertension on ocular blood flow values would have been similar between the two groups. Systemic hypotension is regarded as a

more important risk factor for glaucoma as it results in decreased blood flow (Demailly, P. *et al.*, 1984; Perasalo, R. & Raitta, C., 1990; Kaiser, H. J. *et al.*, 1993b; Hayreh, S. S. *et al.*, 1994; Gramer, E. & Tausch, M., 1995). No subjects were diagnosed with hypotension in either subject group.

9.3 Topographic measurement with the HRT

9.3.1 Accuracy

Overall, accuracy is less of an important factor than reproducibility for the long-term follow-up of disease progression because the same retinal feature is being assessed and any errors in accuracy are relative. The exception to the rule would be when a change in refraction has occurred in the test eye. In such a case it is important that the accuracy of the instrument is sufficient to ensure the change in refraction does not result in distortion of the size of the retinal feature under examination. This was investigated using a simple lens system and template (Chapter 3). The results suggest that the HRT is able to accurately measure an object size during changes in axial length and hence refraction. Other studies have assessed the accuracy of the HRT and it's predecessor, the LTS, and have shown them to be both accurate and valid for topographic measurement (Dreher, A. W. & Weinreb, R. N., 1991; Bartz-Schmidt, K. U. *et al.*, 1994; Janknecht, P. & Funk, J., 1994; Janknecht, P. & Funk, J., 1995).

9.3.2 Reproducibility

The reproducibility of topographic measurement is important for the detection of real change over time. There are several factors known to affect the reproducibility of measurements obtained with the HRT and these are outlined in section 1.11.2.6. Efforts were made to maximise the reproducibility of repeated measurements for the longitudinal study. All pupils were dilated to reduce variability (Zangwill, L. *et al.*, 1997) and maximise the quality of the images. The focus setting was kept constant for within visits and between visits unless a change in refraction occurred in the test eye

(Hosking, S. L. & Flanagan, J. G., 1996). The scan depth was kept constant within visit and only changed between visit if the HRT acquisition software requested it (Hosking, S. L. *et al.*, 1997a). For within visit image acquisition, subjects were requested to keep their heads on the chin rest until all 7 images were obtained. This minimised tilt and misalignment of the laser head and eye (Orgül, S. *et al.*, 1996). Finally, each image was assessed immediately after acquisition to ensure images were of an acceptable quality (well focussed, minimal movement).

9.3.3 Topographic parameters previously identified as useful

A number of studies have highlighted certain parameters as important for classifying between groups of subjects (Mikelberg, F. S. *et al.*, 1995; Zangwill, L. M. *et al.*, 1996; Eid, T. M. *et al.*, 1997; Iester, M. *et al.*, 1997a). Table 9.2. summarises some key studies and the parameters considered important. In particular the parameters third moment in contour, volume above reference and RNFL cross-sectional area appear useful (Brigatti, L. & Caprioli, J., 1995; Mikelberg, F. S. *et al.*, 1995; Eid, T. M. *et al.*, 1997; Iester, M. *et al.*, 1997a; Tole, D. M. *et al.*, 1998).

Eid 1997	**Iester 1997**	**Tole 1998**	**Mikelberg 1995**	**Brigatti 1995**
	Third moment	Third moment	Third moment	Third moment
	Volume above reference	Volume above reference	Volume above reference	
RNFL cross-sectional area	RNFL cross-sectional area	RNFL cross-sectional area	Height Variation of contour	
	Rim area	RNFL thickness		
	Cup area			
	Cup: disc area ratio			

Table 9.2. HRT parameters identified as important for classifying between groups and correlating with visual field loss. The shaded cells identify important parameters common to different studies.

There are few longitudinal studies published that identify which HRT parameters are best for detecting glaucomatous progression. A 1-year follow-up of pre- and post-

trabeculectomy ONH topography showed significant changes (relative improvements) in the HRT parameters third moment in contour, cup volume, mean cup depth and height variation in contour (Topouzis, F. *et al.*, 1999). A recent study followed a group of ocular hypertensive patients (n=13) and a group of normal subjects (n=11) for one year and identified cup:disc area ratio, cup area and rim area as important for detecting change during conversion to POAG (Kamal, D. S. *et al.*, 1999). It should be noted that the group sizes were particularly small in the afore mentioned study and assumptions were based on the comparison of topographic parameters measured at two visits only.

9.3.4 Topographic follow-up of glaucomatous and normal optic nerve heads

A review of the current literature identified a real need for well-designed studies that investigate the potential use of cSLO in the follow-up of glaucoma. It is likely that the parameters shown to be useful for classifying between groups of patients may differ from parameters that are good for detecting change over time in progressive glaucomatous optic neuropathy.

The principle aim of this study was to investigate whether the HRT could detect subtle changes in the ONH due to progressive glaucomatous optic neuropathy. This change was measured against any potential physiological alteration in topography in a normal population followed for the same period. The determination of change in topographic parameters was measured by group comparison, and by identification of change in individual subjects and patients.

Inclusion criteria were adopted to maximise the potential of identifying real change in the glaucoma group. This was important because of the relatively short follow-up period of 16 months and the low incidence of progressive optic neuropathy. It has been reported that less than one in three eyes diagnosed with POAG demonstrate progressive visual field loss when followed for an average period of 6.3 years (Katz, J. L. *et al.*, 1997). In a retrospective study by Pederson, J. E. & Anderson, D. R. (1980),

where the optic disc photographs of 259 patients with raised IOP were followed for 15 years, only 29 showed progression in cupping (generalised expansion of cup). Of these, 50% went on to develop visual field loss in the following 2 years.

The recruitment criteria are summarised in section 7.4. Clearly, change in the glaucoma population would not be identified in cases of end-stage disease. For this reason none of the patients recruited had cup:disc ratios of greater than 0.8. In addition, patients were recruited according to the extent of visual field loss. Studies have shown that clinically detectable nerve fibre loss can occur early on in glaucoma, even before demonstrable visual field loss (Sommer, A. *et al.*, 1991a; Quigley, H. A. *et al.*, 1992). Furthermore, patients with very severe visual field defects demonstrate greater variability of psychophysical measures and as a result progression is more difficult to detect (Hodapp, E. *et al.*, 1993; Katz, J. L. *et al.*, 1997). On this basis, only patients with early to moderate visual field loss as defined by Hodapp, E. *et al.*, (1993) were recruited as it was thought they would most likely show measurable change (see section 7.4.).

The following sections discuss the results obtained for a cross-sectional analysis of baseline data by group, a longitudinal analysis by group and an analysis of individual glaucoma patients and normal subjects.

9.3.5 Cross-sectional comparison between groups at baseline

The global HRT data measured for the POAG patient group at baseline was compared to that of the normal subject group at baseline to give an indication of how the two groups differed topographically (unpaired Student's t-test). Table 8.5. outlines the mean values and standard deviation of each parameter together with p-values. With the exception of disc area, all of the HRT parameters differed significantly between the two groups ($p<0.01$) suggesting their potential use for classifying between glaucomatous and normal optic nerve heads. Tables 9.3. and 9.4. outline the mean HRT parameter values measured in the present study and a number of other studies for normal and POAG subjects respectively.

The subject sample sizes for the normal groups quoted by Zangwill, L. M. *et al.*, (1996), Iester, M. *et al.*, (1997a) and Wollstein, G. *et al.*, (1998) were greater than in the current study and their results may be better representative of a normal and glaucomatous population (Tables 9.3. & 9.4.). It should be noted however, that the afore mentioned studies were cross-sectional in design requiring much bigger sample sizes. The number of normal and POAG subjects recruited for this study were calculated using power statistics (section 7.3.1) and considered adequate for a longitudinal follow-up looking for change in topography. This study was not designed for cross-sectional analysis, but the baseline comparison is of interest for identifying differences between the groups.

The absolute values found in this study for the normal and POAG group are compared to other published data and the individual parameters are discussed in terms of their ability to distinguish between the two subject groups in the following sections.

Parameter	Roff (1999)	Zangwill (1996)	Iester (1997)	Wollstein (1998)
Subject number	**n=31**	**n=46**	**n=59**	**n=81**
C:D area ratio	0.199	0.21	0.28	0.21
Disc area	2.06	2.02	2.43	1.98
Mean height contour	0.010	0.11		
Height variation contour	0.335		0.40	0.37
Volume below surface	0.190			
Volume above surface	0.065			
Volume below reference	0.076	0.10	0.23	0.09
Volume above reference	0.350	0.43	0.48	0.40
Maximum depth	0.477	0.55	0.72	
Third moment	-0.198	-0.19	-0.20	-0.19
RNFL thickness	0.224		0.26	0.24
Mean depth contour	0.096			
Rim area	1.391	1.57	1.73	1.55
Cup area	0.396	0.46	0.71	0.44
Classification	1.665			
Reference height	0.227	0.28	0.3	

Table 9.3. Mean values for HRT parameters measured for normal subjects in the present study (column 1) and 4 other studies

Parameter	Roff (1999)	Zangwill (1996)	Iester (1997)	Wollstein (1998)
Subject number	**n=31**	**n=46**	**n=124**	**n=51**
POAG stage	Early-moderate	Early-moderate	Moderate?	Early
C:D area ratio	0.487	0.47	0.44	0.47
Disc area	2.03	2.00	2.34	1.89
Mean height contour	0.125	0.39		
Height variation contour	0.305		0.37	0.31
Volume below surface	0.489			
Volume above surface	0.045			
Volume below reference	0.314	0.33	0.36	0.29
Volume above reference	0.218	0.23	0.28	0.19
Maximum depth	0.732	0.72	0.71	
Third moment	-0.090	-0.10	-0.11	-0.10
RNFL thickness	0.171		0.2	0.17
Mean depth contour	0.235			
Rim area	1.029	1.03	1.39	0.98
Cup area	1.004	0.97	1.07	0.91
Classification	-0.742			
Reference height	0.296	0.36	0.29	

Table 9.4. Mean values for HRT parameters measured for POAG subjects in the present study (column 1) and 4 other studies.

9.3.5.1 Cup:disc area ratio at baseline

The mean values for the parameter cup:disc area ratio were significantly greater for the POAG group (0.487 ± 0.095) compared to the normal group (0.199 ± 0.115). This finding is in agreement with earlier studies and indicates an increase in the size of the cup and decrease in the amount of healthy rim tissue in the POAG group (Armaly, M. F., 1970; Pederson, J. E. & Anderson, D. R., 1980; Klein, B. E. K. *et al.*, 1985). The mean values for the normal and POAG subjects in this study were very similar to those reported by other studies (Zangwill, L. M. *et al.*, 1996; Iester, M. *et al.*, 1997a; Wollstein, G. *et al.*, 1998) (Tables 9.2. & 9.3.).

9.3.5.2 Cup area, maximum depth and mean depth in contour at baseline

The mean values for the parameters maximum depth, mean depth in contour and cup area were significantly larger for the POAG group (0.732 ± 0.171mm, 0.235 ± 0.084mm, 1.004 ± 0.334mm^2) compared to the normal group (0.477 ± 0.195mm,

0.096 ± 0.061mm, 0.396 ± 0.282mm^2). All of these parameters are related to the depth and size of the cup and indicate large deep cups in the glaucoma group compared to the normal group.

The values reported by other studies for maximum depth and cup area in normal subjects were slightly higher than in this study. This may be the result of different sample sizes between studies. The baseline values for POAG subjects were similar to other published studies thus suggesting that the sample was reflective of a glaucomatous population with early to moderate visual field loss (Zangwill, L. M. *et al.*, 1996; Iester, M. *et al.*, 1997a) (Tables 9.1. & 9.2.).

9.3.5.3 Cup volume at baseline

The two measures of cup volume (volume below reference and volume below surface) were significantly larger for the POAG group (0.314 ± 0.201mm^3, 0.489 ± 0.241mm^3) compared to the normal group (0.076 ± 0.077mm^3, 0.190 ± 0.147mm^3) ($p<0.01$). There was a much larger distinction between the two groups for volume below reference. Other studies report slightly higher values for cup volume in a normal population and similar values for a glaucoma population. The results for these parameters suggest wide and deep optic cups in the POAG group consistent with nerve fibre loss and small, shallow cups for the normal group. The smaller cup measures observed for the normal subject group in this study compared to other studies may account for the high level of significance between the parameters for the normal and POAG subject groups.

9.3.5.4 Rim area and rim volume at baseline

The parameters rim area, volume above reference and volume above surface were smaller for the POAG group (1.029 ± 0.209mm, 0.218 ±0.082mm^3, 0.045 ± 0.022mm^3) compared to the normal group (1.391 ± 0.223mm, 0.352 ± 0.105mm^3, 0.065 ± 0.034mm^3). These findings signify loss of rim tissue for the POAG group and

thicker rim tissue for the normal subject group. Mean values for the rim area and volume above reference parameters were slightly lower for the normal group in comparison to other studies (Zangwill, L. M. *et al.*, 1996; Iester, M. *et al.*, 1997a; Wollstein, G. *et al.*, 1998). Again, the values for the POAG group compared favourably. Volume above surface could not be compared as there was no published data available for that parameter in the studies outlined in Tables 9.3.and 9.4.

9.3.5.5 Height variation in contour and RNFL thickness at baseline

The parameter height variation in contour was significantly lower for the POAG group (0.305 ± 0.080mm) compared to the normal group (0.335 ± 0.075mm). This finding agrees with other studies and is consistent with the flattened rim profile typical of a glaucomatous ONH that occurs as a result of RNFL loss (Iester, M. *et al.*, 1997a; Wollstein, G. *et al.*, 1998). The parameter, RNFL thickness was also significantly smaller for the POAG group (0.171 ± 0.049mm^2) compared to the normal group (0.224 ± 0.055mm^2). A similar result has been previously reported (Eid, T. M. *et al.*, 1997).

9.3.5.6 Mean height in contour and reference height at baseline

The parameters mean height in contour and reference height were significantly higher for the POAG group (0.125 ± 0.051mm, 0.296 ± 0.071mm) compared to the normal group (0.10 ± 0.074mm, 0.227 ± 0.093mm). This finding is consistent with an earlier study that compared normal and glaucomatous optic nerve heads (Zangwill, L. M. *et al.*, 1996). The reference height is, by definition, determined from the mean height of the contour line in the superior-temporal segment. It therefore follows that if the mean height of the contour increases so will the reference height.

9.3.5.7 The classification parameter at baseline

The classification parameter differed significantly between the normal subject group (1.665 ± 1.180) and POAG group (–0.742 ± 1.045). This parameter is derived from

several other parameters and gives an indication of whether or not the ONH is glaucomatous (Mikelberg, F. S. *et al.*, 1995) (see section 1.11.2.8.). A more negative value signifies a glaucomatous ONH. It has been proposed that this system may provide a valuable tool for categorising glaucomatous optic nerves and the results from this analysis suggest that, overall, the classification parameter can differentiate between a normal subject group and a group of patients diagnosed with early to moderate glaucoma. On an individual level, the classification falsely defined 2 normal subjects as glaucomatous (false positive rate of 6.5%) and 7 POAG subjects as normal (false negative rate of 21.2%) (Table 9.5.). On this basis, 2 out of 10 POAG eyes would be misdiagnosed as normal. It is likely that the false negative rate would decrease with more severe glaucoma, but a detection technique is most useful in the early stages of the disease process to aid diagnosis.

	Classified as normal	**Classified as abnormal**
Normal group (n=31)	29 [93.5%]	2 [6.5%]
POAG group (n=33)	7 [21.2%]	26 [78.8]

Table 9.5. Number [and percentage] of normal and POAG subjects diagnosed as normal and abnormal by the classification parameter.

9.3.5.8 Cup shape measure at baseline

The cup shape measure, third moment in contour, differed significantly between the normal (-0.198 ± 0.054) and glaucomatous (-0.090 ± 0.049) subject groups. This parameter is a function of the overall shape of the ONH (see section 1.11.2.4. for definition). Values are typically negative in the normal ONH, characterised by a flat cup and small depth values and are less negative or more positive in the glaucomatous ONH, which has deep slopes and high depth values. The findings from this study for both subject groups are similar to other studies (Zangwill, L. M. *et al.*, 1996; Iester, M. *et al.*, 1997a; Wollstein, G. *et al.*, 1998). This suggests that even though the mean values obtained for cup area, volume and depth measurements were slightly lower for the normal group than previously reported, the overall shape of the cup was similar. Third moment has been highlighted as an important parameter for distinguishing between subject groups and correlating with visual field damage (Mikelberg, F. S. *et*

al., 1995; Iester, M. *et al.*, 1997a). The findings from this study agree that third moment can distinguish between normal and glaucomatous eyes, but other parameters seem equally important.

9.3.6 Baseline comparison of HRT parameters between groups: Summary

With the exception of disc size, all of the measured HRT parameters appeared useful in differentiating between a normal and POAG subject group. In each case, the parameters reached a very high level of significance reflective of the large differences between the two groups at baseline. Of the parameters measured volume below surface, volume below reference, cup area and mean depth in contour presented the highest p-values and appeared particularly useful for distinguishing between a normal and glaucomatous group.

Several cross-sectional studies have highlighted individual parameters as useful for classifying between groups of subjects and for correlation with visual field loss. In particular third moment, volume above surface and RNFL thickness have been identified as important (Tsai, C. S. *et al.*, 1995; Zangwill, L. M. *et al.*, 1996; Eid, T. M. *et al.*, 1997). The results from this study agree with those reported by Zangwill, L. M. *et al.*, (1996) who studied a number of HRT parameters and found they all differed significantly between normal and POAG populations.

Some of the parameter values obtained for the normal group at baseline differed from previous studies. This finding may also account for the highly significant differences observed between the glaucoma and normal group for each HRT parameter. However similar results have been reported and provide reassurance that this is an expected finding between a normal group and group diagnosed with mild to moderate glaucoma (Zangwill, L. M. *et al.*, 1996).

The majority of the POAG patients and normal subjects were classified correctly (78.8% and 93.5% respectively). This suggests the classification parameter provides a reasonable indicator for categorising glaucomatous and normal ONHs with a

conservative degree of overlap. The false negative classifications found for the POAG group means that the system, although useful, must not be completely relied on. The POAG patients in this study had demonstrated visual field loss and untreated raised IOP on more than one occasion aiding an accurate diagnosis. A reliable diagnostic system would need to differentiate early disease when other clinical variables such as IOP and visual fields do not clearly support the diagnosis. However, great variability in the appearance of the ONH, together with the relatively low incidence of the disease would mean such a system would need to be highly specific, sensitive and capable of detecting subtle changes in the optic nerve.

Clearly a rapid and reliable diagnostic system capable of classifying ONHs as glaucomatous would be of great importance, but the results from this study and others suggest there is still some way to go before this becomes a real possibility. A technique that can detect subtle change over-time in the optic nerve may be of more importance clinically and provide crucial information on the progression of disease. Particularly as changes in the nerve have been shown to precede visual loss (Sommer, A. *et al.*, 1991a). The primary aim of this study was to assess the ability the HRT to detect subtle change associated with glaucomatous optic neuropathy when compared to a normal ONH. The parameters identified as important in the long-term follow-up of glaucomatous optic neuropathy are outlined and discussed in the following sections.

9.3.7 Global topographical change over time: by parameter and group

The group-wise analysis provided an initial analysis for identifying parameters that appeared important for detecting change over time in a POAG group compared to a normal group. A number of parameters were identified as significant to ANCOVA ($p<0.01$, $r^2 \geq 0.6$) and these are summarised in Table 9.6. Although ANCOVA gave an indication of which parameters differed significantly over time between the two groups, it gave no indication of the direction of change. In order to see exactly how the groups differed, graphs were plotted of the mean values at each visit. A separate graph is provided in chapter 8 for each significant parameter. r^2 values are given to

demonstrate the level of linear change for each group (Figures 8.1. – 8.6.). Table 9.6. gives the p values for the ANCOVA analysis between groups and the corresponding r^2 values extrapolated from the graphs for each separate parameter and group. Clearly, a good parameter would be one that is significant to ANCOVA, shows change over time for the POAG group ($r^2 \geq 0.6$), but no change for the normal group ($r^2 < 0.6$). The significant parameters are discussed in more detail below.

Parameter	ANCOVA (p-value)	Normal group (r^2-value)	POAG group (r^2-value)
C:D area ratio	0.0026	(+) 0.2344	(+) 0.7982
Volume below surface	0.0020	(+) 0.4780	(+) 0.5230
Volume below reference	0.0065	(+) 0.5920	(+) 0.8616
Mean depth in contour	0.0022	(+) 0.5383	(+) 0.7764
Rim area	0.0068	(-) 0.040	(-) 0.8487
Cup area	0.0050	(+) 0.4986	(+) 0.6644

Table 9.6. Global HRT results are given for parameters significant to ANCOVA analysis ($p<0.01$). r^2 values are shown to demonstrate the linear change over time for each group. The positive or negative sign indicates the increasing or decreasing trend. Shaded boxes represent parameters significant to ANCOVA ($p<0.01$) that also show significant linear change over time for the POAG group ($r^2 \geq 0.6$), but not for the normal group ($r^2 < 0.6$).

9.3.7.1 Parameters demonstrating a significant change over time by group

ANCOVA showed that the global parameters cup:disc area ratio, cup area, rim area, volume below surface, volume below reference and mean depth in contour all showed a significant change over time that differed between the two subject groups ($r^2 \geq 0.6$, $p<0.01$) (Table 9.6.). The graphs showed that with the exception of volume below surface all of the parameters demonstrated a significant linear change for the POAG group, but not for the normal group (Figures 8.1.-8.6.). In each case, the direction of change for the POAG group was consistent with the expected change for disease progression. The significant parameters are discussed in more detail below:

Cup area, rim area and volume below reference are all measured with respect to the reference plane (Table 1.3.b.). Cup area and volume below reference increased and

rim area decreased over time for the glaucoma group. The measured change could be due to one of two things:

1) The height of the reference plane may have been changing over time in the POAG group resulting in larger cup areas and smaller rim areas. This was unlikely because the height of the reference plane did not change significantly in the POAG group. Furthermore the reference plane is located beneath the papillo-macular bundle, which is considered the last retinal area to change in glaucoma. It is therefore proposed to provide the most stable location from which to position the reference plane.
2) There may have been a progressive loss of rim tissue and a concomitant increase in the size of the cup in some of the subjects contained within the POAG group. This was more likely because the change over time was observed for the POAG group only suggesting disease progression was the cause and another parameter, unrelated to the reference plane (mean depth in contour), also showed significant change.

The parameters volume below surface and volume below reference are both measures of cup volume that are determined from different theoretical boundaries. A linear increase in volume below reference, but not volume below surface, over time was evident for the POAG group. There is some speculation as to which boundary, i.e. the reference plane or curved surface is best for volumetric measures (Mikelberg, F. S. *et al.*, 1995). The two reference locations are determined in different ways and it is likely that one is more stable and robust for topographic measurement than the other. Data from the HRT reproducibility study completed on normal and glaucoma subjects, outlined in chapter 2, showed volume below surface to be marginally more reproducible (99.7%, 92.7%) compared to volume below reference (99.2%, 84.5%) (Table 2.2.). However, both parameters performed very well. The results from the baseline analysis discussed earlier (section 9.3.5.3.) show that mean values for the volume below surface parameter are higher than the mean values for volume below reference. This finding is logical because of the very nature of the curved surface (irregular cone shape), which encompasses more tissue than the flat reference plane. It is possible that change in a small volume of tissue will be more obvious than a small

change in a larger volume of tissue. On this basis one might expect volume below reference to show the most change.

The reproducibility study outlined in chapter 2 showed the parameter mean depth in contour to be highly reproducible for normal and glaucoma subjects (99.5% and 97.2% respectively). A linear increase in mean depth in contour was apparent for the POAG group but not for the normal group (Table 9.6., Figure 8.4.) This finding corresponds to an overall increase in the depth of the cup for the POAG group and correlates with the increase in cup volume and area previously discussed. Anatomically, it follows that with increasing loss of ONH axons, the optic cup will become both wider and deeper. The high reproducibility, together with the change evident for the glaucoma group, suggests this parameter is important for detecting glaucomatous progression.

9.3.7.2 Parameters not demonstrating significant change over time by group

The parameters volume above surface and volume above reference, which are both measures of rim volume, fell short of statistical significance ($p>0.01$) but showed a trend towards a reduction over time for the POAG group. RNFL thickness was also unchanged. As previously discussed the parameters which describe cup volume (volume below reference, volume below surface) showed a significant increase over time (ANCOVA). It follows that if the cup volume is increasing, then the rim volume will decrease. The notable and significant decrease in rim area serves to support this (see section 9.3.7.1.).

Results from the HRT reproducibility study (Chapter 2) showed that rim parameters volume above reference and surface are less reproducible (ICC = 95.2% & 98.4% respectively) than the cup parameters volume below reference and surface (99.2% and 99.7% respectively). If rim volume were decreasing in size as the data suggests then the assumption may be made that neither volume above surface or volume above reference were sensitive enough to detect a change over time at the 99% confidence limit.

The reason for the relative lack of sensitivity of these parameters may be related to the small volumes of tissue that are being measured and movement of the boundaries from which these measures are made. If rim volume and RNFL thickness decrease then the contour line, which falls at the boundary of the optic disc, will be repositioned deeper on the z-axis. As such the position of the curved surface and reference plane, which are determined according to the contour line, will be deeper. The repositioning of the measurement boundaries may mask any change in rim volume and RNFL thickness, however the measures of cup volume, which are anatomically larger, may be more robust to changes in the reference locations and more likely to show true change.

The parameters mean height in contour, height variation in contour, maximum depth, third moment, classification and reference height were all non-significant ($p>0.01$). Although all these parameters were capable of distinguishing between a normal and glaucomatous optic nerve at baseline, they were not useful for detecting the subtle change that may be occurring over time in POAG. This may be because the disease has already progressed and hence parameters that are effective in classification may be weaker in progression, or they may not be sensitive enough for follow-up.

9.3.8 Regional topographical change over time: by group

As with the global data, ANCOVA was used to compare change over time for topographic HRT parameters measured regionally for the POAG and normal subject groups. The HRT software allows some parameters to be measured regionally in specific segments of the ONH including the volumetric measures of cup and rim, cup area, maximum depth, mean height in contour and third moment. A number of studies have identified early glaucomatous changes in the superior and inferior poles of the disc which contain the superior and inferior arcuate nerve fibre layer bundles (Weber, J. *et al.*, 1990; Schuman, J. S. *et al.*, 1995; Tsai, C. S. *et al.*, 1995). Furthermore, changes in the superior and inferior poles have been found to correlate highly with

visual field loss (Iester, M. *et al.*, 1997c). The regional measurements of individual parameters have two main uses:

1) They have the potential of detecting localised topographical change that may otherwise be concealed by global measurements.
2) They allow parameters that are significant globally to be looked at in more detail.

Table 9.7. summarises the parameters that were significantly different between the two subject groups according to the area of tissue measured as determined by ANCOVA. Graphs were plotted of the significant parameters (Figures 8.7.-8.16.) and the corresponding r^2 values are given in the table below that describe the direction and magnitude of the linear association between the two variables (visit and parameter). Six regions of the ONH were measured (superior nasal, nasal, inferior nasal, superior temporal, temporal and inferior temporal). The superior temporal, superior nasal, inferior nasal and inferior temporal regions were all 45° sectors whereas the nasal and temporal regions occupied 90°. Significant parameters were identified in the superior nasal and superior temporal regions only. These are discussed in more detail in the following sections.

Parameter	Superior nasal			Superior temporal		
	ANCOVA (p-value)	Normal (r^2)	POAG (r^2)	ANCOVA (p-value)	Normal (r^2)	POAG (r^2)
Volume below surface	0.0033	+0.1956	+0.4446	0.0007	+0.4346	+0.4007
Volume above surface	0.0001	-0.1132	-0.4333	0.0001	-0.2789	-0.6001
Volume below ref	0.0082	+0.1571	+0.7998	0.0001	+0.5303	+0.7563
Volume above ref	0.0065	-0.0854	-0.9656	0.0057	-0.3294	-0.9741
Cup area	0.0003	+0.7212	+0.9754	0.0041	+0.2985	+0.6454

Table 9.7. p-values are given for regional parameters significant to ANCOVA analysis. r^2 values are shown and indicate the magnitude of change over time for each group. Shaded boxes represent parameters significant to ANCOVA ($p<0.01$) that also show significant change over time for the POAG group ($r^2 \geq 0.6$), but not for the normal group ($r^2 < 0.6$).

9.3.8.1 Significant parameters demonstrating change regionally

A significant difference was observed between the normal and POAG group for volume below surface measured superiorly nasally and temporally, but when the results were plotted the r^2 value did not reveal a definite increase (or decrease) for the POAG group or the normal group (Figure 8.7.) This result was consistent with the finding for the global data (section 9.3.7.1.). The parameters volume below reference and cup area were both significantly different between the groups and a linear increase over time was evident for both parameters for the POAG patients, but not for the normal subjects. These results suggest an increase in the size of the cup for the POAG patients over the study period, whilst the same parameters for the normal group remained stable.

The significant change for these parameters was localised in the superior nasal and superior temporal regions of the ONH. Figures 9.1. & 9.2. demonstrate the difference in data measured superiorly and inferiorly for one parameter (volume below reference). Figure 9.1. shows how the increase in volume below reference appeared to be localised in the superior nasal (r^2=0.7992) and superior temporal regions (r^2=0.7563) for the glaucoma group. Slopes for the inferior nasal and inferior temporal regions were not significant (r^2<0.6). The corresponding slopes for the normal subject group showed no change over time ($r^2 < 0.6$) (Figure 9.2.).

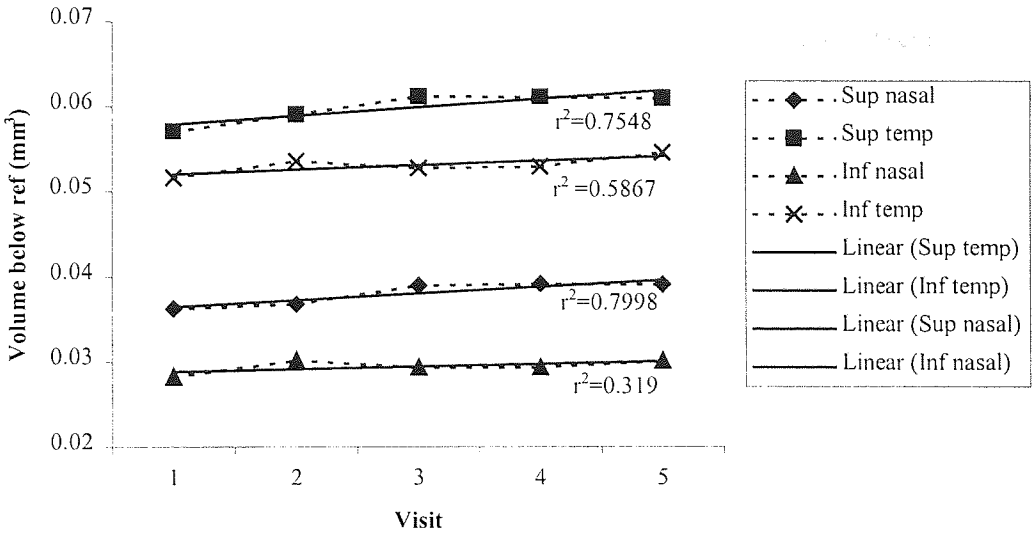

Figure 9.1. Mean values at each visit (POAG group) for volume below reference measured superiorly (nasal and temporal) and inferiorly (nasal and temporal).

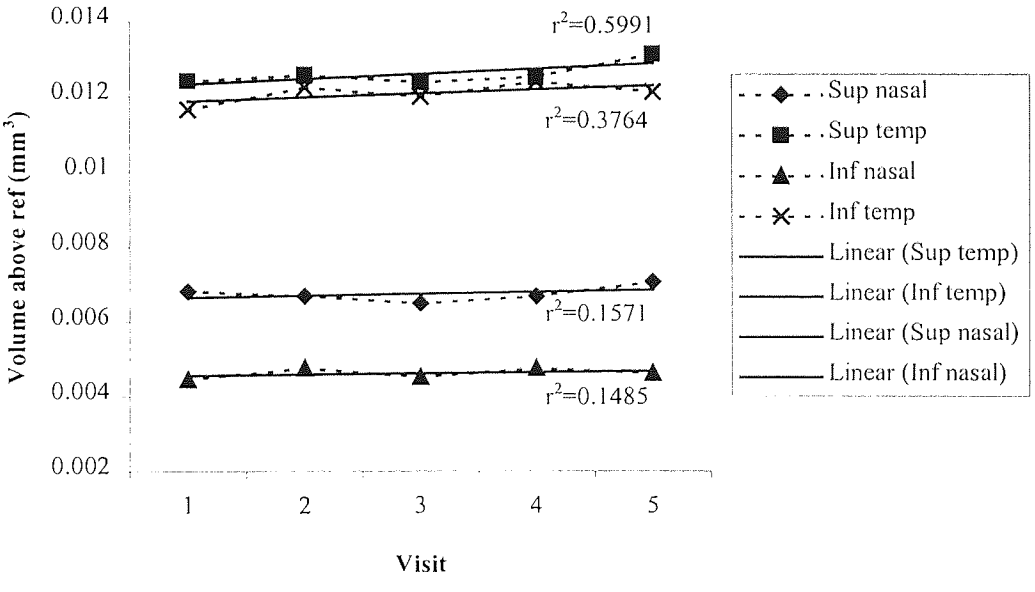

Figure 9.2. Mean values at each visit (normal group) for volume below reference measured superiorly (nasal and temporal) and inferiorly (nasal and temporal).

The results for the parameters volume above surface and volume above reference measured superior nasally and superior temporally showed a significant difference

over time for the POAG group relative to the normal group ($p<0.01$). No significant difference was found when these parameters were measured globally (section 9.3.7.2.) suggesting that the regional measures were more sensitive than the global measures for rim volume.

When graphs were plotted of the mean values, the corresponding r^2 values showed that volume above reference changed significantly throughout the study period for the POAG group but not the normal group in the superior sectors (Figures 8.10. & 8.15.). Volume above surface showed significant change over time superior temporally for the POAG group and again the normal group was stable (Figure 8.13.). Although the ANCOVA results were significant for volume above surface measured superior nasally, this simply implies that the groups were changing differently relative to each other. The graphs show that volume above surface appeared to be decreasing for the normal and POAG group, but not at a level that showed significance (Figure 8.8.)

9.3.8.2 Parameters not demonstrating change regionally by group

The parameters maximum depth, third moment and mean height in contour did not show any evidence of change over time between the two subject groups in any of the regional sectors. Neither were they significant when measured globally. Much of the literature reports the third moment in contour parameter as important for classifying between groups and correlation with visual field loss (Mikelberg, F. S. *et al.*, 1995; Zangwill, L. M. *et al.*, 1996; Iester, M. *et al.*, 1997b). Although the baseline group comparison results from this study agree that this parameter may distinguish between a normal and glaucomatous population, there is no evidence to suggest its usefulness for following glaucomatous progression.

9.3.9 Topographical change over time by group: summary

There are a number of published studies that identify parameters useful for distinguishing between different groups of subjects (i.e., POAG, OHT, suspect

glaucoma & normal subjects). The large majority of studies are cross-sectional in design and there are no reports that define the best parameters for detecting glaucomatous change over time. The results from the group-wise comparison of global and regional topographical data confirmed that there are a number of useful parameters. These are summarised in Table 9.8. Those that appear important regionally only are indicated with †, those that are important both globally and regionally are indicated *† and those that are important, but only measured globally are indicated *.

Rim parameters	Cup parameters	Rim and cup parameters
Rim area *	Cup area *†	Cup:disc area ratio *
Volume above surface †	Volume below reference *†	
Volume above reference †	Mean depth in contour *	

Table 9.8. HRT parameters that appear important for detecting change over time between a normal and POAG group. *† indicates parameters that changed both regionally and globally, † shows parameters that only changed regionally and * indicates parameters that showed change and were only measured globally.

Measures of volume below reference (cup volume) and cup and rim areas were consistently important (globally and regionally) for detecting change over time in a glaucoma group compared to a normal group as was mean depth in contour.

Change over time for the parameters volume above surface and volume above reference (rim volume) were detected regionally but not globally. Most of the literature focuses on HRT parameters measured globally, consequently at the outset of this study it was unknown as to how sensitive parameters would be that were measured regionally. Limiting measurements to individual segments of the ONH may have reduced the variability that would otherwise have been more pronounced globally, thus facilitating the detection of change. However, the change detected regionally in the study was limited to the superior ONH, which is the most variable area anatomically.

There is one potential source of error that may be more pronounced regionally than globally. Tilt of the image in the x,y plane that may occur between images and visits

due to head movement. The HRT software automatically corrects the contour line for tilt by angling it slightly to fit the image. This means that the area measured globally will remain constant. However, the area of tissue measured regionally is predetermined according to an existing axis which is not repositioned and does not account for tilt within the image (Hosking, S. L., 1998b). As a consequence the area being measured regionally as superior nasal in one image may shift slightly for another image of the same subject. The study protocol ensured that head movement was not a factor for within visits, but tilt between visits may have occurred that was not obviously visible to the examiner at the time. Had this been the case, the increase in variability would most likely have masked any true change occurring in specific areas of the ONH. The consistent change observed for the cup and rim volume parameters, measured both regionally and globally, that was evident in the POAG group only, provided reassurance that true change was being detected.

Regional topographic change was consistently localised in the superior nasal and superior temporal sectors. Quigley, H. A. & Anderson, D. R. (1977) reported disruption of axonal transport that was more apparent in the posterior and inferior poles of the disc. Furthermore, localised loss of axonal bundles often occurs temporally to the inferior or (less often) superior poles with corresponding visual field defects (Anderson, D. R., 1983). The results from this study suggest changes in the superior temporal region that are consistent with localised axon loss. No significant change was evident for any of the parameters measured temporally, nasally or inferiorly suggesting that overall, the glaucomatous changes were localised rather than diffuse.

Seven out of the 15 parameters did not show change regionally or globally. Of these, the parameters maximum depth, height variation in contour, third moment and RNFL thickness are all useful for differentiating between groups at baseline, were not reliable indicators of glaucomatous progression (Mikelberg, F. S. *et al.*, 1995; Iester, M. *et al.*, 1996; Zangwill, L. M. *et al.*, 1996; Wollstein, G. *et al.*, 1998). This highlights the important point that parameters useful in discrimination are not necessarily meaningful for the detection of change.

9.3.10 Topographical change over time: by subject

The group-wise comparison between the POAG and normal subjects provided an indication of which HRT parameters appeared important in detecting change in glaucoma over time and a broad indication of the value of the technology in glaucoma monitoring. The analysis also provided some insight into where, topographically, this change was taking place (superior nasally and superior temporally). The ultimate goal was to consider change in individuals. It seemed likely that only a proportion of the subjects diagnosed with POAG would be progressing enough to facilitate the detection of ONH changes. Identifying individual subjects that appear to be progressing would enable other areas to be investigated. For example, could the ONH changes be related to treatment modifications or changes in IOP? Could topographical change be correlated with visual field progression and haemodynamic factors?

Given the duration of the study and subject sample size only a small proportion of POAG patients were expected to show change. A study by Katz, J. L. *et al.*, (1997) showed that approximately 1 in 3-4 POAG patients demonstrated progressive visual field damage when followed-up for a 7 year period. Other studies have reported similar findings (O'Brien, C. *et al.*, 1991; Smith, S. D. *et al.*, 1996). On this basis, it was expected that approximately 10-15% of POAG patients would exhibit deterioration in visual field indices over the 16-month study period. Topographic change of the ONH is thought to precede visual loss (Sommer, A. *et al.*, 1991a) so a greater amount of patients (15%-20%) were expected to change topographically.

Morphological change measured over time for each subject was investigated in two ways; by individual parameter and by factor analysis. The analysis by individual parameters (globally and regionally) resulted in a high proportion of change across both subject groups (see sections 9.3.11.-9.3.12.). Factor analysis reduced this effect and provided a more conservative and perhaps realistic approach for investigating topographical change. The results for the factor analysis are discussed in section 9.4.

9.3.11 Global morphological change: by subject and parameter

64.6% (11) normal subjects showed change in at least one parameter measured globally. This ranged from 6.5% for maximum depth in contour and third moment to 25.8% for C:D ratio and volume above reference (Table 9.9.). Of the POAG subjects, 78.8% (26) showed change in at least one parameter measured globally ranging from 6.1% for third moment in contour, to 42.4% for volume below surface and mean depth in contour (Table 9.10.). Parameters with subjects demonstrating the most change included volume below surface, mean depth in contour, C:D ratio, rim area and mean height in contour. These parameters may be important for detecting topographical glaucomatous progression, alternatively they may be poor because of over-sensitivity.

Tables 9.9. and 9.10. show each normal and POAG subject and their associated change in global HRT parameters. It can be seen from the tables that change is widespread in both groups. The high amount of change observed for the POAG and normal group for each parameter suggests the technique is over-sensitive. Based on the literature, not more than 15-20% change in topographical parameters would be expected in the POAG group consistent with the rate of glaucomatous progression. Some parameters showed change in more than 30% of POAG patients (C:D area ratio, mean height in contour, volume below surface, mean depth in contour), consequently some of this change is likely to represent the error of the technique. This is further reflected by the significant change in parameters evident for the normal group over the study period.

Subject #	C:D area ratio	Mean height contour	Height var contour	Volume below surface	Volume above surface	Volume below ref	Volume above ref	Max depth	Third moment	RNFL thick-ness	Mean depth contour	Rim area	Cup area	Class-ification	Ref height
	1	2	3	4	5	6	7	8	9	10	11	12	13	14	15
1															
2															
3															
4	×		×				×			×		×	×	×	
5					×										×
6															
7															
8		×		×	×	×		×	×		×				
9	×		×		×	×				×		×	×		×
10			×		×						×				×
11				×						×					
12															
13	×	×		×		×	×				×	×	×	×	×
14							×			×					
15	×											×	×		
16															
17				×		×					×	×	×		
18	×											×	×		
19		×		×				×			×				
20															
21															
22															
23					×		×		×					×	×
24															
25															
26		×	×				×								
27	×	×					×			×		×	×		×
28															
29	×				×		×					×	×		
0															
31	×	×	×		×	×	×					×	×		
Total	8	6	5	5	7	5	8	2	2	5	5	9	9	3	6
%	25.8	19.4	16.1	16.1	22.6	16.1	25.8	6.5	6.5	16.1	16.1	29	29	9.7	19.4

Table 9.9. Global HRT parameter change for each normal subject. Ticks indicate significant change ($p<0.01$)

Subject #	C:D area ratio	Mean height contour	Height var contour	Volume below surface	Volume above surface	Volume below ref	Volume above ref	Max depth	Third moment	RNFL thick-ness	Mean depth contour	Rim area	Cup area	Class-ification	Ref height
	1	2	3	4	5	6	7	8	9	10	11	12	13	14	15
32															
33				×		×		×			×				
34		×													
35															
36															
37	×			×							×	×	×		
38												×	×	×	
39		×													
40		×	×	×	×	×	×	×		×	×				×
41															
42															
43	×	×	×	×	×	×	×	×		×	×			×	×
44	×	×		×									×		
45	×											×	×		
46	×	×										×	×		
47				×	×	×		×			×				
48				×		×		×			×				
49				×							×				
50	×						×			×	×	×		×	×
51	×			×			×	×		×	×	×	×		×
52									×					×	
53		×		×	×			×	×	×	×			×	×
54	×											×	×		
55	×	×			×					×		×	×		×
56	×		×		×							×			
57	×	×		×							×	×	×	×	
58			×	×							×				
59															
60		×													
61															
62	×			×	×	×	×			×	×	×	×	×	
63		×		×	×						×				
64		×													
Total	12	12	4	14	8	6	5	7	2	7	14	11	10	7	6
%	36.4	36.4	12.1	42.4	24.2	18.2	15.2	21.2	6.1	21.2	42.4	33.3	30.3	21.2	18.2

Table 9.10 Global parameter change for each POAG subject. Ticks indicate significant change ($p<0.01$).

Missing page(s) from the bound copy

9.3.12 Regional morphological change: by subject and parameter

Change was more common for the parameters determined regionally (Appendix 7.). 93.5% (29) of normal subjects showed change in at least one parameter measured regionally. This ranged from 0% (maximum depth in contour in the superior nasal region) to 35.5% (mean height in contour in the superior temporal region, volume above reference in the inferior nasal region) (Table 8.11, Appendix 7.). A useful parameter is likely to be one that shows no change for the normal subject group and a conservative amount of change for the POAG group. Maximum depth in contour measured superior nasally showed no change for the normal subjects suggesting that it may be of value for detecting topographical shifts associated glaucomatous progression.

97% (32) of POAG subjects showed change in at least one parameter measured regionally (Table 8.10 & Appendix 7.). Cup area showed the most change over the study period when measured regionally in the superior nasal, temporal and inferior nasal and temporal quadrants (33.3%, 39.4%, 42.4%, 39.4%). Third moment in contour, measured in the superior nasal sector, showed the least change over time with only 2 subjects showing change in this parameter (6.1%).

Tables containing parameter change for each POAG patient and each normal subject for the six regions can be found in Appendix 7. Similar to the global results a substantial amount of change was evident in both the normal and POAG group. The change observed for the POAG group exceeded what was expected for disease progression over the study period. The combined regional and global results suggest that topographic parameters measured with the HRT are over-sensitive to subtle ONH change. The large amount of variation observed for many of the parameters measured for the normal subject group gives some indication of the error of the technique. Consequently, the single parameter analysis may not be the best way of monitoring glaucomatous progression for individual patients. The techique of factor analysis is outlined below and presents a more conservative approach for assessing glaucomatous optic neuropathy.

9.4 Factor analysis for determining topographical change

One of the primary objectives of this study was to identify individual subjects that were progressing over time. To facilitate this the statistical method of factor analysis was used to reduce the relatively large number of parameters into a more manageable form that would better describe the data.

The method of factor analysis is described in section 7.9.9. Based on scree plots of the eigenvalues (Figures 8.17. & 8.18.), two factors were appropriate to describe the global and regional data. The individual HRT parameters loaded onto each factor in a logical way. In each case (regionally and globally) the parameters contained in factor 1 described the shape and size of the cup and the parameters contained in factor 2 described the rim and RNFL profile. On this basis, factor 1 was named *cup*, and factor 2 was named *rim*. Table 9.11. summarises the parameters contained within each factor for the regional and global data sets, the parameters are ranked according to how strongly they loaded onto a given factor. In each case the cup shape parameter, third moment in contour was the least important. This finding contrasts with others that have recommended third moment as a most useful parameter for classifying glaucoma and correlating with visual field loss (Mikelberg, F. S. *et al.*, 1995; Zangwill, L. M. *et al.*, 1996; Iester, M. *et al.*, 1997b).

Data Set	**Factor 1 (cup)**	Factor 2 (rim)
Global data (Data set 1)	Mean depth contour (1) Volume below surface (2) Maximum depth (3) Volume below reference (4) Mean height contour (5) Third moment (6)	RNFL thickness (1) Height variation contour (2) Volume above reference (3)
Regional data (Data sets 2-7)	Volume below reference (1) Volume below surface (2) Maximum depth (3) Third moment (4)	Volume above surface (1) Volume above reference (2)

Table 9.11. Factor structure for the global and regional data sets. Parmeters are ranked according to how strongly they load onto a given factor.

9.4.1 Global change in factors over time: by group

Initally, a group-wise analysis was used to look for differences in the factors between the normal and POAG group over time. The results showed that there was no significant difference between the two factors over time between the normal and POAG subject group (ANCOVA). This finding suggests that the factor analysis provided a more conservative approach for investigating the data. Only a modest amount of topographical change was expected in the POAG group over the study period and it was not surprising that the factor model was unable to distinguish between the groups.

The earlier group-wise ANCOVA results for the individual HRT parameters (section 9.3.7.) identified certain parameters as important for detecting change over time between the normal and POAG subject group. Those that were contained within the *cup* factor included volume below surface, volume below reference and mean depth in contour. This left the seemingly less important parameters mean height in contour, maximum depth and third moment still contained within the *cup* factor. Of the parameters contained within *rim*, only one was previously identified as important for detecting change (volume above reference). The other two parameters (height variation in contour and RNFL thickness) were not singled out as useful in the previous analysis. It is possible that the influence of the less important parameters may have masked any change occurring between the two groups. Alternatively, the individual parameters may have been overly sensitive to change (as suggested by the patient analysis) and the factors may provide a more realistic interpretation of the data.

9.4.2 Regional change in factors over time: by group

The parameters in factor 1 (*cup*) and factor 2 (*rim*) for the regional data sets were different to those that made up the global factors. There were fewer parameters contained in each factor. This was because the HRT software only allows a limited number of parameters to be measured regionally. Interestingly the factor structure and content was the same for all of the regional data sets providing strength to the

statistical model. In each case the *cup* factor contained two parameters important in the previous ANCOVA parameter analysis (volume below reference and volume below surface) and two that appeared less important (maximum depth and third moment). In the previous group-wise analysis, the parameters volume below surface and volume below reference appeared useful for detecting change in the superior nasal and superior temporal regions only. On this basis, a possible difference between the normal and POAG groups may be expected in the superior regions. No significant difference between the two groups was observed for factor 1 in any of the regions measured which may imply a masking effect of the less important parameters contained within the factor structure.

The *rim* factor for the regional data sets contained the parameters volume above surface and volume above reference. Both of these parameters appeared important when considered individually in the superior nasal and temporal regions. ANCOVA of the *rim* factor between the normal and POAG group did not reveal a significant difference between the groups for any regions measured. Again, this finding may be related to the conservative approach of the factors and may be a more realistic interpretation of the data.

9.4.3 Global change in factors over time: by subject

The finding that the factors did not differentiate between groups over time was not unexpected. The technique of factor analysis reduces the original number of variables to underlying factors that describe the data and are less likely to detect subtle fluctuations in the data. If one or two POAG subjects showed glaucomatous changes in topography, that change would be masked for the group-wise analysis. It was proposed that the factors would provide a more useful method for detecting true change over time for individual subjects. The reasoning behind this was based on the likelihood that individual POAG patients with progressive optic neuropathy would most likely demonstrate significant change over time for some of the stronger parameters. Change may also occur to a lesser extent for the weaker parameters, but in the same direction, resulting in an overall change in the measured factors.

9.4.3.1 Change for factor 1 (cup): by subject

ANOVA revealed that 33.3 % of POAG subjects and 7% of normal subjects, showed change over the study period for the cup factor measured globally (Table 8.15). It would appear therefore, that on a patient-by-patient basis, the cup factor was able to detect change in the POAG group that was much less apparent in the normal group. This finding suggests that the size and depth of the cup was increasing for the POAG group, consistent with the nerve fibre loss associated with glaucomatous progression. There are three potential reasons that may have accounted for change observed in the normal group:

1) There may have been an age-related decline in cup size.
2) There may have been pathological change in the cup.
3) The change may have represented the error of the measurement technique.

These points will be addressed in turn. Because the analysis was carried out by patient, and each subject acted as their own control, a potential age effect was not corrected for. However, it was possible that some of the change detected in both groups may have been age-related. The normal optic nerve contains between 689,500 and 1,244,005 RGC axons (Balazsi, A. G. *et al.*, 1984; Quigley, H. A. *et al.*, 1988; Mikelberg, F. S. *et al.*, 1989; Repka, M. X. *et al.*, 1989) and a yearly-age related decline of between 4909 and 6723 RGC axons has been reported (Johnson, B. M. *et al.*, 1987; Mikelberg, F. S. *et al.*, 1989). On the assumption that the normal human optic nerve contains approximately 100,000 RGC axons, and that 5,000 are lost yearly this would result in a 0.5% reduction in RGC axons per year and a 0.625% reduction in RGC axons throughout the study period (16 months). Although this may have accounted for some of the change observed for the normal subject group it was highly unlikely that age would be the sole contributor suggesting another underlying reason.

The second possibility was that there might be a pathological (true) change in the size of the cup in some of the normal subjects. On a psychophysical level, only one normal subject showed a significant increase in CPSD (#7). However the glaucoma hemifield

test remained within normal limits and this subject did not show change in any of the topographic factors. It is known that up to 40% of nerve fibre loss precedes visual loss in glaucomatous optic neuropathy (Sommer, A. *et al.*, 1991a), so the absence of visual field defects does not necessarily mean the absence of pathology. None of the normal subjects showing change in factors had a significant change in IOP, however people at risk of developing normal-tension glaucoma would not necessarily demonstrate IOP change. The inclusion criteria (section 7.4.) were designed to minimise the possibility of recruiting people undergoing pathological change. In particular, no diabetes or family history of glaucoma, IOP < 21mmHg, normal visual fields and normal fundus appearance based on an ophthalmic assessment by a consultant ophthalmologist (JMG) were inclusive criteria. On this basis, pathological change in the normal group was highly unlikely, but not an impossibility.

It is highly likely that measurement error accounted for the change observed in the normal group and some of the change for the glaucoma group. Only one other study documents the results for a normal subject group over a 12-month period. They reported no significant change in any of the parameters measured (cup area, C:D area ratio and rim area) for the normal group (n=13) (Kamal, D. S. *et al.*, 1999). These findings agree with the group-wise analysis carried out in this study which found, that overall, the normal group did not show change for the measured parameters. Kamal, D. S. *et al.*, (1999) did not investigate the subjects individually for change over time and there is no other published data which does consider normal subjects for HRT follow-up.

The change over time found for the cup factor in the normal subject group was most probably attributable to measurement error. Cross-sectional analysis has shown the HRT is not foolproof in classifying normality, neither is it foolproof in detecting change over time.

9.4.3.2 Change for factor 2 (rim): by subject

In total 28.1% of POAG subjects showed change over the study period globally for the rim factor and 18.1% of normal subjects showed change (Tables 8.15.). This result indicates a lot of noise in the data, a finding that may be attributable to the factor structure or component parameters. None of the parameters contained within the rim factor were identified as important in the global group-wise analysis and only volume above reference was found to be useful regionally.

9.4.4 Subjects showing change globally for cup and rim factors

During progression of glaucomatous optic nerve atrophy, loss of RGC axons results in loss of rim tissue and a concomitant increase in the size of the cup. As a result, one would expect a proportion of POAG patients to show change in both the rim and cup. None of the normal subjects showed change in both rim and cup. Three POAG patients showed changes in both the global rim factor the global cup factor (subjects #40, #43 & #62). These are discussed below.

Subject #40

Subject #40 showed an improvement in visual field indices. No treatment change was administered and IOP was stable, as such the observed improvement may have been related to a learning effect. ANOVA factor analysis showed both the rim and cup factor to be increasing relative to each other (Figure 9.3.). This finding was not logical and may suggest a measurement artefact for this patient.

Subject #43

Subject #43 showed no change in visual field indices and did not undergo a treatment change. The global cup factor increased and the rim factor decreased over the study

period suggestive of progressive NRR loss and a subsequent increase in the size of the cup that was undetected by perimetry (Figure 9.4.).

Subject #62

Subject #62 demonstrated a deterioration in visual field sensitivity (Figure 9.17.) with a subsequent decrease in rim tissue (factor 2) and increase in cup size (factor 1) (Figure 9.18.). Subject #62 underwent treatment changes and is discussed in section 9.8.4. in relation to visual field progression.

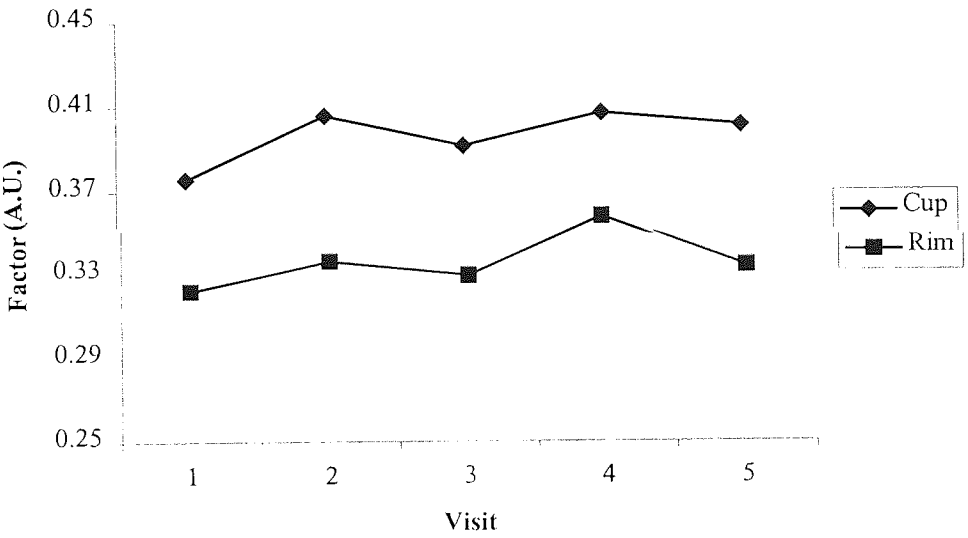

Figure 9.3. POAG subject (#40). There was a significant change over time for both the global cup and rim factors. Both are increasing relative to each other suggestive of an artefact. This patients visual field indices improved over the study period.

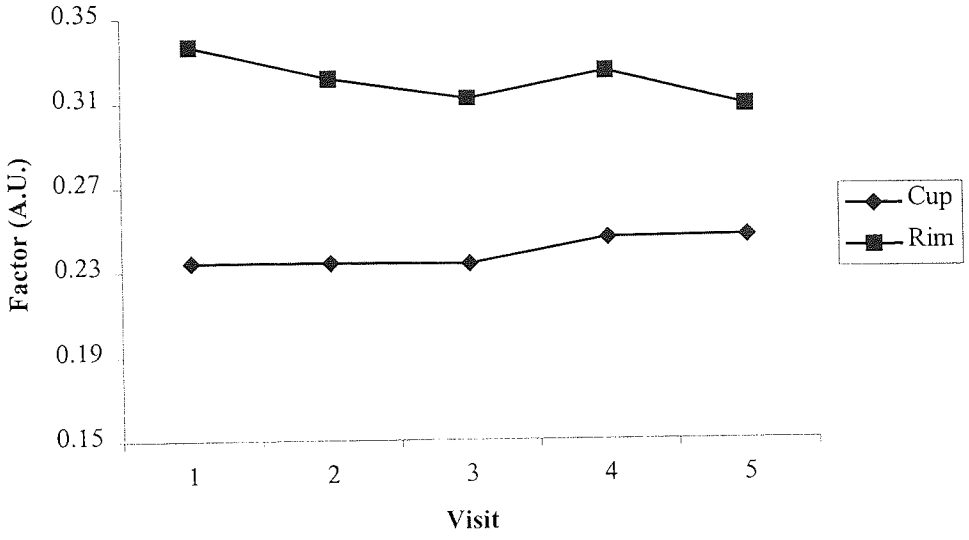

Figure 9.4. POAG subject (#43). There was a significant increase in the global cup factor and decrease in the rim factor over time. There was no change in visual field indices for this patient.

9.4.5 Regional change in factors over time: by subject

9.4.5.1 Change in factor 1 (cup): by subject

The factor structure for the 6 regional data sets differed to that of the global data set. Four rather than 6 parameters were contained within the cup factor, two of which had previously been considered important (volume below surface & volume below reference). The percentage of normal subjects showing change in cup (factor 1) ranged from 3.2% to 16.1% for the regions measured (Table 8.16.). Whereas, the percentage of POAG subjects demonstrating change in factor 1 (cup) ranged from 12.1% to 24.2% for the different regions (Table 8.17.). The most obvious distinction between the two groups was seen for the superior temporal sector where only 1 (3.2%) normal subject showed change, but 8 (24.2%) POAG subjects showed change in the cup factor. This finding agrees with the group-wise analysis which identified the superior temporal region as an important area of change.

9.4.5.2 Change in factor 2 (rim): by subject

The regional rim factor (factor 2) contained only two parameters (volume above reference and volume above surface). The percentage of normal subjects showing change in rim (factor 2) ranged from 3.2% to 19.4% for the different regions whereas the percentage of POAG showing change in rim ranged from 3% to 22.6%. As in the global analysis, no obvious pattern emerged for the rim factor suggesting that this was not a good indicator of glaucomatous change.

9.4.6 Factor analysis for determining topographic change: summary

Factor analysis provides a powerful tool for reducing a relatively large number of parameters into more manageable number of underlying variables. In this study 2 factors were adequate to describe the data and the factor structure followed a logical pattern. Factor 1 contained parameters associated with the cup only and factor 2 contained parameters associated with the rim and RNFL profile. Although the parameters contained within the global factors were different to those contained in the regional factors, the fact that the parameter structure was consistent for all the regional data sets supports the statistical model.

The group-wise analysis for the global and regional factors did not reveal a significant difference between the way in which the two groups changed over time, whereas the group-wise analysis for individual parameters did show significant differences between the groups (sections 9.3.7. & 9.3.8.) and individual parameters were highlighted as important. The factors may provide a more realistic and conservative approach to investigating the data. The small amount of change expected for the POAG group may have been masked by a lack of change for the group overall.

It was thought that the factors would provide a more reliable technique for detecting change in individual subjects. If a POAG patient was progressing then change would be most evident in the stronger parameters and to a lesser extent in the weaker parameters. On the basis of the group-wise parameter analysis, change may be

anticipated globally for the cup factor and regionally for both cup and rim factors in the superior quadrants.

The results showed the global cup factor to be important in distinguishing between the POAG and normal group with 33.3% of POAG subjects showing change over time and only 9.7% of normal subjects showing change. This finding was expected as the factor contained three parameters previously identified as important for detecting change between the two groups (volume below reference, volume below surface and mean depth in contour).

The global rim factor did not distinguish very clearly between the two groups with a similar amount of change evident in each group. This may be related to the factor structure as few of the component parameters were considered important in previous parameter analysis. It may also be related to the area and volumes of tissue being measured which are minute and susceptible to movement of the reference plane.

A total of three POAG subjects showed change in both global factors, two of which appeared to be related to progressive optic neuropathy. No normal subjects exhibited change in both global factors. As such, a change in both factors in the right direction for glaucomatous optic neuropathy might be the main criteria of progression.

In summary, the global cup factor appeared best for differentiating between the normal and glaucoma group and was best for detecting change over time. This result was expected as the factor contained strong parameters that were previously identified by the group-wise parameter analysis (section 9.3.7). The rim factor seemed less sensitive globally with change occurring for both the normal and POAG subjects alike. Regionally, the cup factor appeared best for distinguishing between the normal and POAG subjects and this was most apparent in the superior temporal sector. Finally, a concomitant change in cup and rim factor may be the best criteria for progression, a change in the cup factor alone probably indicates progression whereas a change in rim factor alone must be viewed with caution.

9.5 C:D ratio change over time as measured by the clinician (POAG group)

Direct assessment of the ONH using slit-lamp biomicroscopy is still the most widely used technique to follow-up glaucomatous optic neuropathy. Even in the advent of new technologies, the subjective clinical assessment is useful. The clinical examination provides a stereoscopic three-dimensional view of the ONH which can aid the detection of subtle depth and contour changes (Harper, R., 1995). The disadvantage of the technique lies with the lack of documentation and subjective nature which results in both inter- and intra-observer variation (Lichter, P. R., 1976; Tielsch, J. M. *et al.*, 1988; Pyott, A. A. E. & Montgomery, D. M. I., 1993; Abrams, L. S. *et al.*, 1994). A form was routinely completed by a consultant ophthalmologist at each visit describing the ONH. In particular, notching of the neuroretinal rim, optic disc haemorrhages and subjective measurements of vertical and horizontal C:D ratio were noted. The C:D ratio measurements were statistically analysed for the POAG group as a whole to determine change over time.

9.5.1 Horizontal C:D ratio

ANOVA was used to assess change over time for the POAG group only. The results showed that, overall, horizontal C:D ratio changed significantly throughout the study period ($p<0.05$). Linear regression analysis of the mean values for each visit revealed an r^2 of 0.7358 which suggests a significant increase in horizontal C:D ratio (Figure 8.27.). This finding is consistent with the significant increase for the HRT parameter C:D area ratio which was measured globally.

9.5.2 Vertical C:D ratio

No significant change was observed for the POAG group throughout the study period for vertical C:D ratio measured by ANOVA ($p>0.05$). However linear regression analysis revealed a linear increase in vertical C:D ratio ($r^2=0.6951$) (Figure 8.27.). Clinically, vertical C:D ratio is more readily quoted than horizontal C:D ratio and clinicians are more accustomed to quoting it. It was therefore surprising that

horizontal and not vertical C:D ratio changed significantly over time. HRT measurements showed a global increase in C:D ratio, and regional changes for the POAG group were noted in the superior region of the ONH. In particular regional changes were observed for cup and rim areas and volumes indicating an overall thinning of the neuroretinal rim and elongation of the cup. On this basis, the measurements provided by the HRT appeared more sensitive for detecting subtle changes in the optic disc throughout the study period.

9.5.3 Correlation with HRT parameters, visual field analysis and IOP

A study by Zangwill, L. M. *et al.*, (1995) showed that the HRT measure of C:D ratio (specifically calculated for the study) correlated well with the clinicians estimation of vertical and horizontal C:D ratio. In this study the default measure of C:D area ratio was measured with the HRT. This is a global measure that cannot be directly compared with the ophthalmic assessment. However, an overall increase in horizontal C:D ratio measured by the ophthalmologist for the POAG group agrees with the global increase in C:D area ratio observed for the HRT (Figure 9.5). Regionally, the HRT detected change in the superior nasal and temporal quadrants for the POAG suggesting localised topographic change that was not detected by the clinician.

On an individual patient basis, change in HRT parameters often correlated with a change in C:D ratio (subjectively measured). In particular, subject #41, who had a significant deterioration in visual field sensitivity, also had an increasing vertical (0.8-0.9) and horizontal (0.6-0.8) C:D ratio throughout the study period. These changes correlated with topographic changes in the disc as measured by the HRT (see section 9.8.4.). Two out of the three patients who underwent trabeculectomy (#32 and #54) showed an improvement in both horizontal and vertical C:D ratio following surgery that corresponded with improvements in blood flow parameters, decreased IOP, improved visual field indices and topography. These patients are discussed in detail in section 9.9.3.2. together with the expected changes in topography following trabeculectomy.

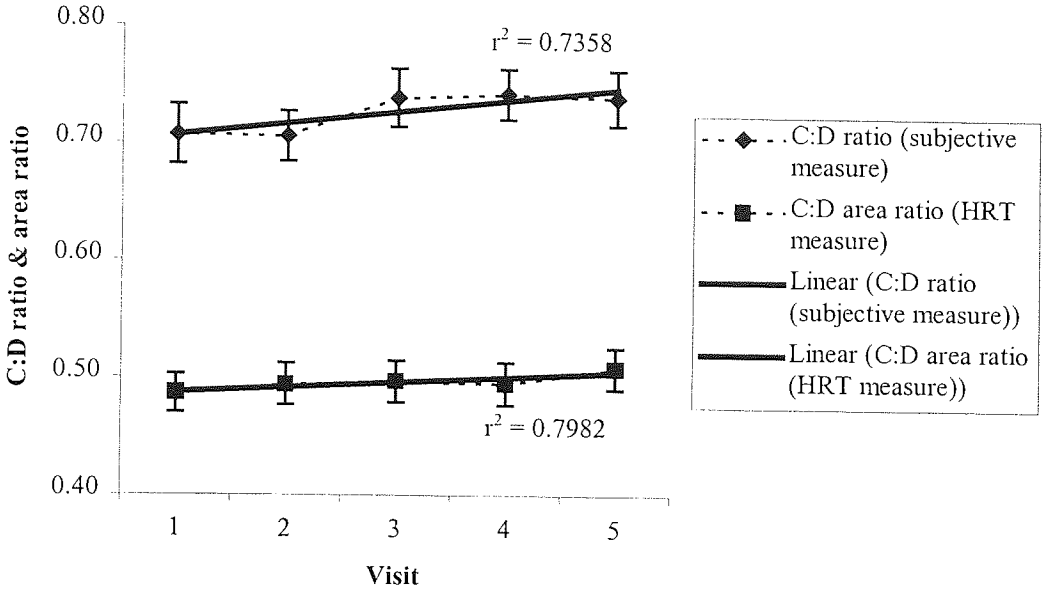

Figure 9.5. C:D ratio measured subjectively and C:D area ratio measured by the HRT for the POAG group over the study period (5 visits).

9.6 Haemodynamic measurement by SLDF

9.6.1 Reproducibility and image acquisition

The inter- and intra-image reproducibility of the HRF has been investigated for optic nerve and peripapillary ocular blood flow measurements in both normal and POAG subjects, and has been extensively reported as good (Michelson, G. & Schmauss, B., 1995; Chauhan, B. C., 1996; Strenn, K. *et al.*, 1997). SLDF may be used to measure ONH blood flow, but imaging of the neuroretinal rim and lamina cribrosa can be difficult due to the depth and high reflectivity of the tissue. It has also been suggested that optic nerve measurements are not as reliable as retinal blood flow measurements (Bohdanecka, Z. *et al.*, 1998). However, a recent method reported by Jonescu-Cuypers, C. *et al.*, (1999), which offsets the temporal rim edge to the lateral border, has been shown to improve neuroretinal rim measurement reliability. SLDF has been repeatedly proven as a reliable technique for the measurement of peripapillary retinal capillary blood flow and for this reason measurements were limited to the

peripapillary retinal bed (Michelson, G. & Schmauss, B., 1995; Michelson, G. *et al.*, 1996b; Nicolela, M. *et al.*, 1997).

An investigation into the intra-image reproducibility of SLDF measurements (Chapter 6) revealed acceptable reproducibility for all measured parameters with ICCs between 60% and 88% (Table 6.3.). There are several factors known to directly affect blood flow measurement with SLDF including cardiac rhythm, eye movement and the distance between the laser head and eye and IOP (Kagemann, L. E. *et al.*, 1996; Kagemann, L. E. *et al.*, 1998). The size of the measurement window and correct relocation of it are also important to the reproducibility (Bohdanecka, Z. *et al.*, 1998).

Efforts were made to maximise the reproducibility of the measurements taken with SLDF. As with the HRT, the subjects were requested to keep their head in the same position throughout imaging. This minimised head movements, maintained posture and ensured the distance between the laser and eye was kept constant. The focus setting was kept constant throughout imaging as this has been shown to be an important factor with the HRT and is likely to be important for the HRF (Hosking, S. L. & Flanagan, J. G., 1996). Pupils were dilated to maximise image quality and only images that were well focussed with minimal eye movement were used in analysis. Subjects were asked to refrain from caffeine-containing products, exercise and smoking prior to measurements.

9.6.2 Validity

A number of validation studies have been carried out with SLDF (Michelson, G. *et al.*, 1996b; Chauhan, B. C. & Smith, F. M., 1997; Strenn, K. *et al.*, 1997). These are discussed in section 1.15.1. There are several methods available for the measurement of ocular blood flow. A study outlined in Chapter 5 investigated the ability of three different ocular blood flow techniques to detect a physiologically induced change in ocular blood flow. The results showed that both CDI and SLDF were capable of detecting change (Roff, E. J. *et al.*, 1998a; Roff, E. J. *et al.*, 1998b). The technique commonly employed to measure the choroidal circulation (POBF) was not sensitive

enough to detect subtle changes in blood flow and would consequently require larger sample sizes to detect differences between groups (Roff, E. J. *et al.*, 1997).

It was proposed that SLDF would provide the best method for the longitudinal follow-up of glaucoma because it was capable of detecting induced changes in blood flow and is both a rapid and non-invasive procedure. Although CDI was capable of detecting changes in blood flow velocities it is a difficult, time consuming and expensive procedure to perform. Furthermore, unless the operator is very experienced, the technique of CDI requires the subject to adopt a supine position, and a change a posture is known to affect both IOP and ocular blood flow measurements (James, C. B. & Smith, S. E., 1991a; Baxter, G. M. *et al.*, 1992; Kothe, A. C. *et al.*, 1992a).

9.7 Haemodynamic parameters

Using SLDF, blood flow, velocity and volume were measured in the four quadrants of the peripapillary retina. The retinal capillary bed was considered the best component of ocular circulation to be measured longitudinally because it provides the most reproducible measures of blood flow (Nicolela, M. *et al.*, 1997). The following sections discuss the results obtained for cross-sectional analysis of baseline data by group, longitudinal analysis by group and analysis of individual glaucoma patients and normal subjects. The haemodynamic findings are discussed relative to psychophysical and morphological change.

9.7.1 Baseline: cross-sectional comparison between groups

A cross-sectional comparison was made between mean blood flow values obtained at baseline for the normal and POAG group; the results are summarised in Table 8.20. A significant difference ($p<0.01$) was observed between the normal and POAG group for blood volume ($p<0.01$) measured in the superior nasal quadrant of the peripapillary retina. A trend towards reduction was observed for blood volume, flow and velocity measured superior temporally ($p<0.05$). In each case the mean blood flow values were less for the POAG group and the standard deviation around the mean was similar

between the two groups. Mean values for blood volume, flow and velocity were not significantly different between the two groups in the inferior temporal and inferior nasal quadrant, however, the mean values were lower for the POAG group than the normal group.

Other investigators have identified significantly reduced blood flow between normal and POAG subjects using SLDF (Michelson, G. *et al.*, 1996a; Nicolela, M. T. *et al.*, 1996b), CDI (Galassi, F. *et al.*, 1992; Harris, A. *et al.*, 1994b; Cellini, M. *et al.*, 1996; Nicolela, M. T. *et al.*, 1996a; Rankin, S. J. A., 1999) and POBF (James, C. B. & Smith, S. E., 1991b; Quaranta, L. *et al.*, 1994). The exact reasons why blood flow is compromised in glaucoma are unclear. There are two principle theories: 1) The IOP pressure theory that proposes changes in the extracellular matrix, induced through mechanical damage to the ONH, may cause blood flow through the capillaries to become compromised (Quigley, H. A., 1995). 2) The autoregulatory dysfunction theory that may be secondary to mechanical damage or due to other influences such as vasospasm or stenosis (Geijer, C. & Bill, A., 1979; Grunwald, J. E. *et al.*, 1984).

Michelson, G. *et al.*, (1996a) showed that blood flow, volume and velocity, as measured by SLDF, was reduced in POAG compared to normal subjects. Although the results from this study identify a significant difference between the normal and POAG subjects for blood volume in the superior nasal quadrant, the difference was not nearly as marked as that reported by Michelson, G. *et al.*, (1996a). In this study, blood volume measured superior nasally was 14.36 ± 3.28 for the normal subject group and 12.51 ± 2.71 for the POAG group. Blood volume measured superior temporally was 16.94 ± 5.33 for the normal group and 14.77 ± 2.96 for the POAG group. Blood volume reported by Michelson, G. *et al.*, (1996a) was 29.38 ± 6.54 for the normal group and 15.74 ± 3.35 for the POAG group.

The sample sizes, mean IOP level and mean visual field defect measured for the POAG group in this study were similar to Michelson's study and we report similar blood flow values for the POAG group. However, the values reported by Michelson, G. *et al.*, (1996a) for the normal subject group were almost twice that found in this

study. The differences in blood flow measures may be accountable, in part, to the lower mean age (50 ± 10 years) of the normal subject group in Michelson's study compared to this study (65 ± 8.3 years). However, it seems unlikely that blood flow levels drop by 50% within fifteen years. There are very few studies that report the effect of age on ocular haemodynamics. However, one study looking at the CRA (using CDI) which supplies the retinal circulation reported a 6-11% decrease in blood flow velocities per decade of life (Groh, M. J. M. *et al.*, 1996). On this basis, the maximum difference between the findings from the present study with those of Michelson's study would have been 16.5%, not 44.3%.

9.7.2 Haemodynamic change over time: by group

ANCOVA was used to compare ocular blood flow parameters over time for the normal and POAG subject group. A correction was made for a potential age effect. The blood flow parameters were determined in 4 regions of the peripapillary retina and the results showed that overall, significant differences between the groups were apparent in the inferior nasal quadrant only. There are no published observations on the longitudinal follow-up of ocular blood flow in normal or POAG subjects using SLDF, so it is impossible to compare these findings with other work.

The concept that ocular blood flow may respond differently in the different areas of peripapillary retina is a recent one brought about by work presented in this thesis (Chapter 5) (Chung, H. S. *et al.*, 1998a; Chung, H. S. *et al.*, 1998b). During the application of a stress test the superior retina, but not the inferior retina, demonstrated efficient autoregulatory activity in normal subjects. As previously discussed, compromised autoregulation has been suggested as a possible mechanism for ONH damage in POAG (Geijer, C. & Bill, A., 1979; Grunwald, J. E. *et al.*, 1984; Pillunat, L. E. *et al.*, 1985; Riva, C. E. *et al.*, 1997a) and the findings from Chapter 5 suggest that autoregulation is less efficient in the inferior retina compared to the superior retina in normal subjects.

The reasons why there is a difference in the autoregulatory capacity of the retina in normal subjects are unknown. There may be an anatomical explanation or possibly a gravitational effect. These findings for normal subjects may have some baring on POAG. In accordance with a vascular theory for optic nerve damage it would seem likely that early blood flow changes in POAG would occur in the less efficient (inferior) area of the retina first. The results for the longitudinal follow-up elegantly demonstrate that overall, differences in peripapillary retinal blood flow between a POAG and normal subject group are detectable in the inferior nasal retinal quadrant only. During the pathogenesis of POAG, characteristic visual field loss has been found to commence primarily in the superior nasal quadrant (McClure, E., 1988). This area corresponds to nerve fibre loss in the inferior retina and the compromised blood flow measured in the inferior retina for the POAG group may go some way to explaining this.

9.7.3 Haemodynamic change over time: by subject

Although the group-wise analysis gives an understanding of the the data it does not enable individual subjects to be investigated. For this reason the haemodynamic parameters, blood flow, velocity and volume were analysed over time for each individual subject.

9.7.3.1 Normal subjects

Table 9.12. shows the total change in parameters for each subject for the normal group. Eleven (35.5%) out of 31 normal subjects did not demonstrate significant changes in blood flow parameters in any area of the peripapillary retina over the duration of the study ($p<0.01$). This still left a high proportion (64.5%) that did show significant change in at least one area of the peripapillary retina. Subjects showed the least change for volume, flow and velocity measured in the inferior nasal quadrant (12.9%, 6.5% & 3.2%) (Figure 9.6.). The most change was seen in the superior nasal quadrant (Figure 9.6.). It is impossible to say whether the change seen in the normal subjects represented true change or simply the error of the instrument. Both the intra-

and inter-reproducibility of SLDF has been reported as good (Michelson, G. *et al.*, 1996b; Nicolela, M. *et al.*, 1997), which supports the detection of true change.

There are many factors known to affect ocular blood flow that may have had a role in the observed results for the normal subject group including diurnal rhythm (Claridge, K. G. & Smith, S. E., 1994; Wang, T. H. *et al.*, 1996), posture (James, C. B. & Smith, S. E., 1991a; Baxter, G. M. *et al.*, 1992; Evans, D. W. *et al.*, 1999a), cigarette smoking (Langhans, M. *et al.*, 1997; Tamaki, Y. *et al.*, 1999), cardiac cycle (Strenn, K. *et al.*, 1997), blood pressure (Robinson, F. *et al.*, 1986), IOP (Pillunat, L. E. *et al.*, 1985; Sperber, G. O. & Bill, A., 1985; Quaranta, L. *et al.*, 1994; Pillunat, E. L. *et al.*, 1996; Lietz, A. *et al.*, 1998), exercise (Harris, A. *et al.*, 1996b; Riva, C. E. *et al.*, 1997b), glycaemia (Grunwald, J. E. *et al.*, 1995), hypercapnia (Ringelstein, E. B. *et al.*, 1992; Schmetterer, L. *et al.*, 1995; Harris, A. *et al.*, 1996c; Schmetterer, L. *et al.*, 1997) and hyperoxia (Fallon, T. J. *et al.*, 1985; Linsenmeier, R. & Yancey, C. M., 1989; Schmetterer, L. *et al.*, 1995). Agents affecting the sympathetic or parasympathetic nervous system (caffeine, alcohol) may also have an affect. An attempt was made to control some factors. Subjects were tested at approximately the same time of day and were requested to avoid caffeine, alcohol and strenuous activity prior to examination and posture was kept the same. Clearly, it is impossible to control for all of these factors and the countless other factors that affect blood flow may account for the change in blood flow observed in normal subjects over time.

9.7.3.2 POAG subjects

Table 9.13. gives the parameter change for each POAG subject. Overall, significant changes in blood flow parameters were evident in at least one quadrant of the peripapillary retina in 26 (78.8%) POAG subjects. A schematic representation of the percentages of POAG and normal subjects showing change in blood flow parameters in the different retinal areas are given in Figure 9.6. The figure shows that, for blood flow parameters measured in the inferior nasal peripapillary retina, considerably more changes in blood volume, flow and velocity occur in the POAG group (24.2%, 30.3%, 33.3%) compared to the normal group (12.9%, 6.5%, 3.2%). This finding agrees with

the ANCOVA analysis by group. Figure 8.22. presents a histogram of the inferior nasal blood flow findings for each group. Of the three parameters, blood velocity provides the largest distinction between the groups.

9.7.4 Correlation with topography, visual fields and IOP

Figure 9.6. shows the percentage of normal and POAG subjects showing change in blood flow parameters measured in the the four peripapillary retinal quadrants relative to accompanying topographic change in factors. The most obvious distinction between the normal and POAG group for heamodynamic change is evident in the inferior nasal region. Interestingly topographic change is most apparent superiorly for the POAG group.

A large number of POAG subjects (66.6%) showed change in at least one haemodynamic parameter and it is impractical to discuss all of the subjects showing change. Some of the more interesting cases that had significant visual field loss or underwent acute IOP reduction throughout the study period are discussed in subsequent sections. Four out of 5 POAG subjects (#41, #44, #57, #58) demonstrating significant deterioration in visual field indices also showed changes in retinal capillary blood flow (Table 9.14.). The results for subject #41 and #58 are discussed relative to their visual field loss in section 9.8.4. Subject #44 underwent trabeculectomy as did subjects #32 and #54. The haemodynamic results for these POAG subjects relative to psychophysical and topographic change are discussed in section 9.9.3.2.

Subject #	Superior Temporal			Superior Nasal			Inferior Temporal			Inferior Nasal		
	Volume	Flow	Velocity	Volume	Flow	Velocity	Volume	Flow	Velocity	Volume	Flow	Velocity
1					×	×						
2										×	×	
3												
4												
5				×	×	×						
6	×	×	×									
7	×	×	×				×	×	×			
8				×	×	×						
9												
10		×	×									
11												
12							×					
13	×			×			×	×	×			
14												
15							×	×				
16												
17										×		
18					×	×		×	×			
19		×	×									
20						×						
21				×	×	×						
22		×	×		×	×				×		
23												
24								×	×			
25												
26										×	×	×
27				×	×	×						
28												
29												
30	×			×								
31												
Total	4	5	5	6	7	8	4	5	4	4	2	1
%	12.9	16.1	16.1	19.4	22.6	35.8	12.9	16.1	12.9	12.9	6.5	3.3

Table 9.12. Blood flow parameter change for each peripapillary retinal quadrant for each normal subject. Ticks represent significant change ($p<0.01$).

Missing page(s) from the bound copy

Subject #	Superior Temporal			Superior Nasal			Inferior Temporal			Inferior Nasal		
	Volume	Flow	Velocity	Volume	Flow	Velocity	Volume	Flow	Velocity	Volume	Flow	Velocity
32	×											
33												
34												
35	×	×	×		×							
36												
37												
38												×
39				×								
40							×					
41										×		
42												
43										×	×	×
44	×	×	×	×								
45	×			×	×	×	×			×	×	×
46				×								
47											×	×
48				×	×	×	×	×	×			
49	×	×	×	×	×	×	×	×	×	×	×	×
50										×	×	×
51										×	×	×
52												
53												
54											×	×
55	×	×	×									
56												
57	×	×	×					×	×			
58	×									×	×	×
59											×	×
60												
61	×	×	×	×	×							
62												
63				×	×	×	×	×	×	×	×	×
64												
Total	9	6	6	8	6	4	5	4	4	8	10	11
%	27.3	18.2	18.2	24.2	18.2	12.1	15.2	12.1	12.1	24.2	30.3	33.3

Figure 9.13. Blood flow parameter change for each peripapillary retinal quadrant for each POAG subject. Ticks represent significant change ($p<0.01$).

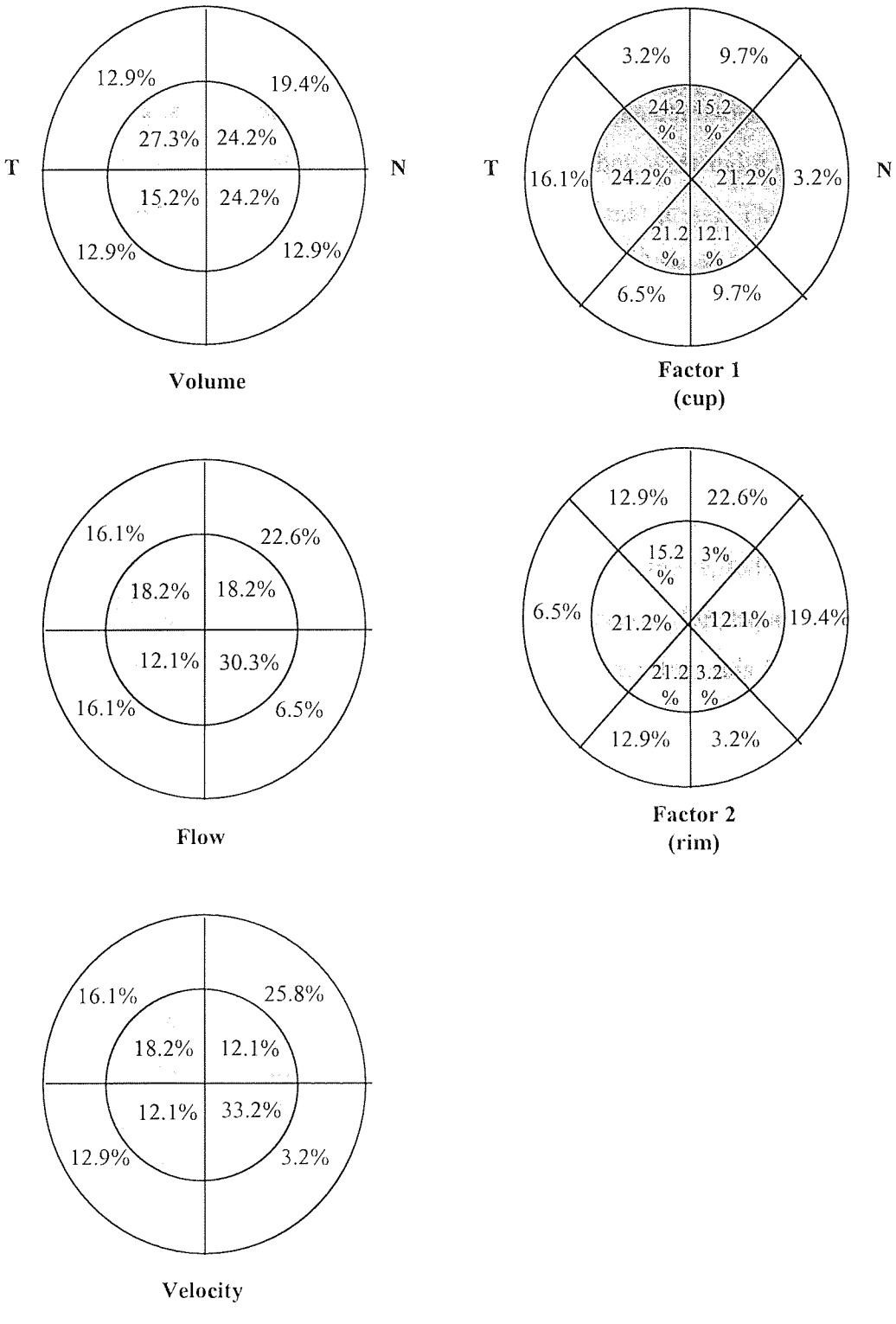

Figure 9.6. Left: schematic representation of the percentage change for blood volume, flow and velocity for the normal vs POAG (shaded areas) subjects. Right: Schematic representation of the percentage change of cup (regional factor 1) and rim (regional factor 2) for the normal and POAG (shaded areas) subjects. T = temporal, N = nasal.

9.7.5 Haemodynamic change over time: summary

The results from this study suggest that changes in blood flow over time at the peripapillary retina are apparent in both a normal and glaucomatous population. Although changes were evident in all areas of the retina, they were more common in the inferior nasal retina for the POAG compared to the normal group. This particular region demonstrates significantly compromised ocular blood flow in POAG subjects over time compared to normal subjects. This is the first time that ocular blood flow measurements have been followed-up longitudinally for a group of POAG and normal subjects and hence the first time that one area of the retina has been singled out as important.

SLDF is a relatively new technique, however earlier studies on the reproducibility and validity of SLDF, together with the significant results observed for the longitudinal follow-up of POAG and normal subjects, provide reassurance that this technique is useful for the detection of subtle changes in ocular blood flow. This study only measured one component of the ocular circulation, the retinal capillary bed. It is possible that changes may have occurred in other areas of the ocular circulation such as the choroid, retrobulbar vessels or ONH, however other techniques would need to be employed to assess this.

Finally, the POAG subjects followed in this study were all diagnosed with HTG. Many studies have focussed on NTG and have reported compromised blood flow in this group of patients (Demailly, P. *et al.*, 1984; James, C. B. & Smith, S. E., 1991b; Durcan, F. J. *et al.*, 1993; Harris, A. *et al.*, 1994b; Ravalico, G. *et al.*, 1994a; Butt, Z. A. *et al.*, 1995; Tomita, G. *et al.*, 1996). Whereas a primary vascular role seems more likely in NTG due to the normal levels of IOP, there is still considerable evidence that points towards a vascular involvement in HTG (Schwartz, B., 1994; Michelson, G. *et al.*, 1996a; Nicolela, M. T. *et al.*, 1996b; Duijm, H. F. A. *et al.*, 1997; Michelson, G. *et al.*, 1998a). The fundamental question of whether the vascular role is primary or secondary to the progression of glaucomatous optic neuropathy is still unknown. The

results from this study add to the knowledge of a vascular involvement in HTG. We have now demonstrated that there are changes in retinal peripapillary blood flow (more so in the inferior nasal quadrant) over time in POAG compared to normal eyes.

9.8 Visual field Indices

Visual field examination serves as an important guide as to whether or not a patients condition is stable. Severe visual field defects (CPSD) show marked intra-visit (short-term) fluctuation and inter-visit (long-term) fluctuation (Hodapp, E. *et al.*, 1993; Katz, J. L. *et al.*, 1997). This can make visual field progression difficult to detect. To facilitate the detection of change, POAG patients with only early to moderate visual field loss were included in the study. During the progression of POAG, loss of nerve fibre axons can result in characteristic visual field deterioration. This occurs in one or more ways (Hodapp *et al.*, 1993):

- A pre-existing defect may deepen.
- A pre-existing defect may expand.
- A new defect may develop in an area that was previously normal.
- The whole visual field may decrease in sensitivity.

In this study the visual field indices MD, PSD and CPSD were assessed for change over time. A decrease in MD indicated a generalised deterioration in the visual field and an increase in PSD and/or CPSD indicated an increase in the irregularity of the visual field that was not diffuse, i.e. it was greater in some areas than others. A minimum criterion for the detection of visual field progression as defined by Hodapp, E. *et al.*, (1993), is a significant decrease in the MD that cannot be explained by developing media opacities or pupil size, or a steadily increasing CPSD.

It was expected that, overall, visual field indices for the normal subject group would remain stable. At most, some individual subjects may exhibit a learning effect which would be apparent through improvements in visual field parameters. It was thought that only a proportion of the POAG subjects would demonstrate visual field progression. A study by Katz, J. L. *et al.*, (1997) showed that approximately 1 in 3-4

POAG patients demonstrated progressive visual field damage when followed-up for a 7 year period. Other studies have reported similar findings (O'Brien, C. *et al.*, 1991; Smith, S. D. *et al.*, 1996) On this basis, it was expected that less than 25% of POAG would exhibit deterioration in visual field indices.

9.8.1 Cross-sectional comparison between groups at baseline

The normal and POAG groups differed significantly at baseline for all measured perimetric indices (Table 8.24.). This was expected and reflected the reduced sensitivity of visual field indices for the POAG group typical of glaucomatous optic neuropathy.

9.8.2 Visual field change over time between groups

ANCOVA was carried out to look for differences between the two subject groups over time. There was a significant difference over time between the two groups for MD, PSD and CPSD when corrected for age ($p<0.05$). Graphs were plotted of the mean values obtained for each group, trend lines are shown together with r^2 values (Figure 8.23. – 8.25.). A decreasing trend in MD was apparent for the POAG group ($r^2=0.592$) over time suggesting a decrease in sensitivity. An increasing trend in MD was observed for the normal group indicative of a learning effect. PSD showed a marked increase over time for the POAG group ($r^2=0.7256$) and a decrease for the normal group ($r^2=0.648$). Whereas MD can indicate change owing to lens opacities, CPSD provided an indication of the change due to glaucomatous progression. CPSD showed a steady increase over time for the POAG group ($r^2=0.9089$) suggesting a gradual deterioration of the visual field in that group consistent with progressive optic neuropathy. The CPSD for the normal group showed a slight decrease after visit 3 consistent with an overall learning effect ($r^2=0.2394$).

9.8.3 Visual field change by subject

The group-wise analysis showed that CPSD and PSD increased significantly and MD decreased significantly over time for the POAG group. This suggests that some patients were demonstrating decreased visual field sensitivity. In order to determine which patients were deteriorating each subject was analysed individually. It was expected that a number of subjects from the normal group would show improvement in visual field indices consistent with a learning effect and a proportion of the POAG patients were expected to show deterioration in visual field indices over time.

In total of 4 (12.9%) subjects from the normal group and 7 (21.2%) subjects from the POAG group demonstrated change in at least one visual field parameter by ANOVA. These are discussed in more detail below.

9.8.3.1 Normal subjects

All four subjects showing change for the normal group did so in one parameter only (Table 8.27). Three out of the 4 subjects demonstrated a relative improvement (2 in MSD and 1 in CPSD) consistent with a learning effect that is commonly observed for the first or second visual field examination (Hodapp, E. *et al.*, 1993). A learning effect was expected in the normal group because the majority of the subjects were unfamiliar with the technique, others had taken part in previous studies and were quite practised. Figure 9.7. gives the MD values at each visit for two of the normal subjects each showing a significant improvement. The subjects had not undergone perimetry testing before. For both subjects the MD for visits 1 and 2 are quite similar, the notable improvement starts at visit 3. This finding agrees with a previous graph plotted for the whole group, where a slight improvement in visual field indices is apparent at visit 3 (Figure 8.23.). The indvidual visual fields for subject #28 are given in Appendix 7.5.

One normal subject showed a significant deterioration in CPSD (Figure 9.8.), however the glaucoma hemifield test remained within normal limits. The IOP for that subject

was stable (12-13mmHg) and no change in topography by HRT parameters or factors were apparent.

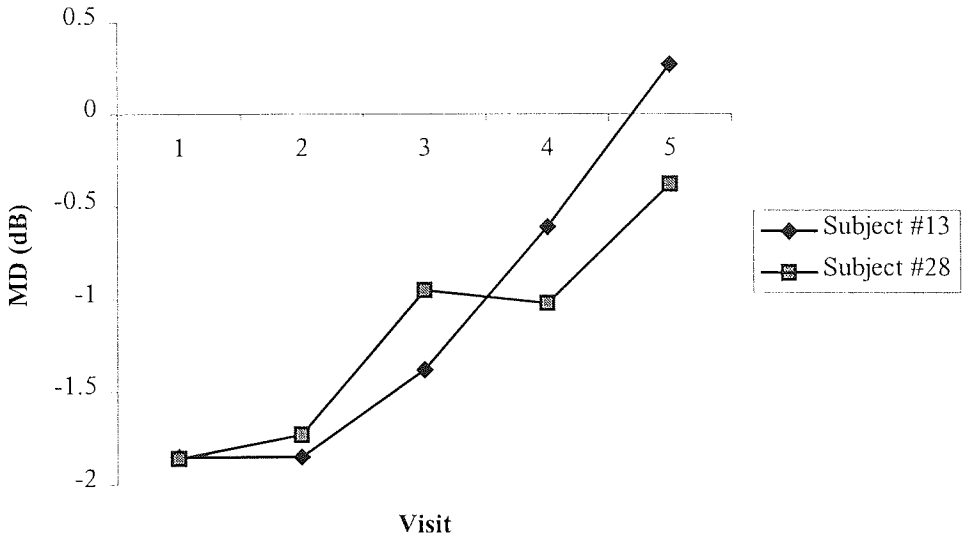

Figure 9.7. Visual field MD for two normal subjects at visits 1-5. The MD increases (improves) over time indicating a learning effect for these subjects.

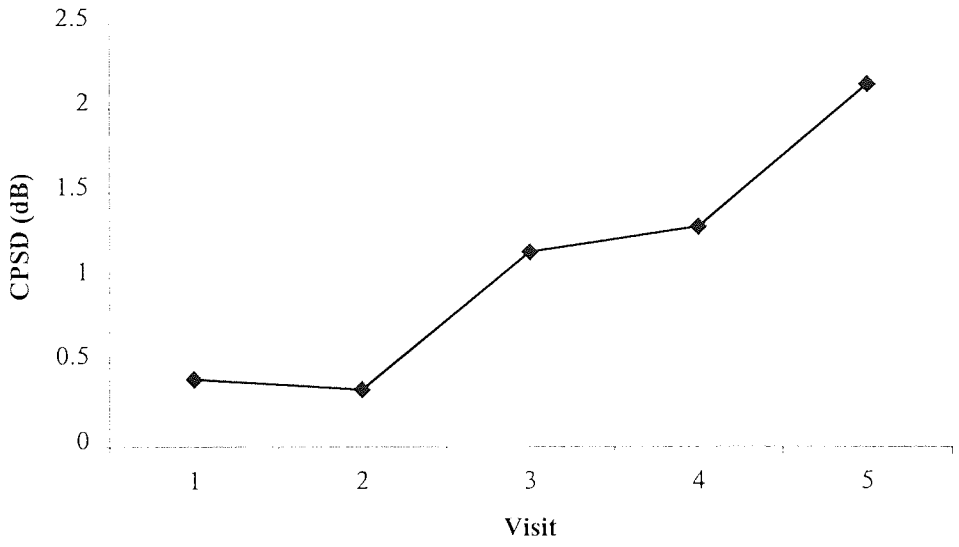

Figure 9.8. Visual field mean CPSD values for visits 1-5 for a normal subject (#7) showed a gradual deterioration over time. The GHT remained within normal limits. Topography and IOP was stable.

9.8.3.2 POAG subjects

Seven POAG subjects demonstrated psychophysical change over time, three of which demonstrated change in more than one visual field parameter (Table 8.28.). Two subjects (#40 & #51) showed a relative improvement in CPSD, one of which (subject #51) had undergone a change in treatment. The change in treatment at visit 2 coincided with the improvement in visual field thereafter (Figure 9.9). The improvement observed for subject #40, who did not undergo treatment changes, was most likely the result of a learning effect.

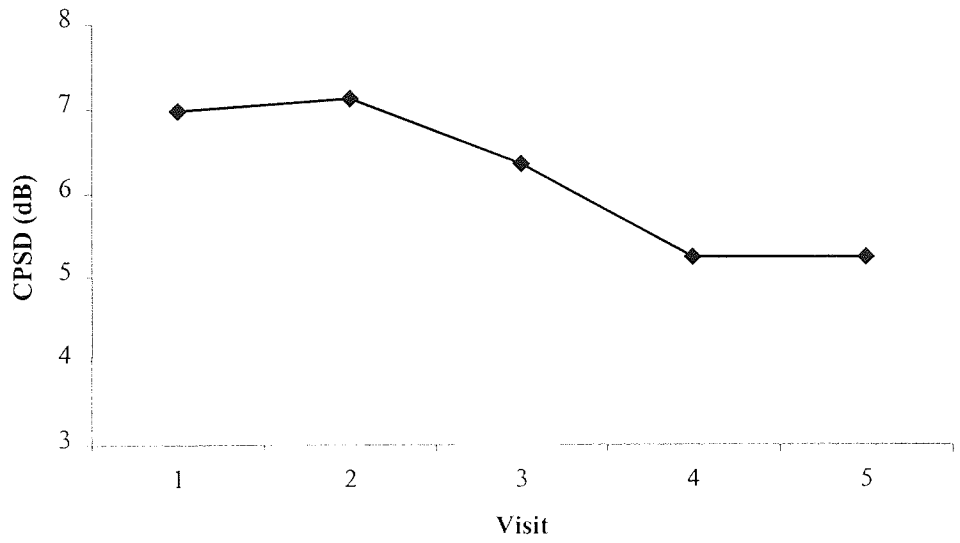

Figure 9.9. Visual field CPSD values at visit 1-5 for a POAG subject (#51). A change in treatment at visit 2 corresponds with an improvement in CPSD thereafter.

The remaining 5 POAG subjects (15%) (subjects #41, 44, 57, 58 & 62) demonstrated a significant deterioration in visual field indices over the follow-up period of the study (Table 8.27.). Katz, J. L. *et al.*, (1997) reported that 1 in 3-4 subjects demonstrated progressive visual field loss in a 7 year follow-up. On this basis, 15% of POAG subjects showing progressive visual field loss during a follow-up period of 16 months is to be expected.

9.8.4 Correlation with change in topography

Four out the 5 subjects who demonstrated deterioration in visual field sensitivity had their treatment modified throughout the study. One subject (#44) underwent trabeculectomy and is discussed in section 9.9.3.2. Of the subjects showing change, 3 showed topographical changes for rim (factor 2), the remainder showed topographical changes for cup (factor 1). These changes were evident globally and regionally. The accompanying topographical changes support the theory that nerve fibre layer loss accompanies visual field loss. All but one subject (#62) showed a change in ocular blood flow parameters. Table 9.14. summarises the psychophysical, topographic and haemodynamic changes for each subject. Three of the patients showing change (#41, #58 & #62) are discussed in more detail below.

Subject	Change in fields	Change in factors		Change in blood flow
		Cup	Rim	
41	MD, PSD, CPSD (superior)		Inf temp	Inf nasal
44	CPSD (diffuse)	Nasal		Sup temp Sup Nasal
57	PSD, CPSD (inferior)	Sup temp Temporal Nasal		Sup temp Inf temp
58	PSD, CPSD (superior)	Sup temp	Global Temporal Inf temporal	Sup temp Inf nasal
62	CPSD (inferior)	Global	Global	

Table 9.14. Visual field changes in POAG patients and corresponding topographic and haemodynamic change throughout the study period.

Subject #41

This subject demonstrated a significant deterioration in CPSD throughout the study period (Figure 9.10., Appendix 7.6.). A significant decrease in blood volume was

evident in the inferior nasal peripapillary retina (Figure 9.10.). IOP was stable (20-21mmHg), but a change in treatment was administered towards the end of the study period on the assumption that the IOP was not low enough due to the deteriorating visual field. Changes in topography for individual HRT parameters were evident inferior nasally and inferior temporally. Changes in the regional rim factor were apparent inferior temporally (Figure 9.11.) suggesting thinning of the neuroretinal rim. Appendix 7.7 shows topography images at visit 1 and 5 for this patient with a subsequent decrease in rim area, volume and retinal nerve fibre layer thickness. Clinical investigation of this patient revealed inferior notching of the rim and an increasing vertical C:D ratio as determined by an ophthalmologist. Finally, in agreement with the ocular blood flow, topographical and clinical findings the visual field showed marked progression in the superior nasal and superior temporal region.

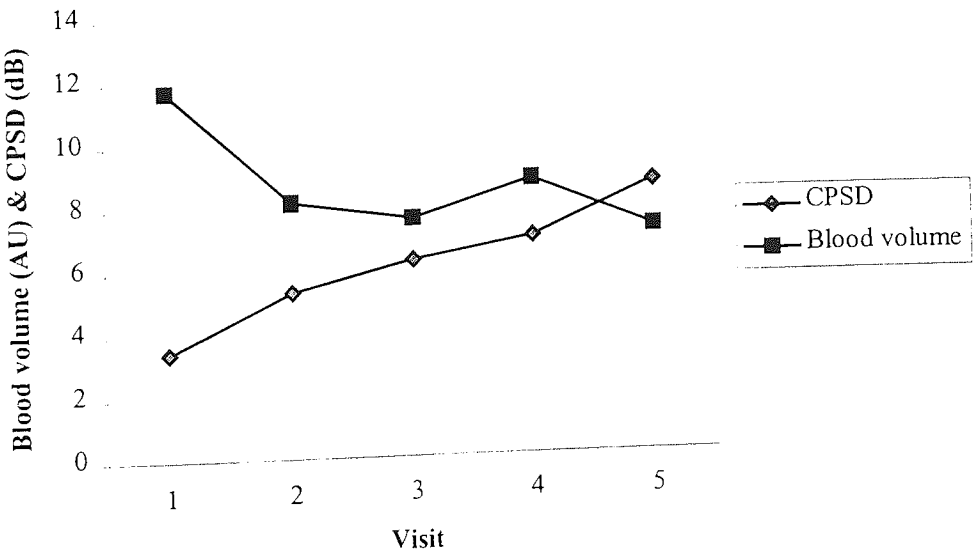

Figure 9.10. Graph of the mean values for blood volume (AU) measured inferior nasally and CPSD (dB) for a POAG subject (#41). As CPSD increases indicating deterioration in visual function, blood volume decreases. This subject underwent a treatment change at visit 4.

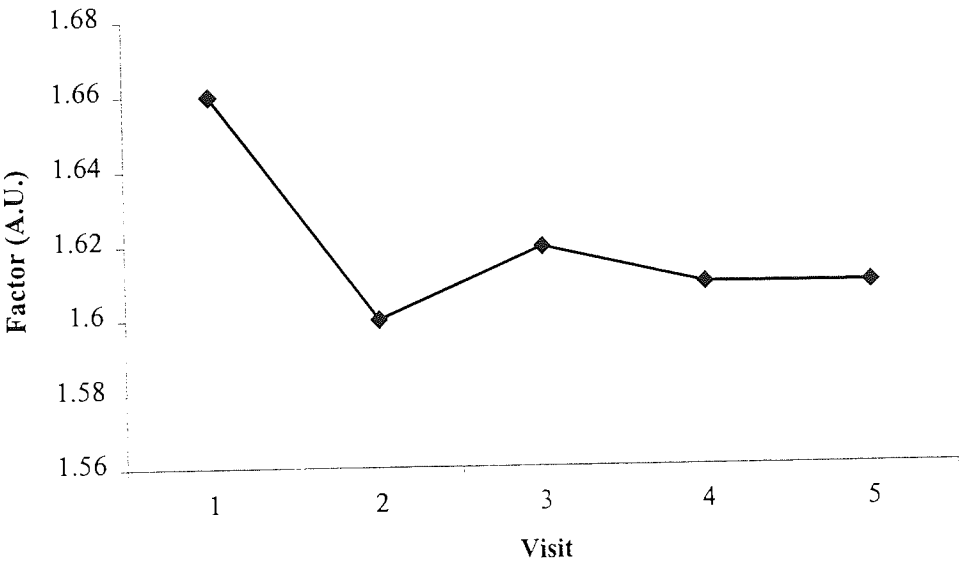

Figure 9.11. POAG subject (#41). Results for topographic rim factor measured inferior temporally throughout the study period. The graph shows a gradual decrease in the rim tissue throughout the study period.

Subject #58

Subject 58 demonstrated a significant decrease in the global rim factor (Figure 9.13., Appendix 7.10.). Significant change was also evident for the regional rim factor in the temporal and inferior temporal sectors (Figure 9.14.). The only change observed for cup was in the superior temporal quadrant. This patient had a superior nasal step defect as verified by perimetry and inferior temporal notching of the neuroretinal rim. A deteriorating CPSD was apparent over the study period (Figure 9.12., Appendix 7.9.). IOP was stable at 18mmHg except for a drop at visit 3 (16mmHg) which may correspond with the relative improvement in CPSD at that time. These combined results suggest a progressive loss of rim tissue localised inferior temporally and temporally despite controlled IOP.

When IOP is controlled and glaucoma continues to progress, other factors such as blood flow may be contributory to the pathogenesis of the disease. Significant blood flow changes were apparent in the superior temporal and nasal quadrants for this patient (Figure 9.15.). A decrease in blood flow was evident for the superior temporal quadrant between visits 1 to 4 after which it increased. The result for visit 5 was most probably erroneous as the overall trend of the readings is downward until that point. This finding may be explained by the sensitivity of blood flow measures to social and environmental factors such as diet, heat and exercise which could not readily be controlled for.

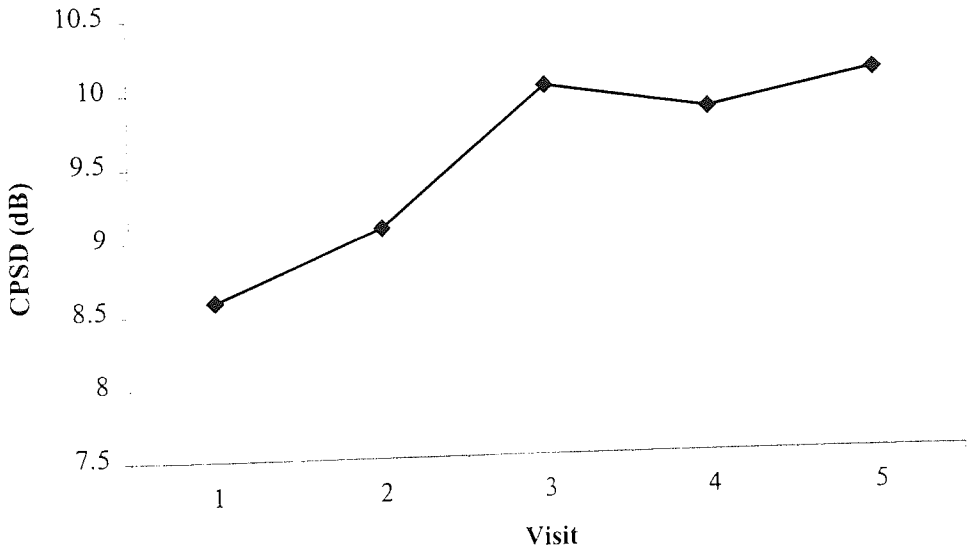

Figure 9.12. **POAG** subject (#58) showing increasing (deterioirating) visual field CPSD throughout the study period. Also see Appendix 7.6. for visual field printouts.

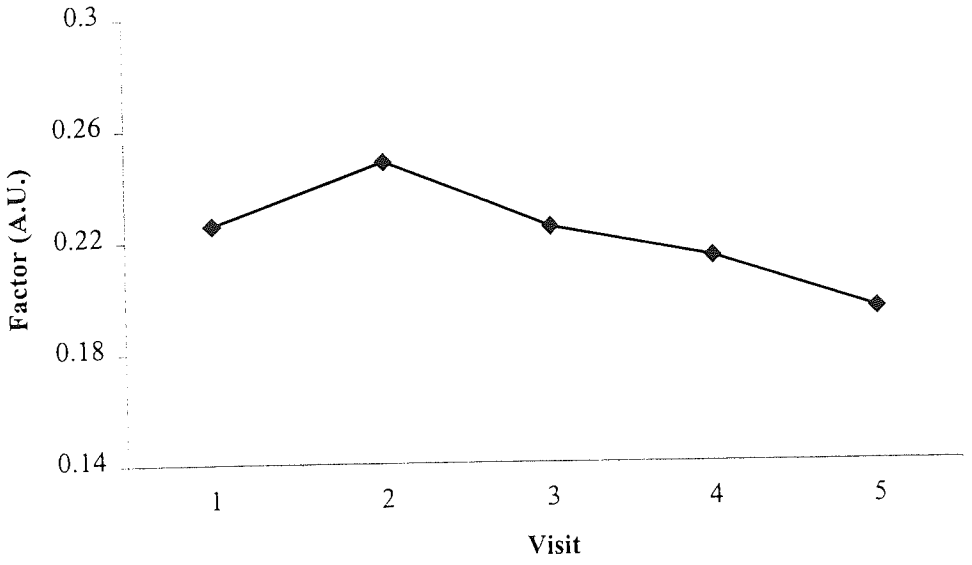

Figure 9.13. POAG subject (#58) showing a steady decrease in rim factor (measured globally) throughout the study period suggestive of rim tissue loss associated with progressive glaucomatous optic neuropathy. See Appendix 7.7 for topography images.

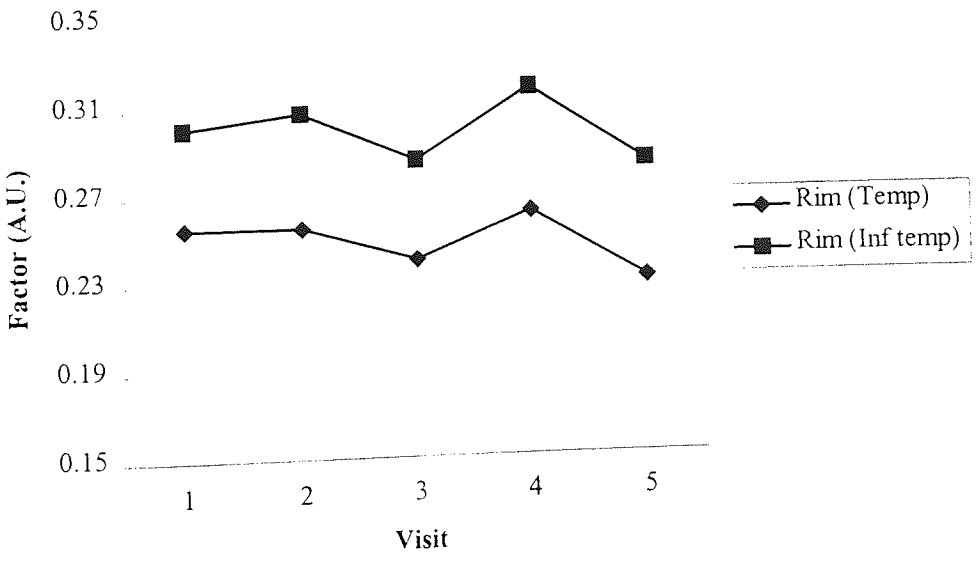

Figure 9.14. POAG subject (#58). Topographic rim factor decreased regionally in the temporal and inferior temporal sectors only for this patient.

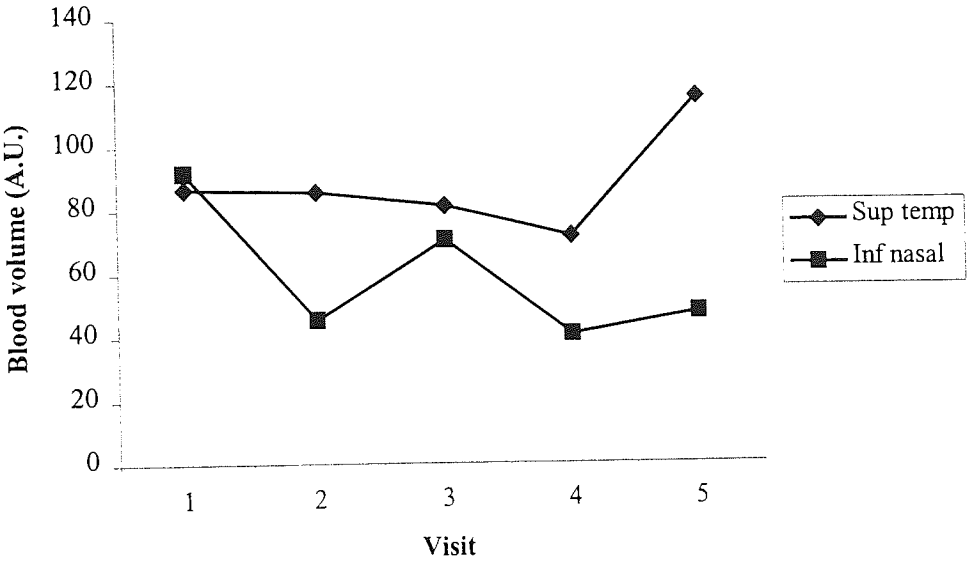

Figure 9.15. POAG subject (#58). Retinal blood volume (as measured by SLDF) in the superior temporal and inferior nasal quadrants over the study period.

Subject #62

Subject #62 demonstrated a significant increase in the global cup factor and a decrease in the global rim factor throughout the study period (Figure 9.18.). IOP increased steadily until a treatment change at visit 4 (addition of Latanaprost to topical therapy) which resulted in a concomitant drop in IOP at visit 5 (Figure 9.16.). The CPSD also increased up to visit 4 after which it stabilised (Figure 9.17.). Likewise, the global rim factor appeared to decrease and then stabilise at visit 5, but the cup factor continued to decrease (Figure 9.18.). Even though the psychophysical and topographic data were changing throughout the study period, no changes in ocular blood flow were evident. This suggests that individual patients may differ in their susceptibility to blood flow (Galassi, F. *et al.*, 1997) and that the mechanism of ONH damage, at least in this patient, may be more related to changes in IOP than changes in blood flow.

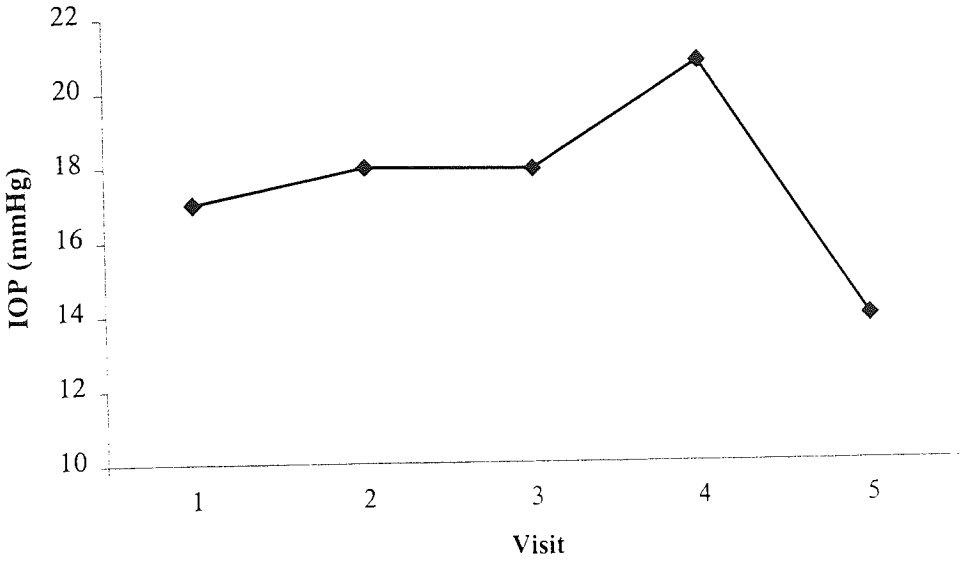

Figure 9.16. POAG subject (#62). IOP at visits 1-5. A treatment change (prostaglandin analogue) was administered at visit 4, effective at visit 5.

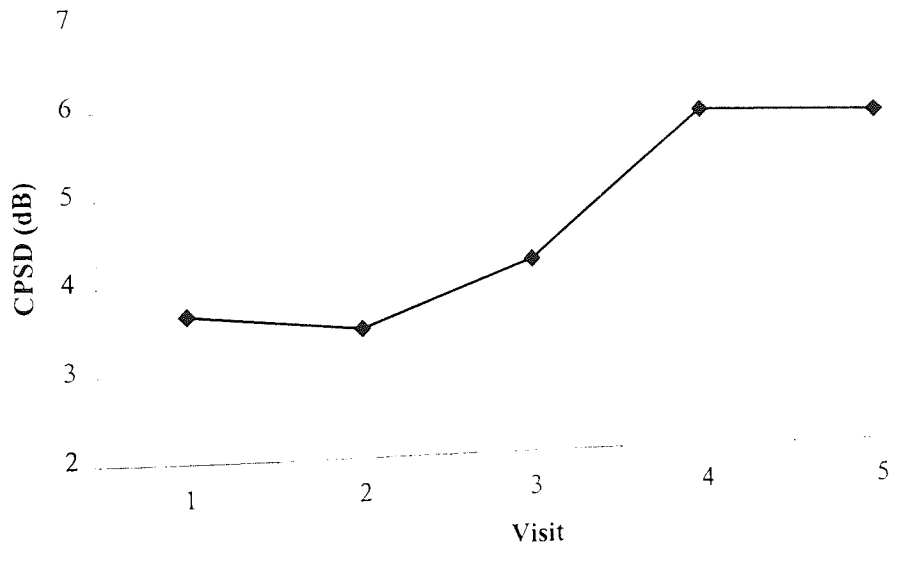

Figure 9.17. POAG subject (#62). Increasing (deteriorating) visual field CPSD over 5 visits which appears to be arrested following a treatment change at visit 4.

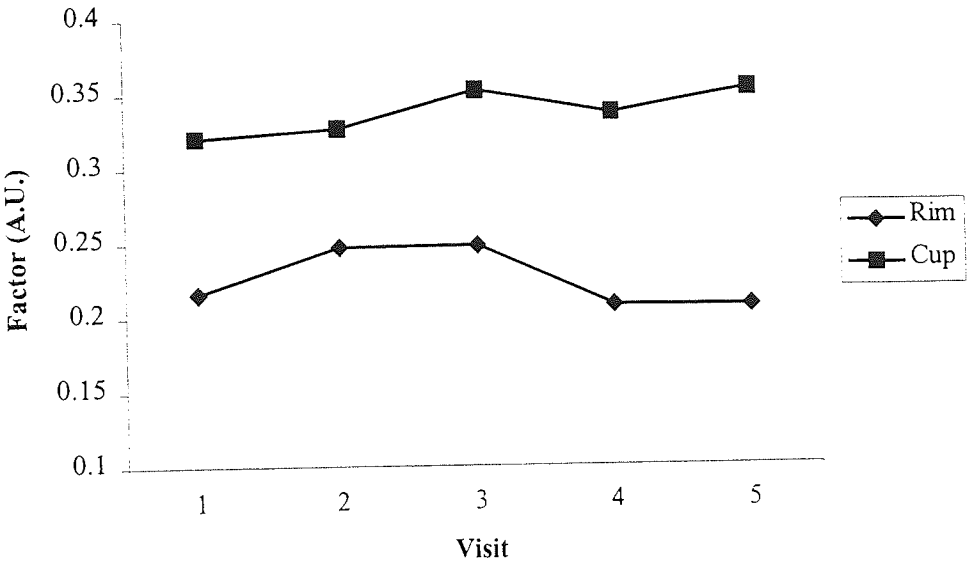

Figure 9.18. POAG subject (#62). Decreasing rim factor and increasing cup factor measured globally consistent with glaucomatous progression. A treatment change (prostaglandin analogue) was effective at visit 5.

9.8.5 Visual field change over time: summary

The group-wise analysis revealed a significant difference between the normal and POAG group for all measured visual field indices over the study period. Investigation by subject showed a proportion of normal subjects that demonstrated a learning effect. A number of POAG patients demonstrated significant progressive visual field loss throughout the study period. In most cases the change in visual field could be related to changes in topography, treatment and haemodynamics.

9.9 IOP

Based on the mechanical theories of optic nerve damage in glaucoma, increased IOP leads to direct compression of optic nerve axons as they exit the eye at the lamina cribrosa (Quigley, H. A. *et al.*, 1980). Alternatively, raised IOP may lead to vascular

insufficiency due to mechanical insult of optic nerve capillaries (Quigley, H. A., 1995). A number of studies have identified topography changes in the optic nerve, such as increased cupping, that are related to increased IOP (Quigley, H. A. *et al.*, 1980; Levy, N. S. *et al.*, 1981; Flammer, J., 1996; Rath, E. Z. *et al.*, 1996; Kulshrestha, M. *et al.*, 1998). Likewise, acute reductions in IOP such as that following trabeculectomy may have the opposite effect (Irak, I. *et al.*, 1996).

9.9.1 Cross-sectional comparison between groups

A cross-sectional comparison of IOP at baseline between the two subject groups showed a significant difference between the normal (15.2 ± 2.1mmHg) and POAG (18.7 ± 2.1mmHg) group ($p<0.001$). The POAG group consisted of patients diagnosed with high-tension POAG. Two subjects had undergone pressure-lowering surgery prior to the study, however the IOP for these subjects had steadily increased following surgery. A further 3 subjects underwent trabeculectomy during the study period and the remainder where administering topical treatment.

9.9.2 IOP change over time: by group.

A significant difference was observed in IOP over the follow-up period of 16 months between the two groups ($p<0.05$). Graphed mean values for each visit showed no change for the normal subject group ($r^2=0.532$) (Figure 8.26.). A significant linear decrease in IOP was evident for the POAG group ($r^2=0.603$). The main drop in IOP occurred between visits 4 and 5 consistent with 2 subjects who underwent trabeculectomy at that time.

9.9.3 IOP change over time: by subject

No significant change in IOP was evident throughout the study period for individual POAG or normal subjects. This finding was expected for the normal subjects. The statistical analysis searched for a linear effect in the data ($r^2 \geq 0.06$). Consequently,

only subjects with a steady increase or decrease in IOP would have resulted in a significant change over time. Three subjects underwent trabeculectomy resulting in a significant drop in IOP that occurred at the end of the study and did not produce a linear effect. These are discussed in section 9.9.3.2.

9.9.3.1 POAG subjects

Not all of the POAG subjects had well-controlled pressure for the duration of the study and if IOP did start to increase then treatment was modified. The result was normally a drop in IOP following the change in treatment. An example of such a patient (#62) is given in Figure 9.16. For the first 4 study visits the IOP steadily increased despite topical therapy consisting of a β-blocker and carbonic anhydrase inhibitor. At visit 4 a prostaglandin analogue was added to the patients therapy, this caused a drop in IOP which was evident at visit 5. Linear regression of the graphed IOP values gives r^2 value of 0.5477. This is not significant, yet it is apparent from the graph that IOP has changed and these changes correlate perfectly with the treatment.

9.9.3.2 Trabeculectomy: psychophysical, haemodynamic and morphological change

Acute reduction in IOP has been shown to produce improvements in optic nerve topography and visual field indices (Shiose, Y., 1990; Mikelberg, F. S., 1993; Spaeth, G. L., 1994b; Azuara-Blanco, A. & Spaeth, G. L., 1997). Relative improvements in topographic parameters measured with the HRT have been reported following trabeculectomy (Irak, I. *et al.*, 1996; Lima, M. C. *et al.*, 1999; Topouzis, F. *et al.*, 1999). This is thought to be due to a reduction in the posterior bowing of the lamina cribrosa (Lusky, M. *et al.*, 1993a). On this basis, reductions in cup depth and size were expected in patients who had undergone trabeculectomy throughout the duration of the study.

Three subjects underwent trabeculectomy throughout the duration of the study period (subjects #32, #44, #54). The maximum percentage change in IOP was defined as the

difference between the highest and lowest IOP values, divided by the highest IOP value (x100 and given in percent). Table 9.15. summarises the maximum IOP change throughout the study period for each patient who underwent trabeculectomy. Related morphological, psychophysical and haemodynamic change following surgery are discussed below.

Subject #	Mean IOP	Min IOP	Max IOP	Max % change
32	17.5	14	22	36.4%
44	19.8	14	23	39.1%
54	18.2	16	21	23.8%

Table 9.15. Maximum percentage change in IOP for subjects who underwent trabeculectomy.

Subject #32

Subject #32 underwent trabeculectomy after visit 4, effective at visit 5 resulting in a 36.4% decrease in IOP (Figure 9.19.). A significant change in blood volume was noted throughout the study period in the superior temporal quadrant (Figure 9.20.). A definite dip in blood volume was apparent at visit 4 (pre-operatively) which may be related to the sharp increase in IOP at this visit. The blood flow increased post-operatively, which may again be related to the decrease in IOP.

Ophthalmic examination revealed inferior notching of the neuroretinal rim with a horizontal CD ratio of 0.8 that decreased to 0.5 following surgery and a vertical C:D ratio of 0.8 that decreased to 0.6 post-operatively. No significant change in topography was evident for regional and global rim or cup factors. However, an increase in volume below reference was noted inferior nasally over the study period (Figure 9.21.). There was no significant (linear) change for visual field parameters, however a notable drop in CPSD between visits 4 and 5 was observed suggesting a relative improvement that may have been related to surgical intervention.

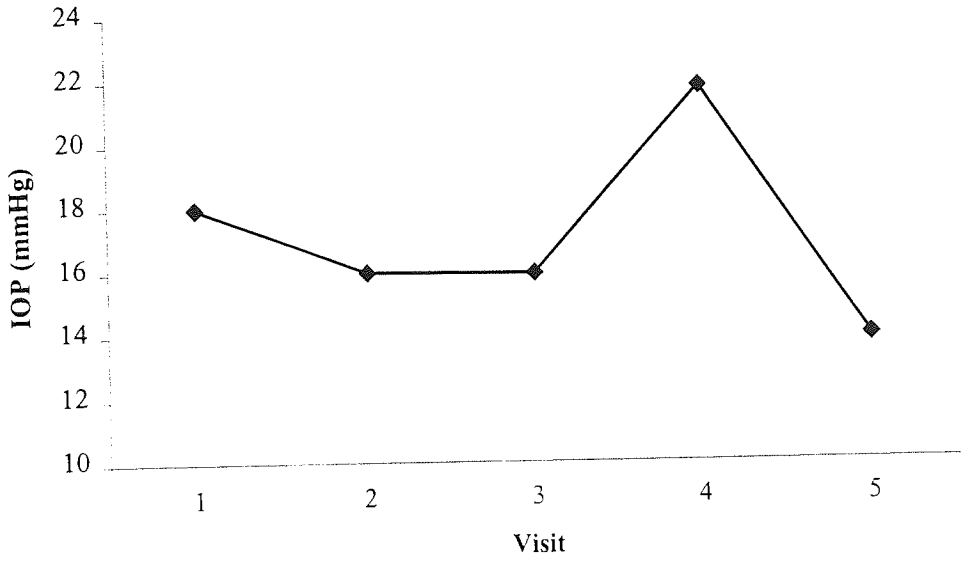

Figure 9.19. POAG subject (#32). IOP throughout the study period. Trabeculectomy was carried out after visit 4 consistent with the sudden drop in IOP.

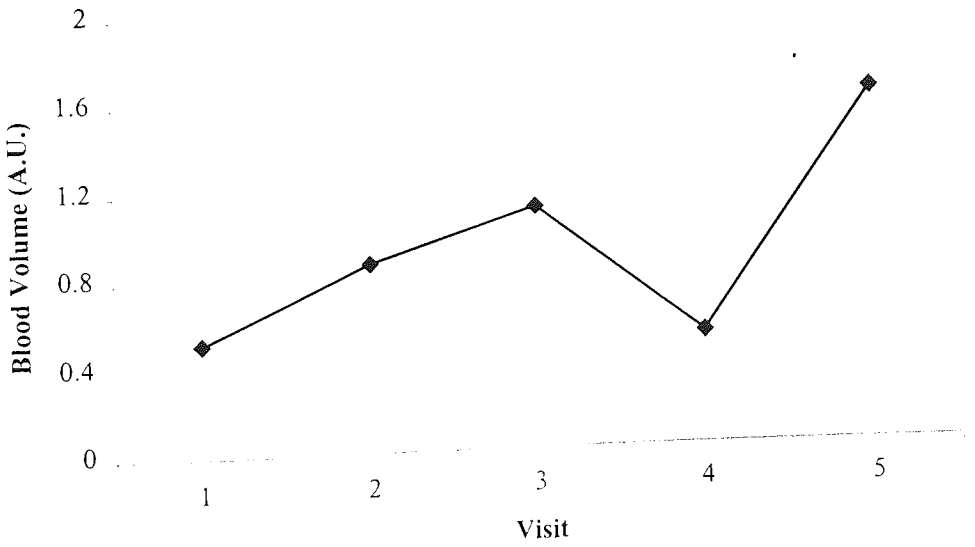

Figure 9.20. POAG subject (#32). Mean blood volume measured superior temporally throughout the study period. Trabeculectomy was effective at visit 5. The drop in blood flow may be related to an increase in IOP at visit 4. Note how this graph is almost a mirror image of the graph given above.

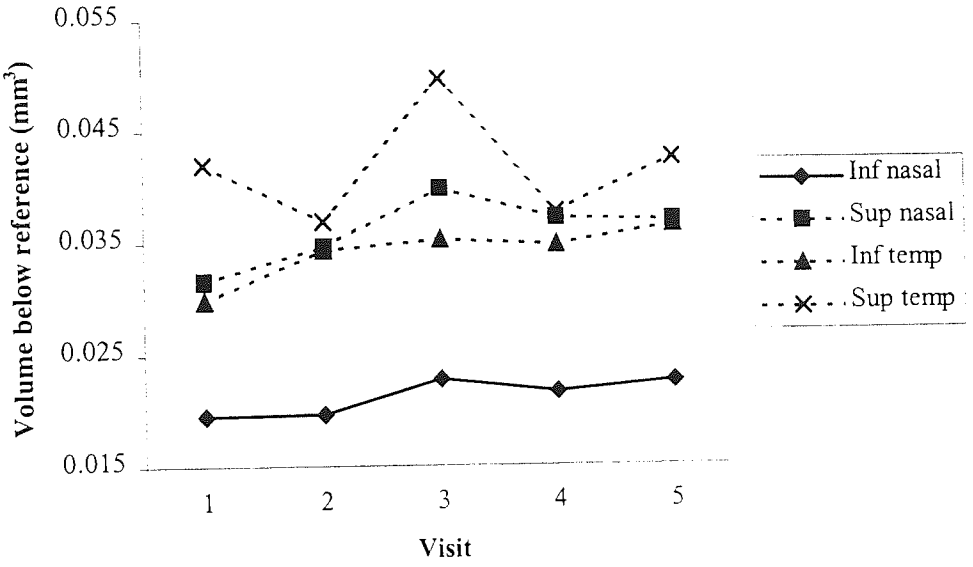

Figure 9.21. POAG subject (#32). Mean values for volume below reference (visits 1-5) in the inferior and superior quadrants. Significant change is indicated by a solid line and was evident in the inferior nasal quadrant only.

Subject #44

Subject #44 underwent trabeculectomy after visit 4 and the change was effective at visit 5 resulting in a 39.1% reduction in IOP. This patient had diffuse visual field loss. A significant deterioration was evident for CPSD over the study period which did not show any signs of improvement following trabeculectomy (Figure 9.22., Appendix 7.10.). Morphologically, a significant decrease in the regional cup factor was evident in the nasal sector after visit 4 (Figure 9.23.). No decrease in horizontal or vertical C:D ratio was observed by slit lamp biomicroscopy. Individual HRT parameters revealed a significant increase followed by a post-operative decrease in volume below surface and maximum cup depth for that region correlating with the change in cup factor. These results indicated a decrease in cup size and depth localised in the nasal region of the ONH that may have been associated with the acute reduction in IOP. No

changes were evident for the rim factors consistent with the known change associated with trabeculectomy which is localised in the cup (Lusky, M. *et al.*, 1993a).

A significant decrease in blood volume, flow and velocity was apparent in the superior temporal quadrant and for blood volume in the superior nasal quadrant ($p<0.01$). Figure 9.24. shows the mean values for blood volume at each visit for the superior temporal and nasal quadrants. The mean values for blood volume measured in the temporal quadrant decreased throughout the study period indicating reduced perfusion in this area. Blood velocity and flow measured in the same quadrant followed a similar pattern. Blood volume in the superior nasal quadrant increased at visit 2 and then decreased for visits 3 and 4, eventually stabilising at visit 5. Overall, the perfusion of the superior retina was reducing throughout the study period, this may or may not be related to the topographic change seen in the ONH. Unlike the topographic measures, but similar to psychophysical measures, no obvious improvement in haemodynamic measures was observed post-operatively in this patient.

Subject #54

Subject #54 underwent trabeculectomy after visit 3 and the change was effective at visit 4 resulting in a 23.8% reduction in IOP. This patient had a superior arcuate visual field defect and although a linear change over time was not identified using ANOVA, graphical representation of the CPSD values for each visit shows a marked improvement for visits 4 and 5 (Figure 9.25.). Ophthalmic examination revealed inferior notching of the neuroretinal rim with a horizontal C:D ratio of 0.7 that decreased to 0.6 following surgery and a vertical C:D ratio of 0.9 that decreased to 0.8 post-operatively.

A significant change over time was apparent for the regional cup factor measured inferior nasally and inferior temporally (Figure 9.26.). The graph shows a gradual increase in cup size until visit 4 where there was a notable decrease. No change was

apparent for rim factors (regionally or globally) for this patient suggesting that the change following surgery was localised to the cup. The individual HRT parameters were examined and significant changes in the cup shape measure third moment in contour were evident for the inferior regions. Thus specific changes in the shape, size, and depth of the cup may have occurred.

Significant changes in blood flow and velocity were identified inferior nasally. Figure 9.27. shows the mean values for blood flow. Mean values for blood velocity followed a similar pattern. The graph shows little change in blood flow pre-operatively, with an increase immediately post-operatively (visit 4) that may have been associated with a change in IOP.

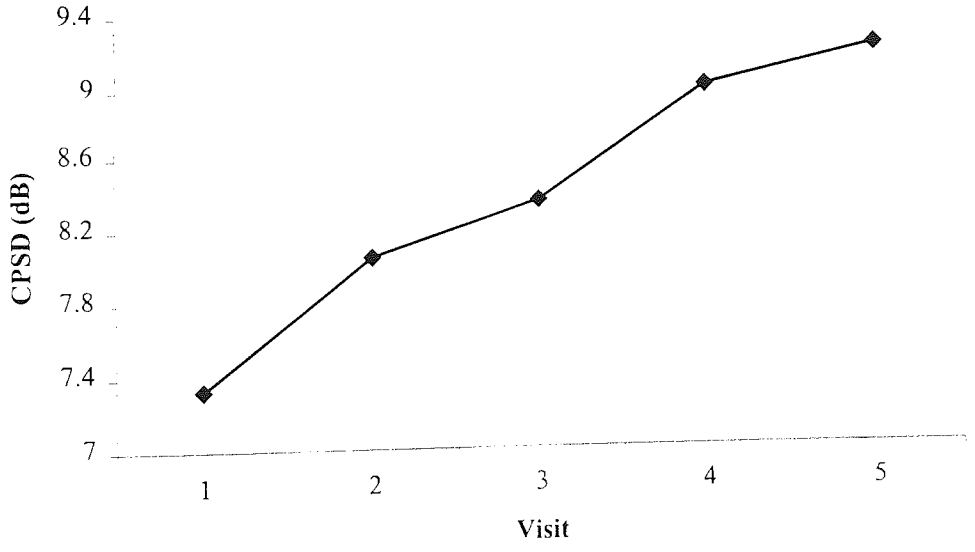

Figure 9.22. POAG subject (#44). Visual field CPSD values for visits 1-5. Acute IOP reduction occurred after visit 4. Also see Appendix 7.10. for visual field printouts.

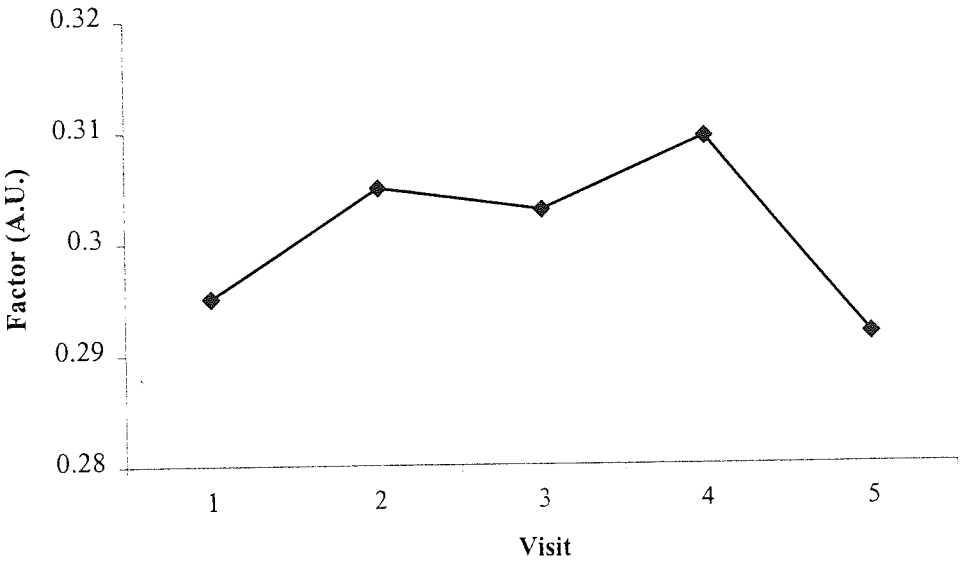

Figure 9.23. POAG subject (#44). Regional change in cup factor over the study period in the nasal sector. Acute IOP reduction was effective after visit 4 and correlates with an overall decrease in the cup factor.

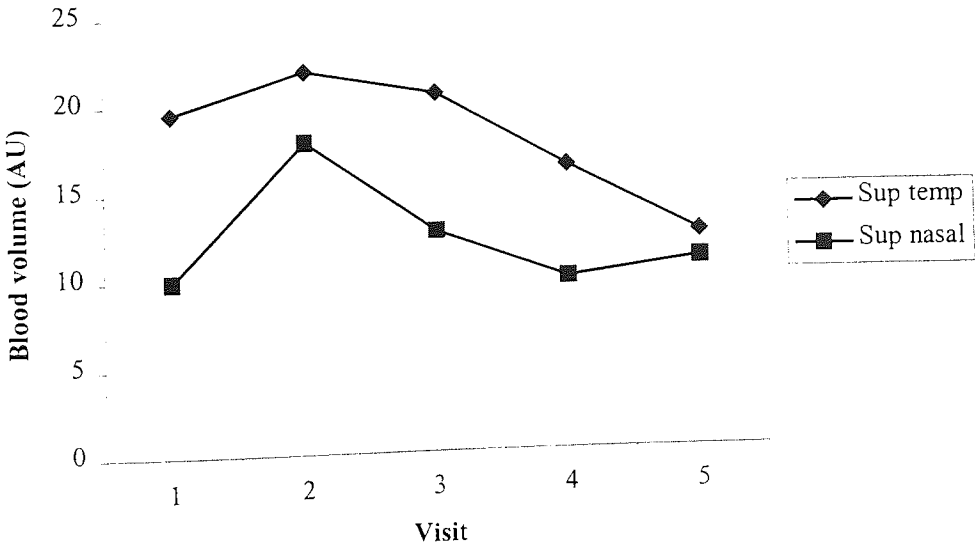

Figure 9.24. POAG subject (#44). Blood volume measured in the superior temporal and superior nasal quadrant.

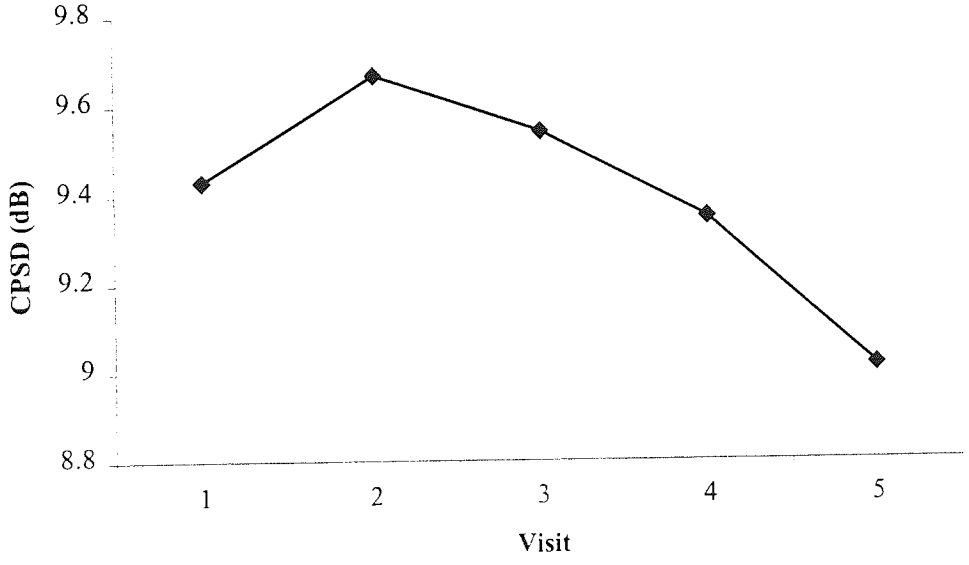

Figure 9.25. POAG subject (#54). Change in visual field CPSD throughout the study period. Trabeculectomy and IOP reduction was effective at visit 4.

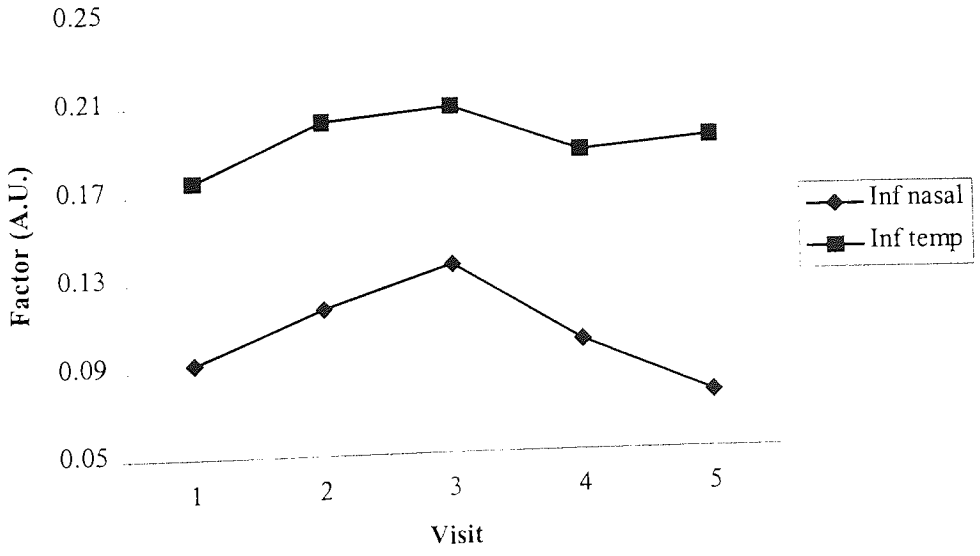

Figure 9.26. POAG subject (#54). Inferior nasal and inferior temporal results for cup factor. Trabeculectomy was carried out at visit 3 and corresponds to a decrease in cup size therafter, particularly apparent in the inferior temporal sector of the optic nerve head.

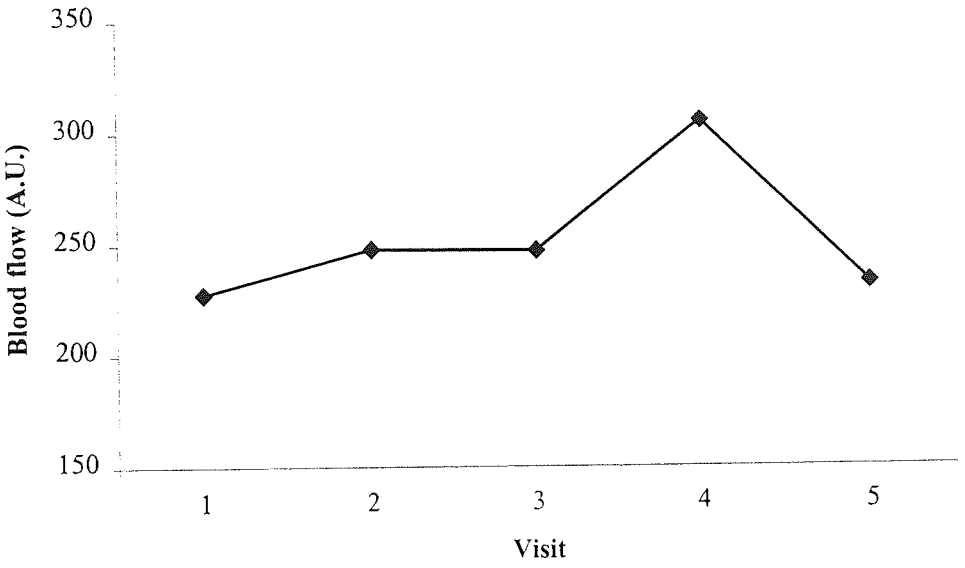

Figure 9.27. POAG subject (#54). Inferior nasal blood flow measured with SLDF. Trabeculectomy was carried out at visit 3, the change was effective at visit 4 corresponding with a increase in blood flow that then decreased again at visit 5 possibly due to a rise in IOP.

9.10 Conclusion

9.10.1 Scanning laser ophthalmoscopy

The group-wise comparison of a normal and POAG subject group at baseline showed that, with the exception of disc area, all measured parameters were useful for differentiating between the groups. Parameters that appeared particularly important in classification included: volume below surface, volume below reference, cup area and mean depth in contour.

Several global parameters were identified as important for detecting change over time between a normal and POAG group including C:D area ratio, cup area, volume below reference, rim area and mean depth in contour. Regionally, the measures of rim volume (volume above surface and volume above reference) were added as important.

Parameter and factor analyses were used to assess change over time in individual subjects. The parameter analysis (global and regional) resulted in a high proportion of

change for normal subjects and glaucoma patients. This suggests that the HRT parameters are oversensitive to subtle topographic fluctuations in the normal optic nerve head and overestimate glaucomatous change.

Factor analysis provided a powerful technique for reducing the relatively large number of HRT parameters into more manageable form that better described the data. Two factors were identified that were measured globally and regionally. In each case factor 1 described the cup and factor 2 the rim. Two POAG patients, but no normal subjects, showed a combined increase in the global cup factor and decrease in the global rim factor. The cup factor measured globally and regionally appeared useful for the detection of change over time in the POAG subjects. A small proportion of change was also noted for the normal subjects suggesting a degree of measurement error or noise associated with the technique. A high proportion of normal and POAG subjects showed change in the rim factor measured globally and regionally suggesting greater variability.

- **Topographic criteria for glaucomatous progression**

It is proposed that a concomitant increase in cup factor and decrease in rim factor may provide the best criteria from which to judge glaucomatous progression. An increase in cup factor alone most probably reflects real change in topography whereas a decrease in rim factor alone may indicate change, but must be viewed with caution.

9.10.2 Scanning laser Doppler flowmetry

Cross-sectional analysis at baseline identified a significant reduction in the perfusion of the peripapillary retinal capillary bed in the superior nasal region and a trend towards reduction in the superior temporal region for POAG subjects. These findings support the literature which reports decreased vascular perfusion in glaucoma.

The group-wise longitudinal analysis of a POAG and normal group identified a significant difference in blood flow, volume and velocity localised in the inferior nasal quadrant of the retina. Assessment of individual subjects showed the same result. The study outlined in chapter 5 identified regional differences in the autoregulatory function of the normal retina and it is proposed that the longitudinal findings may be associated with deficient autoregulatory function in the inferior retina.

9.10.3 Perimetry

By definition, baseline comparison of visual field indices measured for the POAG and normal group identified a significant difference between the two groups. The group-wise analysis of visual field indices showed a significant difference between the normal and POAG group over time. On an individual, basis five (15%) POAG subjects demonstrated a significant deterioration in visual field indices throughout the study period. This compares to 33% of POAG patients showing topographical change in the global cup factor. Although perimetry provides a valuable method for monitoring glaucomatous progression it appears less sensitive to subtle change that may otherwise be detected using topographic means.

9.11 Summary

- cSLO provides a useful technique for both classifying and monitoring the optic nerve head in glaucoma. Statistical factors provide a more realistic and conservative approach to monitoring glaucomatous change than topographical parameters alone.
- SLDF provides a method for monitoring peripapillary retinal blood flow and furthering the understanding of vascular dysfunction in glaucoma.
- Perimetry is of particular value for classifying glaucoma but is less sensitive to monitoring glaucomatous change compared to topographic means.

References

Abrams, L. S., Scott, I. U., Spaeth, G. L., Quigley, H. A. & Varma, R. (1994) Agreement among optometrists, ophthalmologists, and residents in evaluating the optic disc for glaucoma. *Ophthalmology* **101**: 1662-7.

Allen, L. (1964) Ocular fundus photography : Suggestion for achieving consistently good pictures and instrumentation for stereoscopic photography. *American Journal of Ophthalmology* **57**: 13.

Alm, A. & Bill, A. (1973) Ocular and optic nerve head blood flow at normal and increased intraocular pressures in monkeys (*Macaca irus*): a study with radioactively labelled microspheres including flow determinations in brain and some other tissues. *Experimental Eye Research* **15**: 15-29.

Anderson, D. R. (1977) Axonal transport in the retina and optic nerve. **In** Neuroophthalmology. Ed. Glasser, J. S. *CV Mosby Co*, St Louis, .**9**: 140-53.

Anderson, D. R. (1983) What happens to the optic disc and retina in glaucoma? *Ophthalmology* **90**: 766-70.

Anderson, D. R. (1995) Optic nerve blood flow. **In** Optic nerve in glaucoma. Ed. Drance, S. M. *Kulger Publications*, Amsterdam/New York: 311-31.

Anderson, D. R. & Hoyt, W. F. (1969) Ultrastructure of the intraorbital portion of the human and monkey optic nerve. *Archives of Ophthalmology* **82**: 506.

Anton, A., Yamagishi, N., Zangwill, L. M., Sample, P. A. & Weinreb, R. N. (1998) Mapping structural to functional damage in glaucoma with standard automated perimetry and confocal scanning laser ophthalmoscopy. *American Journal of Ophthalmology* **125**: 436-46.

Arend, O., Harris, A., Martin, B. J., Holin, M. & Wolf, S. (1994) Retinal blood velocities during carbogen breathing using scanning laser ophthalmoscopy. *Acta Ophthalmologica* **72**: 332-6.

Arend, O., Harris, A., Sponsel, W. E., Remky, A., Reim, M. & Wolf, S. (1995) Macular capillary particle velocities - a blue field and scanning laser comparison. *Graefe's Archive for Clinical and Experimental Ophthalmology* **233**: 244-9.

Armaly, M. F. (1965) On the distribution of applanation pressure. *Archives of Ophthalmology* **73**: 11-8.

Armaly, M. F. (1970) Optic cup in normal and glaucomatous eyes. *Investigative Ophthalmology* **9**: 425-9.

Armaly, M. F. (1971) Visual field defects in early open angle glaucoma. *Transactions of the American Ophthalmological Society* **69**: 147-62.

Armaly, M. F. & Sayegh, R. E. (1969) The cup/disc ratio. The findings of tonometry and tonography in the normal eye. *Archives of Ophthalmology* **82**: 191-6.

Armstrong, J. R., Daily, R. K., Dobson, H. L. & Girard, L. J. (1960) The incidence of glaucoma in diabetes mellitus. A comparison with the incidence of glaucoma in the general population. *American Journal of Ophthalmology* **50**: 55-63.

Asawaphureekorn, S., Zangwill, L. M. & Weinreb, R. N. (1996) Ranked-segment distribution curve for interpretation of optic nerve topography. *Journal of Glaucoma* **5**: 79-90.

Azuara-Blanco, A., Harris, A. & Cantor, L. B. (1998a) Reproducibility of optic disc topographic measurements with the Topcon ImageNet and the Heidelberg Retina Tomograph. *Ophthalmologica* **212**: 95-8.

Azuara-Blanco, A., Harris, A. & Cantor, L. B. (1998b) Reproducibility of optic disk topographic measurements with the Topcon ImageNet and the Heidelberg retina tomograph. *Ophthalmologica* **212**: 95-8.

Azuara-Blanco, A., Harris, A., Cantor, L. B., Abreu, M. M. & Weinland, M. (1998c) Effects of short term increase of intraocular pressure on optic disc cupping. *British Journal of Ophthalmology* **82**: 880-3.

Azuara-Blanco, A. & Spaeth, G. L. (1997) Methods to objectify reversibility of glaucomatous cupping. *Current Opinion in Ophthalmology* **8**: 50-4.

Azuara-Blanco, A., Spaeth, G. L., Nicholl, J., Lanzl, I. & Augsburger, A. (1999) Comparison between laser scanning tomography and computerised image analysis of the optic disc. *British Journal of Ophthalmology* **83**: 295-8.

Bailey, P. (1973) Cinemaphotography of human retinal vessels. *JAMA* **170**: 1373-5.

Balazsi, A. G., Rootman, J., Drance, S. M., Schulzer, M. & Douglas, G. R. (1984) The effect of age on the nerve-fiber population of the human optic-nerve. *American Journal of Ophthalmology* **97**: 760-6.

Bankes, J. L. K., Perkins, E. S., Tsolakis, S. & Wright, J. E. (1968) Bedford glaucoma survey. *British Medical Journal* **1**: 791-6.

Bartz-Schmidt, K. U., Sengersdorf, A., Esser, P., Walter, P., Hilgers, R. D. & Krieglstein, G. K. (1996) The cumulative normalised rim/disc area ratio curve. *Graefe's Archive for Clinical and Experimental Ophthalmology* **234**: 227-31.

Bartz-Schmidt, K. U., Weber, J. & Heimann, K. (1994) Validity of two-dimensional data obtained with the Heidelberg Retina Tomograph as verified by direct measurements in normal optic nerve heads. *German Journal of Ophthalmolmology* **3**: 400-5.

Baxter, G. M. & Williamson, T. H. (1993) Color Doppler flow imaging in central retinal vein occlusion: a new diagnostic technique? *Radiology* **187**: 847-50.

Baxter, G. M. & Williamson, T. H. (1995) Color Doppler imaging of the eye: normal ranges, reproducibility and observer variation. *Journal of Ultrasound in Medicine* **14**: 91-6.

Baxter, G. M., Williamson, T. H., McKillop, G. & Dutton, G. N. (1992) Color Doppler ultrasound of orbital and optic nerve blood flow: effects of posture and timolol 0.5%. *Investigative Ophthalmology and Visual Science* **33**: 604-10.

Bebie, H. (1995) Introduction to the Doppler effect. **In** Ocular blood flow. Ed. Kaiser, H. J., Flammer, J.& Hendrickson, P. *Karger*, Basel: 93-9.

Becker, B. (1971) Diabetes mellitus and primary open angle glaucoma. *American Journal of Ophthalmology* **71**: 1-16.

Bengtsson, B. (1972) Comparison of schoitz and goldmann applanation tonometry in a population. *Acta Ophthalmologica* **50**: 445-57.

Bengtsson, B. & Krakau, C. E. T. (1992) Correction of optic disc measurements on fundus photographs. *Graefe's Archive for Clinical and Experimental Ophthalmology* **230**: 24-8.

Bennett, A. G., Rudnicka, A. R. & Edgar, D. F. (1994) Improvements on Littmann method of determining the size of retinal features by fundus photography. *Graefe's Archive for Clinical and Experimental Ophthalmology* **232**: 361-7.

Biedner, B., Sachs, U. & David, R. (1983) Interobserver variations in tonometry and optic disc assessment. *Glaucoma* **5**: 160-3.

Bill, A. (1981) Ocular circulation. **In** Adler's Pysiology of the Eye. Ed. Moses, R. A. *Mosby*, St Louis: 184-203.

Bill, A. & Sperber, G. O. (1990) Control of retinal and choroidal blood-flow. *Eye* **4**: 319-25.

Birch, M., Brotchie, D., Roberts, N. & Grierson, I. (1997) The three-dimensional structure of the connective tissue in the lamina cribrosa of the human optic nerve head. *Ophthalmologica* **211**: 183-91.

Bishop, K. I., Werner, E. B., Krupin, T., Kozart, D. M., Beck, S. R., Nunan, F. A. & Wax, M. B. (1988) Variability and reproducibility of the optic disc topographic measurements with the Rodenstock Optic Nerve Head Analyzer. *American Journal of Ophthalmology* **106**: 696-702.

Blaker, J. W. (1980) Toward an adaptive model of the human eye. *Journal of the Optical Society of America* **70**: 223.

Bland, J. M. (1987a) The normal distribution. **In** An Introduction to Medical Statistics. Ed. . *Oxford Medical Publications*, Oxford: 112-33.

Bland, J. M. (1987b) Summarizing data. **In** An Introduction to Medical Statistics. Ed. . *Oxfrod University Press*, Oxford: 66-7.

Bland, J. M. & Altman, D. G. (1995) Multiple significance tests: the Bonferroni method. *British Medical Journal* **21**: 170.

Bland, J. M. & Altman, D. G. (1996a) Measurement error. *British Medical Journal* **312**: 1654.

Bland, J. M. & Altman, D. G. (1996b) Measurement error and correlation coefficients. *British Medical Journal* **313**: 41-2.

Bohdanecka, Z., Orgül, S., Prünte, C. & Flammer, J. (1998) Influence of acquisition parameters on hemodynamic measurements with the Heidelberg retina flowmeter at the optic disc. *Journal of Glaucoma* **7**: 151-7.

Boles Carenini, A., Sibour, G. & Boles Carenini, B. (1994) Differences in the longterm effect of timolol and betaxolol on the pulsatile ocular blood flow. *Survey of Ophthalmology* **38**: S118-S24.

Bonner, R. F. & Nossal, R. (1981) Model for laser Doppler measurements of blood flow in tissue. *Applied Optics* **20**: 2097-107.

Bonner, R. F. & Nossel, R. (1990) Principles of laser Doppler flowmetry. **In** Laser-Doppler blood flowmetry. Ed. Shepherd, A. P.& Oberg, P. A. *Kluwer*, Boston: 17-45.

Booth, A., Churchill, A., Anwar, R., Menage, M. & Markham, A. (1997) The genetics of primary open angle glaucoma. *British Journal of Ophthalmology* **81**: 409-14.

Bothman, L. (1947) Suggestions for accurate records in ophthalmology: Elschnig's classification of normal optic discs. **In** Yearbook of Eye, Ear and Throat. Ed. . *Year book medical publishers, Inc.*, Chicago: 7-13.

Brenton, R. S. & Phelps, C. D. (1981) The normal visual field on the Humphrey Field Analyzer. *Ophthalmologica* **193**: 56-74.

Brigatti, L. & Caprioli, J. (1995) Correlation of visual field with scanning confocal laser optic disc measurements in glaucoma. *Archives of Ophthalmology* **113**: 1191-4.

Broadway, D. C. & Drance, S. M. (1998) Glaucoma and vasospasm. *British Journal of Ophthalmology* **82**: 862-70.

Broadway, D. C., Drance, S. M., Parfitt, C. M. & Mikelberg, F. S. (1998) The ability of scanning laser ophthalmoscopy to identify various optic disc appearances. *American Journal of Ophthalmology* **125**: 593-604.

Broadway, D. C., Nicolela, M. T. & Drance, S. M. (1999) Optic disc appearances in primary open-angle glaucoma. *Survey of Ophthalmology* **43**: S223-S43.

Büchi, E. R. (1996) The blood supply to the optic nerve head. **In** Ocular blood flow. Ed. Kaiser, H. J., Flammer, J.& Hendrickson, P. *Karger*, Basel: 1-8.

Burk, R. O. W., Airaksinen, P. J., Tuulonen, A., Rohrschneider, K., Völcker, H. E. & König, J. (1995) Reference plane for three-dimensional topographic optic disc analysis with the Heidelberg retina tomograph. *Investigative Ophthalmology and Visual Science* **36**: S627.

Burk, R. O. W., Rohrschneider, K., Völcker, H. E. & Zinser, G. (1990) Analysis of three-dimensional optic disc topography by laser scanning tomography. Parameter definition and evaluation of parameter inter-dependence. **In** Scanning laser ophthalmoscopy and tomography. Ed. Nasemann, J. E.& Burk, R. O. W. *Quintessenz*, München: 161-75.

Burk, R. O. W., Tuulonen, A. & Airaksinen, P. J. (1993) Analysis of the three-dimensional topography of retinal nerve fiber layer defects by laser scanning tomography. *Investigative Ophthalmology and Visual Science* **34**: 762.

Burk, R. O. W., Tuulonen, A. & Airaksinen, P. J. (1998) Laser scanning tomography of localised nerve fibre layer defects. *British Journal of Ophthalmology* **82**: 1112-7.

Butt, Z. A., McKillop, G., O'Brien, C., Allen, P. & Aspinall, P. (1995) Measurement of ocular blood flow velocity using color Doppler imaging in low-tension glaucoma. *Eye* **9**: 29-33.

Butt, Z. A. & O'Brien, C. (1995) Reproducibility of pulsatile ocular blood flow measurements. *Journal of Glaucoma* **4**: 214-8.

Cantor, L. B., Azuara-Blanco, A. & Harris, A. (1994) Reproducibility of optic disc topography and RNFLH in the same subjects utilizing the Topcon ImageNet and the Heidelberg retina tomograph. *Investigative Ophthalmology and Visual Science* **35**: 1345.

Caprioli, J. & Miller, J. M. (1989) Measurement of relative nerve fiber layer surface height in glaucoma. *Ophthalmology* **96**: 633-41.

Carel, R. S., Korczyn, A. D., Rock, M. & Goya, I. (1984) Association between ocular pressure and certain health parameters. *Ophthalmology* **91**: 311-4.

Carter, C. J., Brooks, D. E., Doyle, D. L. & Drance, S. M. (1990) Investigations into a vascular etiology for low-tension glaucoma. *Ophthalmology* **97**: 49-52.

Cellini, M., Possati, G. L., Caramazza, N. & Caramazza, R. (1996) Colour Doppler analysis of the choroidal circulation in chronic open-angle glaucoma. *Ophthalmologica* **210**: 200-2.

Chan, A. B., Chauhan, B. C., LeBlanc, R. P., McCormick, T. A. & Shaw, A. M. (1997) Intra- and inter-observer agreement with cumulative defect curves. *Journal of Glaucoma* **6**: 117-22.

Chauhan, B. C. (1996) Confocal scanning laser Doppler flowmetry of the retina and optic nerve head. **In** Encounters in glaucoma research 3. How to ascertain progression and outcome. Ed. Anderson, D. R.& Drance, S. M. *Kugler*, Amsterdam: 263-76.

Chauhan, B. C., Leblanc, R. P., McCormick, F. A. & Rogers, J. B. (1994) Test-retest variability of topographic measurements with confocal scanning laser tomography in patients with glaucoma and control subjects. *American Journal of Ophthalmology* **118**: 9-15.

Chauhan, B. C. & MacDonald, C. A. (1995) Influence of time separation on variability estimates of topographic measurements with confocal scanning laser tomography. *Journal of Glaucoma* **4**: 189-93.

Chauhan, B. C. & McCormick, T. A. (1995) Effect of the cardiac cycle on topographic measurements using confocal scanning laser tomography. *Graefe's Archive for Clinical and Experimental Ophthalmology* **233**: 568-72.

Chauhan, B. C. & Smith, F. M. (1997) Confocal scanning laser Doppler flowmetry: experiments in a model flow system. *Journal of Glaucoma* **6**: 237-45.

Chung, H. S., Harris, A., Evans, D. W., Kagemann, L. E., Garzozi, H. J. & Martin, B. J. (1999a) Vascular aspects in the pathophysiology of glaucomatous optic neuropathy. *Survey of Ophthalmology* **43**: S43-S50.

Chung, H. S., Harris, A., Halter, P. J., Roff, E. J., Kagemann, L. E., Garzozi, H. J., Hosking, S. L. & Martin, B. J. (1998a) Regional differences in retinal vascular reactivity. *Investigative Ophthalmology and Visual Science* **In press**.

Chung, H. S., Harris, A., Kagemann, L. E. & Martin, B. (1999b) Peripapillary retinal blood flow in normal tension glaucoma. *British Journal of Ophthalmology* **83**: 466-9.

Chung, H. S., Harris, A., Roff, E. J., Kagemann, L. E., Evans, D. W. & Halter, P. J. (1998b) Superior and inferior peripapillary retinal vessels respond differently to changing blood level of oxygen and carbon dioxide. *Investigative Ophthalmology and Visual Science* **39**: S263.

Cioffi, G. A., Robin, A. L., Eastman, R. D., Perell, H. F., Sarfarazi, F. A. & Kelman, S. E. (1993) Confocal laser scanning ophthalmoscope

Reproducibility of optic nerve head topographic measurements with the confocal laser scanning ophthalmoscope. *Ophthalmology* **100**: 57-62.

Cioffi, G. A. & Van Buskirk, E. M. (1994) Microvasculature of the anterior optic nerve. *Survey of Ophthalmology* **38**: S107-S17.

Claridge, K. G. (1993) The effect of topical pilcocarpine on pulsatile ocular blood flow. *Eye* **7**: 507-10.

Claridge, K. G. & Smith, S. E. (1994) Diurnal variation in pulsatile ocular blood flow in normal and glaucomatous eyes. *Survey of Ophthalmology* **38**: S198-S205.

Corbett, J. J., Phelps, C. D., Eslinger, P. & Montague, P. R. (1985) The neurological evaluation of patients with low-tension glaucoma. *Investigative Ophthalmology and Visual Science* **26**: 1101-5.

Cranstoun, S. D., Petrig, B. L., Riva, C. E. & Baine, J. (1994) Optic nerve head blood flow in the human eye by laser Doppler flowmetry (LDF). *Investigative Ophthalmology and Visual Science* **35**: 1658.

Crick, R. P., Vogel, R., Newson, R. B., Shipley, M. J., Blackmore, H., Palmer, A. & Bulpitt, C. J. (1989) The visual field in chronic simple glaucoma and ocular hypertension: its character, progress, relationship to the level of intraocular pressure and response to treatment. *Eye* **3**: 536-46.

Demailly, P., Cambien, F., Plouin, F., Baron, P. & Chevallier, B. (1984) Do patients with low tension glaucoma have particular cardiovascular characteristics? *Ophthalmologica* **188**: 65-75.

DeMaio, R., Schweitzer, J., Werner, E. & Piltz, J. (1992) Correlation of peripapillary atrophy, retinal nerve fiber layer, and visual fields among glaucoma and glaucoma suspect patients. *Investigative Ophthalmology and Visual Science* **33**: 885.

Dichtl, A., Jonas, J. B. & Mardin, C. Y. (1996) Comparison between tomographic scanning evaluation and photographic measurement of the neuroretinal rim. *American Journal of Ophthalmology* **121**: 494-501.

Dielemans, I., Vingerling, J. R., Hofman, A., Grobbee, D. E. & de Jong, P. T. V. M. (1994) Reliability of intraocular pressure measurement with the Goldmann applanation tonometer in epidemiological studies. *Graefe's Archive of Clinical Experimentation in Ophthalmology* **232**: 141-4.

Donaldson, D. D. (1964) A new camera for stereoscopic fundus photography. *Trans. Am. Ophthalmol. Soc.* **62**: 429.

Donders, F. C. (1862) *Von Graefe's Archive for Ophthalmology* **8**: 1.

Drance, S. M., Douglas, G. R., Wijsman, K., Schulzer, M. & Britton, R. J. (1988) Response of blood flow to warm and cold in normal and low-tension glaucoma patients. *American Journal of Ophthalmology* **105**: 35-9.

Drance, S. M., Sweeney, V. P., Morgan, R. W. & Feldman, F. (1973) Studies of factors involved in the production of low tension glaucoma. *Archives of Ophthalmology* **89**: 457-65.

Dreher, A. W., Patrick, C. T. & Weinreb, R. N. (1991) Reproducibility of topographic measurements of the normal and glaucomatous optic nerve head with the laser tomographic scanner. *American Journal of Ophthalmology* **111**: 221-9.

Dreher, A. W. & Weinreb, R. N. (1991) Accuracy of topographic measurements in a model eye with the laser tomographic scanner. *Investigative Ophthalmology and Visual Science* **32**: 2992-6.

Duijm, H. F. A., van den Berg, T. J. T. P. & Greve, E. L. (1997) A comparison of retinal and choroidal hemodynamics in patients with primary open-angle glaucoma and normal-pressure glaucoma. *American Journal of Ophthalmology* **123**: 644-56.

Durcan, F. J., Flaharty, P. M., Digre, K. B. & Lundergan, M. K. (1993) Use of color Doppler imaging to assess ocular blood flow in low-tension glaucoma. *Investigative Ophthalmology and Visual Science* **34**: 1388.

Ederer, F. (1975) Why do we need controls? Why do we need to randomize? *American Journal of Ophthalmology* **79**: 758-62.

Eid, T. M., Spaeth, G. L., Katz, L. J., Azuara-Blanco, A., Agusburger, J. & Nicholl, J. (1997) Quantitative estimation of retinal nerve fiber layer height in glaucoma and the relationship with optic nerve head topography and visual field. *Journal of Glaucoma* **6**: 221-30.

Eisenlohr, J. E., Langham, M. E. & Maumenee, A. E. (1962) Manometric studies of the pressure volume relationships in living and enucleated eyes of individual human subjects. *British Journal of Ophthalmology* **46**: 536-48.

Ekström, C. (1996) Prevalence of open-angle glaucoma in central Sweden. *Acta Ophthalmologica Scandinavica* **74**: 107-12.

Ellestad, M. H. (1986) Stress testing, principles and practice *Davis, F.A.*, Philadelphia.

Elliot, R. H. (1922) A treatise on Glaucoma *Henry Frowde and Hodder and Stoughton Ltd.*, London.

Emdadi, A., Zangwill, L. M., Sample, P. A., Kono, Y., Anton, A. & Weinreb, R. N. (1998) Patterns of optic disk damage in patients with early focal visual field loss. *American Journal of Ophthalmology* **126**: 763-71.

Emsley, H. H. (1969) Visual optics. 336.

Erickson, S. J., Hendrix, L. E. & Massaro, B. M. (1989) Color Doppler flow imaging of the normal and abnormal orbit. *Radiology* **173**: 511-6.

Evans, A. & Jeffery, G. (1992) The fascicular organization of the cat optic nerve. *Experimental Brain Research* **91**: 79-84.

Evans, D. W., Harris, A., Garrett, M., Chung, H. S. & Kagemann, L. E. (1999a) Glaucoma patients demonstrate faulty autoregulation of ocular blood flow during posture change. *British Journal of Ophthalmology* **83**: 809-13.

Evans, D. W., Harris, A., Kagemann, L. E. & Chung, H. S. (1999b) Glaucoma patients demonstrate irregularity in nocturnal blood pressure and ocular circulation. *Investigative Ophthalmology and Visual Science* **40**: S509.

Evans, J. (1991) Causes of blindness and partial sight in England and Wales, 1990-1991. London, Office of Population Censuses & Surveys: 1-29.

Fallon, T. J., Maxwell, D. & Kohner, E. M. (1985) Retinal vasculature autoregulation in conditions of hyperoxia and hypoxia using the blue field entoptic phenomenon. *Ophthalmology* **92**: 701-5.

Faraci, F. M., Heistad, D. D. & Mayhan, W. G. (1987) Role of large arteries in regulation of blood flow to brain stem in cats. *Journal of Physiology (London)* **387**: 115-23.

Ferrazzi, E., Vegni, C., Bellotti, M., Borboni, A., Della Peruta, S. & Barbera, A. (1991) Role of umbilical Doppler velocimetry in the biophysical assessment of the growth-retarded foetus - answers from neonatal morbidity and mortality. *Journal of Ultrasound Medicine* **10**: 309-15.

Fitzke, F. W. & McNaught, A. I. (1994) The diagnosis of visual field progression in glaucoma. *Current Opinion in Ophthalmology* **11**: 110-5.

Flaharty, P. M., Sergott, R. C., Lieb, W., Bosley, T. M. & Savino, P. J. (1993) Optic nerve sheath decompression may improve blood flow in anterior ischemic optic neuropathy. *Ophthalmology* **100**: 297-305.

Flammer, J. (1996) To what extent are vascular factors involved in the pathogenesis of glaucoma? **In** Ocular blood flow. Ed. Kaiser, H. J., Flammer, J.& Hendrickson, P. *Karger*, Basel: 12-39.

Fontana, L., Poinoosawmy, D., Bunce, C. V., O'Brien, C. & Hitchings, R. A. (1998) Pulsatile ocular blood flow investigation in asymmetric normal tension glaucoma and normal subjects. *British Journal of Ophthalmology* **82**: 731-6.

Fraser, S. G. (1997) Epidemiology and screening principles in glaucoma. *Optometry Today.* April 4,. 33-6.

Friedman, E. (1970) Choroidal blood flow. Pressure-flow relationships. *Archives of Ophthalmology* **83**: 95-9.

Friedman, E. & Chandra, S. R. (1972) Choroidal blood flow. III: Effects of oxygen and carbon dioxide. *Archives of Ophthalmology* **87**: 70-1.

Friedman, E., Ivry, M., Ebert, E., Glynn, R., Gragoudas, E. & Seddon, J. (1989) Increased scleral rigidity and age-related macular degeneration. *Ophthalmology* **96**: 104-8.

Friedman, E., Smith, T. R. & Kuwabara, T. (1964) Retinal microcirculation *in vivo*. *Investigative Ophthalmology and Visual Science* **3**: 217-26.

Friendenwald, J. S. (1937) Contribution to the theory and practice of tonometry. *American Journal of Ophthalmology* **20**: 985-1024.

Gaasterland, D. E., Ederer, F., Sullivan, K., Caprioli, J. & Cyrlin, M. N. (1994) Advanced glaucoma intervention study. 2. Visual field test scoring and reliability. *Ophthalmology* **101**: 1445-55.

Galassi, F., Nuzzaci, G., Sodi, A., Casi, P. & Vielmo, A. (1992) Color Doppler imaging in evaluation of optic nerve blood supply in normal and glaucomatous subjects. *International Ophthalmology* **16**: 273-6.

Galassi, F., Sodi, A., Rossi, G., Ucci, F. & De Saint Pierre, F. (1997) Ocular haemodynamics in some subgroups of normal pressure glaucoma. *Acta Ophthalmologica Scandinavica* **75**: 35-6.

Gallin-Cohen, P. F., Podos, S. M. & Yablonski, M. E. (1980) Oxygen lowers intraocular pressure. *Investigative Ophthalmology and Visual Science* **19**: 43-8.

Garway-Heath, D. F., Poinoosawmy, D., Wollstein, G., Viswanathan, A. C., Kamal, D. S., Fontana, L. & Hitchings, R. A. (1999) Inter- and intraobserver variation in the analysis of optic disc images: comparison of the Heidelberg retina tomograph and computer assisted planimetry. *British Journal of Ophthalmology* **83**: 664-9.

Garway-Heath, D. F., Rudnicka, A. R., Lowe, T., Foster, P. J., Fitzke, F. W. & Hitchings, R. A. (1998) Measurement of optic disc size: equivalence of methods to correct for ocular magnification. *British Journal of Ophthalmology* **82**: 643-9.

Gasser, P. (1989) Ocular vasospasm: a risk factor in the pathogenesis of low-tension glaucoma. *International Ophthalmology* **13**: 281-90.

Geijer, C. & Bill, A. (1979) Effects of raised intraocular pressure on retinal, prelaminar, laminar and retrolaminar optic nerve blood flow in monkeys. *Investigative Ophthalmology and Visual Science* **18**: 1030-42.

Geijssen, H. C. & Greve, E. L. (1990) Focal ischemic normal pressure glaucoma verses high pressure glaucoma. *Doc Ophthalmol* **75**: 291-302.

Geijssen, H. C. & Greve, E. L. (1995) Vascular concepts in glaucoma. *Current Opinion in Ophthalmology* **6**: 71-7.

Geyer, O., Michaeli-Cohen, A., Silver, D. M., Versano, D., Neudorfer, M., Dzhanov, R. & Lazar, M. (1998) Reproducibility of topographic measures of the glaucomatous optic nerve head. *British Journal of Ophthalmology* **82**: 14-7.

Gibson, J. M., Rosenthal, A. R. & Lavery, J. (1985) A study of the prevalence of eye disease in the elderly in an English community. *Transactions of the Ophthalmological Society of the United Kingdom* **104**: 196-203.

Gidday, J. M. & Park, T. S. (1993) Adenosine-mediated autoregulation of retinal arteriolar tone in the piglet. *Investigative Ophthalmology and Visual Science* **34**: 2713-9.

Gramer, E. & Tausch, M. (1995) The risk profile of the glaucomatous patient. *Current Opinion in Ophthalmology* **6**: 78-88.

Grebe, R., Langham, M. E., Marcus, S. & Hopkins, S. D. (1989) Decreased choroidal blood flow in the diabetic eye. *Investigative Ophthalmology and Visual Science* **30** (Suppl): 89.

Groh, M. J. M., Michelson, G., Langhans, M. J. & Harazny, J. (1996) Influence of age on retinal and optic nerve head blood circulation. *Ophthalmology* **103**: 529-34.

Grunwald, J. E., Riva, C. E., Petrig, B. L., Brucker, A. J., Schwartz, S. S., Braunstein, S. N., DuPont, J. & Grunwald, S. (1995) Strict control of glycaemia: effects on blood flow in the large retinal vessels and in the macular microcirculation. *British Journal of Ophthalmology* **79**: 735-41.

Grunwald, J. E., Riva, C. E., Stone, R. A., Keates, E. U. & Petrig, B. L. (1984) Retinal autoregulation in open-angle glaucoma. *Ophthalmology* **91**: 1690-4.

Grunwald, J. E., Sinclair, S. H. & Riva, C. E. (1982) Autoregulation of retinal circulation in response to decrease of intraocular pressure below normal. *Investigative Ophthalmology and Visual Science* **23**: 124-7.

Guilford, J. P. (1956) Fundamental Statistics in Psychology and Education *McGraw-Hill*, New York.

Gupta, N. & Weinreb, R. N. (1997) New definitions of glaucoma. *Current Opinion in Ophthalmology* **8**: 38-41.

Guthoff, R. F., Berger, R. W., Winkler, P., Helmke, K. & Chumbley, L. C. (1991) Doppler ultrasonography of the ophthalmic and retinal vessels. *Archives of Ophthalmology* **109**: 532-6.

Gutman, I., Melamed, S., Ashkenazi, I. & Blumenthal, M. (1993) Optic nerve compresion by carotid arteries in low-tension glaucoma. *Graefe's Archive for Clinical and Experimental Ophthalmology* **231**: 711-7.

Haefliger, I. O. & Anderson, D. R. (1996) Pericytes and capillary blood flow modulation. **In** Ocular blood flow. Ed. Kaiser, H. J., Flammer, J.& Hendrickson, P. *Karger*, Basel: 74-8.

Haefliger, I. O. & Flammer, J. (1997) The logic of prevention of glaucomatous damage progression. *Current Opinion in Ophthalmology* **8**: 64-7.

Halberg, G. P. (1969) Charting and scoring the optic disc. *Archives of Ophthalmology* **82**: 149-50.

Hardy, P., Pari, K. G., Lahaie, I., Varma, D. R. & Chemtob, S. (1996) Increased nitric oxide synthesis and action preclude choroidal vasoconstriction to hyperoxia in newborn pigs. *Circulation Research* **79**: 504-11.

Harper, R. (1995) The optic disc. Part two - Examination, assessment and measurement. *Optician.* August 11, 17-21.

Harris, A., Arend, O., Arend, S. & Martin, B. (1996a) Effects of topical dorzolamide on retinal and retrobulbar hemodynamics. *Acta Ophthalmologica Scandinavica* **74**: 1-4.

Harris, A., Arend, O., Bohnke, K., Kroepfl, E., Danis, R. & Martin, B. J. (1996b) Retinal blood flow during dynamic exercise. *Graefe's Archive for Clinical and Experimental Ophthalmology* **234**: 440-4.

Harris, A., Arend, O., Kopecky, K., Caldemeyer, K., Wolf, S., Sponsel, W. & Martin, B. J. (1994a) Physiological perturbation of ocular and cerebral blood flow as measured by scanning laser ophthalmoscopy and color Doppler imaging. *Survey of Ophthalmology* **38**: S81-S6.

Harris, A., Ciulla, T. A., Chung, H. S. & Martin, B. J. (1998) Regulation of retinal and optic nerve head blood flow. *Archives of Ophthalmology* **116**: 1491-5.

Harris, A. & Martin, B. J. (1997) Beta-blockers and ocular blood flow: A perspective. *Journal of Glaucoma* **6**: 143-5.

Harris, A., Sergott, R. C., Spaeth, G. L., Katz, J. L., Shoemaker, J. A. & Martin, B. J. (1994b) Color Doppler analysis of ocular vessel blood velocity in normal-tension glaucoma. *American Journal of Ophthalmology* **118**: 642-9.

Harris, A., Spaeth, G. L., Sergott, R. C., Katz, L. J., Cantor, L. B. & Martin, B. J. (1995a) Retrobulbar arterial hemodynamic effects of betaxolol and timolol in normal tension glaucoma. *American Journal of Ophthalmology* **120**: 168-75.

Harris, A., Tippke, S., Sievers, C., Picht, G., Lieb, W. E. & Martin, B. (1996c) Acetazolamide and CO_2: acute effects on cerebral and retrobulbar hemodynamics. *Journal of Glaucoma* **5**: 39-45.

Harris, A., Williamson, T. H., Martin, B., Shoemaker, J. A., Sergott, R. C., Spaeth, G. L. & Katz, J. L. (1995b) Test/retest reproducibility of color Doppler imaging assessment of blood flow velocity in orbital vessels. *Journal of Glaucoma* **4**: 281-6.

Harris, H., Kagemann, L. E. & Cioffi, G. A. (1998) Assessment of human ocular hemodynamics. *Survey of Ophthalmology* **42**: 509-33.

Hart, W. M. & Becker, B. (1982) The onset and evolution of glaucomatous visual field defects. *Ophthalmology* **89**: 268-79.

Harvey, W. J. F. (1997) Classification of the glaucomas. *Optometry Today*. March 7, 1997. 29-34.

Hass, A., Flammer, J. & Schneider, U. (1985) Influence of age on the visual fields of normal subjects. *American Journal of Ophthalmology* **101**: 199-203.

Hayes, A. (1997) Anatomy and physiology of the normal optic nerve head and its changes in glaucoma. *Optometry Today*. Febuary 7, 27-34.

Hayreh, S. S. (1962) The ophthalmic artery. III, Branches. *British Journal of Ophthalmology* **46**: 1962.

Hayreh, S. S. (1969) Blood supply of the optic nerve head and its role in optic atrophy, glaucoma, and oedema of the optic disc. *British Journal of Ophthalmology* **53**: 721-48.

Hayreh, S. S. (1974) The choriocapillaris. *Graefe's Archive for Clinical and Experimental Ophthalmology* **1974**: 165-79.

Hayreh, S. S. & Beach, K. W. (1993) Optic nerve sheath decompression may improve blood flow in anterior ischemic optic neuropathy - discussion. *Ophthalmology* **100**: 303-5.

Hayreh, S. S., Revie, I. H. S. & Edwards, J. (1970) Vasogenic origin of visual field defects and optic nerve changes in glaucoma. *British Journal of Ophthalmology* **54**: 461-72.

Hayreh, S. S., Zimmerman, M. B., Podhajsky, P. & Alward, W. L. M. (1994) Nocturnal arterial hypotension and its role in optic nerve head and ocular ischemic disorders. *American Journal of Ophthalmology* **117**: 603-24.

Hedges, T. R., Reichel, E., Duker, J. S., Puliafito, C. A. & Heggerick, P. A. (1993) Color Doppler imaging identifies different mechanisms of central retinal artery occlusion. *Investigative Ophthalmology and Visual Science* **34**: 842.

Heidelberg (1997) Heidelberg Retina Tomograph: operation manual. January 1997.

Helmholtz, H. (1851) Beschreibung eines augenspiegels zur untersuchung der netzhaut im lebenden auge. Berlin.

Henson, D. B. (1983) Optometric Instrumentation .

Hernandez, M. R. (1992) Ultrastructural immunocytochemical analysis of elastin in the human lamina cribrosa. Changes in elastic fibers in primary open-angle glaucoma. *Investigative Ophthalmology and Visual Science* **33**: 2891-903.

Hernandez, M. R., Luo, X. X., Igoe, F. & Neufeld, A. H. (1987) Extracellular matrix of the human lamina cribrosa. *American Journal of Ophthalmology* **104**: 567-76.

Hill, D. W. (1989) Ocular and retinal blood flow. *Acta Ophthalmologica* **67**: 15-8.

Ho, A. C., Leib, W. E., Flaharty, P. M., Sergott, R. C., Brown, G. C., Bosley, T. M. & Savino, P. J. (1992) Color Doppler imaging of the ocular ischemic syndrome. *Ophthalmology* **99**: 1453-62.

Hodapp, E., Parrish, R. K. & Anderson, D. R. (1993) Clinical decisions in glaucoma *Mosby*, St. Louis.

Hole, J. W. (1992) Essentials of human anatomy and physiology *Wm. C. Brown Publishers*, Dubuque.

Hollows, F. C. & Graham, P. A. (1966) Intraocular pressure, glaucoma and glaucoma suspects in a defined population. *British Journal of Ophthalmology* **50**: 570-86.

Hosking, S. L. (1998a) An A B C of glaucoma, apoptosis, blood flow and confocal imaging. *Ophthalmic and Physiological Optics* **18**: 133-8.

Hosking, S. L. (1998b) Psychophysical and morphological change in progressive glaucomatous optic neuropathy. Department of Ophthalmology. PhD. University of Manchester. Manchester. 292-6.

Hosking, S. L., Chung, H. S., Kagemann, L. E., Pettinger, C., Chabra, A. & Harris, A. (1999) The effect of hypercapnia on ocular haemodynamics in glaucoma patients and normal subjects. *Investigative Ophthalmology and Visual Science* **40**: S509.

Hosking, S. L. & Flanagan, J. G. (1996) Prospective study design for the Heidelberg Retina Tomograph: the effect of change in focus setting. *Graefe's Archive for Clinical and Experimental Ophthalmology* **234**: 306-10.

Hosking, S. L., Flanagan, J. G. & O'Donoghue, E. P. (1997a) The Heidelberg Retina Tomograph (HRT) in optic nerve head assessment: the effect of scan depth settings. Manchester, Manchester Royal Eye Hospital: 1-25.

Hosking, S. L., Flanagan, J. G. & O'Donoghue, E. P. (1997b) Scanning laser tomography detects disease progression in glaucomatous optic neuropathy. *Investigative Ophthalmology* **38**: S828.

Hoyt, W. F., Frisén, L. & Newman, N. M. (1973) Fundoscopy of nerve fiber layer defects in glaucoma. *Investigative Ophthalmology* **121**: 814-29.

Hudson, C., Flanagan, J. G., Turner, G. S. & McLeod, D. (1998) Scanning laser tomography Z profile signal width as an objective index of macular retinal thickening. *British Journal of Ophthalmology* **82**: 121-30.

Iadecola, C., Pellegrino, M. A., Moskowitz, M. A. & Lassen, N. A. (1994) Nitric-oxide synthase inhibition and cerebrovascular regulation. *Journal of Cerebral Blood Flow and Metabolism* **14**: 175-92.

Iester, M., Mikelberg, F. S., Courtright, P. & Drance, S. M. (1996). Correlation between the Heidelberg Retina Tomograph and discriminant analysis formula and visual field indices. *International Heidelberg User's Meeting*, Vancouver .

Iester, M., Mikelberg, F. S., Courtright, P. & Drance, S. M. (1997a) Correlation between the visual field indices and Heidelberg Retina Tomograph parameters. *Journal of Glaucoma* **6**: 78-82.

Iester, M., Mikelberg, F. S. & Drance, S. M. (1997b) The effect of optic disc size on diagnostic precision with the Heidelberg Retina Tomograph. *Ophthalmology* **104**: 545-8.

Iester, M., Swindale, N. V. & Mikelberg, F. (1997c) Sector-based analysis of optic nerve head shape parameters and visual field indices in healthy and glaucomatous eyes. *Journal of Glaucoma* **6**: 371-6.

Irak, I., Zangwill, L. M., Garden, V., Shakiba, S. & Weinreb, R. N. (1996) Change in optic disk topography after trabeculectomy. *American Journal of Ophthalmology* **122**: 690-5.

James, C. B. & Smith, S. E. (1991a) The effect of posture on the intraocular pressure and pulsatile ocular blood flow in patients with non arteretic anterior ischemic optic neuropathy. *Eye* **5**: 309-14.

James, C. B. & Smith, S. E. (1991b) Pulsatile ocular blood flow in patients with low tension glaucoma. *British Journal of Ophthalmology* **75**: 466-70.

Janknecht, P. & Funk, J. (1994) Optic nerve head analyser and Heidelberg Retina Tomograph: accuracy and reproducibility of topographic measurements in a model eye and in volunteers. *British Journal of Ophthalmology* **78**: 760-8.

Janknecht, P. & Funk, J. (1995) Optic nerve head analyzer and Heildelberg Retina Tomograph: relative error and reproducibility of topographic measurements in a model eye with simulated cataract. *Graefe's Archive for Clinical and Experimental Ophthalmology* **233**: 523-9.

Jay, J. L. & Murdoch, J. R. (1993) The rate of visual field loss in untreated primary open angle glaucoma. *British Journal of Ophthalmology* **77**: 176-8.

Johnson, B. M., Miao, M. & Sadun, A. A. (1987) Age-related decline of human optic nerve axon populations. *Age* **10**: 5-9.

Johnson, P. C. (1980a) The microcirculation, and local and humoral control of the circulation. **In** Cardiovascular physiology. Ed. Guyton, A. C.& Jones, C. E. *University Park Press*, Baltimore, .**1**: 163-95.

Johnson, P. C. (1980b) The myogenic response. **In** Handbook of Physiology: The Cardiovascular System. Ed. Bohr, D. F., Somlyo, A. P.& Sparks, H. V. *Waverly Press*, Baltimore, .**2**: 409-42.

Jonas, J. B., Fernández, M. C. & Naumann, O., H (1992) Glaucomatous peripapillary atrophy. Occurrence and correlations. *Archives of Ophthalmology* **110**: 214-22.

Jonas, J. B., Mardin, C. Y. & Gründler, A. E. (1998) Comparison of measurements of neuroretinal rim area between confocal laser scanning tomography and planimetry of photographs. *British Journal of Ophthalmology* **82**: 362-6.

Jonas, J. B. & Papastathopoulos, K. I. (1995) Pressure-dependent changes of the optic disk in primary open-angle glaucoma. *American Journal of Ophthalmology* **119**: 313-7.

Jonescu-Cuypers, C., Chung, H. S., Kagemann, L. E. & Harris, A. (1999) A new reliable method for neuroretinal rim blood flow measurements with the Heidelberg retina flowmeter. *Investigative Ophthalmology and Visual Science* **40**: S276.

Jonescu-Cuypers, C., Thumann, G., Hilgers, R. D., Bartz-Schmidt, K. U., Krott, R. & Krieglstein, G. K. (1998) Long-term fluctuations of the normalised rim/disc area ratio quotient in normal eyes. *Graefe's Archive for Clinical and Experimental Ophthalmology* **237**: 181-6.

Joos, K. M., Kay, M. D., Pillunat, L. E., Harris, A., Gendron, E. K., Feuer, W. J. & Steinwand, B. E. (1999) Effect of acute intraocular pressure changes on short posterior ciliary artery haemodynamics. *British Journal of Ophthalmology* **83**: 33-8.

Kagemann, L. E., Harris, A., Cantor, L. B. & Martin, B. J. (1996) Heidelberg retinal flowmetry: The effect of angle incidence on blood flow measurement. *Investigative Ophthalmology and Visual Science* **37**: 1217.

Kagemann, L. E., Harris, A., Chung, H. S., Evans, D., Buck, S. & Martin, B. J. (1998) Heidelberg retinal flowmetry: factors affecting blood flow measurement. *British Journal of Ophthalmology* **82**: 131-6.

Kagemann, L. E., Harris, A., Chung, H. S., Martin, B. J., Kiesling, K. & Elvambuena, R. (1999) Pointwise analysis reveals that Heidelberg retinal flowmeter measurements of human retinal blood flow are influenced by illumination level. *Investigative Ophthalmology and Visual Science* **40**: S508.

Kahn, H. A., Leibgowitz, H., Ganley, J. P., Kinl, M., Colton, T., Nickerson, R. & Dawber, T. R. (1975) Standardizing diagnostic procedures. *American Journal of Ophthalmology* **79**: 768-75.

Kaiser, H. J., Flammer, J. & Gasser, P. (1993a) Ocular vasospasm in children. *Neuroophthalmology* **13**: 263-7.

Kaiser, H. J., Flammer, J., Graf, T. & Stümpfig, D. (1993b) Systemic blood pressure in glaucoma patients. *Graefe's Archive for Clinical and Experimental Ophthalmology* **231**: 677-80.

Kamal, D. S., Viswanathan, A. C., Garway-Heath, D. F., Hitchings, R. A., Poinoosawmy, D. & Bunce, C. V. (1999) Detection of optic disc changes with the Heidelberg retina tomograph before confirmed visual field change in ocular hypertensives converting to early glaucoma. *British Journal of Ophthalmology* **83**: 290-4.

Kass, M. A. (1983) When to treat ocular hypertension. *Survey of Ophthalmology* **28**: 229-34.

Katz, J. & Sommer, A. (1986) Asymmetry and variation in the normal hill of vision. *Archives of Ophthalmology* **104**: 65-8.

Katz, J. L., Gilbert, D., Quigely, H. A. & Sommer, A. (1997) Estimating progression of visual field loss in glaucoma. *Ophthalmology* **104**: 1017-25.

Kety, S. S. & Schmidt, C. F. (1948) The effects of altered arterial tensions of carbon dioxide and oxygen on cerebral blood flow and cerebral oxygen consumption of normal young men. *Journal of Clinical Investigation* **12**: 484-92.

Khan, M. M., Leibowitz, H. M., Ganley, J. P., Kini, M. M., Colton, T., Nickerson, R. S. & Dawber, T. R. (1977) The Framingham eye survey. I. Outline and major prevalence findings. *American Journal of Epidemiology* **106**: 17-32.

Kiel, J. W. & Shepherd, A. P. (1992) Autroregulation of choroidal blood flow in the rabbit. *Investigative Ophthalmology and Visual Science* **33**: 2399-410.

Kitaya, N., Yoshida, A., Ishiko, S., Mori, F., Abiko, T., Ogasawara, H., Kato, Y. & Nagaoka, T. (1997) Effect of timolol and UF-021 (a prostoglandin-related compound) on pulsatile ocular blood flow in normal volunteers. *Ophthalmic Research* **29**: 139-44.

Klein, B. E. K., Klein, R. & Jensen, S. C. (1994) Open-angle glaucoma and older-onset diabetes

The Beaver Dam eye study. *Ophthalmology* **101**: 1173-7.

Klein, B. E. K., Klein, R., Meuer, S. M. & Goetz, L. A. (1993) Migraine headache and its association with open-angle glaucoma. The Beaver Dam eye study. *Investigative Ophthalmology and Visual Science* **34**: 3024-7.

Klein, B. E. K., Klein, R. & Moss, S. E. (1984) Intraocular pressure in diabetic persons. *Ophthalmology* **91**: 1356-60.

Klein, B. E. K., Klein, R., Sponsel, W. E., Franke, T., Cantor, L. B., Martone, J. & Menage, M. J. (1992) Prevalence of glaucoma: The Beaver-Dam eye study. *Ophthalmology* **99**: 1499-504.

Klein, B. E. K., Magli, Y. L., Richie, K. A., Moss, S. E., Meuer, S. M. & Klein, R. (1985) Quantification of optic disc cupping. *Ophthalmology* **92**: 1654-6.

Klingbeil, A. P. U. & Schödel, W. R. C. (1990) Scanning Ophthalmic Imaging. **In** Scanning laser ophthalmoscopy and tomography. Ed. Nasemann, J. E.& Burk, R. O. W. *Quintessenz*, München: 23-33.

Klingbeil, U. (1989) Fundus geometry measured with the analyzing stereo video ophthalmoscope. **In** Noninvasive diagnostic techniques in ophthalmology. Ed. Masters, B. R. *Springer*, Berlin: 410-37.

Kono, Y., Zangwill, L. M., Sample, P. A., Jonas, J. B., Emdadi, A., Gupta, N. & Weinreb, R. N. (1999) Relationship between peripapillary atrophy and visual field abnormality in primary open-angle glaucoma. *American Journal of Ophthalmology* **127**: 674-80.

Kontos, H. (1971) Role of hypercapnic acidosis in the local regulation of blood flow in skeletal muscle. *Circulation Research* **28**: 1-98.

Kothe, A. C. (1993) Ocular hemodynamics. I. Choroidal blood flow. *Canadian Journal of Ophthalmology* **55**: 160-5.

Kothe, A. C. (1994) The effect of posture on intraocular pressure and pulsatile ocular blood flow in normal and glaucomatous eyes. *Survey of Ophthalmology* **38**: S191-S7.

Kothe, A. C., Lovasik, J. V. & Kergoat, H. (1992a) Postural effects on ocular hemodynamics as a function of age. *Investigative Ophthalmology and Visual Science* **33**: 808.

Kothe, A. C., Vachon, N. & Woo, S. (1992b) Factors affecting pulsatile ocular blood flow: Axial length and ocular rigidity. *Optometry and Vision Science* **69** (Suppl): 74.

Krakau, C. E. T. (1992) Calculation of the pulsatile ocular blood flow. *Investigative Ophthalmology and Visual Science* **33**: 2754-6.

Krakau, C. E. T. (1995) A model for pulsatile and steady ocular blood-flow. *Graefe's Archive for Clinical and Experimental Ophthalmology* **233**: 112-8.

Krammer, T. R. & Langham, M. E. (1989) Reduced ciliary/choroidal blood flow and neovascularization in central retinal vein occlusion. *Investigative Ophthalmology and Visual Science* **30** (Suppl): 477.

Kronfeld, P. C. (1967) The optic nerve. **In** Symposium on Glaucoma. Transactions of the New Orelans Academy of Ophthalmology. Ed. . *CV Mosby Co.*, St. Louis: 64-7.

Kruse, F. E., Burk, R. O. W., Völcker, H. E., Zinser, G. & Harbarth, U. (1989) Reproducibility of topographic measurements of the optic nerve head with laser tomographic scanning. *Opthalmology* **96**: 1320-4.

Kulshrestha, M., Roff, E. J., Sedgwick, G. & Ainsworth, J. (1998) Demonstration of reversibility of optic disc topography by scanning laser ophthalmoscopy. *Archives of Ophthalmology*, **In press**.

Lacey, B. & Rankin, S. J. A. (1997) The effect of increased intrathoracic pressure on pulsatile ocular blood flow. *Investigative Ophthalmology* **38**: S781.

Langer, S. Z. (1995) Aspects of vascular pharmocology related to ocular blood flow. **In** Optic nerve in glaucoma. Ed. Drance, S. M. *Kugler Publications*, Amsterdam/New York: 301-10.

Langham, M. E. (1967) Manometric, pressure-cup, and tonographic procedures in the evaluation in intraocular dynamics. **In** Glaucoma Symposium. Ed. . *Tutzing Castle, Karger*, New York: 126-50.

Langham, M. E. (1975) Vascular pathopysiology of the ocular postural response. A pneumotonographic study. *Trans Ophthalmol Soc UK* **95**: 281-7.

Langham, M. E. (1990) The influence of timolol, clonidine and aminoclonidine on ocular blood flow in the rabbit and human subjects. *Investigative Ophthalmology and Visual Science* **31** (Suppl): 378.

Langham, M. E., Farrell, R., O'Brien, V., Silver, D. & Shilder, P. (1989a) Non-invasive measure of pulsatile blood flow in the human eye. **In** Ocular Blood Flow in Glaucoma. Ed. Lambrou, G. N.& Greve, E. L. *Kugler Publications*, Amsterdam: 93-9.

Langham, M. E., Farrell, R. A., O'Brien, V., Silver, D. M. & Schilder, P. (1989b) Blood flow in the human-eye. *Acta Ophthalmologica* **67**: 9-13.

Langham, M. E. & Kramer, T. (1990) Decreased choroidal blood-flow associated with retinitis pigmentosa. *Eye* **4**: 374-81.

Langham, M. E. & McCarthy, E. (1968) A rapid pneumatic applanation tonometer. Comparative findings and evaluation. *Archives of Ophthalmology* **79**: 389-99.

Langhans, M., Michelson, G. & Groh, M. J. M. (1997) Effect of breathing 100% oxygen on retinal and optic nerve head capillary blood flow in smokers and non-smokers. *British Journal of Ophthalmology* **81**: 365-9.

Leske, M. C., Connell, A. M. S., Schachat, A. P. & Hyman, L. (1994) The Barbados eye study. Prevalence of open-angle glaucoma. *Archives of Ophthalmology* **112**: 821-9.

Leske, M. C. & Podgor, M. J. (1983) Intraocular pressure, cardiovascular risk variables, and visual field defects. *American Journal of Epidemiology* **118**: 280-7.

Levy, N. S., Crapps, E. E. & Bonney, R. C. (1981) Displacement of the optic nerve head. Response to acute intraocular pressure elevation in primate eyes. *Archives of Ophthalmology* **99**: 2166-74.

Lichter, P. R. (1976) Variability of expert observers in evaluating the optic disc. *Transactions of the American Ophthalmological Society* **74**: 532-72.

Lieb, W. E. (1996) Color Doppler imaging of the eye and orbit. **In** Ocular blood flow: New insights and pathogenesis. Ed. Kaiser, H. J., Flammer, J.& Hendrickson, P. *Karger*, Basel: 100-13.

Lieb, W. E., Cohen, S. M., Merton, D. A., Shields, J. A., Mitchell, D. G. & Goldberg, B. B. (1991) Color Doppler imaging of the eye and orbit. *Archives of Ophthalmology* **109**: 527-31.

Lieb, W. E., Shields, J. A., Cohen, S. M., Merton, D. A., Mitchell, D. G., Shields, C. L. & Goldberg, B. B. (1990) Color Doppler imaging in the management of intraocular tumors. *Ophthalmology* **97**: 1660-4.

Lieberman, M. F., Maumenee, A. E. & Green, W. R. (1976) Histological studies of the vasculature of the anterior optic nerve. *American Journal of Ophthalmology* **82**: 405-23.

Lietz, A., Hendrickson, P., Flammer, J., Orgül, S. & Haefliger, I. O. (1998) Effect of carbogen, oxygen and intraocular pressure on Heidelberg retina flowmeter parameter 'flow' measured at the papilla. *Ophthalmologica* **212**: 149-52.

Lima, M. C., Paranho, A., Jr., Salim, S., Osorio, P., Caprioli, J. & Shields, M. B. (1999) Heidelberg retina tomograph measurements and intraocular pressure before and after trabeculectomy - regression analysis. *Investigative Ophthalmology and Visual Science* **40**: S74.

Linsenmeier, R. & Yancey, C. M. (1989) Effects of hyperoxia on the oxygen distribution in the intact cat retina. *Investigative Ophthalmology and Visual Science* **30**: 612-8.

Littmann, H. (1982) Zur bestimmung der wahren Größe eines Objektes auf dem Hintergrund des lebenden Auges. *Klin. Mbl. Augenheilk* **180**: 286-9.

Liu, C. J., Chou, Y.-H., Chou, J. C., Chiou, H.-J., Chiang, S.-C. & Liu, J.-H. (1997) Retrobulbar haemodynamic changes studied by colour Doppler imaging in glaucoma. *Eye* **11**: 818-26.

Lovasik, J. V. & Kergoat, H. (1994) Gravity-induced homeostatic reactions in the macular and choroidal vasculature of the human eye. *Aviation, Space, and Environmental Medicine* **65**: 1010-4.

Lundberg, L., Uettreil, K. & Linner, E. (1980) Ocular hypertension. A 20 year follow up at Skovde. *Survey of Ophthalmology* **25**: 136.

Lusky, M., Bosem, M. E. & Weinreb, R. N. (1993a) Effects of intraocular pressure reduction on optic nerve head topography. *Current Opinion in Ophthalmology* **4**: 40-3.

Lusky, M., M.E., B. & Weinreb, R. N. (1993b) Reproducibility of optic nerve head topography measurements in eyes with undilated pupils. *Journal of Glaucoma* **2**: 104-9.

Lusky, M., Taylor, J., Bosem, M. E. & Weinreb, R. N. (1992) Reproducibility of topographic measurements of the optic nerve head with the retina tomograph. *Investigative Ophthalmology and Visual Science* **33**: 885.

Mackenzie, W. A. (1830) A practical treatise on the diseases of the eye *Longman*, London.

Mackie, S. W., Jay, J. L., Ackerley, R. & Walsh, G. (1996) Clinical comparison of the Keeler Pulsair 2000, American Optical MkII and Goldmann applanation tonometers. *Ophthalmic and Physiological Optics* **16**: 171-7.

Mainster, M. A., Timberlake, G. T., Webb, R. H. & Hughes, G. W. (1982) Scanning laser ophthalmoscopy - clinical applications. *Ophthalmology* **89**: 852-7.

Mansberger, S., Harris, A., Arend, O., Wolf, S., Sponsel, W. E. & Shoemaker, J. A. (1993) Small PCO_2 changes significantly alter retinal flow indices as measured by the scanning laser ophthalmoscope. *Investigative Ophthalmology and Visual Science* **34**: 1395.

Mardin, C. Y. & Horn, F. K. (1998) Influence of optic disc size on the sensitivity of the Heidelberg Retina Tomograph. *Graefe's Archive for Clinical and Experimental Ophthalmology* **236**: 641-5.

Mardin, C. Y., Horn, F. K., Jonas, J. B. & Budde, W. M. (1999) Preperimetric glaucoma diagnosis by confocal scanning laser tomography of the optic disc. *British Journal of Ophthalmology* **83**: 299-304.

McBain, E. H. (1958) Tonometer calibration. II. Ocular rigidity. *Archives of Ophthalmology* **60**: 1080-91.

McClure, E. (1988) Visual fields. **In** Optometry. Ed. Edwards, K.& Llewellyn, R. *Butterworth & Co. Ltd.*, Cambridge: 355-79.

McKinnon, S. J. (1997) Glaucoma, apoptosis, and neuroprotection. *Current Opinion in Ophthalmology* **8**: 28-37.

Menezes, A. V., Giunta, M., Chisholm, L., Harvey, P. T., Tuli, R. & Devenyi, R. G. (1995) Reproducibility of topographic measurements of the macula with a scanning laser ophthalmoscope. *Ophthalmology* **102**: 230-5.

Meyer, J. H., Brandi-Dohrn, J. & Funk, J. (1996) Twenty four hour blood pressure monitoring in normal tension glaucoma. *British Journal of Ophthalmology* **80**: 864-7.

Meyer, P., Haefliger, I. O., Flammer, J. & Lüscher, T. F. (1996) Endothelium-dependent regulation in ocular vessels. **In** Ocular blood flow. Ed. Kaiser, H. J., Flammer, J.& Hendrickson, P. *Karger*, Basel: 64-73.

Michelson, G., Langhans, M. J. & Groh, M. J. M. (1996a) Perfusion of the juxtapapillary retina and the neuroretinal rim area in primary open angle glaucoma. *Journal of Glaucoma* **5**: 91-8.

Michelson, G., Langhans, M. J., Harazny, J. & Dichtl, A. (1998a) Visual field defect and perfusion of the juxtapapillary retina and the neuroretinal rim area in primary open-angle glaucoma. *Graefe's Archive for Clinical and Experimental Ophthalmology* **236**: 80-5.

Michelson, G. & Schmauss, B. (1995) Two dimensional mapping of the perfusion of the retina and optic nerve head. *British Journal of Ophthalmology* **79**: 1126-32.

Michelson, G., Schmauss, B., Langhans, M. J., Harazny, J. & Groh, M. J. M. (1996b) Principle, validity, and reliability of scanning laser Doppler flowmetry. *Journal of Glaucoma* **5**: 99-105.

Michelson, G., Welzenbach, J., Pal, I. & Harazny, J. (1998b) Automatic full field analysis of perfusion images gained by scanning laser Doppler flowmetry. *British Journal of Ophthalmology* **82**: 1294-300.

Miglior, S., Rossetti, L., Brigatti, L., Bujtar, E. & Orzalesi, N. (1994) Reproducibility of retinal nerve fiber layer evaluation by dynamic scanning laser ophthalmoscopy. *American Journal of Ophthalmology* **118**: 16-23.

Mikelberg, F. S. (1992) Do computerised visual fields and automated optic disc analysis assist in the choice of therapy in glaucoma? *Eye* **6**: 47-9.

Mikelberg, F. S. (1993) Intraocular pressure and glaucoma. *Canadian Journal of Ophthalmology* **28**: 251-2.

Mikelberg, F. S., Drance, S. M., Schulzer, M., Yidegiligne, H. M. & Weis, M. M. (1989) The normal human optic nerve. Axon count and axon diameter distribution. *Ophthalmology* **96**: 1325-8.

Mikelberg, F. S., Parfitt, C. M., Swindale, N. V., Graham, S. L., Drance, S. M. & Gosine, R. (1995) Ability of the Heidelberg Retina Tomograph to detect early glaucomatous visual field loss. *Journal of Glaucoma* **4**: 242-7.

Mikelberg, F. S., Wijsman, K. & Schulzer, M. (1993) Reproducibility of topographic parameters obtained with the Heidelberg Retina Tomograph. *Journal of Glaucoma* **2**: 101-3.

Miles, R. D., Menke, J. A., Bashiru, M. & Colliver, J. A. (1987) Relationships of five Doppler measures with flow in an in vitro model and clinical findings in newborn infants. *Journal of Ultrasound in Medicine* **6**: 597-9.

Miller, K. N. & Quigley, H. A. (1988) The clinical appearance of the lamina cribrosa as a function of the extent of glaucomatous optic nerve damage. *Ophthalmology* **95**: 135-8.

Morgan, R. K., Feuer, W. J. & Anderson, D. R. (1991) Statpac 2 glaucoma change probability. *Archives of Ophthalmology* **109**: 1690-2.

Moses, R. A. (1975) Intraocular pressure. **In** Adler's Physiology of the Eye: Clinical Application. Ed. Moses, R. A. *Mosby*, St Louis: 179.

Mulholland, D. A., Craig, J. J. & Rankin, S. J. A. (1998) Use of scanning laser ophthalmoscopy to monitor papilloedema in idiopathic intracranial hypertension. *British Journal of Ophthalmology* **82**: 1301-5.

Murdoch, I. E., Morris, S. S. & Cousens, S. N. (1998) People and eyes: statistics in ophthalmology. *British Journal of Ophthalmology* **82**: 971-3.

Navarro, R., Santamaría, J. & Bescós, J. (1985) Accommodation-dependent model of the human eye with aspherics. *Journal of the Optical Society of America* **2**: 1273-81.

Neetens, A. (1994) Vascular supply of the optic nerve - a practical survey for the clinician. *Neuro-ophthalmology* **14**: 113-20.

Nicolela, M., Hnik, P., Schulzer, M. & Drance, S. M. (1997) Reproducibility of retinal and optic nerve head blood flow measurements with scanning laser Doppler flowmetry. *Journal of Glaucoma* **6**: 157-64.

Nicolela, M. T., Drance, S. M., Rankin, S. J. A., Buckley, A. R. & Walman, B. E. (1996a) Color Doppler imaging in patients with asymmetric glaucoma and unilateral visual field loss. *American Journal of Ophthalmology* **121**: 502-10.

Nicolela, M. T., Hnik, P. & Drance, S. M. (1996b) Scanning laser Doppler flowmeter study of retinal and optic disk blood flow in glaucomatous patients. *American Journal of Ophthalmology* **122**: 775-83.

Norman, G. R. & Streiner, D. L. (1994) Biostatistics. The bare essentials *Mosby*, St. Louis.

Nuzzi, R. & Cerruti, A. (1995) Epidemiological aspects, development and management of prevention in ophthalmology in relation to different ages. *Panminerva Medica* **37**: 28-37.

Nyman, K., Tomita, G., Raitta, C. & Kawamura, M. (1994) Correlation of asymmetry of visual field loss with optic disc topography in normal-tension glaucoma. *Archives of Ophthalmology* **112**: 349-53.

O'Brien, C. & Schwartz, B. (1993) Point by point linear regression analysis of automated visual fields in primary open angle glaucoma. **In** Perimetry update. Ed. Mills, R. P. *Kugler & Ghedini*, Amsterdam: 143-5.

O'Brien, C., Schwartz, B., Takamoto, T. & Wu, D. C. (1991) Intraocular pressure and the rate of visual field loss in chronic open-angle glacucoma. *American Journal of Ophthalmology* **111**: 492-500.

Okada, M., Takamatsu, M., Suzuki, M., Nii, H. & Mishima, H. K. (1999) Comparison of two scanning laser ophthalmoscope techniques for glaucomatous optic nerve head - Heidelberg retina tomograph vs TopSS. *Investigative Ophthalmology and Visual Science* **40**: 658.

Onda, E., Cioffi, G. A., Bacon, D. R. & Van Buskirk, E. M. (1995) Microvasculature of the anterior human optic nerve. *American Journal of Ophthalmology* **120**: 92-102.

Oppenheim, B., Dickersin, K., Min, Y. I. & Schocket, S. (1993) Reliability of measurements using the Langham ocular blood flow system. *Investigative Ophthalmology and Visual Science* **34**: 940.

Orgül, S., Cioffi, G. A., Bacon, D. R. & Van Buskirk, E. M. (1996) Sources of variability of topometric data with a scanning laser ophthalmoscope. *Archives of Ophthalmology* **114**: 161-4.

Orgül, S., Cioffi, G. A. & Van Buskirk, E. M. (1997) Variability of contour line alignment on sequential images with the Heidelberg Retina Tomograph. *Graefe's Archive for Clinical and Experimental Ophthalmology* **235**: 82-6.

Orgül, S., Flammer, J. & Gasser, P. (1995) Female preponderance in normal-tension glaucoma. *Ann Ophthalmol Glaucoma* **27**: 355-9.

Park, K. H., Tomita, G., Liou, S. Y. & Kitazawa, Y. (1996) Correlation between peripapillary atrophy and optic nerve damage in normal-tension glaucoma. *Ophthalmology* **103**: 1899-906.

Pawson, P. & Vernon, S. A. (1995) The optic disc in glaucoma. *Optometry Today*. November 6. 20-6.

Pederson, J. E. & Anderson, D. R. (1980) The mode of progressive disc cupping in ocular hypertension and glaucoma. *Archives of Ophthalmology* **98**: 490-5.

Perasalo, R. & Raitta, C. (1990) Low blood pressure: a risk factor for nerve fiber loss in institutionalized geriatric glaucoma patients. *Acta Ophthalmologica* **68**: 65-7.

Perkins, E. S. (1973) The Bedford glaucoma survey. I Long-term follow -up of borderline cases. *British Journal of Ophthalmology* **57**: 179-85.

Petrig, B. L. & Riva, C. E. (1996) Optic nerve head laser Doppler flowmetry: principles and computer analysis. **In** Ocular blood flow. Ed. Kaiser, H. J., Flammer, J.& Hendrickson, P. *Karger*, Basel: 120-7.

Phelps, C. D. & Corbett, J. J. (1985) Migraine and low-tension glaucoma. A case control study. *Investigative Ophthalmology and Visual Science* **26**: 1105-8.

Phillips, C. I. (1972) Aetiology of angle-closure glaucoma. *British Journal of Ophthalmology* **56**: 248-?

Pickard, R. (1923) A method of recording disc alterations and a study of the growth of normal and abnormal disc cups. *British Journal of Ophthalmology* **7**: 81-90.

Pillunat, E. L., Anderson, D. R., Knighton, R. W., Joos, K. M. & Feuer, W. J. (1996) Effect of increased intraocular pressure on optic nerve head blood flow. **In** Ocular blood flow. Ed. Kaiser, H. J., Flammer, J.& Hendrickson, P. *Karger*, Basel: 138-44.

Pillunat, L. E., Stodtmeister, R., Wilmanns, I. & Christ, T. H. (1985) Autoregulation of ocular blood flow during changes in intraocular pressure. *Graefe's Archive for Clinical and Experimental Ophthalmology* **223**: 219-23.

Pourcelot, L. (1974) Applications cliniques de l'examinen Doppler transcutane. *INSERM* **34**: 213-40.

Pournaras, C. J. (1996) Autoregulation of ocular blood flow. **In** Ocular Blood Flow. Ed. Kaiser, H. J., Flammer, J.& Hendrickson, P. *Karger*, Basel: 40-50.

Price, E. L., Gray, L. S. & Button, N. F. (1999) Sources of variation in the measurement of pulsatile ocular blood flow. *Investigative Ophthalmology and Visual Science* **40**: S507.

Priestly-Smith (1885) On a case of chronic glaucoma of unusually long duration. *Ophthalmic Rev (Lond)* **4**: 261-6.

Pyott, A. A. E. & Montgomery, D. M. I. (1993) Inter-observer variation in clinical optic disc biometry. *Eye* **7**: 452-6.

Quaranta, L., Harris, A., Donato, F., Cassamali, M., Semeraro, F., Nascimbeni, G., Gandolfo, E. & Quaranta, C. A. (1997) Color Doppler imaging of ophthalmic artery blood flow velocity

A study of repeatability and agreement. *Ophthalmology* **104**: 653-8.

Quaranta, L., Manni, G., Donato, F. & Bucci, M. G. (1994) The effect of increased intraocular pressure on pulsatile ocular blood flow in low tension glaucoma. *Survey of Ophthalmology* **38**: S177-S82.

Quigley, H. A. (1993) Medical progress - open-angle glaucoma. *New England Journal of Medicine* **328**: 1097-106.

Quigley, H. A. (1995) Overview and introduction to session on connective tissue of the optic nerve head in glaucoma. **In** Optic nerve in glaucoma. Ed. Drance, S. M. *Kuger publications*, Amsterdam / New York: 15-36.

Quigley, H. A. (1996) Number of people with glaucoma worldwide. *British Journal of Ophthalmology* **80**: 389-93.

Quigley, H. A., Addicks, E. M. & Green, W. R. (1982) Optic nerve damage in human glaucoma. III. Quantitative correlation of nerve fibre loss and visual field defect in glaucoma, ischemic neuropathy, papilledema, and toxic neuropathy. *Archives of Ophthalmology* **100**: 135-46.

Quigley, H. A. & Anderson, D. R. (1977) Distribution of axonal transport blockade by acute intraocular pressure elevation in the primate optic nerve head. *Investigative Ophthalmology and Visual Science* **16**: 640-4.

Quigley, H. A., Dunkelberger, G. R. & Green, W. R. (1988) Chronic human glaucoma causing selectively greater loss of large optic nerve axons. *Ophthalmology* **95**: 357-63.

Quigley, H. A., Flower, R. W., Addicks, E. M. & McLeod, D. S. (1980) The mechanism of optic nerve damage in experimental acute intraocular pressure elevation. *Investigative Ophthalmology and Visual Science* **19**: 505-17.

Quigley, H. A., Guy, J. & Anderson, D. R. (1979) Blockade of rapid axonal transport. Effect of intraocular pressure elevation in primate optic nerve. *Archives of Ophthalmology* **97**: 525-31.

Quigley, H. A., Hohman, R. M., Addicks, E. M. & Green, W. R. (1984) Blood vessels of the glaucomatous optic disc in experimental primate and human eyes. *Investigative Ophthalmology and Visual Science* **25**: 918-31.

Quigley, H. A., Hohman, R. M., Addicks, E. M., Massof, R. W. & Green, W. R. (1983) Morphologic changes in the lamina cribrosa correlated with neural loss in open-angle glaucoma. *American Journal of Ophthalmology* **95**: 673-91.

Quigley, H. A., Katz, J. L., Derick, R. J., Gilbert, D. & Sommer, A. (1992) An evaluation of optic disc and nerve fiber layer examinations in monitoring progression of early glaucoma damage. *Ophthalmology* **99**: 19-28.

Quigley, H. A. & Langham, M. E. (1975) Comparative intraocular pressure measurements with the pneumatonograph and the Goldmann tonometer. *American Journal of Ophthalmology* **80**: 266-73.

Quigley, H. A., Nickells, R. W., Kerrigan, L. A., Pease, M. E., Thibault, D. J. & Zack, D. J. (1995) Retinal ganglion cell death in experimental glaucoma and after axotomy occurs by apoptosis. *Investigative Ophthalmology and Visual Science* **36**: 774-86.

Quigley, H. A., Reacher, M., Katz, J. L., Strahlman, E., Gilbert, D. & Scott, R. (1993) Quantitative grading of nerve fiber layer photographs. *Ophthalmology* **100**: 1800-7.

Rankin, S. J. A. (1999) Color Doppler imaging of the retrobulbar circulation in glaucoma. *Survey of Ophthalmology* **43**: S176-S82.

Rankin, S. J. A. & Drance, S. M. (1996) Peripapillary focal retinal arteriolar narrowing in open angle glaucoma. *J Glaucoma* **5**: 22-28.

Rath, E. Z., Shin, D. H., Kim, C., Tsai, C. S., Zeiter, J. H. & Hong, Y. J. (1996) Relationship between optic disc cupping change and intraocular pressure control in adult glaucoma patients. *Graefe's Archive for Clinical and Experimental Ophthalmology* **234**: 434-9.

Ravalico, G., Pastori, G., Toffoli, G. & Crocè, M. (1994a) Visual and blood flow responses in low-tension glaucoma. *Survey of Ophthalmology* **38**: S173-S6.

Ravalico, G., Toffoli, G., Pastori, G. & Crocè, M. (1994b) Age-related ocular blood flow changes. *Ophthalmology* **37**: 2645-50.

Repka, M. X., Quigley, H. A. & Sadun, A. A. (1989) The effect of age on normal human optic nerve fiber number and diameter. *Ophthalmology* **96**: 26-32.

Repo, L. P., Suhonen, M. T., Teräsvirta, M. E. & Koivisto, K. J. (1995) Color Doppler imaging of the ophthalmic artery blood flow spectra of patients who have had a transient ischemic attack. *Ophthalmology* **102**: 1199-205.

Rhoades, R. (1995) Respiratory physiology: gas transfer and transport. **In** Medical Physiology. Ed. Rhoades, R. & Tanner, G. *Little, Brown*, Boston, .**2**: 386-98.

Ringelstein, E. B., Van Eyck, S. & Mertens, I. (1992) Evaluation of cerebral vasomotor reactivity by various vasodilating stimuli: comparison of CO_2 to acetazolamide. *Journal of Cerebral Blood Flow and Metabolism* **12**: 162-8.

Riva, C. E., Cranstoun, S. D., Grunwald, J. E. & Petrig, B. L. (1994) Choroidal blood flow in the foveal region of the human ocular fundus. *Investigative Ophthalmology and Visual Science* **35**: 4273-81.

Riva, C. E., Grunwald, J. E. & Petrig, B. L. (1986) Autoregulation of human retinal blood flow. An investigation with laser Doppler velocimetry. *Investigative Ophthalmology and Visual Science* **27**: 1706-12.

Riva, C. E., Grunwald, J. E. & Sinclair, S. H. (1983) Laser Doppler velocimetry study of the effect of pure oxygen breathing on retinal blood flow. *Investigative Ophthalmology and Visual Science* **24**: 47-51.

Riva, C. E., Grunwald, J. E., Sinclair, S. H. & Petrig, B. L. (1985) Blood velocity and volumetric flow-rate in human retinal vessels. *Investigative Ophthalmology and Visual Science* **26**: 1124-32.

Riva, C. E., Harino, S., Petrig, B. L. & Shonat, R. D. (1992) Laser Doppler flowmetry in the optic nerve. *Experimental Eye Research* **55**: 499-506.

Riva, C. E., Hero, M., Titze, P. & Petrig, B. L. (1997a) Autoregulation of human optic nerve head blood flow in response to acute changes in ocular perfusion pressure. *Graefe's Archive for Clinical and Experimental Ophthalmology* **235**: 618-26.

Riva, C. E., Sinclair, S. H. & Grunwald, J. E. (1981) Autoregulation of retinal circulation in response to decrease of perfusion pressure. *Investigative Ophthalmology and Visual Science* **21**: 34-8.

Riva, C. E., Titze, P., Hero, M., Movaffaghy, A. & Petrig, B. L. (1997b) Choroidal blood flow during isometric exercises. *Investigative Ophthalmology and Visual Science* **38**: 2338-43.

Riva, C. E., Titze, P., Hero, M. & Petrig, B. L. (1997c) Effect of acute decreases of perfusion pressure on choroidal blood flow in humans. *Investigative Ophthalmology and Visual Science* **38**: 1752-60.

Robinson, F., Riva, C. E., Grunwald, J. E., Petrig, B. L. & Sinclair, S. H. (1986) Retinal blood flow autoregulation in response to an acute increase in blood pressure. *Investigative Ophthalmology and Visual Science* **27**: 722-6.

Roche, M., Brigatti, L. & Caprioli, J. (1994) Does optic nerve cupping increase in normal eyes with age? *Investigative Ophthalmology and Visual Science* **35**: 1342.

Roff, E. J., Harris, A., Chung, H. S., Hosking, S. L., Halter, P. J. & Kagemann, L. E. (1998a) The effect of blood gas perturbation on retrobulbar heamodynamics measured with color doppler imaging. *Investigative Ophthalmology and Visual Science* **39**: S477.

Roff, E. J., Harris, A., Chung, H. S., Hosking, S. L., Morrison, A. M., Halter, P. J. & Kagemann, L. E. (1998b) Comprehensive assessment of retinal, choroidal and retrobulbar haemodynamics during blood gas perturbation. *Graefe's Archive for Clinical and Experimental Ophthalmology* **In press**.

Roff, E. J., Harris, A., Morrison, A. M., Halter, P. J., Chung, H.S., Hosking, S. L. & Kagemann, L. E. (1997) Ocular blood flow changes measured by colour Doppler imaging and pulsatile ocular blood flow during blood gas perturbation. *Ophthalmic and Physiological Optics* **18**: 384-5.

Rohrschneider, K. & Burk, R. O. W. (1993) Three-dimensional analysis of the optic nerve head: Comparison of two laser tomographic scanning systems. *Ophthalmolge* **90**: 613-9.

Rohrschneider, K., Burk, R. O. W., Kruse, F. E. & Völkner, H. E. (1994) Reproducibility of the optic nerve head topography with a new laser tomographic scanning device. *Ophthalmology* **101**: 1044-9.

Rohrschneider, K., Burk, R. O. W., Völcker, H. E., Zinser, G. & Harbarth, U. (1990) Factors influencing three-dimensional data in follow-up studies with the laser topographic scanner. **In** Scanning laser ophthalmoscopy and tomography. Ed. Nasemann, J. E. & Burk, R. O. W. *Quintessenz*, München: 183-92.

Rojanapongpun, P. & Drance, S. M. (1993) The response of blood flow velocity in the ophthalmic artery and blood flow of the finger to warm and cold stimuli in glaucomatous patients. *Graefe's Archive for Clinical and Experimental Ophthalmology* **231**: 375-7.

Rosenberg, L. F. (1995) Glaucoma: early detection and therapy for prevention of vision loss. *American Family Physician* **52**: 2289-98.

Rudnicka, A. R., Burk, R. O. W., Edgar, D. F. & Fitzke, F. W. (1998) Magnification characteristics of fundus imaging systems. *Ophthalmology* **105**: 2186-92.

Satomura, S. (1957) Ultrasononic Doppler method for the inspection of cardiac functions. *Journal of the Acoustic Society of America* **29**: 1181-5.

Schmetterer, L., Findl, O., Strenn, K., Graselli, U., Kastner, J., Eichler, H.-G. & Wolzt, M. (1997) Role of NO in the O_2 and CO_2 responsiveness of cerebral and ocular circulation in humans. *American Journal of Physiology* **273**: R2005-R12.

Schmetterer, L., Wolzt, M., Lexer, F., Alschinger, C., Gouya, G. & Zanaschka, G. (1995) The effect of hyperoxia and hypercapnia on fundus pulsations in the macular and optic disc region in healthy young men. *Experimental Eye Research* **61**: 685-90.

Schnabel, J. (1905) Entwicklungsgeschichte der glaucomatosen exkavation. *Z Augelheilkd* **14**: 1.

Schulzer, M. (1994) Errors in the diagnosis of visual field progression in normal tension glaucoma. *Ophthalmology* **101**: 1589-95.

Schuman, J. S., Hee, M. R., Puliafito, C. A., Wong, C., Pedut-Kloizman, T., Lin, C. P., Hertzmark, E., Izatt, J. A., Swanson, E. A. & Fujimoto, J. G. (1995) Quantification of nerve fiber layer thickness in normal and glaucomatous eyes using optical coherence tomography. *Archives of Ophthalmology* **113**: 586-96.

Schwartz, B. (1994) Circulatory defects of the optic disc and retina in ocular hypertension and high pressure open-angle glaucoma. *Survey of Ophthalmology* **38**: S23-S34.

Shields, M. B., Tiedeman, J. S., Miller, K. N., Hickingbotham, D. & Ollie, A. R. (1989) Accuracy of topographic measurements with the Optic Nerve Head Analyzer. *American Journal of Ophthalmology* **107**: 273-9.

Shiose, Y. (1990) Intraocular pressure. New perspectives. *Survey of Ophthalmology* **34**: 413-35.

Shonat, R. D., Wilson, D. F., Riva, C. E. & Cranstoun, S. D. (1992) Effect of acute increases in intraocular pressure on intravascular optic nerve head oxygen tension in cats. *Investigative Ophthalmology and Visual Science* **33**: 3174-80.

Silver, D. M. & Farrell, R. A. (1994) Validity of pulsatile ocular blood flow measurements. *Survey of Ophthalmology* **38**: 572-80.

Silver, D. M., Farrell, R. A., Langham, M. E., O'Brien, V. & Schilder, P. (1989) Estimation of pulsatile ocular blood flow from intraocular pressure. *Acta Ophthalmologica* **67**: 25-9.

Singh, S. & Dass, R. (1960) The central artery of the retina. *British Journal of Ophthalmology* **44**: 193-212.

Smith, S. D., Katz, J. & Quigley, H. A. (1996) Analysis of progressive change in automated visual fields in glaucoma. *Investigative Ophthalmology and Visual Science* **37**: 1419-28.

Sommer, A., Katz, J. L., Quigley, H. A., Miller, N. R., Robin, A. L., Richter, R. C. & Witt, K. A. (1991a) Clinically detectable nerve fiber atrophy precedes the onset of glaucomatous field loss. *Archives of Ophthalmology* **109**: 77-83.

Sommer, A., Tielsch, J. M., Katz, J. L., Quigley, H. A., Gottsch, J. D., Javitt, J. C. & Singh, K. (1991b) Relationship between intraocular pressure and primary open angle glaucoma among white and black Americans. *Archives of Ophthalmology* **109**: 1090-5.

Spaeth, G. L. (1994a) A new classification of glaucoma including focal glaucoma. *Survey of Ophthalmology* **38**: S9-S-17.

Spaeth, G. L. (1994b) Reversible changes in the optic disc and visual field in glaucoma. *Current Opinion in Ophthalmology* **5**: 36-45.

Spencer, A. F., Sadiq, S. A., Pawson, P. & Vernon, S. A. (1995) Vertical optic disc diameter: discrepancy between planimetric and SLO measurements. *Investigative Ophthalmology and Visual Science* **36**: 796-803.

Spencer, A. F. & Vernon, S. A. (1994) Optic disc measurement with the Zeiss four mirror contact lens. *British Journal of Ophthalmology* **78**: 775-80.

Spencer, A. F. & Vernon, S. A. (1995) Optic disc measurement: a comparison of indirect ophthalmoscopic methods. *British Journal of Ophthalmology* **79**: 910-5.

Spencer, A. F. & Vernon, S. A. (1996) Optic disc height measurement with the Zeiss 4-mirror contact lens and 78 dioptre lens compared. *Eye* **10**: 371-6.

Spencer, J. A. D., Guissani, D. A., Moore, P. J. & Hanson, M. A. (1991) In vitro validation of Doppler indices using blood and water. *Journal of Ultrasound in Medicine* **10**: 305-8.

Sperber, G. O. & Bill, A. (1985) Blood flow and glucose consumption in the optic nerve, retina and brain: effects of high intraocular pressure. *Experimental Eye Research* **41**: 639-53.

Sponsel, W. E., Kaufman, P. L. & Blum, F. G., Jr. (1997a) Association of retinal capillary perfusion with visual status during chronic glaucoma therapy. *Ophthalmology* **104**: 1026-32.

Sponsel, W. E., Zetlan, S. R., Stodtmeister, R. & Kaufman, P. L. (1997b) Retinal capillary hemodynamics and VEP/pressure tolerance: evidence of retinal microcirculatory compromise in treated glaucomatous eyes. *Ophthalmologica* **211**: 172-7.

Spraul, C. W., Lang, G. E., Ronzani, M., Högel, J. & Lang, G. K. (1998) Reproducibility of measurements with a new slit lamp-mounted ocular blood flow tonograph. *Graefe's Archive for Clinical and Experimental Ophthalmology* **236**: 274-9.

Spry, P. (1996) Tonometry with a difference. *Optician*. . 24-6.

Stewart, W. C. (1995) The effect of lifestyle on the relative risk to develop open-angle glaucoma. *Current Opinion in Ophthalmology* **6**: 3-9.

Strenn, K., Menapace, R., Rainer, G., Findl, O., Wolzt, M. & Schmetterer, L. (1997) Reproducibility and sensitivity of scanning laser Doppler flowmetry during graded changes in PO_2. *British Journal of Ophthalmology* **81**: 360-4.

Sullivan, P., Cioffi, G. A., Wang, L., Johnson, C. A., Van Buskirk, E. M., Sherman, K. R. & Bacon, D. R. (1999) The influence of ocular pulsatility on scanning laser Doppler flowmetry. *American Journal of Ophthalmology* **128**: 81-7.

Tamaki, Y., Araie, M., Nagahara, M. & Tomita, K. (1999) Acute effects of cigarette smoking on tissue circulation in human optic nerve head and choroid-retina. *Ophthalmology* **106**: 564-9.

Tamaki, Y., Nagahara, M., Yamashita, H. & Kikuchi, M. (1993) Analysis of blood flow velocity of ophthalmic artery with color Doppler imaging. 1. Studies on normal human eyes. *Acta Societatis Ophthalmologicae Japonicae* **97**: 175-80.

Tate, G. & Lynn, J. (1977) Principles of quantitative perimetry *Grune and Stratton*, New York.

Thomson, S. (1994) Retinal topography with the Heidelberg retina tomograph. *Journal of Audiovisual Media in Medicine* **17**: 156-60.

Thornburn, W. (1978) The accuracy of clinical applanation tonometry. *Acta Ophthalmologica* **56**: 1-5.

Thylefors, B. & Negrel, A.-D. (1994) The global impact of glaucoma. *Bulletin of the World Health Organization* **72**: 323-6.

Tielsch, J. M. (1991) The epidemiology of primary open angle glaucoma. *Ophthalmol. Clin. North Am* **4**: 649-57.

Tielsch, J. M., Katz, J. L., Quigley, H. A., Miller, N. R. & Sommer, A. (1988) Intraobserver and interobserver agreement in measurement of optic disc characteristics. *Ophthalmology* **95**: 350-6.

Tielsch, J. M., Katz, J. L., Sommer, A., Quigley, H. A. & Javitt, J. C. (1994) Family history and risk of primary open angle glaucoma - the Baltimore eye survey. *Archives of Ophthalmology* **112**: 69-73.

Tielsch, J. M., Katz, J. L., Sommer, A., Quigley, H. A. & Javitt, J. C. (1995) Hypertension, perfusion pressure and primary open angle glaucoma. *Archives of Ophthalmology* **113**: 216-21.

Tielsch, J. M., Sommer, A., Katz, J. L., Qigley, H. A., Royall, R. M. & Javitt, J. C. (1991) Racial variations in the prevalance of primary open angle glaucoma - the Baltimore eye survey. *Journal of the American Medical Association* **266**: 369-74.

Tole, D. M., Edwards, M. P., Davey, K. G. & Menage, M. J. (1998) The correlation of the visual field with scanning laser ophthalmoscope measurements in glaucoma. *Eye* **12**: 686-90.

Tomita, G., Park, K. H., Lion, S. Y. & Kitazawa, Y. (1996) Optic nerve head blood flow evaluated by scanning laser Doppler flowmetry in normal-tension glaucoma with interocular asymmetric visual field loss. *Investigative Ophthalmology and Visual Science* **37**: 1209.

Topouzis, F., Peng, F., Kotas-Neumann, R., Garcia, R., Sanguinet, J., Yu, F. & Coleman, A. (1999) Longitudinal changes in optic disc topography of adult patients after trabeculectomy. *Ophthalmology* **106**: 1147-151.

Trew, D. R., James, C. B., Thomas, S. H. L., Sutton, R. & Smith, S. E. (1991) Factors influencing the ocular pulse - the heart rate. *Graefe's Archive for Clinical and Experimental Ophthalmology* **229**: 553-6.

Trew, D. R. & Smith, S. E. (1991a) Postural studies in pulsatile ocular blood flow: I. Ocular hypertension and normotension. *British Journal of Ophthalmology* **75**: 66-70.

Trew, D. R. & Smith, S. E. (1991b) Postural studies in pulsatile ocular blood flow: II. Chronic open angle glaucoma. *British Journal of Ophthalmology* **75**: 71-5.

Trible, J. R., Sergott, R. C., Spaeth, G. L., Wilson, R. P., Katz, L. J., Moster, M. R. & Schmidt, C. M. (1994) Trabeculectomy is associated with retrobulbar hemodynamic changes: a color Doppler analysis. *Ophthalmology* **101**: 340-51.

Trokel, S. (1965) Respiratory gases and the choroidal hemodynamics. *Archives of Ophthalmology* **73**: 838-92.

Tsacopoulos, M., Baker, R. & Levy, S. (1976) Studies on retinal oxygenation. *Advances in Experimental Medical Biology* **75**: 413-6.

Tsacopoulos, M. & David, N. (1973) The effect of arterial PCO2 on relative retinal blood flow. *Investigative Ophthalmology and Visual Science* **12**: 335-47.

Tsai, C. S., Ritch, R., Shin, D. H., Wan, J. Y. & Chi, T. (1992) Age-related decline of disc rim area in visually normal subjects. *Ophthalmology* **99**: 29-35.

Tsai, C. S., Zangwill, L. M., Sample, P. A., Garden, V., Bartsch, D.-U. & Weinreb, R. N. (1995) Correlation of peripapillary retinal height and visual field in glaucoma and normal subjects. *Journal of Glaucoma* **4**: 110-6.

Vachon, N. & Kothe, A. C. (1992) Mechanisms mediating the postural effect of the pulsatile ocular blood flow. *Optometry and Vision Science* **69** (Suppl): 51-2.

van Norren, D. & van de Kraats, J. (1989) Imaging retinal densitometry with a confocal scanning laser ophthalmoscope. *Vision Research* **29**: 1825-30.

Varma, R., Skaf, M. & Barron, E. (1996) Retinal nerve fiber layer thickness in normal human eyes. *Ophthalmology* **103**: 2114-9.

Varma, R., Spaeth, G. L., Steinmann, W. C. & Katz, L. J. (1989) Agreement between clinicians and an image analyzer in estimating cup-to-disc ratios. *Archives of Ophthalmology* **107**: 526-9.

Varma, R., Steinmann, W. C. & Scott, I. U. (1992) Expert agreement in evaluating the optic disc in glaucoma. *Ophthalmology* **99**: 215-21.

Varma, R., Tielsch, J. M., Quigley, H. A., Hilton, S. C., Katz, J. L., Spaeth, G. L. & Sommer, A. (1994) Race-, age-, gender-, and refractive error-related differences in the normal optic disc. *Archives of Ophthalmology* **112**: 1068-76.

Vernon, S. A. (1996) Disc and nerve fiber layer examination in early glaucoma. *Eye News* **2**: 7-10.

Vihanninjoki, K., Tuulonen, A., Burk, R. O. W. & Airaksinen, P. J. (1997) Comparison of optic disc measurements by Heidelberg Retina Tomograph and manual planimetric techniques. *Acta Ophthalmologica Scandinavica* **75**: 512-5.

Vogel, R., Crick, R. P., Newson, R. B., Shipley, M., Blackmore, H. & Bulpitt, C. J. (1990) Association between intraocular pressure and loss of visual field in chronic simple glaucoma. *British Journal of Ophthalmology* **74**: 3-6.

Von Briba, H., Stempfle, H. U. & Poll, A. (1990) Erfassung von verschiedener Dopplertechniken in der erfassung von flußgeschwindigkeiten. Untershuchgen in vitro. *K Kardiol* **79**: 73-82.

Von Graefe, A. (1857) Uber die iridektomie bei glaukom. Und uber den glaukomatosen process. *Von Graefe's Archive for Opthalmology* **3**: 456.

Wallece, J. & Lowell, G. G. (1969) Glaucoma and intraocular pressure in Jamaica. *American Journal of Ophthalmology* **67**: 93-100.

Wang, Q., Pellegrino, D. A., Baughman, V. L., Koenig, H. M. & Albrecht, R. F. (1995) The role of neuronal nitric oxide synthase in regulation of cerebral blood flow in normocapnia and hypercapnia in rats. *Journal of Cerebral Blood Flow and Metabolism* **15**: 774-8.

Wang, T. H., Hung, P. T., Hwang, J. K. & Shih, Y. F. (1996) Diurnal blood flow change of optic disc and macula in normal subjects by scanning laser Doppler flowmetry. *Investigative Ophthalmology and Visual Science* **37**: S266.

Webb, R. H., Hughes, G. W. & Delori, F. C. (1987) Confocal scanning laser ophthalmoscope. *Applied Optics* **26**: 1492-9.

Webb, R. H., Hughes, G. W. & Pomerantzeff, O. (1980) Flying spot TV ophthalmoscope. *Applied Optics* **19**: 2991-7.

Weber, A. (1855) *Arch für Ophthalmologie* **2**: 133.

Weber, J., Dannheim, F. & Dannheim, D. (1990) The topographical relationship between the optic disc and visual field in glaucoma. *Acta Ophthalmol* **68**: 568-74.

Weinreb, R. N. (1992) Why study the ocular microcirculation in glaucoma? *Journal of Glaucoma* **1**: 145-7.

Weinreb, R. N., Dreher, A. W., Coleman, A., Quigley, H. A., Shaw, B. & Reiter, K. (1990) Histopathologic validation of fourier-ellipsometry measurements of retinal nerve fiber layer thickness. *Archives of Ophthalmology* **108**: 557-60.

Weinreb, R. N., Lusky, M., Bartsch, D.-U. & Morsman, D. (1993) Effect of repetitive imaging on topographic measurements of the optic nerve head. *Archives of Ophthalmology* **111**: 636-8.

Weinreb, R. N., Shakiba, S. & Zangwill, L. M. (1995) Scanning laser polarimetry to measure the nerve fiber layer of normal and glaucomatous eyes. *American Journal of Ophthalmology* **119**: 627-36.

Werner, E. B., Petrig, B., Krupin, T. & Bishop, K. I. (1989) Variability of automated visual fields in clinically stable glaucoma patients. *Investigative Ophthalmology and Visual Science* **30**: 1083-9.

Wild, J. M., Hutchings, N., Hussey, M. K., Flanagan, J. G. & Trope, G. E. (1997) Pointwise univariate linear regression of perimetric sensitivity against follow-up time in glaucoma. *Ophthalmology* **104**: 808-15.

Wilke, K. (1972) Effects of repeated tonometry: genuine and sham measurements. *Acta Ophthalmologica* **50**: 574-82.

Williams, F. (1992) Reasoning with statistics *T Buchholz*, .

Williamson, T. H., Baxter, G. M. & Dutton, G. N. (1993) Color Doppler velocimetry of the arterial vasculature of the optic nerve head and orbit. *Eye* 7: 74-9.

Williamson, T. H. & Harris, A. (1996) Color Doppler ultrasound imaging of the eye and orbit. *Survey of Ophthalmology* **40**: 255-67.

Wilson, R., Walker, A. M., Dueker, D. K. & Crick, R. P. (1982) Risk factors for rate of progression of glaucomatous visual field loss. A computer-based analysis. *Archives of Ophthalmology* **100**: 737-41.

Wilson, R. P., Chang, W. J., Sergott, R. C., Moster, M. R., Schmidt, C. M., Bond, J. B. & Harris, A. (1997) A color Doppler analysis of nifedipine-induced posterior ocular blood flow changes in open-angle glaucoma. *Journal of Glaucoma* **6**: 231-6.

Winder, A. F., Paterson, G. & Miller, S. J. H. (1974) Biochemical abnormalities associated with ocular hypertension and low-tension glaucoma. *Trans. ophthal. Soc. U.K.* **94**: 518-24.

Wollstein, G., Garway-Heath, D. F. & Hitchings, R. A. (1998) Identification of early glaucoma cases with the scanning laser ophthalmoscope. *Ophthalmology* **105**: 1557-63.

Woon, W. H., Fitzke, F. W., Bird, A. C. & Marshall, J. (1992) Confocal imaging of the fundus using a scanning laser ophthalmoscope. *British Journal of Ophthalmology* **76**: 470-4.

Yan, D. B., Flanagan, J. G., Farra, T., Trope, G. E. & Ethier, C. R. (1998) Study of regional deformation of the optic nerve head using scanning laser tomography. *Current Eye Research* **17**: 903-16.

Yang, Y. C., Hulbert, M. F. G., Batterbury, M. & Clearkin, L. G. (1997a) Pulsatile ocular blood flow measurements in healthy eyes: reproducibility and reference values. *Journal of Glaucoma* **6**: 175-9.

Yang, Y. C., Kent, D., Fenerty, C. H., Kosmin, A. S. & Damato, B. E. (1997b) Pulsatile ocular blood flow in eyes with untreated choroidal melanoma. *Eye* **11**: 331-4.

Yücel, Y. H., Gupta, N., Kalichman, M. W., Mizisin, A. P., Hare, W., de Souza Lima, M., Zangwill, L. M. & Weinreb, R. N. (1998) Relationship of optic disc topography to optic nerve fiber number in glaucoma. *Archives of Ophthalmology* **116**: 493-7.

Zambarakji, H. J., Amoaku, W. M. K. & Vernon, S. A. (1998) Reproducibility of volumetric measurements of normal maculae with the Heidelberg retina tomograph. *British Journal of Ophthalmology* **82**: 884-91.

Zangwill, L., Irak, I., Berry, C. C., Garden, V., Lima, M. D. & Weinreb, R. N. (1997) Effect of cataract and pupil size on image quality with confocal scanning laser ophthalmoscopy. *Archives of Ophthalmology* **115**: 983-90.

Zangwill, L. M., Bowd, C., Berry, C. C., Williams, J. M. & Weinreb, R. N. (1999) Discriminating between normal and glaucomatous eyes using the Heidelberg Retina Tomograph, GDx/ Nerve Fiber Analyzer and Optical Coherence Tomograph. *Investigative Ophthalmology and Visual Science* **40**: S983.

Zangwill, L. M., Shakiba, S., Caprioli, J. & Weinreb, R. N. (1995) Agreement between clinicians and a confocal scanning laser ophthalmoscope in estimating cup/disk ratios. *American Journal of Ophthalmology* **119**: 415-21.

Zangwill, L. M., van Horn, S., Souza Lima, M., Sample, P. A. & Weinreb, R. N. (1996) Optic nerve head topography in ocular hypertensive eyes using confocal scanning laser ophthalmoscopy. *American Journal of Ophthalmology* **122**: 520-5.

Zeimer, R., Asrani, S. G., Gieser, D. K. & Wilensky, J. T. (1994) The variability in diurnal Intraocular Pressure is a risk factor for Glaucomatous progression. *Investigative Ophthalmology and Visual Science* **35**: 1856.

Zeltan, S. R., Sponsel, W. E. & Stodtmeister, R. (1989) Evaluation of normal and glaucomatous eyes using the VEP/pressure tolerance test and leukocyte flow analysis. *Investigative Ophthalmology and Visual Science* **30** Suppl: 179.

Appendices

Appendix 1 Publications arising from this work

Academic Journal Papers and Abstracts

Roff, E.J., Harris, A., Chung, H.S., Hosking, S.L., Morrison, A.M., Halter, P.J., Kagemann, L. (1999) Comprehensive assessment of retinal, choroidal and retrobulbar haemodynamics during blood gas perturbation. *Graefes Archive for Clinical Experimental Ophthalmology* **237:** 984-990.

Chung, H.S., Harris, A., Halter, P.J., Kagemann, L., **Roff E.J.,** Garzozi, H.J., Hosking, S.L., Martin, B. (1999) Regional differences in retinal vascular reactivity. *Investigative Ophthalmology and Visual Science* **40:** 2448-2453.

Roff, E. J., Hosking, S. L., Barnes, D. A., Gibson, J. M. (1999) The influence of contour line size and location on the reproducibility of topographic measurement with the Heidelberg Retina Tomograph. *Ophthalmic and Physiological Optics* (in press).

Roff, E.J., Harris, A., Chung, H.S., Hosking, S.L., Halter, P.J., Kagemann, L.E. (1998) The effect of blood gas perturbation on retrobulbar haemodynamics measured with colour Doppler imaging. *Investigative Ophthalmology and Visual Science* **39:** (4) Supl. S477.

Chung, H.S., Harris, A., **Roff, E.J.,** Kagemann, L., Evans, D.W., Halter, P.J. (1998) Superior and inferior peripapillary retinal vessels respond differently to changing blood level of oxygen and carbon dioxide. *Investigative Ophthalmology and Visual Science* **39:** (4) Supl. S263.

Roff, E.J., Harris, A., Morrison, A.M., Halter, P.J., Chung, H.S., Hosking, S.L., Kagemann, L.E. (1998) Ocular Blood Flow Changes measured by Colour Doppler Imaging and Pulsatile Ocular Blood Flow during Blood Gas Perturbation. *Ophthalmic and Physiological Optics.* **18:** (4) 384-385.

Roff, E. J., Hosking, S. L., Barnes, D. A., Gibson, J. M. (1997) Reproducibility of topographic measurements of the optic nerve head with the Heidelberg Retina Tomograph using separate and imported contour lines. *Ophthalmic and Physiological Optics* **17:** (2) 172.

Roff, E. J., Hosking, S. L., Barnes, D. A., Gibson, J. M. (1997) Contour line position influences the reproducibility of optic nerve head measurement using the Heidelberg Retina Tomograph. *Investigative Ophthalmology and Visual Science* **38:** (4) Supl. S826.

Conference proceedings and presentations

Roff, E.J., Harris, A., Morrison, A.M., Halter, P.J., Chung, H.S., Hosking, S.L., Kagemann, L.E. (1998) Detection of Ocular Blood Flow Changes using Color Doppler Imaging and Pulsatile Ocular Blood Flow During Blood Gas Perturbation. *Proceedings of the 5th Workshop on the Quantification of Ocular Blood Flow.* Florence, Italy.

Roff, E.J., Harris, A., Morrison, A.M., Halter, P.J., Chung, H.S., Hosking, S.L., Kagemann, L.E. (1998) Detection of Ocular Blood Flow Changes during Blood Gas Perturbation. *Glaucoma Society 18th Annual Meeting,* London.

Roff, E. J., Hosking, S. L., Barnes, D. A. and Gibson, J. M. (1996) Reproducibility of Normal and Glaucomatous Optic Nerve Head Parameters with the Heidelberg Retina Tomograph using Separate and Imported Contour Lines. *Glaucoma Society 17th Annual Meeting,* London.

Appendix 2. HRT reproducibility summary tables

	2	3	4	5	6	7	8	9	10	11	12
Cup area	0.023	0.024	0.025	0.027	0.027	0.027	0.027	0.027	0.027	0.028	0.029
C:D ratio	0.011	0.012	0.012	0.013	0.013	0.013	0.013	0.013	0.013	0.013	0.014
Rim area	0.023	0.024	0.025	0.027	0.027	0.027	0.027	0.027	0.027	0.028	0.029
Height Var Contour	0.014	0.017	0.018	0.022	0.022	0.023	0.022	0.023	0.023	0.023	0.024
Volume below ref	0.006	0.006	0.007	0.007	0.007	0.007	0.007	0.007	0.007	0.007	0.007
Volume above ref	0.013	0.016	0.018	0.020	0.020	0.020	0.020	0.020	0.020	0.020	0.022
Mean cup depth	0.005	0.005	0.006	0.006	0.007	0.007	0.007	0.007	0.007	0.007	0.007
Max cup depth	0.014	0.016	0.019	0.020	0.020	0.023	0.024	0.025	0.025	0.026	0.026
Third moment	0.009	0.011	0.013	0.013	0.015	0.016	0.016	0.016	0.016	0.017	0.017
Mean RNFL thick	0.008	0.011	0.012	0.014	0.014	0.014	0.014	0.013	0.014	0.014	0.014
RNFL cross-sectional area	0.040	0.051	0.056	0.066	0.067	0.067	0.065	0.065	0.066	0.066	0.069
Classification	0.149	0.199	0.206	0.227	0.255	0.262	0.280	0.280	0.279	0.293	0.293
Effective area	0.014	0.019	0.021	0.024	0.025	0.026	0.026	0.028	0.030	0.030	0.030
Mean Height in Contour	0.004	0.006	0.007	0.008	0.009	0.009	0.009	0.009	0.009	0.009	0.010
Volume below surface	0.005	0.006	0.007	0.008	0.008	0.008	0.008	0.008	0.008	0.008	0.009
Volume above surface	0.003	0.003	0.004	0.004	0.004	0.004	0.004	0.004	0.004	0.004	0.004
Mean depth in contour	0.003	0.003	0.004	0.004	0.004	0.004	0.004	0.004	0.004	0.004	0.004
Ref height	0.119	0.178	0.235	0.293	0.349	0.405	0.460	0.516	0.572	0.628	0.683

Mean SD of HRT parameters for 2-12 images for the normal group. 7 images were defined as optimum.

	2	3	4	5	6	7	8	9	10	11	12
Cup area	0.022	0.021	0.024	0.025	0.029	0.030	0.030	0.033	0.033	0.033	0.032
C:D ratio	0.043	0.041	0.046	0.047	0.055	0.057	0.063	0.071	0.069	0.069	0.067
Rim area	0.041	0.038	0.038	0.040	0.047	0.051	0.051	0.054	0.054	0.054	0.053
Height Var Contour	0.031	0.031	0.034	0.037	0.041	0.044	0.043	0.044	0.044	0.043	0.043
Volume below ref	0.016	0.015	0.018	0.019	0.022	0.024	0.027	0.030	0.029	0.028	0.027
Volume above ref	0.024	0.021	0.024	0.024	0.027	0.027	0.027	0.028	0.028	0.028	0.028
Mean cup depth	0.010	0.010	0.011	0.011	0.011	0.012	0.012	0.013	0.014	0.014	0.014
Max cup depth	0.018	0.021	0.021	0.024	0.024	0.025	0.024	0.033	0.033	0.035	0.035
Third moment	0.010	0.012	0.012	0.015	0.015	0.015	0.015	0.016	0.017	0.018	0.018
Mean RNFL thick	0.021	0.019	0.020	0.021	0.023	0.024	0.023	0.025	0.025	0.026	0.026
RNFL cross-sectional area	0.101	0.093	0.100	0.105	0.111	0.115	0.114	0.120	0.122	0.126	0.125
Classification	0.205	0.237	0.262	0.284	0.328	0.338	0.360	0.359	0.373	0.388	0.383
Effective area	0.020	0.024	0.028	0.027	0.031	0.030	0.031	0.039	0.039	0.039	0.038
Mean Height in Contour	0.011	0.014	0.016	0.017	0.017	0.019	0.018	0.020	0.021	0.021	0.021
Volume below surface	0.011	0.014	0.014	0.014	0.016	0.017	0.017	0.021	0.021	0.022	0.022
Volume above surface	0.004	0.005	0.005	0.005	0.005	0.005	0.005	0.006	0.006	0.006	0.006
Mean depth in contour	0.006	0.008	0.008	0.008	0.008	0.009	0.009	0.010	0.011	0.011	0.011
Ref height	0.028	0.027	0.029	0.031	0.031	0.033	0.033	0.037	0.036	0.035	0.035

Mean SD of HRT parameters for 2-12 images for the POAG group. 7 images were defined as optimum.

Parameter	Sum of squares		
	Subject	Residual	Total
C:D area ratio	2.755	0.035	2.97
Disc area	23.974	0.000	23.974
Cup area	18.247	0.163	18.41
Rim area	5.120	0.163	5.283
RNFL thickness	0.296	0.030	0.326
RNFL cross-sectional thickness	4.724	0.772	5.506
Volume above surface	0.220	0.003	0.223
Volume below surface	4.942	0.014	4.956
Volume above reference	1.538	0.066	1.604
Volume below reference	1.656	0.011	1.667
Effective area	40.675	0.123	40.798
Mean cup depth	0.913	0.008	0.921
Mean height in contour	1.068	0.013	1.081
Height variation of contour	0.478	0.090	0.568
Maximum depth in contour	0.117	0.104	0.221
Mean depth in contour	0.748	0.003	0.751
Third moment	0.714	0.046	0.76
Classification	295.629	11.842	307.471
Reference height	1.015	0.046	1.061

ANOVA sums of squares results for HRT parameters measured for the normal subject group (used to calculate ICC).

Parameter	Sum of squares		
	Subject	Residual	Total
C:D area ratio	0.913	0.068	0.981
Disc area	1.814	0.000	1.814
Cup area	2.051	0.280	2.331
Rim area	6.800	0.228	7.028
RNFL thickness	0.119	0.037	0.156
RNFL cross-sectional thickness	3.405	0.889	4.294
Volume above surface	0.016	0.002	0.018
Volume below surface	0.284	0.019	0.303
Volume above reference	6.800	0.228	7.028
Volume below reference	2.051	0.280	2.331
Effective area	1.104	0.075	1.179
Mean cup depth	0.252	0.010	0.262
Mean height in contour	0.205	0.026	0.231
Height variation of contour	0.228	0.123	0.351
Maximum depth in contour	0.652	0.044	0.696
Mean depth in contour	0.200	0.005	0.205
Third moment	0.183	0.015	0.198
Classification	118.1	8.263	126.3
Reference height	0.202	0.040	0.242

ANOVA sums of squares results for HRT parameters measured for the POAG subject group (used to calculate ICC).

Appendix 3. ANOVA summary tables

Parameter	Sum of squares		
	Subject	Residual	Total
C:D area ratio	1.459	0.015	1.474
Cup volume	9.496	0.011	9.507
Rim volume	0.541	0.050	0.591
Rim area	3.378	0.183	3.561
RNFL thickness	0.212	0.019	0.231
Volume above surface	0.121	0.002	0.123
Volume below surface	12.386	0.005	12.391
Reference height	0.469	0.023	0.492

Sum of Squares calculated from one way analysis of variance (ANOVA). Results are for intra-image reproducibility for the POAG group (contour line redrawn 7 times on one image).

Parameter	Sum of squares		
	Subject	Residual	Total
C:D area ratio	1.202	0.024	1.226
Cup volume	2.095	0.022	2.117
Rim volume	0.709	0.082	0.791
Rim area	18.250	0.218	18.468
RNFL thickness	0.170	0.023	0.193
Volume above surface	0.038	0.003	0.041
Volume below surface	3.772	0.009	3.781
Reference height	0.323	0.035	0.358

Sum of Squares calculated from one way analysis of variance (ANOVA). Results are for intra-image reproducibility for the normal group (contour line redrawn 7 times on one image).

Parameter	Sum of squares		
	Subject	Residual	Total
C:D area ratio	1.383	0.035	1.418
Cup volume	10.230	0.048	10.278
Rim volume	0.611	0.118	0.729
Rim area	3.153	0.233	3.386
RNFL thickness	0.276	0.046	0.322
Volume above surface	0.133	0.019	1.152
Volume below surface	14.403	0.062	14.465
Reference height	0.598	0.093	0.691

Sum of Squares calculated from one way analysis of variance (ANOVA). Results are for inter-image reproducibility for the POAG group (contour line redrawn separately for each of 7 images).

Parameter	Sum of squares		
	Subject	Residual	Total
C:D area ratio	1.248	0.038	1.286
Cup volume	2.179	0.203	2.38
Rim volume	0.894	0.204	1.098
Rim area	4.588	0.328	4.916
RNFL thickness	0.153	0.053	0.206
Volume above surface	0.035	0.016	0.051
Volume below surface	3.989	0.088	4.077
Reference height	0.598	0.093	0.691

Sum of Squares calculated from one way analysis of variance (ANOVA). Results are for inter-image reproducibility for the normal group (contour line redrawn separately for each of 7 images).

Parameter	Contour position	Sum of squares		
		Subject	Residual	Total
C:D area ratio	-50 μm	2.483	0.036	2.519
	Elschnig's	1.757	0.043	1.801
	+50 μm	1.243	0.033	1.276
	+100 μm	1.246	0.034	1.279
Cup volume	-50 μm	10.187	0.046	10.233
	Elschnig's	10.585	0.034	10.619
	+50 μm	10.275	0.027	10.302
	+100 μm	11.604	0.041	11.645
Rim volume	-50 μm	12.826	0.156	12.981
	Elschnig's	11.279	0.282	11.561
	+50 μm	5.654	0.107	5.761
	+100 μm	15.700	0.130	15.830
Rim area	-50 μm	11.143	0.115	11.258
	Elschnig's	4.274	0.162	4.435
	+50 μm	4.811	0.170	4.981
	+100 μm	6.937	0.279	7.216
RNFL thickness	-50 μm	3.285	0.105	3.390
	Elschnig's	1.993	0.107	2.100
	+50 μm	0.765	0.036	0.802
	+100 μm	0.803	0.038	0.841
Volume above surface	-50 μm	0.083	0.011	0.094
	Elschnig's	0.085	0.008	0.093
	+50 μm	0.122	0.011	0.133
	+100 μm	0.366	0.017	0.383
Volume below surface	-50 μm	9.689	3.833	13.522
	Elschnig's	9.994	3.976	13.970
	+50 μm	10.257	4.058	14.315
	+100 μm	11.004	4.449	15.453
Reference height	-50 μm	5.591	0.151	5.742
	Elschnig's	3.312	0.157	3.469
	+50 μm	1.399	0.072	1.471
	+100 μm	1.370	0.086	1.456

Sum of Squares (ANOVA) results for the POAG group using 4 contour line positions 1) Elschnig's ring; 2) Radius < 50 μm; 3) Radius > 50 μm; 4) Radius > 100 μm.

Parameter	Contour position	Sum of squares		
		Subject	Residual	Total
C:D area ratio	-50 μm	1.026	0.092	1.118
	Elschnig's	1.013	0.056	1.069
	+50 μm	1.007	0.032	1.039
	+100 μm	0.954	0.022	0.976
Cup volume	-50 μm	1.584	0.095	1.680
	Elschnig's	2.112	0.401	2.513
	+50 μm	2.092	0.072	2.164
	+100 μm	2.460	0.055	2.516
Rim volume	-50 μm	0.661	0.124	0.785
	Elschnig's	0.711	0.362	1.073
	+50 μm	0.674	0.127	0.801
	+100 μm	0.831	0.134	0.965
Rim area	-50 μm	2.574	0.494	3.067
	Elschnig's	3.296	0.511	3.807
	+50 μm	3.530	0.198	3.729
	+100 μm	4.714	0.485	5.199
RNFL thickness	-50 μm	2.112	0.401	2.513
	Elschnig's	0.134	0.112	0.246
	+50 μm	0.101	0.038	0.140
	+100 μm	0.180	0.480	0.661
Volume above surface	-50 μm	3.971	0.069	4.040
	Elschnig's	4.139	0.062	4.201
	+50 μm	4.411	0.083	4.494
	+100 μm	5.309	0.130	5.439
Volume below surface	-50 μm	0.038	0.011	0.049
	Elschnig's	0.037	0.012	0.049
	+50 μm	0.041	0.018	0.059
	+100 μm	0.060	0.017	0.077
Reference height	-50 μm	0.600	0.221	0.821
	Elschnig's	0.470	0.186	0.656
	+50 μm	0.375	0.065	0.440
	+100 μm	0.285	0.038	0.323

Sum of Squares (ANOVA) results for the normal group using 4 contour line positions 1) Elschnig's ring; 2) Radius < 50 μm; 3) Radius > 50 μm; 4) Radius > 100 μm.

Appendix 4. Blood gas procedures

4.1. Baseline procedure

1. The Subject was instructed to rest for 5 minutes in an upright sitting position.
2. Subject briefed on the procedure to follow in the event that they felt unwell.
3. Pulse oximeter placed on the forefinger of the left hand.
4. The subject was requested to sterile wear nose clips and breath normal room air through a mouth-piece for 5 minutes to stabilise breathing.
5. Thumbs up requested from subject to initiate baseline measurement.
6. End-tidal CO_2 and O_2 levels monitored continuously via a sample line leading from the mouth-piece to the POET II gas analyser.
7. After 5 minutes acclimatisation, the following baseline measurements were recorded over a 1 minute period:

- End-tidal CO_2 (continuous)
- End-tidal O_2 (continuous)
- Heart rate (single measure)
- Saturated O_2 content (single measure)
- Breathing rate (over 1 minute)
- Blood pressure (single measure)

8. The appropriate ocular blood flow measurement procedure then followed.

4.2. Hyperoxia procedure

1. Steps 1-3 of baseline procedure followed.
2. The subject was requested to wear sterile nose clips and breath through a mouth-piece that was connected to a mixing chamber and balloon reservoir fed by an oxygen tank containing 100% O_2.
3. A controlled amount of O_2, monitored via a flow meter by a single operator (PJH), was allowed to flow into the mixing chamber. In order to ensure there was enough gas in the chamber at any one time a balloon reservoir was kept inflated, this acted as an over-spill for the mixing chamber ensuring that it was always full of gas (see Figure 5.1).
4. 100% O_2 breathing was maintained until end-tidal O_2 levels exceeded 70% above baseline levels.
5. The subjects' end-tidal CO_2, O_2, heart rate, O_2 saturation and breathing rate was monitored continuously.
6. If the end-tidal CO_2 level fell between 0.5%-1% then CO_2 was added to the mixing chamber to prevent hyperventilation.

7. When the subjects' end-tidal O_2 content reached 70% above baseline, 5 minutes acclimatisation was allowed before any ocular blood flow measurements were taken.
8. Following acclimatisation, blood pressure was measured and recorded and the appropriate ocular blood flow measurement procedure followed.

4.4. Hypercapnia procedure

1. Steps 1-3 of baseline procedure followed.
2. The subject was requested to wear sterile nose clips and breath through a mouth-piece that was connected to a mixing chamber fed by a mixture of tanked CO_2 and normal room air. The balloon reservoir used during hyperoxia was removed during this part of the experiment, thereby allowing normal room air to flow in. A controlled amount of CO_2 was trickled into the mixing chamber.
3. One operator (PJH) simultaneously monitored the subjects' end-tidal gases and the amount of CO_2 in the mixing chamber until the end-tidal CO_2 content reached 15% above baseline.
4. The subjects end-tidal CO_2, O_2, heart rate, O_2 saturation and breathing rate was monitored continuously.
5. If the end-tidal CO_2 level raised above 15% then O_2 was added to the mixing chamber to reduce the end-tidal CO_2 level and prevent hyperventilation.
6. When the subjects' end-tidal CO_2 content reached 15% above baseline, 5 minutes acclimatisation was allowed before any ocular blood flow measurements were taken.
7. Following acclimatisation, blood pressure was measured and recorded and the appropriate ocular blood flow measurement procedure followed.

4.5. Baseline summary tables for CDI, SLDF and OBF topography

Quadrant	Parameter	Baseline 1	Baseline 2	p-value
Superior temporal	Volume	17.56 ± 3.46	18.35 ± 3.95	0.437
	Flow	231.79 ± 58.61	252.39 ± 72.30	0.456
	Velocity	0.84 ± 0.20	0.89 ± 0.29	0.508
Superior nasal	Volume	14.58 ± 4.46	16.00 ± 6.73	0.422
	Flow	211.53 ± 91.56	230.76 ± 118.63	0.524
	Velocity	0.76 ± 0.32	0.80 ± 0.39	0.667
Inferior temporal	Volume	19.59 ± 6.92	19.09 ± 8.04	0.489
	Flow	281.94 ± 130.88	266.05 ± 149.73	0.598
	Velocity	0.98 ± 0.44	0.92 ± 0.48	0.753
Inferior nasal	Volume	14.06 ± 4.09	14.28 ± 4.49	0.828
	Flow	215.01 ± 104.44	198.54 ± 86.38	0.389
	Velocity	83.44 ± 36.37	0.70 ± 0.29	0.382

Mean ± SD SLDF results for Baseline 1 (pre-hyperoxia) and baseline 2 (pre-hypercapnia).

Vessel group	Parameter	Baseline 1	Baseline 2	p-value
OA	PSV	35.07 ± 5.77	32.65 ± 7.29	0.106
	EDV	7.09 ± 1.82	6.79 ± 1.56	0.555
	RI	0.79 ± 0.05	0.79 ± 0.03	0.742
CRA	PSV	6.68 ± 1.28	6.56 ± 1.18	0.703
	EDV	1.40 ± 0.54	1.34 ± 0.59	0.597
	RI	0.79 ± 0.08	0.80 ± 0.07	0.598
SPCA	PSV	5.80 ± 1.1	5.94 ± 0.92	0.550
	EDV	1.53 ± 0.36	1.44 ± 0.30	0.571
	RI	0.73 ± 0.06	0.75 ± 0.00	0.359

Mean ± SD CDI results for Baseline 1 (pre-hyperoxia) and baseline 2 (pre-hypercapnia). Peak systolic velocity = PSV, end diastolic velocity = EDV, resistance index = RI.

Parameter	Baseline 1	Baseline 2	p-value
IOP	16.03 ± 1.7	16.05 ± 2.22	0.957
Pulse amplitude	1.94 ± 0.54	1.81 ± 0.46	0.317
Pulse volume	4.04 ± 1.23	3.84 ± 0.82	0.541
Pulse rate	73.67 ± 12.23	71.25 ± 4.97	0.459
POBF	619.96 ± 154.99	596.75 ± 131.68	0.488

Mean ± SD OBF tonograph results for Baseline 1 (pre-hyperoxia) and baseline 2 (pre-hypercapnia).

4.6. SLDF results during gas perturbation

Mean of all 4 quadrants				
Parameter	Baseline	Hypercapnia	% change	p-value
Volume	16.93 ± 6.33	18.22 ± 6.54	7.61	0.075
Flow	236.94 ± 113.73	266.86 ± 130.91	12.62	0.033
Velocity	0.83 ± 0.37	0.92 ± 0.42	11.62	0.028

SLDF results for baseline and hypercapnia. Mean values for all quadrants.

Superior temporal quadrant				
Parameter	Baseline	Hypercapnia	% change	p-value
Volume	18.35 ± 3.95	23.05 ± 6.96	25.58	0.004
Flow	252.39 ± 72.30	351.40 ± 144.22	39.23	0.003
Velocity	0.89 ± 0.29	1.19 ± 0.45	34.06	0.003

SLDF results for baseline and hypercapnia. Mean values for the superior temporal quadrant.

Superior nasal quadrant				
Parameter	Baseline	Hypercapnia	% change	p-value
Volume	16.00 ± 6.73	15.59 ± 4.88	2.6	0.72
Flow	230.76 ± 118.63	223.72 ± 103.37	3.05	0.73
Velocity	0.80 ± 0.39	0.785 ± 0.33	2.2	0.79

SLDF results for baseline and hypercapnia. Mean values for the superior nasal quadrant.

Inferior temporal quadrant				
Parameter	Baseline	Hypercapnia	% change	p-value
Volume	19.09 ± 8.04	19.63 ± 5.35	2.85	0.76
Flow	266.05 ± 149.73	280.49 ± 109.6	5.43	0.65
Velocity	0.92 ± 0.48	0.98 ± 0.36	6.54	0.54

SLDF results for baseline and hypercapnia. Mean values for the inferior temporal quadrant.

Inferior nasal quadrant				
Parameter	**Baseline**	**Hypercapnia**	**% change**	**p-value**
Volume	14.28 ± 4.49	14.61 ± 4.99	3.25	0.77
Flow	198.54 ± 86.38	211.81 ± 113.27	15.1	0.56
Velocity	0.70 ± 0.29	0.75 ± 0.38	16	0.59

SLDF results for baseline and hypercapnia. Mean values for the inferior nasal quadrant.

Mean of all 4 quadrants				
Parameter	**Baseline**	**Hyperoxia**	**% change**	**p-value**
Volume	16.51 ± 5.41	15.92 ± 5.88	3.6	0.46
Flow	237.23 ± 104.17	235.61 ± 124.68	0.68	0.92
Velocity	0.84 ± 0.35	0.83 ± 0.41	0.75	0.91

SLDF results for baseline and hyperoxia. Mean values for all 4 quadrants.

Superior temporal quadrant				
Parameter	**Baseline**	**Hyperoxia**	**% change**	**p-value**
Volume	17.56 ± 3.46	19.92 ± 5.67	13.41	0.21
Flow	231.79 ± 58.61	295.45 ± 130.59	24.25	0.15
Velocity	0.84 ± 0.20	1.03 ± 0.41	22.15	0.13

SLDF results for baseline and hyperoxia. Mean values for the superior temporal quadrant.

Superior nasal quadrant				
Parameter	**Baseline**	**Hyperoxia**	**% change**	**p-value**
Volume	14.58 ± 4.46	13.46 ± 4.64	7.67	0.01
Flow	211.53 ± 91.56	180.36 ± 91.56	14.74	0.001
Velocity	0.76 ± 0.32	0.64 ± 0.32	14.92	0.001

SLDF results for baseline and hyperoxia. Mean values for the superior nasal quadrant.

Inferior temporal quadrant				
Parameter	**Baseline**	**Hyperoxia**	**% change**	**p-value**
Volume	19.59 ± 6.92	16.89 ± 5.96	13.77	0.13
Flow	281.94 ± 130.88	256.81 ± 141.97	8.91	0.45
Velocity	0.98 ± 0.44	0.91 ± 0.47	7.98	0.48

SLDF results for baseline and hyperoxia. Mean values for the inferior temporal quadrant.

Inferior nasal quadrant				
Parameter	**Baseline**	**Hyperoxia**	**% change**	**p-value**
Volume	14.06 ± 4.09	13.53 ± 4.55	3.75	0.70
Flow	215.01 ± 104.44	210.14 ± 94.49	2.26	0.84
Velocity	83.44 ± 36.37	0.75 ± 0.33	1.50	0.88

SLDF results for baseline and hyperoxia. Mean values for the inferior nasal quadrant.

4.7. CDI results during gas perturbation

PCAs				
Parameter	**Baseline**	**Hypercapnia**	**% change**	**p-value**
PSV	5.94 ± 0.92	6.43 ± 1.17	9	0.025
EDV	1.44 ± 0.30	1.78 ± 0.47	23	0.006
RI	0.75 ± 0.00	0.72 ± 0.06	5	0.004

CDI results for baseline and hypercapnia. Mean values for the PCAs.

OA				
Parameter	**Baseline**	**Hypercapnia**	**% change**	**p-value**
PSV	32.65 ±	34.93 ± 6.89	6.99	0.06
EDV	6.79 ± 1.56	7.06 ± 1.30	4.02	0.312
RI	0.79 ± 0.03	0.80 ± 0.02	0.90	0.273

CDI results for baseline and hypercapnia. Mean values for the OA.

CRA				
Parameter	**Baseline**	**Hypercapnia**	**% change**	**p-value**
PSV	6.56 ± 1.18	7.06 ± 1.19	7.67	0.199
EDV	1.34 ± 0.59	1.57 ± 0.44	17.68	0.062
RI	0.80 ± 0.07	0.77 ± 0.06	3.04	0.088

CDI results for baseline and hypercapnia. Mean values for the CRA.

PCAs				
Parameter	**Baseline**	**Hyperoxia**	**% change**	**p-value**
PSV	5.80 ± 1.1	6.24 ± 1.21	7.59	0.23
EDV	1.53 ± 0.36	1.67 ± 0.47	8.83	0.16
RI	0.73 ± 0.06	0.73 ± 0.06	0.01	0.94

CDI results for baseline and hyperoxia. Mean values for the PCAs.

OA				
Parameter	**Baseline**	**Hyperoxia**	**% change**	**p-value**
PSV	35.07 ± 5.77	32.69 ± 6.77	6.79	0.043
EDV	7.09 ± 1.82	6.39 ± 1.24	9.93	0.07
RI	0.79 ± 0.05	0.80 ± 0.05	0.63	0.578

CDI results for baseline and hyperoxia. Mean values for the OA.

CRA				
Parameter	**Baseline**	**Hyperoxia**	**% change**	**p-value**
PSV	6.68 ± 1.28	6.51 ± 1.48	2.50	0.742
EDV	1.40 ± 0.54	1.54 ± 0.6	10.08	0.364
RI	0.79 ± 0.08	0.71 ± 0.06	2.90	0.160

CDI results for baseline and hyperoxia. Mean values for the CRA.

4.7. OBF tonograph results during blood gas perturbation

Parameter	**Baseline**	**Hyperoxia**	**% change**	**p-value**
IOP	16.05 ± 2.22	15.25 ± 2.37	4.98	0.052
Pulse amplitude	1.81 ± 0.46	1.85 ± 0.61	2.10	0.321
Pulse volume	3.84 ± 0.82	4.10 ± 1.31	6.73	0.141
Pulse rate	71.25 ± 4.97	72.76 ± 5.06	2.12	0.129
POBF	596.75 ± 131.68	637.83 ± 179.42	6.88	0.232

OBF tonograph results for baseline and hyperoxia.

Parameter	Baseline	Hypercapnia	% change	p-value
IOP	16.03 ± 1.7	13.57 ± 1.39	15.34	0.000
Pulse amplitude	1.94 ± 0.54	1.92 ± 0.43	0.74	0.866
Pulse volume	4.04 ± 1.23	4.64 ± 1.09	14.96	0.008
Pulse rate	73.67 ± 12.23	69.1 ± 11.59	6.2	0.000
POBF	619.96 ± 154.99	652.21 ± 141.40	5.2	0.080

OBF tonograph results for baseline and hyperoxia.

Appendix 5. HRF reproducibility summary tables

	Normal subject group								
Flow	**2**	**3**	**4**	**5**	**6**	**7**	**8**	**9**	**10**
Sup nasal	18.04	20.78	32.57	32.57	31.97	34.13	32.60	33.54	33.33
Sup temporal	34.13	37.49	37.81	37.36	39.45	38.78	39.52	40.21	39.94
Cen nasal	24.43	35.41	37.99	39.96	38.67	41.15	40.40	40.97	40.69
Cen temporal	20.11	38.67	41.49	42.64	41.64	42.90	44.08	44.43	44.46
Inf nasal	28.15	31.58	36.25	36.78	36.34	35.72	34.83	36.27	36.65
Inf temp	26.80	31.35	33.03	34.59	35.57	35.83	36.66	36.45	38.06

Mean standard deviations for the HRF parameter flow at 2-10 images in 6 peripapillary locations for the normal group (n=19).

	POAG subject group								
Flow	**2**	**3**	**4**	**5**	**6**	**7**	**8**	**9**	**10**
Sup nasal	30.33	48.49	52.91	53.18	59.05	55.88	54.90	57.78	57.64
Sup temporal	29.70	36.10	54.94	60.83	63.52	64.90	64.09	63.58	62.64
Cen nasal	29.59	52.55	54.33	56.24	60.34	59.72	57.52	64.92	64.23
Cen temporal	21.86	46.85	53.47	58.38	63.41	62.59	65.42	63.86	63.91
Inf nasal	45.12	52.33	54.35	56.77	67.45	65.47	67.63	68.19	68.55
Inf temp	26.77	32.32	42.47	46.65	50.69	53.39	52.49	53.75	53.74

Mean standard deviations for the HRF parameter flow at 2-10 images in 6 peripapillary locations for the POAG group (n=10).

	Normal subject group								
Volume	**2**	**3**	**4**	**5**	**6**	**7**	**8**	**9**	**10**
Sup nasal	1.15	1.16	1.47	1.59	1.64	1.79	1.74	1.81	1.85
Sup temporal	1.63	1.82	1.79	1.85	1.92	2.01	2.04	2.08	2.09
Cen nasal	1.14	1.69	1.97	2.13	2.11	2.14	2.10	2.16	2.14
Cen temporal	1.27	1.90	1.91	2.13	2.11	2.14	2.23	2.25	2.28
Inf nasal	1.75	1.86	2.01	2.04	2.09	2.07	2.01	2.11	2.10
Inf temp	1.66	2.10	2.12	2.16	2.17	2.16	2.22	2.22	2.24

Mean standard deviation for the HRF parameter volume for 2-10 images in 6 peripapillary retinal locations for the normal group (n=19).

	POAG subject group								
Volume	**2**	**3**	**4**	**5**	**6**	**7**	**8**	**9**	**10**
Sup nasal	1.06	1.84	2.17	2.27	2.40	2.32	2.37	2.44	2.45
Sup temporal	1.10	1.19	2.19	2.70	2.97	3.02	2.95	2.90	2.93
Cen nasal	1.50	2.26	2.41	2.61	2.64	2.59	2.51	2.73	2.80
Cen temporal	0.74	2.01	2.21	2.44	2.57	2.74	2.76	2.75	2.81
Inf nasal	1.76	2.37	2.49	2.53	2.71	2.70	2.77	2.77	2.82
Inf temp	1.18	1.82	2.40	2.53	2.58	2.65	2.66	2.65	2.65

Mean standard deviations for the HRF parameter volume at 2-10 images in 6 peripapillary locations for the POAG group (n=10).

	Normal subject group								
Velocity	**2**	**3**	**4**	**5**	**6**	**7**	**8**	**9**	**10**
Sup nasal	0.06	0.07	0.10	0.11	0.11	0.12	0.11	0.11	0.11
Sup temporal	0.12	0.13	0.13	0.13	0.13	0.13	0.13	0.14	0.14
Cen nasal	0.08	0.12	0.13	0.14	0.13	0.14	0.14	0.14	0.14
Cen temporal	0.07	0.14	0.14	0.15	0.14	0.15	0.15	0.15	0.15
Inf nasal	0.11	0.12	0.12	0.13	0.12	0.12	0.12	0.13	0.13
Inf temp	0.10	0.11	0.12	0.12	0.13	0.13	0.13	0.13	0.13

Mean standard deviation for the HRF parameter velocity for 2-10 images in 6 peripapillary retinal locations for the normal group (n=19).

	POAG subject group								
Velocity	**2**	**3**	**4**	**5**	**6**	**7**	**8**	**9**	**10**
Sup nasal	0.11	0.17	0.18	0.18	0.20	0.19	0.19	0.20	0.20
Sup temporal	0.11	0.13	0.19	0.21	0.22	0.22	0.22	0.22	0.22
Cen nasal	0.11	0.18	0.19	0.18	0.19	0.20	0.19	0.22	0.22
Cen temporal	0.08	0.16	0.18	0.20	0.22	0.22	0.22	0.22	0.22
Inf nasal	0.15	0.18	0.19	0.19	0.23	0.22	0.23	0.23	0.23
Inf temp	0.09	0.11	0.14	0.16	0.17	0.18	0.18	0.18	0.18

Mean standard deviation for the HRF parameter velocity for 2-10 images in 6 peripapillary retinal locations for the POAG group (n=10).

Region	**Parameter**	Sum of squares		
		Subject	**Residual**	**Total**
Superior	**Nasal volume**	1193.23	108.03	1301.26
	Temp volume	693.17	239.13	932.30
Central	**Nasal volume**	908.62	221.76	1130.38
	Temp volume	970.32	313.99	1284.31
Inferior	**Nasal volume**	984.79	333.95	1318.74
	Temp volume	614.93	300.40	915.32
Superior	**Nasal flow**	419800.97	36373.75	456174.72
	Temp flow	546903.76	129615.37	676519.13
Central	**Nasal flow**	3180330.56	107469.69	425500.25
	Temp flow	469934.50	130328.93	600263.43
Inferior	**Nasal flow**	272603.88	90698.87	363302.74
	Temp flow	456502.76	85292.62	541795.38
Superior	**Nasal velocity**	4.67	0.43	5.13
	Temp velocity	6.23	1.4	7.66
Central	**Nasal velocity**	3.54	1.26	4.8
	Temp velocity	4.27	1.53	5.8
Inferior	**Nasal velocity**	3.53	1.15	4.68
	Temp velocity	3.05	0.97	4.03

ANOVA sums of squares results for HRF parameters for the normal group (used to calculate ICC).

Region	Parameter	Sum of squares		
		Subject	Residual	Total
Superior	Nasal volume	418.44	87.88	506.23
	Temp volume	413.48	57.04	470.51
Central	Nasal volume	450.74	214.40	665.14
	Temp volume	524.79	135.41	660.20
Inferior	Nasal volume	577.75	189.76	767.52
	Temp volume	644.14	119.84	763.97
Superior	Nasal flow	155962.60	58140.99	214103.59
	Temp flow	112118.84	48778.93	160897.74
Central	Nasal flow	195931.33	125067.03	320998.35
	Temp flow	348233.95	79108.35	427342.29
Inferior	Nasal flow	234661.15	73255.99	307917.13
	Temp flow	229417.67	37142.72	266560.38
Superior	Nasal velocity	1.84	0.55	2.39
	Temp velocity	1.32	0.61	1.93
Central	Nasal velocity	2.50	1.53	4.03
	Temp velocity	1.32	0.61	1.93
Inferior	Nasal velocity	2.62	0.86	3.48
	Temp velocity	2.65	0.40	3.06

ANOVA sums of squares results for HRF parameters for the POAG group (used to calculate ICC).

Appendix 6. Normality data for the regional HRT parameters.

	Superior nasal data set					
	Normal		Without outliers		With outliers	
Parameter	Normal	POAG	Normal	POAG	Normal	POAG
Mean height contour	4 [80]	5 [100]			1 [20]	
Volume below surface			4 [80]	2 [40]	1 [20]	3 [60]
Volume above surface	1 [20]		1 [20]		3 [60]	5 [100]
Volume below reference			5 [100]	2 [40]		3 [60]
Volume above reference	5 [100]	5 [100]				
Maximum depth	5 [100]	5 [100]				
Third moment	4 [80]	5 [100]	1 [20]			
Cup area		1 [20]	5 [100]	1 [20]		3 [60]
Mean	**19 [47.5 %]**	**21 [52.5%]**	**16 [40%]**	**5 [12.5%]**	**5 [12.5%]**	**14 [35%]**

	Superior temporal data set					
	Normal		Without outliers		With outliers	
Parameter	Normal	POAG	Normal	POAG	Normal	POAG
Mean height contour	3 [60]	5 [100]			2 [40]	
Volume below surface	2 [40]	1 [20]	1 [20]		2 [40]	4 [80]
Volume above surface				3 [60]	5 [100]	2 [40]
Volume below reference			4 [80]	2 [40]	1 [20]	3 [60]
Volume above reference	5 [100]	4 [80]				1 [20]
Maximum depth	5 [100]	4 [80]				1 [20]
Third moment	5 [100]	5 [100]				
Cup area		3 [60]	5 [100]	1 [20]		1 [20]
Mean	**20 [50%]**	**22 [55%]**	**10 [25%]**	**6 [15%]**	**10 [25%]**	**12 [30%]**

	Temporal data set					
	Normal		Without outliers		With outliers	
Parmeter	Normal	POAG	Normal	POAG	Normal	POAG
Mean height contour	5 [100]	5 [100]				
Volume below surface	2 [40]	4 [80]	2 [40]	1 [20]	1 [20]	
Volume above surface	1 [20]		1 [20]	2 [40]	3 [60]	3 [60]
Volume below reference			5 [100]	2 [40]		3 [60]
Volume above reference	5 [100]	4 [80]				1 [20]
Maximum depth	5 [100]	4 [80]				1 [20]
Third moment	5 [100]	5 [100]				
Cup area		5 [100]	3 [60]		2 [40]	
Mean	**23 [57.5%]**	**27 [67.5%]**	**11 [27.5%]**	**5 [12.5%]**	**6 [15%]**	**8 [20%]**

	Nasal data set					
	Normal		Without outliers		With outliers	
Parmeter	Normal	POAG	Normal	POAG	Normal	POAG
Mean height contour	5 [100]	5 [100]				
Volume below surface			4 [80]	5 [100]	1 [20]	
Volume above surface	3 [60]		1 [20]	4 [80]	1 [20]	1 [20]
Volume below reference			5 [100]	5 [100]		
Volume above reference	5 [100]	5 [100]				
Maximum depth	2 [40]	5 [100]			3 [60]	
Third moment	4 [80]	2 [40]			1 [20]	3 [60]
Cup area			5 [100]	3 [60]		2 [40]
Mean	**19 [47.5%]**	**17 [42.5%]**	**15 [37.5%]**	**17 [42.5%]**	**6 [15%]**	**6 [15%]**

	Inferior nasal data set					
	Normal		Without outliers		With outliers	
Parameter	Normal	POAG	Normal	POAG	Normal	POAG
Mean height contour	4 [80]	5 [100]			1 [20]	
Volume below surface			3 [60]	2 [40]	2 [40]	3 [60]
Volume above surface	1 [20]		1 [20]	3 [60]	3 [60]	2 [40]
Volume below reference			5 [100]	4 [80]		1 [20]
Volume above reference	5 [100]	5 [100]				
Maximum depth		4 [80]			5 [100]	1 [20]
Third moment	5 [100]	5 [100]				
Cup area		4 [80]	5 [100]			1 [20]
Mean	**15 [37.5%]**	**23 [57.5%]**	**14 [35%]**	**9 [22.5%]**	**11 [27.5%]**	**8 [20%]**

	Inferior temporal data set					
	Normal		Without outliers		With outliers	
Parameter	Normal	POAG	Normal	POAG	Normal	POAG
Mean height contour	5 [100]	5 [100]				
Volume below surface		1 [20]			5 [100]	4 [80]
Volume above surface			5 [100]	4 [80]		1 [20]
Volume below reference			5 [100]	2 [40]		3 [60]
Volume above reference	5 [100]			1 [20]		4 [80]
Maximum depth	5 [100]	5 [100]		1 [20]		
Third moment	4 [80]	5 [100]			1 [20]	
Cup area		5 [100]			5 [100]	
Mean	**19 [47.5%]**	**21 [52.5%]**	**10 [25%]**	**8 [20%]**	**11 27.5%]**	**12 [30%]**

Appendix 7. Individual subject change in regional HRT parameters. Examples of visual fields and topography images for individual patients

7.1. Normal subject group: nasal data.

7.2. Normal subject group: temporal data.

7.3. POAG subject group: nasal data.

7.4. POAG subject group: temporal data.

7.5. Visual field change for normal subject (#28).

7.6. Visual field progression for a POAG subject (#41).

7.7. Topography images for a POAG subject (#41).

7.8 Visual field progression for a POAG subject (#58).

7.9 Topography images for a POAG subject (#58).

7.10 Visual field progression for a POAG subject (#44).

Subject #	Mean height contour 2			Volume below surface 4			Volume above surface 5			Volume below reference 6			Volume above reference 7			Maximum depth 8			Third moment 9			Cup area 13		
	SN	N	IN	SN	N	IN	SN	N	IN	SN	N	IN	SN	N	IN	SN	N	IN	SN	N	IN	SN	N	IN
1	×																							
2			×						×															
3				×																		×		
4											×		×		×							×		×
5								×					×	×										
6												×												
7																								
8	×				×																			
9	×			×			×			×			×		×				×		×	×		
10							×								×							×		×
11									×															
12																								
13	×		×	×	×								×		×						×	×		
14			×											×	×									
15															×									
16		×																						
17																				×				
18			×					×																
19	×	×	×				×																	
20																								
21		×									×			×										
22											×												×	
23				×				×	×				×	×	×							×	×	
24																								
25			×				×	×																
26			×												×									
27		×				×							×		×		×						×	×
28																								
29		×		×		×		×						×								×	×	
30							×					×								×				
31	×		×		×			×						×	×			×			×	×		×
Total	6	5	8	5	3	2	5	6	3	1	3	2	6	6	10	0	1	1	1	2	4	8	4	4

Appendix 7.1. Regional HRT data measured superior nasally, nasally and inferior nasally for the normal subject group.

Subject #	Mean height contour 2			Volume below surface 4			Volume above surface 5			Volume below reference 6			Volume above reference 7			Maximum depth 8			Third moment 9			Cup area 13		
	ST	T	IT	ST	T	IT	ST	T	IT	ST	T	IT	ST	T	IT	ST	T	IT	ST	T	IT	ST	T	IT
1	x						x											x						
2	x						x					x				x								
3				x			x	x		x	x	x	x							x		x		x
4																				x				
5																			x					
6	x	x			x				x															
7																								
8				x	x	x							x	x		x	x		x					x
9	x	x		x					x	x	x			x	x								x	x
10										x					x		x							x
11				x	x								x											
12															x									
13	x	x			x						x		x	x					x	x			x	
14	x	x									x												x	
15													x		x									
16									x															
17	x	x			x						x		x									x		
18			x																					
19	x		x	x	x												x							
20			x																					
21									x															
22						x																		
23		x	x							x			x	x			x					x		x
24																								
25	x		x												x									
26	x							x	x						x									x
27			x						x			x												x
28	x														x									
29													x											
30				x																				
31							x			x	x		x						x			x		
Total	11	6	6	6	6	2	4	2	6	4	7	3	9	4	7	2	4	1	4	3	0	4	3	7

Appendix 7.2. Regional HRT data measured superior temporally, temporally and inferior temporally for the normal subject group.

Subject #	Mean height contour 2			Volume below surface 4			Volume above surface 5			Volume below reference 6			Volume above reference 7			Maximum depth 8			Third moment 9			Cup area 13		
	SN	N	IN	SN	N	IN	SN	N	IN	SN	N	IN	SN	N	IN	SN	N	IN	SN	N	IN	SN	N	IN
32												×												
33																×	×	×						
34		×	×	×						×	×					×	×			×		×		
35																								
36									×													×	×	×
37			×	×		×						×			×									×
38												×												×
39		×																						
40			×		×			×	×			×		×	×		×				×			
41						×						×												×
42																								
43	×	×			×	×		×			×		×	×	×	×	×	×				×	×	×
44		×		×	×										×		×							×
45				×		×				×												×		×
46		×																		×				
47				×						×		×			×	×			×					×
48				×	×	×				×		×			×	×	×	×	×			×	×	×
49						×																		
50			×								×			×	×						×		×	
51						×					×			×	×			×						×
52				×						×					×	×				×		×		×
53				×												×								
54				×				×		×											×	×		
55	×				×		×						×								×		×	
56		×	×	×		×	×	×	×	×	×	×			×	×		×					×	
57		×	×														×							
58	×				×								×							×				
59				×		×				×		×				×		×						
60																	×				×	×		
61								×		×			×						×		×	×		×
62	×				×			×		×	×	×	×	×	×						×	×	×	×
63	×	×	×	×	×	×	×	×	×			×					×							×
64			×																			×		
Total	5	8	8	12	8	10	3	7	4	10	6	11	5	5	11	9	9	6	3	4	7	11	7	14

Appendix 7.3. Regional HRT data measured superior nasally, nasally and inferior nasally for the POAG subject group

#	Mean height contour 2			Volume below surface 4			Volume above surface 5			Volume below reference 6			Volume above reference 7			Maximum depth 8			Third moment 9			Cup area 13		
	ST	T	IT	ST	T	IT	ST	T	IT	ST	T	IT	ST	T	IT	ST	T	IT	ST	T	IT	ST	T	IT
32																								
33	×			×	×					×	×	×				×	×	×						
34			×																	×				×
35		×																				×		
36															×								×	×
37				×	×									×	×				×		×	×	×	×
38									×			×			×									×
39																					×	×		
40	×	×	×	×	×		×	×		×	×	×	×		×	×	×	×	×			×		×
41																		×						
42																								
43	×	×		×	×	×	×		×		×		×		×		×		×	×	×	×		
44	×			×						×								×		×				
45				×			×	×		×			×	×								×		×
46																								
47				×						×						×			×	×				
48				×	×	×				×		×				×	×	×			×			×
49					×	×		×		×		×					×	×					×	×
50		×											×									×	×	
51						×	×							×	×		×	×		×	×		×	×
52															×									×
53	×	×	×	×			×								×				×			×		
54													×								×	×		×
55		×					×		×															
56							×									×			×	×		×	×	
57	×		×	×	×					×	×									×		×		×
58	×			×	×				×				×				×	×				×		
59																						×		
60			×											×								×		
61													×							×	×			
62												×		×		×				×				×
63	×					×	×							×					×		×		×	×
64			×				×					×	×											
Total	8	6	6	11	8	5	9	3	4	7	5	7	7	6	8	5	8	8	7	9	8	14	7	14

Appendix 7.4. Regional HRT data measured superior temporally, temporally and inferior temporally for the POAG subject group.

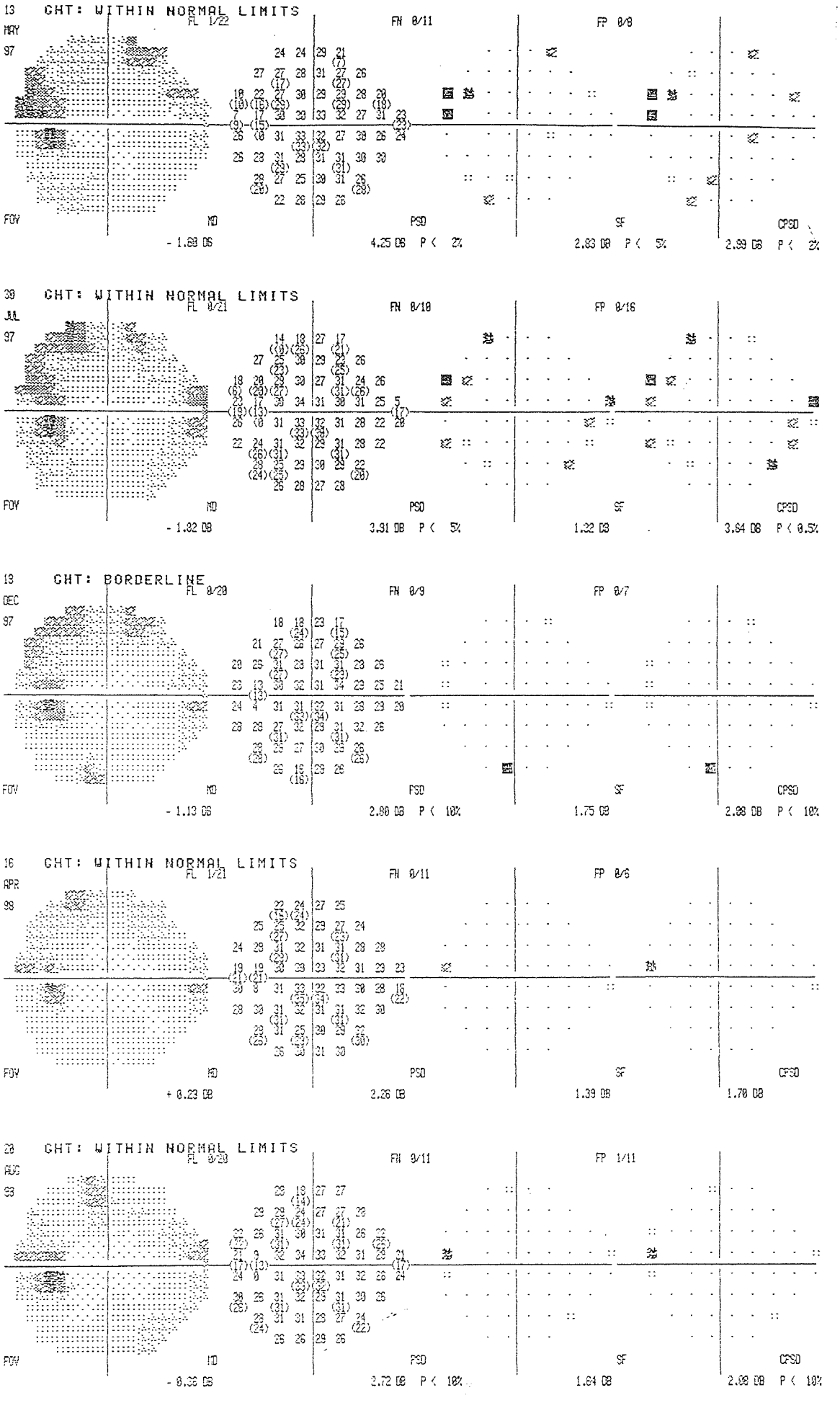

Appendix 7.5. Visual field change for normal subject (#28). CPSD increased significantly over the study period indicative of a learning effect.

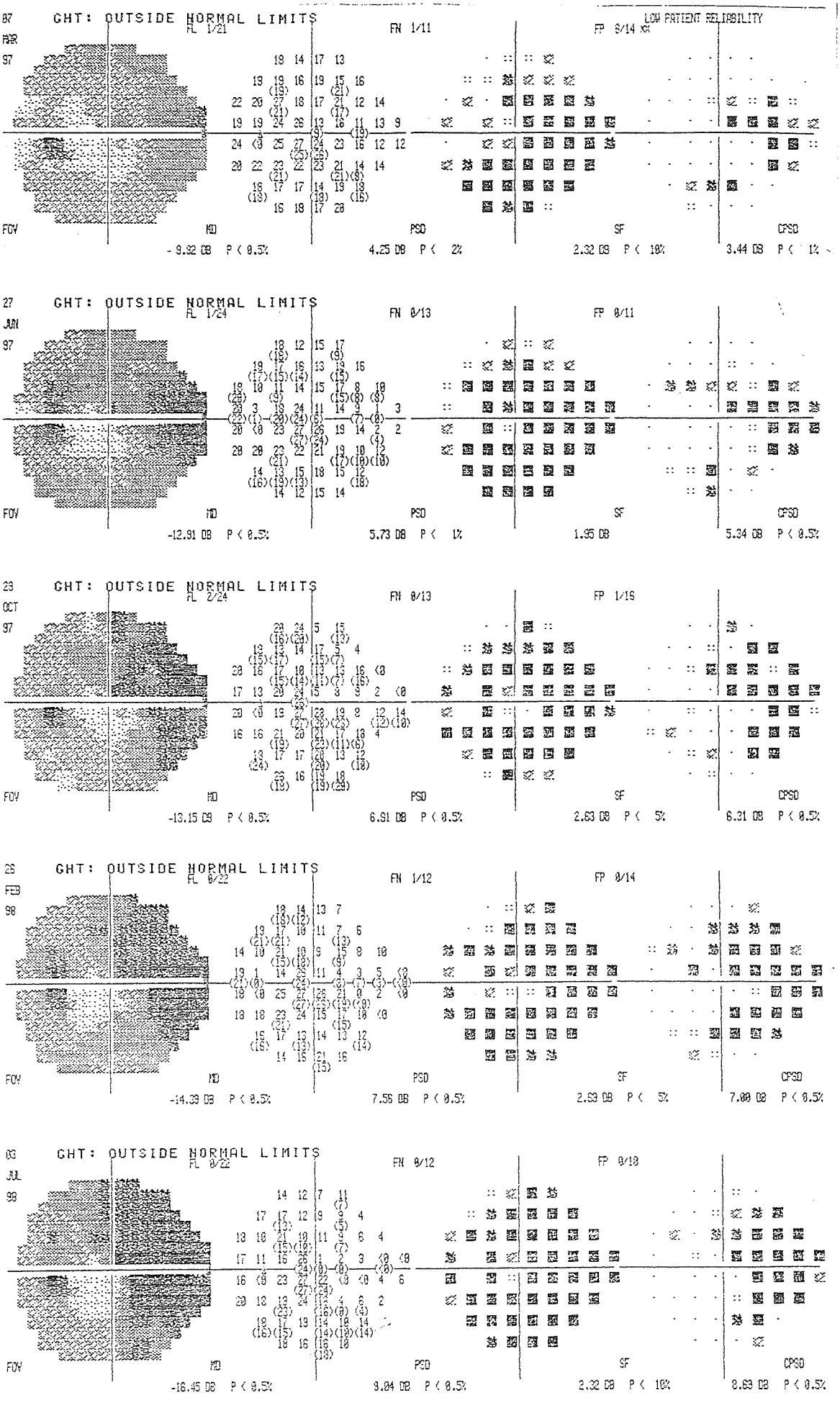

Appendix 7.6. Visual field progression for POAG subject (#41). CPSD decreased and MD increased significantly over the study period. Morphological change in disc topography was evident

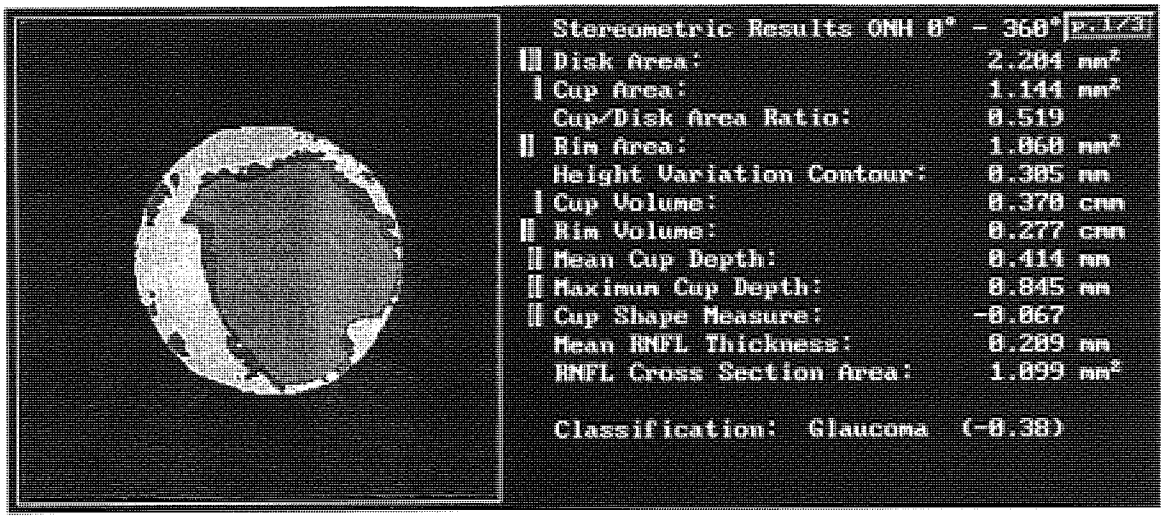

Visit 1

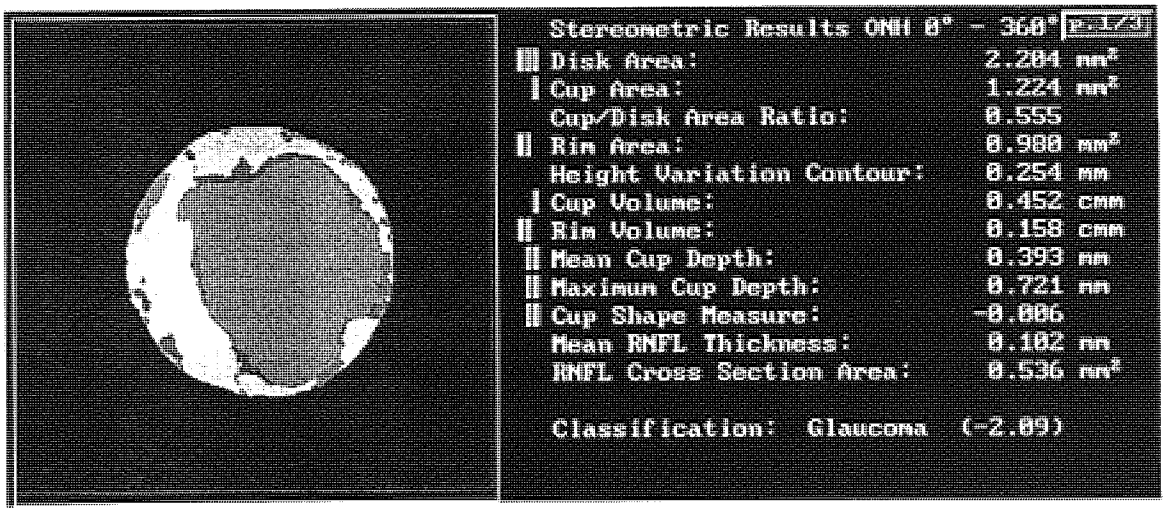

Visit 5

Appendix 7.7. Visit 1 and visit 5 HRT topography images for a POAG subject (#41). This patient had an increasing visual field CPSD (appendix) throughout the study period together with a morphological change in rim factor. Note the decrease in rim area, rim volume and retinal nerve fibre layer thickness between visits 1 and 5. The cup parameters also appear to be increasing indicting glaucomatous progression.

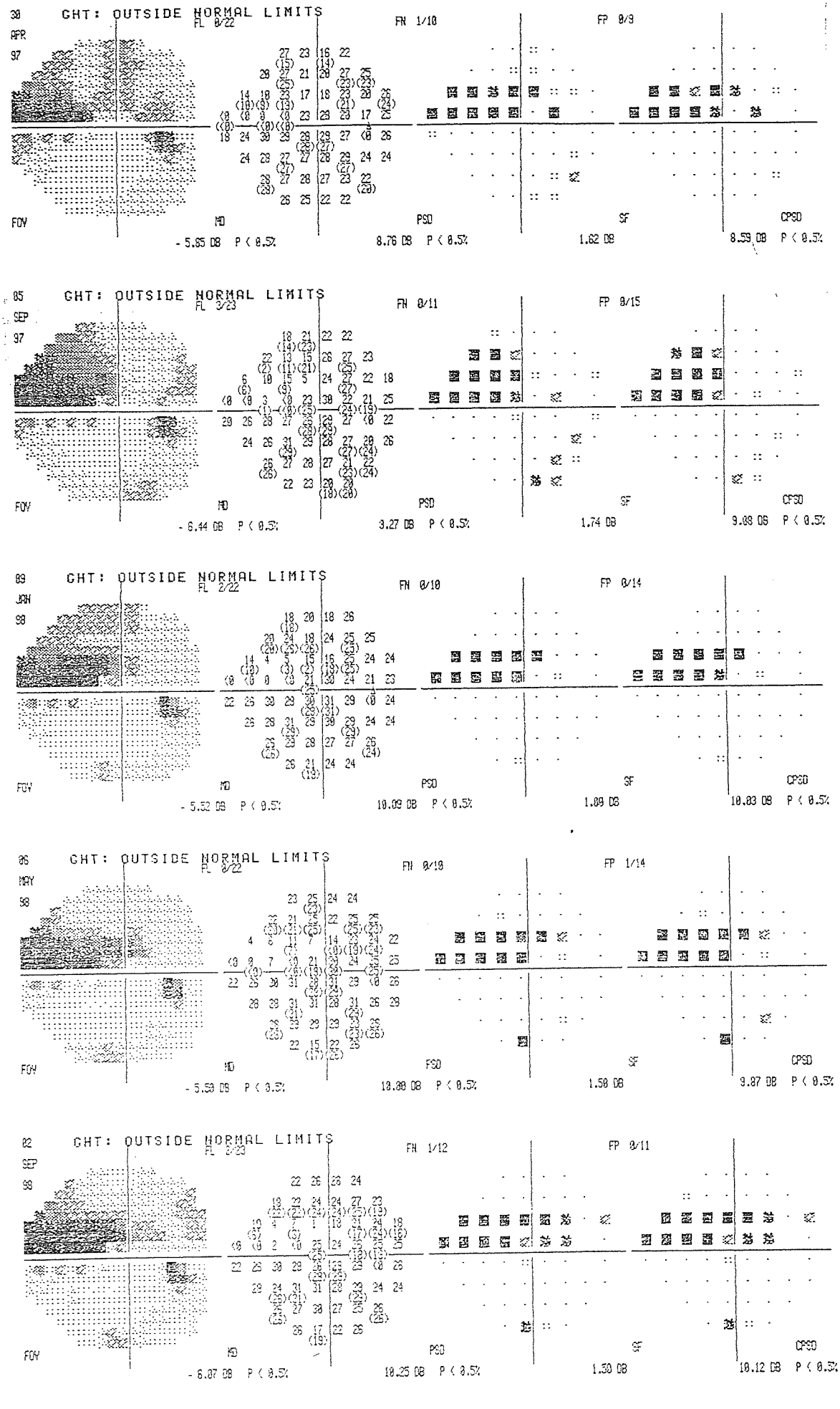

Appendix 7.8. Visual field progression for POAG subject (#58). CPSD decreased significantly over the study period and is consistent with morphological change in disc topography.

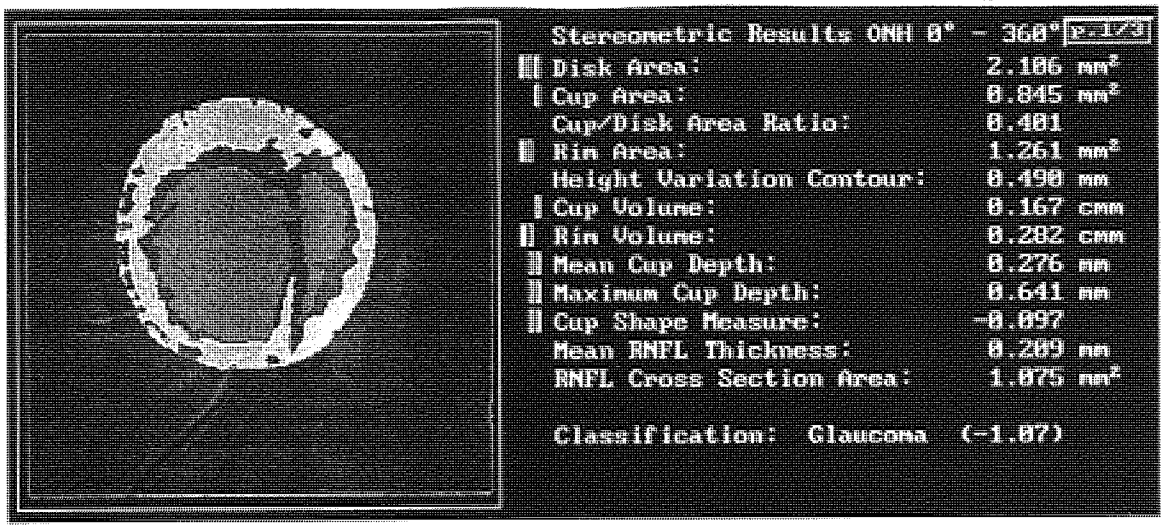

Visit 1

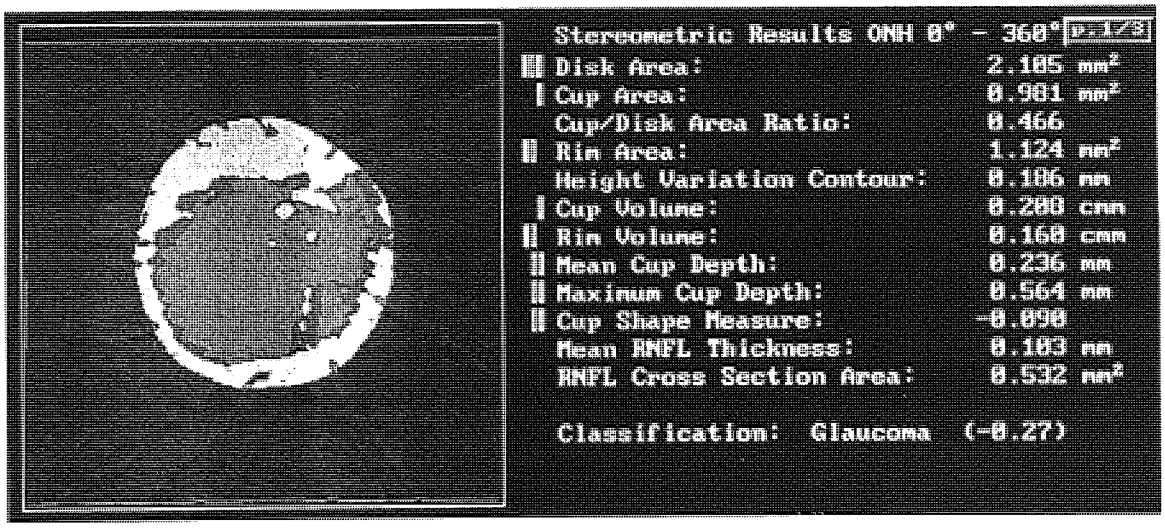

Visit 5

Appendix 7.9. Visit 1 and visit 5 HRT topography images for a POAG subject (#58). This patient had an increasing (deteriorating) visual field CPSD (appendix) throughout the study period together with a morphological change in rim factor. Note the decrease in rim area, rim volume and retinal nerve fibre layer thickness between visits 1 and 5.

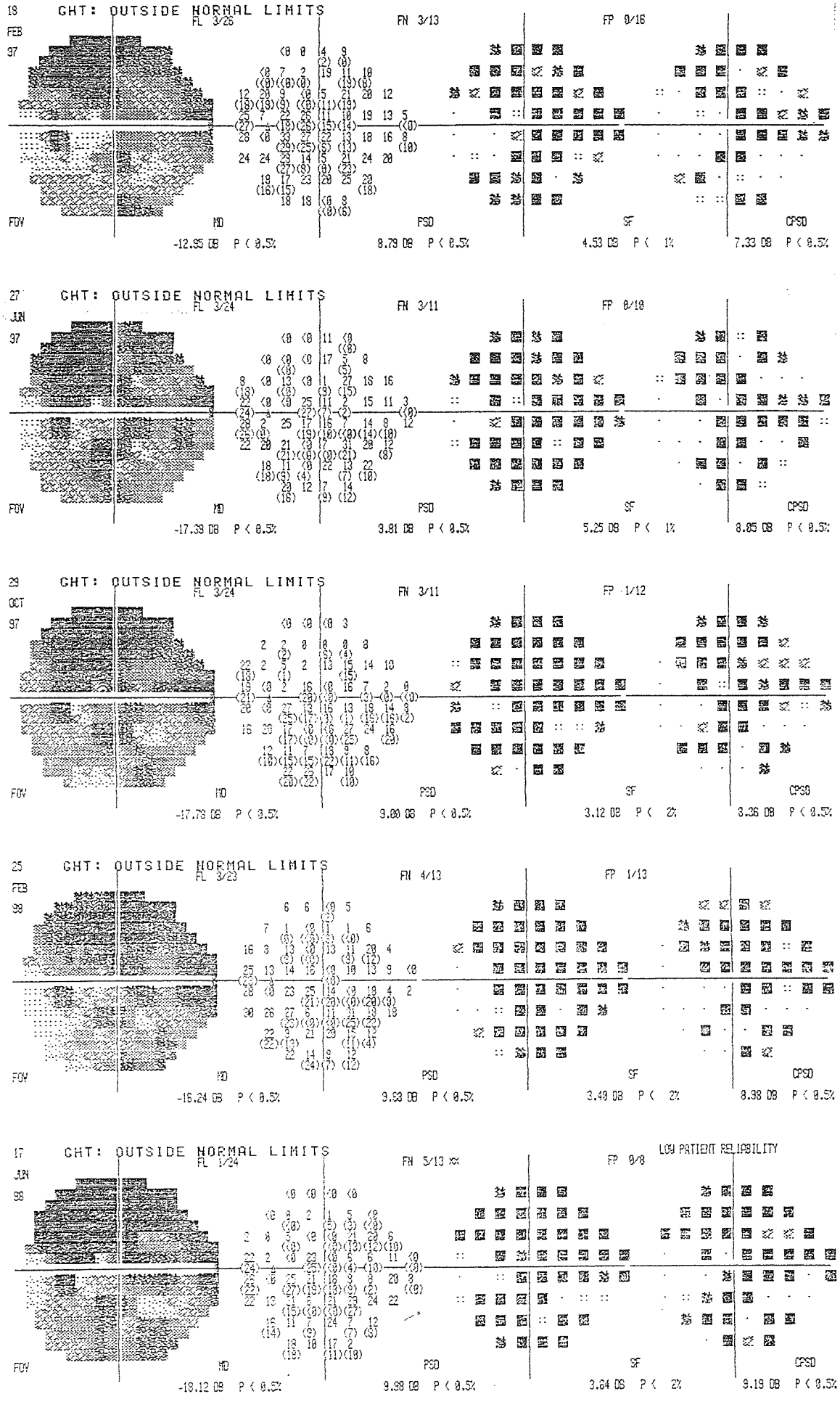

Appendix 7.10. Visual fields for POAG subject (#44), showing a deterioration in CPSD over the study period.